Boston College

Morrissey Graduate School of Arts and Sciences

Department of Chemistry

Pd/AZABORINE-BIARYL PHOSPHINE COMPLEXES: REACTION DEVELOPMENT, MECHANISTIC ANALYSIS, AND INVESTIGATIONS INTO METAL-LIGAND COORDINATION DYNAMICS

A dissertation

By

YUANZHE ZHANG

Submitted in partial fulfillment of the requirements

for the degree of

Doctor of Philosophy

May 2021

Pd/AZABORINE-BIARYL PHOSPHINE COMPLEXES: REACTION DEVELOPMENT, MECHANISTIC ANALYSIS, AND INVESTIGATIONS INTO METAL-LIGAND COORDINATION DYNAMICS

By

YUANZHE ZHANG

Dissertation Advisor:

Professor Shih-Yuan Liu

Abstract: Described herein are three research projects that focused on 1) the catalytic activities of Pd/azaborine-derived biary phosphine (Senphos) complexes in 1,3-enyne difunctionalization reactions and 2) the coordination behaviors of these Pd/Senphos complexes. In the first chapter, expansion of the substrate scope and mechanistic studies of the reported Pd/Senphos catalyzed site-, regio- and *trans*-selective hydroboration of 1,3-enynes are described. In the second chapter, the first intermolecular site-, regio- and *trans*-selective chloroboration and cyanoboration of enynes that are enabled by the Pd/Senphos catalytic system are presented. The cyanoboration products, namely vicinal boron-substituted alkenylnitriles, are demonstrated as versatile synthetic building blocks. In the last chapter, the κ^2-*P*-η^2-B,C coordination behavior in a series of 1,2-, 1,3- and 1,4-Senphos ligated Pd(0) or Pd(II) complexes are evaluated based on solid-state structures and variable-temperature NMR measurements.

TABLE OF CONTENTS

ACKNOWLEDGMENTS

Every single day in lab is unpredictable, however, after several years, these unpredictable days together constitute a rather predictable and amazing PhD journey. And this accomplishment is closely related to the wonderful people around me. I am grateful to my advisor, Prof. Shih-Yuan Liu, for his guidance throughout my graduate school. Being a great scientific research supervisor, Prof. Liu's passion in chemistry, broad and deep knowledge and creative ideas benefit me a lot, and more importantly, being a wonderful life mentor, Prof. Liu's critical thinking and meticulous attitude are great spiritual digest for me. I would also like to thank my committee members, Professor Marc Snapper and Professor Masayuki Wasa, for their time reviewing this dissertation and rendering invaluable insights.

I want to especially thank my mentor, Dr. Senmiao Xu for his discussions and encouragement during my PhD study, and thank Dr. Zhiqiang Liu, Dr. Xuguang Liu, Dr. Jacob Ishibashi, Dr. Zachary Giustra, Dr. Cameron McConnell, Yao Liu, Xinyu Yang, Kevin Byrne and the rest of the Liu group members, past and present, with whom working in the lab becomes enjoyable.

My research would be impossible without the instrumentation and administration support from the department and university, where I greatly appreciate Dr. Bo Li, Dr. Thusitha Jayasundera (TJ), Dr. Jing Jin, Marek Domin, Dale Mahoney, Lynne Pflaumer and Dr. Ian Parr.

Finally, I am deeply indebted to my family. During these years even though I spent little time with them, they always provided me with love and support unconditionally across the Pacific Ocean.

LIST OF ABBREVIATIONS

9-BBN: 9-borabicyclo[3.3.1]nonane

ATR: attenuated total reflectance

BCF: tris(pentafluorophenyl)borane

^{n}Bu: *n*-butyl

CAAC: cyclic (alkyl)(amino)carbene

COD: 1,5-cyclooctadiene

Cp: cyclopentadienyl

Cp*: pentamethylcyclopentadienyl

CuTc: copper(I)-thiophene-2-carboxylate

Cy: cyclohexyl

dan: 1,8-diaminonaphthalene

DART: direct analysis in real time

dba: dibenzylideneacetone

DBU: 1,8-diazabicyclo[5.4.0]undec-7-ene

DFT: density functional theory

DDQ: 2,3-dichloro-5,6-dicyanobenzoquinone

dipp: 2,6-di-*iso*-propylphenyl

DPEphos: bis[(2-diphenylphosphino)phenyl] ether

dppe: 1,2-bis(diphenylphosphino)ethane

dppf: 1,1'-bis(diphenylphosphino)ferrocene

DTBP: di-*tert*-butyl peroxide

ESI: electrospray ionization

Et: ethyl

EtOAc: ethyl acetate

eq.: equation

equiv.: equivalent

FLP: frustrated Lewis pair

GC-MS: gas chromatography-mass spectrometry

$G^{\neq}$: Gibbs free energy of activation

HBCat: catecholborane

HB(pin) pinacolborane

HOMO: highest occupied molecular orbital

HRMS: high resolution mass spectrometry

h: Planck's constant.

^{i}Pr: *iso*-propyl

IR: infrared

κ: transmission coefficient

k_B: Boltzmann's constant,

KHMDS: potassium bis(trimethylsilyl)amide

KIE: kinetic isotope effect

LAH: lithium aluminum hydride

LDA: lithium di-*iso*-propyl amide

LiTMP: lithium tetramethylpiperidide

LUMO: lowest unoccupied molecular orbital

Me: methyl

Mes: 2,4,6-trimethylphenyl

MAP: 2-(diphenylphosphino)-2′-dimethylamino-1,1′-binaphthyl

MOP: 2-(diphenylphosphino)-2′-methoxy-1,1′-binaphthyl

MP2: second-order Møller-Plesset perturbation theory

MW: molecular weight

nbd: 2,5-norbornadiene

NHC: *N*-heterocyclic carbene

NMR: nuclear magnetic resonance

NRT: natural resonance theory

o-DCB: 1,2-dichlorobenzene

ORTEP: Oak Ridge thermal ellipsoid plot

o-xylene: 1,2-dimethylbenzene

PES: potential energy surface

Ph: phenyl

PMHS: polymethylhydrosiloxane

ppm: parts per million

p-tol: *para*-tolyl

R: gas constant

RCM: ring closing metathesis

RDS: rate determining step

RPKA: reaction progress kinetic analysis

RT: room temperature

SIPr: 1,3-bis(2,6-di-*iso*-propylphenyl)imidazolidin-2-ylidene

^{t}Bu: *tert*-butyl

TBS: *tert*-butyldimethylsilyl

TfOH: trifluoromethanesulfonic acid

TBS: *tert*-butyldimethylsilyl

TBDPS: *tert*-butyldiphenylsilyl

THF: tetrahydrofuran

TMEDA: *N, N, N′, N′*-tetramethylethylenediamine

TMS: trimethylsilyl

VT: variable temperature

XPhos: 2-di-cyclohexylphosphino-2′,4′,6′-tri-*iso*-propylbiphenyl

Chapter One. Pd/Senphos Catalyzed *trans*-Selective Hydroboration of 1,3-Enynes: Condition Re-optimization and Mechanistic Investigations

1.1. Introduction

The replacement of a C=C bond unit with an isoelectronic and isosteric B–N bond unit is an exemplary illustration of BN/CC isoterism (Figure 1.1, top).[1] Even though C=C and B–N bond units are similar in shapes and have the same overall electron count, their corresponding compounds differ in physical and chemical properties as a result of distinct electronic structure differences.[2] When applying BN/CC isoterism to aromatic systems such as benzene (i.e., the replacement of any two carbon atoms with one boron and one nitrogen), three isoelectronic and isosteric permutations can be envisioned, namely 1,2-dihydro-1,2-azaborine, 1,3-dihydro-1,3-azaborine and 1,4-dihydro-1,4-azaborine (abbreviated as 1,2-azaborine, 1,3-azaborine and 1,4-azaborine, respectively) (Figure 1.1, bottom). These isosteres differ in physical and chemical properties from benzene as well as among themselves, for example, in the aspect of thermodynamic stability and

[1] (a) Liu, Z.; Marder, T. B. *Angew. Chem. Int. Ed.* **2008**, *47*, 242-244; (b) Bosdet, M. J. D.; Piers, W. E. *Can. J. Chem.* **2009**, *87*, 8-29; (c) Campbell, P. G.; Marwitz, A. J.; Liu, S.-Y. *Angew. Chem. Int. Ed.* **2012**, *51*, 6074-6092; (d) Belanger-Chabot, G.; Braunschweig, H.; Roy, D. K. *Eur. J. Inorg. Chem*. **2017**, (*38-39*), 4353-4368; (e) Giustra, Z. X.; Liu, S. -Y. *J. Am. Chem. Soc.* **2018**, *140*, 1184-1194.

[2] (a) Campbell, P. G.; Marwitz, A. J. V.; Liu, S.-Y. *Angew. Chem. Int. Ed.* **2012**, 51, 6074-6092; (b) Knack, D. H.; Marshall, J. L.; Harlow, G. P.; Dudzik, A.; Szaleniec, M.; Liu, S.-Y.; Heider, J. *Angew. Chem. Int. Ed.* **2013**, 52, 2599-2601.

aromaticity.[3] Therefore, BN/CC isosterism has the potential to significantly expand and provide new opportunities for discovery of new functions.

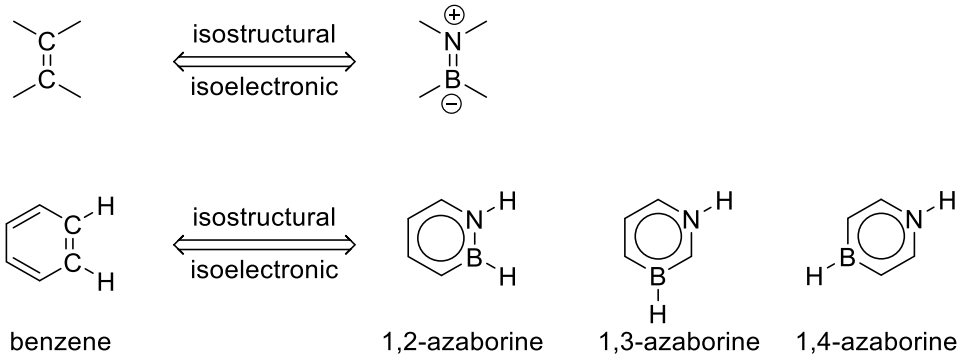

Figure 1.1. BN/CC isoterism and its application in benzene.

1.1.1. Development of 1,2-, 1,3- and 1,4-azaborines

The history of 1,2-azaborine family can be traced back to 1958, when Dewar synthesized the very first polycyclic 1,2-azaborine **1.1**.[4] Several years later Dewar and White reported the first examples of monocyclic 1,2-azaborine **1.2** and **1.3**, respectively.[5] 1,2-Azaborines received quite significant attention in the 1960s and 1970s,[6] however, in the subsequent decades, interest in this field has waned, arguably due to the synthetic limitations of accessing this type of compounds.

---

[3] (a) Kranz, M.; Clark, T. *J. Org. Chem*. **1992**, *57,* 5492-5500; (b) Matus, M. H.; Liu, S.-Y.; Dixon, D. A. *J. Phys. Chem. A* **2010**, *114*, 2644-2654; (c) Ghosh, D.; Periyasamy, G.; Pati, S. K. *Phys. Chem. Chem. Phys.* **2011**, *13*, 20627-20636; (d) Xu, S.; Mikulas, T. C.; Zakharov, L. N.; Dixon, D. A; Liu, S.-Y. *Angew. Chem. Int. Ed.* **2013**, *52*, 7527-7531; (e) Baranac-Stojanovic, M. *Chem. Eur. J.* **2014**, *20*, 16558-16565; (f) Papadopoulos, A. G.; Charistos, N. D.; Kyriakidou, K.; Sigalas, M. P. *J. Phys. Chem. A* **2015**, *119*, 10091-10100; (g) Baranac-Stojanović, M. *J. Org. Chem.* **2019**, *84*, 21, 13582-13594; (h) Baranac-Stojanović, M.; Stojanović, M. *Phys. Chem. Chem. Phys*. **2019**, *21*, 9465-9476; (i) Iwaki, R. A.; Udagawa, T. *Chem. Phys. Lett.* **2020**, *745*, 137271-137275.

[4] (a) Dewar, M. J. S.; Kubba, V. P.; Pettit, R. *J. Chem. Soc.* **1958**, 3073-3076; (b) Dewar, M. J. S.; Dietz, R. *J. Chem. Soc.* **1959**, 2728-2730.

[5] (a) Dewar, M. J. S.; Marr, P. A. *J. Am. Chem. Soc.* **1962**, *84*, 3782-3782; (b) White, D. G. *J. Am. Chem. Soc.* **1963**, *85*, 3634-3636.

[6] Fritsch, A. J. *Chem. Heterocycl. Compd.* **1977**, *30*, 381-440.

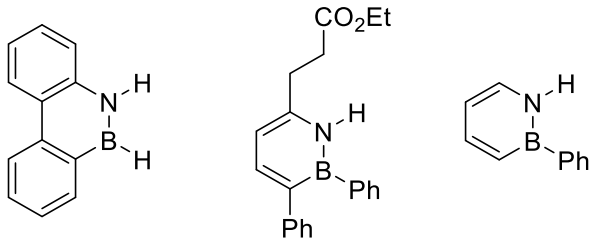

1.1 **1.2** **1.3**

1958 1962 1963

Figure 1.2. Early examples of polycyclic and monocyclic 1,2-azaborines.

In the beginning of the new millennium, the field has been reinvigorated by significant advances in RCM (ring-closing metathesis).[7] The Ashe group developed two novel synthetic routes towards 1,2-azaborines with much milder reaction conditions.[8] The first route starts with allyltributyltin, which affords the B–N adduct **1.4** via transmetalation and amine condensation. Substitution of the boron position with phenyllithium results in compound **1.5**, which undergoes RCM with Grubbs 1st generation catalyst. Subsequent oxidation with DDQ (2,3-dichloro-5,6-dicyanobenzoquinone) delivers *N*–Et-*B*–Ph 1,2-azaborine **1.7**.

[7] (a) Fürstner, A. *Angew. Chem. Int. Ed.* **2000**, *39*, 3012-3043; (b) Grubbs, R. H. *Tetrahedron* **2004**, *60*, 7117-7140; (c) Schrock, R. R.; Hoveyda, A. H. *Angew. Chem. Int. Ed.* **2003**, *42*, 4592-4633.

[8] (a) Ashe, A. J.; Fang. *Org. Lett.* **2000**, *2*, 2089-2091; (b) Ashe, A. J.; Fang, X.; Fang, X.; Kampf, J. W. *Organometallics* **2001**, *20*, 5413-5418.

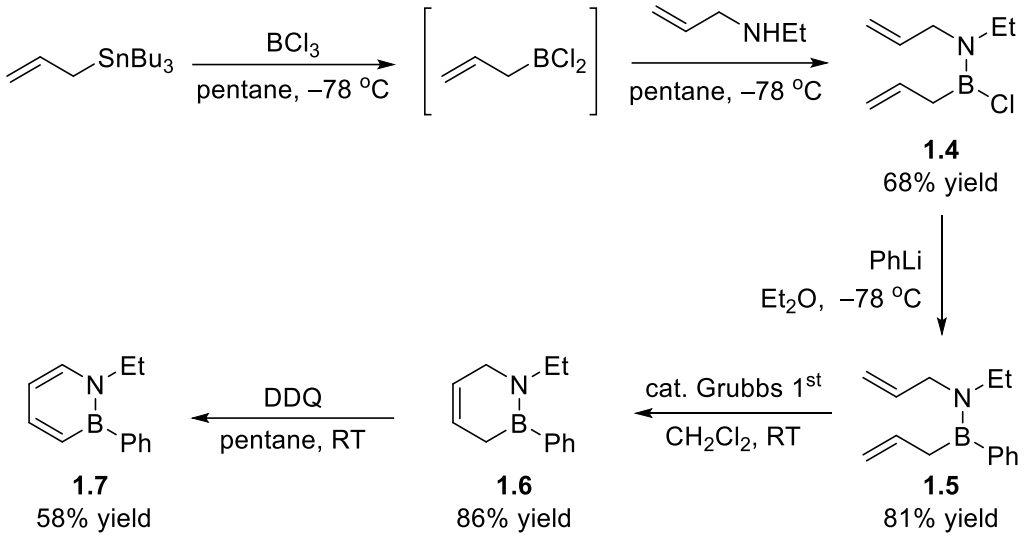

Scheme 1.1. Ashe's synthesis of 1,2-azaborine via RCM/oxidation sequence.

In their second synthesis route[8b] (Scheme 1.2), the RCM reaction occurs on diene **1.8** to deliver B,N-cyclopentene **1.9**. Subsequent LDA-mediated (lithium di-isopropyl amide) deprotonation in the α-position to the nitrogen atom leads to 1,2-azaborolide **1.10**. Further addition of excess CD_2Cl_2 and LDA at low temperature affords 1,2-azaborine **1.11** through a ring expansion pathway.

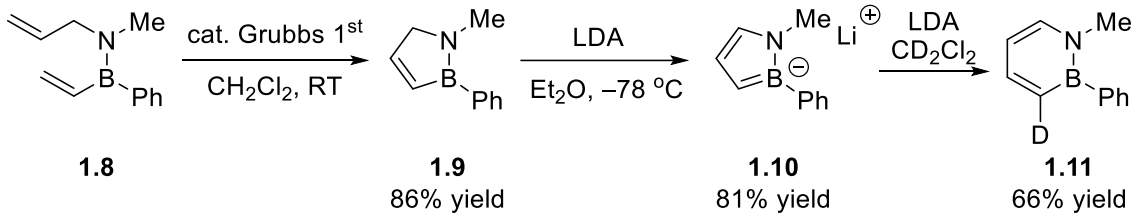

Scheme 1.2. Ashe's synthesis of 1,2-azaborine via ring expansion.

These two routes of 1,2-azaborine synthesis, though novel at the time, suffer from limited scope and modularity. Aiming to develop a versatile 1,2-azaborine synthon, our

group envisioned the synthesis of *N*–TBS-*B*–Cl 1,2-azaborine **1.15** (Scheme 1.3).[9] Triallylborane **1.12** comproportionates with BCl_3 to deliver allyldichloroborane, which then condenses with *N*–TBS (*tert*-butyldimethylsilyl) allylamine to yield adduct **1.13**. Adduct **1.13** undergoes smooth RCM reaction and dehydrogenation reaction to generate 1,2-azaborine **1.15**, where both the nitrogen and boron are easily subjected to further functionalization as demonstrated in the synthesis towards the parental 1,2-azaborine **1.16**.[9b,10] Our group also developed a series of site-selective C–H functionalizations around the 1,2-azaborine ring.[11] Due to its thermodynamic stability and versatile and modular synthesis, the 1,2-azaborine heterocycle has been the most investigated family among the azaborines, where tremendous advances in the application of the 1,2-azaborine scaffold in biomedical research[2b, 12] and material science[13] have been reported in the last two decades.[1c,1e,11d]

[9] (a) Brown, A. N. "Late-Stage Functionalization of 1,2-Dihydro-1,2-Azaborines", PhD Dissertation, Boston College, 2015. http://hdl.handle.net/2345/bc-ir:104564; (b) Marwitz, A. J. V.; Matus, M. H.; Zakharov, L. N.; Dixon, D. A.; Liu, S.-Y. *Angew. Chem. Int. Ed.* **2009**, *48*, 973-977.

[10] Abbey, E. R.; Lamm, A. N.; Baggett, A. W.; Zakharov, L. N.; Liu, S.-Y. *J. Am. Chem. Soc.* **2013**, *135*, 12908-12913.

[11] (a) Baggett, A. W.; Vasiliu, M.; Li, B.; Dixon, D. A.; Liu, S.-Y. *J. Am. Chem. Soc.* **2015**, *137*, 5536-5541; (b) Brown, A. N.; Li, B.; Liu, S.-Y. *J. Am. Chem. Soc.* **2015**, *137*, 8932-8935; (c) McConnell, C. R.; Haeffner, F.; Baggett, A. W.; Liu, S.-Y. *J. Am. Chem. Soc.* **2019**, *141*, 9072-9078; (d) McConnell, C. R.; Liu, S.-Y. *Chem. Soc. Rev*. **2019**, *48*, 3436-3453.

[12] (a) Lee, H.; Fischer, M.; Shoichet, B. K.; Liu, S.-Y. *J. Am. Chem. Soc.* **2016**, *138*, 12021-12024; (b) Zhao, P.; Nettleton, D. O.; Karki, R. G.; Zecri, F. J.; Liu, S.-Y. *ChemMedChem* **2017**, *12*, 358-361; (c) Boknevitz, K.; Italia, J. S.; Li, B.; Chatterjee, A.; Liu, S.-Y. *Chem. Sci.* **2019**, *10,* 4994-4998; (d) Liu, Y.; Liu, S.-Y. *Org. Biomol. Chem.* **2019**, *17*, 7002-7006.

[13] (a) Wang, X.-Y.; Wang, J.-Y.; Pei, J. *Chem. Eur. J.* **2015**, *21*, 3528-3539; (b) Wang, J.-Y.; Pei, J. *Chin. Chem. Lett.* **2016**, *27*, 1139-1146; (c) Liu, Z.; Ishibashi, J. S. A.; Darrigan, C.; Dargelos, A.; Chrostowska, A.; Li, B.; Vasiliu, M.; Dixon, D. A.; Liu, S.-Y. *J. Am. Chem. Soc.* **2017**, *139*, 6082-6085.

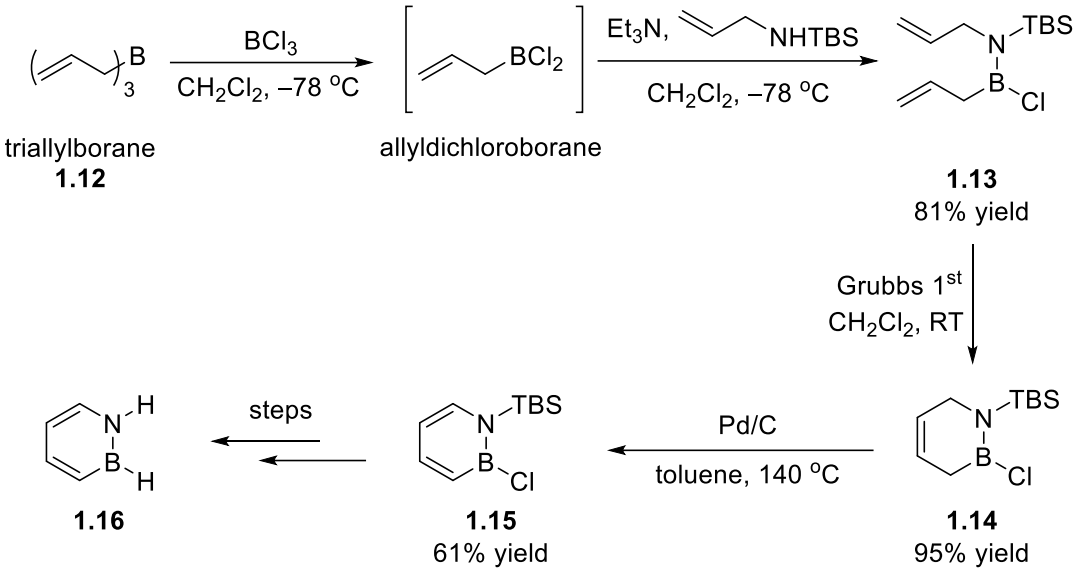

Scheme 1.3. Synthesis of a versatile 1,2-azaborine synthon.

Comparing to 1,2-azaborines, 1,3-azaborine chemistry is still in its early stages of development. In 2011, our group reported the synthesis towards the very first monocyclic 1,3-azaborine (Scheme 1.4).[14] The reaction of *N*–methyl-*N*–allylamine with 1,2,3-benzotriazole and formaldehyde yields tertiary amines **1.17** and **1.17'** in a 4:1 ratio. The 1,2,3-benzotriazole, acting as a good leaving group, is substituted by tributyltin moiety to yield organotin **1.18**. Subsequent lithium tin exchange followed by addition of the boron electrophile vinyl–B(N^iPr_2)Cl delivers diene **1.19**. To avoid the nucleophilic amine group poisoning the Grubbs 1st generation catalyst,[15] diene **1.19** is first converted to its ammonium salt by treating with TfOH, and then converted back to the free amine form with DBU (1,8-diazabicyclo[5.4.0]undec-7-ene) after the RCM step to reveal 1,3-B,N cyclohexene **1.20**. The final dehydrogenation step is challenging since two *meta*-

[14] (a) Xu, S.; Zakharov, L.N.; Liu, S.-Y. *J. Am. Chem. Soc*. **2011**, *133*, 20152-20155; (b) Xu, S.; Mikulas, T. C.; Zakharov, L. N.; Dixon, D. A.; Liu, S.-Y. *Angew. Chem. Int. Ed*. **2013**, *52*, 7527-7531.
[15] Deiters, A.; Martin, S. F. *Chem. Rev.* **2004**, *104*, 2199-2238.

positioned hydrogen atoms need to be eliminated in a six-membered ring. Fortunately, by carefully evaluating the reaction conditions, 1,3-azaborine **1.21** is obtained in a satisfactory yield in the presence of Pd/C in benzene at 120 °C.

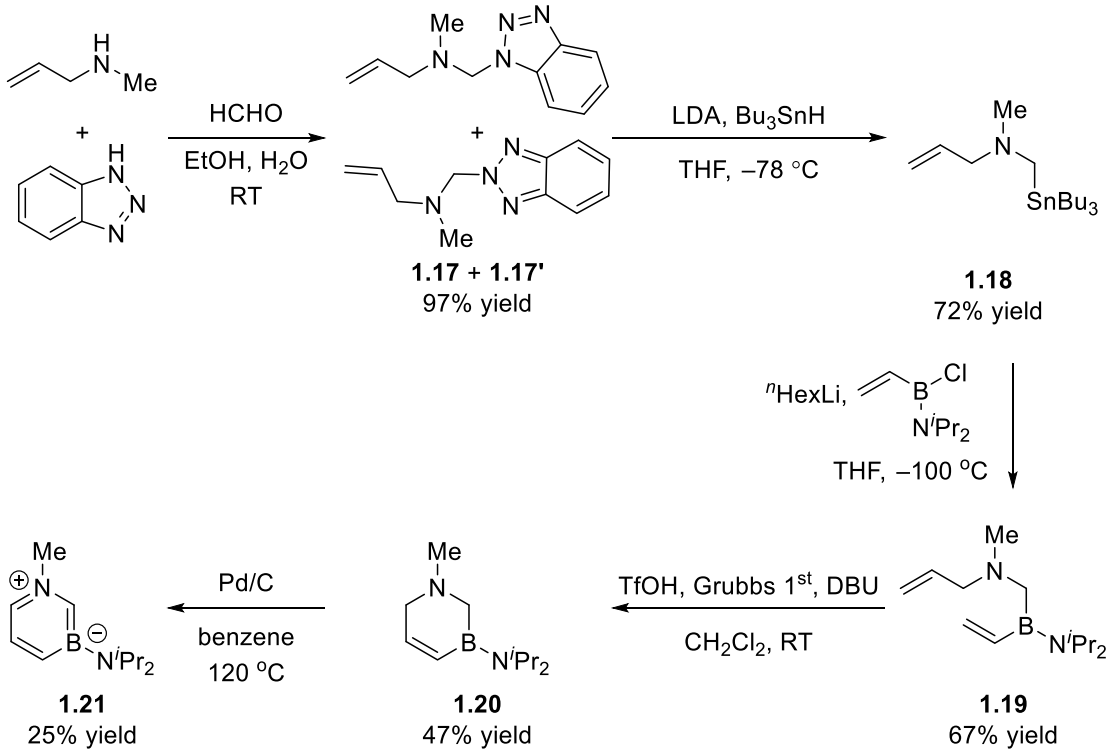

Scheme 1.4. Synthesis of monocyclic 1,3-azaborine.

The Erker group developed an alternative synthesis towards multi-substituted monocyclic 1,3-azaborines.[16] Sequential hydroboration and isonitrile insertion between (Fmes)BH_2·SMe_2, alkyne and isonitrile leads to either compound **1.22**, if the stoichiometry of borane and alkyne is 1:2, or compound **1.25**, if it is 1:1. Subsequent bora-Nazarov cyclization and H-shift result in mono-substituted or dihydro-1,3-azaboroles **1.23** and **1.26**,

[16] (a) Li, J.; Daniliuc, C. G.; Mück-Lichtenfeld, C.; Kehr, G.; Erker, G. *Angew. Chem. Int. Ed.* **2019**, *58*, 15377-15380; (b) Li, J.; Daniliuc, C. G.; Kartha, K. K.; Fernández, G.; Kehr, G.; Erker, G. *J. Am. Chem. Soc*. **2021**, *143*, 2059-2067.

some of which exhibit AIE (aggregation-induced emission) effects. Treating 1,3-azaboroles with additional equivalent of isonitrile leads to 1,3-azaborine **1.24**.

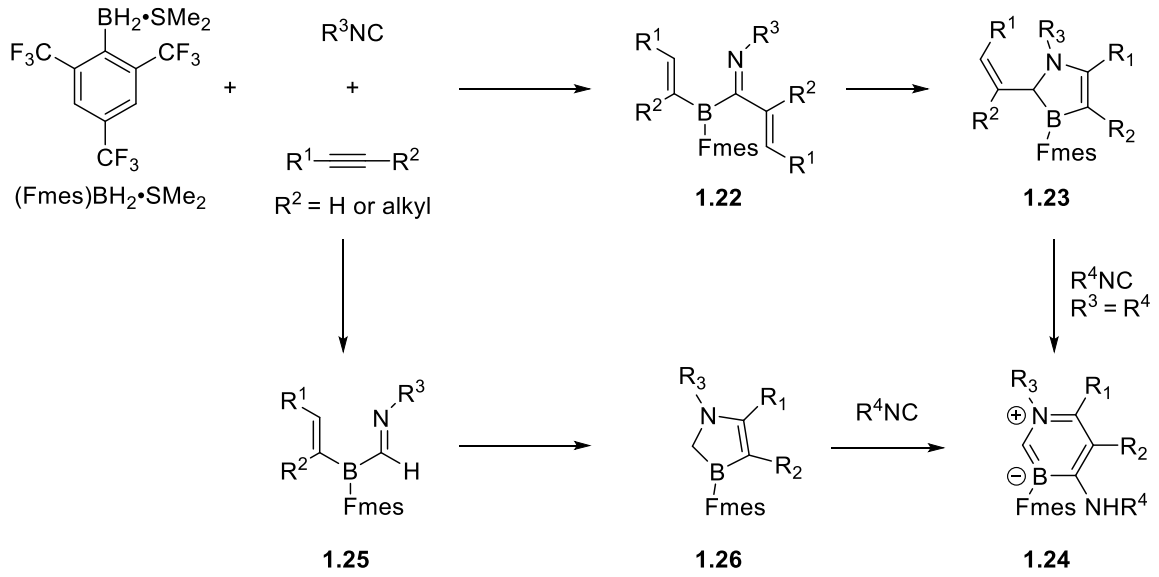

Scheme 1.5. Erker's synthesis of monocyclic 1,3-azaborine.

For the preparation of polycyclic 1,3-azaborines the only report is from the Wang group. [17] B,N-heterocycle **1.27** is prepared by double deprotonations of 1,3-bis(mesityl)imidazolium chloride with ^{n}BuLi in the presence of TMEDA (*N, N, N′, N′*-tetramethylethylenediamine) and quenching with $BMes_2F$. Subsequent photo-elimination of mesitylene is accomplished by 300 nm UV (ultraviolet) light to afford polycyclic 1,3-azaborine **1.28**.

[17] McDonald, S. M.; Mellerup, S. K.; Peng, J.; Yang, D.; Li, Q.-S.; Wang, S. *Chem. Eur. J.* **2015**, *21*, 13961-13970.

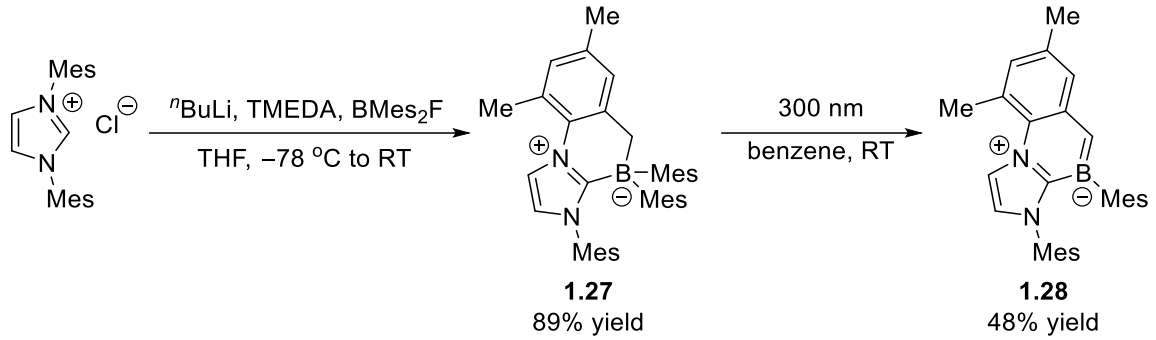

Scheme 1.6. Wang's synthesis of polycyclic 1,3-azaborine.

Interest in the 1,4-azaborine family occurred around the same time as 1,2-azaborine, when the Maitlis group reported the synthesis of the first 1,4-azaborine in 1961.[18] To date, predominant work has focused on this dibenzofused 1,4-azaborine framework due to the easy accessibility of the starting bis-(2-halophenyl)amines (X = Br or I).[19] Recent advances even simplify the starting amines to un-halogenated ones (X = H) which is used in *B*-Friedel-Crafts type reactions.[20]

[18] Maitlis, P. M. *J. Chem. Soc*. **1961**, 425-429.

[19] For selective examples, see: (a) Kranz, M.; Hampel, F.; Clark, T. *J. Chem. Soc., Chem. Commun*. **1992**, 1247-1248; (b) Agou, T.; Sekine, M.; Kobayashi, J.; Kawashima, T. *Chem. Commun.* **2009**, 1894-1896; (c) Tomohiro, A.; Hiroki, A.; Takayuki, K. *Chem. Lett.* **2010**, *39*, 612-613; (d) Agou, T.; Kojima, T.; Kobayashi, J.; Kawashima, T. *Org. Lett*. **2009**, *11*, 3534-3537; (e) Dimitrijević, E.; Cusimanoa, M.; Taylor, M. S. *Org. Biomol. Chem*. **2014**, *12,* 1391-1394; (f) Oda, S.; Kawakami, B.; Kawasumi, R.; Okita, R.; Hatakeyama, T. *Org. Lett*. **2019**, *21*, 9311-9314.

[20] (a) Matsui, K.; Oda, S.; Yoshiura, K.; Nakajima, K.; Yasuda, N.; Hatakeyama, T. *J. Am. Chem. Soc.* **2018**, *140*, 1195-1198; (b) Mitsudo, K.; Shigemori, K.; Mandai, H.; Wakamiya, A.; Suga. S. *Org. Lett.* **2018**, *20*, 7336-7340; (c) Liang, X.; Yan, Z.-P.; Han, H.-B.; Wu, Z.-G.; Zheng, Y.-X.; Meng, H.; Zuo, J.-L.; Huang, W. *Angew.Chem. Int. Ed.* **2018**, *57*, 11316-11320; (d) Oda, S.; Ueura, K.; Kawakami, B.; Hatakeyama, T. *Org. Lett*. **2020**, *22*, 700-704; (e) Suresh, S. M.; Duda, E.; Hall, D.; Yao, Z.; Bagnich, S.; Slawin, A. M. Z.; Bässler, H.; Beljonne, D.; Buck, M.; Olivier, Y.; Köhler, A.; Zysman-Colman, E. *J. Am. Chem. Soc.* **2020**, *142*, 6588-6599.

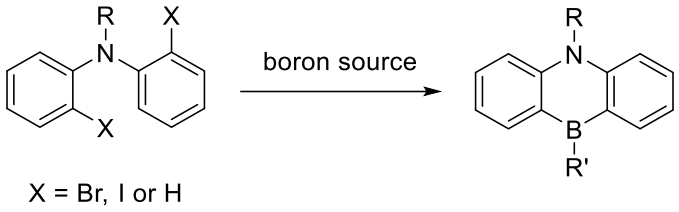

Scheme 1.7. Synthesis of dibenzofused 1,4-azaborines.

Monobenzofused 1,4-azaborines, unlike dibenzofused 1,4-azaborines, are less explored potentially due to the difficulty in preparing the *cis*-β-bromo enamine precursors. To date the only two methods are reported by our group.[21] The first synthesis route, inspired by the RCM strategy in other azaborine syntheses, was disclosed in 2014.[21a] Two consecutive alkylation reactions of the commercially available 2-bromoaniline affords tertiary amine **1.29**. Subsequent alkene isomerization leads to the thermodynamically more stable enamine **1.30** in excellent yield. Then, installation of the vinyl boron moiety generates the RCM precursor diene **1.31**. After carefully evaluating the reaction conditions, Grubbs 2nd generation catalyst is found to effectively close the ring, providing 1,4-azaborine **1.32** in a satisfactory yield.

[21] (a) Xu, S.; Haeffner, F.; Li, B.; Zakharov, L. N.; Liu, S.-Y. *Angew. Chem. Int. Ed.* **2014**, *53*, 6795-6799; (b) Xu, S.; Zhang, Y.; Li, B.; Liu, S.-Y. *J. Am. Chem. Soc.* **2016**, *138*, 14566-14569.

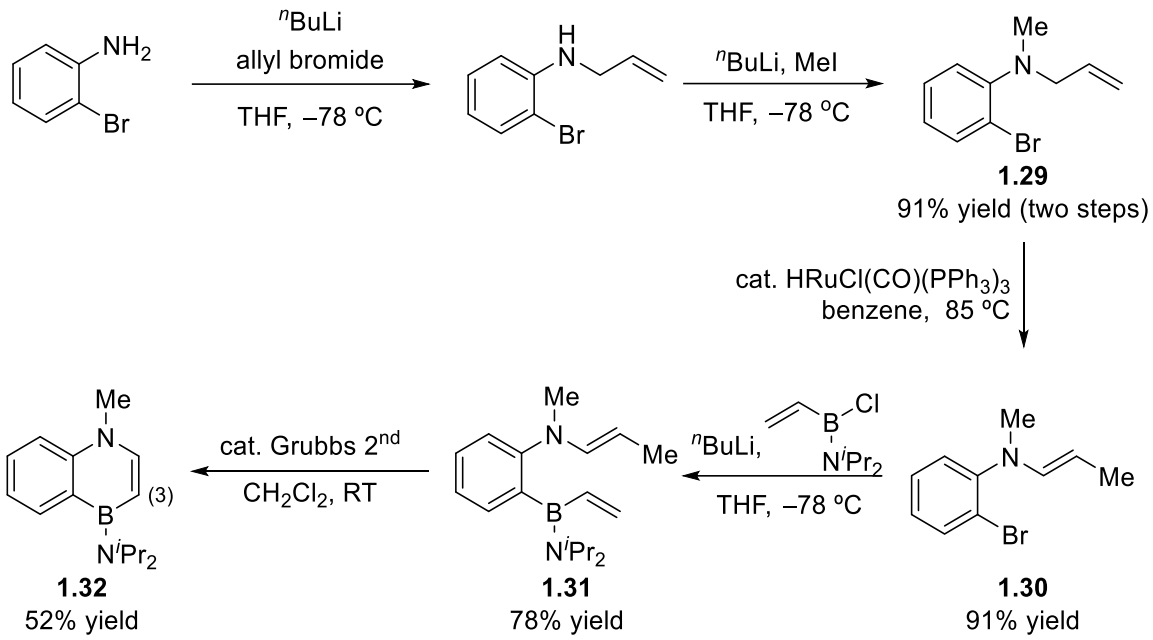

Scheme 1.8. Synthesis of monobenzofused 1,4-azaborine via isomerization/RCM sequence.

Although straightforward, this route is somehow limited to the modularity of the C(3) substituent. To solve this problem, an improved, while also scalable route was reported.[21b] As depicted in Scheme 1.9, an Ir-catalyzed stereo-convergent reduction of tertiary amide with PMHS (polymethylhydrosiloxane) affords the (*E*)-enamine **1.34**. Attaching the boron moiety after lithium-halogen exchange provides intermediate **1.35**, which undergoes a cyclization reaction, reminiscing of Dewar's synthesis of the first 2,1-borazaro-naphthalene, to generate 1,4-azaborine **1.36**-Me.[22] The weak B–Cl bond in 1,4-azaborine **1.36** greatly facilitates further functionalizations. By simply changing the substituent of the starting amide, a series of C(3) alkyl substituted monobenzofused 1,4-azaborines can be obtained.

[22] Dewar, M. J. S.; Dietz, R. *J. Chem. Soc*. **1959**, 2728-2730.

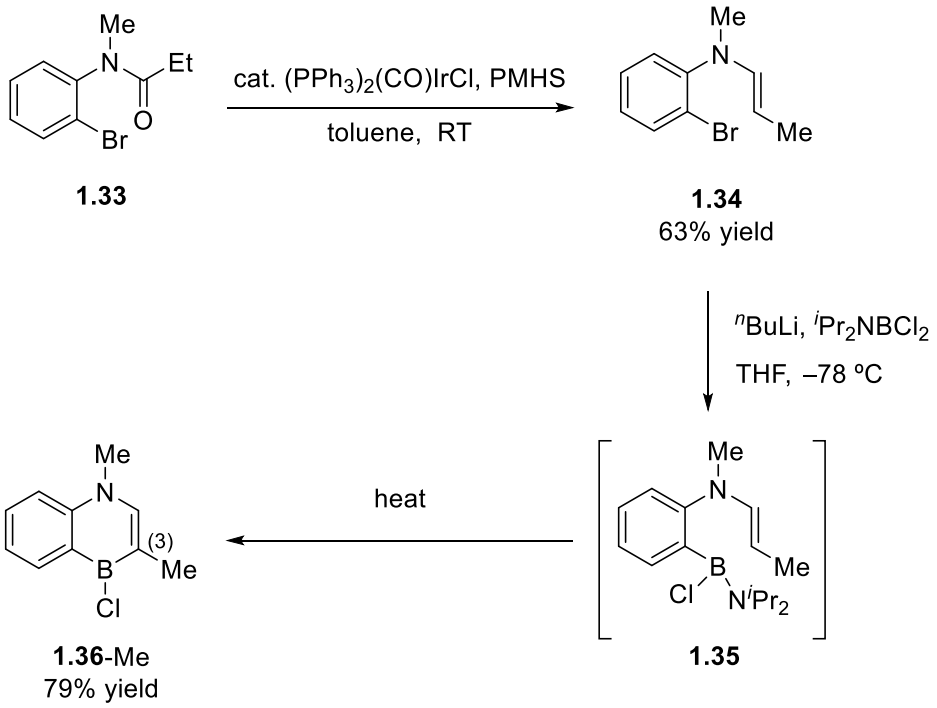

Scheme 1.9. Synthesis of monobenzofused 1,4-azaborine via cyclization.

When it comes to monocyclic 1,4-azaborine, the first example was not achieved until 2012 by Braunschweig.[23] Phosphine-rhodium-catalyzed [2+2] cycloaddition of di-^{t}butyliminoborane with acetylene leads to a rhodium η^4-1,2-azaborete complex **1.37**. In the presence of excess acetylene, further [4+2] cycloaddition of complex **1.37** yields 1,4-azaborine **1.38**. This one-step method is straightforward, however, restrictions with regard to the installation of nitrogen and boron substituents have limited its utility.

[23] (a) Braunschweig, H.; Damme, A.; Jimenez-Halla, J. O. C.; Pfaffinger, B.; Radacki, K.; Wolf, J. *Angew. Chem. Int. Ed.* **2012**, *51*, 10034-10037; (b) Schäfer, M.; Beattie, N. A.; Geetharani, K.; Schäfer, J.; Ewing, W. C.; Krahfuß, M.; H rl, C.; Dewhurst, R. D.; Macgregor, S. A.; Lambert, C.; Braunschweig, H. *J. Am. Chem. Soc*. **2016**, *138*, 8212-8220.

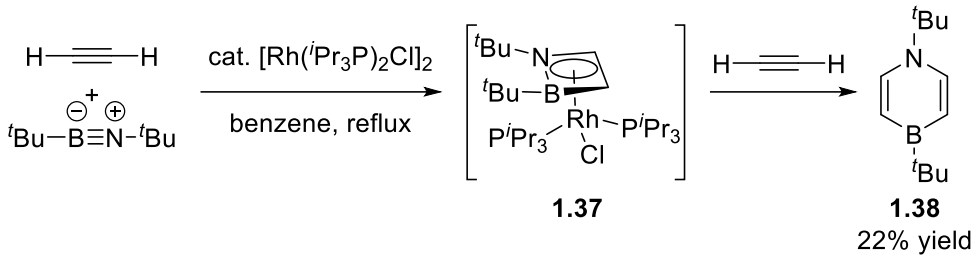

1.37 **1.38**
22% yield

Scheme 1.10. Braunschweig's synthesis of monocyclic 1,4-azaborine.

As a complement to Braunschweig's method, our group reported a more general route towards *B*-functionalized monocyclic 1,4-azaborines (Scheme 1.11).[24] Dialkylation reaction of methylamine with 2,3-dibromopropene affords alkenyl bromide **1.39**, which is further converted to 1,4-B,N-cyclohexane **1.40** through lithium-bromide exchange and quenched with $^{i}Pr_2NBCl_2$. Ruthenium-catalyzed isomerization and MeOH alcoholysis of 1,4-B,N-cyclohexane **1.40** furnishes a versatile 1,4-azaborine synthon **1.42**, from where a variety of *B*-functionalized 1,4-azaborines can be obtained through nucleophilic substitution reaction.

[24] Liu, X.; Zhang, Y.; Li, B.; Zakharov, L. N.; Vasiliu, M.; Dixon, D. A.; Liu, S.-Y. *Angew. Chem. Int. Ed.* **2016**, *55*, 8333-8337.

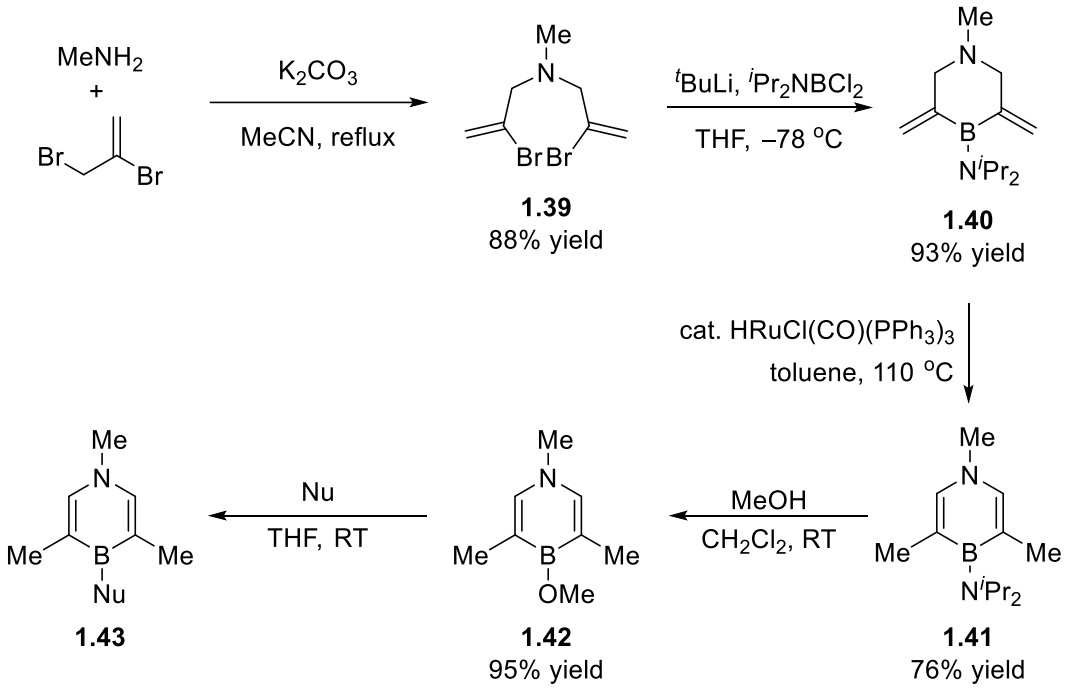

Scheme 1.11. Synthesis of *B*-functionalized monocyclic 1,4-azaborines.

1.1.2. Unique coordination mode in Senphos-containing metal complexes

The development of ligand-supported metal-catalyzed reactions have been a popular subject in modern organic chemistry.[25] And in the field of ligand design, benzene structure is a popular subunit.[26] Consequently, azaborines would provide an opportunity to expand the available ligand chemical space[27] and possibly facilitate the discovery of new reactivity. Due to the scalability and modularity of monobenzofused 1,4-azaborine scaffold,

[25] For recent reviews, see: (a) Huang, L.; Arndt, M.; Gooßen, K.; Heydt, H.; Gooßen, L. J. *Chem. Rev.* **2015**, *115*, 2596-2697; (b) Zhang, K.; Liu, X.; Feng, X. *Chem. Rev*. **2018**, *118*, 7586-7656; (c) Biffis, A.; Centomo, P.; Del Zotto, A.; Zecca, M. *Chem. Rev.* **2018**, *118*, 2249-2295; (d) Nájera, C.; Beletskaya, I. P.; Yus, M. *Chem. Soc. Rev*. **2019**, *48*, 4515-4618; (e) Chaudhari, M. B.; Gnanaprakasam, B. *Chem. Asian J*. **2019**, *14,* 76-93; (f) Chen, W.-M.; Shang, R. *ACS Catal.* **2020**, *10*, 9170-9196.

[26] (a) Gavrilova, A. L.; Bosnich, B. *Chem. Rev*. **2004**, *104*, 349-384; (b) Steel, P. J. *Acc. Chem. Res*. **2005**, *38*, 243-250; (c) Watt, M. M.; Collins, M. S.; Johnson, D. W. *Chem. Res*. **2013**, *46*, 955-966; (d) Bryant, D. J.; Zakharov, L. N.; Tyler, D. R. *Organometallics* **2019**, *38*, 3245-3256; (e) Stradiotto, M.; Lundgren, R. J. *Ligand Design in Metal Chemistry: Reactivity and Catalysis*, 1st ed.; John Wiley & Sons, Ltd., 2016.

[27] McConnell, C. R.; Campbell, P. G.; Fristoe, C. R.; Memmel, P.; Zakharov, L. N.; Li, B.; Darrigan, C.; Chrostowska, A.; Liu, S.-Y. *Eur. J. Inorg. Chem*. **2017**, *2017*, 2207-2210.

our group chose this framework for our initial work into ligand development. A versatile 1,4-azaborine precursor **1.44** can be synthesized by substituting the di-isopropylamino group of 1,4-azaborine **1.32** with a methoxy group. From here, two 1,4-azaborine ligands containing a pyridyl (**1.45**) or phosphine group (**1.46**) were synthesized, respectively.[21]

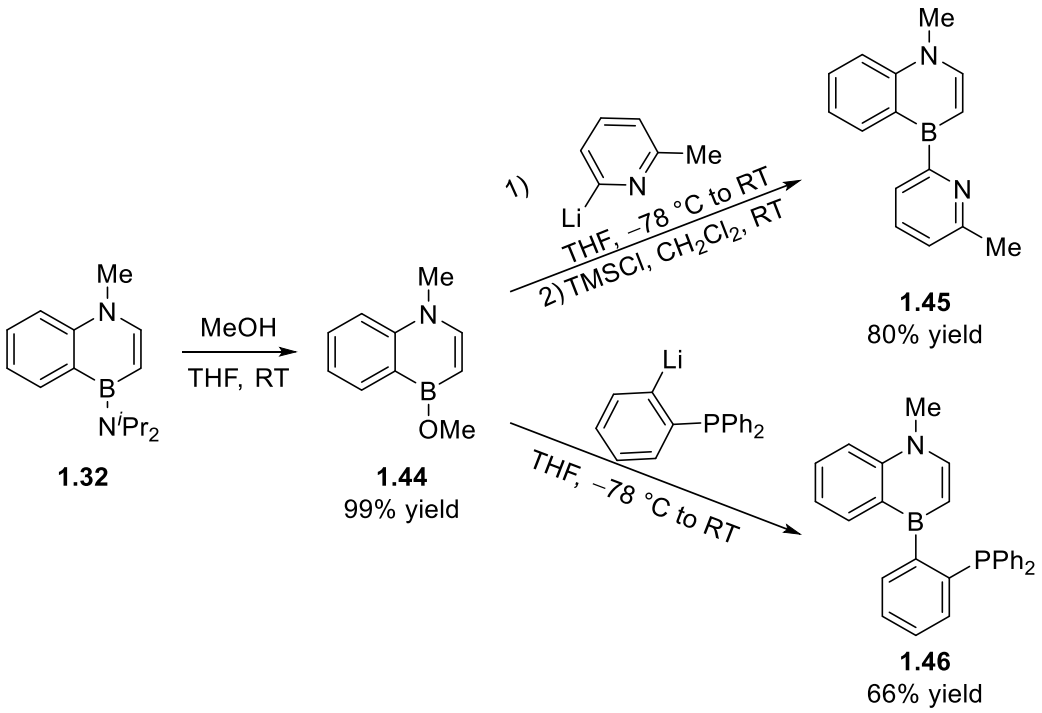

Scheme 1.12. Synthesis of monobenzofused 1,4-azaborine ligands.

Considering the rich chemistry of platinum and palladium catalysis,[28] Pt and Pd precursors were treated with ligands **1.45** and **1.46**, respectively. The two resulting complexes **1.47** and **1.48** both showed an unusual κ^2-η^2-B,C coordination to the metal[29]

[28] For recent reviews, see: (a) Johansson Seechurn, C. C. C.; Kitching, M. O.; Colacot, T. J.; Snieckus, V. *Angew. Chem. Int. Ed.* **2012**, *51*, 5062-5085; (b) Molander, G. A.; Larhed, M.; Wolfe, J. *Cross-Coupling Reactions, Workbench Edition, Science of Synthesis Series*, 1st ed.; Thieme Chemistry: Stuttgart, 2013; (c) Biffis, A.; Centomo, P.; Zotto, A. D.; Zecca, M. *Chem. Rev.* **2018**, *118*, 2249-2295; (d) Fürstner, A**.** *Chem. Soc. Rev***. 2009**, *38*, 3208-3221; (e) Labinger, J. A. *Chem. Rev.* **2017**, *117*, 8483-8496.

[29] 1,2- and 1,3-azaborines have been demonstrated to engage in metal η^1, η^5 or η^6 coordination modes, see: ref. 8b, 9b, 14a and (a) Pan, J.; Kampf, J. W.; Ashe, A. J. *Organometallics* **2004**, *23*, 5626-5629; (b) Pan, J.; Kampf, J. W.; Ashe, A. J. *Organometallics* **2008**, *27*, 1345-1347.

where the azaborine ring coordinates via what can be considered a borataalkene group ($[R_2B{=}CR_2]^-$).[30] NMR study and X-ray crystallography analysis of the complexes support our structure assignment. Ligands similar to **1.46** are named as Senphos ligands to acknowledge its initial developer Dr. Senmiao Xu.

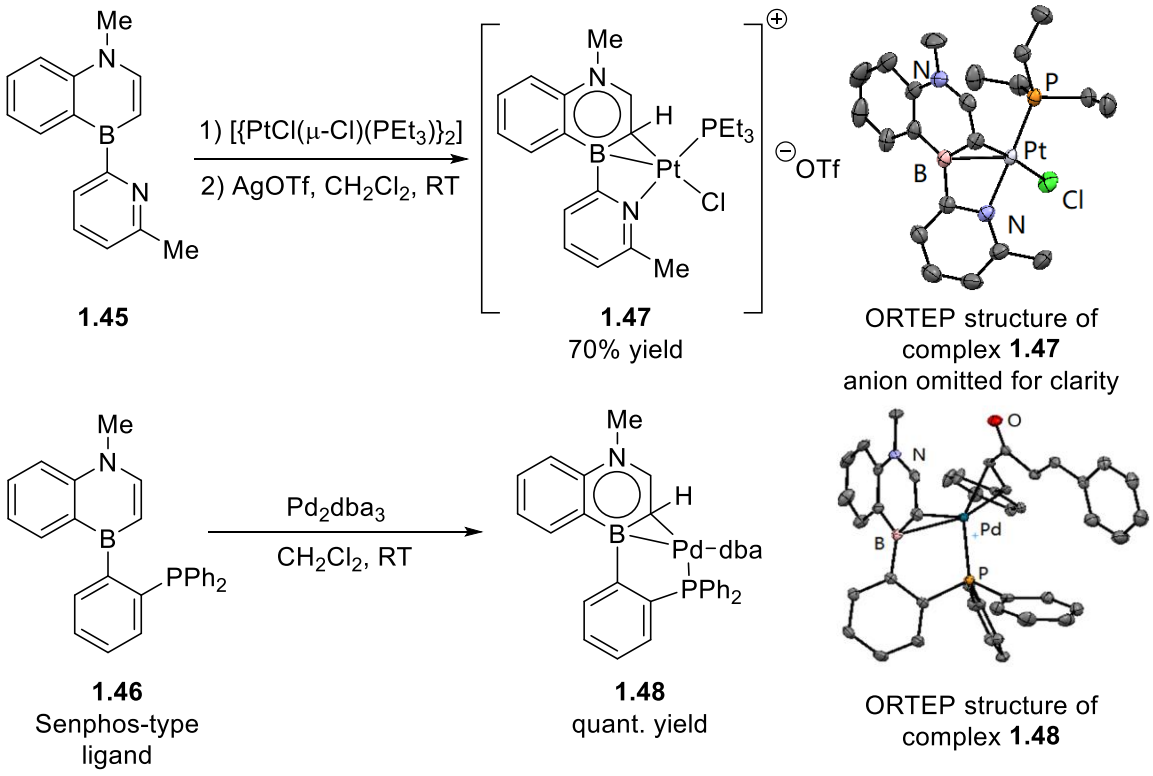

Scheme 1.13. κ^2-η^2-BC binding in azaborine-metal complexes.

The supporting ligand has profound impact on the reactivity and selectivity of the metal center.[31] As a specific example, Hayashi demonstrated that in palladium-catalyzed

[30] Borataalkenes are usually regarded as anionic species, but here the borataalkene motif is masked as zwitterionic iminium borataalkene. For an overview on borataalkene, see: Emslie, D. J. H.; Cowie, B. E.; Kolpin, K. B. *Dalton Trans.* **2012**, *41*, 1101-1117.

[31] For the ligand effects on specific reactions, see: (a) Gorin, D. J.; Sherry, B. D.; Toste, F. D. *Chem. Rev.* **2008**, *108*, 3351-3378; (b) Barder, T. E.; Walker, S. D.; Martinelli, J. R.; Buchwald, S. L. *J. Am. Chem. Soc.* **2005**, *127*, 4685-4696; (c) Krasovskiy, A.; Lipshutz, B. H. *Org. Lett.* **2011**, *13*, 3818-3821; (d) Lu, G.-P.; Voigtritter, K. R.; Cai, C.; Lipshutz, B. H. *J. Org. Chem.* **2012**, *77*, 3700-3703; (e) Matsumoto, Y.; Naito, M.; Hayashi, T. *Organometallics*, **1992**, *11*, 2732-2734; (f) Ojha, D. P.; Prabhu, K. R. *Org. Lett.* **2016**, *18*, 432-435.

hydroboration reaction of enyne the product distribution is dependent on the ligand structure (Table 1.1). When mono-dentate ligand PPh_3 is engaged, allene **1.53** is the major product whereas the engagement of bi-dentate ligand dppf (1,1'-bis(diphenylphosphino)ferrocene) results in the *cis*-hydroboration product **1.52** exclusively (entries 1 and 2).[31e] On the other hand, when Pd(0)/Senphos complex **1.48** (Scheme 1.13) is applied, the *trans*-hydroboration product **1.51** becomes the major product (entry 3). The carbonaceous analogue ligand **1.54** performs more similar to PPh_3 ligand.

Table 1.1. Unique selectivity in Pd(0)/Senphos catalyzed hydroboration of 1,3-enyne.

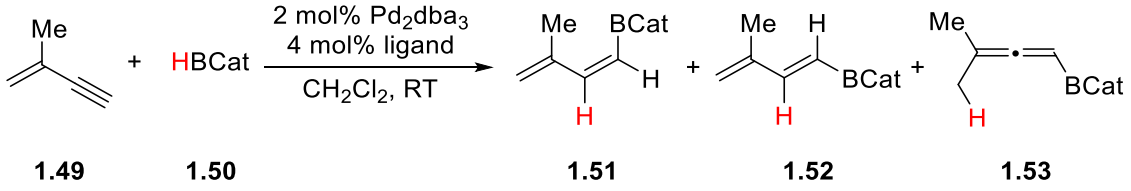

1.49 **1.50** **1.51** **1.52** **1.53**

entry	ligand[a]	yield (%)[b]	ratio **1.51/1.52/1.53**
1	PPh_3	22	8/0/92
2	dppf	89	0/100/0
3	**1.46**	84	82/12/6
4	**1.54**	42	10/19/71

[a] Ratio of Pd and L is set to 1:1. [b] Yield determined by ^1H NMR against a calibrated internal standard.

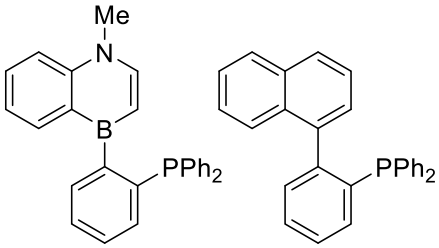

1.46 **1.54**

Hayashi rationalized the reaction outcomes of PPh_3 and dppf originate from the coordination environment of the Pd(II) intermediate (Figure 1.3).[31e] Since the number of coordination site around the square planar Pd(II) is limited, the enyne would act as either a mono- or bi-dentate ligand to palladium depending on the denticity of the phosphine ligand. Thus, a mono-dentate ligand has the potential for 1,4-hydroboration via complex **1.55** after oxidative insertion of LPd(0) to the borane. On the other hand, a bidentate ligand would be restricted to *cis*-1,2-hydroboration via complex **1.56**. In palladium/Senphos

complexes the η^2-B,C coordination is hemi-labile.[32] The distinct electronic structure and hemi-labile nature of Senphos-type ligands enable the observed *trans*-1,2-hydroboration selectivity.

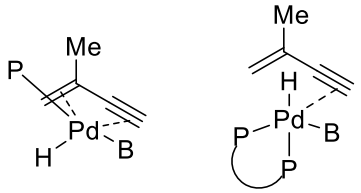

1.55 **1.56**

Figure 1.3. Proposed key intermediates in Hayashi's hydroboration reaction of enyne.

1.1.3. Alkyne hydroboration reactions

As a versatile organic synthon, organoboron compounds have attracted much attention more than half a century.[33] Alkenyl boronates, in particular, are flexible precursors in constructing a series of alkenyl carbon and heteroatom bonds.[34] Among various practical methods for accessing such compounds, alkyne hydroboration stands out due to its atom-economy[35] and starting alkyne preparation.[36] To date, a large variety of hydroboration reagents (HBR_2) has been investigated, as shown in Figure 1.4.[37-39]

---

[32] See chapter 3 for a detailed discussion about the coordination capability of Senphos-type ligands.

[33] For recent reviews, see: (a) Fyfe, W. B. J.; Watson, A. J. B. *Chem*. **2017**, *3*, 31-55: (b) Nguyen, V. D.; Nguyen, V. T.; Jin, S.; Dang, H. T.; Larionov, O. V. *Tetrahedron*, **2019**, *75*, 584-602; (c) Wen, Y.; Deng, C.; Xie, J.; Kang, X. *Molecules* **2019**, *24*, 101-116; (d) Fernández, E. *Advances in Organoboron Chemistry towards Organic Synthesis,* 1st ed.; Thieme: Stuttgart, Germany, 2020.

[34] For reviews, see: (a) Miyaura, N.; Suzuki, A. *Chem. Rev.* **1995**, *95*, 2457-2483; (b) Yun, J. *Asian J. Org. Chem.* **2013**, *2*, 1016-1025; (c) Roscales, S.; Csákÿ, A. G. *Chem. Soc. Rev*. **2014**, *43*, 8215-8225; (d) Leonori, D.; Aggarwal, V. K. *Angew. Chem. Int. Ed*. **2015**, *54,* 1082-1096; (e) Royes, J.; Cuenca, A. B.; Fernández, E. *Eur. J. Org. Chem*. **2018**, *2018*, 2728-2739; (f) Namirembe, S.; Morken, J. P. *Chem. Soc. Rev.* **2019**, *48,* 3464-3474; (g) Carreras, J.; Caballero, A.; Pérez, P. J. *Chem. Asian J.* **2019**, *14*, 329-343; (h) Wu, D.; Taguchi, J.; Tanriver, M.; Bode, J. W. *Angew. Chem. Int. Ed.* **2020**, *132*, 16993-17004; (i) Lennox, A. J. J.; Lloyd-Jones, G. C. *Chem. Soc. Rev*. **2014**, *43,* 412-443.

[35] Trost, B. M. *Angew. Chem. Int. Ed. Engl.* **1995**, *34*, 259-281.

[36] For recent reviews, see: (a) Heravi, M. M.; Dehghani, M.; Zadsirjan, V.; Ghanbarian, M. *Curr. Org. Synth.* **2019**, *16,* 205-243; (b) Shaw, R.; Elagamy, A.; Althagafi, I.; Pratap, R. *Org. Biomol. Chem*. **2020**, *18,* 3797-3817.

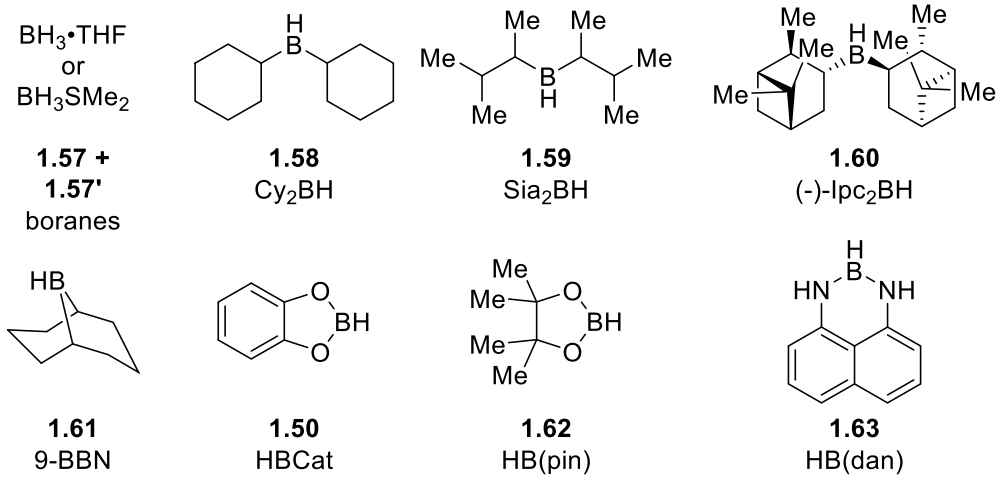

Figure 1.4. Selective examples of alkyne hydroboration reagents.

The hydroboration of an alkyne results in two pairs of diastereomers (Scheme 1.14). In the following sections, the *cis*- and *trans*-hydroboration reactions are summarized and discussed, respectively.

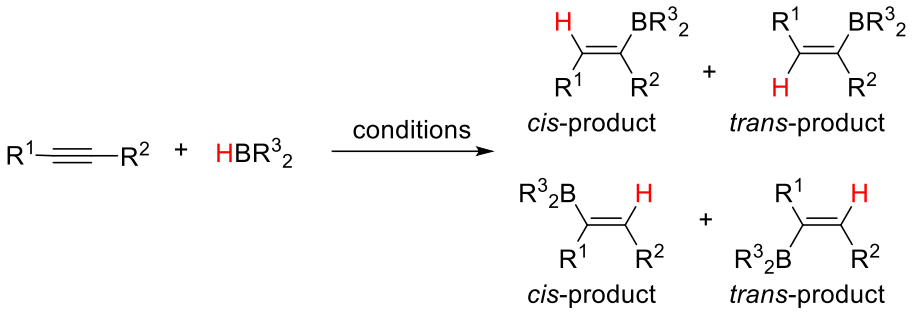

Scheme 1.14. Illustration of the outcomes in hydroboration reaction of an alkyne.

1.1.3.1. *Cis*-hydroboration reaction of alkynes

After Brown's initial report in 1959,[37] *cis*-hydroboration reactions of alkynes have been studied intensively. Non-catalyzed reactions proceed readily with reactive boranes (i.e., compounds **1.57**-**1.61**) through a four-membered transition state to yield the expected

[37] Brown, H. C.; Zweifel, G. *J. Am. Chem. Soc*. **1959**, *81*, 1512-1512.

product.[38] However, undesired regio-isomers as well as diborylated products are also generated.[39c] Aiming at a more selective *cis*-hydroboration reaction, numerous catalytic systems have been developed.[39] In such reaction setup, the reaction conditions are more benign, providing products in high regio- and *cis*-selectivity.

1.1.3.2. *Trans*-hydroboration reaction of alkynes

In stark contrast to the enormous advances in alkyne *cis*-hydroboration reaction, the *trans*-hydroboration reaction is relatively underdeveloped. Several methods have been uncovered, and their mechanisms, unlike the intuitive *cis*-hydroboration mechanism, usually varies.

1.1.3.2.1. Formal *trans*-hydroboration via 1,1-hydroboration reaction

In formal *trans*-hydroboration via 1,1-hydroboration reactions, both the hydride and boron from the hydroboration reagent end up on the terminal carbon. Miyaura developed the very first *trans*-hydroboration of terminal alkynes that are catalyzed by rhodium or iridium complexes.[40] Labeling experiment confirmed that the original alkyne terminal proton has relocated to the β-carbon in the product. For the reaction mechanism, the phosphine-supported rhodium or iridium center is able to oxidatively insert into the terminal C–H bond and then isomerizes to vinylidene **1.65**. Subsequent oxidative insertion

---

[38] Brown, H. C.; Chandrasekharan, J.; Wang, K. K. *Pure Appl. Chem.* **1983**, *55*, 1387-1414.

[39] For reviews, see: (a) Trost, B. M.; Ball, Z. T. *Synthesis* **2005**, *2005*, 853-887; (b) Beletskaya, I.; Pelter, A. *Tetrahedron* **1997**, *53*, 4957-5026; (c) Barbeyron, R.; Benedetti, E.; Cossy, J.; Vasseur, J.-J.; Arseniyadis, S.; Smietana, M. *Tetrahedron* **2014**, *70*, 8431-8452; (d) Yoshida, H. *ACS Catal.* **2016**, *6*, 1799-1811; (e) Geier, S. J.; Vogels, C. M.; Westcott, S. A. *Current Developments in the Catalyzed Hydroboration Reaction. Boron Reagents in Synthesis*; ACS Symposium Series 1236; American Chemical Society: Washington, DC, 2016; Chapter 6, pp 209-225; (f) Obligacion, J. V.; Chirik, P. J. *Nat. Rev. Chem*. **2018**, *2*, 15-34; (g) Saptal, V. B.; Wang, R.; Park, S. *RSC Adv*. **2020**, *10*, 43539-43565.

[40] (a) Ohmura, T.; Yamamoto, Y.; Miyaura, N. *J. Am. Chem. Soc*. **2000**, *122*, 4990-4991; (b) Cid, J.; Carbó, J. J.; Fernández, E. *Chem. Eur. J*. **2012**, *18*, 1512-1521.

with borane followed by α-migratory insertion of the boryl group affords intermediate **1.67**. Reductive elimination of this intermediate closes the catalytic cycle. The authors proposed Et_3N as a key reagent for suppressing *cis*-hydroboration product via minimizing the oxidative insertion process between the metal and H–BX_2.

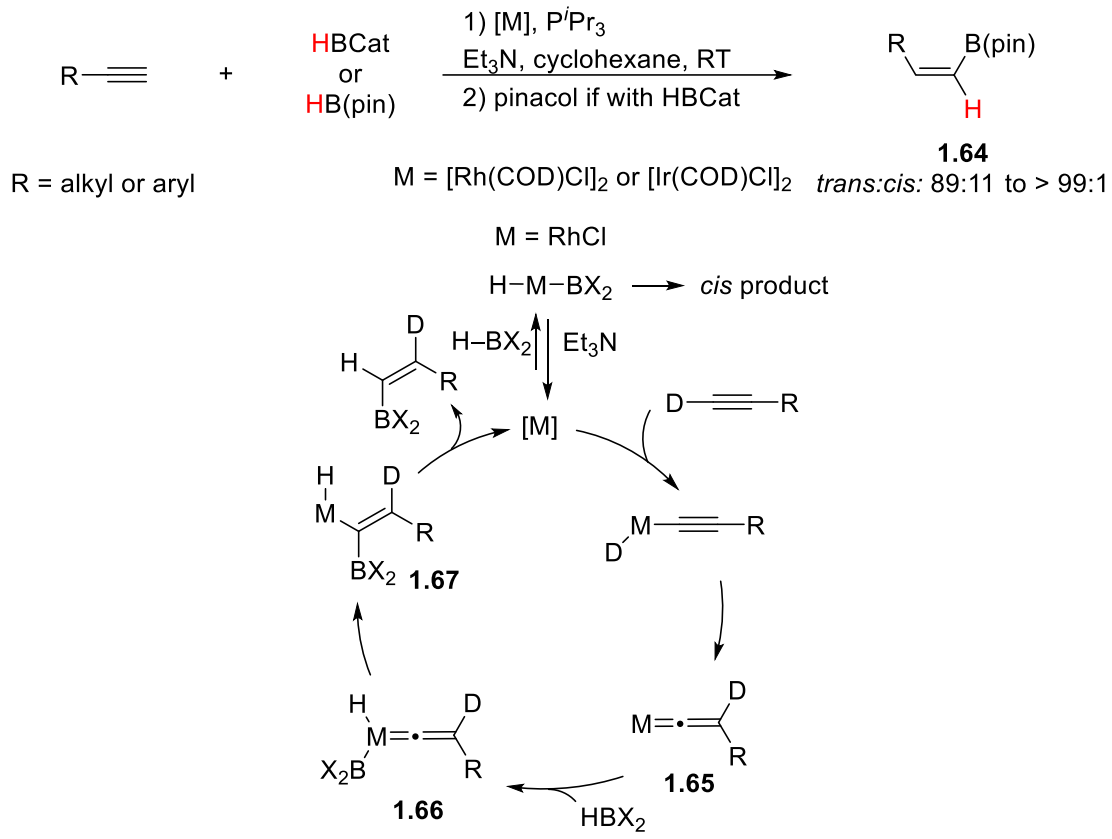

Scheme 1.15. Miyaura's Rh-catalyzed 1,1-*trans*-hydroboration reaction.

Ruthenium[41] and iron[42] polyhydride PNP-pincer complexes effectively catalyze *trans*-hydroboration reactions of terminal alkynes with HB(pin), respectively (Scheme 1.16). Pre-catalyst **1.68** or **1.69** first undergoes ligand exchange with HB(pin) to provide

[41] Gunanathan, C.; H lscher, M.; Pan, F.; Leitner, W. *J. Am. Chem. Soc*. **2012**, *134*, 14349-14352.

[42] (a) Gorgas, N.; Alves, L. G.; Stöger, B.; Martins, A. M.; Veiros, L. F.; Kirchner, K. *J. Am. Chem. Soc*. **2017**, *139*, 8130-8133; (b) Gorgas, N.; St ger, B.; Veiros, L. F.; Kirchner, K. *ACS Catal*. **2018**, *8*, 7973-7982; (c) Garhwal, S.; Fridman, N.; de Ruiter, G. *Inorg. Chem*. **2020**, *59*, 13817-13821.

intermediate **1.70**, which features two bridging hydrides. Then, alkyne coordination induces the release of H_2 followed by isomerization to yield vinylidene intermediate **1.71**. Subsequent α-migratory insertion of the boryl group and σ-bond metathesis complete the catalytic cycle.

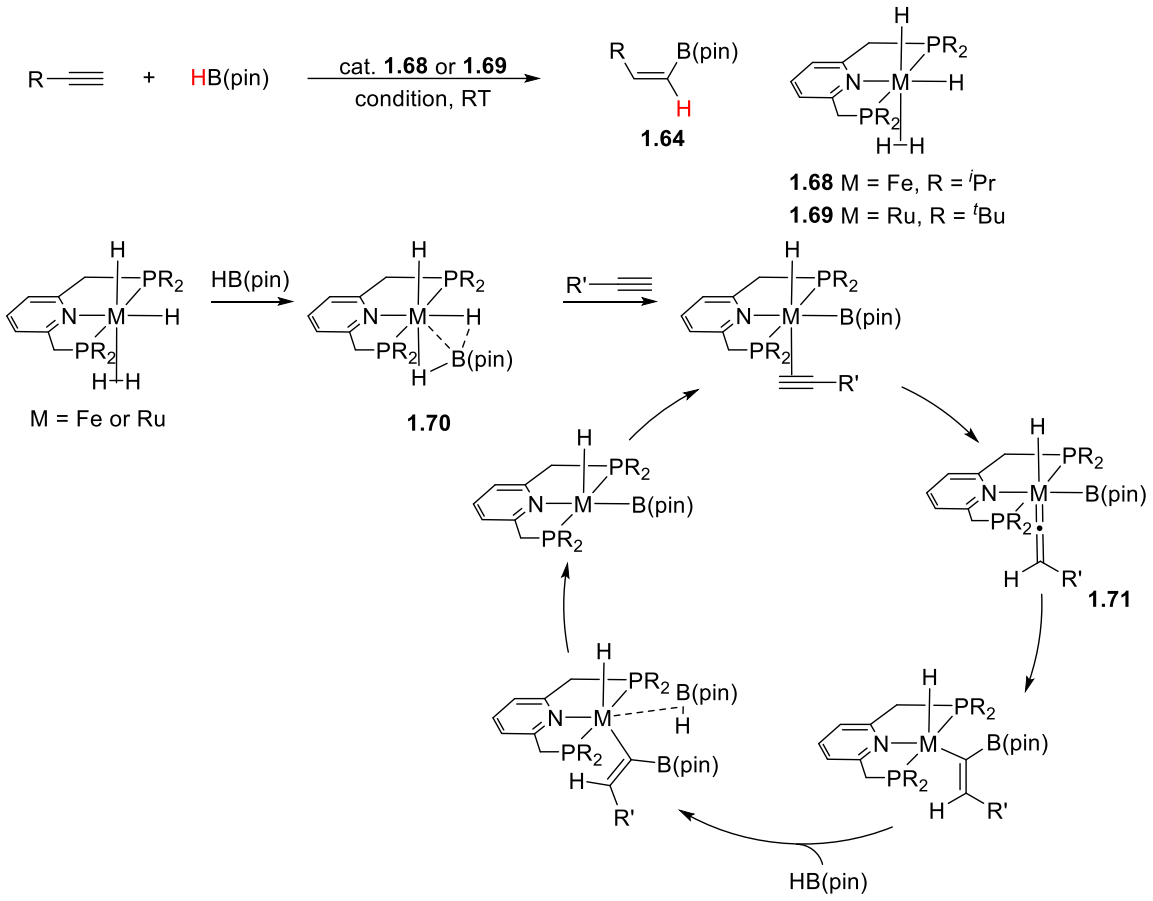

Scheme 1.16. Leitner and Kirchner's Ru/Ir PNP-pincer catalyzed 1,1-*trans*-hydroboration reaction.

Chirik and coworkers reported the application of bis(imino)pyridine cobalt complex **1.72** for *trans*-hydroboration reaction of terminal alkyne.[43] Unlike the previous

[43] Obligacion, J. V.; Neely, J. M.; Yazdani, A. N.; Pappas, I.; Chirik, P. J. *J. Am. Chem. Soc*. **2015**, *137*, 5855-5858.

vinylidene pathways, this reaction involves a Co–H β-migratory insertion into alkynyl boronates. Complex **1.72** is first activated by the alkyne with the release of methane, resulting in the active catalyst **1.73**. The cobalt center oxidatively inserts into HB(pin), which is then followed by C–B bond reductive elimination to provide alkynyl boronate **1.75**. *Cis*-hydrometalation then occurs on complex **1.75** to deliver intermediate **1.76-Pro-*anti***, which is in equilibrium with intermediate **1.76-Pro-*syn***, and both intermediates can undergo a proto-demetalation process. Experimental evidence suggests when R is an alkyl group, the reaction is under Curtain-Hammett control whereas when R is an aryl group, the proto-demetalation rate in **1.76-Pro-*anti*** is much faster than the equilibrium rate. Therefore, in both cases the *trans*-hydroboration product is the major one.

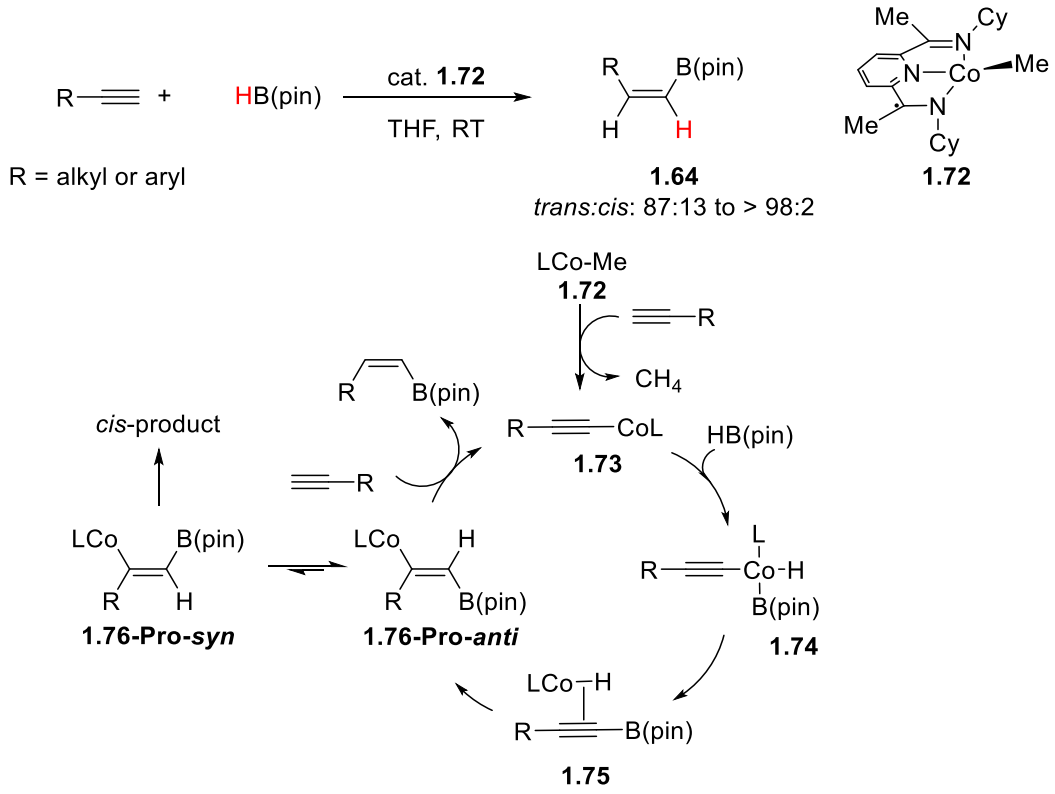

Scheme 1.17. Chirik's Co-catalyzed 1,1-*trans*-hydroboration reaction.

1.1.3.2.2. 1,2-*Trans*-hydroboration reactions via *cis*-*trans* isomerization

In 1,2-*trans*-hydroboration reactions the hydride and boron from the hydroboration reagent end up on different carbons. The initial addition of the metal-hydride or metal-boryl complex to the alkyne follows the *cis*-addition pathway, which then isomerizes to the *trans*-intermediate in subsequent steps due to sterics. Therefore, the overall reaction leads to the *trans*-hydroboration product.

Yun and coworkers reported a ligand-dependent copper-catalyzed hydroboration reaction of aryl-substituted terminal alkynes (Scheme 1.18).[44] The proposed catalytic cycle starts from copper hydride that is generated *in situ* from CuTc/DPEphos and HB(dan) (Tc: thiophene-2-carboxylate, DPE: bis[(2-diphenylphosphino)phenyl] ether, dan: 1,8-diaminonaphthalene). Coordination and β-migratory insertion provide intermediate **1.78-Pro-*syn***, which is in equilibrium with intermediate **1.78-Pro-*anti*** via a zwitterionic carbene-copper intermediate **1.79**. Both intermediates have the capability to undergo copper-boryl exchange, and which side would prevail is largely determined by the combination of ligand and borane reagent. For example, the SIPr-HB(dan) (SIPr: 1,3-bis(2,6-di-isopropylphenyl)imidazolidin-2-ylidene) and DPEphos-HB(pin) ligand-borane combinations favor the *cis*-product, while DPEphos-HB(dan) ligand-borane combination favors the *trans*-product.

[44] Jang, W. J.; Lee, W. L.; Moon, J. H.; Lee, J. Y.; Yun, J. *Org. Lett*. **2016**, *18*, 1390-1393.

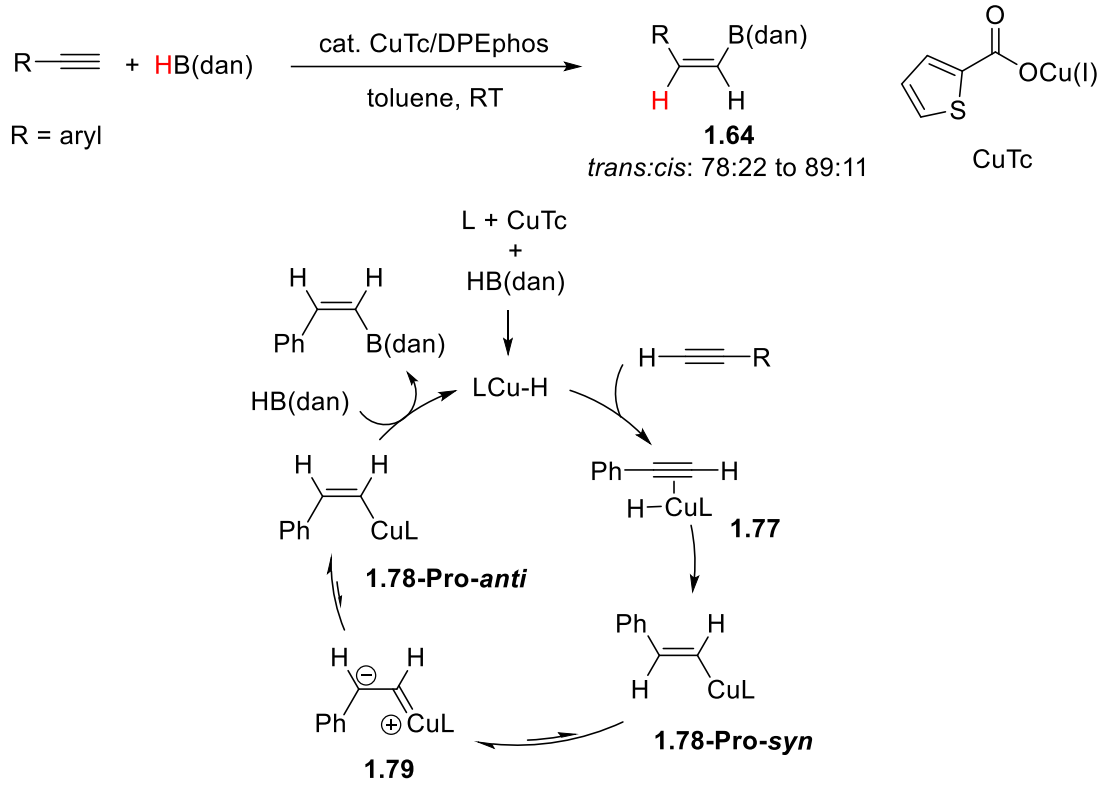

Scheme 1.18. Yun's Cu-catalyzed 1,2-*trans*-hydroboration reaction via *cis-trans* isomerization.

The Saito group developed a Ru-catalyzed *trans*-hydroboration reaction of terminal alkynes (Scheme 1.19, eq.1).[45] The NHC (*N*-heterocyclic carbene) ligated Ru pre-catalyst **1.80** first hydrometalates the alkyne, and a subsequent σ-bond metathesis with HB(dan) generates the active catalyst **1.82**. Alkyne coordination followed by boryl β-migratory insertion affords intermediate **1.83-Pro-*syn***. Due to the steric repulsions between NHC and B(dan) groups, this intermediate undergoes isomerization through either a metallacyclopropene intermediate **1.84** or a zwitterionic intermediate **1.85** to intermediate **1.83-Pro-*anti***. σ-Bond metathesis with HB(dan) produces the *trans*-product with the

[45] Yamamoto, K.; Mohara, Y.; Mutoh, Y.; Saito, S. *J. Am. Chem. Soc.* **2019**, *141*, 17042-17047.

regeneration of the catalyst. Apart from terminal alkynes, catalyst **1.80**-^{t}Bu exhibits *trans*-hydroboration activity towards diphenylacetylene, an internal alkyne, although it results in inferior diastereoselectivity (eq. 2).

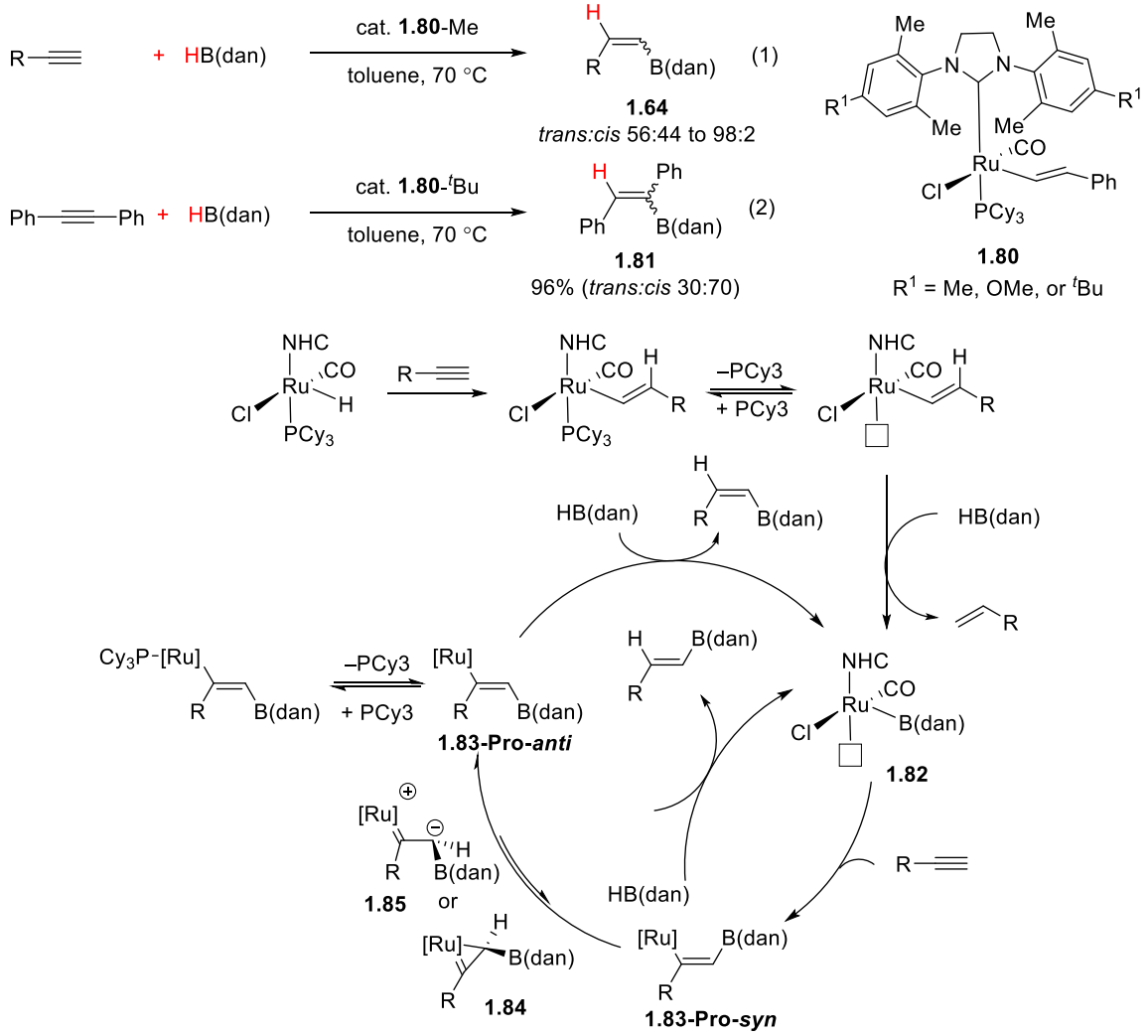

Scheme 1.19. Saito's Ru-catalyzed 1,2-*trans*-hydroboration reaction via *cis-trans* isomerization.

The only reported *trans*-selective hydroboration of internal alkynes system is reported by the Fürstner group.[46] As shown in Scheme 1.20, with $[Cp^*Ru(MeCN)_3]PF_6$

[46] Sundararaju, B.; Fürstner, A. *Angew. Chem. Int. Ed.* **2013**, *125*, 14050-14054.

(Cp*: pentamethylcyclopentadienyl) as the catalyst, symmetric alkynes usually afford good to excellent diastereoselectivity while sterically- or electronically-biased unsymmetrical alkynes lead to moderate selectivity. Additionally, terminal alkynes and enynes are not suitable substrates. In terms of the mechanism, alkyne and HB(pin) displace the labile acetonitriles on the metal. And then, the hydride is delivered to the alkyne in an inner-sphere fashion, forming metallacyclopropene **1.86**. As a configurationally labile complex, intermediate **1.88** is then formed via an η^1 zwitterionic intermediate **1.87** driven by the steric repulsion between the bulky Cp^* and R^1 group. Boryl 1,2-migration along the *anti*-side to the hydrogen atom and ligand exchange release the *trans*-hydroboration product. The overall mechanism pathway here is adapted from the alkyne *trans*-hydrosilylation mechanism.[47]

[47] Chung, L.; Wu, Y.-D.; Trost, B. M.; Ball, Z. T. *J. Am. Chem. Soc*. **2003**, *125*, 11578-11582.

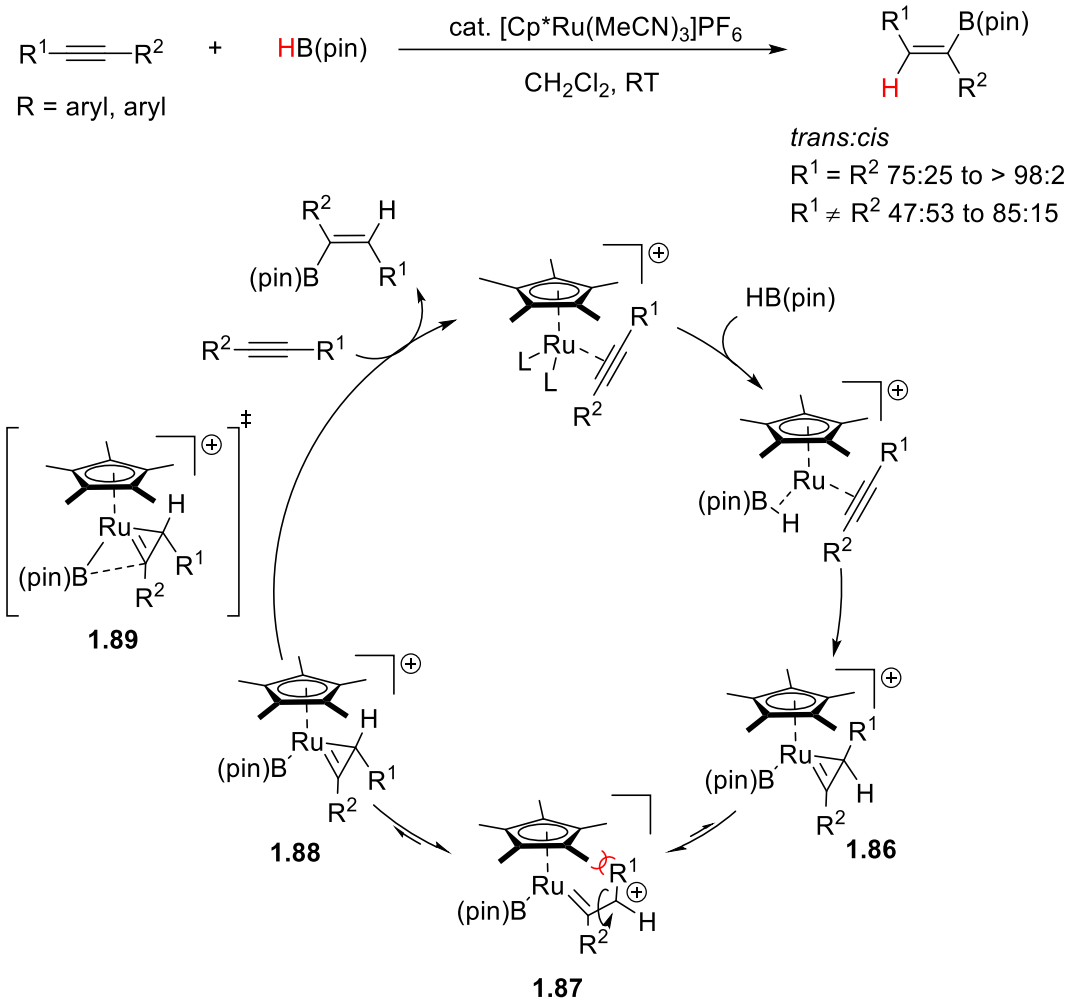

Scheme 1.20. Fürstner's Ru-catalyzed 1,2-*trans*-hydroboration of symmetrical alkynes.

In the follow-up works, the alkyne substrates can be expanded to protected propargylic alcohols with $[Cp^*RuCl]_4$ as the catalyst (Scheme 1.21).[48] Since the substrate is not symmetrical, two regio-isomeric *trans*-hydroboration products **1.91** and **1.92** are obtained, and their ratio is dictated by the steric repulsions between the two alkyne substituents rather than the directing effect of the peripheral group (i.e., oxygen coordination to boron). In other words, the boron group would preferentially add to the less

[48] (a) Longobardi, L. E.; Fürstner, A. *Chem. Eur. J.* **2019**, *25,* 10063-10068; (b) Murakami, S.; Matsubara, R.; Hayashi, M. *J. Organomet. Chem.* **2021**, *933*, 121653.

sterically hindered carbon. Inspired by this finding, the authors further tested sterically-biased alkyne **1.93** and successfully obtained product **1.94** in good regio- and diastereoselectivity.

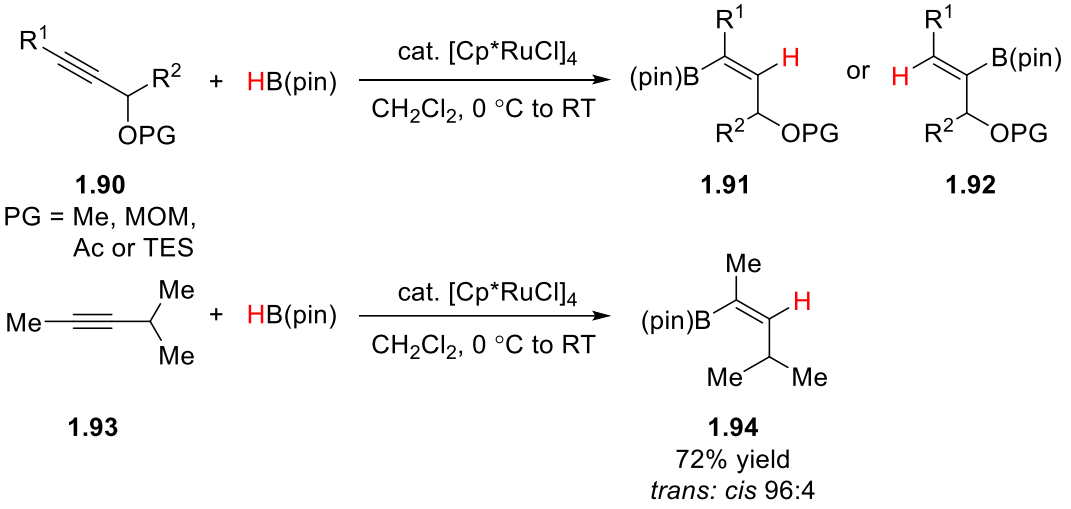

Scheme 1.21. Fürstner's Ru-catalyzed 1,2-*trans*-hydroboration of unsymmetrical alkynes.

1.1.3.2.3. 1,2-*Trans*-hydroboration reactions directed by neighboring group

Installing a Lewis basic group in proximity to the alkyne is another strategy to conduct alkyne 1,2-*trans*-hydroboration reactions. The directing group is able to form the Lewis acid-base adduct with borane, thus entropically lowering the energy as well as activating the alkyne if conjugated. Most reactions in this category are accomplished in transition metal free conditions.

In 2014 Shi and coworkers showed a gold-catalyzed amine-directed *trans*-hydroboration reaction of propargylamine-borane **1.95** (Scheme 1.22).[49] The electrophilic

[49] Wang, Q.; Motika, S. E.; Akhmedov, N. G.; Petersen, J. L. Shi, X. *Angew. Chem. Int. Ed*. **2014**, *53*, 5418-5422.

gold is crucial for activating the alkyne and facilitating boron hydride *trans*-delivery to afford intermediate **1.97**. Subsequent cyclization leads to 1,2-B,N-cyclopentenes **1.96**.

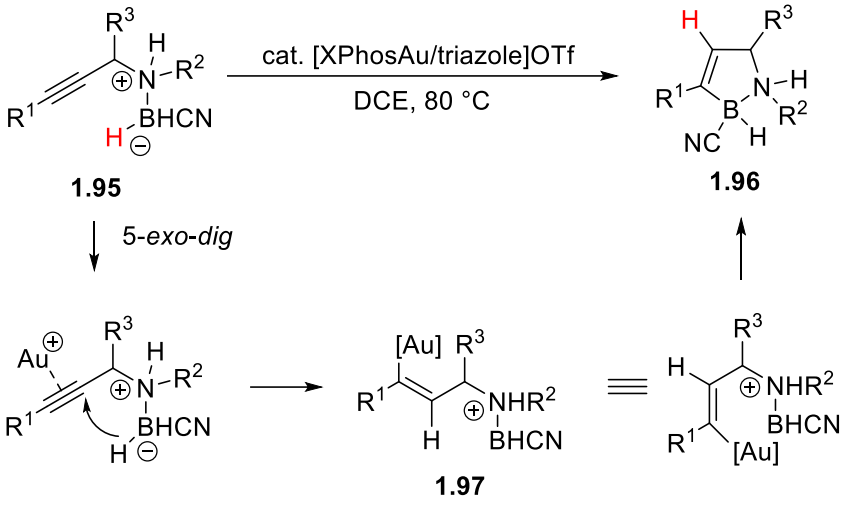

Scheme 1.22. Shi's amine-directed *trans*-hydroboration reaction.

Trialkylphosphines have been demonstrated as effective organocatalysts in enabling *trans*-hydroboration reaction of a large variety of conjugated alkynes such as alkynoates, alkynylamides and ynones (Scheme 1.23).[50] When HB(pin) is added to the system, it first coordinates to the Lewis basic heteroatoms (O or N), assisting the phosphine conjugate addition and forming zwitterionic intermediate **1.99**. Phosphonium ylides **1.100** and **1.101** are then generated through a 1,4-hydride shift and isomerization. Intramolecular nucleophilic attack of the ylide carbon to boron forms the five-membered ring **1.102**, which then undergoes a simultaneous ring-opening/phosphine extrusion process to produce alkenyl boronates **1.98**.

[50] (a) Nagao, K.; Yamazaki, A.; Ohmiya, H.; Sawamura, M. *Org. Lett.* **2018**, *20*, 1861-1865; (b) Zi, Y.; Schömberg, F.; Seifert, F.; Görlsb, H.; Vilotijevic, I. *Org. Biomol. Chem.* **2018**, *16*, 6341-6349; (c) Fritzemeier, R.; Gates, A.; Guo, X.; Lin, Z.; Santos, W. L. *J. Org. Chem*. **2018**, *83*, 10436-10444.

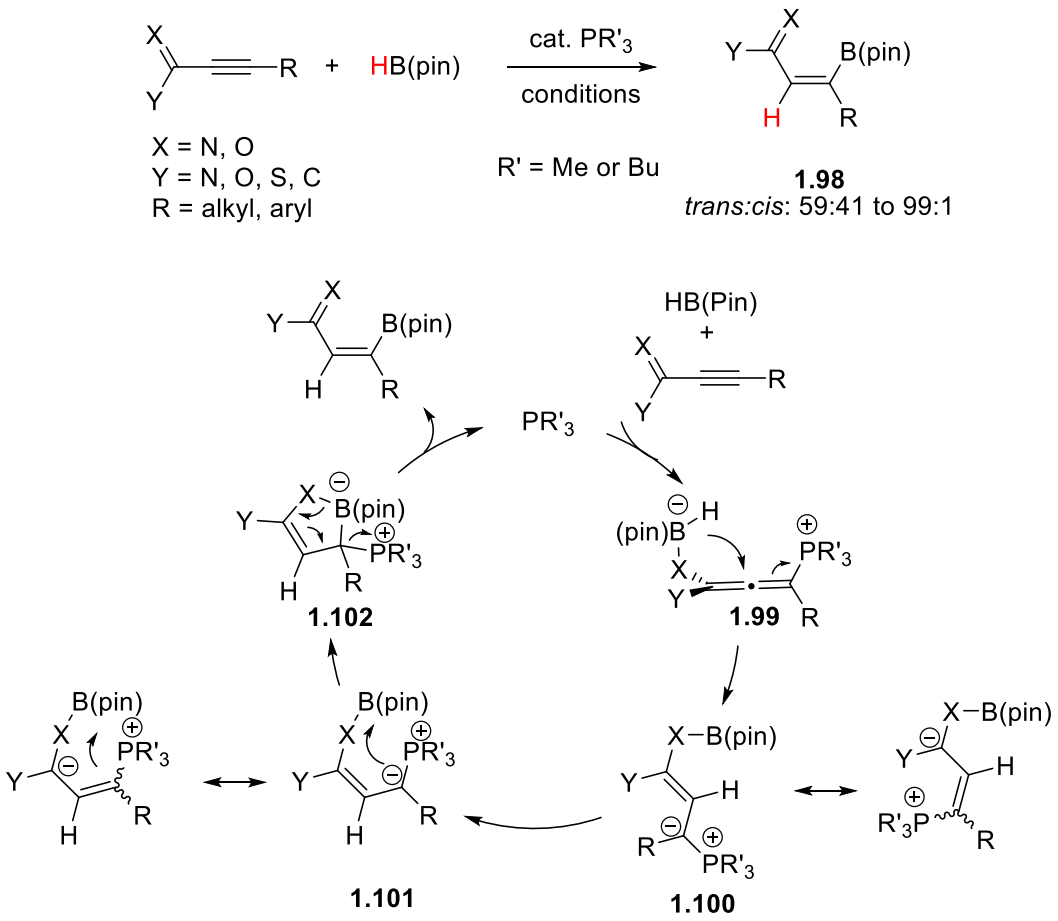

Scheme 1.23. Trialkylphosphine catalyzed oxygen/nitrogen directed *trans*-hydroboration reaction.

The Santos group showed that for propiolamides **1.103**, *trans*-hydroboration can take place without any catalysts.[51] Deprotonation of the substrate and coordination with HB(pin) provides intermediate **1.105**, which undergoes 1,4-hydride shift and isomerization to afford carbanion **1.106**. Carbanion **1.106** undergoes a boron migration followed by quenching with a proton to form the *trans*-hydroboration product **1.104**.

[51] Justin Grams, R.; Fritzemeier, R. G.; Slebodnick, C.; Santos, W. L. *Org. Lett.* **2019**, *21*, 6795-6799.

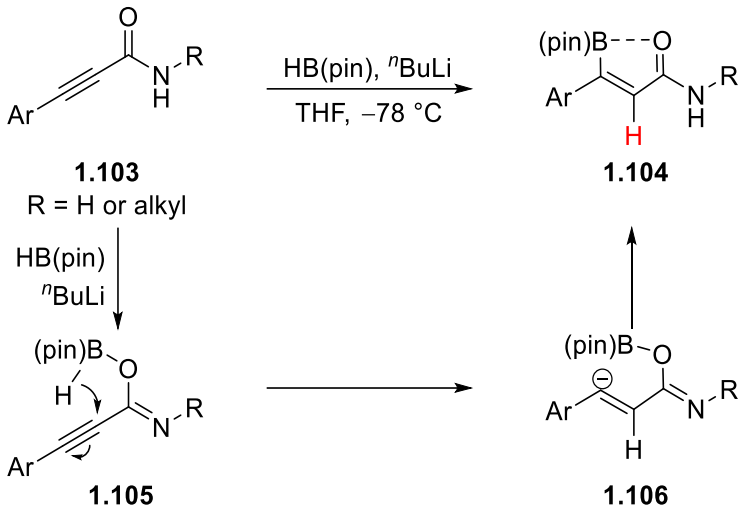

Scheme 1.24. Santo's oxygen-directed *trans*-hydroboration reactions.

With 2-pyridyl as the directing group, the *trans*-hydroboration reaction occurs on 2-pyridyl phenylacetylenes **1.107**, yielding B,N-indene **1.108** (Scheme 1.25).[52] The reaction follows a similar mechanism as described with propiolamides.

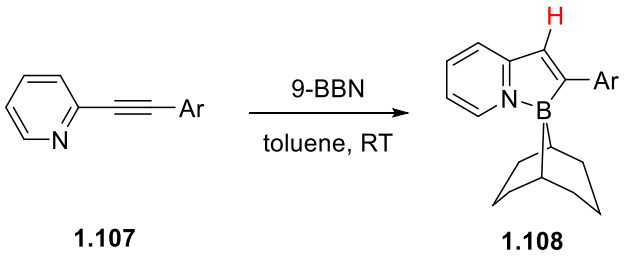

Scheme 1.25. Wang's pyridine-directed *trans*-hydroboration reaction.

A zinc-mediated *trans*-hydroboration reaction of ynamides with NHC bound borane is also reported (Scheme 1.26).[53] Even though a radical chain pathway is possible, the experimental evidence is consistent with an ionic pathway. The authors take the advantage of the equilibrium between ynamide **1.109** and keteniminium **1.111** and propose

[52] Yuan, K.; Suzuki, N.; Mellerup, S. K.; Wang, X.; Yamaguchi, S.; Wang, S. *Org. Lett*. **2016**, *18*, 720-723.
[53] Wang, K.; Zhuang, Z.; Ti, H.; Wu, P.; Zhao, X.; Wang, H. *Chin. Chem. Lett*. **2020**, *31,* 1564-1567.

the hydride in NHC bound borane attacking the electrophilic carbon. The resulting enamide anion is further trapped by $ZnEt_2$ to form intermediate **1.112**, which then combines with the previously generated borenium cation to afford the product **1.110**.

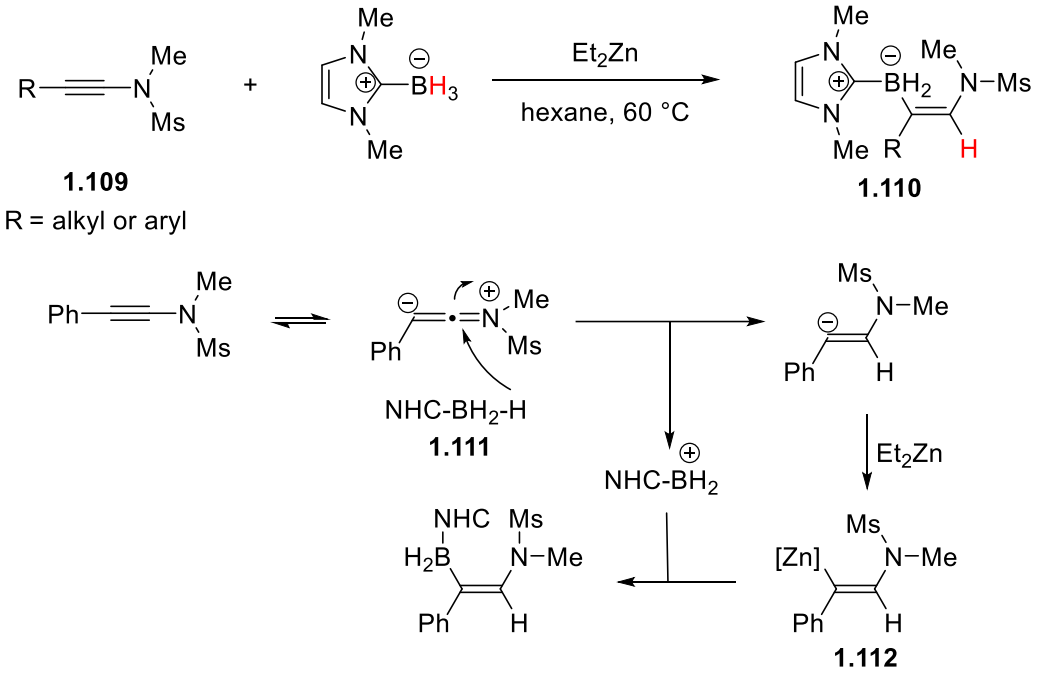

Scheme 1.26. Wang's *trans*-hydroboration reaction of ynamide.

1.1.3.2.4. Miscellaneous

The Ingleson group developed a BCF (tris(pentafluorophenyl)borane) catalyzed reaction with NHC bound 9-BBN (9-borabicyclo[3.3.1]nonane) as the hydroboration reagent, affording the *trans*-hydroboration product exclusively (Scheme 1.27).[54] For the mechanism, BCF first abstracts a hydride from NHC bound 9-BBN, resulting in borenium **1.114**. This borenium cation is then captured by the alkyne, leading to the linear alkenyl

[54] McGough, J. S.; Butler, S. M.; Cade, I. A.; Ingleson, M. J. *Chem. Sci.* **2016**, *7*, 3384-3389.

cation **1.115**. Finally, vinyl cation **1.115** is quenched by H–BCF anion from the least sterically hindered side to close the catalytic cycle.

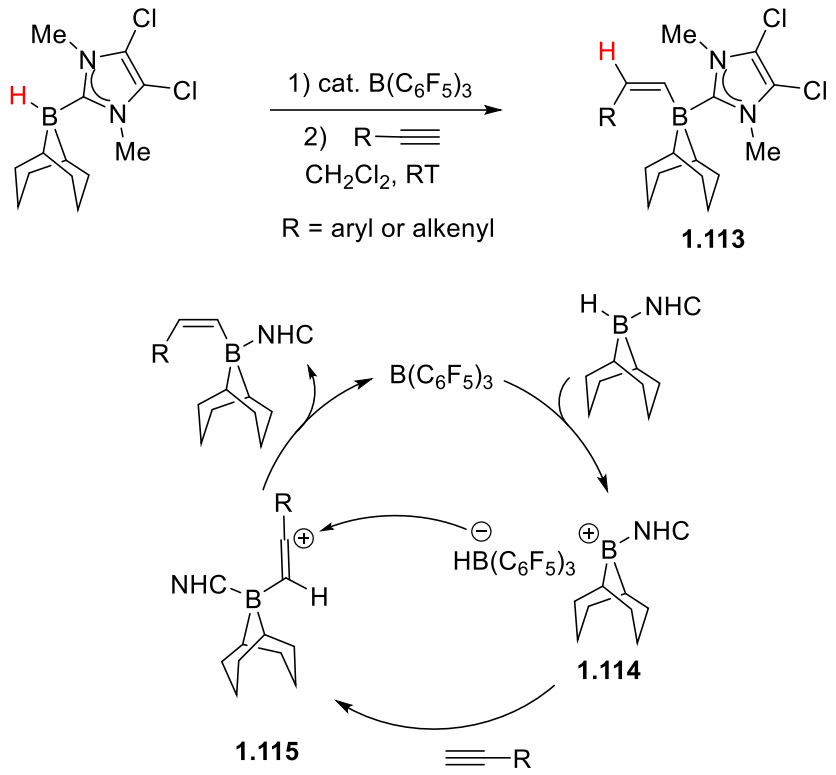

Scheme 1.27. Ingelson's BCF-catalyzed *trans*-hydroboration reaction.

A similar system was later developed by the Erker group, which is compatible for both terminal and internal alkynes (Scheme 1.28).[55] Though the reaction condition for the internal alkynes are more forcing, good yield and diastereoselectivity are maintained. Another BCF-catalyzed t*rans*-hydroboration of alkynyl-phosphine derivatives is reported by Stephan, following a similar mechanism.[56]

[55] Wang, T.; Jentgens, X.; Daniliuc, C. G.; Kehr, G.; Erker, G. *ChemCatChem* **2017**, *9*, 651-658.
[56] Fan, L.; Stephan, D. W. *Dalton Trans*. **2016**, *45*, 9229-9234.

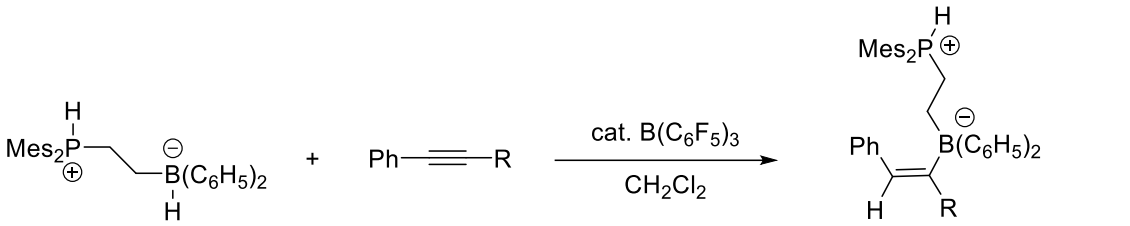

1.116 R = H, RT, 90% yield
1.117 R = Me, 60 °C, 93% yield

Scheme 1.28. Erker's BCF-catalyzed *trans*-hydroboration reaction.

All the reactions described above are classified as two-electron chemistry. To date there is only one reported system of one-electron chemistry for alkyne *trans*-hydroboration. NHC boranes have been long known as radical precursors,[57] but its application in the field of *trans*-hydroboration emerged only recently where DTBP (di-*tert*-butyl peroxide) is chosen as a suitable radical initiator.[58] In initiation steps *tert*-butoxide radical, resulting from the homolytic cleavage of DTBP, abstracts a hydrogen from adduct **1.118**, affording boryl radical **1.120**. In propagation steps, radical **1.120** adds to the alkyne substrate to form alkenyl radical **1.121**, which then abstracts a hydrogen atom from NHC bound borane **1.118** to furnish the *trans*-hydroboration product **1.119**. Although the reaction follows a radical chain mechanism, stoichiometric DTBP is necessary to ensure a good yield probably due to the short chain lengths in propagating steps.

[57] Ueng, S.-H.; Brahmi, M. M.; Derat, É.; Fensterbank, L.; Lacôte, E.; Malacria, M.; Curran, D. P. *J. Am. Chem. Soc.* **2008**, *130*, 10082-10083.
[58] (a) Shimoi, M.; Watanabe, T.; Maeda, K.; Curran, D. P.; Taniguchi, T. *Angew. Chem. Int. Ed*. **2018**, *57*, 9485-9490; (b) Takahashi, K.; Geib, S. J.; Maeda, K.; Curran, D. P.; Taniguchi, T. *Org. Lett.* **2021**, *23*, 1071-1075.

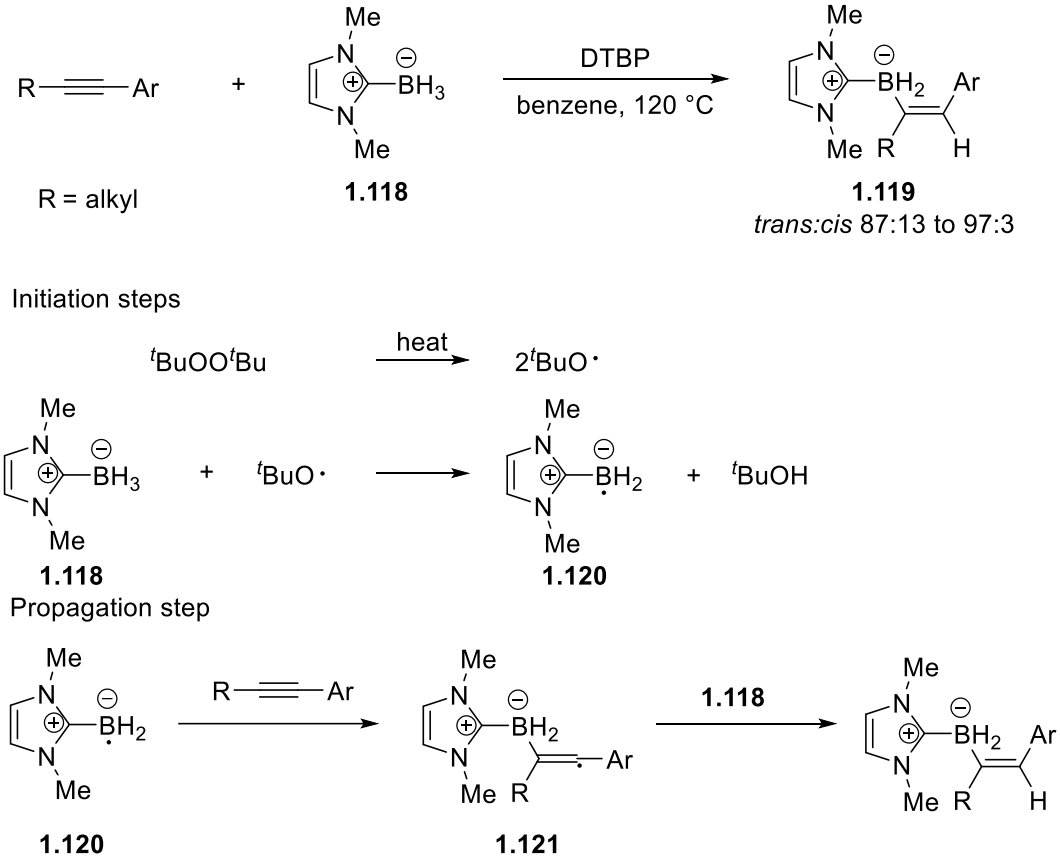

Scheme 1.29. Taniguchi's *trans*-hydroboration reaction via radical pathway.

1.2. Pd/Senphos catalyzed site-selective and stereoselective *trans*-hydroboration of 1,3-enynes

In view of the current limitations of alkyne *trans*-hydroboration reactions that only symmetrical or strongly sterically biased alkynes are suitable substrates and no general method for both terminal and internal alkynes as well as enynes,[59] we continued to optimize the reaction conditions from our initial discovery (chapter 1.1.2). Evidenced by X-ray diffraction structure (Scheme 1.13) that the palladium metal and C(3) substituent of the

[59] (a) Sasaki, Y.; Horita, Y.; Zhong, C.; Sawamura, M.; Ito, H. *Angew. Chem. Int. Ed*. **2011**, *50*, 2778-2782; (b) Mao, L.; Bose, S. K. *Adv. Synth. Catal.* **2020**, *362*, 4174-4188.

Senphos ligand are in close proximity, a series of C(3) alkyl substituted ligands (ligand **1.46**, **1.122-1.126**) were synthesized according to Scheme 1.30. The phosphine containing southern fragment of the ligands can be easily attached to 1,4-azaborines by *in situ* generation of the lithiated precursor and subsequent quenching with precursors **1.44** or **1.36**.

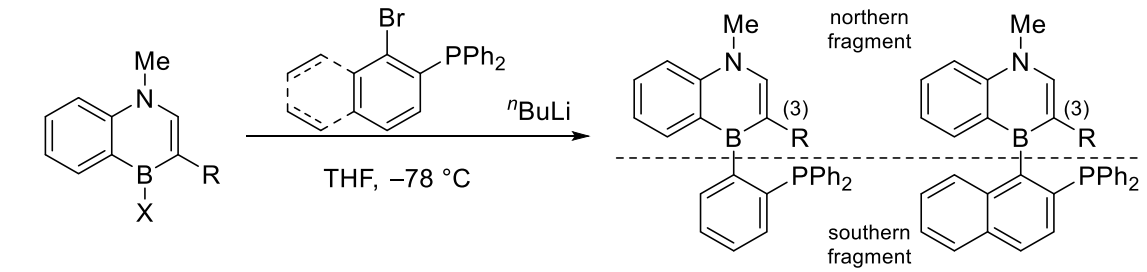

1.44 X = OMe, R = H
1.36 X = Cl, R = alkyl

1.46 R = H
1.122 R = Me
1.123 R = Et
1.124 R = ^{i}Pr

1.125 R = Me
1.126 R = Et

Scheme 1.30. Syntheses of Senphos ligands.

1.2.1. Results and discussion[60]

With 1,3-enyne **1.127** as the model substrate, the ligand effects on *trans*-hydroboration diastereoselectivity were investigated and summarized in Table 1.2. No background reaction was observed in the absence of the catalyst under otherwise identical reaction conditions. The C(3) substituent plays a small but noticeable role in the product diastereoselectivity (entries 1-4), and the best result was obtained with Senphos **1.124** (entry 4) which bears a sterically hindered ^{i}Pr group. No obvious trends in either reactivity or stereoselectivity is observed by changing the southern fragment from the *o*-diphenylphosphinophenyl to 2-diphenylphosphinonaphth-1-yl group (entry 2 *vs* 5, entry 3

[60] Part of this section is adapted from ref. 21b.

vs 6). With Senphos **1.124** as the ligand and 1.5 equivalent HBCat, the desired product was obtained in 86% yield (entry 4 *vs* 7) while maintaining diastereoselectivity (> 98:2).

Table 1.2. Ligand survey of Pd/Senphos catalyzed *trans*-hydroboration of terminal 1,3-enyne.[a]

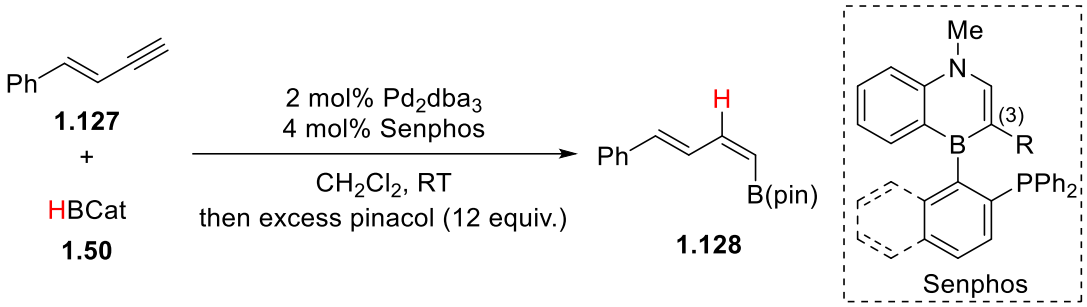

entry	Senphos	*trans*-hydroboration selectivity[b]	yield (%)[c]
1	**1.46** (R = H)	93:7	59
2	**1.122** (R = Me)	92:8	60
3	**1.123** (R = Et)	96:4	56
4	**1.124** (R = ^{i}Pr)	>98:2	62
5	**1.125** (R = Me)	96:4	59
6	**1.126** (R = Et)	94:6	68
7[d]	**1.124** (R = ^{i}Pr)	>98:2	86

[a] Reaction was setup with 1.0 equiv. enyne **1.127**, 1.0 equiv. HBCat and 4 mol% Pd(0)/Senphos catalyst in CH_2Cl_2 (0.25 M). [b] The diastereomeric ratio was determined by ^{1}H NMR of crude material before addition of pinacol. [c] Yield of isolated product, based on enyne **1.127**. [d] 1.5 equiv. of HBCat was applied.

With the optimal conditions in hand, we further expanded the reaction system to a large variety of terminal and internal 1,3-enynes, which all proceeded readily with good yields and high diastereoselectivities. Selected examples are shown in Table 1.3.[61] Different functional groups such as aryl halides (entries **1.130**, **1.131**, **1.137**), alkene (entry **1.133**) and silyl protected alcohol (entry **1.136**) were well tolerated in the reaction system.

[61] For complete substrate scope tables, see ref. 21b.

Table 1.3. Pd/Senphos catalyzed *trans*-hydroboration of 1,3-enynes.[a,b]

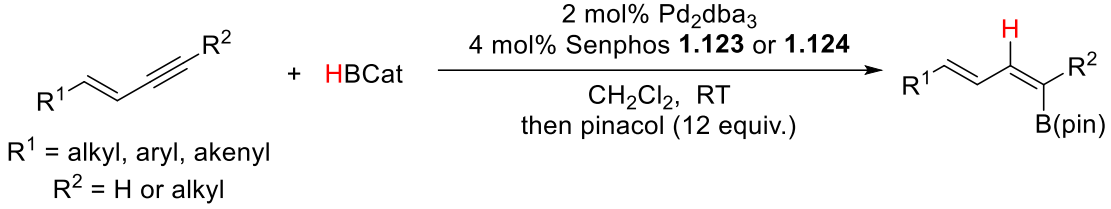

R^1 = alkyl, aryl, akenyl
R^2 = H or alkyl

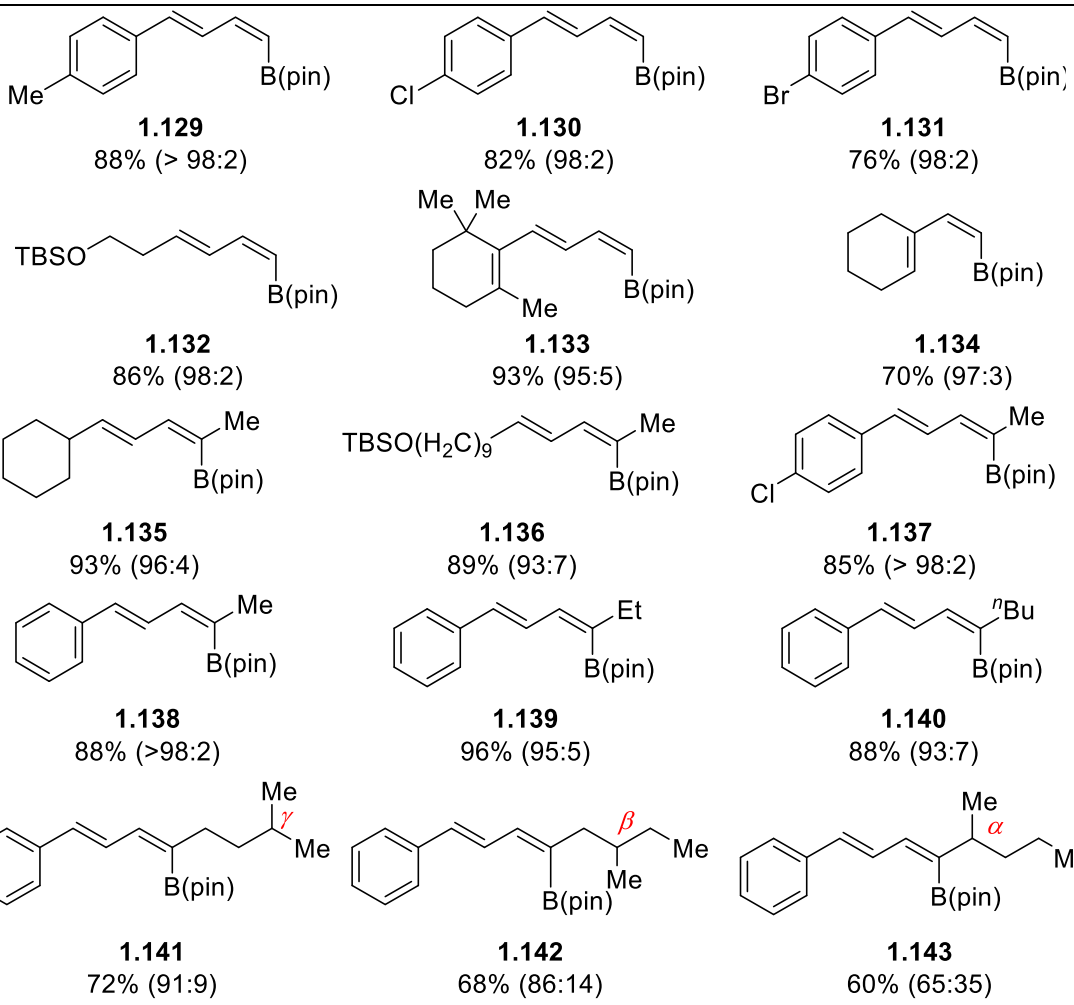

[a] Yield of isolated product (average of 2 runs), based on enyne. The diastereomeric ratio in parentheses was determined by ^{1}H NMR of crude material before addition of pinacol. [b] For internal 1,3-enynes Senphos **1.123** was determined to be the optimal ligand.

We observed an erosion in diastereoselectivity as the R^2 group becomes more sterically demanding. For example, from products **1.138** to **1.140**, increasing the size of the

R^2 group (A-value: methyl: 1.70, ethyl: 1.75)[62] results in a decrease in diastereoselectivity. And a more drastic observation is found in a series of branched products **1.141** to **1.143**. γ-Branched enyne-**1.141** had the least steric influence on the reactive site, resulting in a 91:9 diastereoselectivity ratio. On the other hand, α-branched enyne-**1.143** exhibits a 65:35 diastereoselectivity.

1.2.2. Reaction condition re-optimization for sterically hindered 1,3-enynes

To tackle the low diastereoselectivity in 1,3-enynes with sterically hindered alkynyl groups, we initiated reaction condition re-optimization with α-branched enyne-**1.143** and catalyst Pd(0)/Senphos **1.123** as the model reaction (Table 1.4). The relationship between the sterics on catecholborane and reaction diastereoselectivity was investigated first (entries 1-4). When 4-*t*butylcatecholborane **1.144** was applied, the reaction outcome improved slightly (entry 1 *vs*. 2). Installing an extra *t*butyl group *ortho* to oxygen (**1.145**) led to a higher selectivity (entry 1 *vs.* entry 3). However, increasing the sterics additionally at the C(6) position led to no reaction even under refluxing condition (entry 4). Based on these unsuccessful modifications on catecholborane, we turned our attention to the solvent screening since it can influence both the thermodynamics and kinetics of a reaction.[63] Seven solvents were further evaluated (entries 5-11). Common solvents such as benzene, Et_2O, THF and MeCN gave unsatisfactory results in terms of yield and selectivity. However, a clear trend in diastereoselectivity was observed with chlorinated solvents

[62] Eliel, E. L.; Wilen, S. H.; Mander, L. N. *Stereochemistry of Organic Compounds,* 1st ed.; New York: Wiley, 1994.

[63] (a) Slakman, B. L.; West, R. H. *J. Phys. Org. Chem.* **2019**, *32*, e3904; (b) Cainelli, G.; Galletti, P.; Giacomini, D. *Chem. Soc. Rev.* **2009**, *38*, 990-1001; (c) Varghese, J. J.; Mushrif, S. M**.** *React. Chem. Eng.* **2019**, *4*, 165-206; (d) Anslyn, E. V.; Dougherty, D. A. *Modern Physical Organic Chemistry,* 1st ed.; University Science Books, 2006.

(entries 1, 9-11). And it appears that the more chlorine atoms in the solvent molecule, the better selectivity can be obtained. Eventually, $(CHCl_2)_2$ was determined to be the best solvent, providing 86% NMR yield with a *trans:cis* ratio of 97:3.

Table 1.4. Optimization of reaction conditions with sterically hindered 1,3-enyne as the substrate.[a]

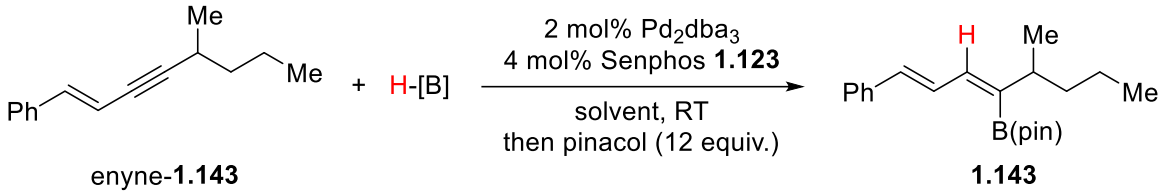

enyne-**1.143** **1.143**

entry	H–[B]	solvent	NMR yield (*trans*:*cis*)[b]
1	HBCat	CH_2Cl_2	60% (65:35)
2	**1.144**	CH_2Cl_2	62% (66:34)
3[c]	**1.145**	CH_2Cl_2	65% (86:14)
4[d]	**1.146**	CH_2Cl_2	No reaction
5	HBCat	benzene	83% (12:88)
6	HBCat	Et_2O	42% (19:81)
7	HBCat	THF	90% (21:79)
8	HBCat	MeCN	71% (82:18)
9	HBCat	$(CH_2Cl)_2$	88% (65:35)
10	HBCat	$CHCl_3$	82% (82:18)
11	HBCat	$(CHCl_2)_2$	86% (97:3)

[a] Reaction was setup with 1.0 equiv. enyne-**1.143**, 1.5 equiv. H-[B] and 4 mol% Pd(0)/Senphos **1.123** in solvent (1.25 M). [b] The yield and diastereomeric ratio were determined by ^{1}H NMR of crude mixture after silica gel plug with hexamethylbenzene as the internal standard. [c] Reaction time was extended to 14 hours. [d] Under refluxing condition, 12 hours.

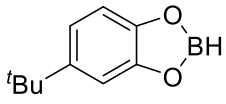

1.144

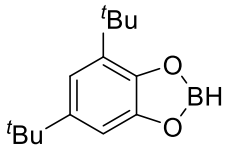

1.145

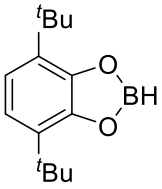

1.146

Enynes with sterically hindered alkynyl group R^2 were examined under the optimal reaction conditions (Table 1.5).[64] High *trans*-selectivity was observed for various R^2 alkyl (entries **1.143**, **1.147**) and aryl (entries **1.148**-**1.151**) substituted enynes. The tolerance of a

[64] I acknowledge Johnny Wang for helping prepare some of the substrates and perform several *trans*-hydroboration reactions.

2-chlorophenyl (entry **1.150**) and alkenyl silane group[65] (entry **1.151**) would facilitate further functionalizations toward complex molecules.

Table 1.5. *Trans*-hydroboration of sterically hindered 1,3-enynes.[a]

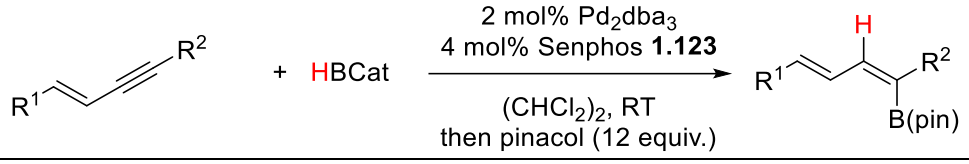

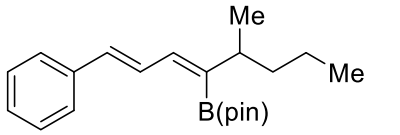

1.143
80% (97:3)

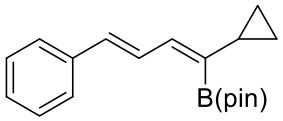

1.147
66% (95:5)

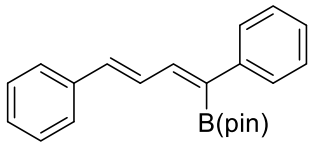

1.148
76% (96:4)

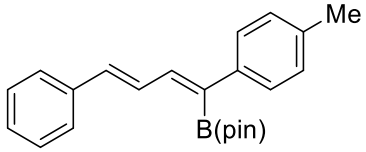

1.149
73% (96:4)

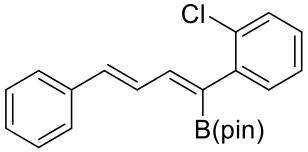

1.150
83% (>98:2)

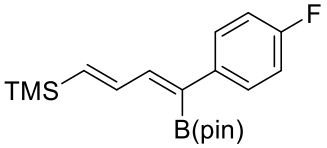

1.151
77% (98:2)[b]

[a] Reaction was setup with 1.0 equiv. enyne, 1.5 equiv. HBCat and 4 mol% Pd(0)/Senphos **1.123** in $(CHCl_2)_2$ (1.25 M). Yield of isolated product (average of 2 runs) based on the enyne. The diastereomeric ratio in parentheses was determined by ^{1}H NMR of crude material after addition of pinacol. [b] With 10 mol% catalyst loading.

1.3. Mechanistic studies towards Pd/Senphos catalyzed *trans*-hydroboration reaction of 1,3-enyne

1.3.1. Proposed catalytic cycles

With the established excellent diastereoselectivity in Pd/Senphos catalyzed *trans*-hydroboration reaction of both terminal and internal 1,3-enynes, we turned our attention to elucidating the reaction mechanism. We envisioned two possible mechanisms, namely the

[65] Goh, K. K.; Kim, S.; Zard, S. Z. *J. Org. Chem.* **2013**, *78*, 12274-12279.

inner-sphere oxidative addition mechanism and the outer-sphere[39g] oxidative addition mechanism.

The inner-sphere oxidative addition mechanism (Scheme 1.31): LPd(0) complex **1.152** first oxidatively inserts into HBCat to provide intermediate **1.153**.[66] Then, subsequent enyne coordination and β-migratory insertion affords intermediate **1.154-Pro-*syn***. Next, the steric repulsion between the LPd(II) moiety and the boryl group leads to a *cis*-*trans* isomerization[67] to form intermediate **1.154-Pro-*anti*** via a palladium alkylidene intermediate **1.155**. Finally, reductive elimination of intermediate **1.154-Pro-*anti*** yields the *trans*-product.

[66] The oxidative insertion product between metal and HBCat has been proposed previously, see ref. 31e, 40a. For experimental evidence, see: (a) Westcott, S. A.; Taylor, N. J.; Marder, T. B.; Baker, R. T.; Jones, N. J.; Calabrese, J. C. *J. Chem. Soc., Chem. Commun*. **1991**, 304-305; (b) Shimada, S.; Batsanov, A. S.; Howard, J. A. K.; Marder, T. B. *Angew. Chem. Int. Ed*. **2001**, *40*, 2168-2171; (c) Segawa, Y.; Yamashita, M.; Nozaki, K. *J. Am. Chem. Soc.* **2009**, *131*, 9201-9203; (d) Segawa, Y.; Yamashita, M.; Nozaki, K. *Organometallics* **2009**, *28*, 6234-6242.

[67] For the isomerization of alkenyl palladium intermediates, see: (a) Daini, M.; Yamamoto, A.; Suginome, M. *J. Am. Chem. Soc.* **2008**, *130*, 2918-2919; (b) Wisthoff, M. F.; Pawley, S. B.; Cinderella, A. P.; Watson, D. A. *J. Am. Chem. Soc.* **2020**, *142*, 12051-12055; (c) Lv, W.; Liu, S.; Chen, Y.; Wen, S.; Lan, Y.; Cheng, G. *ACS Catal.* **2020**, *10,* 10516-10522.

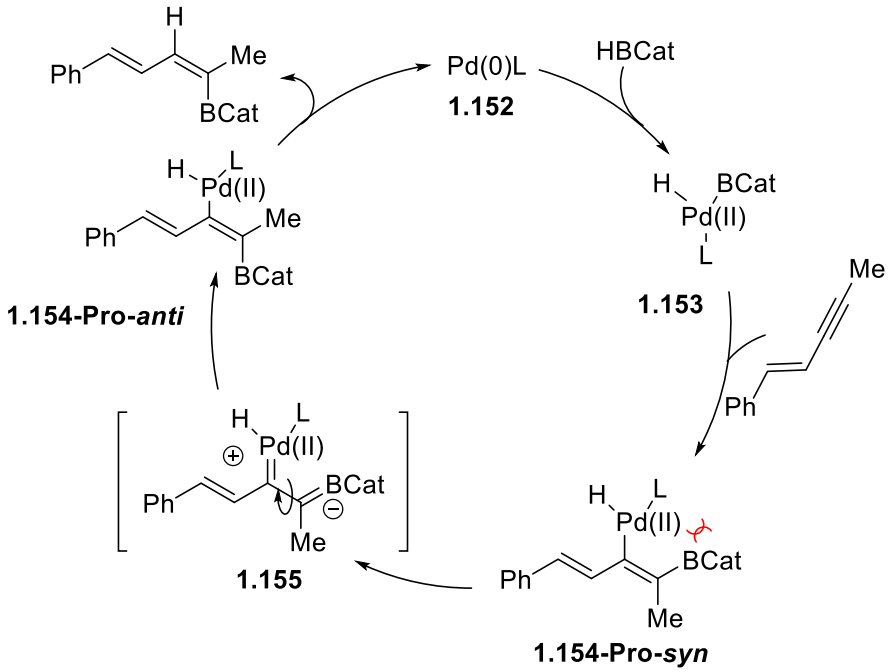

Scheme 1.31. Inner-sphere oxidative addition mechanism.

The outer-sphere oxidative addition mechanism (Scheme 1.32): LPd(0) complex **1.152** first coordinates with enyne to form the enyne-Pd(0) complex **1.156**, which is then activated by HBCat to yield palladium π-allyl zwitterion **1.157**. Next, the pendant hydride on the borate is shuttled to the palladium by the second HBCat via intermediate **1.158** to afford intermediate **1.159.** Finally, reductive elimination of the Pd(II) leads to the *trans*-product.

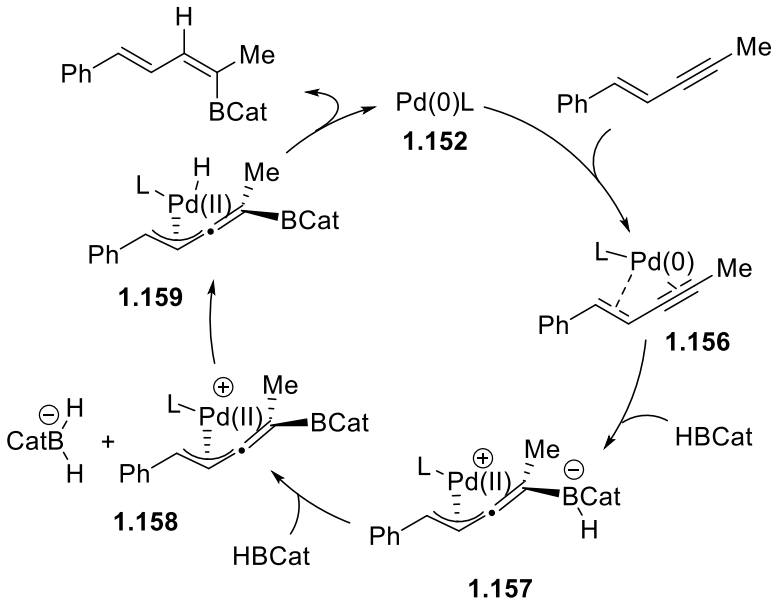

Scheme 1.32. Outer-sphere oxidative addition mechanism.

Aiming at identifying the most plausible mechanism, we further conducted the reaction mechanistic studies in the following three sections. Specially, we performed 1) double crossover experiments to probe the hydride shuttle mechanism; 2) kinetic studies to help identify the resting state and RDS (rate determining step) of the catalytic cycle; and 3) spectroscopic characterization to elucidate possible reaction intermediates.

1.3.2. Double crossover experiment

In the outer-sphere oxidative addition mechanism, the HBCat is proposed to serve as a hydride shuttle thus allowing a mechanism for scrambling (intermediates **1.157** to **1.159**, Scheme 1.32), and such process is absent in the inner-sphere oxidative addition mechanism. Therefore, we designed a double crossover experiment with two equal amount of isotopically labeled catecholboranes **1.161** and **1.162** (which are assumed to have very similar chemical reactivities, labeled as HBCat and DBCat in Scheme 1.35 and Scheme 1.36), and the scrambling or absence of scrambling of the labels in the products distribution

(Scheme 1.33, A to D) can potentially distinguish between the two proposed reaction mechanisms. The reaction outcome can be analyzed by the products mass distribution via GC-MS (gas chromatography-mass spectrometry) where the unscrambled product A and D have a molecular weight of 269 and 271, respectively, and both the scrambled products B and C have a molecular weight of 270.

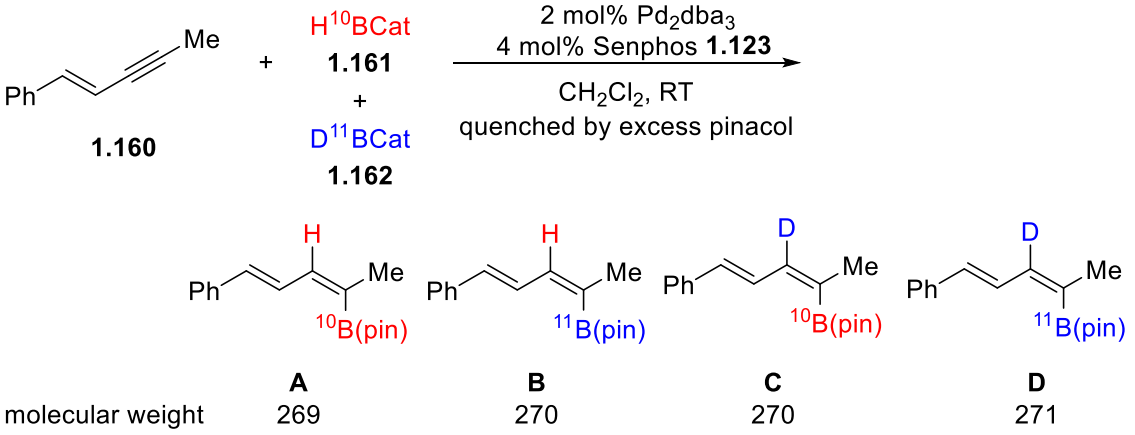

Scheme 1.33. Design of the double crossover experiment.

We commenced with the syntheses of two isotopically labeled catecholboranes (Scheme 1.34). Two commercially available boric acids, $^{10}B(OH)_3$ and $^{11}B(OH)_3$, undergo esterification reaction with butanol followed by reduction in presence of amine to afford Et_3N bound borane **1.163** and **1.164**, respectively.[68] Subsequent reaction with metal hydride delivers the isotopically pure metal borohydrides **1.165** and **1.166**, which can be readily incorporated into catecholborane **1.161** and **1.162**.[69,70]

[68] Safronov, A. V.; Jalisatgi, S. S.; Hawthorne, M. F. *Inorg. Chem.* **2016**, *55*, 5116-5117.

[69] (a) Narayana, C.; Periasamy, M. *J. Organomet. Chem.* **1987**, *323*, 145-147; (b) Suseela, Y.; Prasad, A. S. B.; Periasamy, M. *J. Chem. Soc., Chem. Commun.* **1990**, 446-447.

[70] 4-^{t}Butylcatechol is chosen to facilitate the product purification.

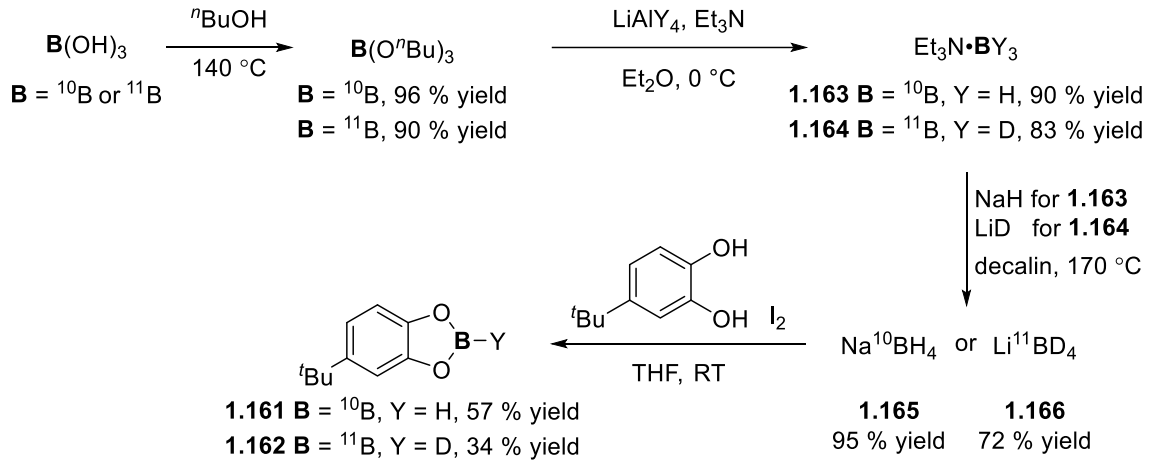

Scheme 1.34. Synthesis of two isotopically labeled 4-*t*butylcatecholborane.

For Pd/Senphos catalyzed *trans*-hydroboration reaction of internal enyne **1.160** (Scheme 1.33), if the inner-sphere oxidative addition mechanism is followed, we propose hydride-boron scrambling will less likely occur (Scheme 1.35). Thus, the crossover products B and C are not expected to be observed, and the product mass distribution of molecular weight 269, 270 and 271 would be 1:0:1 (A : (B + C) : D).

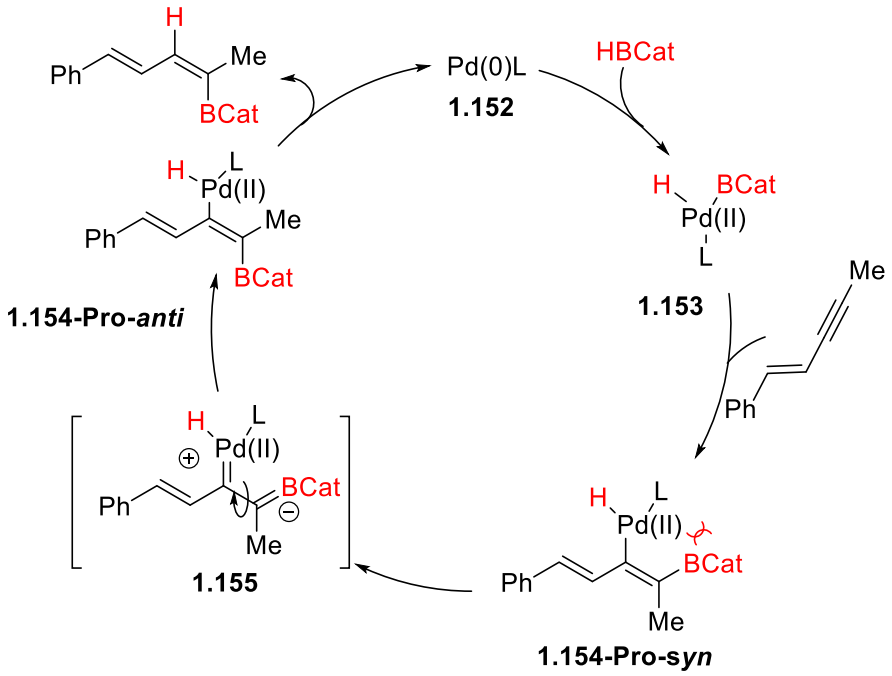

Scheme 1.35. Double crossover analysis in inner-sphere oxidative addition mechanism.

If the outer-sphere oxidative addition mechanism is followed, after the incorporation of $H^{10}BCat$ in complex **1.157**, either $H^{10}BCat$ or $D^{11}BCat$ can abstract the pendent hydride. If $D^{11}BCat$ serves as the shuttle and abstract the H, the resulting catecholborohydride anion in intermediate **1.158** would possess H and D, both of which have the same possibility to attack the palladium. In the case of D attacking, product with D-$^{10}BCat$ combination would form. Thus, the crossover products B and C are expected to be observed, and the product mass distribution of molecular weight 269, 270 and 271 would be 1:2:1 (A : (B + C) : D).

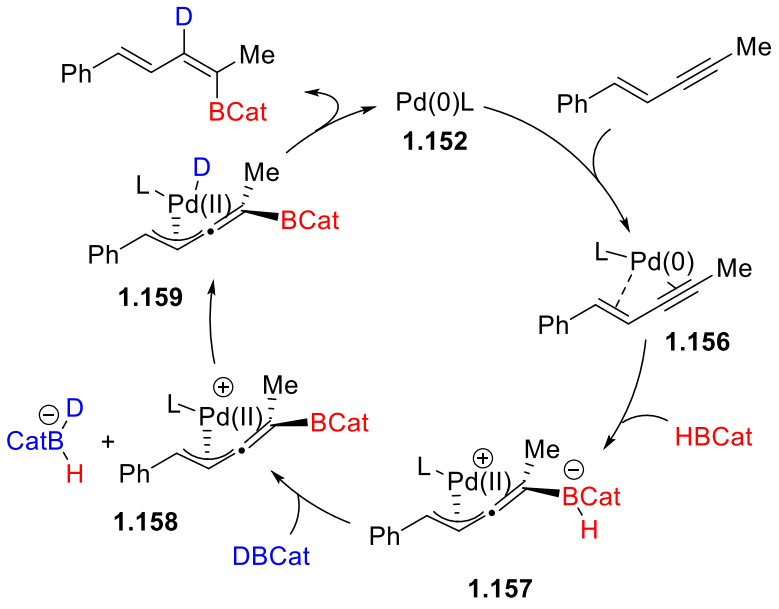

Scheme 1.36. Double crossover analysis in outer-sphere oxidative addition mechanism.

To extract the correct information from the double crossover experiment, the background borane scrambling needs to be considered.[71] We used the mass distribution within the *cis*-hydroboration product, a side product which is proposed to form in the absence of borane scrambling, as a background borane scrambling indicator.[31e, 72] As shown in Table 1.6, when the reaction is conducted in condition 1 (where both the borane and catalyst are low in concentration compared to the standard setup), the *cis*-product with molecular weight 269, 270 and 271 has a mass distribution of 1.0:0.5:0.8, indicating the background borane scrambling occurs to some extent, and the *trans*-product has a mass distribution of 1.0:1.9:1.1, showing substantial amount of scrambled products and being

[71] We used diluted reaction conditions and quenched the reaction in its early conversion to suppress the background scrambling between boranes **1.161** and **1.162**, however, it still occurs to some extent as monitored by ^{11}B NMR during a two-minute time period (see Experimental section). For a related investigation into the background scrambling of HBCat, see: Brown, J. M.; Lloyd-Jones, G. C. *J. Am. Chem. Soc*. **1994**, *116*, 866-878.

[72] Yang, Y.; Jiang, J.; Yu, H.; Shi, J. *Chem. Eur. J*. **2018**, *24*, 178-186.

consistent with outer-sphere oxidative addition mechanism.[73,74] On the other hand, in condition 2 (where the borane concentration is doubled compared to condition 1), the background scrambling is accelerated as indicated by the 1.0:1.0:1.0 mass distribution in *cis*-product, and the *trans*-product displays the same mass distribution pattern as in condition 1. In a positive control experiment where the two isotopically labeled boranes are pre-scrambled, both the *cis*- and *trans*-product are formed with similar mass distribution. Therefore, we conclude the observed mass distribution in *trans*-hydroboration product is more consistent with the outer-sphere oxidative addition mechanism.

[73] Our GC-MS system with 19091S-433UI column is able to separate the *cis*- and *trans*-product, but unable to separate their corresponded four isotopically labeled products.

[74] Due to the low concentration of borane and catalyst loading in condition 1 and control experiment, the reaction *trans:cis* selectivity is almost 1:1 in the first 2-minute period. However, in condition 2 the *trans:cis* selectivity increases to 7:1.

Table 1.6. Products mass distributions in double crossover experiment.[75]

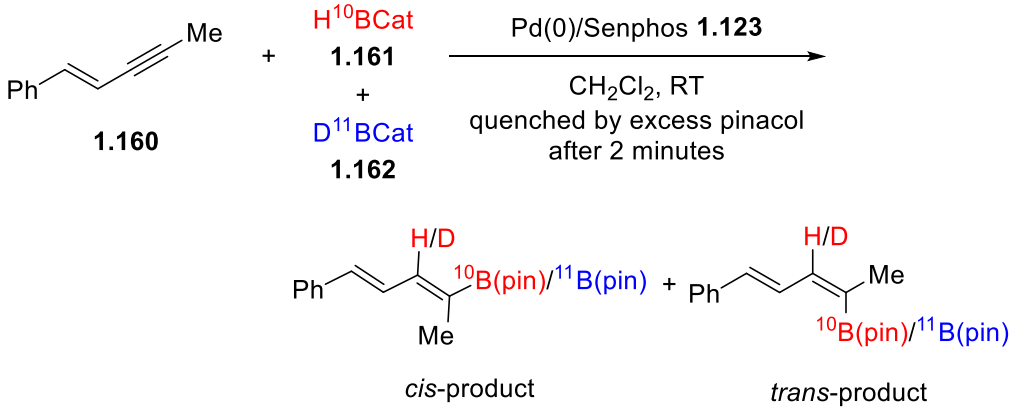

mass 269:270:271	*cis*-product	*trans*-product
condition 1[a]	1.0:0.5:0.8	1.0:1.9:1.1
condition 2[b]	1.0:1.0:1.0	1.0:2.0:1.2
control[c]	1.0:1.7:1.0	1.0:2.0:1.2

[a] Reaction was setup with enyne **1.160** (1.25 M) and Pd/Senphos **1.123** (0.5 mol%) with boranes **1.161** and **1.162** (0.07 M each) in CH_2Cl_2. [b] Reaction was setup with enyne **1.160** (1.25 M) and Pd/Senphos **1.123** (0.5 mol%) with boranes **1.161** and **1.162** (0.14 M each) in CH_2Cl_2. [c] Same as condition 1, but the two boranes are pre-mixed in neat for 4 hours at room temperature.

1.3.3. Investigation of reaction kinetic profile

In this section the reaction orders and the KIE (kinetic isotope effect) were studied with the model reaction setup in Scheme 1.37. To avoid any non-innocent behavior of the dba ligand,[76] Pd(COD)($CH_2TMS)_2$ was chosen as the precatalyst instead of Pd_2dba_3.

[75] The ratios reported in Table 1.6 represent the directly observed relative intensities of the species with the corresponding molecular weights (269, 270, 271) from the MS instrument. Corrections for natural abundance (i.e., 1% 13C for a 17-carbon compound) have not been made. We estimate that accounting for these corrections would lead to an error of ± 10%, which would make this method unsuitable for evaluating small kinetic isotope effects. For examples of KIE determination via mass spectrometry, see (a) Perrin, C. L.; Zhao, C. *Org. Biomol. Chem.* **2008**, *6*, 3349-3353; (b) Liuni, P.; Olkhov-Mitsel, E.; Orellana, A.; Wilson, D. J. *Anal. Chem.* **2013**, *85*, 3758-3764; (c) Iannone, R.; Anderson, R. S.; Vogel, A.; Eby, P. S.; Whiticar, M. J.; Rudolph, J. *J. Atmos. Chem.* **2005**, *50*, 121-138; (d) Kline, P. C.; Rezaee, M.; Lee, T. A. *Anal. Biochem.* **1999**, *275*, 6-10.

[76] (a) Fairlamb, I. J. S.; Kapdi, A. R.; Lee, A. F.; McGlacken, G. P.; Weissburger, F.; de Vries, A. H. M.; Schmieder-van de Vondervoort, L. *Chem. Eur. J.* **2006**, *12*, 8750-8761; (b) Colletto, C.; Burés, J.; Larrosa, I. *Chem. Commun.* **2017**, *53*, 12890-12893; (c) Fairlamb, I. J. S. *Org. Biomol. Chem.* **2008**, *6*, 3645-3656; (d) Amaya, T.; Maegawa, Y.; Masuda, T.; Osafune, Y.; Hirao, T. *J. Am. Chem. Soc.* **2015**, *137*, 10072-10075.

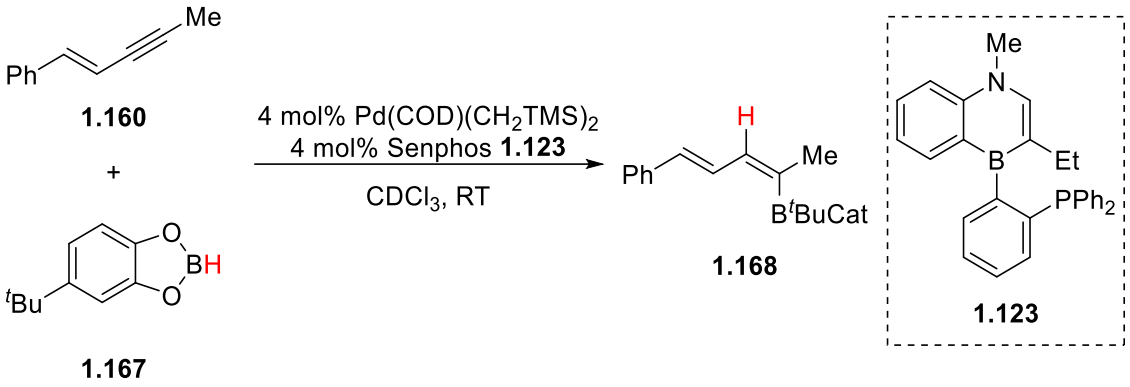

Scheme 1.37. Model reaction setup in the investigation of reaction kinetic profile.

First, same excess experiment was conducted. It contains parallel experiments where the initial concentrations of one reactant are different but the initial concentration differences between the two reactants remains the same.[77] We performed such analysis for the reaction in Scheme 1.37 where enyne **1.160** was the limiting reagent and its initial concentration difference to catecholborane **1.167** was kept at 0.36 M. As shown in Figure 1.5, the green trace, which is generated via the time-adjustment method from the blue trace,[78] overlays with the orange trace. This is an indication that there is no catalyst deactivation or product inhibition.

[77] Blackmond, D. G. *Angew. Chem. Int. Ed*. **2005**, *44*, 4302-4320.

[78] (a) Baxter, R. D.; Sale, D.; Engle, K. M.; Yu, J.-Q.; Blackmond, D. G. *J. Am. Chem. Soc.* **2012**, *134*, 4600-4606; (b) Blackmond, D. G. *J. Am. Chem. Soc.* **2015**, *137*, 10852-10866.

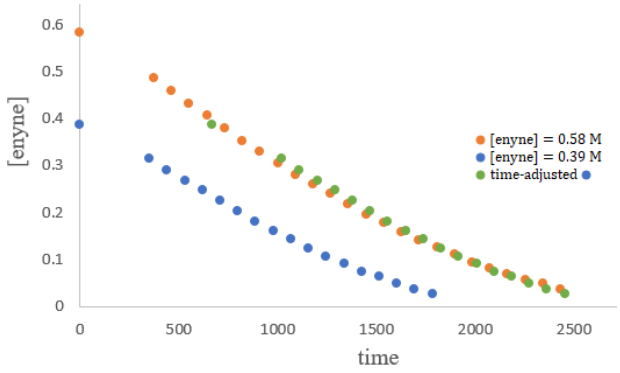

Figure 1.5. Same excess experiment of *trans*-hydroboration reaction.

Then, different excess experiments were conducted. It contains parallel experiments where the initial concentrations of one reactant remains the same but the initial concentration differences between the two reactants are different.[77] By doing so the reaction order of the reactant with varying concentrations can be obtained by analyzing the corresponding reaction rates. Reaction rates are traditionally obtained via initial concentration-time plots,[79] which however only utilize the data at the initial stage (< 10% conversion). Newer methods such as RPKA (reaction progress kinetic analysis)[80] rely on mathematic manipulation of selected physical parameters throughout the reaction that may require sophisticated instrumentation. Recently Burés proposed a variable time normalization analysis which conveniently utilizes NMR to acquire necessary signals and determines the reaction orders by visualizing overlap.[81] Due to its simplicity, this method was considered here (for the theory behind this method, see Experimental section).

---

[79] For applications, see (a) Avidan-Shlomovich, S.; Ghosh, H.; Szpilman, A. M. *ACS Catal.* **2015**, *5*, 336-342; (b) Bartoszewicz, A.; Miera, G. G.; Marcos, R.; Norrby, P.-O.; Martín-Matute, B. *ACS Catal.* **2015**, *5*, 3704-3716; (c) Ziegler, D. T.; Riesgo, L.; Ikeda, T.; Fujiwara, Y.; Fu, G. C. *Angew. Chem. Int. Ed.* **2014**, *53*, 13183-13187; (d) Jiang, Y.; Li, F.; Zhang, B.; Li, X.; Wang, X.; Huang, F.; Sun, L. *Angew. Chem. Int. Ed.* **2013**, *52*, 3398-3401.

[80] (a) Blackmond, D. G. *J. Am. Chem. Soc.* **2015**, *137*, 10852-10866; (b) Blackmond, D. G. *Angew. Chem. Int. Ed*. **2005**, *44*, 4302-4320.

[81] (a) Burés, J. *Angew. Chem. Int. Ed.* **2016**, *55*, 2028-2031; (b) Burés J. *Angew. Chem. Int. Ed*. **2016**, *55*, 16084-16087.

By maintaining the initial concentrations of catecholborane **1.167** as 0.94 M and the catalyst as 0.024 M, and varying the initial concentration of enyne **1.160**, plots with different possible reaction orders in enyne **1.160** are summarized in Figure 1.6. And the most suitable order for the enyne is determined to be zero order.

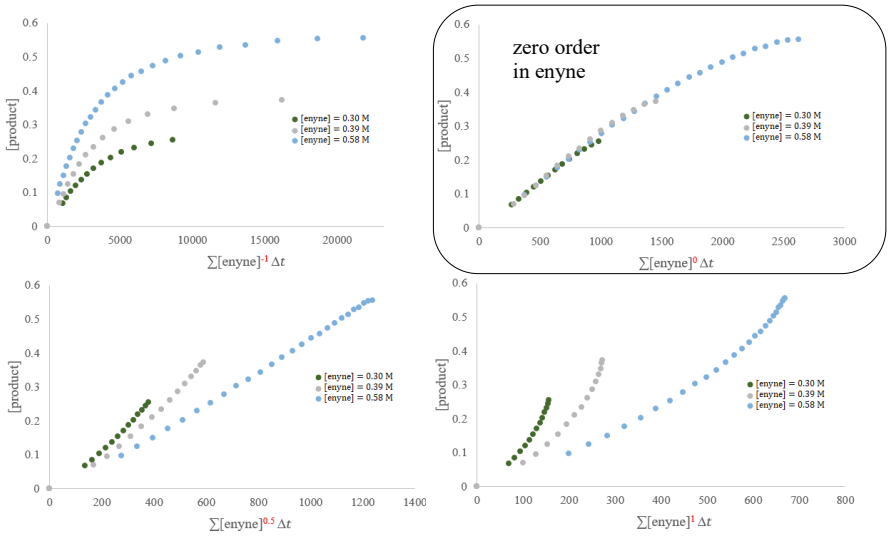

Figure 1.6. Determination of order in enyne.

By maintaining the initial concentrations of enyne **1.160** as 0.58 M and the catalyst as 0.024 M, and varying the initial concentration of catecholborane **1.167**, plots with different possible reaction orders in catecholborane **1.167** are summarized in Figure 1.7. And the most suitable order for the catecholborane is determined to be first order.

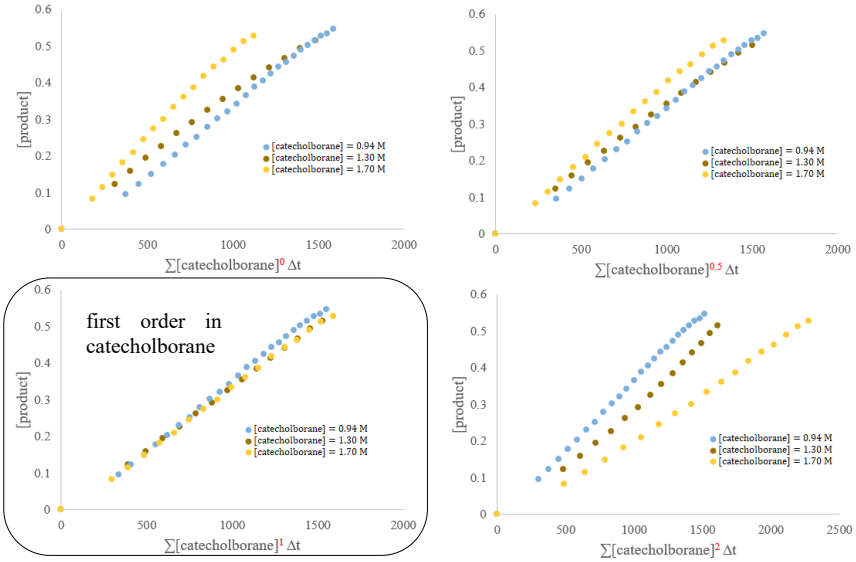

Figure 1.7. Determination of order in catecholborane.

By maintaining the initial concentrations of enyne **1.160** as 0.58 M and catecholborane **1.167** as 0.94 M, and varying the catalyst concentration, plots with different possible reaction orders in catalyst were summarized in Figure 1.8. And the most suitable order for the catalyst is determined to be first order.

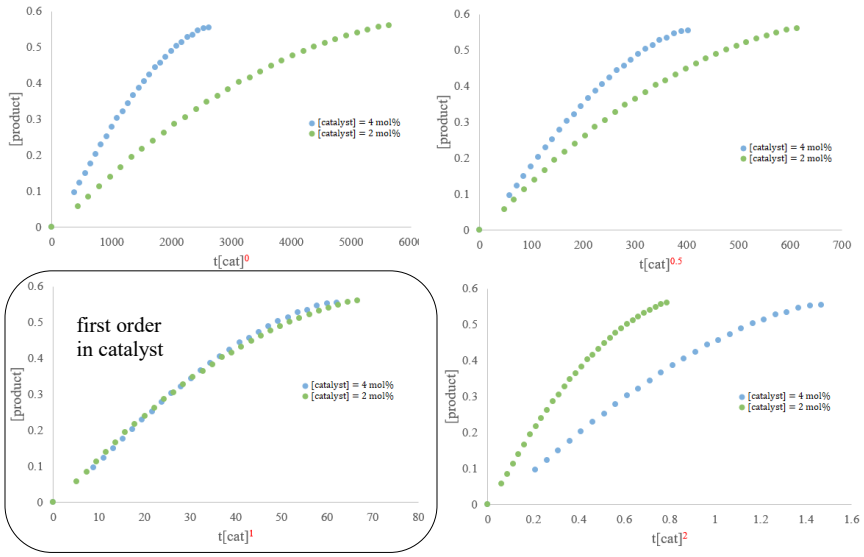

Figure 1.8. Determination of order in catalyst.

Our kinetic analysis leads to the rate expression for reaction in Scheme 1.37 as:

$$\text{rate} = k[\text{enyne}]^0[\text{HB}^t\text{BuCat}]^1[\text{catalyst}]^1.$$

And the rate constant k_H was calculated as 0.90 ± 0.042 $M^{-1}\cdot min^{-1}$.[82]

KIE experiment was performed with catecholborane **1.169** (deuterated version of catecholborane **1.167)** (Scheme 1.38), and the rate constant k_D is calculated as 0.79 ± 0.016 $M^{-1}\cdot min^{-1}$. Thus a k_H/k_D value of 1.1 is determined.

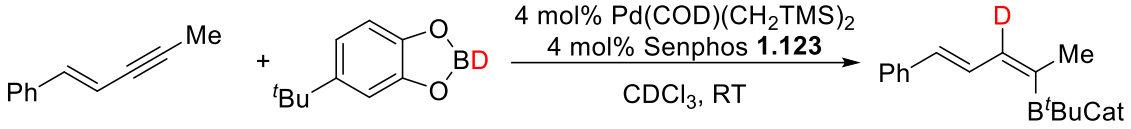

1.160 **1.169** **1.170**

Scheme 1.38. KIE experiment of the *trans*-hydroboration reaction.

The kinetic isotope effect of C–H bond is different from the B–H bond (Table 1.7).[83-86] In C–H bonds, a primary KIE results in a large value (3-7), and a secondary C–H KIE involving hybridization change from C_{sp3}–H to C_{sp2}–H results in a normal KIE value (1.1-1.5) due to a decrease in out-of-plane bending mode frequency (from 1350 cm^{-1} to 800 cm^{-1}).[63d] However, in B–H bonds, the primary B–H KIE has a small magnitude (usually less than 2),[83] due to either very early or very late transition states,[84] and a secondary B–H KIE involving hybridization change from B_{sp3}–H to B_{sp2}–H results in inverse KIE value

[82] According to ref. 81b, the rate constant equals to the linear fitting slope in Figure 1.7 bottom left corner divided by the catalyst concentration.

[83] (a) Wigfield, D. C.; Phelps, D. J. *Can. J. Chem*. **1972**, *50*, 388-394; (b) Hawthorne, M. F.; Lewis, E. S. *J. Am. Chem. Soc*. **1958**, *80*, 4296-4299.

[84] Leitao, E. M.; Stubbs, N. E.; Robertson, A. P.; Helten, H.; Cox, R. J.; Lloyd-Jones, G. C.; Manners, I. *J. Am. Chem. Soc*. **2012**, *134*, 16805-16816.

due to an increase in vibration frequency.[85,86] When a polyhydride boron species undergoes both a B–H bond break and a boron sp^3 to sp^2 hybridization change, the observed KIE value would be in the range around 1.0 (0.7-1.4).[85-85] Therefore, the 1.1 value we observed in *trans*-hydroboration KIE study is consistent with a B–H primary KIE plus an inverse secondary B–H KIE.

Table 1.7. Illustration of KIE differences between C–H bond and B–H bond.

effect	C–H	B–H
primary KIE	3-7	< 2
secondary KIE with hybridization change from sp^3 to sp^2	1.1-1.5	< 1

The obtained reaction orders and KIE value can help us distinguish between the inner-sphere and outer-sphere oxidative addition mechanisms. For inner-sphere oxidative addition mechanism, the zero order in enyne and first order in borane leaves the palladium oxidative insertion step to be the only possible RDS (complex **1.152** to **1.153**, Scheme 1.31) with Pd(0)L as the resting state, although the experimental KIE value is less consistent with a primary KIE value. For outer-sphere oxidative addition mechanism, the reaction orders leave two possibilities for the RDS: either the outer-sphere oxidative addition step (complex **1.156** to **1.157**, Scheme 1.32, with the resting state being the enyne bound Pd(0) complex **1.156**) or the hydride delivery step (complex **1.157** to **1.158**, or complex **1.157** to **1.159**, both with the resting state being the outer-sphere oxidative addition adduct **1.157**). However, the experimental KIE value suggests the RDS involves a boron hybridization

[85] (a) Davis, R. E.; Kibby, C. L.; Swain, C. G. *J. Am. Chem. Soc.* **1960**, *82*, 5950-5951; (b) Davis, R. E.; Bromles, E.; Kibby, C. L. *J. Am. Chem. Soc*. **1962**, *84*, 885-892; (c) Davis, R. E.; Kenson, R. E.; Kibby, C. L.; Lloyd, H. H. *Chem. Commun. (London)* **1965**, 593-595.

[86] Our collaboration with Prof. Miqueu in DFT calculation shows the B–H vibration frequencies are 2400 cm^{-1} for intermediate **1.157**, 2292 cm^{-1} and 2400 cm^{-1} for intermediate **1.158** and 2768 cm^{-1} for free catecholborane in outer-sphere oxidative addition mechanism.

change from sp^3 to sp^2 as well as a B–H bond breaking process, which is more consistent with the hydride delivery process (complex **1.158** to **1.159**). Overall, the kinetic study is more consistent with the outer-sphere oxidative addition mechanism with complex **1.157** as the resting state and its transformation to complex **1.159** to be the RDS.

1.3.4. Spectroscopic characterization of possible reaction intermediates

Monitoring a reaction by adding one reactant at a time rather than combining everything at once in one pot allows for the spectroscopic characterization of possible reaction intermediates. Senphos ligand **1.171** where its southern fragment is the *o*-dicyclohexylphoshinophenyl (PCy_2) group instead of an *o*-diphenylphoshinophenyl (PPh_2) group is used in this study (Scheme 1.39).[87]

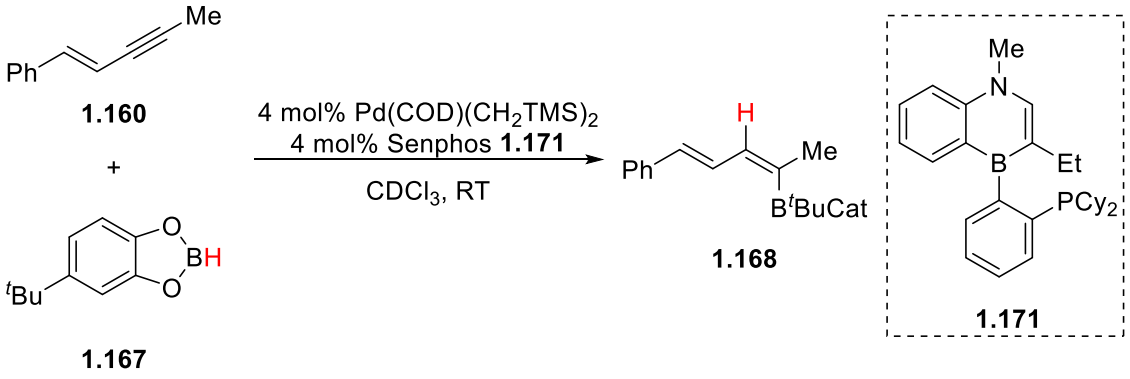

Scheme 1.39. Model reaction setup in spectroscopic characterization of possible reaction intermediates.

The reaction setup can be divided into three stages: Stage 1: complexation between 4.2 mol% Pd(0) and 4.2 mol% Senphos **1.171** in solvent $CDCl_3$; Stage 2: addition of 1.0 equiv. of enyne **1.160** into the solution obtained from Stage 1; and Stage 3: addition of 1.5

[87] Utilizing Senphos **1.171** as the ligand gave clean ^{31}P NMR signals, and the *trans*-hydroboration reaction catalyzed by Pd/Senphos **1.171** still provides good yield and diastereoselectivity.

equiv. catecholborane **1.167** into the solution obtained from Stage 2 to commence the *trans*-hydroboration reaction. Spectra of Stage 3 were collected when the reaction reached around 20% conversion.

Figure 1.9 shows the stacked ^{1}H spectra of the three stages. An efficient way to interpret the ^{1}H signals is by looking at the ligand's C(2) proton (abbreviated as H_a) signal, which is more downfield (> 8.5 ppm) due to its iminium character in Pd-bound complexes *vs*. in the free ligand (7.6 ppm). In Stage 1, as evidenced by the new H_a signal at 8.9 ppm, some of the ligand readily displaces the COD in the palladium precursor and induces the reductive elimination,[88,89] while some free ligand still floating around. In Stage 2, no free ligand can be observed, and the H_a exhibits exactly the same chemical shift as in Stage 1. This is consistent with no formation of a new complex, such as enyne bound Pd(0) complex **1.156** (Scheme 1.32) upon addition of the enyne. Adding HB^{t}BuCat **1.167** into the solution triggers the *trans*-hydroboration reaction, and the H_a signal of 8.9 ppm quickly disappears with the formation of two new sets of H_a signals appearing around 8.75 ppm, which persist throughout the reaction. These two signals disappear after the completion of reaction. Thus, we propose these two signals belong to the resting state species in the reaction mixture.

[88] (a) Pan, Y.; Young, G. B. *J. Organomet. Chem.* **1999**, *577*, 257-264; (b) Sergeev, A. G.; Schulz, T.; Torborg, C.; Spannenberg, A.; Neumann, H. *Angew. Chem. Int. Ed*. **2009**, *48*, 7595-7599; (c) Lee, H. G.; Milner, P. J.; Buchwald, S. L. *Org. Lett*. **2013**, *15*, 5602-5605; (d) Lee, H. G.; Milner, P. J.; Buchwald, S. L. *J. Am. Chem. Soc*. **2014**, *136*, 3792-3795; (e) Takahashi, R.; Kubota, K.; Ito, H. *Chem. Commun*. **2020**, *56*, 407-410.

[89] The reductive elimination product $TMSCH_2CH_2TMS$ is detected by ^{1}H NMR, which shows a 1:1 ratio to the Senphos iminium peak (8.9 ppm). For the product reference, see: Shtelman, A. V.; Becker, J. V. *J. Org. Chem.* **2011**, *76*, 4710-4714. See the Spectra Library for more information.

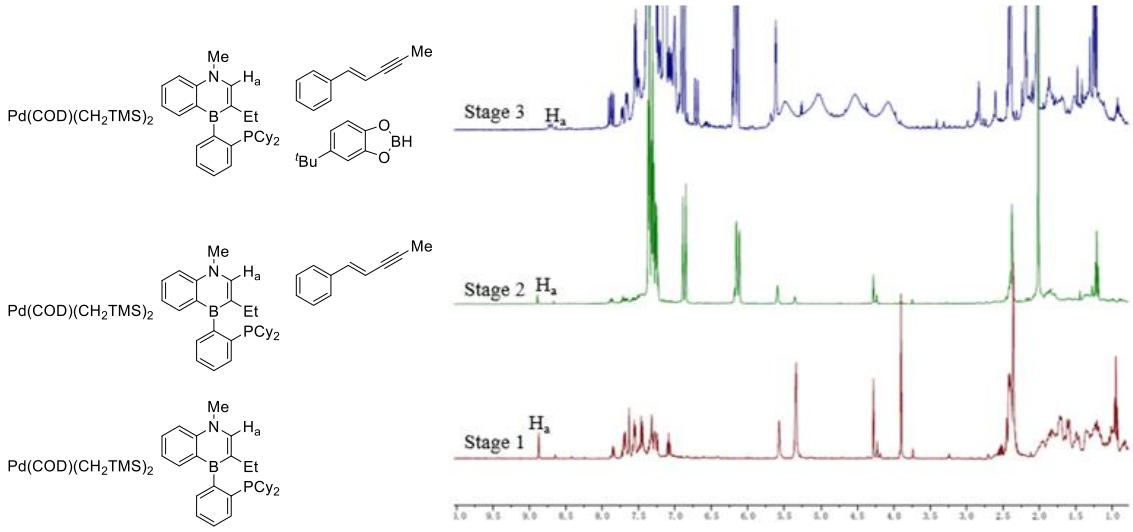

Figure 1.9. Stacked ^{1}H NMR in $CDCl_3$ from Stage 1 to Stage 3.

The stacked ^{31}P spectra of the three stages are shown in Figure 1.10. In Stage 1, some ligand coordinates to the palladium (39 ppm) while some free ligand can still be seen (–3 ppm). In Stage 2, enyne addition does not result in a change of the 39 ppm signal. And in Stage 3, a downfield shifted signal at 59 ppm was observed. A control experiment shows that a Senphos-bound Pd(II) complex **1.172** exhibits a ^{31}P NMR signal at 57 ppm (Scheme 1.40). Thus, we propose that the resting state signal is more consistent with a Senphos ligated Pd(II) species.

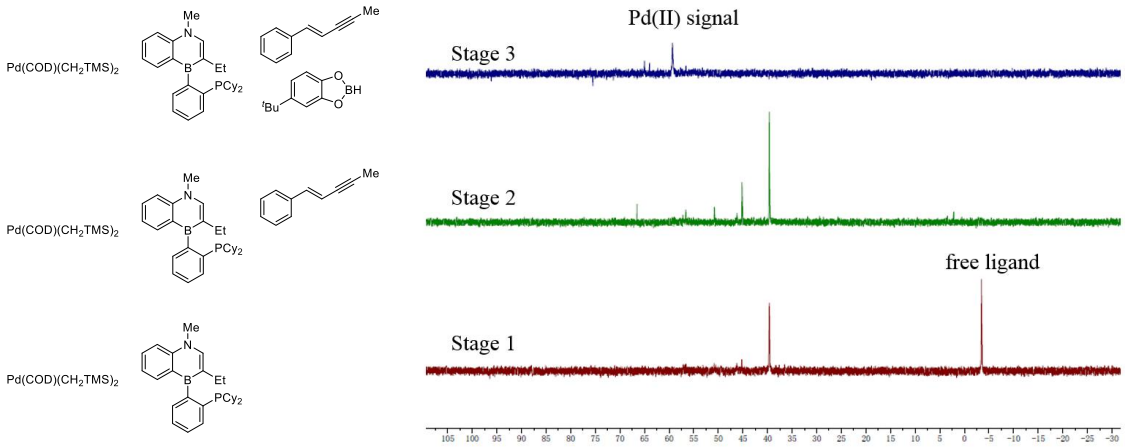

Figure 1.10. Stacked ^{31}P NMR in $CDCl_3$ from Stage 1 to Stage 3.

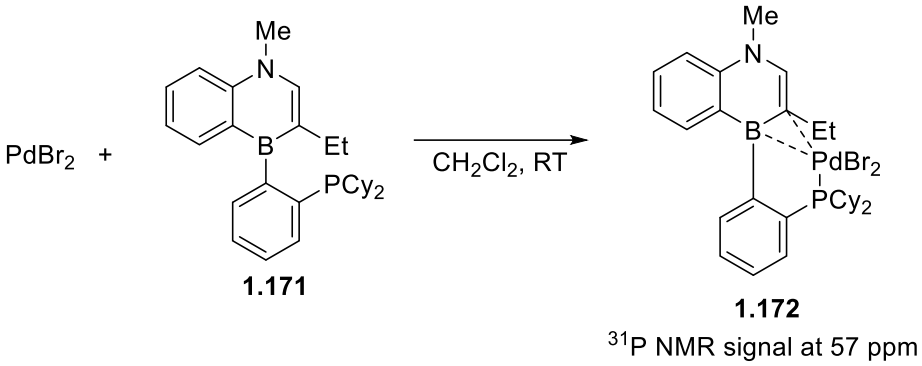

Scheme 1.40. Synthesis of Senphos **1.171** bound $PdBr_2$ complex **1.172**.

^{11}B NMR of the solution in Stage 3 is also collected. With the proton coupled technique, a doublet at –12.6 ppm (d, J = 170 Hz) was observed. This signal is consistent with a B–H containing intermediate.[90]

[90] Lu, Z.; Hausmann, H.; Becker, S.; Wegner, H. A. *J. Am. Chem. Soc.* **2015**, *137*, 5332-5335.

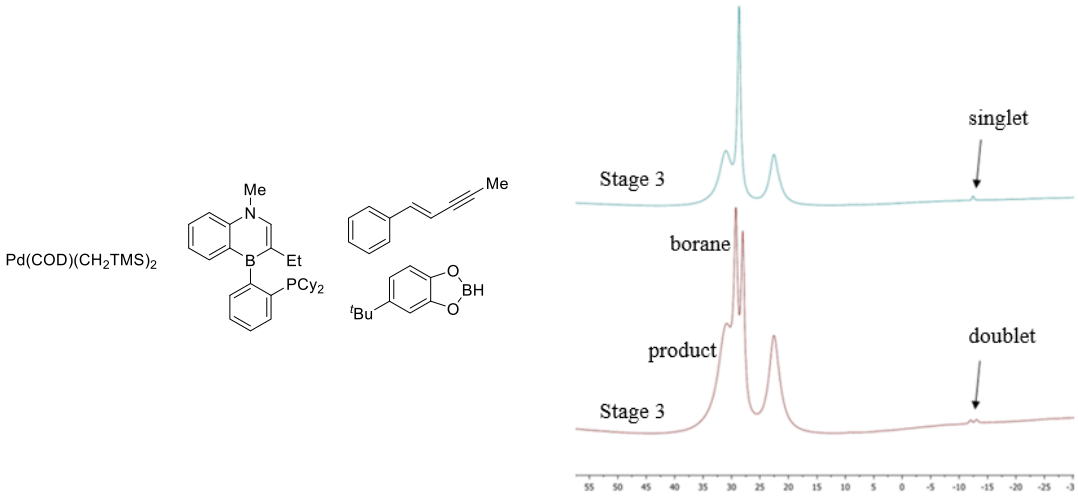

Figure 1.11. Proton coupled and decoupled ^{11}B NMR in $CDCl_3$ at Stage 3.

To further support the outer-sphere oxidative addition mechanism, we synthesized Pd(II)/Senphos **1.171**-enyne-BCF complex **1.173** (Scheme 1.41) following the pathway where BCF first activates the Pd(0)/Senphos **1.171** enyne complex (similar to complex **1.156**, Scheme 1.32) and then induces the oxidative addition process in an outer-sphere fashion. In $CDCl_3$, the H_a proton in complex **1.173** has a chemical shift of 8.75 ppm, which is in the same range as the observed H_a signals in Stage 3 (Figure 1.9) and is consistent with the assignment of the outer-sphere oxidative addition adduct (complex **1.157**, Scheme 1.32) as the resting state at stage 3. The bond connectivity in complex **1.173** is confirmed by the X-ray structure of a similar complex **1.174**.[91]

[91] Unpublished work from Ziyong Wang.

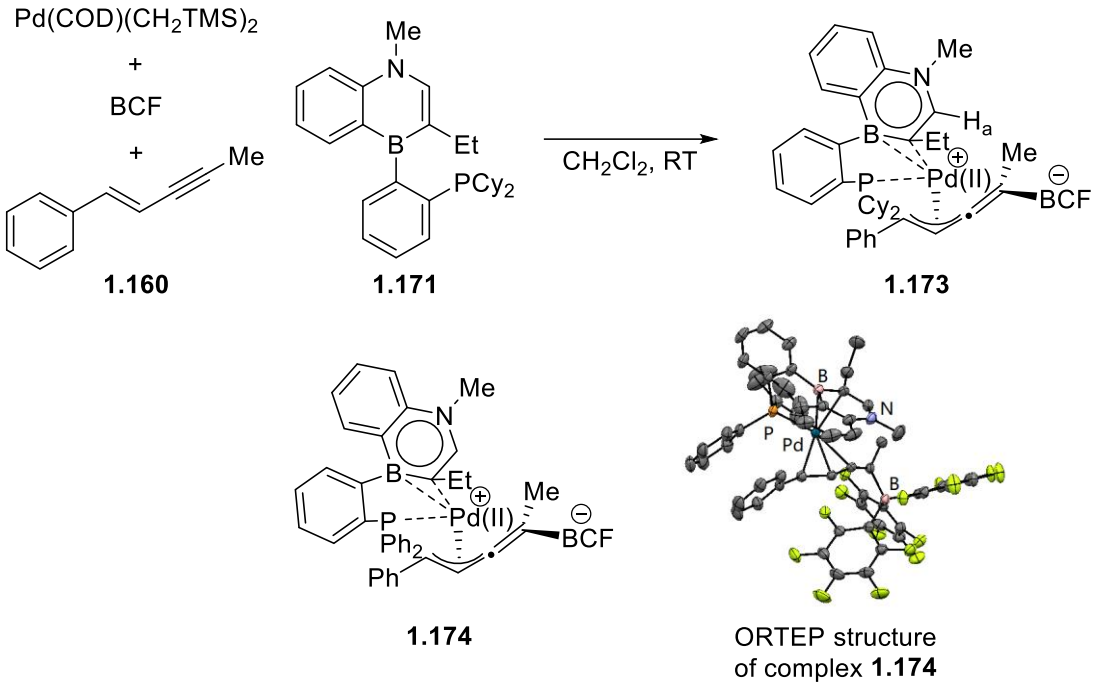

Scheme 1.41. Synthesis of LPd(II)-enyne-BCF complex.

In this section the resting state is observed as a Pd(II) species with a B–H moiety, which is consistent with intermediate **1.157** (Scheme 1.32) in the outer-sphere oxidative addition mechanism. This intermediate is further validated by the synthesis of analog complex **1.173**.

1.3.5. Conclusion

We investigated the mechanism of *trans*-hydroboration reaction encompassing double crossover experiment, kinetic studies and spectroscopic characterization of possible reaction intermediates, and all the observations are consistent with the outer-sphere oxidative addition mechanism. The reaction resting state is determined to be the outer-sphere oxidative addition product **1.157** (Scheme 1.32) and the RDS to be the hydride delivery step (complex **1.158** to **1.159**, Scheme 1.32).

1.4. Summary

Pd/Senphos complexes, which contain a unique κ^2-η^2-B,C coordination mode, are demonstrated as highly effective catalysts in *trans*-hydroboration reactions of both terminal and internal enynes. The reaction mechanism is consistent with an outer-sphere oxidative addition mechanism, and the corresponding resting state as well as the RDS are determined. These in-depth mechanistic underpinnings reveal critical reaction intermediates and point toward unexplored reaction manifolds that can be developed with Pd/Senphos catalytic system.

1.5. Experimental section

1.5.1. General information

^{1}H, ^{13}C, ^{31}P and ^{19}F spectra were recorded on Varian 400, 500 or 600 MHz spectrometers and ^{11}B spectra were on Inova 500 MHz spectrometers at ambient temperature. ^{1}H NMR spectra were reported with the solvent resonance as internal standard. ^{13}C NMR spectra were reported with the solvent resonance as internal standard. ^{11}B NMR spectra were reported with BF_3•Et_2O (δ 0 ppm) as externally reference. ^{31}P NMR spectra were reported with H_3PO_4 (δ 0 ppm) as externally reference. IR spectra were recorded on a Bruker FTIR Alpha (ATR mode) spectrometer. High-resolution mass spectroscopy data were obtained at the Mass Spectroscopy Facilities at Chemistry Department of Boston College with DART ion source in positive ion mode. Gas chromatography–mass spectrometry was performed using helium as carrier gas on an Agilent 7890B GC system instrument equipped with 19091S-433UI column and Agilent 5977B EI detector.

All oxygen- and moisture-sensitive manipulations were carried out under N_2 atmosphere with standard Schlenk techniques or in N_2 glovebox.

Solvents used under N_2 atmosphere (pentane, THF, benzene, Et_2O, MeCN and CH_2Cl_2) were purified by passing through a neutral alumina column under argon. Decalin was dried over CaH_2, distilled, subjected to three freeze-pump-thaw cycles, and stored in a Schlenk flask in a nitrogen glovebox. Commercially available HBCat was purified via distillation before using. All other chemicals and solvents were purchased and used as received.

1.5.2. Experimental procedures

1.5.2.1. Experiment for reaction condition re-optimization

General procedure for Table 1.4: To a 4-mL vial charged with enyne-**1.143** (0.100 mmol, 19.8 mg, 1.00 equiv.) and catalyst solution (Pd_2dba_3/Senphos **1.123**, 0.05 M in CH_2Cl_2, 0.08 mL, 0.004 mmol, 4 mol%) was put under high vacuum for 15 minutes, and then the indicated solvent (0.08 mL) was added along with indicated H-[B] **1.144-1.146**[92] (0.15 mmol, 1.5 equiv.) and hexamethylbenzene (internal standard, 3 mg). The resulting mixture was allowed to stir for 6 hours at room temperature. At the conclusion of the reaction, a pinacol solution (1.20 mmol, 142 mg, 12.0 equiv. in 0.5 mL CH_2Cl_2) was added and the new mixture was allowed to stir for another 12 hours. At the conclusion of reaction, the crude mixture was passed through a silica gel plug using hexanes/EtOAc (5/1) as the eluent, the yield and *trans:cis* ratio were obtained through ^{1}H NMR against the internal standard.

[92] (a) Uehara, K.; Wagner, C.; Vogler, T.; Luftmann, H.; Studer, A. *Angew. Chem. Int. Ed.* **2010**, *49*, 3073-3076; (b) Baban, J. A.; Goodchild, N. J.; Roberts, B. P. J. *Chem. Soc. Perkin Trans. 2*, **1986**, 157-161; (c) Chesnokov, S. A.; Cherkasov, V. K.; Abakumov, G. A.; Kurskii, Y. A.; Shurygina, M. P.; Mamysheva, O. N.; Shavyrin, A. S. *Russ. Chem. Bull.* **2003**, *52,* 718-724.

Entry 1: The general procedure was followed with HBCat (18 mg, 0.15 mmol, 1.5 equiv.). ^{1}H NMR analysis indicated the reaction yield is 60% with a *trans:cis* ratio of 65:35.

Entry 2: The general procedure was followed with 4-*t*butylcatecholborane **1.144** (27 mg, 0.15 mmol, 1.5 equiv.). ^{1}H NMR analysis indicated the reaction yield is 62% with a *trans:cis* ratio of 66:34.

Entry 3: The general procedure was followed with 3,5-di-*t*butylcatecholborane **1.145** (34 mg, 0.15 mmol, 1.5 equiv.) and the reaction time was prolonged to 14 hours. After adding pinacol solution, the resulting mixture was allowed to heat at 40 °C to facilitate the transesterification reaction. ^{1}H NMR analysis indicated the reaction yield is 65% with a *trans:cis* ratio of 86:14.

Entry 4: The general procedure was followed with 3,6-di-*t*butylcatecholborane **1.146** (34 mg, 0.15 mmol, 1.5 equiv.) and the reaction was allowed to heat at 40 °C for 12 hours. ^{1}H NMR analysis before adding the pinacol solution indicated no hydroboration reaction occurred.

Entry 5: The general procedure was followed with HBCat (18 mg, 0.15 mmol, 1.5 equiv.) and benzene (0.08 mL). ^{1}H NMR analysis indicated the reaction yield is 83% with a *trans:cis* ratio of 12:88.

Entry 6: The general procedure was followed with HBCat (18 mg, 0.15 mmol, 1.5 equiv.) and Et_2O (0.08 mL). ^{1}H NMR analysis indicated the reaction yield is 42% with a *trans:cis* ratio of 19:81.

Entry 7: The general procedure was followed with HBCat (18 mg, 0.15 mmol, 1.5 equiv.) and THF (0.08 mL). ^{1}H NMR analysis indicated the reaction yield is 90% with a *trans:cis* ratio of 21:79.

Entry 8: The general procedure was followed with HBCat (18 mg, 0.15 mmol, 1.5 equiv.) and MeCN (0.08 mL). ^{1}H NMR analysis indicated the reaction yield is 71% with a *trans:cis* ratio of 82:18.

Entry 9: The general procedure was followed with HBCat (18 mg, 0.15 mmol, 1.5 equiv.) and $(CH_2Cl)_2$ (0.08 mL). ^{1}H NMR analysis indicated the reaction yield is 88% with a *trans:cis* ratio of 65:35.

Entry 10: The general procedure was followed with HBCat (18 mg, 0.15 mmol, 1.5 equiv.) and $CHCl_3$ (0.08 mL). ^{1}H NMR analysis indicated the reaction yield is 82% with a *trans:cis* ratio of 82:18.

Entry 11: The general procedure was followed with HBCat (18 mg, 0.15 mmol, 1.5 equiv.) and $(CHCl_2)_2$ (0.08 mL). ^{1}H NMR analysis indicated the reaction yield is 86% with a *trans:cis* ratio of 97:3.

Syntheses of enynes in Table 1.5: Enyne-**1.147** to enyne-**1.149** and enyne-**1.151** were synthesized following the literature procedure.[93] Synthesis of enyne **1.143** and **1.150**: Under nitrogen $PdCl_2(PPh_3)_2$ (84 mg, 0.12 mmol, 0.030 equiv.) and CuI (38 mg, 0.20 mol, 0.050 equiv.) were placed in a 50-mL round bottom flask. To this flask ^{i}Pr$_2$NH (20 mL), *(E)*-styrenyl bromide (0.73 g, 4.0 mmol, 1.0 equiv.) and terminal alkyne (4.8 mmol, 1.2 equiv.) were added, respectively. The mixture was allowed to heat at 55 °C for 16 h. At the conclusion of reaction, Et_2O (15 mL) along with H_2O (15 mL) were added to the crude mixture, and the organic layer was separated. Additional Et_2O (10 mL) was used to

[93] (a) Mokar, B. D.; Liu, R. S. *Chem. Commun.* **2014**, *50*, 8966-8969; (b) Zhang, Y.; Li, B.; Liu, S.-Y. *Angew. Chem. Int. Ed.* **2020***, 59,* 15928-15932.

wash the aqueous layer. Then, the organic layers were combined, concentrated and further purified by silica gel chromatography using hexanes as the eluent to afford the enynes.

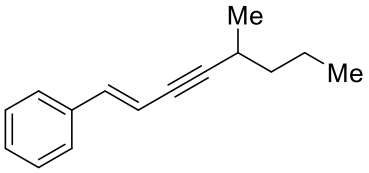

91% yield. NMR (500 MHz, $CDCl_3$) δ 7.36 (dd, J = 8.4, 1.4 Hz, 2H), 7.31 (dd, J = 8.4, 6.7 Hz, 2H), 7.29 – 7.21 (m, 1H), 6.87 (d, J = 16.2 Hz, 1H), 6.18 (dd, J = 16.3, 2.1 Hz, 1H), 2.69 – 2.50 (m, 1H), 1.58 – 1.38 (m, 4H), 1.22 (d, J = 6.8 Hz, 3H), 0.95 (t, J = 6.9 Hz, 3H); ^{13}C NMR (126 MHz, $CDCl_3$) δ 140.0, 136.8, 128.8, 128.3, 126.2, 109.1, 97.6, 80.0, 39.3, 26.7, 21.2, 20.8, 14.1; IR (ATR) 3059, 3027, 2959, 2929, 2915, 2870, 2217, 1490, 1448, 1376, 1333, 950, 745, 689, 597, 517 cm^{-1}; HRMS (DART) calcd for $C_{15}H_{19}$ ($[M+H]^+$) 199.14813, found 199.14843.

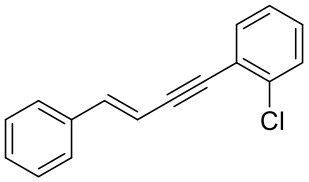

69% yield. ^{1}H NMR (500 MHz, $CDCl_3$) δ 7.54 – 7.49 (m, 1H), 7.46 – 7.40 (m, 3H), 7.38 – 7.34 (m, 2H), 7.33 – 7.28 (m, 1H), 7.26 – 7.20 (m, 2H), 7.11 (d, J = 16.3 Hz, 1H), 6.44 (d, J = 16.3 Hz, 1H); ^{13}C NMR (126 MHz, $CDCl_3$) δ 142.3, 136.3, 135.9, 133.4, 129.4, 129.3, 128.9, 128.9, 126.6, 126.6, 123.5, 107.9, 94.2, 88.5; IR (ATR) 3059, 3027, 2198, 1472, 1446, 1436, 1126, 1065, 1033, 949, 744, 688, 675, 512 cm^{-1}; HRMS (DART) calcd for $C_{16}H_{12}Cl$ ($[M+H]^+$) 239.06220, found 239.06237.

General procedure for Table 1.5: To a 4-mL vial charged with enyne (0.20 mmol, 1.0 equiv.) and catalyst solution (Pd_2dba_3/Senphos **1.123**, 0.050 M in CH_2Cl_2, 0.16 mL, 0.080 mmol, 4.0 mol%) was put under high vacuum for 15 minutes, then $(CHCl_2)_2$ (0.16 mL) was added along with HBCat (0.30 mmol, 36 mg, 1.5 equiv.). The resulting mixture was allowed to stir for 6 hours at room temperature. At the conclusion of reaction, a CH_2Cl_2 solution (1 mL) of pinacol (2.40 mmol, 283 mg, 12.0 equiv.) was added and the new

mixture was allowed to stir for another 12 hours. The crude mixture was then concentrated, and the resulting crude residue was purified by silica gel chromatography using hexanes/EtOAc (200/1 to 50/1 gradient) as the eluent to afford the desired *trans*-hydroboration products as solids.

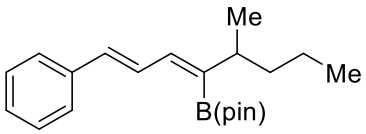

80% yield (run1: 77%, run2: 83%), 97:3. ^{1}H NMR (600 MHz, $CDCl_3$) δ 7.55 (ddd, *J* = 15.5, 11.0, 1.0 Hz, 1H), 7.41 – 7.37 (m, 2H), 7.34 – 7.29 (m, 2H), 7.23 – 7.18 (m, 1H), 6.68 (d, *J* = 11.0 Hz, 1H), 6.54 (d, *J* = 15.5 Hz, 1H), 2.38 (h, *J* = 7.0 Hz, 1H), 1.53 – 1.47 (m, 1H), 1.34 (d, *J* = 1.0 Hz, 12H), 1.32 – 1.23 (m, 3H), 1.09 (dd, *J* = 6.9, 1.0 Hz, 3H), 0.89 (td, *J* = 7.2, 1.0 Hz, 3H); ^{13}C NMR (151 MHz, $CDCl_3$) δ 141.8, 138.1, 133.4, 129.5, 128.7, 127.4, 126.6, 83.2, 40.6, 39.2, 25.1, 21.1, 20.9, 14.4 (*B*-alkenyl carbon signal was not observed); ^{11}B NMR (160 MHz, $CDCl_3$) δ 30.5; IR (ATR) 2975, 2931, 2872, 1076, 1473, 1451, 1372, 1329, 1142, 980, 851, 749, 696, 672 cm^{-1}; HRMS (DART) calcd for $C_{21}H_{32}BO_2$ ($[M+H]^+$) 327.24899, found 327.24832.

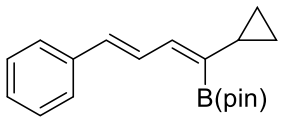

66% yield (run1: 69%, run2: 62%), 95:5. ^{1}H NMR (500 MHz, $CDCl_3$) δ 7.57 (dd, *J* = 15.5, 11.1 Hz, 1H), 7.41 – 7.36 (m, 2H), 7.31 (t, *J* = 7.8 Hz, 2H), 7.21 (td, *J* = 7.8, 1.3 Hz, 1H), 6.63 (d, *J* = 11.1 Hz, 1H), 6.51 (d, *J* = 15.5 Hz, 1H), 1.65 – 1.57 (m, 1H), 1.34 (s, 12H), 0.77 – 0.71 (m, 2H), 0.67 – 0.60 (m, 2H); ^{13}C NMR (126 MHz, $CDCl_3$) δ 140.7, 138.1, 133.0, 129.2, 128.7, 127.3, 126.6, 83.4, 25.1, 17.1, 8.0 (*B*-alkenyl carbon signal was not observed); ^{11}B NMR (160 MHz, $CDCl_3$) δ 30.0; IR (ATR) 2977, 2932, 1583, 1448, 1407, 1370, 1292, 1270, 1139, 1019, 964, 849, 808, 748, 690, 510 cm^{-1}; HRMS (DART) calcd for $C_{19}H_{26}BO_2$ ($[M+H]^+$) 297.20204, found 297.20198.

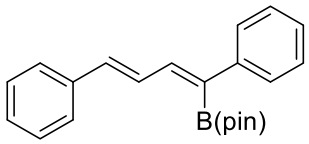

76% yield (run1: 78%, run2: 74%), 96:4. ^{1}H NMR (500 MHz, CD_2Cl_2) δ 7.72 (dd, *J* = 15.5, 11.2 Hz, 1H), 7.47 (dd, *J* = 8.0, 1.3 Hz, 2H), 7.41 (dd, *J* = 8.3, 1.3 Hz, 2H), 7.39 – 7.28 (m, 4H), 7.30 – 7.19 (m, 2H), 7.11 (d, *J* = 11.2 Hz, 1H), 6.75 (d, *J* = 15.5 Hz, 1H), 1.40 (s, 12H); ^{13}C MR (151 MHz, CD_2Cl_2) δ 145.5, 145.5, 143.7, 138.0, 136.7, 129.5, 129.2, 128.7, 128.4, 128.1, 127.2, 84.4, 25.3 (*B*-alkenyl carbon signal was not observed); ^{11}B NMR (160 MHz, CD_2Cl_2) δ 30.5; IR (ATR) 2976, 1492, 1389, 1308, 1295, 1247, 1206, 1138, 967, 852, 764, 690, 511 cm^{-1}; HRMS (DART) calcd for $C_{22}H_{26}BO_2$ ($[M+H]^+$) 333.20204, found 333.20184.

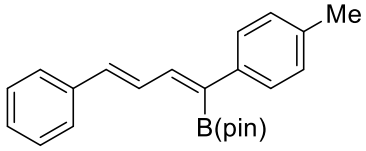

73% yield (run1: 78%, run2: 69%), 96:4. ^{1}H NMR (600 MHz, $CDCl_3$) δ 7.69 (dd, *J* = 15.5, 11.2 Hz, 1H), 7.45 (d, *J* = 7.2 Hz, 2H), 7.36 – 7.34 (m, 4H), 7.27 – 7.24 (m, 1H), 7.15 (d, *J* = 7.9 Hz, 2H), 7.12 (d, *J* = 11.2 Hz, 1H), 6.72 (d, *J* = 15.5 Hz, 1H), 2.36 (s, 3H), 1.41 (s, 12H); ^{13}C NMR (151 MHz, $CDCl_3$) δ 144.2, 140.2, 137.8, 136.5, 135.8, 129.2, 129.1, 128.8, 127.8, 127.4, 126.8, 83.8, 25.1, 21.3 (*B*-alkenyl carbon signal was not observed); ^{11}B NMR (160 MHz, $CDCl_3$) δ 30.7; IR (ATR) 2977, 2925, 1510, 1448, 1386, 1295, 1246, 1204, 1140, 969, 852, 816, 749, 691 cm^{-1}; HRMS (DART) calcd for $C_{23}H_{28}BO_2$ ($[M+H]^+$) 347.21769, found 347.21773.

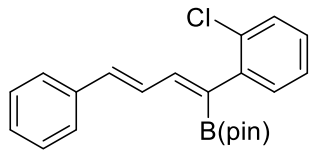

83% yield (run1: 85%, run2: 80%), >98:2. ^{1}H NMR (600 MHz, $CDCl_3$) δ 7.80 (dd, *J* = 15.5, 11.2 Hz, 1H), 7.51 – 7.42 (m, 2H), 7.38 – 7.35 (m, 3H), 7.30 (td, *J* = 7.6, 1.6 Hz, 2H), 7.29 – 7.23 (m, 1H), 7.20 (td, *J* = 7.6, 1.6 Hz, 1H), 6.91 (d, *J* = 11.2 Hz, 1H), 6.73 (d, *J* = 15.6 Hz, 1H), 1.39 (s, 12H); ^{13}C NMR (151 MHz, $CDCl_3$) δ 147.3, 143.1, 137.5, 137.0, 133.3, 130.0,

129.1, 128.8, 128.6, 128.1, 128.1, 127.1, 126.9, 83.9, 25.1(*B*-alkenyl carbon signal was not observed); ^{11}B NMR (160 MHz, $CDCl_3$) δ 29.8; IR (ATR) 2978, 2929, 1580, 1389, 1317, 1295, 1258, 1138, 1055, 1034, 968, 849, 801, 749, 734, 690, 670 cm^{-1}; HRMS (DART) calcd for $C_{22}H_{25}BO_2Cl$ ($[M+H]^+$) 367.16306, found 367.16441.

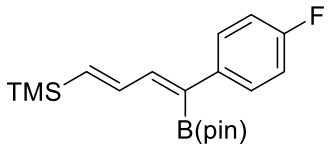

With 10 mol% catalyst loading. 77% yield (run1 72%, run2: 82%), 98:2. ^{1}H NMR (400 MHz, $CDCl_3$) δ 7.39 – 7.24 (m, 3H), 7.04 – 6.93 (m, 2H), 6.89 (d, *J* = 10.8 Hz, 1H), 6.10 (dd, *J* = 18.2, 0.9 Hz, 1H), 1.37 (s, 12H), 0.13 (s, 9H); ^{13}C NMR (101 MHz, $CDCl_3$) δ 162.2 (d, *J* = 245.7 Hz), 146.7 (d, *J* = 1.5 Hz), 143.4, 138.9, 138.7 (d, *J* = 3.3 Hz), 129.0 (d, *J* = 7.9 Hz), 115.2 (d, *J* = 21.3 Hz), 84.0, 25.1, –1.2 (*B*-alkenyl carbon signal was not observed); ^{11}B NMR (128 MHz, $CDCl_3$) δ 30.8; ^{19}F NMR (376 MHz, $CDCl_3$) δ –116.27 – –116.40 (m); IR (ATR) 2978, 2955, 1506, 1380, 1220, 1159, 1141, 1122, 968, 857, 835, 738, 726, 693, 580, 526 cm^{-1}; HRMS (DART) calcd for $C_{19}H_{29}BO_2FSi$ ($[M+H]^+$) 347.20084, found 347.20114.

1.5.2.2. Experimental procedure for double crossover experiment

Syntheses of boranes in Scheme 1.34:

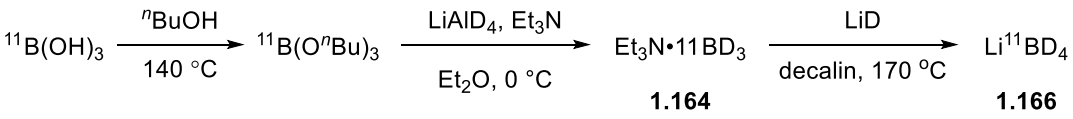

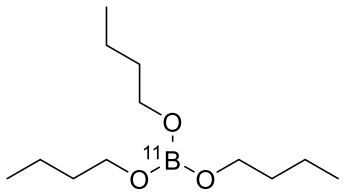

To a 100-mL round bottom flask charged with $^{11}B(OH)_3$ (1.86g, 30.0 mmol, 1.00 equiv.) was added 1-butanol (24 mL). And the resulting mixture was allowed to stir at 140 °C for 8 hours under nitrogen atmosphere. At the conclusion of reaction, all volatiles were removed under vacuum and $^{11}B(O^nBu)_3$ was obtained by distillation under

attenuated pressure (200 mTorr, 70 °C) as a colorless liquid (90% yield). ^{1}H NMR (500 MHz, $CDCl_3$) δ 3.77 (t, J = 6.6 Hz, 6H), 1.57 – 1.43 (m, 6H), 1.42 – 1.28 (m, 6H), 0.91 (t, J = 7.4 Hz, 9H); ^{13}C NMR (126 MHz, $CDCl_3$) δ 63.1, 33.9, 19.2, 14.0; ^{11}B NMR (160 MHz, $CDCl_3$) δ 18.2; IR (ATR) 2958, 2934, 2874, 1482, 1466, 1414, 1326, 1294, 1259, 1231, 1071, 1028, 664 cm^{-1}; HRMS (DART) calcd for $C_{12}H_{27}{}^{11}BO_3$ ([M+H]$^+$) 231.21260, found 231.21446.

$Et_3N\cdot{}^{11}BD_3$ To a 250-mL round bottom flask charged with $LiAlD_4$ (0.907g, 21.6 mmol, 0.800 equiv.), triethylamine (3.00 g, 29.7 mmol, 1.10 equiv.) and Et_2O (100 mL) was added $^{11}B(O^nBu)_3$ (6.2 g, 27 mmol, 1.0 equiv.) in a dropwise fashion during 20 minutes at 0 °C. After allowing the mixture to stir for additional 30 minutes at room temperature, the formed precipitate was filtered off, and the filtrate was concentrated. The desired product was afforded by distillation under attenuated pressure (200 mTorr, 50 °C) as a colorless liquid (83% yield). ^{1}H NMR (400 MHz, $CDCl_3$) δ 2.78 (q, J = 7.3 Hz, 6H), 1.19 (t, J = 7.3 Hz, 9H); ^{13}C NMR (126 MHz, $CDCl_3$) δ 52.4, 8.7; ^{11}B NMR (160 MHz, $CDCl_3$) δ –13.8; IR (ATR) 3001, 2979, 2945, 1775, 1720, 1658, 1460, 1390, 1381, 1188, 1167, 1095, 1043, 1021, 895, 769 cm^{-1}; HRMS (DART) calcd for $C_6H_{15}D_3BN$ ([M-D]$^+$) 116.1580, found 116.1586.

$Li^{11}BD_4$ To a 50-mL round bottom flask charged with $Et_3N\cdot{}^{11}BD_3$ (2.64 g, 22.4 mmol, 1.10 equiv.) and decalin (9 mL) was added and LiD (0.183 g, 20.3 mmol, 1.00 equiv.), and the resulting mixture was allowed to stir at 170 °C for 4 hours. At the conclusion of reaction, triethylamine was distillated off at 110 °C under nitrogen. Then, the precipitate was filtrated, washed with pentane (20 mL) and dried under high vacuum to

afford $Li^{11}BD_4$ as a white powder (72% yield). ^{11}B NMR (160 MHz, THF-d_8) δ –41.7; IR (ATR) 3433, 1716, 1632, 633, 537, 496 cm^{-1}.

Synthesis of isotopically labeled catecholboranes:

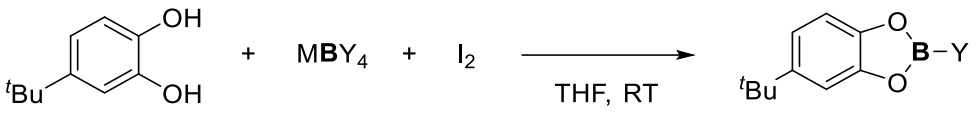

$MBY_4 = Na^{10}BH_4$ or $Li^{11}BD_4$

4-^{t}Bu-catechol (0.33 g, 2.0 mmol, 1.0 equiv.) along with THF (2 mL) were added into a 5-mL round bottom flask under nitrogen. Isotopically labeled diborane, which was generated via addition of a diglyme (3 mL) solution of iodine (0.64 g, 2.5 mmol, 1.25 equiv.) into a diglyme (5 mL) solution of metal borohydride $Na^{10}BH_4$ **1.165**[68] or $Li^{11}BD_4$ **1.166** (5 mmol, 2.5 equiv.) during a 4-hour period, was slowly passed through the catechol THF solution during 4 hours at room temperature. At the conclusion of reaction, all volatiles were then removed under vacuum and the isotopically labeled catecholborane was obtained by distillation under attenuated pressure (300 mTorr, 30 °C) as a colorless liquid.

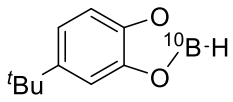

57% yield. ^1H NMR (600 MHz, CD_2Cl_2) δ 7.34 (d, J = 1.9 Hz, 1H), 7.25 – 7.10 (m, 2H), 4.68 (m, br, 1H), 1.32 (d, J = 0.9 Hz, 9H); ^{13}C NMR (151 MHz, CD_2Cl_2) δ 147.9, 147.6, 145.6, 120.5, 112.1, 110.5, 35.3, 32.0; ^{11}B NMR (160 MHz, CD_2Cl_2) δ 28.3 (d, J = 187.9 Hz); IR (ATR) 2963, 2908, 2870, 2673, 2602, 1487, 1429, 1307, 1255, 1225, 1155, 877, 824, 812, 653 cm^{-1}; HRMS (DART) calcd for ($[M+H]^+$)176.10451, found 176.07519.

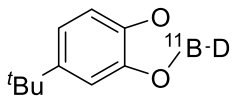

34% yield. ^1H NMR (600 MHz, CD_2Cl_2) δ 7.34 (d, J = 1.8 Hz, 1H), 7.22 – 7.13 (m, 2H), 1.32 (s, 9H); ^{13}C NMR (151 MHz, CD_2Cl_2) δ 147.9, 147.6, 145.6, 120.5, 112.1, 110.5, 35.3, 32.0; ^{11}B NMR (160 MHz, CD_2Cl_2) δ 28.3;

IR (ATR) 2962, 2908, 2870, 2010, 1989, 1975, 1487, 1427, 1268, 1245, 1223, 1152, 1092, 833, 812, 734, 652 cm^{-1}; HRMS (ESI) calcd for ($[M]^+$) 177.10714, found 177.07144.

Procedure for background experiment via ^{11}B NMR in Table 1.6: To a screw cap NMR tube charged with catalyst solution (Pd_2dba_3/Senphos **1.123**, 0.05 M in CH_2Cl_2, 0.01 mL, 0.0005 mmol) was added CH_2Cl_2 (0.4 mL). Then, the two isotopically labeled boranes **1.161** and **1.162** (5 mg each, 0.057 mmol total) were added simultaneously, and the scrambling reaction was monitored by proton coupled ^{11}B NMR, taking the advantage of the broad singlet signal of ^{11}B–D containing compound compared to its ^{11}B–H analog (doublet signal).[94] The representative traces were collected at time zero, 63 s, 162 s, 261 s and 90 min, respectively. As can be seen from Figure 1.12, the scrambling is complete around 261 s after mixing.

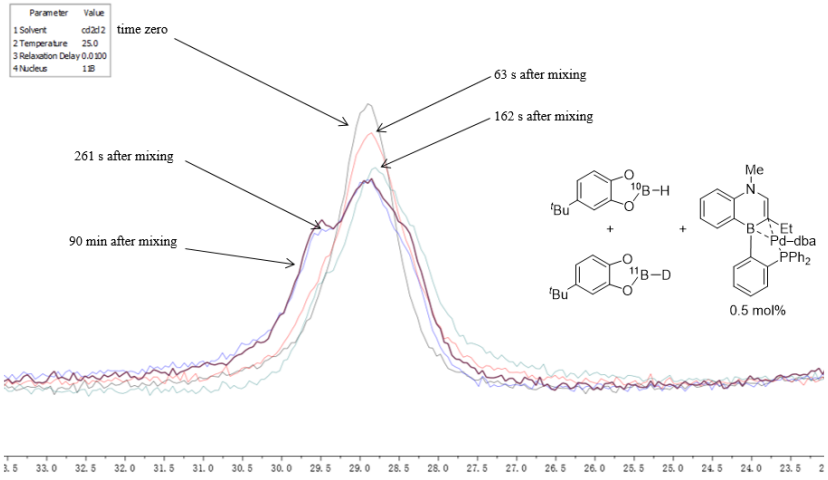

Figure 1.12. Background scrambling of 4-tbutylcatecholboranes in the presence of Pd(0)/Senphos complex via ^{11}B NMR**.**

[94] In boron NMR spectroscopy, though both boron nuclei (^{10}B and ^{11}B) are NMR active, ^{11}B has a higher sensitivity due to its higher natural abundancy and lower quadrupole moment than ^{10}B. Besides, compounds containing ^{11}B–D moiety usually show a singlet signal in coupled ^{11}B-NMR due to the large relaxation rate of ^{11}B and D, see: Eaton, G. R. *J. Chem. Educ.* **1969**, *46*, 547-556.

Procedure for experiment in Table 1.6: To a 4-mL vial charged with catalyst solution (Pd_2dba_3/Senphos **1.123**, 0.05 M in CH_2Cl_2, 0.01 mL, 0.0005 mmol) was added enyne **1.160** (71.0 mg, 1.00 mmol) and CH_2Cl_2 (0.4 mL). Then, the indicated isotopically labeled boranes **1.161** and **1.162** were added simultaneously. The new mixture was allowed to stir for 120 s, and quenched by a CH_2Cl_2 (0.5 m) solution of pinacol (120 mg, 1.00 mmol) and Et3N (50 mg, 0.50 mmol). After allowing the new mixture to stir for 4 hours at room temperature, all volatiles were removed under vacuum and the residue was analyzed by GC-MS after passing through a silica gel plug using hexanes/EtOAc (5/1) as the eluent. In the GC-MS trace, the *trans*-product has a retention time of 12.9 min, the *cis*-product has a retention time of 13.5 min and the allene has a retention time of 13.0 min. The ratios of mass 269, 270 and 271 in *trans*-product and *cis*-product were extracted by the ion extraction method and calculated by their integrals (labeled at the top of peak, bold).

Condition 1: Boranes **1.161** and **1.162** (5.0 mg, 0.057 mmol in total) were added to the mixture simultaneously. GC-MS trace showed the mass distribution of 269, 270 and 271 in *trans*-product is 1.0:1.9:1.1 and the distribution in *cis*-product is 1.0:0.5:0.8 (Figure 1.13).

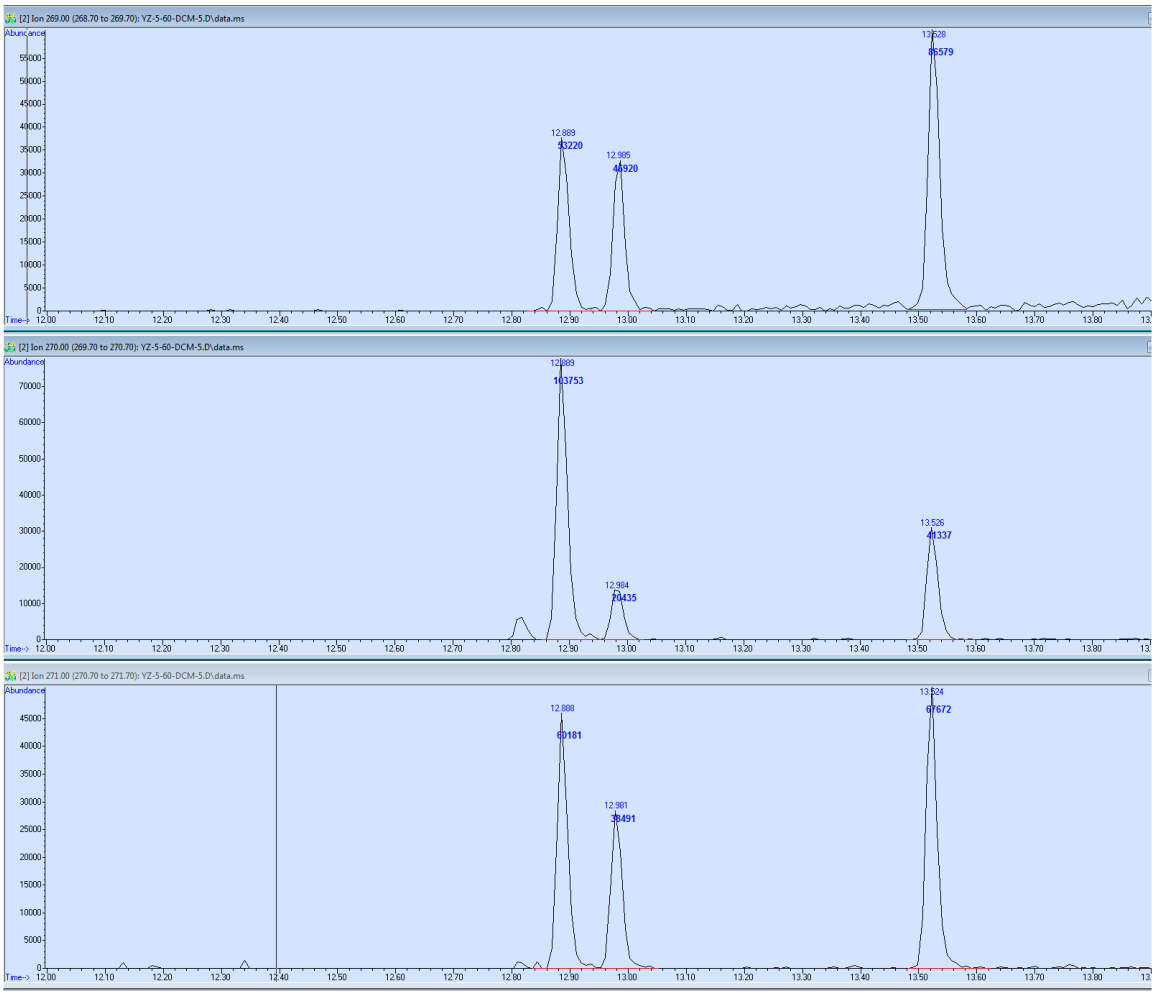

Figure 1.13. GC-MS traces of mass distribution of ion 269, 270 and 271 of *trans*- and *cis*-product in reaction condition 1.

Condition 2: Boranes **1.161** and **1.162** (10 mg, 0.11 mmol in total) were added to the mixture simultaneously. GC-MS trace showed the mass distribution of 269, 270 and 271 in *trans*-product is 1.0:2.0:1.2 and the distribution in *cis*-product is 1.0:1.0:1.0 (Figure 1.14).

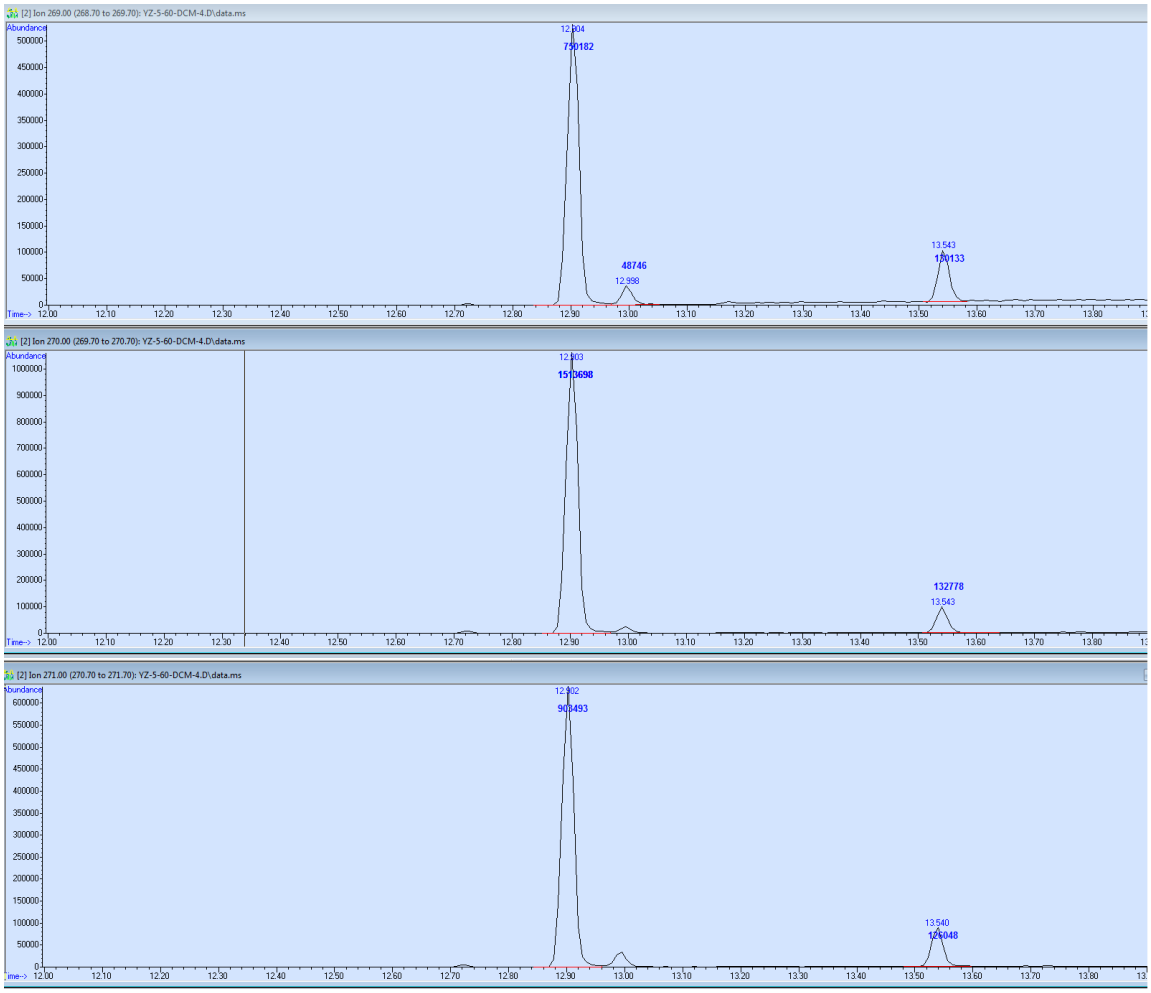

Figure 1.14. GC-MS traces of mass distribution of ion 269, 270 and 271 of *trans*- and *cis*-product in reaction condition 2.

Control: Boranes **1.161** and **1.162** (5 mg, 0.057 mmol in total) were pre-mixed together in neat for 4 hours at room temperature, and then they were added to the mixture together. GC-MS trace showed the mass distribution of 269, 270 and 271 in *trans*-product is 1.0:1.7:1.0 and the distribution in *cis*-product is 1.0:2.0:1.2 (Figure 1.15).

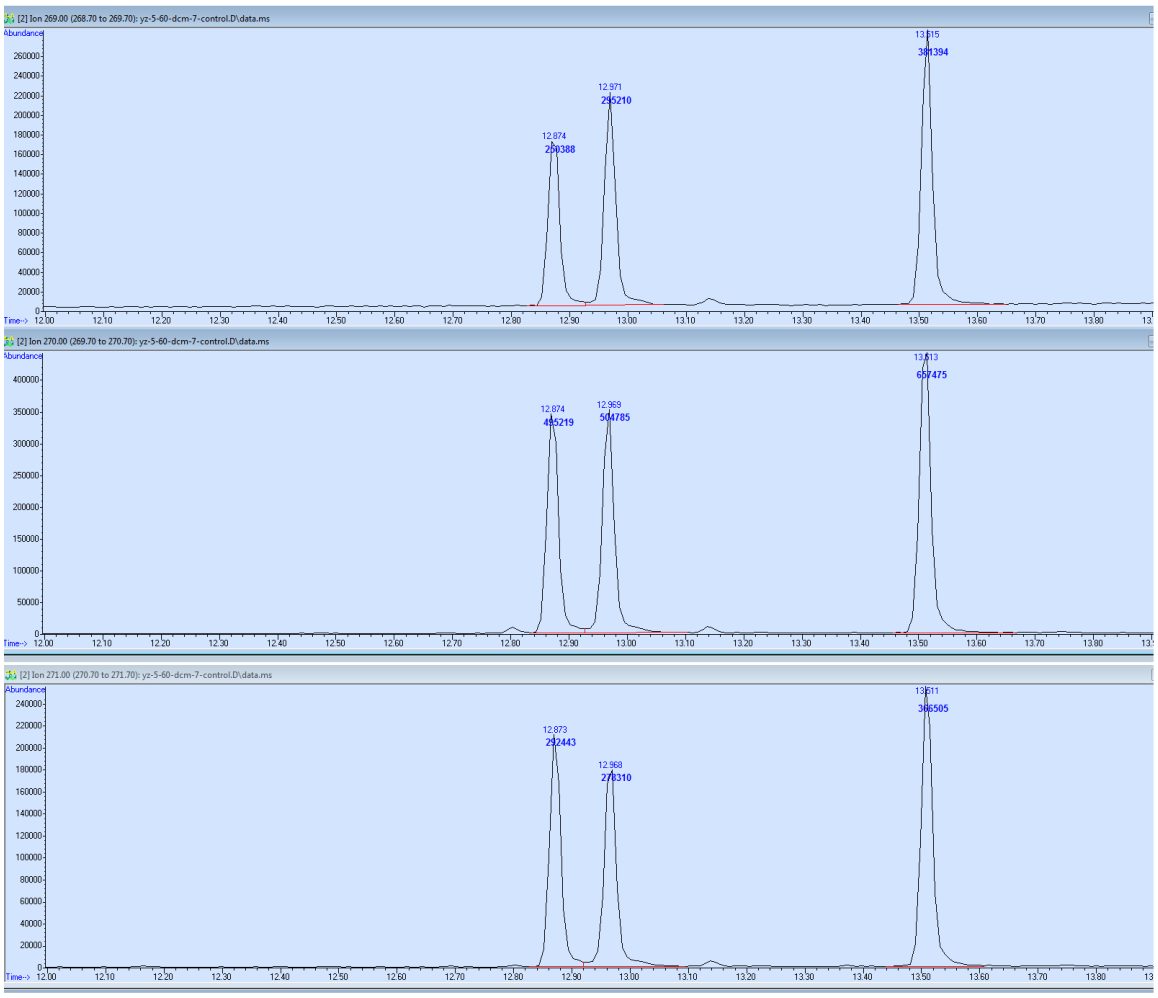

Figure 1.15. GC-MS traces of mass distribution of ion 269, 270 and 271 of *trans*- and *cis*-product in reaction control experiment.

1.5.2.3. Theory for Burés' variable time normalization analysis

The conclusions are excerpted from ref. 81b. For a catalyzed reaction between A and B (eq. 1), the formation of P in the differential form is expressed as eq. 2 (k is the a constant).

$$\mathrm{A} + \mathrm{B} \xrightarrow{\text{catalyst}} P \quad (\text{eq. } 1)$$

$$\mathrm{d}P = k[\mathrm{A}]^{\alpha}[\mathrm{B}]^{\beta}\,\mathrm{d}t \quad (\text{eq. } 2)$$

When plotting P *vs.* t, the slope at any given time is $k[\mathrm{A}]_t^{\alpha}[\mathrm{B}]_t^{\beta}$. In different excess experiment where $[\mathrm{A}]_0$ remains the same and $[\mathrm{B}]_0$ is different, the corresponding P-t traces will not overlay with each other since all slopes are different. However, if the horizontal axis can be manipulated to f(t), where it accounts for the concentration changing in [B] (eq.3), analyzing the previous data sets in terms of the P-f(t) plots will result in the overlay of all traces if the correct β value is applied, since now at any given time, the slope is only a function of $[\mathrm{A}]^{\alpha}$ (eq.4). The manipulated horizontal axis f(t) can be conveniently calculated as the sum of a series of trapezoid areas shown in eq.5.

$$f(t) = \int_0^{t_n} [\mathrm{B}]^{\beta}\,\mathrm{d}t \quad (\mathrm{eq.}\,3)$$

$$\mathrm{d}P = k[\mathrm{A}]^{\alpha}\mathrm{d}f(t) \quad (\mathrm{eq.}\,4)$$

$$\mathrm{f}(\mathrm{t}_n) = \sum_{\mathrm{i}=1}^{n}\left(\frac{[\mathrm{B}]_\mathrm{i}+[\mathrm{B}]_{\mathrm{i}-1}}{2}\right)^{\beta}(\mathrm{t}_\mathrm{i} - \mathrm{t}_{\mathrm{i}-1}) \quad (\mathrm{eq.}\,5)$$

1.5.2.4. Experimental procedure for investigation of reaction kinetic profile

General procedure: To a screw-cap NMR tube charged with $Pd(COD)(CH_2TMS)_2$ (4.6 mg, 12 μmol, 4.2 mol%), Senphos **1.123** (5.2 mg, 12 μmol, 4.2 mol%), trimethoxybenzene (internal standard, 10 mg) was added $CDCl_3$ (0.50 mL). And the resulting mixture was allowed to sit for 15 minutes, and then enyne **1.160** (41 mg, 0.29 mmol, 1.0 equiv.) was added. After allowing to sit for another 5 minutes, ^{t}Bu-catecholborane **1.167** (83 mg, 0.47 mmol, 1.6 equiv.) was added to start the reaction, which was close monitored by ^{1}H NMR and processed according to ref. 81b.

For Figure 1.5: One additional set of experiment with enyne **1.160** (28 mg, 0.20 mmol, 1.0 equiv.) and ^{t}Bu-catecholborane **1.167** (67 mg, 0.38 mmol, 1.9 equiv.) was done and processed according to ref 78.

For Figure 1.6: Two additional sets of experiment with enyne **1.160** (21 mg, 0.15 mmol, 1.0 equiv.) and enyne **1.160** (28 mg, 0.20 mmol, 1.0 equiv.) were done, respectively.

For Figure 1.7: Two additional sets of experiment with ^{t}Bu-catecholborane **1.167** (114 mg, 0.648 mmol, 2.24 equiv.) and ^{t}Bu-catecholborane **1.167** (150 mg, 0.852 mmol, 2.93 equiv.) were done, respectively.

For Figure 1.8: One additional set of experiments with $Pd(COD)(CH_2TMS)_2$ (2.3 mg, 6 μmol, 2.1 mol%), Senphos **1.123** (26 mg, 6.00 μmol, 2.1 mol%) was done.

For Scheme 1.38: One additional set of experiments with *B*–D-^{t}Bu-catecholborane **1.169** [95] (83 mg, 0.47 mmol, 1.6 equiv.) was done. K_{obs} data for reactions in Scheme 1.37 and Scheme 1.38 were obtained after linear fitting, according to ref. 81b.

$k_H = \overline{slope}/[\text{catalyst}] = [(3.73+3.42+3.46) * 10^{-4}/3/0.024] * 60 = 0.90 \pm 0.042\ M^{-1}\cdot min^{-1}$

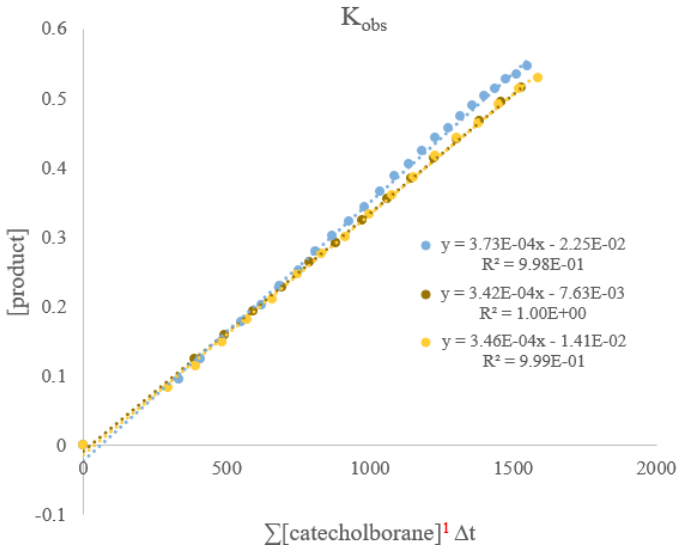

[95] Lantero, D. R.; Ward, D. L.; Smith, M. R. *J. Am. Chem. Soc.* **1997**, *119*, 9699-9708.

Figure 1.16. Linear fitting for data in Scheme 1.37 with variable time normalization analysis.

$$k_D = \overline{slope}/[\text{catalyst}] = [(3.08+3.28) *10^{-4}/2/0.024] *60 = 0.79 \pm 0.016\ M^{-1}\cdot min^{-1}$$

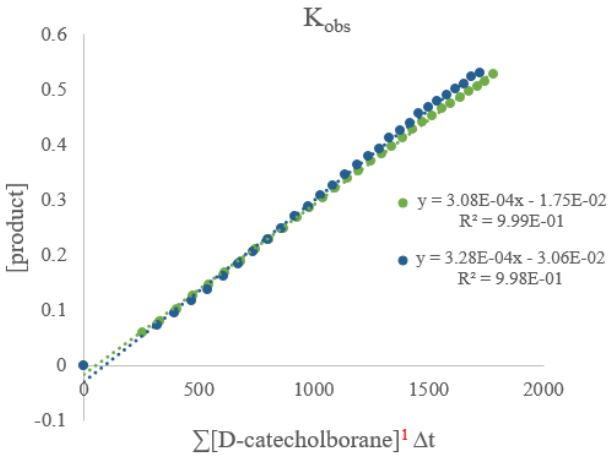

Figure 1.17. Linear fitting for data in Scheme 1.38 with variable time normalization analysis.

1.5.2.5. Experimental data for spectroscopic characterization of possible reaction intermediates

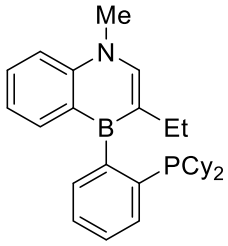

Synthesis of Senphos **1.171** : To a 100-mL round bottom flask charged with 2-bromophenyl dicyclohexylphosphine (706 mg, 2.00 mmol, 1.00 equiv.) and Et_2O (15 mL) was added *n*butyl lithium (0.80 mL, 2.5 M in hexanes, 2.0 mmol, 1.0 equiv.) at –78 °C. After allowing the mixture to stir at –78 °C for an hour, 1,4-azaborine **1.36**-Et (411 mg, 2.0 mmol, 1.0 equiv.) in THF (3 mL) was added, and the resulting mixture was allowed to warm to room temperature in 2 hours. At the conclusion of reaction, all volatiles were removed under vacuum, and the crude residue was purified by silica gel chromatography under nitrogen using pentane/Et_2O (20/1 to 10/1 gradient) as the eluent to afford ligand **1.171** as a white

solid (36% yield). ^{1}H NMR (500 MHz, $CDCl_3$) δ 7.71 (dd, *J* = 7.8, 1.7 Hz, 1H), 7.65 (s,1H), 7.62 – 7.54 (m, 2H), 7.47 (d, *J* = 8.6 Hz, 1H), 7.39 – 7.29 (m, 2H), 7.29 (dd, *J* =5.5, 3.2 Hz, 1H), 7.11 (t, *J* = 7.3 Hz, 1H), 3.92 (s, 3H), 2.55 (dq, *J* = 14.8, 7.5 Hz, 1H), 2.35 (dq, *J* = 14.7, 7.5 Hz, 1H), 2.08 – 1.94 (m, 1H), 1.79 – 0.79 (m, 24H); ^{13}C NMR (101 MHz, $CDCl_3$) δ 146.0, 143.2, 137.6, 137.2 (d, *J* = 11.0 Hz), 132.2 (d, *J* = 15.4 Hz), 131.7 (d, *J* = 2.5 Hz), 130.5, 127.3, 125.6, 120.1, 114.3, 42.1, 35.3 (d, *J* = 13.8 Hz), 33.5 (d, *J* = 12.3 Hz), 30.7 (d, *J* = 14.0 Hz), 30.3 (d, *J* = 15.9 Hz), 30.0 (d, *J* = 11.3Hz), 29.1 (d, *J* = 5.7 Hz), 27.7, 27.6 (d, *J* = 1.5 Hz), 27.6 (d, *J* = 3.7 Hz), 27.5 (d, *J* = 8.6 Hz), 26.8, 26.6 (d, *J* = 4.3 Hz), 26.6, 16.5 (three signals of aromatic carbons attached to boron are not observed); ^{11}B NMR(160 MHz, $CDCl_3$) δ 47.1; ^{31}P NMR (202 MHz, $CDCl_3$) δ –3.6; IR (ATR) 3040, 2924, 2850, 1604, 1585, 1491, 1448, 1375, 1266, 1223, 1105, 912, 764, 750, 733, 663 cm^{-1}; HRMS (DART) calcd for $C_{29}H_{40}BNP([M+H]^+)$ 444.29859, found 444.29726.

Reaction setup for Stage 1, 2 and 3: Stage 1: To a screw-cap NMR tube charged with $Pd(COD)(CH_2TMS)_2$ (4.6 mg, 12 μmol, 4.2 mol%), Senphos **1.171** (5.3 mg, 12 μmol, 4.2 mol%), was added $CDCl_3$ (0.50 mL). The resulting mixture was allowed to sit for 15 minutes. Stage 2: Enyne **1.160** (41 mg, 0.29 mmol, 1.0 equiv.) was added to the solution from Stage 1, and the resulting mixture was allowed to sit for 30 minutes. Stage 3: *t*Bu-catecholborane **1.167** (83 mg, 0.47 mmol, 1.6 equiv.) was added to the solution from Stage 2 to start the reaction.

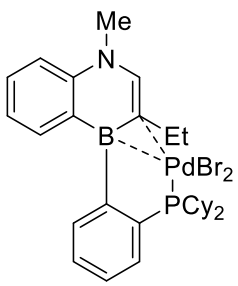

Synthesis of complex **1.172**: To a 4-mL vial charged with $PdBr_2$ (3.0 mg, 0.011 mmol, 1.1 equiv.) was added Senphos **1.171** (4.4 mg, 0.010 mmol, 1.0 equiv.) and CH_2Cl_2 (1.0 mL). After allowing the mixture to stir for 14 hours, the resulting red solution was filtered and

the filtrate was concentrated to provide the complex. 95% yield. ^{1}H NMR (400 MHz, $CDCl_3$) δ 9.46 (s, 1H), 8.01 (d, *J* = 7.6 Hz, 1H), 7.74 – 7.65 (m, 2H), 7.56 – 7.40 (m, 4H), 7.26 (d, *J* = 7.6 Hz, 1H), 4.20 (s, 3H), 3.32 – 3.15 (m, 1H), 2.57 – 2.26 (m, 2H), 2.11 – 0.74 (m, 21H), 0.64 (t, *J* = 7.4 Hz, 3H); ^{13}C NMR (101 MHz, $CDCl_3$) δ 182.8, 140.5, 136.8, 133.8 (d, *J* = 41.2 Hz), 132.5 (d, *J* = 19.7 Hz), 131.5, 131.1 (d, *J* = 2.6 Hz), 130.5, 127.3 (d, *J* = 6.9 Hz), 126.3, 117.5, 45.4, 38.3 (d, *J* = 31.3 Hz), 37.8 (d, *J* = 25.7 Hz), 30.4, 29.7, 28.6 (d, *J* = 7.1 Hz), 27.7 (d, *J* = 13.4 Hz), 27.5 (d, *J* = 11.0 Hz), 27.0, 26.9, 26.8 (d, *J* = 2.6 Hz), 26.7, 26.2, 25.9 (d, *J* = 1.7 Hz), 18.7 (three signals of aromatic carbons attached to boron are not observed); ^{11}B NMR (160 MHz, $CDCl_3$) δ 36.7; ^{31}P NMR (162 MHz, $CDCl_3$) δ 57.5; IR (ATR) 2929, 2852, 2223, 1591, 1535, 1487, 1449, 1349, 1245, 1205, 1126, 1113, 911, 767, 730, 635 cm^{-1}; HRMS (DART) calcd for $C_{29}H_{40}BNPPdBr_2$ ($[M+H]^+$) 710.03, not found.

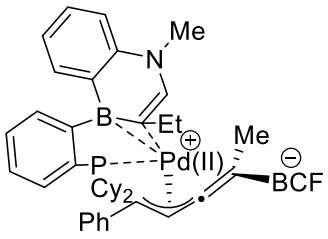

Synthesis of complex **1.173**: To a 4-mL vial charged with Pd(COD)($CH_2TMS)_2$ (11.7 mg, 30.0 μmol, 1.00 equiv.) and Senphos **1.171** (13.2 mg, 30.0 μmol, 1.00 equiv.) in CH_2Cl_2 (0.5 mL) was added enyne **1.160** (8.5 mg, 60 μmol, 2.0 equiv.). The resulting mixture was allowed to stir for an hour at room temperature. Then, BCF (15.4 mg, 30.0 μmol, 1.00 equiv.) was added to the previous solution and the new mixture was allowed to stir for 30 minutes. At the conclusion of reaction, pentane (2 mL) was carefully added by the vial wall and the titled compound was obtained after recrystallization at –30 °C under N_2 atomsphere. ^{11}B NMR (160 MHz, $CDCl_3$) δ 39.3, –12.0; ^{31}P NMR (243 MHz, $CDCl_3$) δ 39.1; ^{19}F NMR (564 MHz, $CDCl_3$) δ –161.09 (t, *J* = 20.1 Hz), –165.03 (s), –165.64 (s).

1.5.3. NMR Spectra of New Compounds

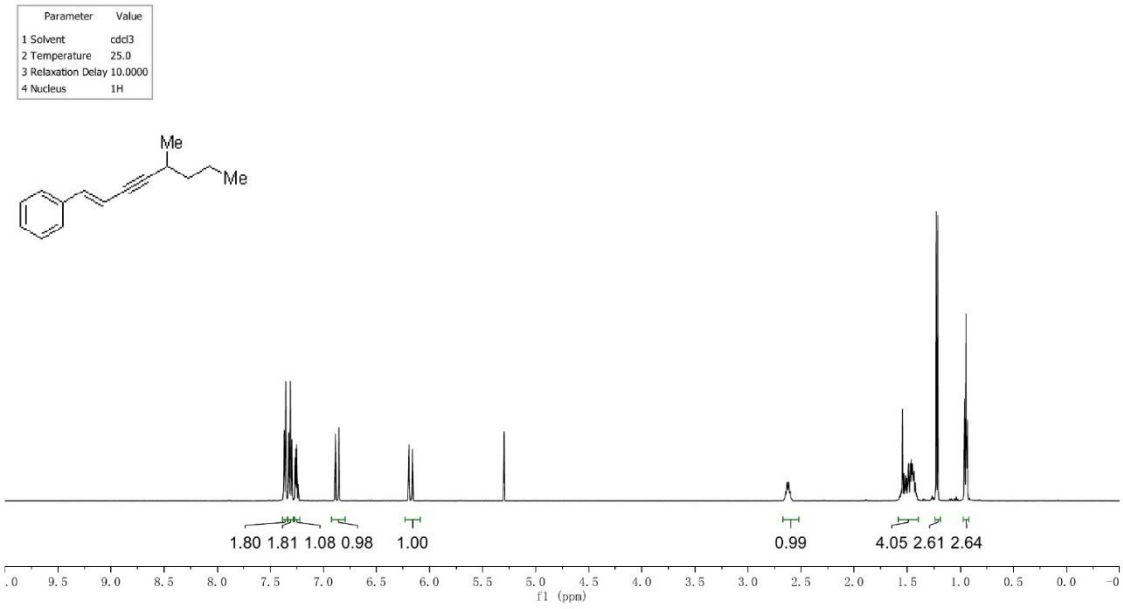

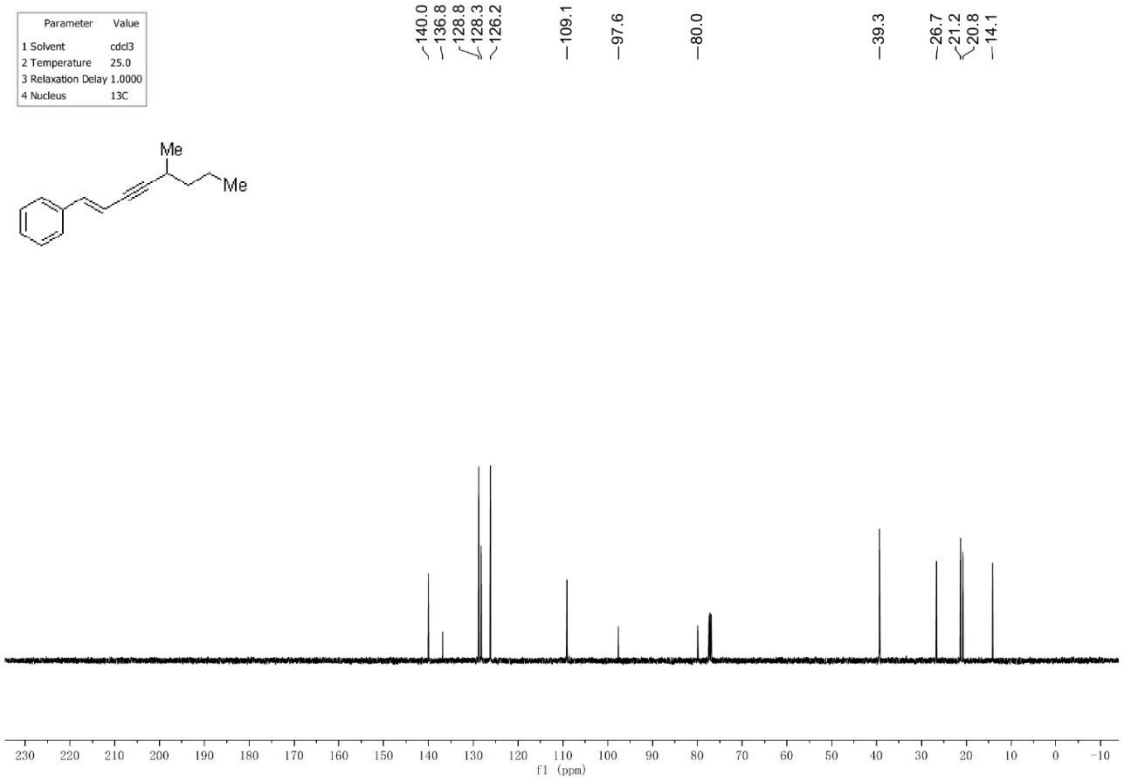

Parameter	Value
1 Solvent	cdcl3
2 Temperature	25.0
3 Relaxation Delay	10.0000
4 Nucleus	1H

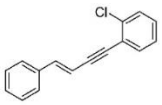

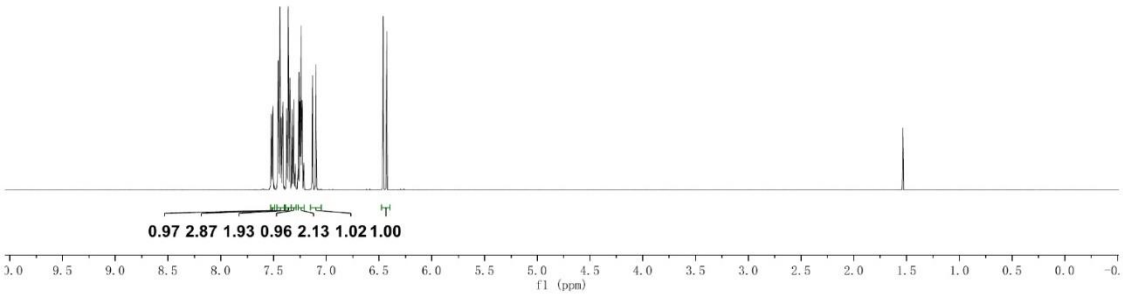

Parameter	Value
1 Solvent	cdcl3
2 Temperature	25.0
3 Relaxation Delay	1.0000
4 Nucleus	13C

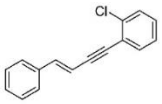

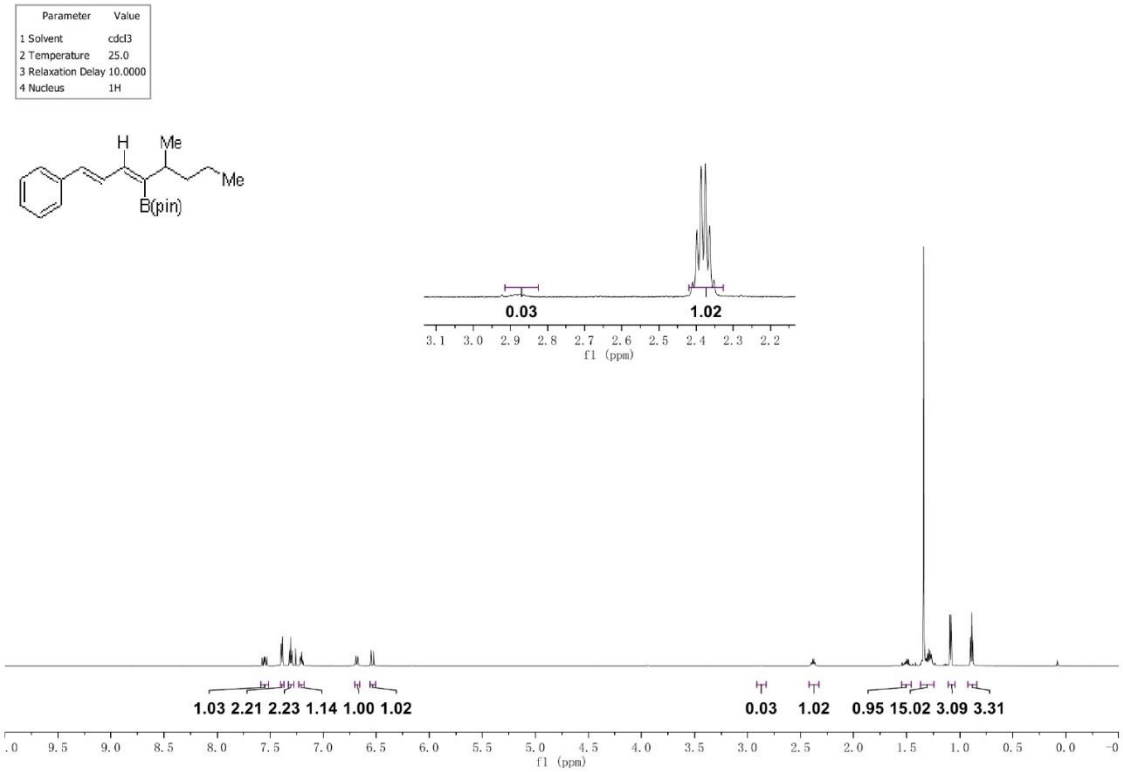
Parameter Value
1 Solvent cdcl3
2 Temperature 25.0
3 Relaxation Delay 10.0000
4 Nucleus 1H
H
Me
Me
B(pin)
0.03
1.02
f1 (ppm)
1.03 2.21 2.23 1.14 1.00 1.02
0.03 1.02 0.95 15.02 3.09 3.31
f1 (ppm)

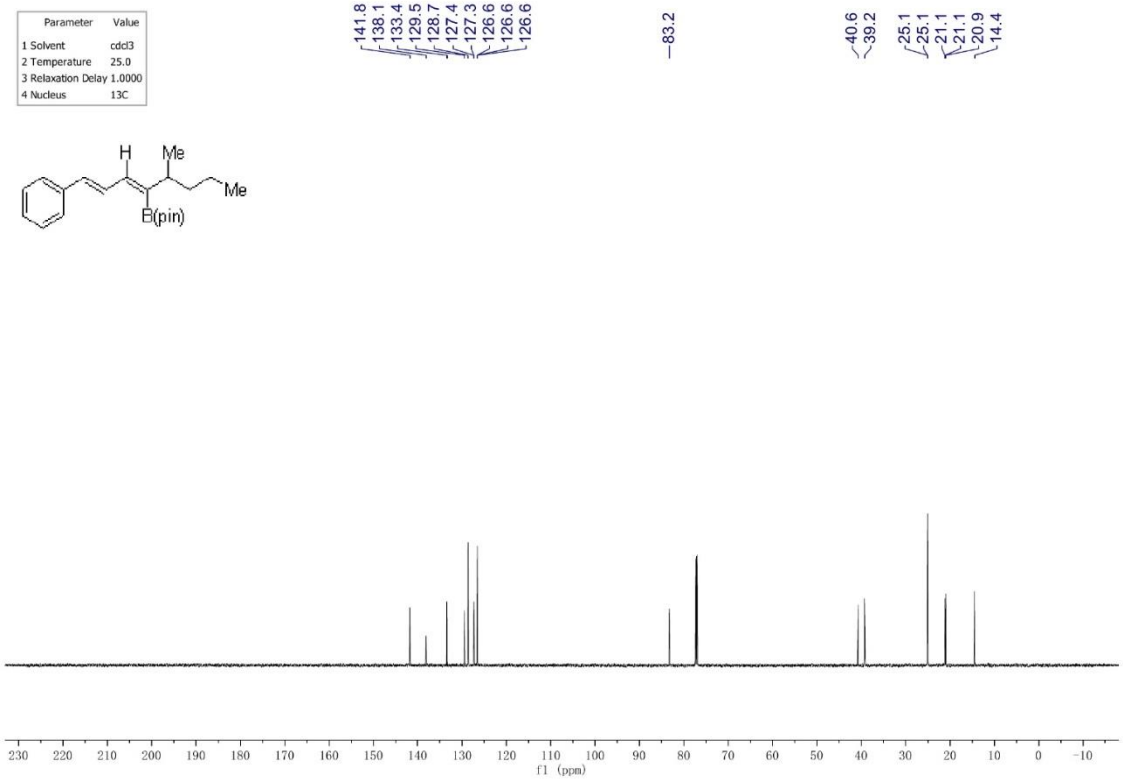
Parameter Value
1 Solvent cdcl3
2 Temperature 25.0
3 Relaxation Delay 1.0000
4 Nucleus 13C
141.8
138.1
133.4
129.5
128.7
127.4
127.3
126.6
126.6
126.6
83.2
40.6
39.2
25.1
25.1
21.1
21.1
20.9
14.4
H
Me
Me
B(pin)
f1 (ppm)

Parameter	Value
1 Solvent	cdcl3
2 Temperature	25.0
3 Relaxation Delay	0.0100
4 Nucleus	11B

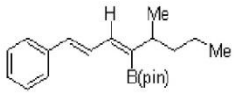

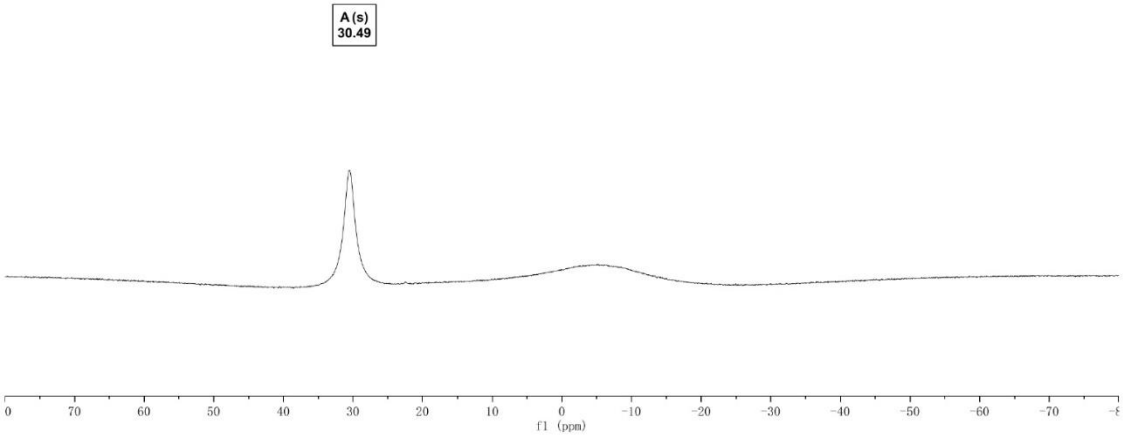

Parameter	Value
1 Solvent	cdcl3
2 Temperature	25.0
3 Relaxation Delay	10.0000
4 Nucleus	1H

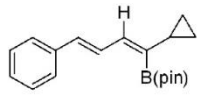

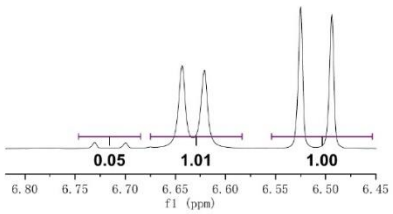

Parameter	Value
1 Solvent	cdcl3
2 Temperature	25.0
3 Relaxation Delay	1.0000
4 Nucleus	13C

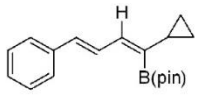

Parameter	Value
1 Solvent	cdcl3
2 Temperature	25.0
3 Relaxation Delay	0.0100
4 Nucleus	11B

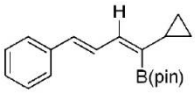

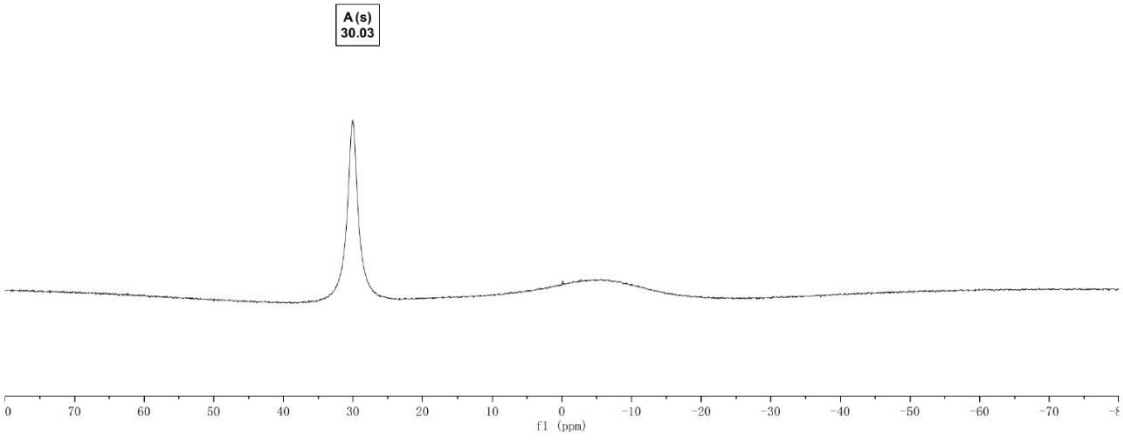

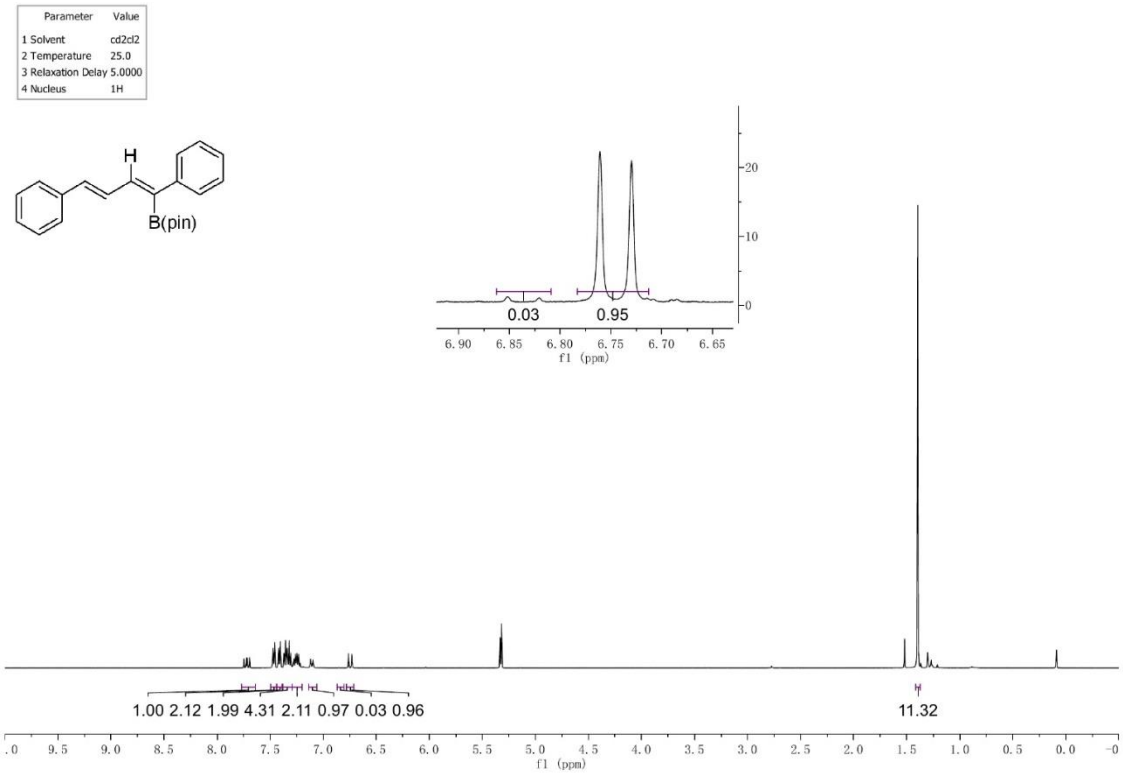
Parameter Value
1 Solvent cd2cl2
2 Temperature 25.0
3 Relaxation Delay 5.0000
4 Nucleus 1H
H
B(pin)
0.03
0.95
6.90 6.85 6.80 6.75 6.70 6.65
f1 (ppm)
1.00 2.12 1.99 4.31 2.11 0.97 0.03 0.96
11.32
f1 (ppm)

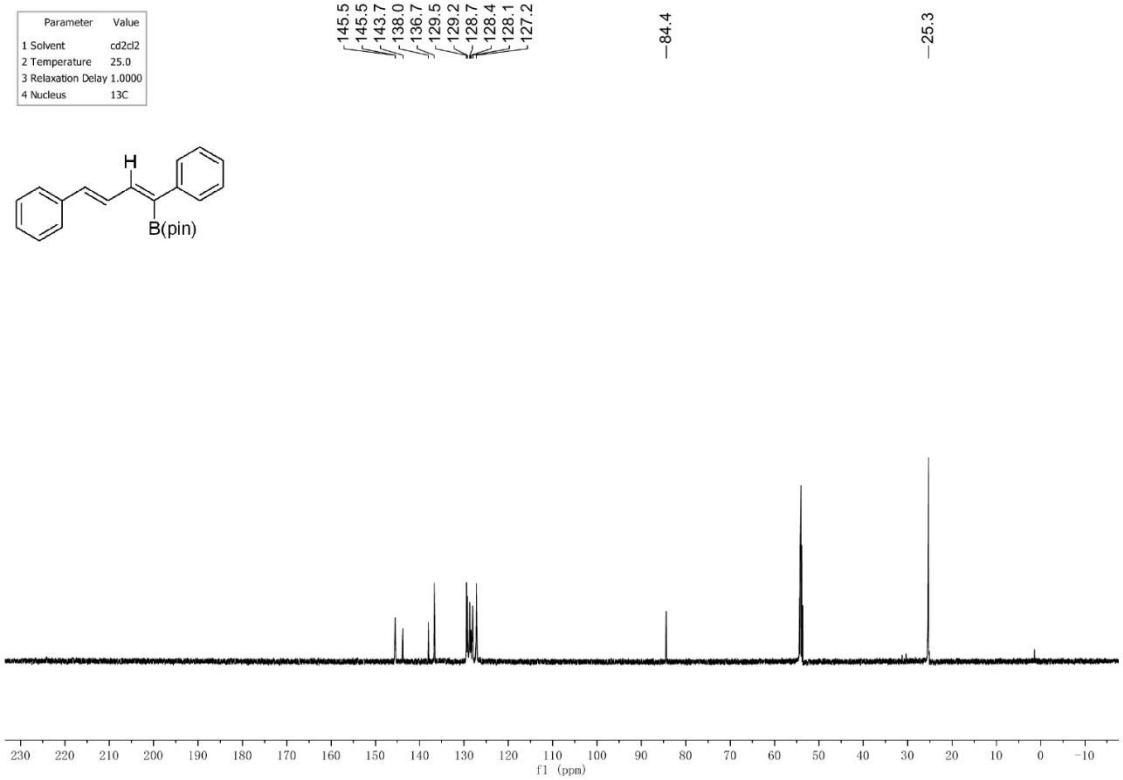
Parameter Value
1 Solvent cd2cl2
2 Temperature 25.0
3 Relaxation Delay 1.0000
4 Nucleus 13C
H
B(pin)
145.5
145.5
143.7
138.0
136.7
129.5
129.2
128.7
128.4
128.1
127.2
84.4
25.3
f1 (ppm)

Parameter	Value
1 Solvent	cd2cl2
2 Temperature	25.0
3 Relaxation Delay	0.0100
4 Nucleus	11B

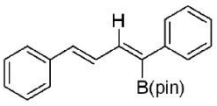

A (s)
30.5

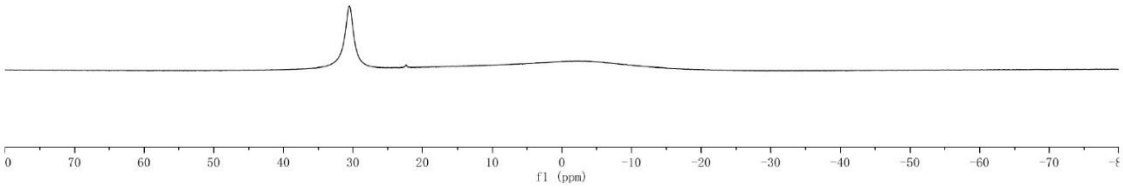

Parameter	Value
1 Solvent	cdcl3
2 Temperature	25.0
3 Relaxation Delay	10.0000
4 Nucleus	1H

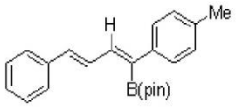

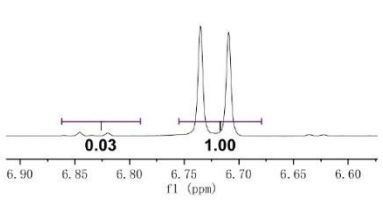

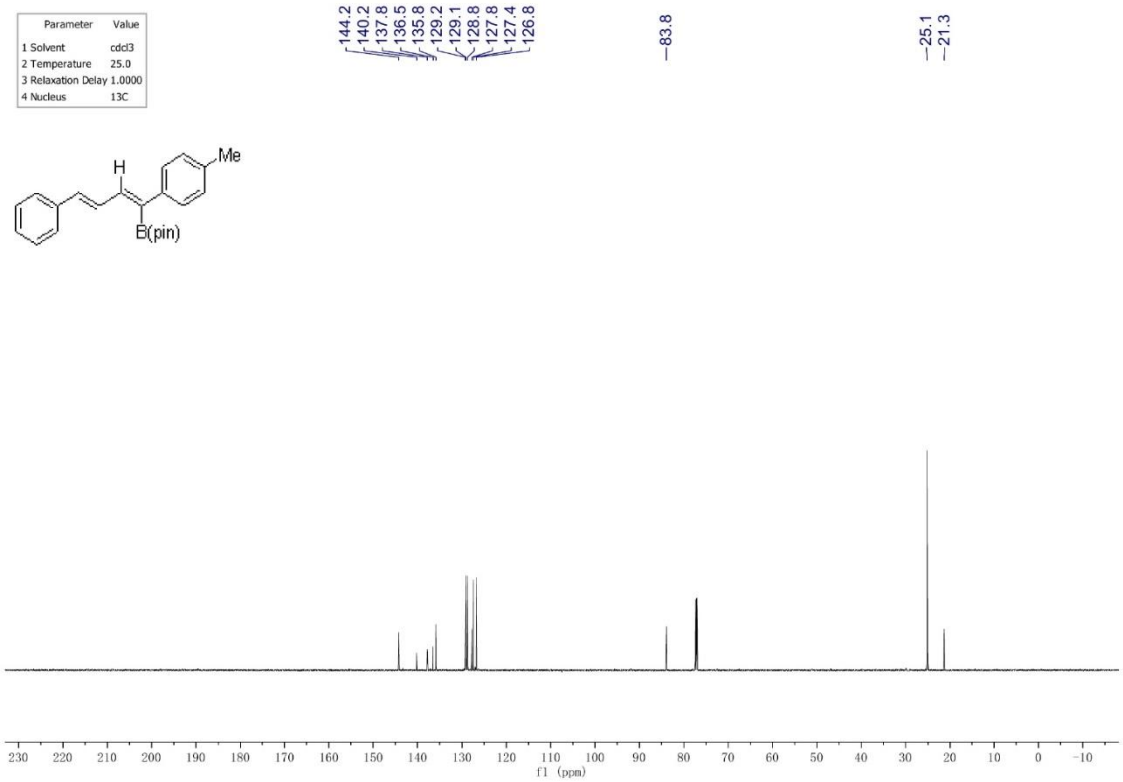
Parameter Value
1 Solvent cdcl3
2 Temperature 25.0
3 Relaxation Delay 1.0000
4 Nucleus 13C
144.2
140.2
137.8
136.5
135.8
129.2
129.1
128.8
127.8
127.4
126.8
83.8
25.1
21.3
H
Me
B(pin)
f1 (ppm)

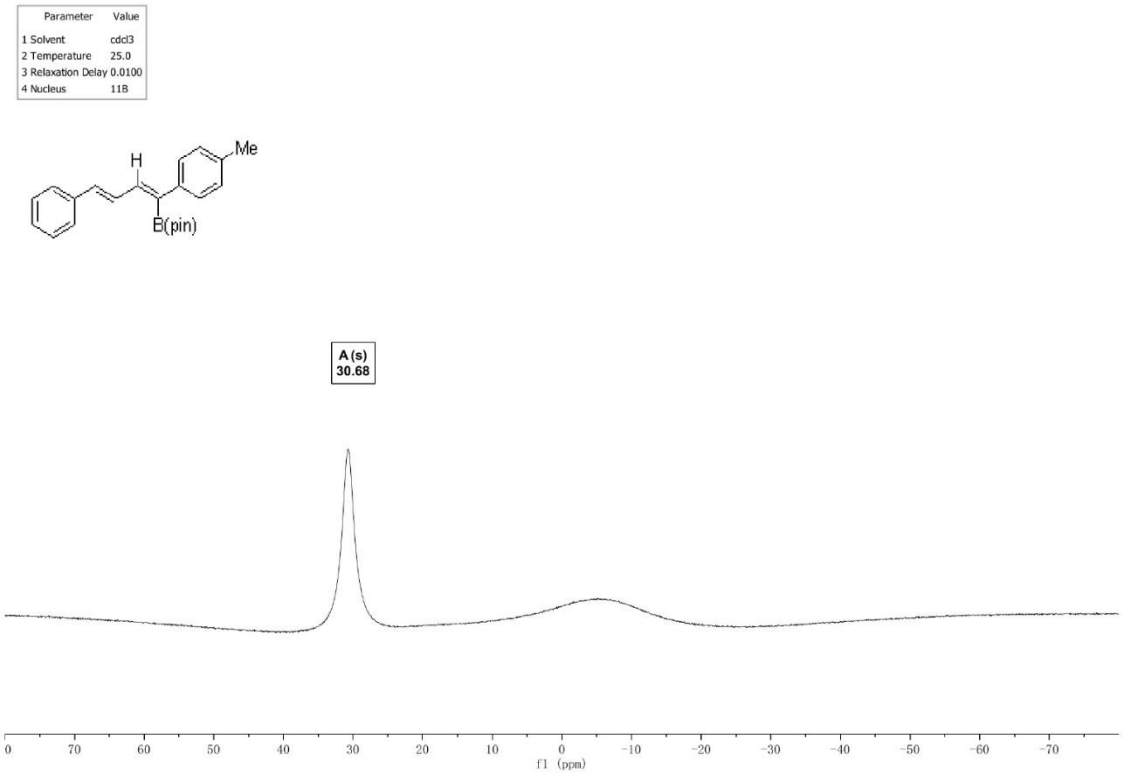
Parameter Value
1 Solvent cdcl3
2 Temperature 25.0
3 Relaxation Delay 0.0100
4 Nucleus 11B
H
Me
B(pin)
A(s)
30.68
f1 (ppm)

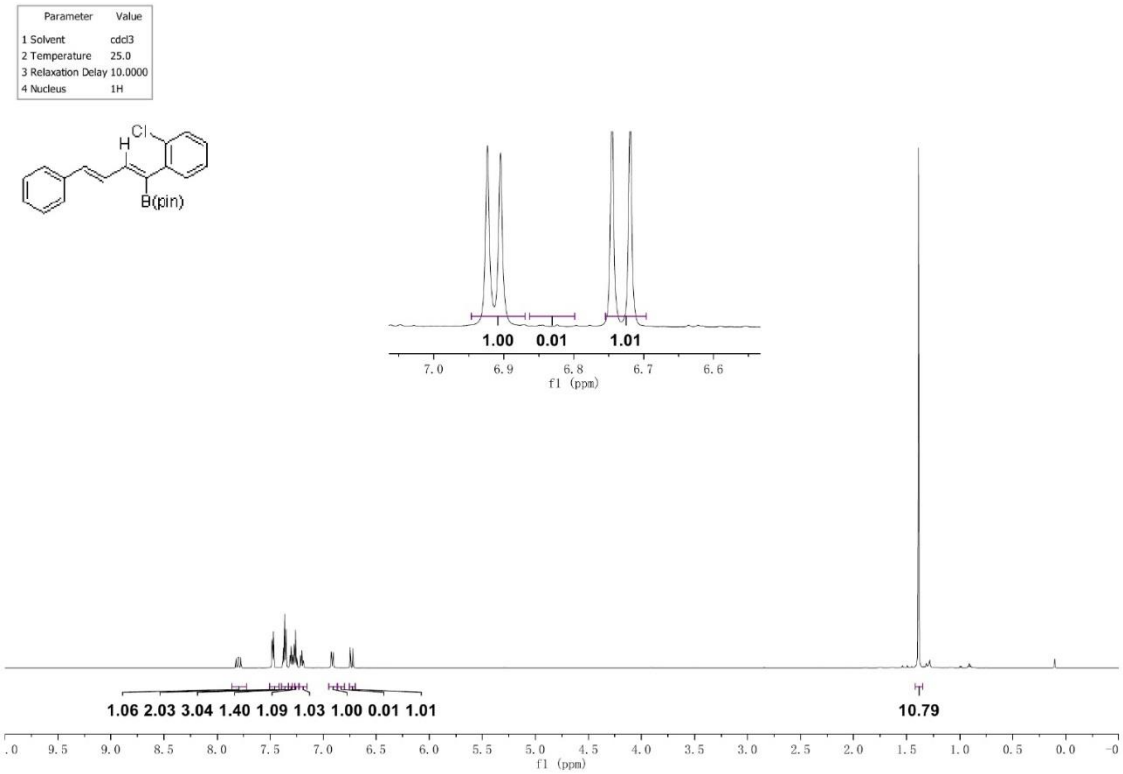
Parameter Value
1 Solvent cdcl3
2 Temperature 25.0
3 Relaxation Delay 10.0000
4 Nucleus 1H
Cl
H
B(pin)
1.00 0.01 1.01
f1 (ppm)
1.06 2.03 3.04 1.40 1.09 1.03 1.00 0.01 1.01
10.79
f1 (ppm)

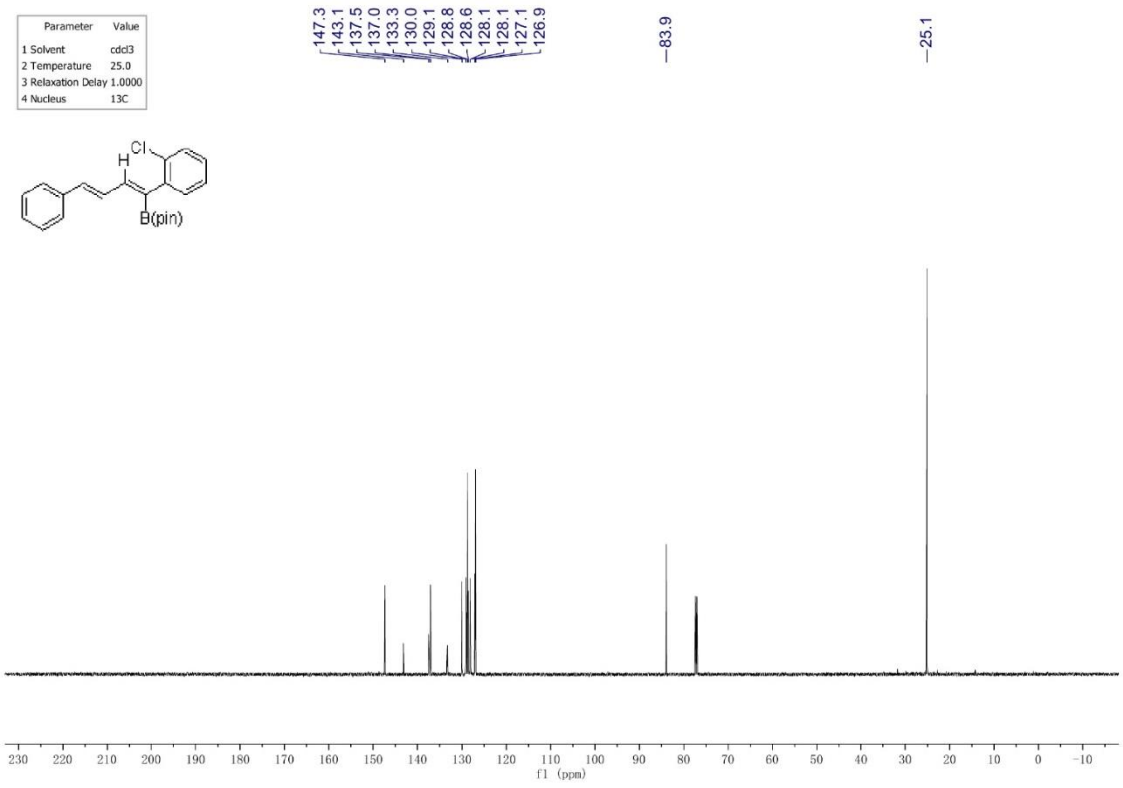
Parameter Value
1 Solvent cdcl3
2 Temperature 25.0
3 Relaxation Delay 1.0000
4 Nucleus 13C
Cl
H
B(pin)
147.3
143.1
137.5
137.0
133.3
130.0
129.1
128.8
128.6
128.1
128.1
127.1
126.9
83.9
25.1
f1 (ppm)

Parameter	Value
1 Solvent	cdcl3
2 Temperature	25.0
3 Relaxation Delay	0.0100
4 Nucleus	11B

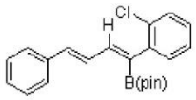

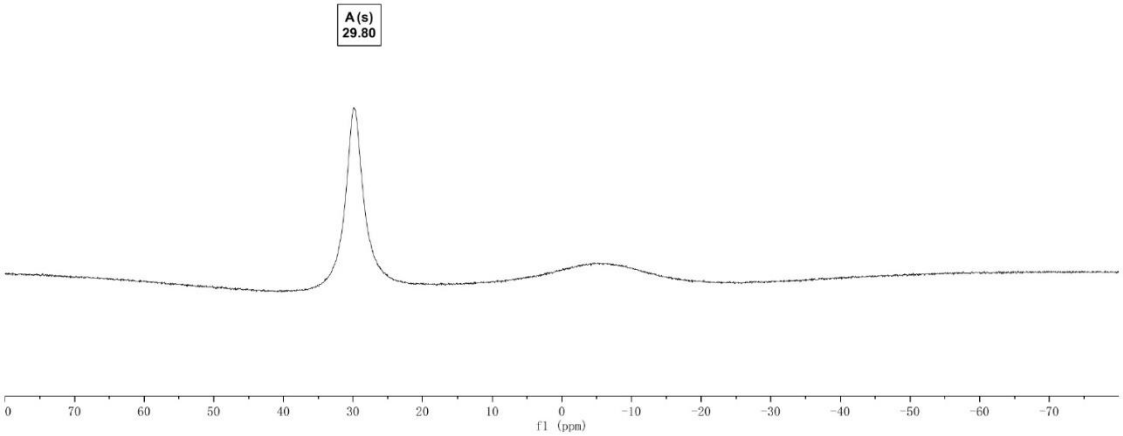

Parameter	Value
1 Solvent	cdcl3
2 Temperature	25.0
3 Relaxation Delay	10.0000
4 Nucleus	1H

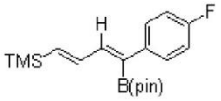

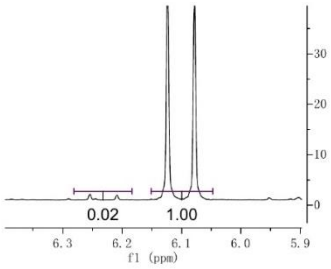

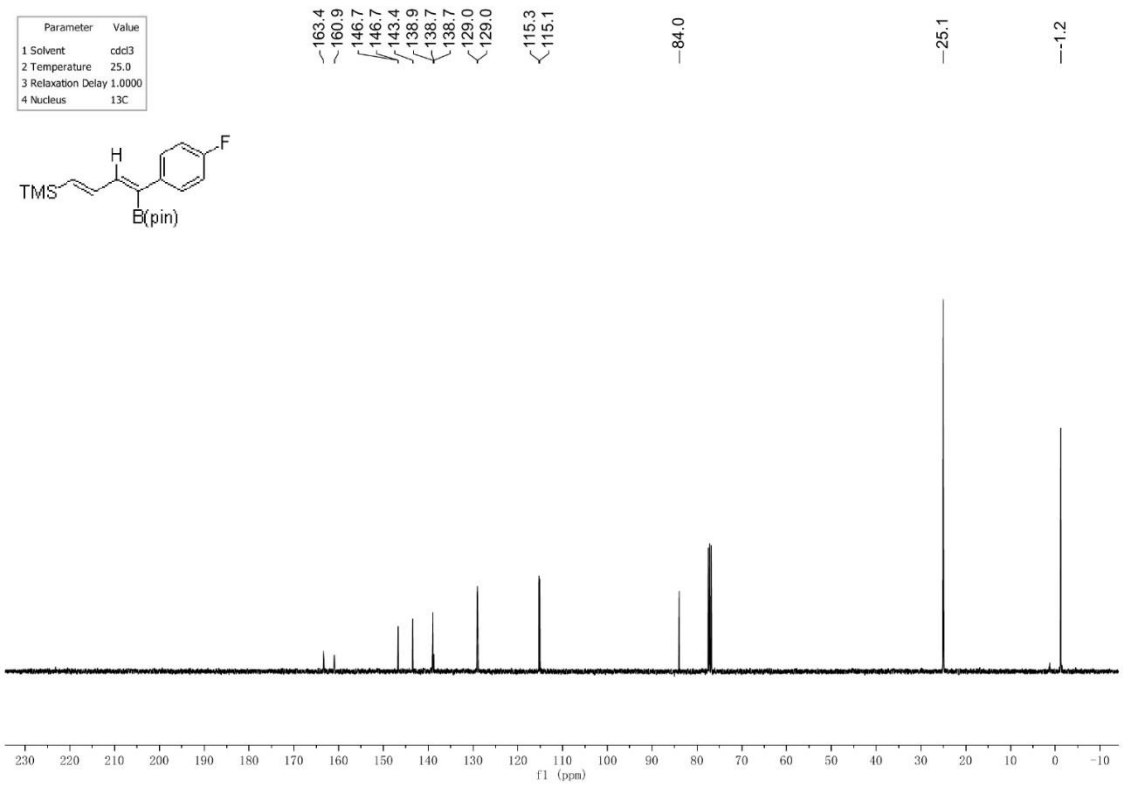
Parameter Value
1 Solvent cdcl3
2 Temperature 25.0
3 Relaxation Delay 1.0000
4 Nucleus 13C
163.4
160.9
146.7
146.7
143.4
138.9
138.7
138.7
129.0
129.0
115.3
115.1
84.0
25.1
-1.2
H
F
TMS
B(pin)
f1 (ppm)

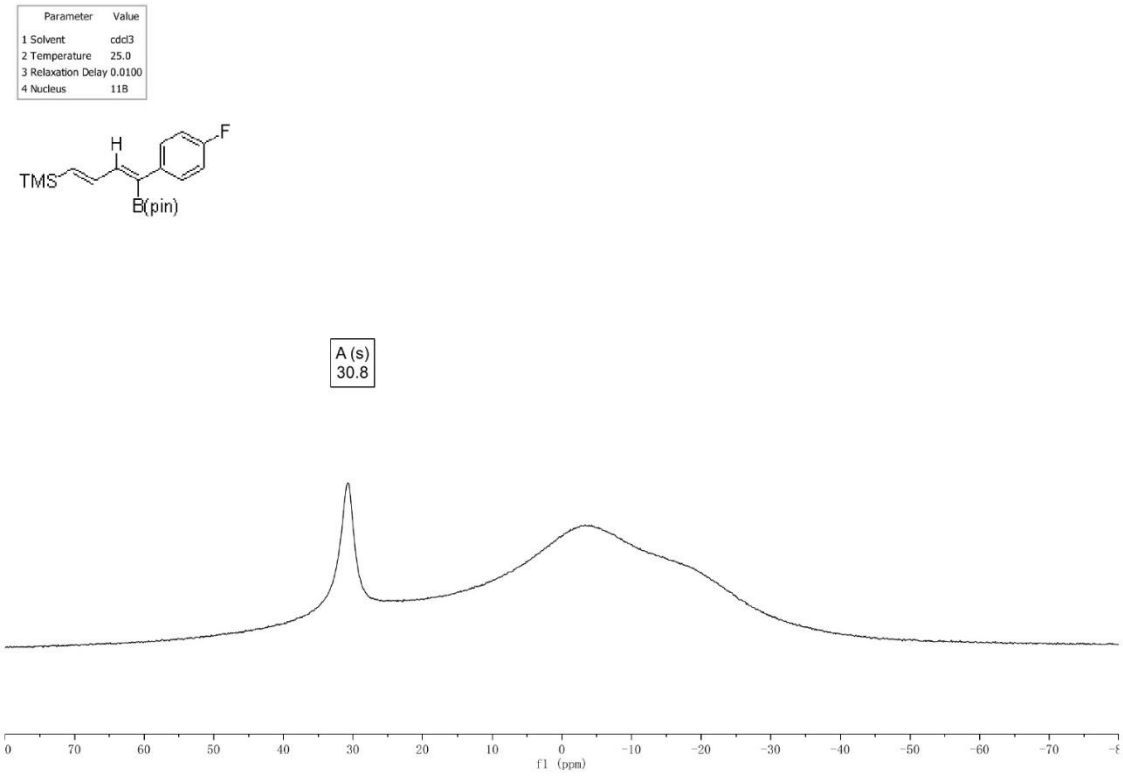
Parameter Value
1 Solvent cdcl3
2 Temperature 25.0
3 Relaxation Delay 0.0100
4 Nucleus 11B
H
F
TMS
B(pin)
A (s)
30.8
f1 (ppm)

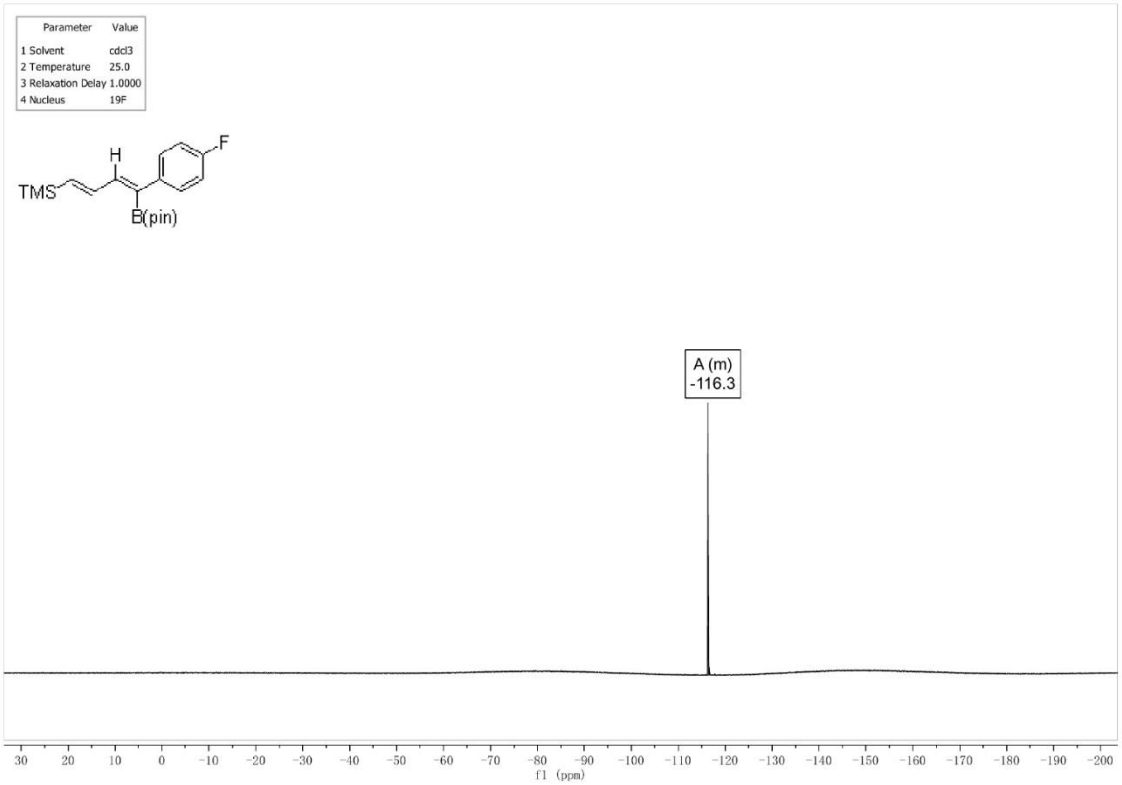
Parameter Value
1 Solvent cdcl3
2 Temperature 25.0
3 Relaxation Delay 1.0000
4 Nucleus 19F
H
F
TMS
B(pin)
A (m)
-116.3
f1 (ppm)

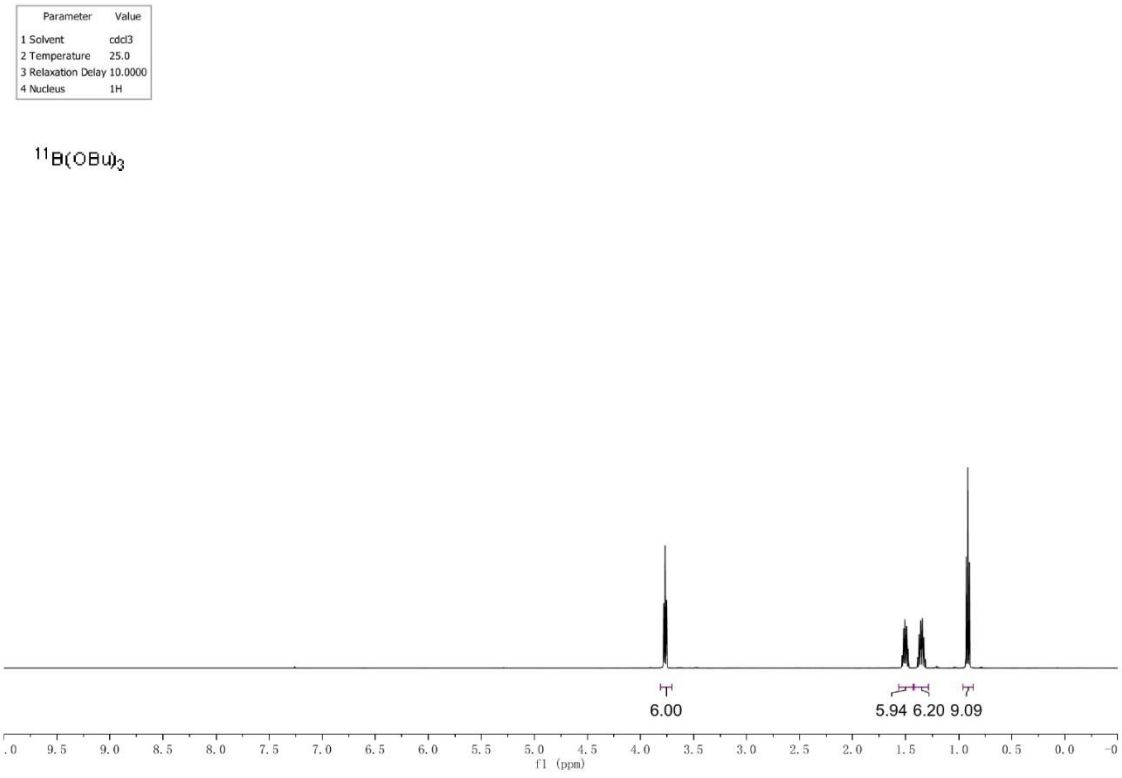
Parameter Value
1 Solvent cdcl3
2 Temperature 25.0
3 Relaxation Delay 10.0000
4 Nucleus 1H
$^{11}B(OBu)_3$
6.00
5.94 6.20 9.09
f1 (ppm)

Parameter	Value
1 Solvent	cdcl3
2 Temperature	25.0
3 Relaxation Delay	1.0000
4 Nucleus	13C

$^{11}B(OBu)_3$

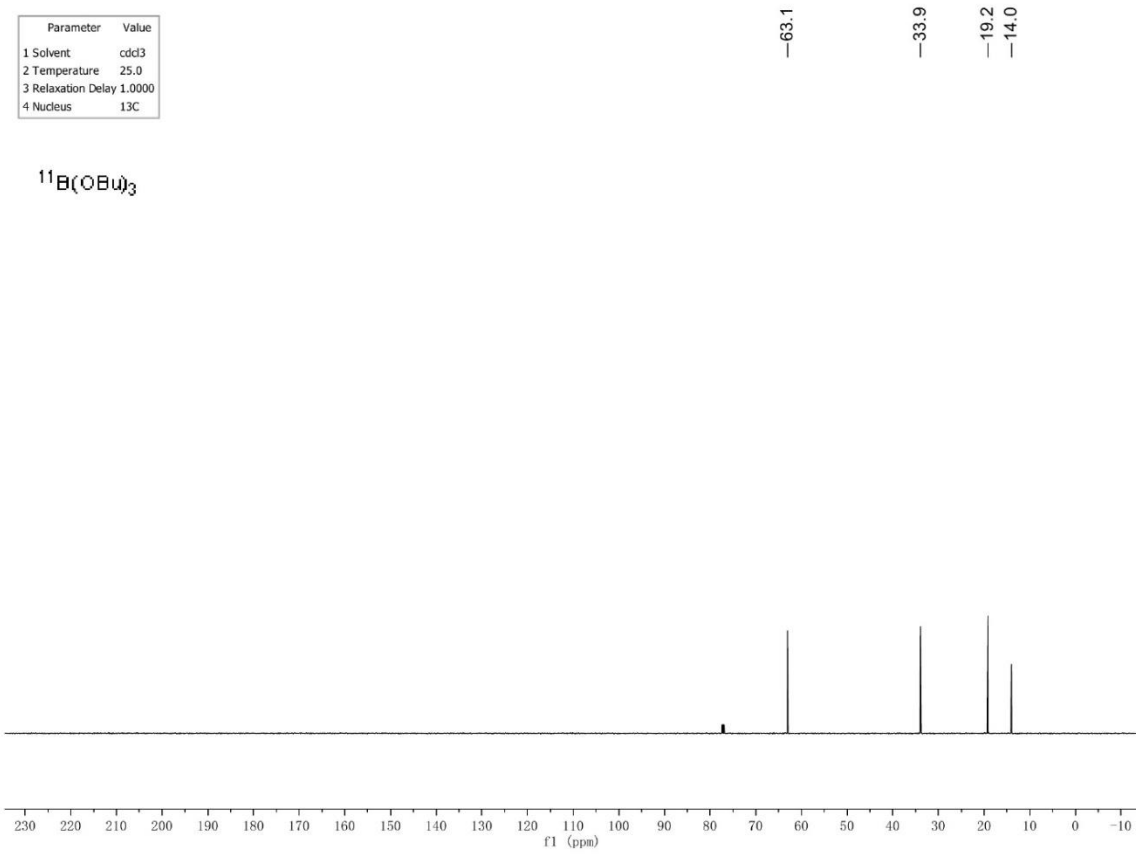

Parameter	Value
1 Solvent	cdcl3
2 Temperature	25.0
3 Relaxation Delay	0.0100
4 Nucleus	11B

$^{11}B(OBu)_3$

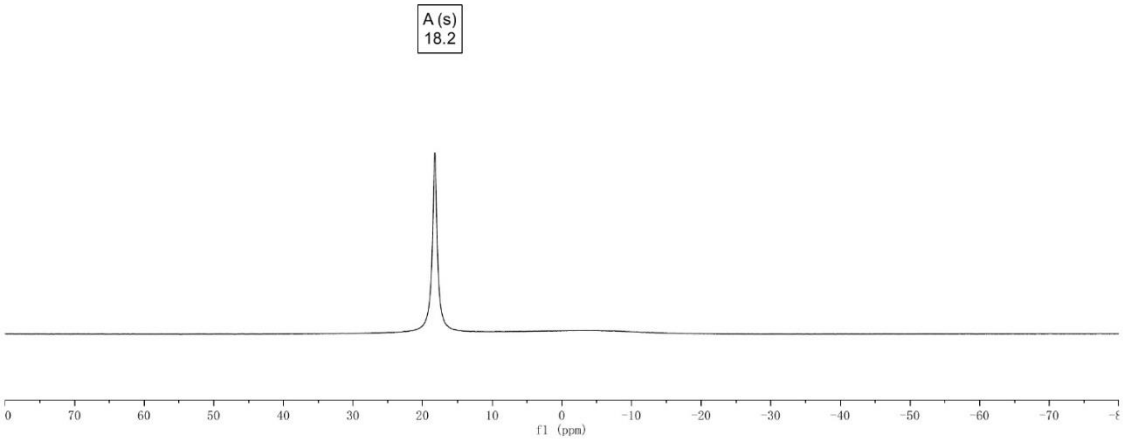

Parameter	Value
1 Solvent	cdcl3
2 Temperature	25.0
3 Relaxation Delay	10.0000
4 Nucleus	1H

$Et_3N{\cdot}^{11}BD_3$

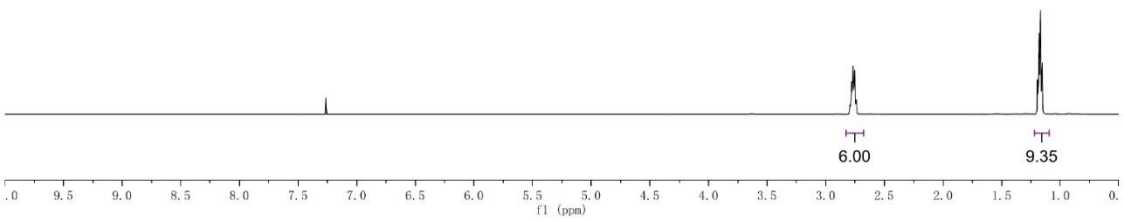

Parameter	Value
1 Solvent	cdcl3
2 Temperature	25.0
3 Relaxation Delay	1.0000
4 Nucleus	13C

52.4

8.7

$Et_3N{\cdot}^{11}BD_3$

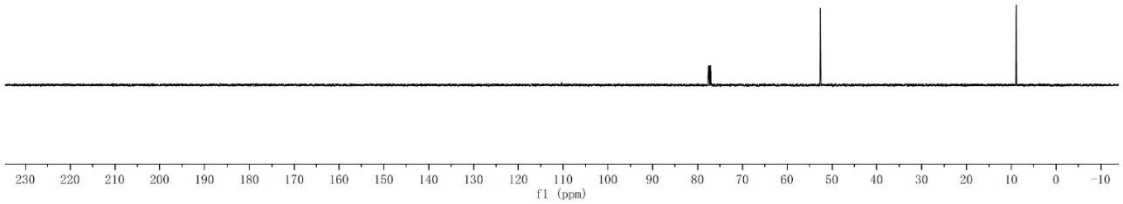

Parameter	Value
1 Solvent	cdcl3
2 Temperature	25.0
3 Relaxation Delay	0.0100
4 Nucleus	11B

$Et_3N{\cdot}^{11}BD_3$

A (s)
-13.8

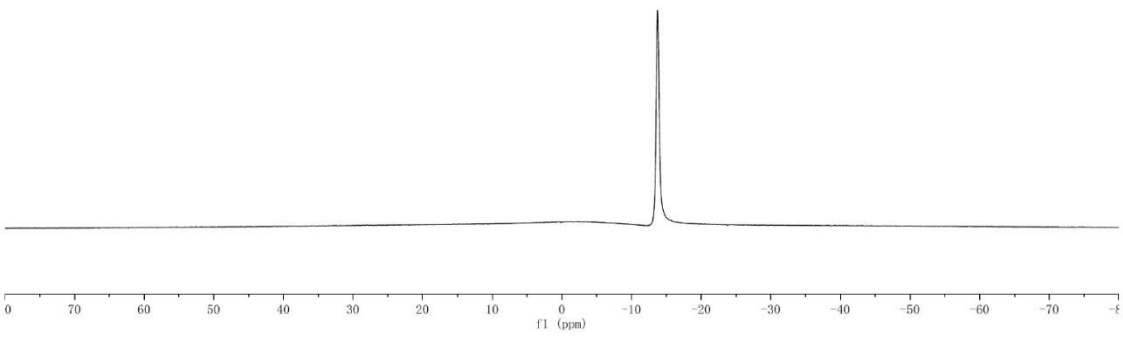

Parameter	Value
1 Solvent	thf
2 Temperature	25.0
3 Relaxation Delay	0.0100
4 Nucleus	11B

$Li^{11}BD_4$

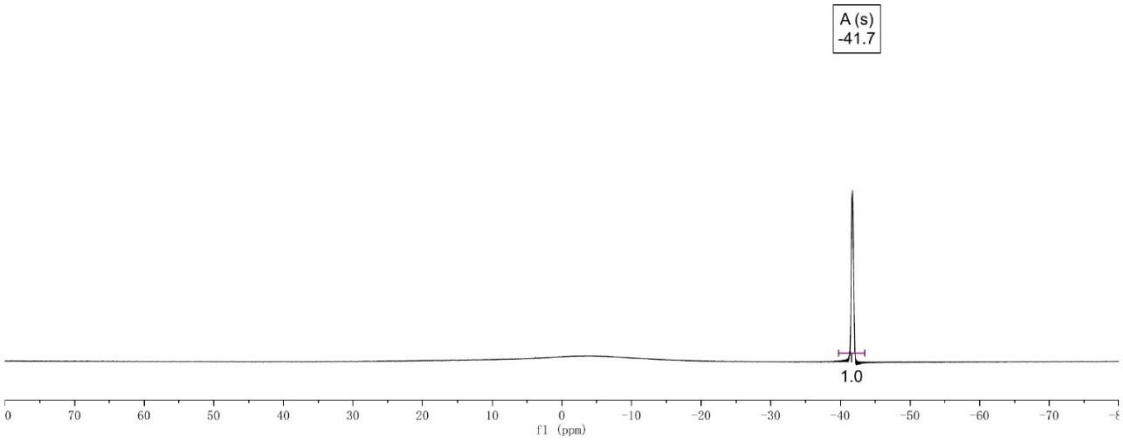

Parameter	Value
1 Solvent	cd2cl2
2 Temperature	25.0
3 Relaxation Delay	5.0000
4 Nucleus	1H

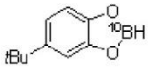

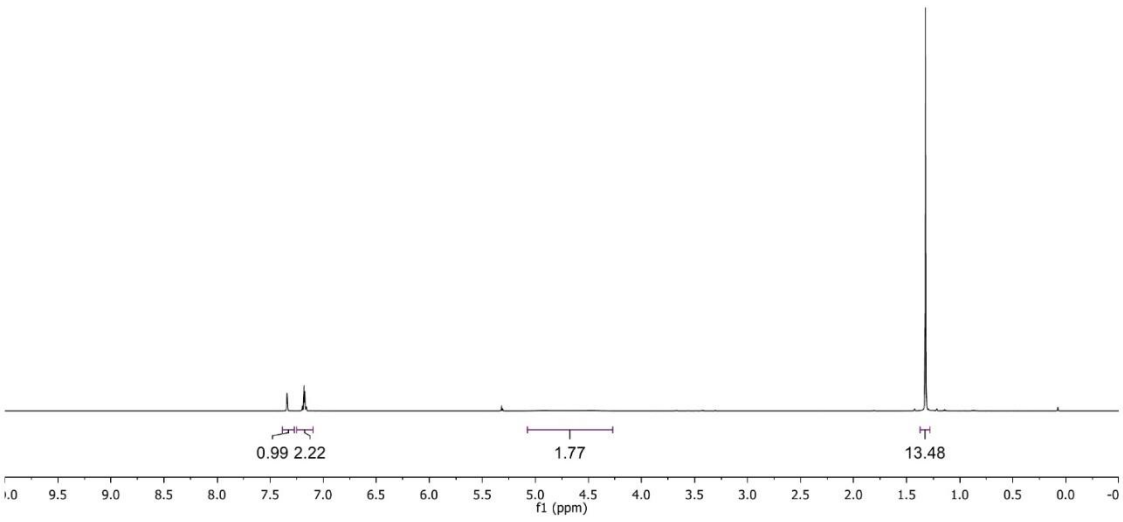

Parameter	Value
1 Solvent	cd2cl2
2 Temperature	25.0
3 Relaxation Delay	1.0000
4 Nucleus	13C

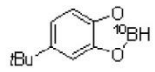

Parameter	Value
1 Solvent	cd2cl2
2 Temperature	25.0
3 Relaxation Delay	0.0100
4 Nucleus	11B

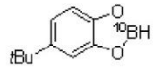

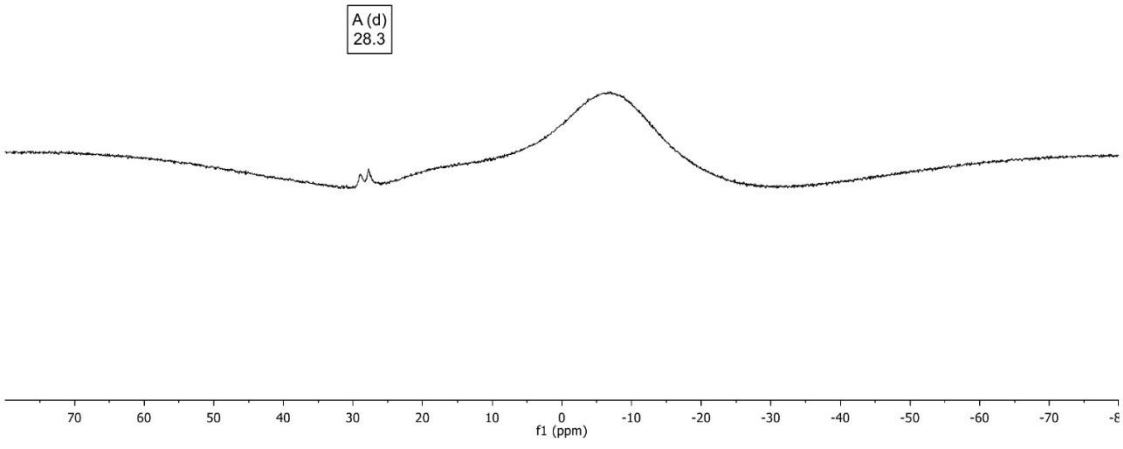

Parameter	Value
1 Solvent	cd2cl2
2 Temperature	25.0
3 Relaxation Delay	0.0100
4 Nucleus	11B

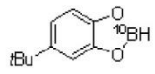

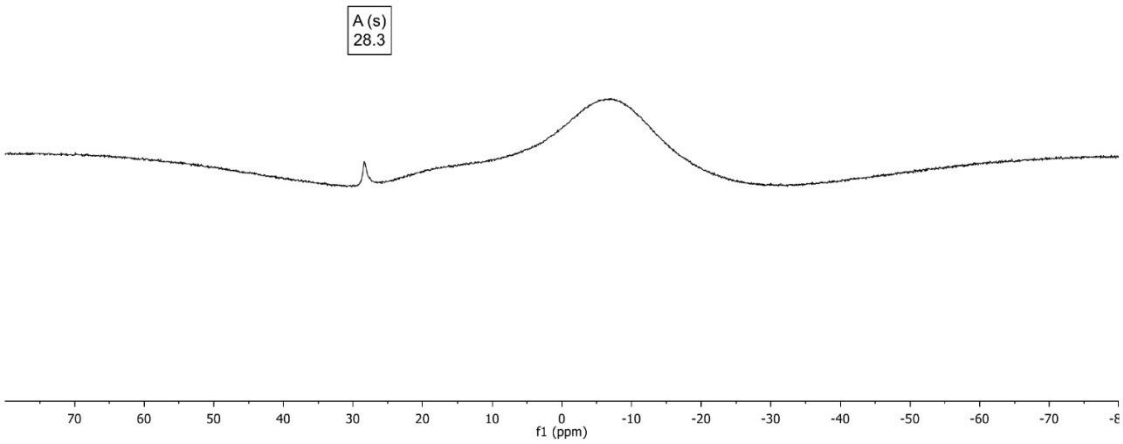

Parameter	Value
1 Solvent	cd2cl2
2 Temperature	25.0
3 Relaxation Delay	5.0000
4 Nucleus	1H

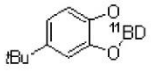

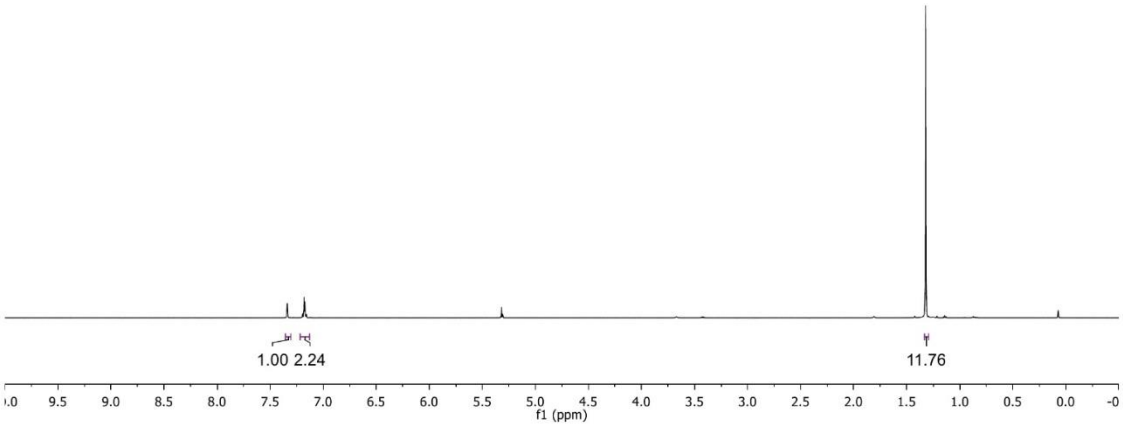

Parameter	Value
1 Solvent	cd2cl2
2 Temperature	25.0
3 Relaxation Delay	1.0000
4 Nucleus	13C

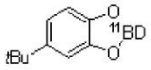

147.9
147.6
145.6
120.5
112.1
110.5
35.3
32.0

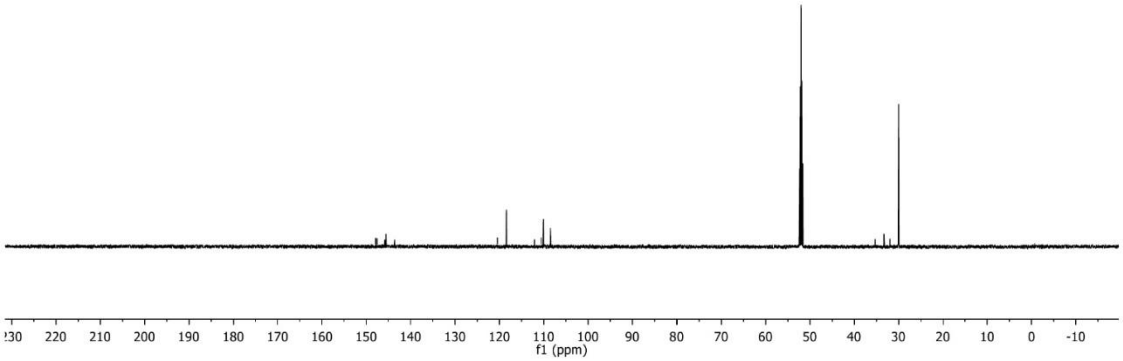

Parameter	Value
1 Solvent	cd2cl2
2 Temperature	25.0
3 Relaxation Delay	0.0100
4 Nucleus	11B

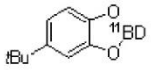

A (s)
28.34

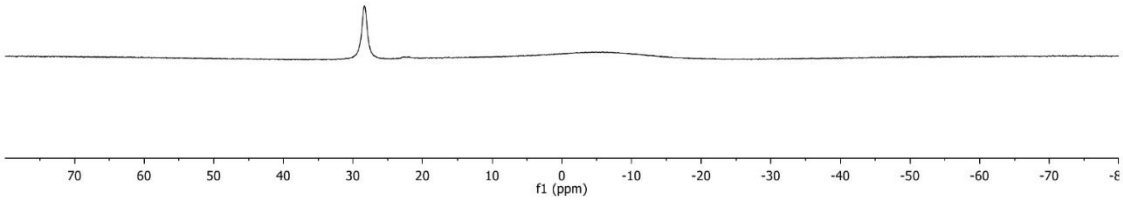

Stacked ^{1}H NMR of Pd(COD)($CH_2TMS)_2$ and ^{1}H NMR at Stage 1

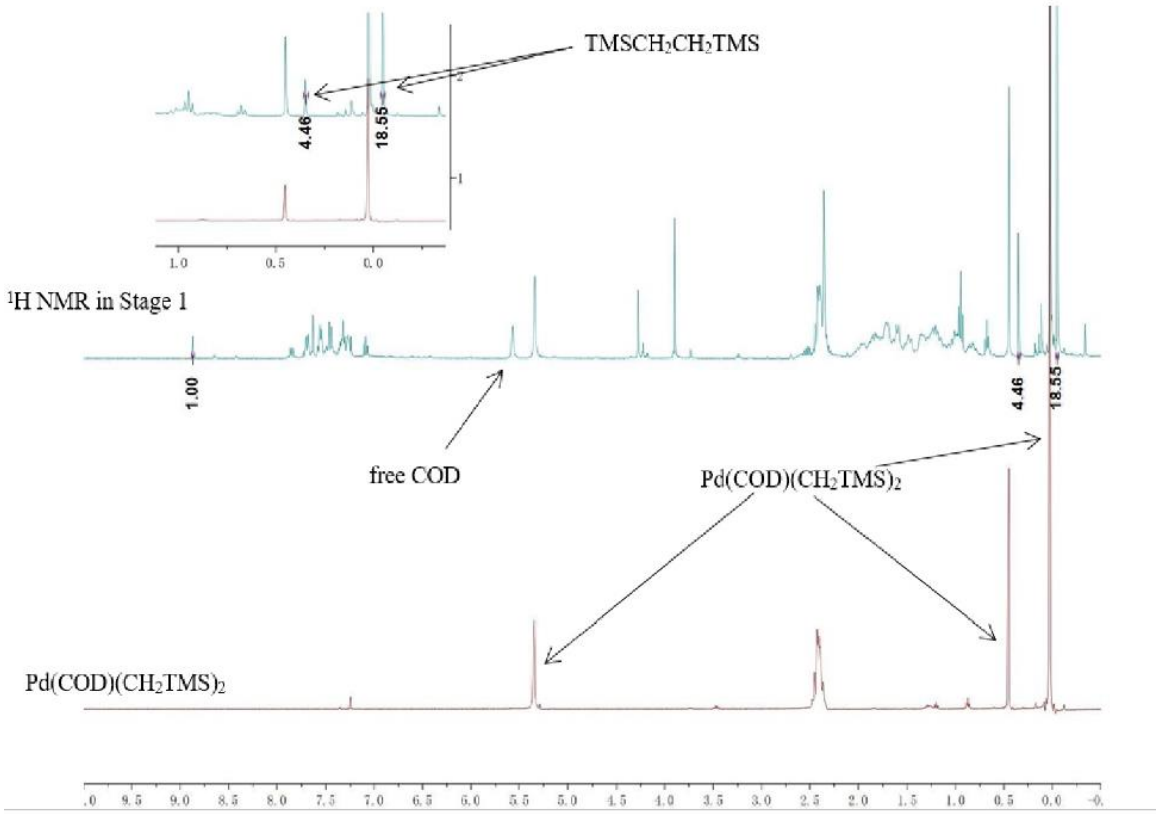

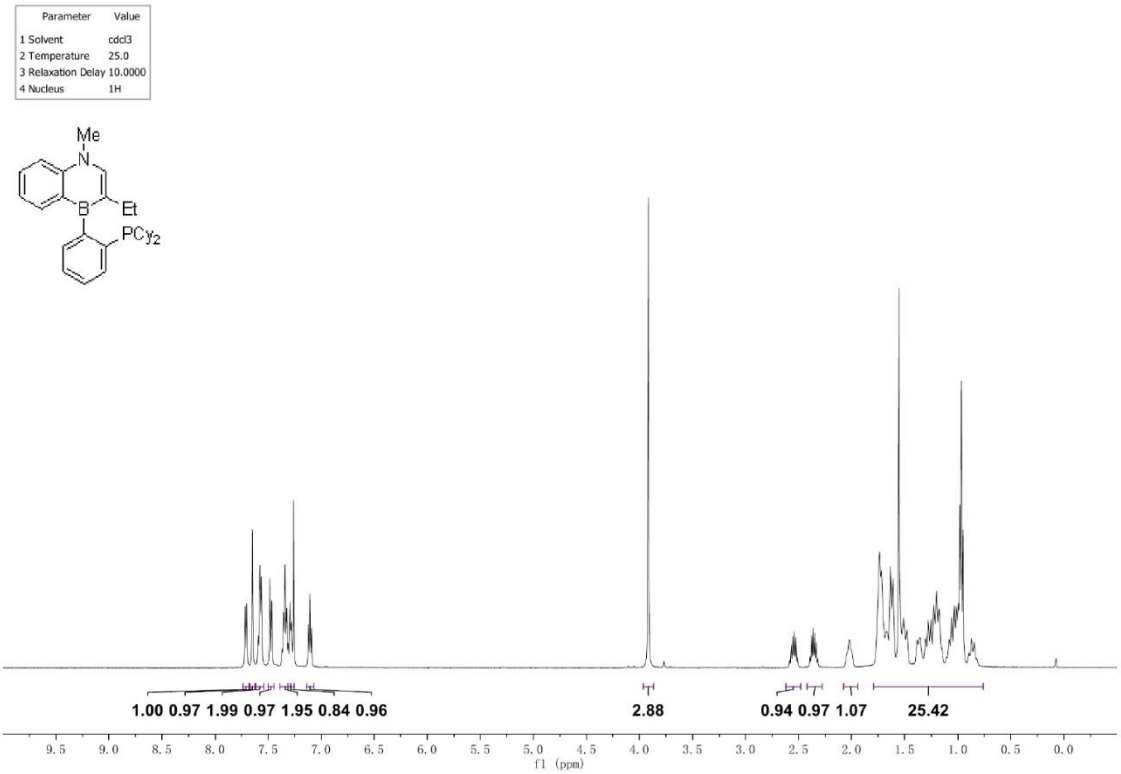
Parameter Value
1 Solvent cdcl3
2 Temperature 25.0
3 Relaxation Delay 10.0000
4 Nucleus 1H
Me
N
B
Et
PCy2
1.00 0.97 1.99 0.97 1.95 0.84 0.96
2.88
0.94 0.97 1.07
25.42
f1 (ppm)

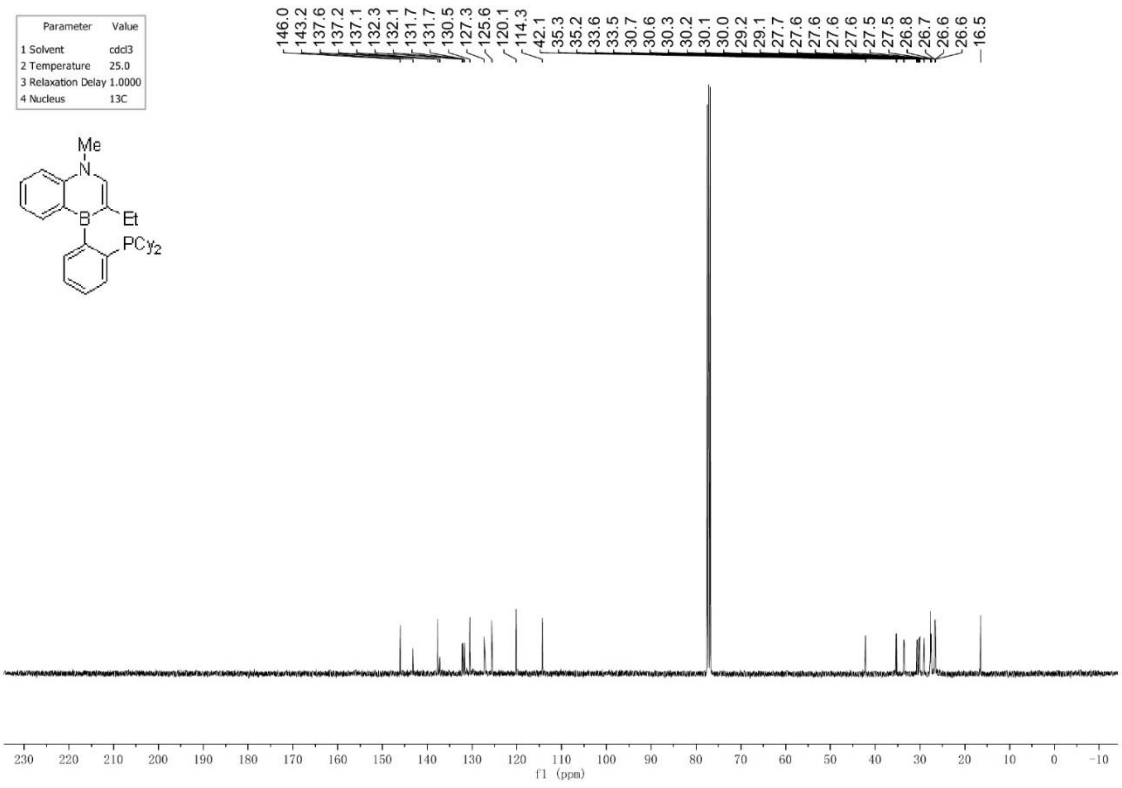
Parameter Value
1 Solvent cdcl3
2 Temperature 25.0
3 Relaxation Delay 1.0000
4 Nucleus 13C
Me
N
B
Et
PCy2
146.0
143.2
137.6
137.2
137.1
132.3
132.1
131.7
131.7
130.5
127.3
125.6
120.1
114.3
42.1
35.3
35.2
33.6
33.5
30.7
30.6
30.3
30.2
30.1
30.0
29.2
29.1
27.7
27.6
27.6
27.6
27.6
27.5
27.5
26.8
26.7
26.6
26.6
16.5
f1 (ppm)

Parameter	Value
1 Solvent	cdcl3
2 Temperature	25.0
3 Relaxation Delay	0.0100
4 Nucleus	11B

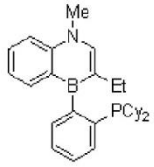

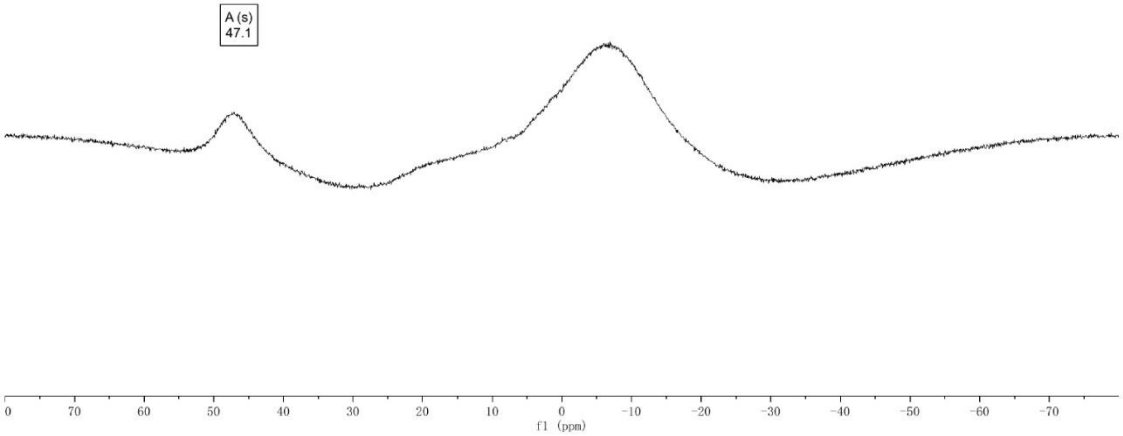

Parameter	Value
1 Solvent	cdcl3
2 Temperature	25.0
3 Relaxation Delay	1.0000
4 Nucleus	31P

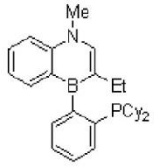

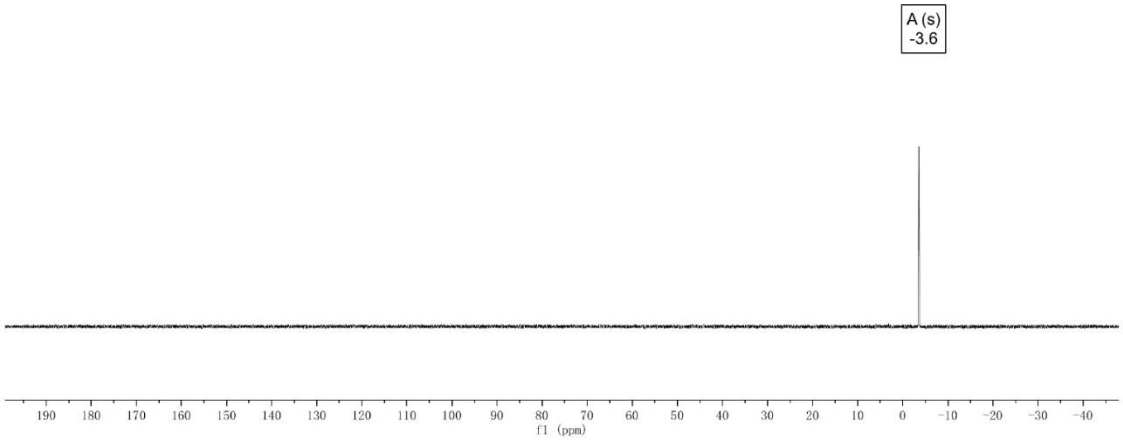

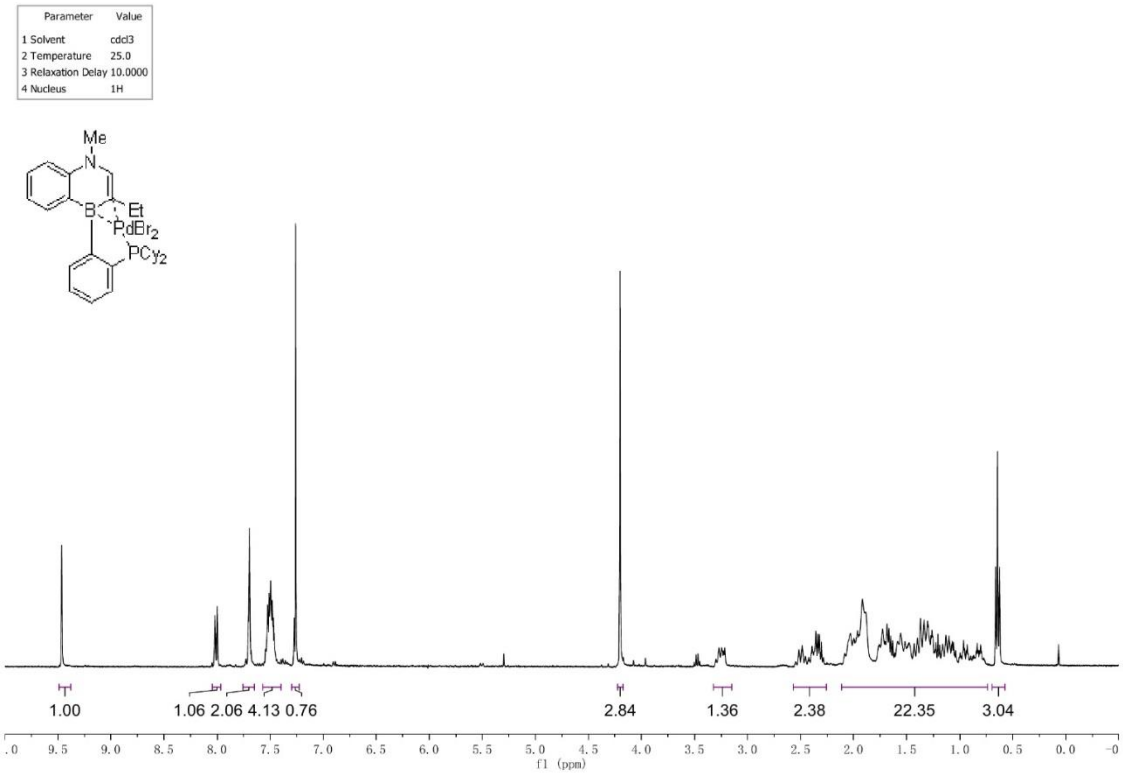
Parameter Value
1 Solvent cdcl3
2 Temperature 25.0
3 Relaxation Delay 10.0000
4 Nucleus 1H
Me
N
B
Et
PdBr2
PCy2
1.00
1.06 2.06 4.13 0.76
2.84
1.36
2.38
22.35
3.04
f1 (ppm)

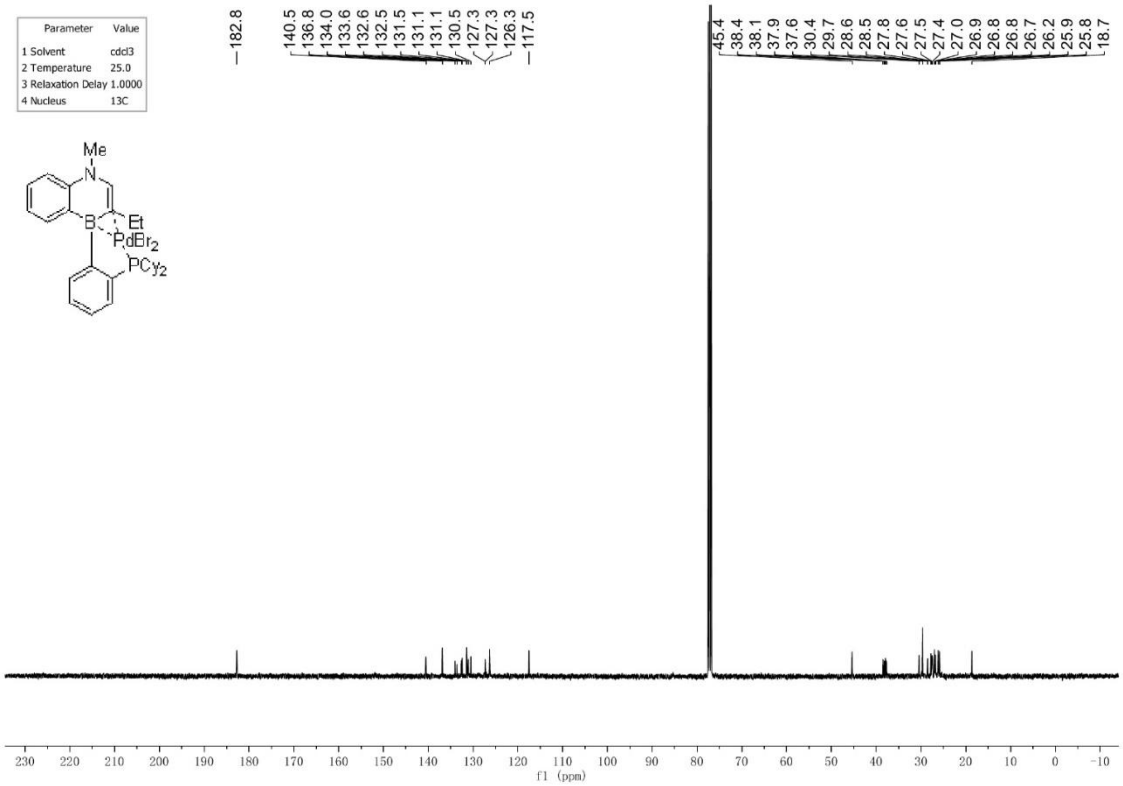
Parameter Value
1 Solvent cdcl3
2 Temperature 25.0
3 Relaxation Delay 1.0000
4 Nucleus 13C
Me
N
B
Et
PdBr2
PCy2
182.8
140.5
136.8
134.0
133.6
132.6
132.5
131.5
131.1
131.1
130.5
127.3
127.3
126.3
117.5
45.4
38.4
38.1
37.9
37.6
30.4
29.7
28.6
28.5
27.8
27.6
27.5
27.4
27.0
26.9
26.8
26.8
26.7
26.2
25.9
25.8
18.7
f1 (ppm)

Parameter	Value
1 Solvent	cdcl3
2 Temperature	25.0
3 Relaxation Delay	0.0100
4 Nucleus	11B

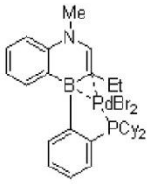

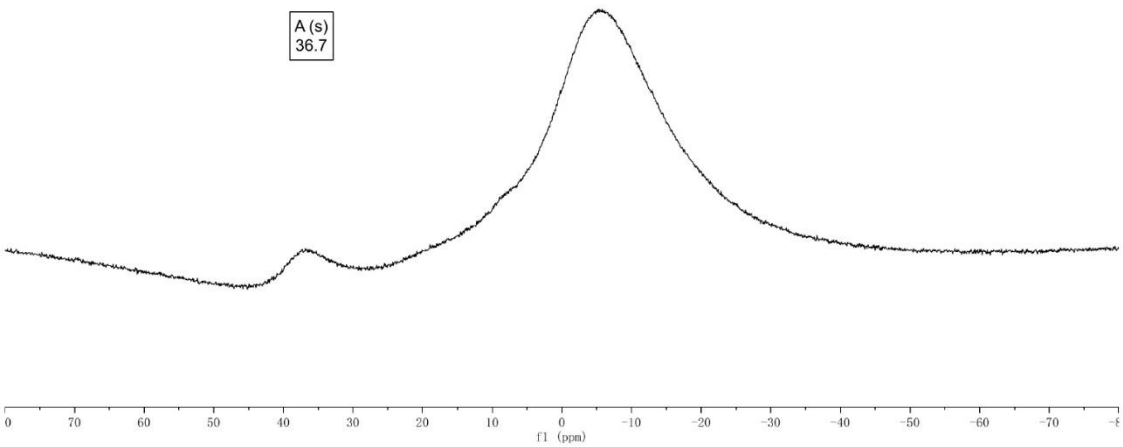

Parameter	Value
1 Solvent	cdcl3
2 Temperature	25.0
3 Relaxation Delay	1.0000
4 Nucleus	31P

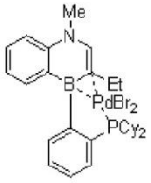

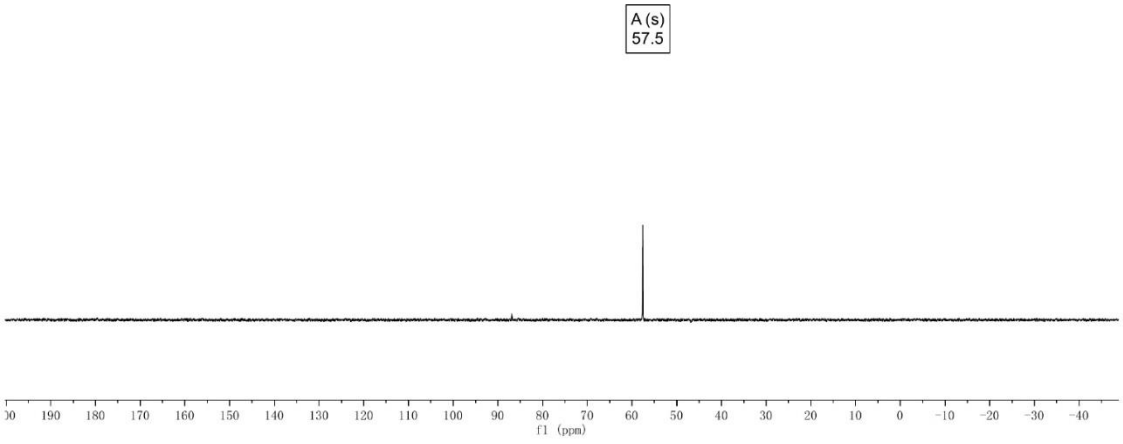

Parameter	Value
1 Solvent	cdcl3
2 Temperature	25.0
3 Relaxation Delay	1.0000
4 Nucleus	1H

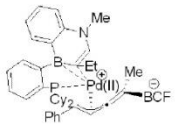

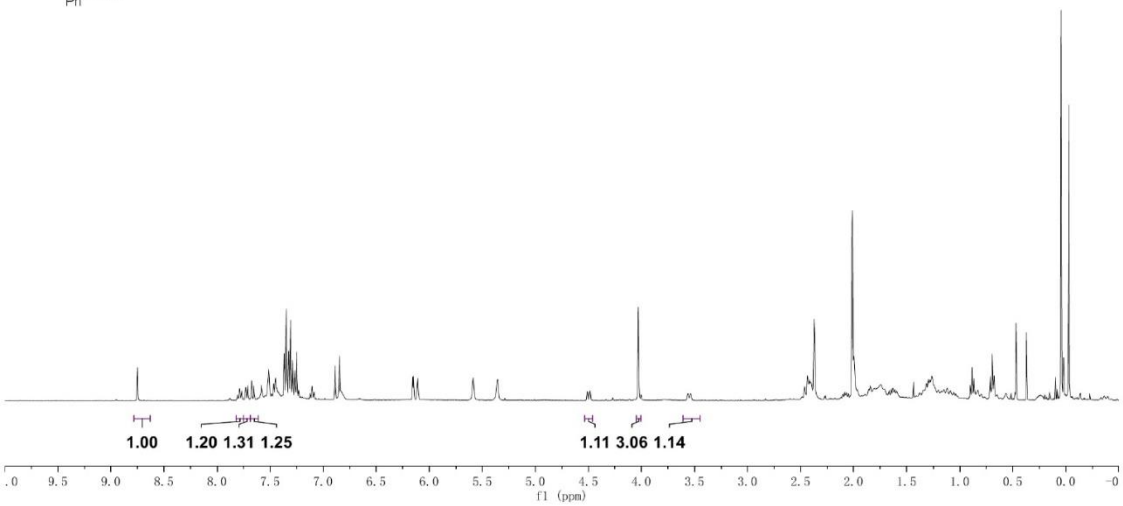

Parameter	Value
1 Solvent	cdcl3
2 Temperature	25.0
3 Relaxation Delay	1.0000
4 Nucleus	13C

157.5

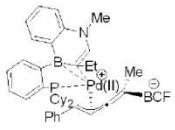

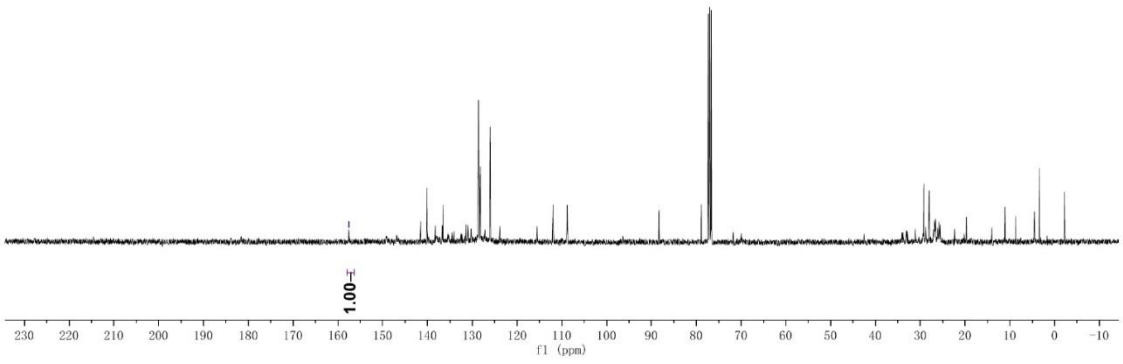

Parameter	Value
1 Solvent	cdcl3
2 Temperature	25.0
3 Relaxation Delay	0.0100
4 Nucleus	11B

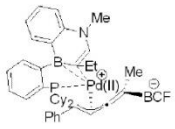

Parameter	Value
1 Solvent	cdcl3
2 Temperature	25.0
3 Relaxation Delay	1.0000
4 Nucleus	31P

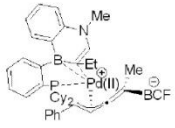

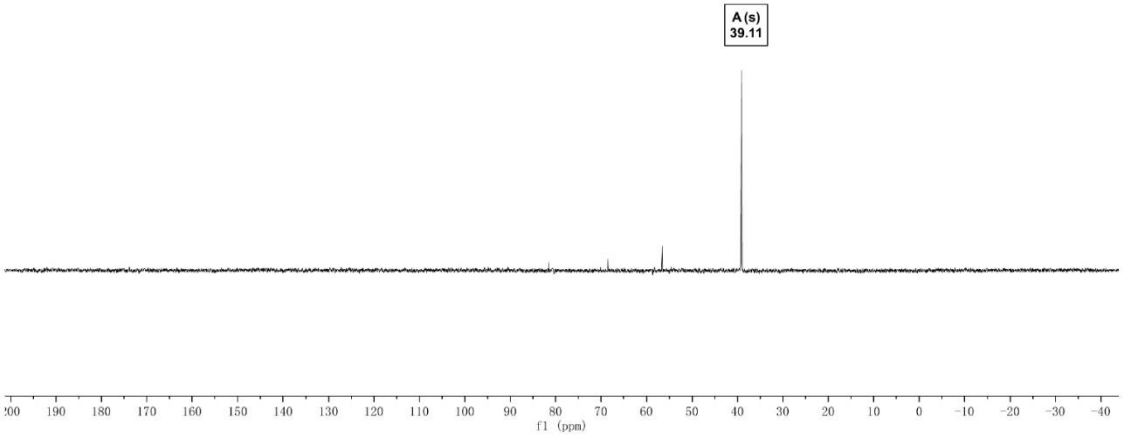

Parameter	Value
1 Solvent	cdcl3
2 Temperature	25.0
3 Relaxation Delay	1.0000
4 Nucleus	19F

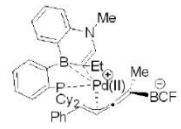

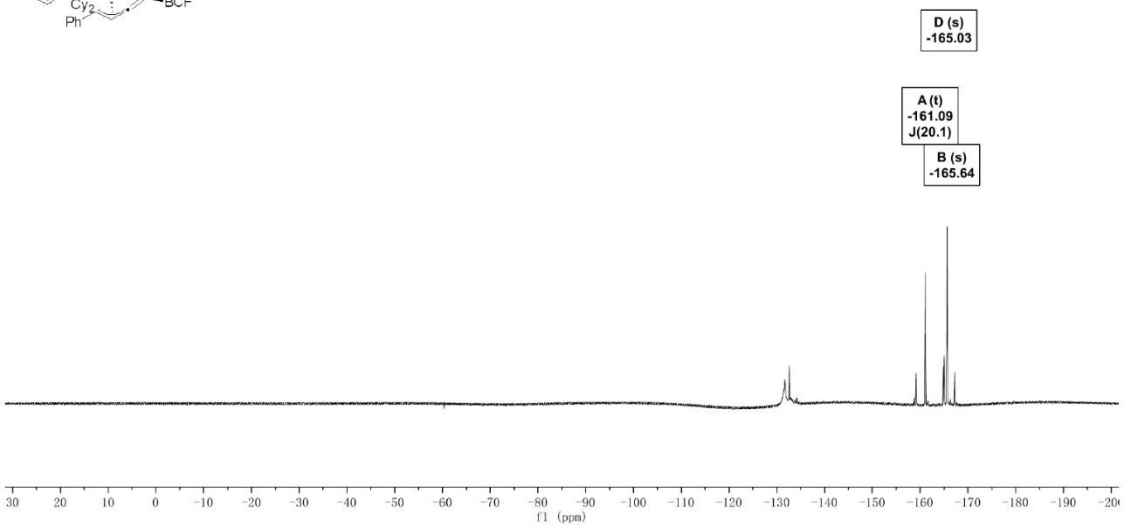

Chapter 2. Palladium/Senphos Catalyzed *trans*-Selective Chloroboration and Cyanoboration of 1,3-Enynes

2.1. Palladium/Senphos catalyzed *trans*-selective chloroboration of 1,3-enynes

2.1.1. Introduction

Multi-substituted alkenes are key building blocks in organic syntheses.[1] Thus, the stereoselective syntheses towards these motifs are desirable but challenging.[2] Among various methods, alkyne difunctionalization reactions provide a useful route to multi-substituted alkenes[3] because of their highly atom-economical and versatile nature and the ease in starting alkyne preparation.[4] To enable selective downstream derivations of the resulting alkenes, it would be ideal if the two installed groups are chemically distinguishable from one another. An illustrative example would be alkyne haloboration

[1] For recent reviews, see: (a) Ogba, O. M.; Warner, N. C.; O'Leary, D. J.; Grubbs, R. H. *Chem. Soc. Rev.* **2018**, *47*, 4510-4544; (b) Obligacion, J. V.; Chirik, P. J. *Nat. Rev. Chem*. **2018**, *2*, 15-34; (c) Kalck, P.; Urrutigoïty, M. *Chem. Rev*. **2018**, *118*, 3833-3861; (d) Lee, J. H.; Choi, S.; Hong, K. B. *Molecules* **2019**, *24*, 2634-2656; (e) Kaur, N.; Wu, F.; Alom, N.-E.; Ariyarathna, J. P.; Saluga, S. J.; Li, W. *Org. Biomol. Chem*. **2019**, *17*, 1643-1654; (f) Fiorito, D.; Scaringi, S.; Mazet, C. *Chem. Soc. Rev*. **2021**, *50*, 1391-1406.

[2] For reviews, see: (a) Flynn, A.B.; Ogilvie W. W. *Chem. Rev.* **2007**, *107*, 4698-4745; (b) Negishi, E.; Huang, Z.; Wang, G.; Mohan, S.; Wang, C.; Hattori, H. *Acc. Chem. Res.* **2008**, *41*, 1474-1485; (a) Eissen, M.; Lenoir, D. *ACS Sustainable Chem. Eng.* **2017**, *5*, 10459-10473; (d) Polák, P.; Váňová, H.; Dvořák, D.; Tobrman, T. *Tetrahedron Lett.* **2016**, *57*, 3684-3693; (e) Chinchilla, R.; Najera, C. *Chem. Rev.* **2014**, *114*, 1783-1826.

[3] For reviews, see: (a) Trost, B. M. *Angew. Chem. Int. Ed*. **1995**, *34*, 259-281; (b) Ansell, M. B.; Navarro, O.; Spencer, J. *Coord. Chem. Rev*. **2017**, *336*, 54-77; (c) Murakami, K.; Yorimitsu, H. *Beilstein J. Org. Chem*. **2013**, *9*, 278-302; (d) Yoshida, H. *ACS Catal.* **2016**, *6*, 1799-1811; (e) Bottcher, S. E.; Hutchinson, L. E.; Wilger, D. J. *Synthesis* **2020**, *52*, 2807-2820; (f) Yao, H.; Hu, W.; Zhang, W. *Molecules* **2021**, *26*, 105-135.

[4] For recent reviews, see: (a) Heravi, M. M.; Dehghani, M.; Zadsirjan, V.; Ghanbarian, M. *Curr. Org. Synth.* **2019**, *16,* 205-243; (b) Shaw, R.; Elagamy, A.; Althagafi, I.; Pratap, R. *Org. Biomol. Chem*. **2020**, *18,* 3797-3817.

reaction. In the corresponding product, the two alkenyl carbons possess different reactivities engendered by the installed halogen and boron groups (Figure 2.1). [5]

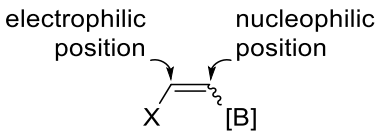

Figure 2.1. Reactivity differences in alkyne haloboration product.

2.1.2. Haloboration reaction of alkynes

Although discovered more than 80 years ago,[6] the alkyne haloboration reaction is still not well developed, presumably due to the unpredictable, and not so readily controllable reaction outcome in terms of selectivity. [7] The haloboration reaction of alkynes can lead to two diastereomers (Scheme 2.1),[8] which are summarized in the following sections, respectively.

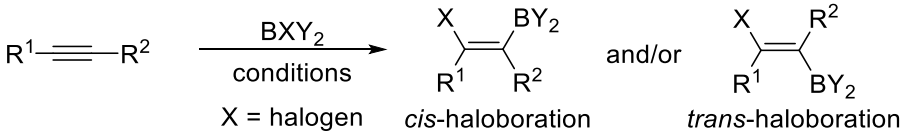

Scheme 2.1. Two possible outcomes of alkyne haloboration reaction.

[5] (a) Liu, C.; Zhang, H.; Shi, W.; Lei, A. *Chem. Rev.* **2011**, *111*, 3, 1780-1824; (b) Everson, D. A.; Weix, D. J. *J. Org. Chem.* **2014**, *79*, 11, 4793-4798; (c) Guinchard, X.; Bugaut, X.; Cook, C.; Roulland, E. *Chem. Eur. J.* **2009**, *15*, 5793-5798.

[6] (a) Arnold, H. R. New Organoboron Compounds. U. S. Patent 2402589, June 25, 1946; *Chem. Abstr.* **1946**, *40*, 5769; (b) Jensen, R. J.; Hayes, J. K.; Cluff, C. L.; Thorne, J. M. *IEEE J. Quantum Electron*. **1980**, *16*, 1352-1356.

[7] Kirschner, S.; Yuan, K.; Ingleson, M. J. *New J. Chem*. **2021**, Advance Article, doi:10.1039/D0NJ02908D.

[8] For 1,1-haloboration reaction, see: K. Yuan, K.; Kahan, R. J.; Si, C.; Williams, A.; Kirschner, S.; Uzelac, M.; Zysman-Colman, E.; Ingleson, M. J. *Chem. Sci.* **2020**, *11*, 3258-3267.

2.1.2.1. *Cis*-haloboration reaction of alkynes

The Lappert group[9] and the Blackborow group[10] first demonstrated the *cis*-haloboration reaction of aryl and alkyl substituted terminal alkynes. The reactions proceed readily with the boron group preferentially adding to the less sterically hindered carbon. However, small amount of regioisomers and multi-chloroboration products are always observed (Scheme 2.2).

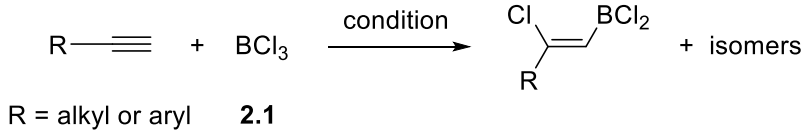

Scheme 2.2. *Cis*-chloroboration of terminal alkynes with BCl_3.

To minimize the formation of multi-chloroboration products, less Lewis acidic B–Cl containing reagents are used, such as $PhBCl_2$ **2.2** and Ph_2BCl **2.4**.[9] However, neither of them improved the selectivity, even worse, additional products such as *cis*-carboboration products **2.3** and **2.5** are observed (Scheme 2.3).

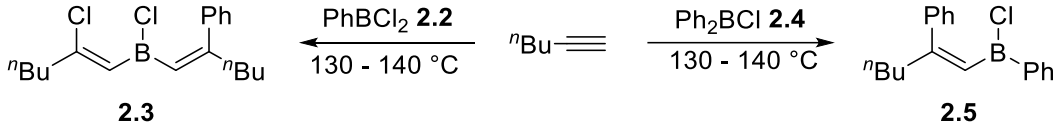

Scheme 2.3. Alkyne *cis*-carboborations with phenyl substituted chloroboranes.

Electronically or sterically biased mono-chloro boron reagents such as Cl–BCat **2.6**,[9] *B*–Cl-9-BBN (BBN: 9-borabicyclo[3.3.1]nonane) **2.7**[11] and $Cl–B(C_6F_5)_2$ **2.8**[12] have been discovered to suppress the multi-chloroboration products. However, in the latter

[9] Lappert, M. F.; Prokai, B. *J. Organomet. Chem.* **1964**, *1*, 384-400.
[10] (a) Blackborow, J. R. *J. Organomet.Chem.* **1977**, *128*, 161-166; (b) Blackborow, J. R. *J. Chem. Soc., Perkin Trans. 2* **1973**, 1989-1993.
[11] (a) Suzuki, A. *Pure and Applied Chemistry* **1986**, *58*, 629-638; (b) Hara, S.; Satoh, Y.; Ishiguro, H.; Suzuki, A *Tetrahedron Lett*. **1983**, *24*, 735-738.
[12] Ueno, A.; Li, J.; Daniliuc, C. G.; Kehr, G.; Erker, G. *Chem. Eur. J.* **2018**, *24*, 10044-10048.

case, the resulting $C_{alkenyl}$–B bond is susceptible to undergo alkyne insertion reaction to form polyenes.

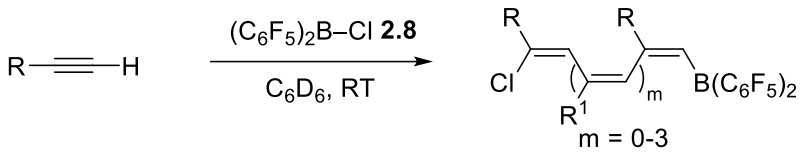

Scheme 2.4. Synthesis of polyenes through *cis*-chloroboration reactions.

To achieve a more selective *cis*-haloboration reaction with an easily accessible haloboration reagent, BBr_3 **2.9** was examined. A close study of the bromoboration reaction of 1-hexyne reveals that the reaction is highly dependent on the reaction temperature.[10a] As shown in Scheme 2.5, conducting the reaction at –20 ℃ affords a mixture of *cis*- and *trans*-bromoboration products whereas at –80 ºC the desired *cis*-product is obtained with high diastereoselectivity (98:2).

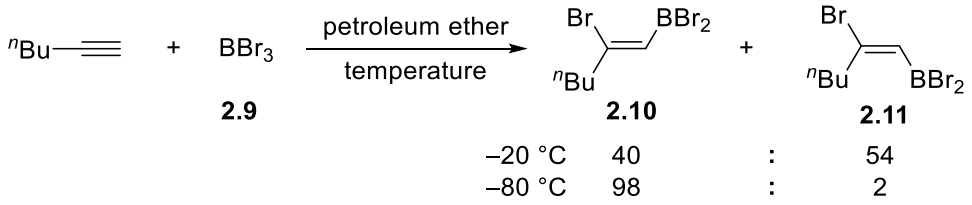

Scheme 2.5. Temperature-dependent *cis*-bromoboration reaction of terminal alkynes.

The superior diastereoselectivity plus the abundant BBr_3 feedstock allow the alkyne *cis*-bromoboration reaction to be utilized in organic syntheses,[13] including natural product syntheses.[14] For example, *cis*-bromoboration reaction of alkyne **2.12** yields a

[13] (a) Hara, S.; Kato, T.; Shimizu, H.; Suzuki, A. *Tetrahedron Lett*. **1985**, *26*, 1065-1068; (b) Satoh, Y.; Serizawa, H.; Miyaura, N.; Hara, S.; Suzuki, A. *Tetrahedron Lett.* **1988**, *29*, 1811-1814; (c) Yamashina, N.; Hyuga, S.; Hara, S.; Suzuki, A. *Tetrahedron Lett.* **1989**, *30*, 6555-6558; (d) Yao, M. L.; Reddy, M. S.; Zeng, W.; Hall, K.; Walfish, I.; Kabalka, G. W. *J. Org. Chem.* **2009**, *74*, 1385-1387.

[14] (a) Wang, K. K.; Wang, Z.; Tarli, A.; Gannett, P. *J. Am. Chem. Soc.* **1996**, *118*, 10783-10791; (b) Xu, Z.; Negishi, E. *Org. Lett.* **2008**, *10*, 4311-4314; (c) Wang, C.; Tobrman, T.; Xu, Z.; Negishi, E. *Org. Lett.* **2009**, *11*, 4092-4095.

versatile organic intermediate **2.13** where both carbon–heteroatom bonds are engaged in the following stereo-retentive cross-coupling reactions to afford yellow scale pheromone **2.14** in 6 steps (Scheme 2.6).[14b]

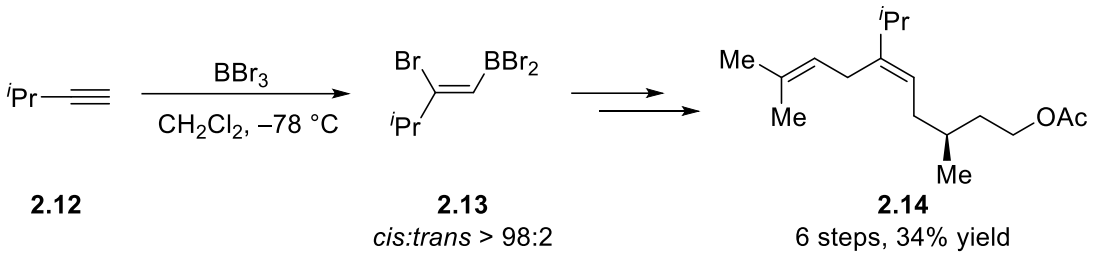

Scheme 2.6. Application of *cis*-bromoboration reaction in the total synthesis of a natural product.

Diaryl acetylenes, such as diphenylacetylene, are inert toward BCl_3 at room temperature.[9] On the other hand, the *cis*-bromoboration reactions of diaryl acetylenes take place smoothly in the presence of a stronger Lewis acid such as BBr_3[8,9] or $PhBBr_2$ (Scheme 2.7).[15] The corresponding products (compounds **2.16** and **2.19)** are regarded as kinetic products, and with extended reaction period, they tend to isomerize to the thermodynamically more stable 1,1-bromoboration product **2.15** and *cis*-carboboration product **2.18** (Scheme 2.7, eq. 1 and 2), respectively. Such transformation is absent in the *cis*-iodoboration product of diphenylacetylene (Scheme 2.7, eq. 3).[16]

[15] Eisch, J. J.; Gonsior, L. J. *J. Organomet. Chem.* **1967**, *8*, 53-64.
[16] Eisch, J. J.; Becker, H. P. *J. Organomet. Chem*. **1979**, *171*, 141-153.

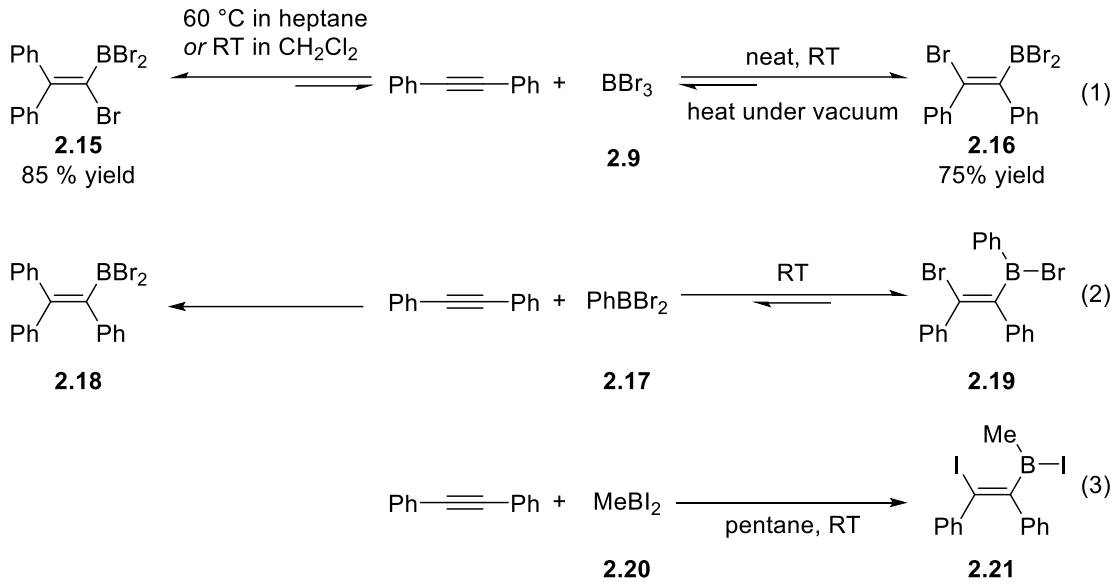

Scheme 2.7. Haloboration reactions of diaryl acetylenes.

The c*is*-haloboration products of dialkyl acetylenes exhibit different isomerization pathways.[17] Similar to the diphenylacetylene scenario where the *cis*-bromoboration products are formed initially, compound **2.22**, the *cis*-bromoboration product of 3-hexyne, isomerizes to the thermodynamically more stable *trans*-product **2.23** after several days (Scheme 2.8).

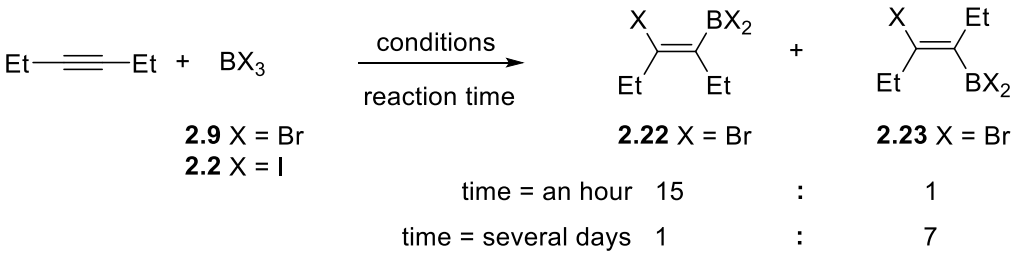

Scheme 2.8. Haloboration reactions of dialkyl acetylenes.

The origin of the *cis*-selectivity in alkyne haloboration reaction are elucidated by MP2 (second-order Møller-Plesset perturbation theory) level calculations with propyne as

[17] (a) Wrackmeyer, B. *Polyhedron* **1986**, *5*, 1709-1721; (b) Nie, Y.; Schwiegk, S.; Pritzkow, H.; Siebert, W. *Eur. J. Inorg. Chem*. **2004**, 2004, 1630-1638.

the model substrate (Scheme 2.9).[18] In terms of the mechanism, electrophilic BX_3 first forms a weak Van der Waals complex with propyne, which then yields the π-bonded complex in the case of the more electrophilic BBr_3 and BI_3. Next, two regioisomers are formed via the corresponding four-membered transition states (Scheme 2.9). The top transition state is lower in energy than the bottom one due to the extra stabilization of the partially positively charged carbon through methyl hyperconjugation and the minimized steric interactions between the methyl and the boron group. The authors also discovered that the transition state barrier is closely related to the electrophilicity of the boron reagent where BCl_3 leads to the highest barrier among the BX_3 series (X = Cl, Br and I). Therefore, the existence of a sterically crowded and very electrophilic boron group would help achieve highly regioselective alkyne haloboration reactions under mild reaction conditions.

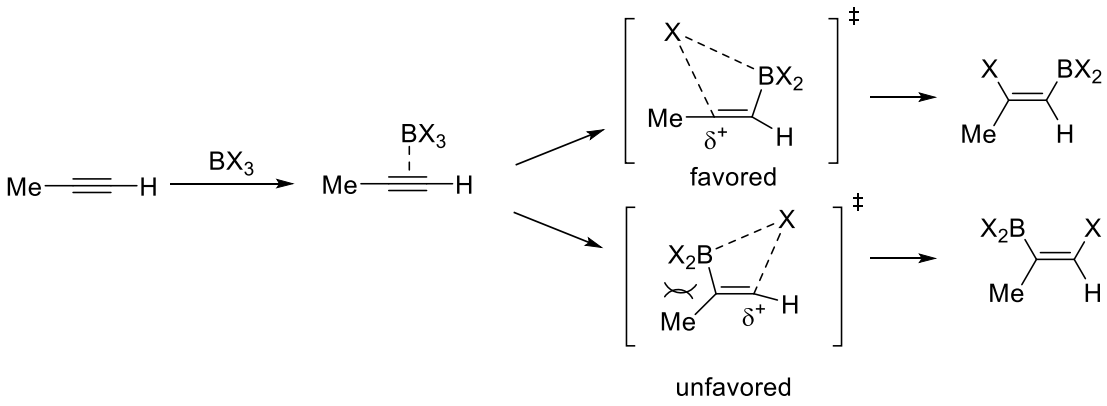

Scheme 2.9. Mechanistic illustration of the regioselectivity in terminal alkyne *cis*-haloboration reactions.

[18] Wang, C.; Uchiyama, M. *Eur. J. Org. Chem.* **2012**, *2012*, 6548-6554.

Inspired by this computational discovery, Ingleson successfully applied a series of highly electrophilic borenium **2.24** and boronium **2.25** reagents [19] in alkyne *cis*-chloroboration reactions (Scheme 2.10). [20] Terminal, symmetrical and unsymmetrical internal alkynes are viable substrates, providing the *cis*-chloroboration products as single stereoisomers. Assisted by DFT calculations, the reaction is proposed to involve a vinyl cation intermediate **2.26** followed by an exothermic chloride 1,3-migration to form intermediate **2.27**. The coordination of a pendant base, although not essential, stabilizes the boron group thus avoiding possible side reactions.

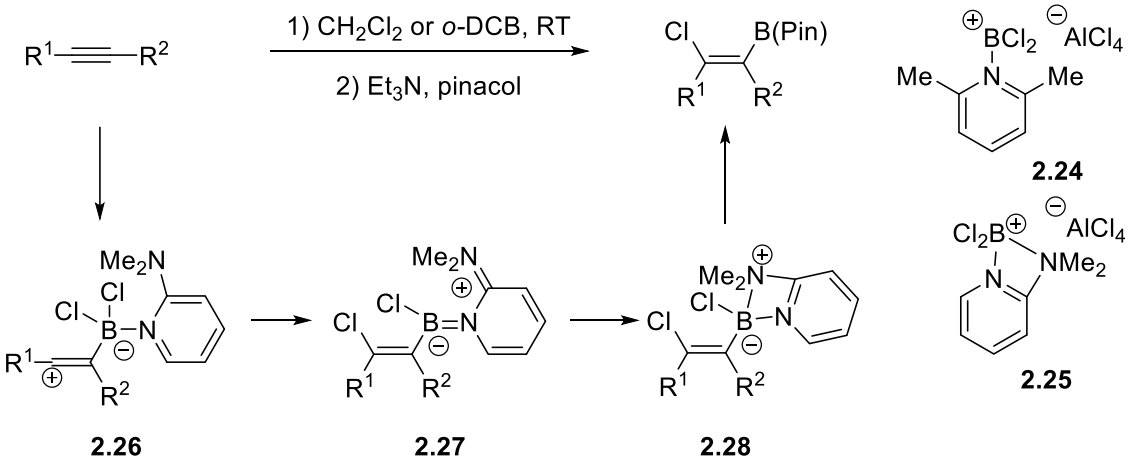

Scheme 2.10. *cis*-Chloroboration of alkynes with boronium and borenium reagents.

[19] Piers, W. E.; Bourke, S. C.; Conroy, K. D. *Angew. Chem. Int. Ed.* **2005**, *44,* 5016-5036; (b) De Vries, T. S.; Prokofjevs, A.; Vedejs, E. *Chem. Rev*. **2012**, *112*, 4246-4282; (c) Solomon, S. A.; Del Grosso, A.; Clark, E. R.; Bagutski, V.; McDouall, J. J. W.; Ingleson, M. J. *Organometallics* **2012**, *31*, 1908-1916.

[20] Lawson, J. R.; Clark, E. R.; Cade, I. A.; Solomon, S. A.; Ingleson, M. J. *Angew. Chem. Int. Ed.* **2013**, *52*, 7518-7522.

2.1.2.2. *Trans*-haloboration reaction of alkynes

Trans-haloboration reaction of alkynes are less developed comparing to the *cis* version. Ethyne was discovered to undergo *trans*-selective haloboration reactions with BCl_3 [6,21] and BBr_3[9] without any traces of product isomerization.

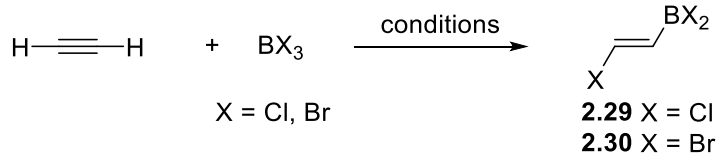

Scheme 2.11. *Trans*-haloboration reactions of ethyne.

Aided by calculations, the origin of the *trans*-selectivity of ethyne is disclosed and an addition/elimination pathway is proposed (Scheme 2.12).[18] First, two consecutive *cis*-bromoboration reactions occur with ethyne, providing geminal dibromoalkane **2.31**. Then the rotation of the C–C σ-bond leads to a less sterically hindered conformer **2.32**. Finally, a Br–BBr_2 *syn*-elimination yields the *trans*-product **2.30**.

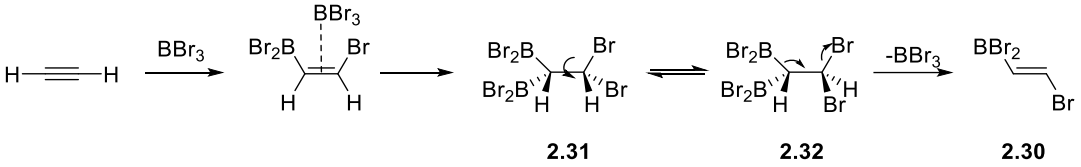

Scheme 2.12. *Trans*-bromoboration reaction of ethyne via addition/elimination pathway.

Recently, the Mazal group reported the inconsistency of the experimental observations with the previous computation results.[22] Their observation shows that the *trans:cis* ratio of the ethyne bromoboration product remains unchanged with extra BBr_3 but changes with HBr, a contaminant in BBr_3 reagent. Therefore, possible species related

[21] (a) Gipstein, E.; Kippur, P. R.; Higgins, M. A.; Clark, B. F. *J. Org. Chem*. **1961**, *26*, 943.
[22] Polášek, J.; Paciorek, J.; Stošek, J.; Semrád, H.; Munzarová, M.; Mazal, C. *J. Org. Chem.* **2020**, *85*, 6992-7000.

to HBr, namely bromide anion and bromine radical, are proposed to facilitate the formation of *trans*-product. Three pathways (Scheme 2.13) are validated by MP2 calculations: 1) *cis*-bromoboration reaction of ethyne occurs first, followed by bromine radical addition to yield radical **2.33**. Subsequent C–C σ-bond rotation and bromine radical extrusion affords *trans*-product **2.30**; 2) bromine radical adds to ethyne first and then the resulting vinyl radical **2.35** undergoes *cis*-bromoboration reaction to yield intermediate **2.34** in pathway 1; 3) a polar *trans*-addition reaction of ethyne with BBr_3 and a bromide anion yields alkene **2.36**, which then eliminates a bromide anion to generate the final product. All pathways are consistent with the experimental observations and are not distinguishable from one another.

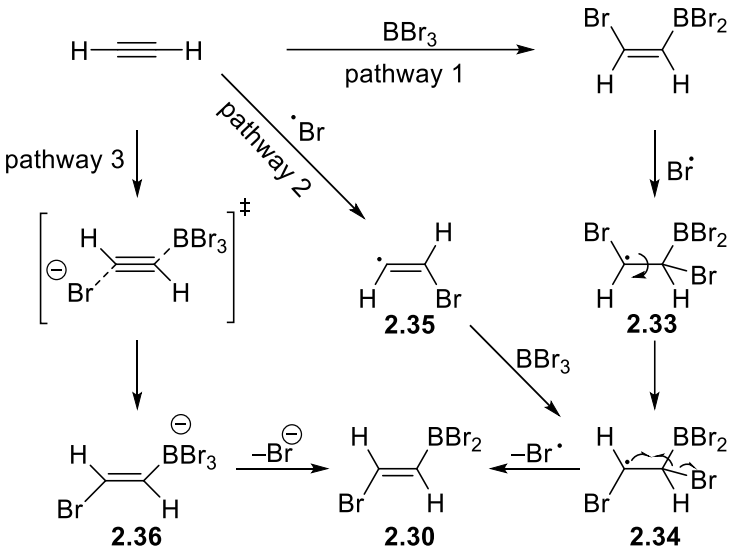

Scheme 2.13. Alternative mechanisms of ethyne *trans*-bromoboration reaction.

Terminal alkynes, as shown in chapter 2.1.2.1, usually undergo *cis*-haloboration reactions. However, in rare cases the *trans*-haloboration products are observed as the

major products (Scheme 2.14).[23] One common condition in these reactions is the presence of excess BX_3 reagents.

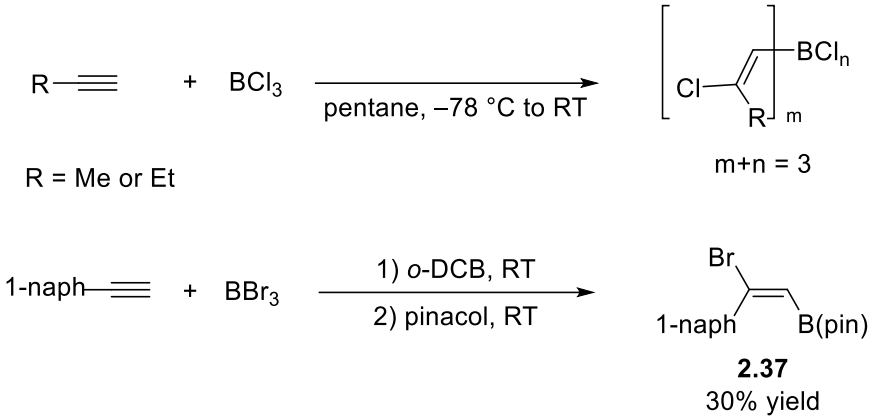

Scheme 2.14. *Trans*-haloboration reactions of terminal alkynes.

For *trans*-haloboration reaction of internal alkynes, only directed version has been reported which requires a Lewis base in proximity to the alkyne. The Yamato group reported the first directed *trans*-bromoboration reaction of di-*o*-anisylacetylene derivative **2.38** with BBr_3 (Scheme 2.15, top).[24] By the same token, *trans*-chloroborations of diaryl acetylene derivatives **2.40** and **2.41** are also achieved (Scheme 2.15, bottom).[25] Evidenced by both NMR (nuclear magnetic resonance) and X-ray crystallography analyses, in the products the boron group interacts with the adjacent Lewis base.

[23] (a) Bayer, M. J.; Pritzkow, H.; Siebert, W. *Z. Naturforsch. B* **2002**, *57*, 295-300; (b) Kahan, R. J.; Crossley, D. L.; Cid, J.; Radcliffe, J. E.; Ingleson, M. J. *Angew. Chem. Int. Ed.* **2018**, *57*, 8084-8088.
[24] Uchikawa, Y.; Tazoe, K.; Tanaka, S.; Feng, X.; Matsumoto, T.; Tanaka, J.; Yamato, T. *Can. J. Chem.* **2012**, *90*, 441-449.
[25] Warner, A. J.; Churn, A.; McGough, J. S.; Ingleson, M. J. *Angew. Chem. Int. Ed*. **2017**, *56*, 354-358.

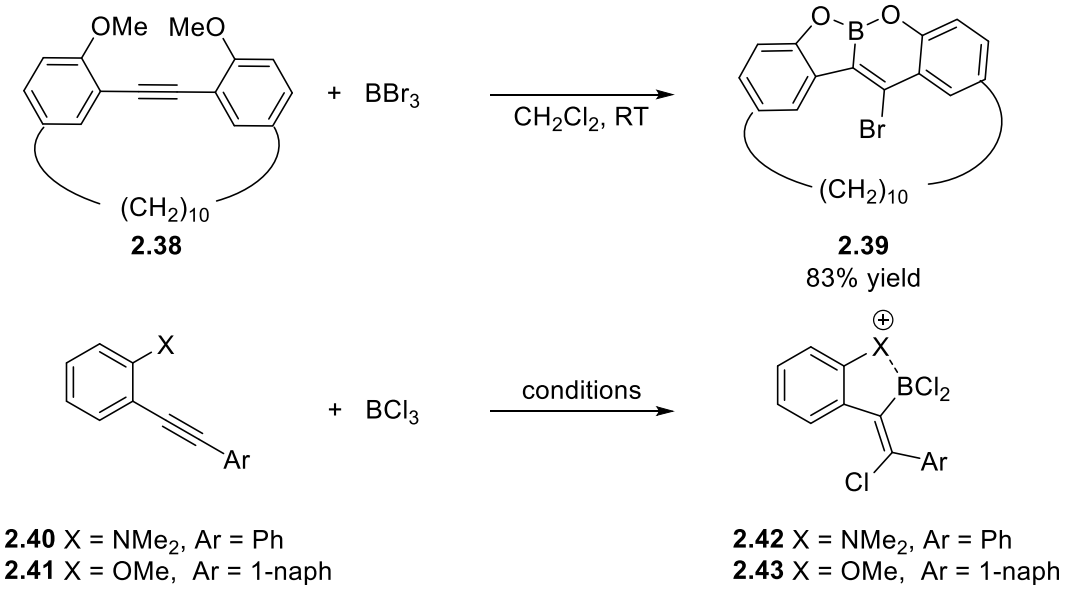

Scheme 2.15. Oxygen or nitrogen directed *trans*-haloboration reaction of alkynes.

A less Lewis basic alkyne can also act as a directing group. Ingleson reported a BCl_3 triggered annulative 1,4-*trans*-chloroboration reaction of bis-phenylacetylene **2.44**, affording benzofulvene **2.45** with two functional handles (Scheme 2.16).[26]

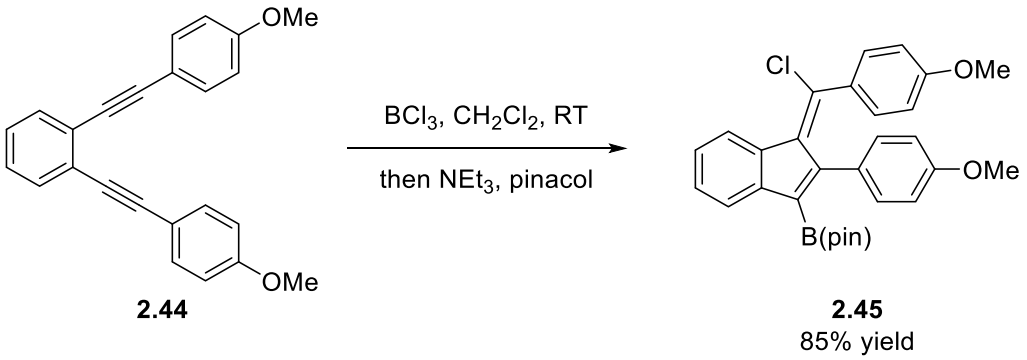

Scheme 2.16. Alkyne directed *trans*-haloboration reactions of bis-phenylacetylene.

A series of halogenated 2,1-borazaronaphthalenes **2.46** and **2.47** are obtained through *trans*-haloboration reactions of 2-ethynylaniline where the halogens come from

[26] Warner, A. J.; Enright, K. M.; Cole, J. M.; Yuan, K.; McGough, J. S.; Ingleson, M. J. *Org. Biomol. Chem.* **2019**, *17*, 5520-5525.

the ammonium salts NBu_4X (X = Br or I).[27] After $PhBCl_2$ condensation with aniline, the alkyne is activated by the adjacent boron group thus facilitating a halogen attack in a *trans* fashion to afford compounds **2.46** and **2.47**. Following the same mechanism, a double *trans*-chloroboration of diyne is reported, affording bis-1,2-azaborines.[28]

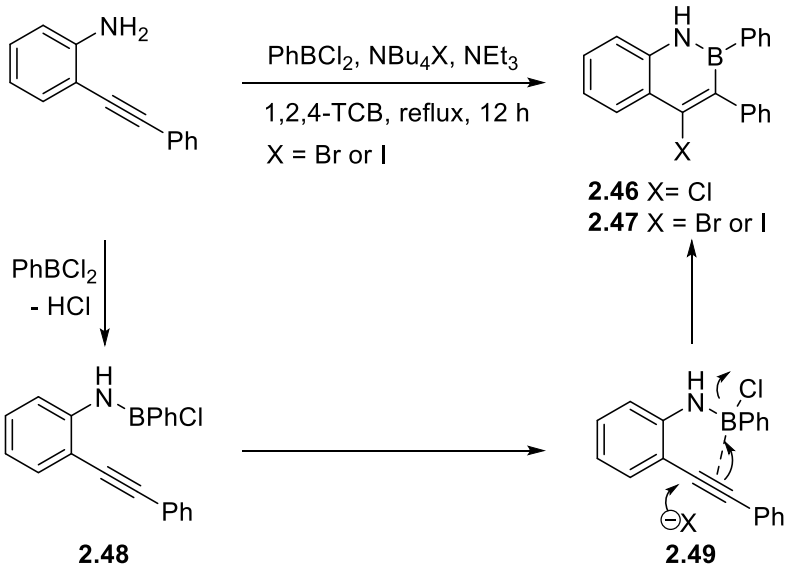

Scheme 2.17. Syntheses of 1,2-azaborines via *trans*-haloboration reactions.

2.1.3. Palladium/Senphos catalyzed *trans*-selective chloroboration of 1,3-enynes

Despite these advances in *trans*-haloboration reaction of alkynes, significant challenges still remain with respect to generality and substrate scope. In participle, a non-directed *trans*-haloboration reaction of internal alkyne has remained elusive. Inspired by our previous developments in *trans*-selective difunctionalization of 1,3-enynes,[29] we

[27] Zhuang, F.-D.; Han, J.-M.; Tang, S.; Yang, J.-H.; Chen, Q.-R.; Wang, J.-Y.; Pei, J. *Organometallics* **2017**, *36*, 2479-2482.
[28] Pati, P. B.; Jin, E.; Kim, Y.; Kim, Y.; Mun, J.; Kim, S. J.; Kang, S. J.; Choe, W.; Lee, G.; Shin, H.-J.; Park, Y. S. *Angew. Chem. Int. Ed*. **2020**, *59*, 14891-14895.
[29] (a) Xu, S.; Haeffner, F.; Li, B.; Zakharov, L. N.; Liu, S.-Y. *Angew. Chem. Int. Ed.* **2014**, *53*, 6795-6799; (b) Xu, S.; Zhang, Y.; Li, B.; Liu, S.-Y. *J. Am. Chem. Soc.* **2016**, *138*, 14566-14569.

focused on the expansion of Pd/Senphos catalytic system to address this unsolved 1,3-enyne *trans*-haloboration reaction.

2.1.3.1. Reaction optimization and discussion

With Cl–BCat **2.6** as the chloroboration reagent, Senphos **2.50** bound Pd(0) as the catalyst, and enyne **2.52** as the substrate, we commenced the optimization of the *trans*-chloroboration reaction. No reaction is detected at room temperature (Table 2.1, entry 1).[30] Heating the system at 110 °C leads to the formation of *trans:cis* stereoisomers in a ratio of 73:27 (entry 2). Varying the Pd precursor to Pd(COD)(CH_2TMS)$_2$ (COD: 1,5-cyclooctadiene) results in an inferior diastereoselectivity (entry 3). Among various solvents, *o*-DCB (1,2-dichlorobenzene) was determined to be the optimal reaction solvent (entries 4-7), providing a *trans:cis* ratio of 88:12 (entry 7). We found the reaction diastereoselectivity correlates to reaction temperature where higher temperature affords a higher *trans:cis* selectivity (entries 7-9). With a bulkier Senphos ligand **2.51**, the product diastereoselectivity is improved to over 98:2 (entries 10).

[30] At room temperature the palladium catalyst might be arrested by Cl–BCat via a reversible low-barrier oxidative insertion reaction, see: (a) Onozawa, S.-Y.; Tanaka, M. *Organometallics* **2001**, *20*, 2956-2958; (b) Braunschweig, H.; Gruss, K.; Radacki, K.; Uttinger, K. *Eur. J. Inorg. Chem*. **2008**, *2008*, 1462-1466; (c) Reid, W. B.; Spillane, J. J.; Krause, S. B.; Watson, D. A. *J. Am. Chem. Soc*. **2016**, *138*, 5539-5542.

Table 2.1. Optimization of Pd/Senphos catalyzed *trans*-chloroboration of 1,3-enyne.[a]

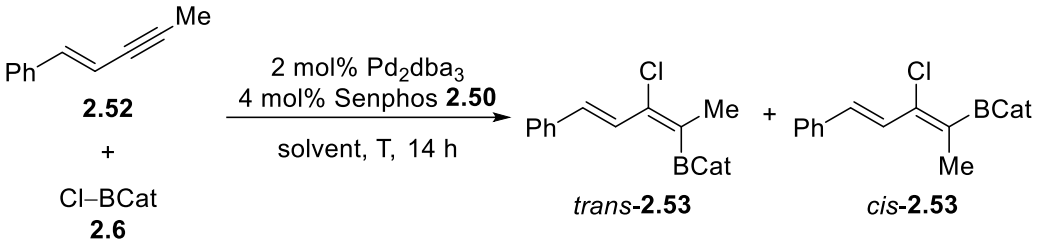

entry	T (°C)	solvent	Senphos	*trans*:*cis*[b]
1	25	$PhCH_3$	**2.50**	ND
2	110	$PhCH_3$	**2.50**	73:27
3[c]	110	$PhCH_3$	**2.50**	66:33
4	110	$(CHCl_2)_2$	**2.50**	55:45
5	110	$PhCF_3$	**2.50**	77:23
6	110	*o*-xylene	**2.50**	87:13
7	110	*o*-DCB	**2.50**	88:12
8	80	*o*-DCB	**2.50**	82:18
9	130	*o*-DCB	**2.50**	97:3[d]
10	130	*o*-DCB	**2.51**	> 98:2[e]

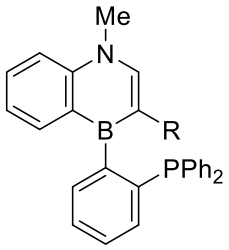

2.50 R = Et
2.51 R = ^{t}Bu

[a] Reaction was setup with 1.0 equiv. enyne **2.52**, 1.5 equiv. Cl–BCat **2.6** and 4 mol% catalyst loading in solvent (1 M) for 14 hours at the indicated temperature. [b] The diastereomeric ratio was determined by ^{1}H NMR of crude mixture. [c] $Pd(COD)(CH_2TMS)_2$ was used instead of Pd_2dba_3. [d] 70% ^{1}H NMR yield. [e] 54% ^{1}H NMR yield.

At current stage, isolation of the product *trans*-**2.53** appears to be non-trivial. After transesterification reaction of *trans*-**2.53** with pinacol, the desired pinacol ester **2.54** was observed in both ^{1}H NMR and HRMS (high resolution mass spectrometry). However, its purification through either silica gel or neutral alumina oxide column gave the starting enyne **2.52** exclusively.[31] A *trans*-elimination pathway is proposed where weak nucleophiles such as water or silica gel might facilitate such process. Similar transformations have been reported (Scheme 2.19, eq. 1 and 2),[23b,25] and this pathway is

[31] Converting product **2.53** to its BF_3K salt or engaging it *in situ* Suzuki-Miyaura cross coupling also leads to the generation of the starting enyne.

even utilized in the purification of pinacol ester (*Z*)-**2.57** from the *E*/*Z* mixture. (Scheme 2.19, eq. 3).[22]

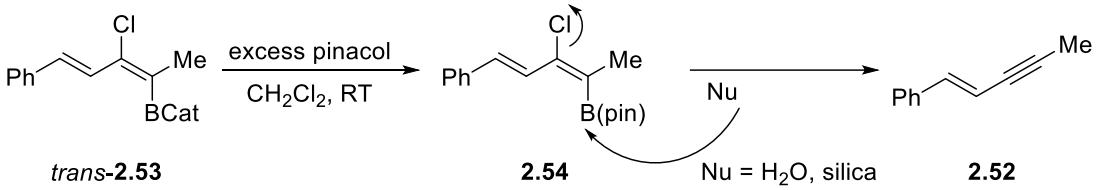

Scheme 2.18. Proposed *trans*-elimination pathway.

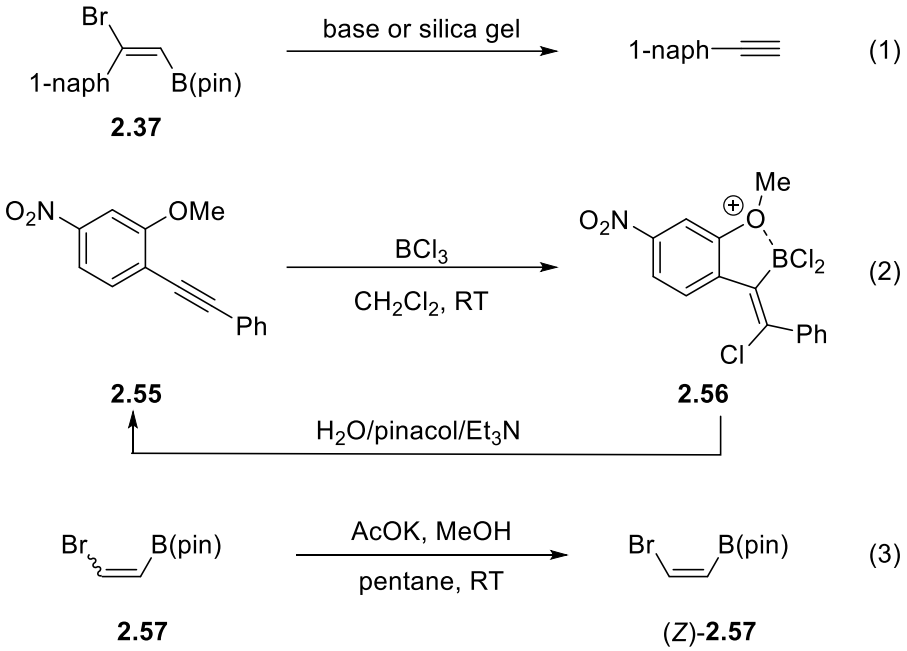

Scheme 2.19. Precedented *trans*-elimination process.

We further transformed product **2.53** to its dan (1,8-diaminonaphthlene) protected analog **2.58**.[32] After silica gel chromatography the product was isolated in good diastereoselectivity, albeit in poor yield (5%). The bond connectivity in product **2.58** was supported by single crystal X-ray diffraction analysis. The high propensity for *trans*-

[32] Noguchi, H.; Hojo, K.; Suginome, M. *J. Am. Chem. Soc.* **2007**, *129*, 758-759.

haloboration products to re-form to the alkyne significantly limit its synthetic utility, and we decided not to pursue its further development.

Table 2.2. Pd/Senphos catalyzed *trans*-chloroboration reaction of 1,3-enynes.

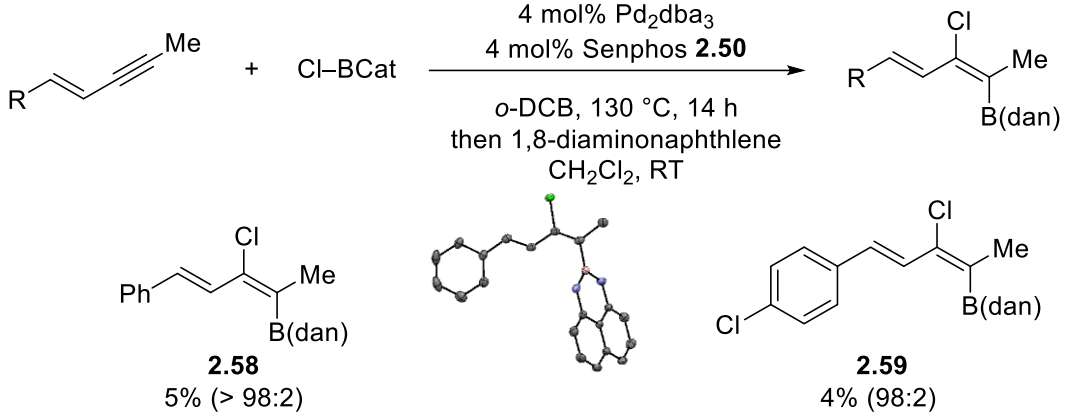

2.58
5% (> 98:2)

2.59
4% (98:2)

2.2. Palladium/Senphos catalyzed *trans*-selective cyanoboration of 1,3-enynes

2.2.1. Working hypothesis of Pd/Senphos catalyzed *trans*-difunctionalization of 1,3 enynes

The current Pd/Senphos catalyzed *trans*-chloroboration reaction of 1,3-enynes, though novel, is less practical in two folds: 1) the formation of C–Cl bond via Pd(II) reductive elimination is highly endothermic thus requiring harsh reaction conditions[33] and 2) the alkenyl chloro group the in product would facilitate the undesired *trans*-elimination process during the product purification. Therefore, bypassing the formation of a $C_{alkenyl}$–Cl bond would be the key to these issues. The Suginome group reported a series of alkyne *cis*-carboboration reactions starting from B–Cl containing reagents (Scheme 2.20,

[33] For reviews, see: (a) Vigalok, A. *Chem. Eur. J.* **2008**, *14*, 5102-5108; (b) Sheppard T. D. *Org. Biomol. Chem*. **2009**, *7*, 1043-1052; (c) Furuya, T.; Kamlet, A. S.; Ritter, T. *Nature* **2011**, *473*, 470-477; (d) Engle, K. M.; Mei, T.-S.; Wang, X.; Yu, J.-Q. *Angew. Chem. Int. Ed.* **2011**, *50*, 1478-1491; (e) Jiang, X.; Liu, H.; Gu, Z. *Asian J. Org. Chem*. **2012**, *1*, 16-24; (f) Chen, C.; Tong, X. *Org. Chem. Front.* **2014**, *1,* 439-446; (g) Petrone, D. A.; Ye, J.; Lautens, M. *Chem. Rev*. **2016**, *116*, 8003-8104.

left).[34] In a generic mechanism, Pd(0) oxidative insertion followed by β-migratory insertion affords complex **2.62**, which preferentially transmetalates with a broad range of carbon based nucleophiles rather than reductively eliminates to yield alkenyl chloride (Scheme 2.20, right). We envisioned such strategy would be applied to Pd/Senphos catalyzed *trans*-difunctionalization of 1,3 enynes with Cl–BCat as a relay reagent.

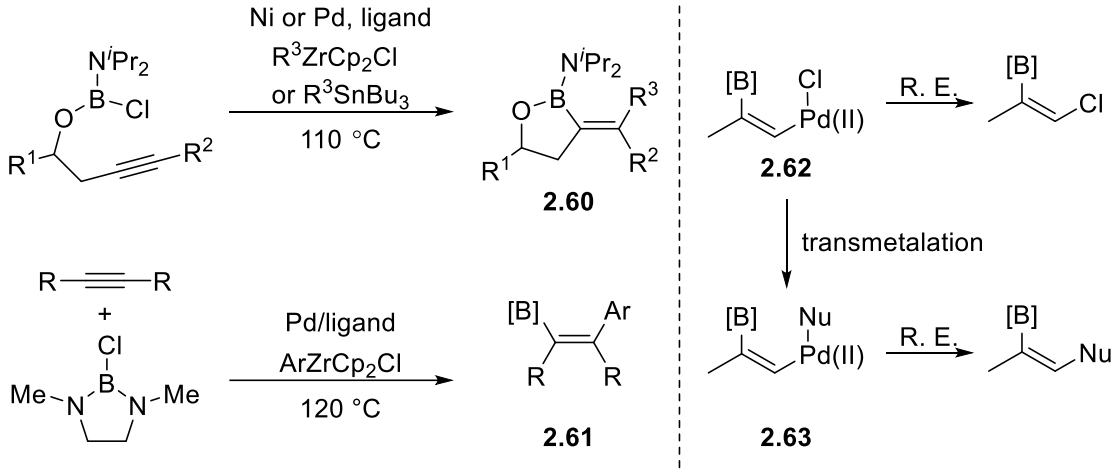

Scheme 2.20. Suginome's transmetalation on Pd(II) species.

Thus, with Cl–BCat as the boron source, Senphos **2.50** bound Pd(0) as the catalyst, and enyne **2.52** as the model substrate, we carried out the discovery of suitable transmetalation reagents (Table 2.3). Organo-zirconium, silyl enol ether or organo-tin reagents are not capable to afford the desired products (entries 1-3). On the other hand, when simple metal cyanide salts are engaged, the desired *trans*-cyanoboration product can be detected via ^{1}H NMR (entries 4-6). In contrast, tetrabutylammonium cyanide and tributyltin cyanide fail to transmetalate the cyanide to palladium (entries 7-8), emphasizing the importance of a transition metal cation.

[34] (a) Daini, M.; Yamamoto, A.; Suginome, M. *J. Am. Chem. Soc.* **2008**, *130*, 2918-2919; (b) Daini, M.; Yamamoto, A.; Suginome, M. *Asian J. Org. Chem.* **2013**, *2*, 968-976; (c) Nakada, K.; Daini, M.; Suginome, M. *Chem. Lett*. **2013**, *42*, 538-540; (d) Daini, M.; Suginome, M. *Chem. Commun*. **2008**, 5224-5226.

Table 2.3. Survey of transmetalation reagents in Pd/Senphos catalyzed *trans*-selective difunctionalization reaction of 1,3-enyne.[a]

entry	transmetalation reagent	^{1}H NMR observation (NMR yield)
1	PhCH=CHZr(Cp)$_2$Cl	ND[b]
2	vinyl-OTMS	ND[b]
3	^{n}Bu$_3$Sn-vinyl	NR[c]
4[d]	AgCN	*trans*-cyanoboration (5%)
5[d]	Zn(CN)$_2$	*trans*-cyanoboration (12%)
6[d]	CuCN	*trans*-cyanoboration (44%)
7	Bu$_4$NCN	NR[c]
8	Bu$_3$SnCN	NR[c]

[a] Reaction was setup with 1.0 equiv. enyne **2.52**, 1.5 equiv. Cl–BCat **2.6**, 1.5 equiv. transmetalation reagent and 4 mol% catalyst in *o*-DCB for 14 hours at 130 °C. [b] Not determined, enyne decomposition. [c] No reaction occurred. [d] Yields were determined by ^{1}H NMR of the crude mixture against internal standard.

2.2.2. Alkyne X–CN difunctionalizations

Alkenyl nitriles play an important role in the field of polymers,[35] pharmaceutics,[36] and agrochemistry.[37] Thus, the stereoselective syntheses toward substituted alkenyl nitriles have attracted significant attention. Among various methods, the alkyne X–CN difunctionalization is attractive because the concomitant installed cyano and X functional groups provide handles for possible structural diversifications.[38] Based on the relative position of X and CN in the product, the reaction can be categorized as *cis*- and *trans*-selective alkyne difunctionalizations.

[35] Brazdil, J. F. Acrylonitrile. In Ullmann's Encyclopedia of Industrial Chemistry, Wiley-VCH Verlag GmbH & Co. KGaA: Weinheim, Germany, 2012.

[36] (a) Fleming, F. F. *Nat. Prod. Rep.* **1999**, *16*, 597-606; (b) Fleming, F. F.; Yao, L.; Ravikumar, P. C.; Funk, L.; Shook, B. C. *J. Med. Chem.* **2010**, *53*, 7902-7917.

[37] Van Boven, M.; Blaton, N.; Cokelaere, M.; Daenens, P. *J. Agric. Food. Chem.* **1993**, *41*, 1605-1607.

[38] (a) Nakao, *Chem. Rev.* **2021**, *121*, 327-344; (b) Iyori, Y.; Ueno, R.; Morishige, A; Chatani, N. *Chem. Sci.* **2021**, 12, 1772-1777.

2.2.2.1. *Cis*-selective alkyne X–CN difunctionalizations

Cis-selective alkyne X–CN difunctionalizations have been widely studied and a large variety of functional groups can be installed along with the cyano group such as B,[39] C,[40] N,[41] O,[42] halogen,[43] Si,[44] S,[45] Se[45d] and Ge.[46]

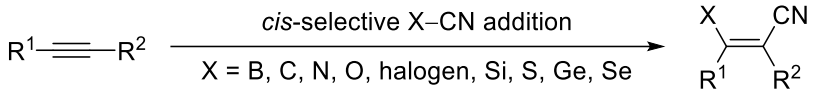

Scheme 2.21. *Cis*-selective alkyne X–CN difunctionalizations.

Among these difunctionalization methods, the *cis*-cyanoboration of alkynes is particularly appealing due to the rich functionalization chemistry of organoboron

[39] (a) Suginome, M.; Yamamoto, A.; Murakami, M. *J. Am. Chem. Soc.* **2003**, *125*, 6358-6359; (b) Suginome, M.; Yamamoto, A.; Murakami, M. *Angew. Chem. Int. Ed.* **2005**, *44*, 2380-2382; (c) Suginome, M.; Yamamoto, A.; Murakami, M. *J. Organomet. Chem.* **2005**, *690*, 5300-5308; (d) Ohmura, T.; Awano, T.; Suginome, M.; Yorimitsu, H.; Oshima, K. *Synlett* **2008**, 423-427.

[40] (a) Liu, B.; Wang, Y.; Chen, Y.; Wu, Q.; Zhao, J.; Sun, J. *Org. Lett.* **2018**, *20*, 3465-3468; (b) Arai, S.; Sato, T.; Koike, Y.; Hayashi, M.; Nishida, A. *Angew. Chem. Int. Ed.* **2009**, *48*, 4528-4531; (c) Arai, S.; Koike, Y.; Nishida, A. *Adv. Synth. Catal.* **2010**, *352*, 893-900; (d) Arai, S.; Sato, T.; Nishida, A. *Adv. Synth. Catal.* **2009**, *351*, 1897-1904; (e) Igarashi, T.; Arai, S.; Nishida, A. *J. Org. Chem.* **2013**, *78*, 4366-4372. For reviews, see: (f) Chen, P. H.; Billett, B. A.; Tsukamoto, T.; Dong, G. *ACS Catal.* **2017**, *7*, 1340-1360; (g) Wen, Q.; Lu, P.; Wang, Y. *RSC Adv.* **2014**, *4*, 47806-47826; (h) Kou, X.; Fan, J.; Tong, X.; Shen, Z. *Chin. J. Org. Chem.* **2013**, *33*, 1407-1422; (i) Tobisu, M.; Chatani, N. *Chem. Soc. Rev.* **2008**, *37*, 300-307.

[41] (a) Chen, L.; Cao, S.; Zhang, J.; Wang, Z. *Tetrahedron Lett.* **2019**, *60*, 1678-1681; (b) Liao, Z.-Y.; Liao, P.-Y.; Chien, T.-C. *Chem. Commun*. **2016**, *52*, 14404-14407; (c) Qiu, G.; Qiu, X.; Liu, J.; Wu, J. *Adv. Synth. Catal.* **2013**, *355*, 2441-2446.

[42] (a) Wang, X.; Studer, A. *J. Am. Chem. Soc.* **2016**, *138*, 2977-2980; (b) Zhu, Y.; Shen, Z. *Adv. Synth. Catal.* **2017**, *359*, 3515-3519.

[43] (a) Moreau, P.; Commeyras, A. *J. Chem. Soc., Chem. Commun.* **1985**, 817-818; (b) Murai, M.; Hatano, R.; Kitabata, S.; Ohe, K. *Chem. Commun.* **2011**, *47*, 2375-2377; (c) Barrado, A. G.; Zielinski, A.; Goddard, R.; Alcarazo, M. *Angew. Chem. Int. Ed.* **2017**, *56*, 13401-13405; (d) Lukashev, N. V.; Kazantsev, A. V.; Borisenko, A. A.; Beletskaya, I. P. *Tetrahedron* **2001**, *57*, 10309-10317.

[44] (a) Chatani, N.; Hanafusa, T. *J. Chem. Soc., Chem. Commun.* **1985**, 838-839; (b) Chatani, N.; Takeyasu, T.; Horiuchi, N.; Hanafusa, T. *J. Org. Chem.* **1988**, *53*, 3539-3548; (c) Suginome, M.; Kinugasa, H.; Ito, Y. *Tetrahedron Lett.* **1994**, *35*, 8635-8638.

[45] (a) Kamiya, I.; Kawakami, J.; Yano, S.; Nomoto, A.; Ogawa, A. *Organometallics* **2006**, *25*, 3562-3564; (b) Lee, Y. T.; Choi, S. Y.; Chung, Y. K. *Tetrahedron Lett.* **2007**, *48*, 5673-5677; (c) Bürger, M.; Loch, M. N.; Jones, P. G.; Werz, D. B. *Chem. Sci.* **2020**, *11*, 1912-1917; (d) Ozaki, T.; Nomoto, A.; Kamiya, I.; Kawakami, J.; Ogawa, A. *Bull. Chem. Soc. Jpn.* **2011**, *84*, 155-163.

[46] Chatani, N.; Horiuchi, N.; Hanafusa, T. *J. Org. Chem*. **1990**, *55*, 3393-3395.

derivatives.[47] The Suginome group reported the first intra- and inter-molecular *cis*-cyanoboration reaction of alkynes that catalyzed by Pd or Ni/ligand system (Scheme 2.22).[39a,b] And in the intermolecular case, various sterically- and electronically-biased cyanoboration reagents (compounds **2.67**-**2.70**) can be engaged to achieve good to excellent diastereoselectivity of both terminal and internal alkynes.

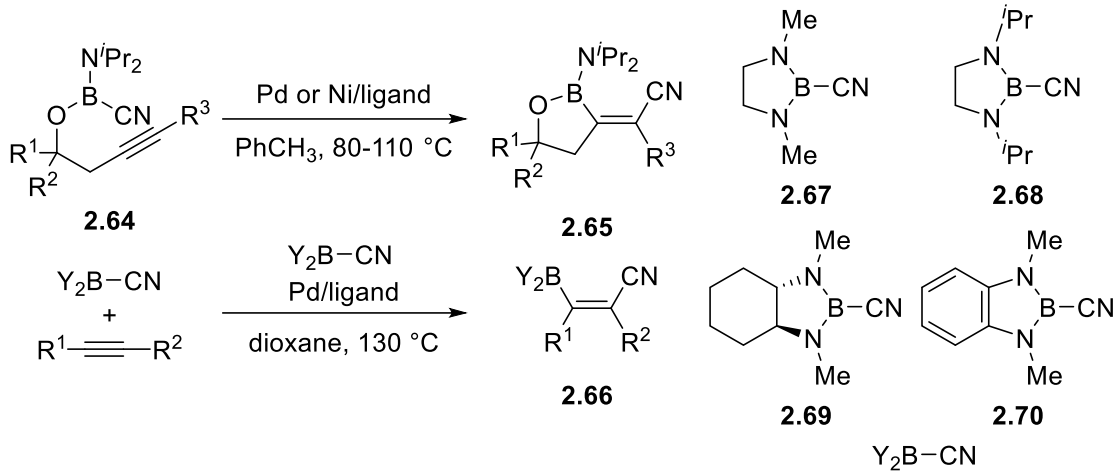

Scheme 2.22. Suginome's *cis*-cyanoboration reaction of alkynes.

The corresponding alkyne *cis*-cyanoboration mechanism is investigated in detail.[48] As shown in Scheme 2.23, palladium first coordinates with alkyne followed by a reversible oxidative insertion of Y_2B–CN to form intermediate **2.71**. Then β-migratory insertion occurs to provide intermediate **2.72**, which is in equilibrium with an 18-electron palladium species **2.73**. Subsequent reductive elimination of intermediate **2.72** provides the *cis*-cyanoboration product.

[47] For recent reviews, see: (a) Fyfe, W. B. J.; Watson, A. J. B. *Chem*, **2017**, *3*, 31-55: (b) Nguyen, V. D.; Nguyen, V. T.; Jin, S.; Dang, H. T.; Larionov, O. V. *Tetrahedron*, **2019**, *75*, 584-602; (c) Wen, Y.; Deng, C.; Xie, J.; Kang, X. *Molecules* **2019**, *24*, 101-116; (d) Pattison, G. *Org. Biomol. Chem.* **2019**, *17*, 5651-5660; (e) Yang, X.; Kalita, S. J.; Maheshuni, S.; Huang, Y.-Y. *Coord. Chem. Rev.* **2019**, *392*, 35-48.
[48] Suginome, M.;Yamamoto, A.; Sasaki, T.; Murakami, M. *Organometallics* **2006**, *25*, 2911-2913.

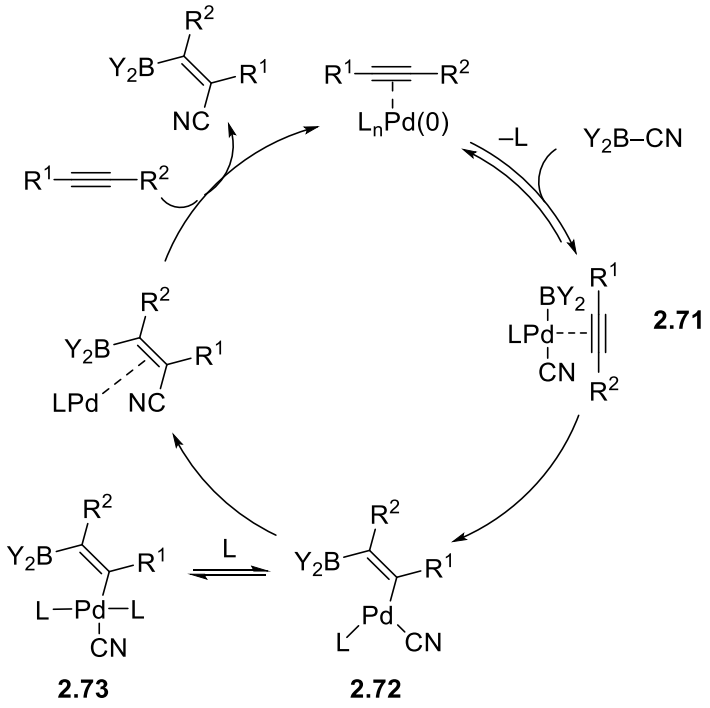

Scheme 2.23. Proposed mechanism of Suginome's alkyne *cis*-cyanoboration reaction.

2.2.2.2. *Trans*-selective alkyne X–CN difunctionalizations

In comparison to the numerous *cis*-selective alkyne X–CN difunctionalizations, the *trans*-selective version is less common. Tsuji and co-workers reported the first example where $PtCl_2(PPh_3)_2$ effectively catalyzes the *trans*-cyanostannylation reaction between tributyltin cyanide and dimethyl acetylenedicarboxylate (Scheme 2.24).[49] The transformation requires highly π-acidic di-substituted alkynes as the substrates, and mono-substituted alkynes only lead to the stannylation on the alkyne terminal position. The origin of the *trans*-selectivity is unknown.

[49] Obora, Y.; Baleta, A. S.; Tokunaga, M.; Tsuji, Y. *J. Organomet. Chem.* **2002**, *660*, 173-177.

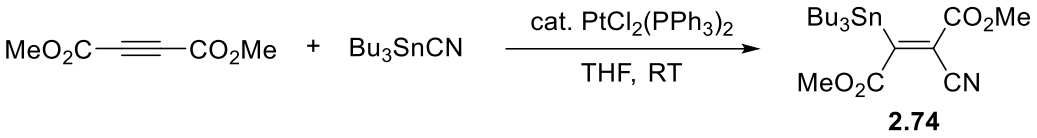

Scheme 2.24. Tsuji's platinum-catalyzed *trans*-cyanostannylation reaction.

The Ohe group disclosed a *trans*-selective iodocyanation reaction of alkynoates (Scheme 2.25).[50] The reaction between CuI and ICN **2.76** yields CuCN and I_2, which is rapidly consumed by alkynoates to generate and the (*E*)-di-iodo acrylate **2.77**. The ester oxygen then directs CuCN toward the oxidative insertion of the distal C–I bond while leaving the proximal C–I bond intact. Subsequent reductive elimination of complex **2.78** provides the *trans*-product. Simple alkynes that lack the ester directing group, such as 3-phenyl-1-propyne, result in a non-regioselective iodocyanation reaction.

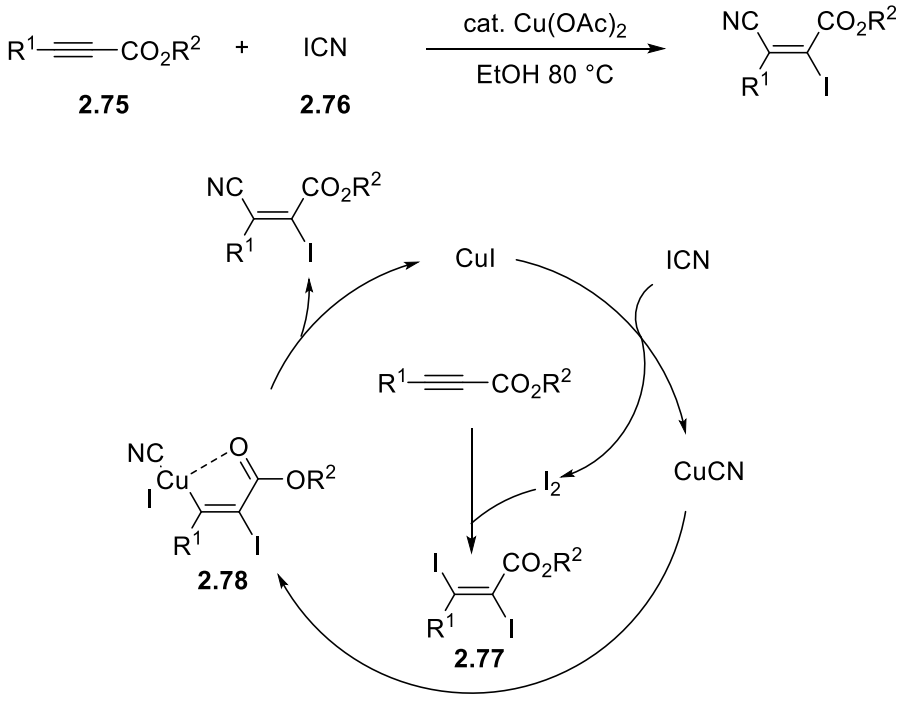

Scheme 2.25. Ohe's copper-catalyzed *trans*-iodocyanation reaction.

[50] Sakata, N.; Sasakura, K.; Matsushita, G.; Okamoto, K.; Ohe, K. *Org. Lett.* **2017**, *19*, 3422-3425.

A PPh_2Me catalyzed *trans*-selective acylcynantion reaction of alkynoates was reported by Sawamura (Scheme 2.26).[51] 1,4-Conjugate addition of alkynoate with PPh_2Me and trapping with acyl cyanide **2.79** forms phosphonium **2.81** via a zwitterionic allenolate intermediate **2.80**. Cyanide initiates another conjugate addition to intermediate **2.81** providing the zwitterion **2.82**, which then undergoes PPh_2Me extrusion to generate the product.

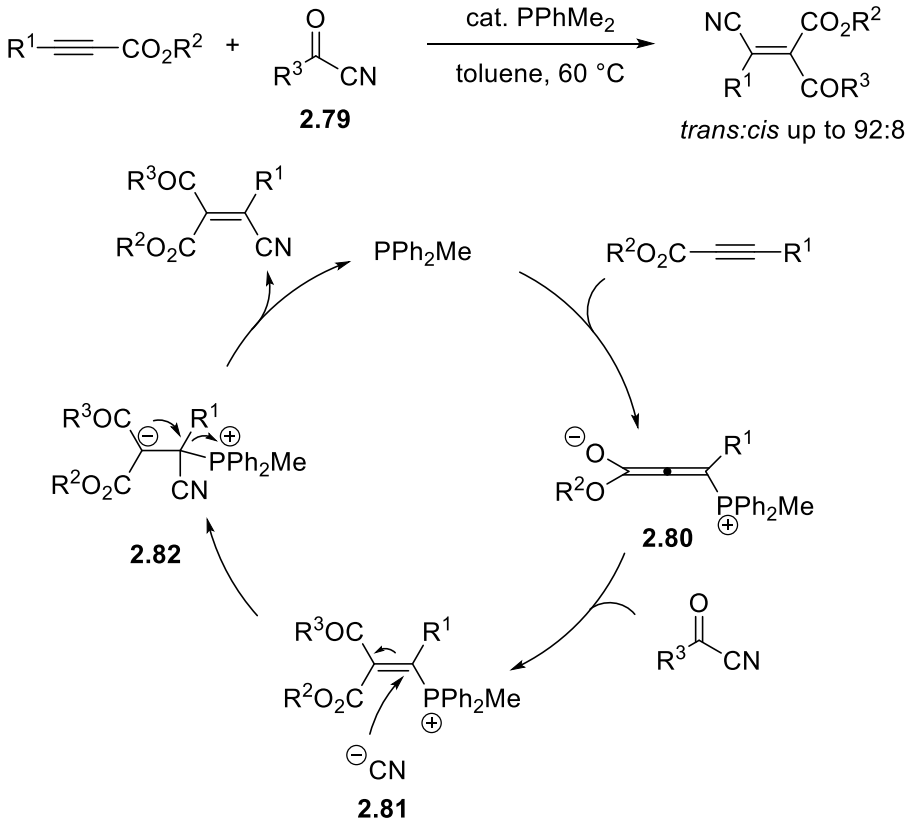

Scheme 2.26. Sawamura's phosphine-catalyzed *trans*-acylcynantion reaction.

Alkyne *trans*-selective X–CN addition can also be achieved under radical mechanism, as demonstrated in Liang's copper-mediated *trans*-cyano-difluoroalkylation

[51] Murayama, H.; Nagao, K.; Ohmiya, H.; Sawamura, M. *Org. Lett.* **2016**, *18*, 1706-1709.

reaction (Scheme 2.27).[52] Single electron transfer between Cu(0) and ICF_2CO_2Et yields CuI and CF_2CO_2Et radical, which subsequently adds to the alkyne to form vinyl radical **2.84**. Then, radical **2.84** reacts with TMSCN and CuI from the least sterically hindered site to form complex **2.85**, which reductively eliminates to furnish the *trans*-product **2.83**.

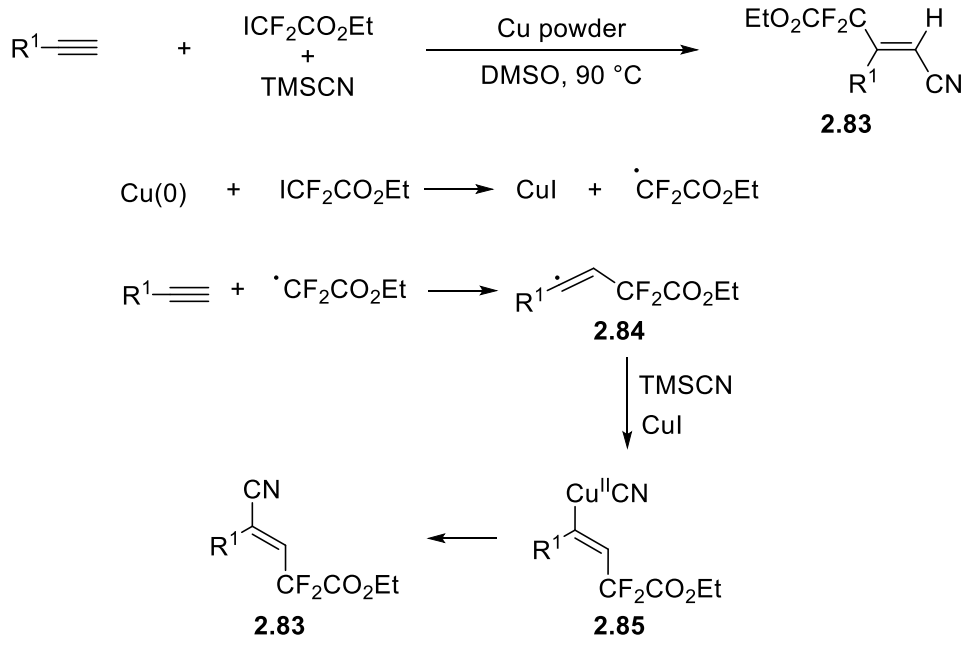

Scheme 2.27. Liang's copper-mediated *trans*-cyano-difluoroalkylation reaction.

The Ogawa group reported a palladium-catalyzed cyanothiolation reaction of symmetrical internal alkynes (Scheme 2.28).[53] As for the mechanism, palladium first oxidatively inserts into the disulfide, followed by β-migratory insertion into the alkyne to provide intermediate **2.86**. ^{t}Butyl isocyanide then coordinates to palladium with subsequent α-migratory insertion to provide intermediate **2.87-Pro-*syn***, which is in equilibrium with intermediate **2.87-Pro-*anti*** through an enamine intermediate. Both

[52] He, Y. T.; Li, L. H.; Wang, Q.; Wu, W.; Liang, Y. M. *Org. Lett.* **2016**, *18*, 5158-5161.
[53] Higashimae, S.; Kurata, D.; Kawaguchi, S. I.; Kodama, S.; Sonoda, M.; Nomoto, A.; Ogawa, A. *J. Org. Chem.* **2018**, *83*, 5267-5273.

diastereomers are able to undergo β-alkyl elimination/reductive elimination to afford the products.

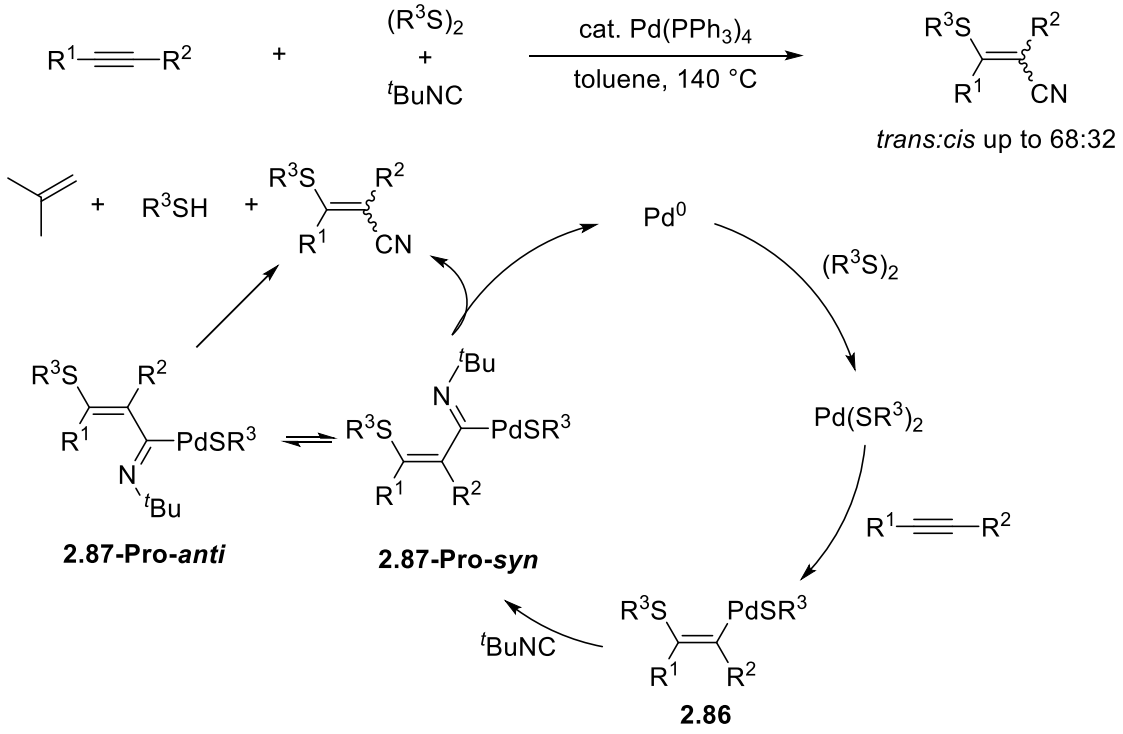

Scheme 2.28. Ogawa's palladium-catalyzed cyanothiolation reaction.

Despite the current advances in *trans*-selective alkyne X–CN difunctionalizations, no *trans*-selective cyanoboration reaction of alkynes has been reported where the installed boron group would be a useful handle for further transformations. With our preliminary result in a site-, regio- and *trans*-selective enyne cynaoboration reaction, we continued to optimize the reaction conditions.

2.2.3. Senphos as a unique ligand for *trans*-selective cyanoboration of 1,3-enynes[54]

2.2.3.1. Reaction optimization

With Cl–BCat **2.6** as the boron source, CuCN as the cyanide source and enyne **2.52** as the model substrate, the reactivity and selectivity of *trans*-cyanoboration was evaluated in terms of the ligand structure. In all cases the chloroboration product *trans*-**2.53** is determined to be the major side product. As shown in Table 2.4, the absence of a supporting ligand does not lead to a productive and chemo-selective reaction (entry 1). The presence of a monodentate phosphine ligand ($PhPCy_2$) or Buchwald ligand (XPhos: 2-dicyclohexylphosphino-2′,4′,6′-triisopropylbiphenyl) promotes the formation of both products, albeit in low yields (entries 2 and 3). On the other hand, the presence of a bidentate phosphine ligand (dppe: 1,2-bis(diphenylphosphino)ethane) aids the generation of *trans*-chloroboration product and shuts down the *trans*-cyanoboration pathway (entry 4). The use of Senphos as supporting ligands leads to a substantial increase in the *trans*-cyanoboration product yield, with greater than 95:5 *trans:cis* selectivity while minimizing the formation of *trans*-chloroboraion product (entries 5-10). The substituent R at the C(3) position of the ligand has a profound influence on reaction yield, presumably due to its proximity to the catalytically active palladium center. When Senphos **2.89** that bears the methyl group at the C(3) position, is employed as the ligand, the reaction gives the desired product in superior yield (entry 6) compared to those with bigger (entries 7-9) and smaller (entry 5) R substituents. Switching the boron substituent from the *o*-dicyclohexyl-phosphinophenyl to *o*-diphenyl-phosphinophenyl group results in diminished reactivity (Table 1, entry 6 *vs*. 10). We determined that ligand **CC-2.89**, the

[54] This section is partially adapted from Zhang, Y.; Li, B.; Liu, S.-Y. *Angew. Chem. Int. Ed.* **2020**, *59*, 15928-15932.

carbonaceous analogue of the best performing Senphos ligand, is inferior to Senphos **2.89** with regard to reaction efficiency and selectivity (entry 11 *vs*. entry 6), highlighting the importance of the unique electronic structure of the 1,4-azaborine motif in promoting the reaction.

Table 2.4. Pd-catalyzed *trans*-cyanoboration as a function of ligand structure.[a]

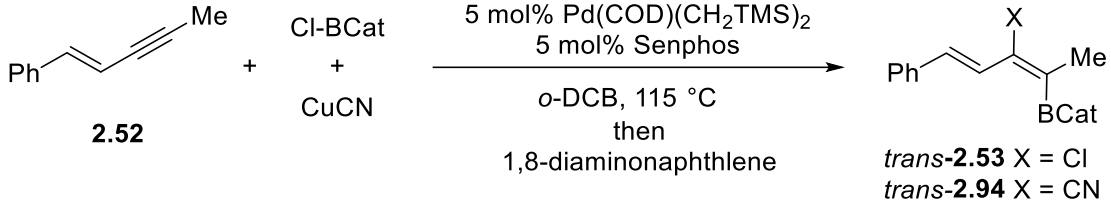

Entry	L	**2.53** Yield *(trans:cis)* [a]	**2.94** Yield *(trans:cis)* [b]
1	none	3% (75:25)	3% (89:11)
2	$PhPCy_2$	4% (77:23)	13% (95:5)
3	XPhos	7% (59:41)	10% (90:10)
4	dppe	12% (66:34)	0.3% (ND)
5	**2.88**	2% (69:31)	79% (97:3)
6	**2.89**	1% (78:22)	92% (96:4)
7	**2.90**	2% (73:27)	69% (95:5)
8	**2.91**	5% (71:29)	48% (95:5)
9	**2.92**	5% (71:29)	24% (95:5)
10	**2.93**	3% (66:34)	46% (96:4)
11	**CC-2.89**	13% (81:19)	6% (89:11)

[a] Determined by ^{1}H NMR of the crude mixture *vs.* a calibrated internal standard in crude NMR. [b] Determined by ^{1}H NMR of the crude mixture after quenching with 1,8-diaminonaphthlene.

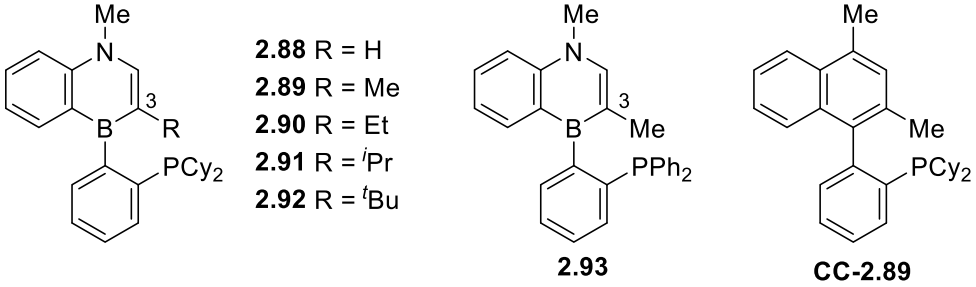

2.2.3.2. Substrate scope and discussion

Under optimized reaction conditions, various alkyl substituted (*E*)-1,3-enynes (R^2 = alkyl) were subjected to the Pd/Senphos catalyzed *trans*-cyanoboration reaction followed by quenching with 1,8-diaminonaphthalene or pinacol, and the results are summarized in Table 2.5. High *trans*-selectivity was observed consistently with an array of electronically (e.g., entries **2.98**-**2.104**) and sterically different (e.g., entries **2.97** and **2.106**) substituents on the alkene. In addition to arenes, the R^1 position also tolerates heteroarenes (entries **2.107** and **2.108**) and alkyl groups (entries **2.109**-**2.113**). Functional groups such as aryl halides (entries **2.101**-**2.103**), alkyl chloride (entry **2.110**), esters (entries **2.104** and **2.113**), methoxy (entry **2.98**), and alcohol (with pre-treatment with HBCat; entry **2.112**) are also tolerated. When the steric demand of the R^2 substituent is increased from Me to Et, a slight decrease in diastereoselectivity was observed (entry **2.95** *vs*. **2.114**). For 2-furyl substituted 1,3-enyne substrate, Senphos **2.93** was a superior ligand compared to Senphos **2.89** with regard to reaction selectivity (entry **2.107**).[55] The terminal enyne substrate required higher catalyst loading at a lower reaction temperature and shorter reaction time (entry **2.115**). The bond connectivity and stereochemistry of two *trans*-cyanoboration products **2.96** and **2.105** were confirmed by single crystal X-ray diffraction analysis.

[55] When the reaction was performed with Senphos **2.89** as the ligand, the product **2.107** was obtained in 81% yield 94:6 (*trans*:*cis)* ratio.

Table 2.5. Pd/Senphos catalyzed *trans*-cyanoboration of alkyl/terminal 1,3-enynes (R^2 = alkyl/H).[a]

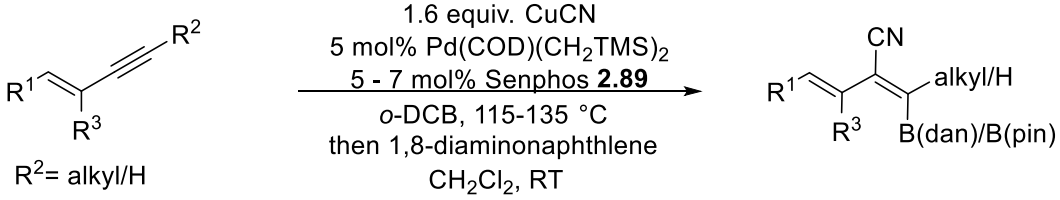

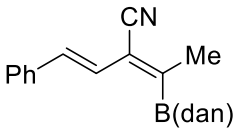

2.95
86% (96:4)

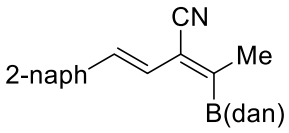

2.96
77% (98:2)

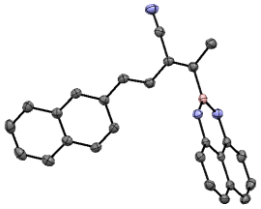

X-ray structure of **2.96**

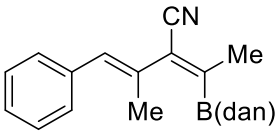

2.97
63% (>98:2)

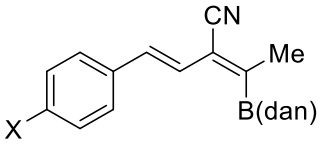

2.98 X = OMe 64% (96:4)
2.99 X = Me 87% (97:3)
2.100 X = CF_3 80% (>98:2)
2.101 X = F 66% (96:4)
2.102 X = Cl 84% (>98:2)
2.103 X = Br 55 % (95:5)
2.104 X = CO_2Et 69% (>98:2)

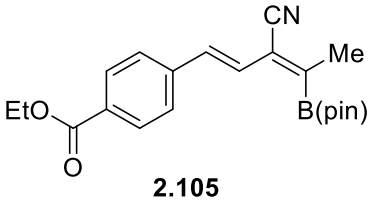

2.105
56% (>98:2)

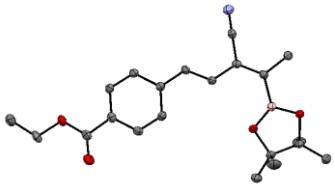

X-ray structure of **2.105**

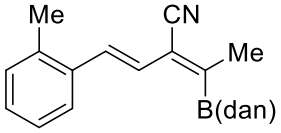

2.106
58% (94:6)[b]

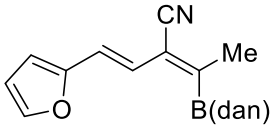

2.107
71% (98:2)[b]

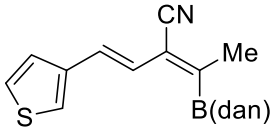

2.108
72% (97:3)

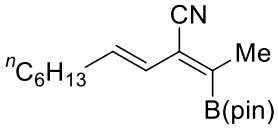

2.109
60% (96:4)

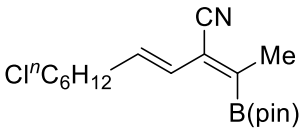

2.110
55% (96:4)

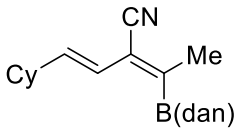

2.111
60% (93:7)

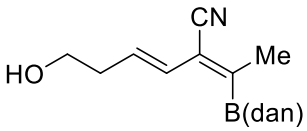

2.112
35% (98:2)[c]

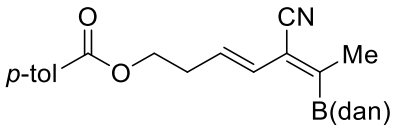

2.113
73% (96:4)

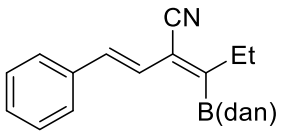

2.114
66% (93:7)

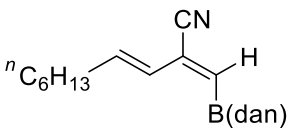

2.115
66% (93:7)[d]

[a] Yields of isolated isomerically pure *trans*-product (average of 2 runs) based on the starting enyne. The diastereomeric ratio in parenthesis (*trans:cis*) was determined by ^{1}H NMR of the crude material after addition of 1,8-diaminonaphthalene or pinacol. [b] Senphos **2.93** was used instead of Senphos **2.89**. [c] The substrate enyne was first pre-treated with HBCat before subjecting it to the reaction conditions. [d] 10 mol% catalyst loading, 90 °C, 40 min reaction time.

For aryl (*E*)-1,3-enynes (R^2 = Ar) , we determined that Senphos **2.93** was a superior ligand compared to Senphos **2.89**.[56] The diastereoselectivity of the reaction for diaryl 1,3-enynes (R^1 = Ar, R^2 = Ar) substrates is dependent on the electronic nature of the R^2 substituent, where electron deficient R^2 groups resulting in higher *trans*-selectivity (entry **2.119** and **2.118** *vs*. **2.117** and **2.116**). On the other hand, for monoaryl 1,3-enynes (R^1 = alkyl or heteroatom, R^2 = Ar), the observed *trans*-cyanoboration selectivity remains excellent (>94:6) regardless of the electronic nature of the R^2 substituent (entries **2.120-2.124**). Good diastereoselectivity was also observed for the alkenyl silane and alkenyl chloride substrates, albeit with diminished yields (entries **2.123** and **2.124**). For terminal 1,3-enyne (R^1 = H, R^2 = Ar), diminished yield and diastereoselectivity were observed (entry **2.125**). The X-ray crystal structure of product **2.122** was obtained, thus unambiguously establishing connectivity and diastereoselectivity.

[56] When the reaction was performed with Senphos **2.89** as the ligand, the product **2.121** was obtained in 46% yield with (91:9) *trans*:*cis* ratio.

Table 2.6. Pd/Senphos catalyzed *trans*-cyanoboration of aryl 1,3-enynes (R^2 = Ar).[a]

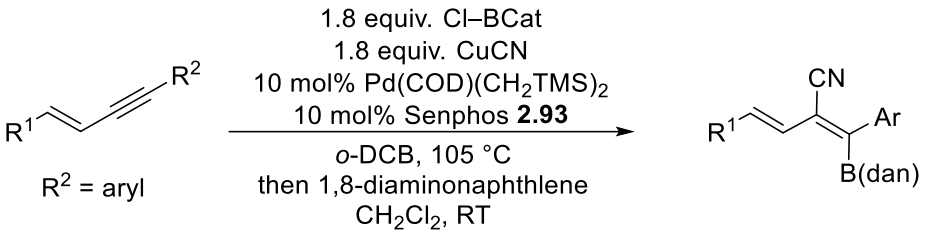

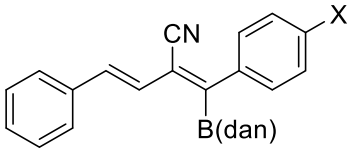

2.116 X = H 60% (86:14)
2.117 X = Me 48% (75:25)
2.118 X = CF_3 84% (93:7)

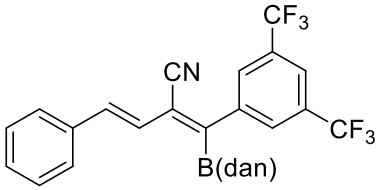

2.119
86% (>98:2)

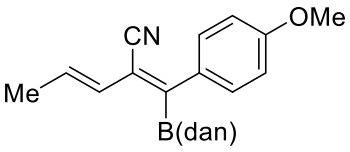

2.120
71% (94:6)

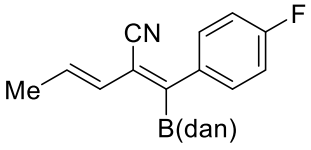

2.121
70% (95:5)

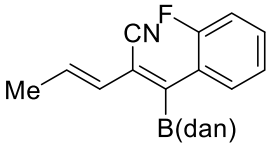

2.122
63% (98:2)

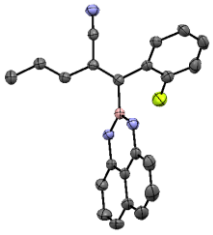

X-ray structure of **2.122**

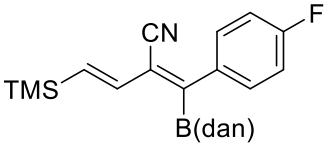

2.123
38% (94:6)

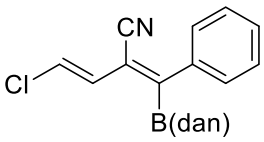

2.124
28% (96:4)[b]

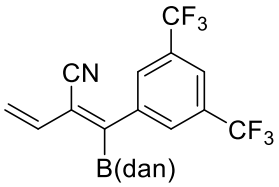

2.125
27% (66:34)

[a] Yields of isolated isomerically pure *trans*-product (average of 2 runs), based on the starting enyne. The diastereomeric ratio in parenthesis (*trans*:*cis*) was determined by ^{1}H NMR of the crude material after addition of 1,8-diaminonaphthalene. [b] 15 mol% catalyst loading, 1.2 equiv. CuCN, 1.6 equiv. Cl–BCat, 90 °C, 25 min.

We note several limitations with regard to the scope of the substrate (Figure 2.2). For example, (*E*)-1,3-enynes with free or protected allylic alcohol moiety compounds

2.126-2.128 are not viable substrates (enyne decompositions were observed). Moreover, the steric hindrance around enyne plays an important role as little reactivity is observed with alkynyl ^{t}Bu substituted enyne **2.129** or geminal disubstituted enyne **2.130**.

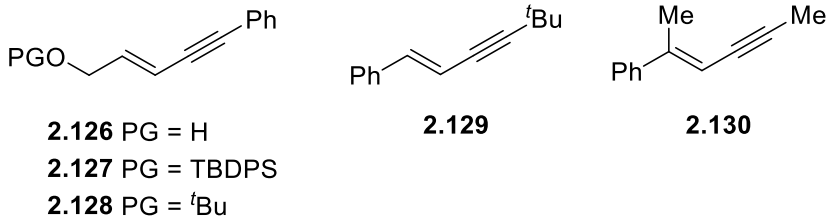

2.126 PG = H
2.127 PG = TBDPS
2.128 PG = ^{t}Bu

2.129 **2.130**

Figure 2.2. Challenging 1,3-enyne substrates in Pd/Senphos catalyzed *trans*-cyanoboration reaction.

2.2.3.3. Derivatizations of 1,3-enyne *trans*-cyanoboration products

The Pd/Senphos catalyzed *trans*-cyanoboration reactions afford various vicinal boron-substituted alkenylnitriles, which are versatile synthesis building blocks (Scheme 2.29). For example, *trans*-cyanoboration product **2.95** undergoes hydrolysis followed by Pd/XPhos catalyzed Suzuki-Miyaura coupling with bromobenzene or 4-*B*(dan)-bromobenzene to furnish tetra-substituted alkenes **2.132** and **2.133** in 86% and 85% yield, respectively, with complete retention of olefin stereochemistry. Furthermore, fluorination of boronic acid **2.131** with Selectfluor[57] produces a novel (*E*)-2-nitrile-fluorodiene motif **2.134**. The boron-substituted alkenylnitriles are also demonstrated to undergo regioselective hydrogenation. For example, when *trans*-cyanoboration product **2.122** is subjected to Pd/C catalyzed hydrogenation condition, tetra-substituted borylated alkenylnitrile **2.135** is obtained after transesterification with pinacol (Scheme 2.29, eq. 1).

[57] Furuya, T.; Ritter, T. *Org. Lett.* **2009**, *11*, 2860-2863.

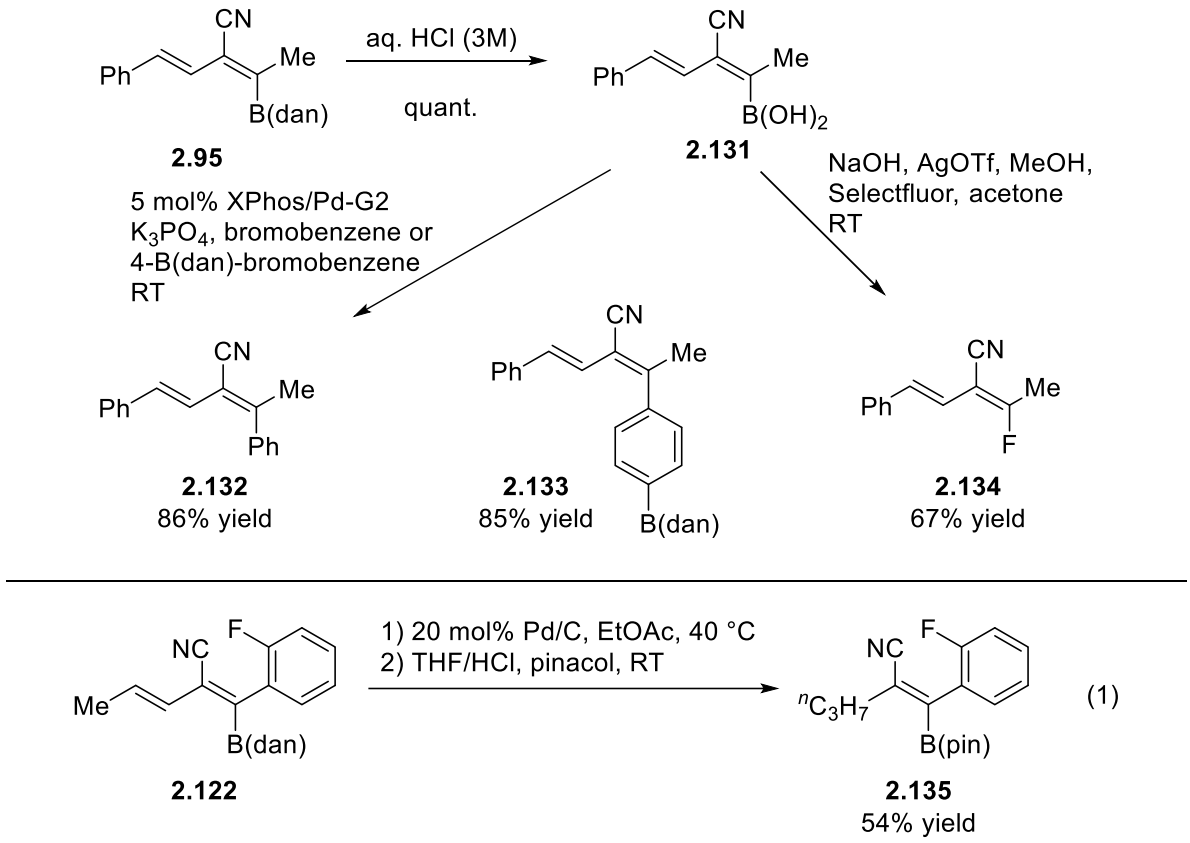

Scheme 2.29. Functionalization of *trans*-cyanoboration products.

Finally, we applied our *trans*-selective cyanoboration reaction to the synthesis of Satigrel **2.138**, an anti-platelet aggregating agent that contains a tetra-substituted acrylonitrile core.[58,59] The original synthesis starts with the condensation between 4,4'-di-

[58] (a) Fujimori, T. H.; K.; Saeki, T.; Kogushi, M.; Akasaka, K.; Yamagishi, Y.; Yamatsu, I. *Arzneim. Forsch.* **1987**, *37*, 1143-1148; (b) Hoshi, S.; Goto, M.; Koyama, N.; Nomoto, K.; Tanaka, H. *J. Biol. Chem.* **2000**, *275*, 883-889; (c) Nakajima, T.; Kitajima, I.; Shin, H.; Matsumoto, W.; Soejima, Y.; Maruyama, I. *Biochem. Biophys. Res. Commun.* **1994**, *203*, 1181-1187; (d) Fujimori, T.; Harada, K.; Saeki, T.; Kogushi, M.; Katayama, K.; Satoh, M. *Cardiovasc. Drug Rev.* **1991**, *9*, 264-284.

[59] For bioactive molecules containing multi-substituted alkenylnitrile motif, see (a) Carpenter, C.; Sorenson, R. J.; Jin, Y.; Klossowski, S.; Cierpicki, T.; Gnegy, M.; Showalter, H. D. *Bioorg. Med. Chem*. **2016**, *24*, 5495-5504; (b) Sit, S. Y.; Parker, R. A.; Motoc, I.; Balasubramanian, W. H. N.; Catt, J. D.; Brown, P. J.; Harte, W. E.; Thompson, M. D.; Wright, J. J. *J. Med. Chem*. **1990**, *33*, 2982-2999; (c) Benjahad, A.; Courté, K.; Guillemont, J.; Mabire, D.; Coupa, S.; Poncelet, A.; Csoka, I.; Andries, K.; Pauwels, R.; de Béthune, M.-P.; Monneret, C.; Bisagni, E.; Nguyen, C. H.; Grierson, D. S. *J. Med. Chem*. **2004**, *47*, 5501-5514; (d) Ruchelman, A. L.; Man, H. W.; Chen, R.; Liu, W.; Lu, L.; Cedzik, D.; Zhang, L.; Leisten, J.; Collette, A.; Narla, R. K.; Raymon, H. K.; Muller, G. W. *Bioorg. Med. Chem*. **2011**, *19*, 6356-6374.

methoxy benzophenone **2.136** and α-bromo-nitrile ester **2.137** in the presence of Zn metal followed by saponification to afford Satigrel (Scheme 2.30). Although concise, a mixture of diastereomers would be likely obtained if unsymmetrical benzophenones are utilized in the condensation step.

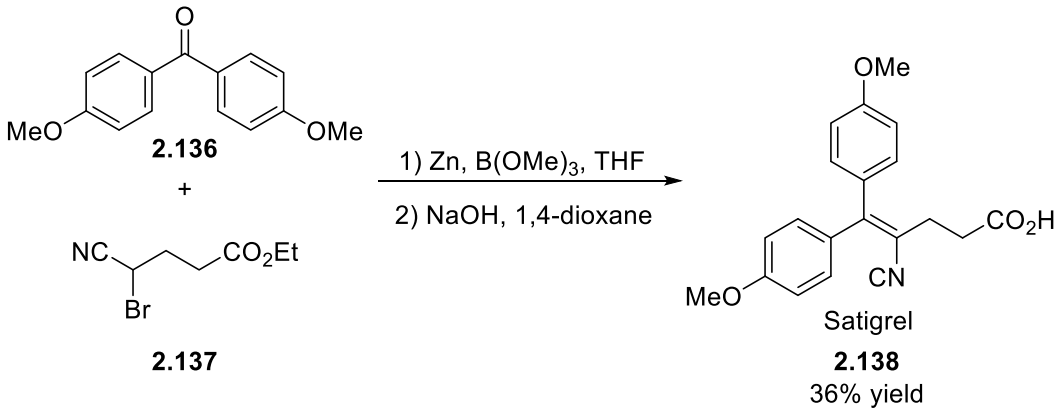

Scheme 2.30. Original synthesis route of Satigrel.

Now with a stereoselective method for the construction of tetra-substituted acrylonitriles at our disposal, we reasoned that Satigrel could be synthesized from *trans*-cyanoboration product **2.120** in a straightforward fashion (Scheme 2.31).

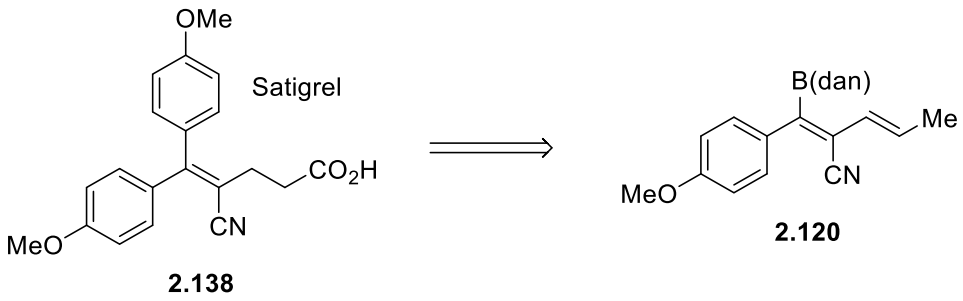

Scheme 2.31. Retrosynthesis of Satigrel from *trans*-cyanoboration product.

We commenced with the transesterification of *trans*-cyanoboration product **2.120** with pinacol followed by Suzuki-Miyaura cross coupling to produce a variety of bis-aryl substituted dienenitriles **2.139-2.141** in a stereospecific manner (Scheme 2.32). The bis-

4-methoxy-phenyl dienenitrile **2.139** was then subjected to oxidation condition[60] to yield carboxylic acid **2.142**. Finally, catalytic hydrogenation[61] selectively reduced the more accessible alkene to furnish Satigrel **2.138**. This synthesis offers a modular and stereoselective approach towards bis-aryl substituted dienenitriles, taking advantage of the versatile boron functional handle.

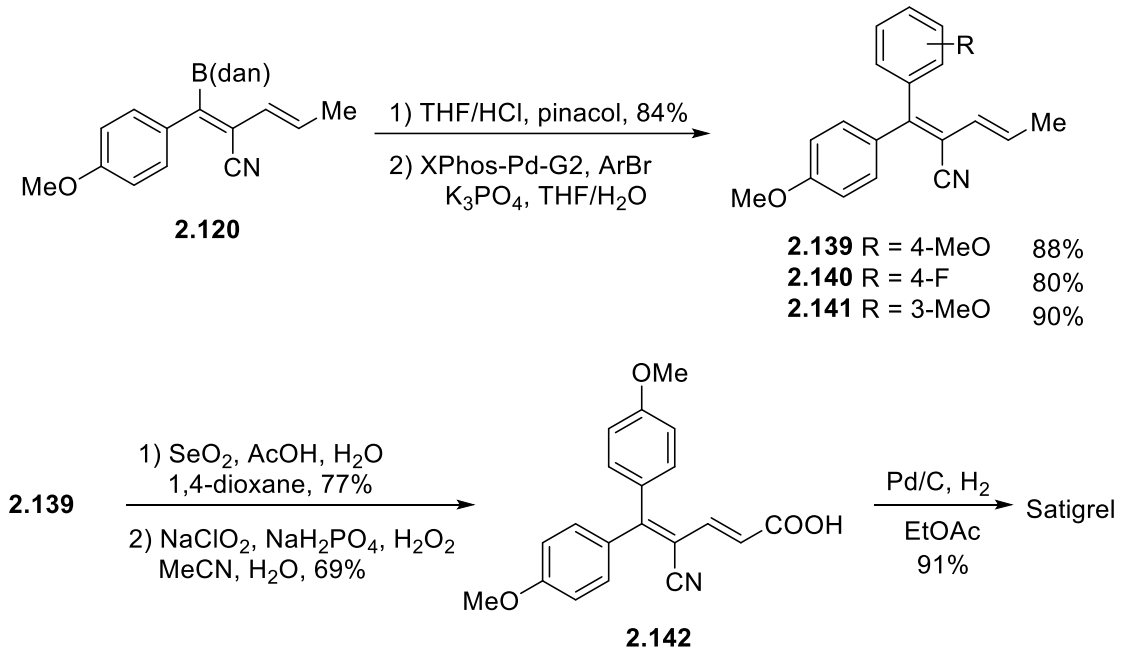

Scheme 2.32. Synthesis of Satigrel.

2.2.4. Reaction mechanism investigation

The Suginome group reported the *cis*-cyanoboration reaction of alkynes utilizing B–CN containing cyanoboration reagents (Scheme 2.22),[39a,b] whereas in our example the boron and cyanide groups are from different molecules. To exclude the possibility of the *in situ* generated BCat–CN **2.143** as the active reagent, we independently synthesized

[60] (a) Moazami, Y.; Gulledge, T. V.; Laster, S. M.; Pierce, J. G. *Bioorg. Med. Chem. Lett.* **2015**, *25*, 3091-3094; (b) Huang, Q.; Pennington, J. D.; Williams, H. J.; Scott, A. I. *Synth. Commun.* **2006**, *36*, 2577-2585; (c) Dalcanale, E.; Montanari, F. *J. Org. Chem.* **1986**, *51*, 567-569.
[61] Majetich, G.; Yu, J. *Can. J. Chem.* **2012**, *90*, 75-84.

BCat–CN from Cl–BCat and TMSCN (Scheme 2.33, eq. 1). The reaction went smoothly, generating a new ^{11}B NMR signal at 22 ppm that corresponds to the target molecule **2.143**.[62] By conducting the standard Pd/Senphos catalyzed *trans*-cyanoboration reaction of 1,3-enyne **2.52** (without Cl–BCat and CuCN) with the crude mixture of BCat–CN **2.143**, we observed a 51% conversion of the starting enyne and a 17% formation of the desired product with a *trans:cis* ratio of 94:6 (Scheme 2.33, eq. 2). The similar diastereoselectivity (compared to the standard reaction outcome in Table 2.4, entry 6) plus a slower reaction rate indicate BCat–CN is a chemically competent, but not a kinetically competent species.

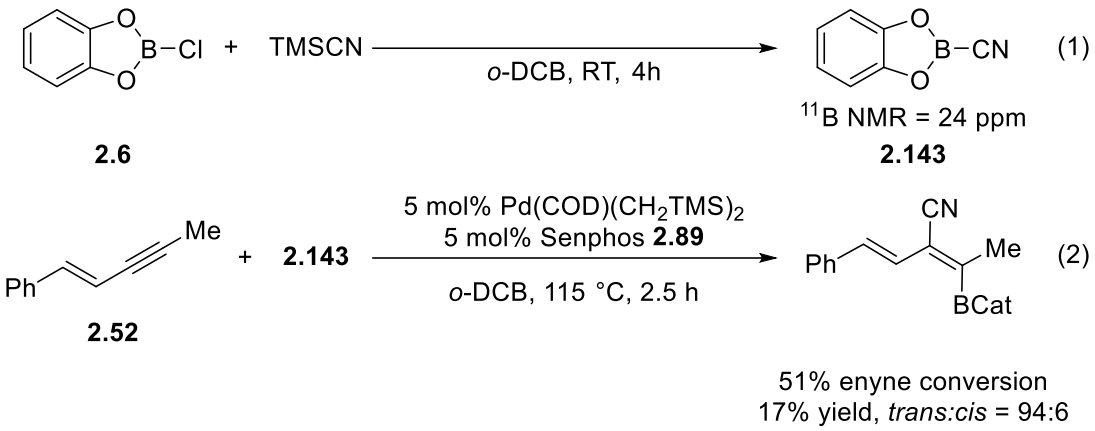

Scheme 2.33. Synthesis of BCat–CN and its performance as the cyanoboration reagent.

The Pd/Senphos catalyzed *trans*-cyanoboration reaction mechanism is adapted from the established *trans*-hydroboration mechanism in Chapter 1 (Scheme 2.34). Pd(0) complex **2.144** first coordinates with enyne to form the enyne-Pd(0) complex **2.145**, which is then activated by Cl–BCat to yield palladium π-allyl zwitterion **2.146**. Next,

[62] BCat–CN is not a known compound. Its 24 ppm chemical shift in ^{11}B NMR, which is upfield shifted compared to Cl–BCat (31 ppm), is consistent with the shielding effect of the cyanide group. For similar compounds, see: (a) Jiang, B.; Kan, Y.; Zhang, A. *Tetrahedron*, **2001**, *57*, 1581-1584; (b) Suginome, M.; Yamamoto, A.; Ito, Y. *Chem. Commun*. **2002**, 1392-1393; (c) Weber, L.; Domke, I.; Greschner, W.; Miqueu, K.; Chrostowska, A.; Baylère, P. *Organometallics* **2005**, *24*, 5455-5463.

transmetalation with CuCN with concomitant elimination of CuCl furnishes complex **2.147**. Finally, reductive elimination results in the desired *trans*-product.

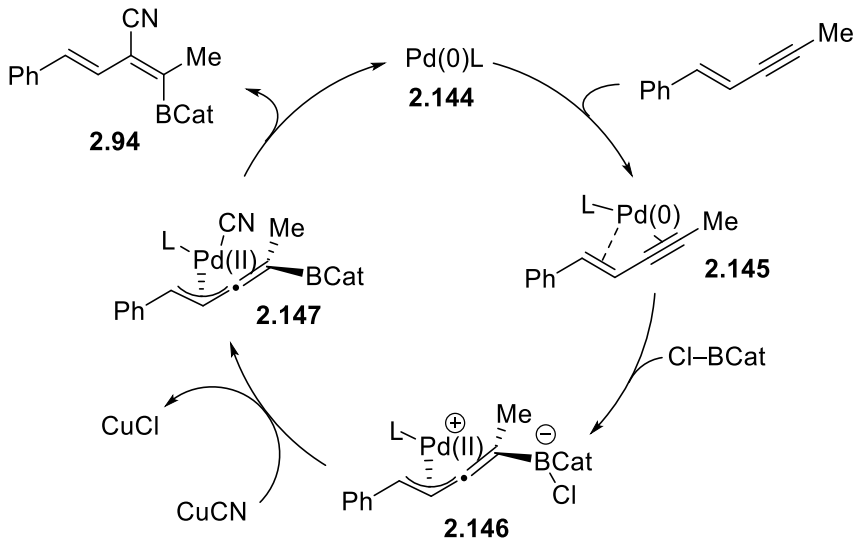

Scheme 2.34. Proposed mechanism of Pd/Senphos catalyzed *trans*-cyanoboration reaction of 1,3-enynes.

2.3. Summary

The first *trans*-selective chloroboration and cyanoboration reaction of 1,3-enynes catalyzed by Pd/Senphos system have been developed. These site-, regio- and diastereoselective reactions provide access to vicinal boron-substituted alkenyl chloride and alkenyl nitriles, respectively, in a straightforward fashion. The *trans*-cyanoboration products are versatile organic synthon and its utility in the synthesis of Satigrel is described.

2.4. Experimental Section

2.4.1. General information

^{1}H, ^{13}C, ^{31}P and ^{19}F spectra were recorded on Varian 400, 500 or 600 MHz spectrometers, and ^{11}B spectra were on an Inova 500 MHz spectrometer at ambient

temperature. ^{1}H NMR spectra were reported with the solvent resonance as internal standard. ^{13}C NMR spectra were reported with the solvent resonance as internal standard. ^{11}B NMR spectra were reported with BF_3•Et_2O (δ 0 ppm) as the external reference. ^{31}P NMR spectra were reported with H_3PO_4 (δ 0 ppm) as the external reference. IR spectra were recorded on a Bruker FTIR Alpha (ATR mode) spectrometer. High-resolution mass spectroscopy data were obtained at the Mass Spectroscopy Facilities at Chemistry Department of Boston College with DART ion source in positive ion mode.

All oxygen- and moisture-sensitive manipulations were carried out under N_2 atmosphere with standard Schlenk techniques or in N_2 glovebox. Hexanes were purified by distillation before using in column chromatography. Solvents used under N_2 atmosphere (pentane, THF, benzene and CH_2Cl_2) were purified by passing through a neutral alumina column under argon. 1,8-diaminonaphthlene was purified by distillation under attenuated pressure followed by recrystallization with hexanes/EtOAc. *o*-DCB was purified by drying with CaH_2 and subsequent distillation under attenuated pressure. All other chemicals and solvents were purchased and used as received.

2.4.2. Experimental procedures

2.4.2.1. Experimental procedure for Senphos ligands syntheses

Synthesis of 1,4-azaborine B–Cl precursors **2.51-S3** and **2.88-S3**:

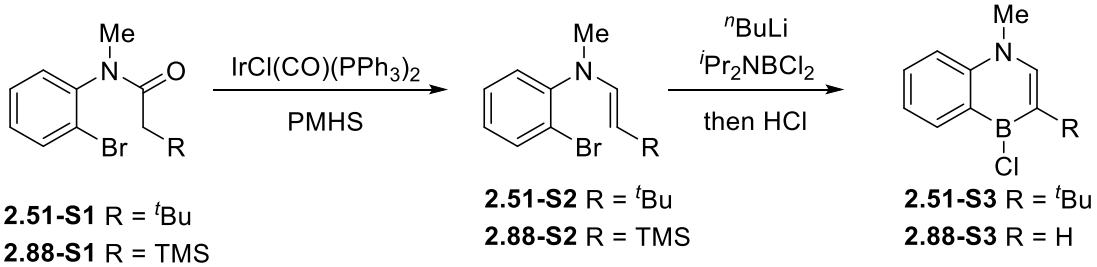

2.51-S1 R = ^{t}Bu
2.88-S1 R = TMS

2.51-S2 R = ^{t}Bu
2.88-S2 R = TMS

2.51-S3 R = ^{t}Bu
2.88-S3 R = H

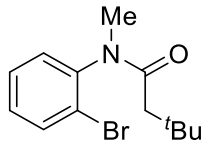

Synthesis of amide **2.51-S1**: To a solution of 2-bromoaniline (5.10 g, 30.0 mmol, 1.00 equiv.) in CH_2Cl_2 (100 mL) was added pyridine (2.50 g, 31.5 mmol, 1.05 equiv.) and *t*butylacetyl chloride (4.24 g, 31.5 mmol, 1.05 equiv.) in a dropwise fashion at 0 °C, and the mixture was allowed to stir for 4 hours at the same temperature. At the conclusion of reaction, H_2O (50 mL) was added, and the organic layer was separated, which was further washed with brine (60 mL) and dried with Na_2SO_4. After removing all volatiles *in vacuo*, a white solid was obtained, which was used for next step without further purification. THF (80 mL) was added to this white solid and then NaH (1.80 g, 60% in oil, 45.0 mmol, 1.50 equiv.) was added in 5 portions in 20 minutes, and the resulting mixture was allowed to stir for another 30 minutes at room temperature, followed by the addition of MeI (6.40 g, 45.0 mmol, 1.50 equiv.). After allowing the new mixture to stir for 2 hours, H_2O (60 mL) along with Et_2O (30 mL) were added. The organic layer was separated and washed with brine (50 mL) and dried with Na_2SO_4. After removing all volatiles, **2.51-S1** was obtained by distillation under attenuated pressure (130 °C, 250 mmTor) as a white solid (88% yield). ^{1}H NMR (500 MHz, $CDCl_3$) δ 7.66 (dt, J = 8.0, 1.5 Hz, 1H), 7.37 (tt, J = 7.5, 1.3 Hz, 1H), 7.25 – 7.19 (m, 2H), 3.16 (d, J = 1.6 Hz, 3H), 1.89 (t, J = 1.1Hz, 2H), 0.97 (d, J = 1.7 Hz, 9H); ^{13}C NMR (126 MHz, $CDCl_3$) δ 171.8, 143.4, 133.9, 130.2, 129.5, 128.9, 123.6, 45.6, 35.8, 31.2, 29.9; IR (ATR) 2952, 2866, 1661, 1475, 1433, 1372, 1361, 1280, 1249, 1117, 1064, 1030, 765, 728, 690, 568, 457 cm^{-1}; HRMS (DART) calcd for $C_{13}H_{19}NOBr$ ($[M+H]^+$) 284.06445, found 284.06500.

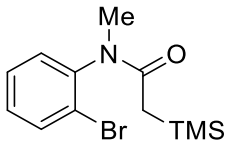

Synthesis of amide **2.88-S1**:To a 100-mL round bottom flask charged with HN^{i}Pr$_2$ (1.1 g, 11 mmol, 1.1 equiv.) and THF (40 mL)

was added ^{n}BuLi (4.4 mL, 2.5 M in hexanes, 11 mmol, 1.1 equiv.) at –78 °C. After allowing the mixture to stir at the same temperature for 15 minutes, a THF (5 mL) solution of *N*-(2-bromophenyl)-*N*-methylacetamide (synthesized according to previous literature[63]) (2.28 g, 10.0 mmol, 1.00 equiv.) was added at once, and the new mixture was allowed to stir for another 2 hours. Then TMSCl (1.09 g, 10.0 mmol, 1.00 equiv.) was added to quench the reaction and the mixture was allowed to gradually warm to room temperature during two hours. At the conclusion of reaction, all volatiles were removed under vacuum and the crude residue was purified by silica gel chromatography under using hexane/EtOAc (15/1 to 5/1 gradient) as the eluent to afford amide **2.88-S1** as yellow oil (51% yield). ^{1}H NMR (600 MHz, $CDCl_3$) δ 7.65 (dt, *J* = 8.0, 1.0 Hz, 1H), 7.39 – 7.33 (m, 1H), 7.24 – 7.18 (m, 2H), 3.16 (s, 3H), 1.70 (d, *J* = 13.3 Hz, 1H), 1.59 (d, *J* = 13.3 Hz, 1H), 0.03 (d, *J* = 0.8 Hz, 9H); ^{13}C NMR (151 MHz, $CDCl_3$) δ 172.7, 144.0, 134.0, 130.2, 129.5, 128.8, 123.7, 36.0, 25.8, –0.7; IR (ATR): 2954. 2897, 1644, 1475, 1423, 1345, 1302, 1246, 1111, 1049, 1029, 843, 764, 727, 700, 624 cm^{-1}; HRMS (DART) calcd for $C_{12}H_{19}NOSiBr$ ([M+H]$^{+}$) 300.04138, found 300.04241.

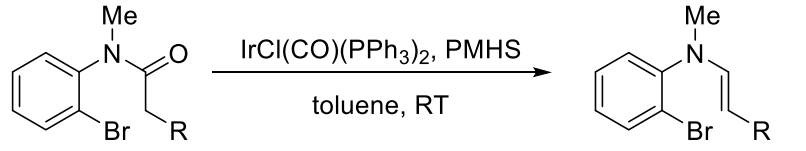

2.51-S1 R = ^{t}Bu
2.88-S1 R = TMS

2.51-S2 R = ^{t}Bu
2.88-S2 R = TMS

To a 250-mL round bottom flask charged with tertiary amide (10.0 mmol, 1.00 equiv.), toluene (30 mL), and PMHS (polymethylhydrosiloxane) (2.60 g, MW 1700-3200, 40.0 mmol, 4.00 equiv.) was added a toluene (5 mL) solution of $IrCl(CO)(PPh_3)_2$ (4 mg,

[63] Cheng, H.-C.; Hou, W.-J.; Li, Z.-W.; Liua, M.-Y.; Guan, B.-T. *Chem. Commun.* **2015**, *51*, 17596-17599.

5 μmol, 0.0005 equiv.) in a dropwise fashion under nitrogen at room temperature. Gelation was observed in 5 minutes, and the reaction mixture was allowed to stir for another 30 minutes. Then, Et_2O (60 mL) was added, and the mixture was passed through a celite pad. The filter cake was further washed with Et_2O (30 mL) for two times, and the filtrates were combined. All volatiles were then removed under vacuum and the enamines were obtained by distillation under attenuated pressure as colorless liquids.

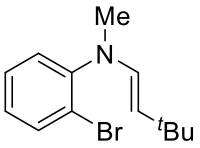

Distilled at 95 °C, 280 mmTor with 90% yield. ^{1}H NMR (600 MHz, $CDCl_3$) δ 7.57 (dd, *J* = 8.0, 1.5 Hz, 1H), 7.26 (tdd, *J* = 7.2, 1.6, 0.6 Hz, 1H), 7.09 (dd, *J* = 8.0, 1.6 Hz, 1H), 6.97 (tdd, *J* = 7.2, 1.6, 0.6 Hz, 1H), 6.15 (d, *J* = 14.1 Hz, 1H), 4.64 (d, *J* = 14.1 Hz, 1H), 2.98 (s, 3H), 1.08 (s, 9H); ^{13}C NMR (151 MHz, $CDCl_3$) δ 148.8, 134.0, 132.9, 128.3, 126.3, 125.5, 119.9, 115.2, 38.4, 31.9, 31.3; IR (ATR) 2952, 2900, 2864, 1650, 1584, 1481, 1461, 1420, 1356, 1320, 1251, 1238, 1129, 1117, 1026, 981, 937, 753, 723, 656, 446 cm^{-1}; HRMS (DART) calcd for $C_{13}H_{19}NBr$ ($[M+H]^+$) 268.06954, found 268.06955.

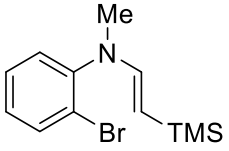

Distilled at 100 °C, 300 mmTor with 76% yield. ^{1}H NMR (600 MHz, $CDCl_3$) δ 7.59 (ddd, *J* = 8.0, 1.6, 0.7 Hz, 1H), 7.29 (tdd, *J* = 7.3, 1.5, 0.7 Hz, 1H), 7.13 (ddd, *J* = 7.9, 1.7, 0.6 Hz, 1H), 7.03 (dddd, *J* = 8.0, 7.4, 1.6, 0.7 Hz, 1H), 6.45 (dd, *J* = 16.6, 0.7 Hz, 1H), 4.19 (d, *J* = 16.5 Hz, 1H), 3.07 (s, 3H), 0.09 (d, *J* = 0.7 Hz, 9H); ^{13}C NMR (151 MHz, $CDCl_3$) δ 147.8, 146.6, 134.1, 128.4, 127.4, 126.5, 120.5, 92.4, 37.5, 0.1; IR (ATR): 2951, 2892, 1599, 1579, 1480, 1440, 1354, 1243, 1198, 1047, 1028, 868, 829, 755, 737, 720, 686, 581 cm^{-1}; HRMS (DART) calcd for $C_{12}H_{19}NSiBr$ ($[M+H]^+$) 284.04647, found 284.04681.

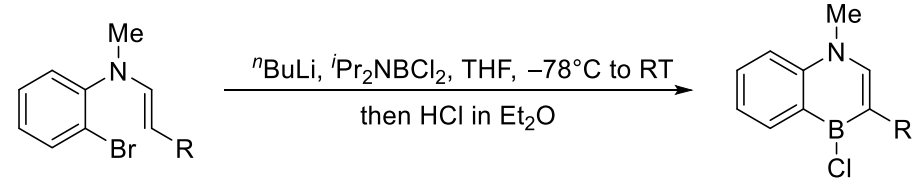

2.51-S2 R = ^{t}Bu
2.88-S2 R = TMS

2.51-S3 R = ^{t}Bu
2.88-S3 R = H

To a 100-mL round bottom flask charged with enamine (9.00 mmol, 1.00 equiv.) and THF (30 mL) was added ^{n}butyl lithium (3.60 mL, 2.50 M in hexanes, 9.00 mmol, 1.00 equiv.) at –78°C. After allowing the mixture to stir at –78 °C for 20 minutes, a THF (3 mL) solution of ^{i}Pr$_2$NBCl$_2$ (1.64 g, 9.00 mmol, 1.00 equiv.) was added. And the resulting reaction mixture was allowed to warm to room temperature in 2 hours. Then, HCl (4.5 mL, 2.0 M in Et$_2$O, 9.0 mmol, 1.0 equiv.) was added, and the mixture was allowed to stir for an hour. At the conclusion of reaction, the solution was passed through an acrodisc under an inert atmosphere and the filtrate was concentrated and re-dissolved in CH_2Cl_2 (10 mL) and filtered and concentrated again. The resulting residue was purified by recrystallization from pentane/CH_2Cl_2 to furnish *N*–Me-*B*–Cl.

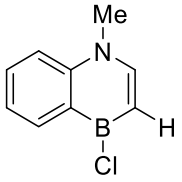

Due to the presence of inseparable mixtures after recrystallization, **2.88-S3** was used in next step without further purification.[1]H NMR (500 MHz, $CDCl_3$) δ 8.40 (dd, *J* = 7.8, 1.7 Hz, 1H), 7.84 (d, *J* = 9.4 Hz, 1H), 7.76 – 7.69 (m, 1H), 7.56 – 7.50 (m, 1H), 7.38 (ddd, *J* = 7.8, 7.0, 0.9 Hz, 1H), 6.19 (d, *J* = 9.4 Hz, 1H), 3.91 (s, 3H); HRMS (DART) calcd for $C_9H_{10}BNCl$ ($[M+H]^+$) 178.05893, found 178.05927.

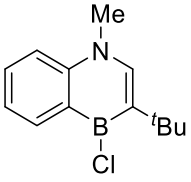

36% yield. [1]H NMR (500 MHz, $CDCl_3$) δ 8.55 (dd, *J* = 7.9, 1.7 Hz, 1H), 7.78 (s, 1H), 7.69 (ddd, *J* = 8.6, 6.9, 1.7 Hz, 1H), 7.46 (d, *J* =

8.6 Hz, 1H), 7.35 (ddd, J = 7.9, 6.9, 1.0 Hz, 1H), 3.89 (s, 3H), 1.50 (s, 9H); ^{13}C NMR (126 MHz, $CDCl_3$) δ 145.8, 143.2, 134.0, 133.7 (br), 131.6, 128.4 (br), 121.4, 114.6, 42.4, 34.9, 31.0; ^{11}B NMR (160 MHz, $CDCl_3$) δ 44.4; IR (ATR): 2959, 2867, 1582, 1457, 1374, 1264, 1096, 922, 760, 734, 702, 637 cm^{-1}; HRMS (DART) calcd for $C_{13}H_{18}BNCl$ ($[M+H]^+$) 234.12153, found 234.12340.

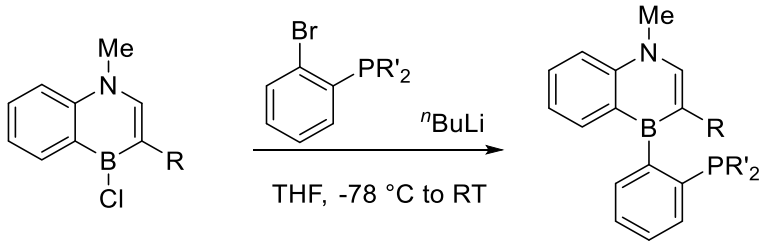

R = H, Me, ^{i}Pr, ^{t}Bu
R' = Cy, Ph

Senphos **2.50**, **2.90** and **2.93** were synthesized in Chapter 1. *N*–Me-*B*–Cl 1,4-Azaborines *B*–Cl where R = Me and ^{i}Pr were synthesized according to previous literature.[29] To a 100-mL round bottom flask charged with 2-bromophenyl dicyclohexylphosphine or 2-bromophenyl diphenylphosphine (2.00 mmol, 1.00 equiv.) and Et_2O (15 mL) was added ^{n}butyllithium (0.80 mL, 2.5 M in hexanes, 2.0 mmol, 1.0 equiv.) at –78 °C. After allowing the mixture to stir at –78 °C for an hour, the corresponding 1,4-azaborine *B*–Cl (2.0 mmol, 1.0 equiv.) in THF (3 mL) was added, and the resulting mixture was allowed to warm to room temperature in 2 hours. At the conclusion of reaction, all volatiles were removed under vacuum, and the crude residue was purified by silica gel chromatography under inert atmosphere using pentane/Et_2O (25/1 to 10/1 gradient) as the eluent to afford the desired ligand as white solids.

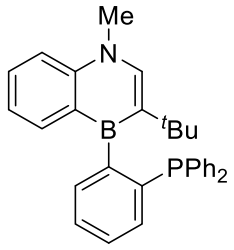

65% yield. ^{1}H NMR (400 MHz, $CDCl_3$) δ 7.89 (s, 1H), 7.50 – 7.29 (m, 7H), 7.29 – 7.16 (m, 5H), 7.17 – 7.04 (m, 5H), 6.68 (ddd, J = 7.8, 6.4, 1.3 Hz, 1H), 3.94 (s, 3H), 1.27 (s, 9H); ^{13}C NMR (101 MHz, $CDCl_3$) δ 157.6 (br, d, J = 49.4 Hz), 145.0, 141.9, 139.2, 139.0, 138.6, 138.5, 138.1 (d, J = 12.1 Hz), 137.6, 135.5 (br), 134.4, 134.2, 134.1 (d, J = 2.2 Hz), 133.0, 132.9, 132.2 (br), 132.1 (d, J = 16.7 Hz), 130.5, 128.2, 128.0 (d, J = 1.6 Hz), 128.0, 128.0, 127.5, 126.2, 120.0, 113.7, 42.5, 35.8, 32.8 (d, J = 1.3 Hz); ^{11}B NMR (128 MHz, $CDCl_3$) δ 46.6; ^{31}P NMR (162 MHz, $CDCl_3$) δ –10.2; IR (ATR) 3052, 2948, 2862, 1604, 1579, 1459, 1433, 1375, 1264, 1221, 1087, 1026, 919, 739, 696, 669, 510 cm^{-1}; HRMS (DART) calcd for $C_{31}H_{32}BNP$ ($[M+H]^+$) 460.23599, found 460.23641.

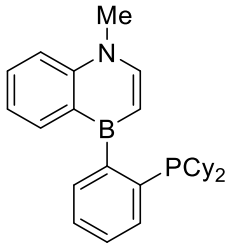

15% yield. ^{1}H NMR (500 MHz, $CDCl_3$) δ 7.83 (d, J = 9.1 Hz, 1H), 7.77 (dd, J = 7.7, 1.6 Hz, 1H), 7.66 – 7.61 (m, 2H), 7.52 (d, J = 8.6 Hz, 1H), 7.41 – 7.29 (m, 3H), 7.19 (t, J = 7.3 Hz, 1H), 6.28 (d, J = 9.0 Hz, 1H), 3.90 (s, 3H), 1.97 – 1.85 (m, 2H), 1.84 – 1.54 (m, 10H), 1.35 – 0.94 (m, 10H); ^{13}C NMR (101 MHz, $CDCl_3$) δ 156.6 (br, d, J = 46.5 Hz), 147.1, 143.8, 137.2 (d, J = 10.9 Hz), 137.1, 131.8 (d, J = 4.2 Hz), 131.8 (d, J = 21.7 Hz), 131.5 (br), 130.8, 127.3 (d, J = 1.5 Hz), 125.8, 121.0, 116.1 (br), 114.7, 42.1, 34.8 (d, J = 13.4 Hz), 34.3 (d, J = 12.8 Hz), 30.7 (d, J = 15.6 Hz), 30.4 (d, J = 15.7 Hz), 29.4, 29.3, 27.6, 27.5 (d, J = 4.2 Hz), 27.4, 27.3, 26.6, 26.6; ^{11}B NMR (160 MHz, $CDCl_3$) δ 46.9; ^{31}P NMR (202 MHz, $CDCl_3$) δ –5.08; IR (ATR) 3036, 2919, 2847, 1605, 1578, 1493, 1448, 1433, 1368, 1221, 1001, 892, 798, 764, 736, 635 cm^{-1}; HRMS (DART) calcd for $C_{27}H_{36}BNP$ ($[M+H]^+$) 416.26729, found 416.26737.

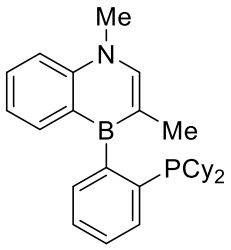

42% yield. ^{1}H NMR (500 MHz, $CDCl_3$) δ 7.74 (dd, *J* = 7.8, 1.6 Hz, 1H), 7.67 (s, 1H), 7.61 – 7.55 (m, 2H), 7.48 (d, *J* = 8.6 Hz, 1H), 7.40 – 7.31 (m, 2H), 7.28 – 7.24 (m, 1H), 7.13 (ddd, *J* = 7.8, 6.8, 0.9 Hz, 1H), 3.90 (s, 3H), 2.06 (d, *J* = 0.9 Hz, 3H), 2.01 (ddd, *J* = 11.1, 5.1, 3.0 Hz, 1H), 1.81 – 1.59 (m, 8H), 1.60 – 1.48 (m, 2H), 1.47 – 0.78 (m, 11H); ^{13}C NMR (126 MHz, $CDCl_3$) δ 146.6, 143.2, 137.6, 137.3 (d, *J* = 11.0 Hz), 131.7 (d, *J* = 15.4 Hz), 131.7 (d, *J* = 2.6 Hz), 130.8 (br), 130.4, 127.5, 125.6, 122.9 (br), 120.2, 114.3, 42.0, 35.1 (d, *J* = 13.7 Hz), 33.6 (d, *J* = 12.4 Hz), 30.7 (d, *J* = 14.2 Hz), 30.3 (d, *J* = 15.9 Hz), 30.0 (d, *J* = 10.6 Hz), 29.2 (d, *J* = 6.0 Hz), 27.7, 27.6 (d, *J* = 6.4 Hz), 27.6, 27.5 (d, *J* = 3.6 Hz), 26.7, 26.6, 19.6 (d, *J* = 4.3 Hz) (one signal of aromatic carbon attached to boron is not observed); ^{11}B NMR (160 MHz, $CDCl_3$) δ 47.3; ^{31}P NMR (202 MHz, $CDCl_3$) δ –3.2; IR (ATR) 3039, 2922, 2849, 1605, 1586, 1491, 1447, 1369, 1269, 1225, 1102, 908, 891, 764, 732, 647 cm^{-1}; HRMS (DART) calcd for $C_{28}H_{38}BNP$ ($[M+H]^+$) 430.28294, found 430.28290.

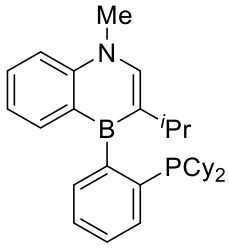

48% yield. ^{1}H NMR (500 MHz, $CDCl_3$) δ 7.71 – 7.64 (m, 2H), 7.62 – 7.53 (m, 2H), 7.47 (d, *J* = 8.6 Hz, 1H), 7.40 – 7.29 (m, 3H), 7.10 (t, *J* = 7.3 Hz, 1H), 3.93 (s, 3H), 2.89 (hept, *J* = 7.2 Hz, 1H), 1.96 (tt, *J* = 12.1, 3.5 Hz, 1H), 1.80 – 1.59 (m, 8H), 1.56 (d, *J* = 9.0 Hz, 3H), 1.43 (d, *J* = 13.2 Hz, 1H), 1.34 – 0.79 (m, 15H); ^{13}C NMR (126 MHz, $CDCl_3$) δ 144.3, 143.1, 137.7, 137.5 (d, *J* = 11.0 Hz), 134.9 (br), 132.1 (d, *J* = 15.3 Hz), 131.8 (d, *J* = 2.8 Hz), 131.3 (br), 130.5, 127.3, 125.6, 120.1, 114.3, 42.4, 35.2 (d, *J* = 14.0 Hz), 34.1 (d, *J* = 12.9 Hz), 30.6 (d, *J* = 14.2 Hz), 30.4 (d, *J* = 16.0 Hz), 29.9 (d, *J* = 10.3 Hz), 29.7 (d, *J* = 2.4 Hz), 29.3 (d, *J* = 6.7 Hz), 27.7, 27.6, 27.5, 27.5, 27.1, 26.7, 26.6, 22.7 (one

signal of the aromatic carbon attached to boron is not observed); ^{11}B NMR (160 MHz, $CDCl_3$) δ 47.5; ^{31}P NMR (202 MHz, $CDCl_3$) δ –4.3; IR (ATR) 3039, 2923, 2849, 1605, 1585, 1491, 1457, 1428, 1383, 1372, 1265, 1223, 908, 765, 750, 733, 667 cm^{-1}; HRMS (DART) calcd for $C_{30}H_{42}BNP$ ($[M+H]^+$) 458.31424, found 458.31565.

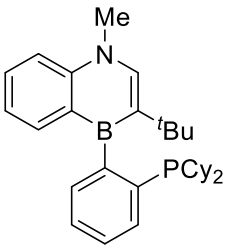

38% yield. ^{1}H NMR (600 MHz, $CDCl_3$) δ 7.83 (s, 1H), 7.57 – 7.49 (m, 2H), 7.46 – 7.37 (m, 3H), 7.36 – 7.28 (m, 2H), 7.04 (ddd, *J* = 7.9, 6.8, 1.0 Hz, 1H), 3.93 (s, 3H), 2.10 (tdd, *J* = 11.1, 6.7, 3.1 Hz, 1H), 1.83 – 0.70 (m, 30H); ^{13}C NMR (126 MHz, $CDCl_3$) δ 145.1, 142.1, 138.8 (d, *J* = 9.7 Hz), 138.1, 132.2 (d, *J* = 14.9 Hz), 131.2 (d, *J* = 2.3 Hz), 130.5, 126.5, 125.2, 119.9, 113.8, 42.5, 36.0 (d, *J* = 14.7 Hz), 35.9, 33.6 (d, *J* = 14.1 Hz), 33.0 (d, *J* = 1.6 Hz), 32.0 (d, *J* = 16.6 Hz), 31.1 (d, *J* = 13.3 Hz), 30.5 (d, *J* = 15.7 Hz), 28.3 (d, *J* = 4.9 Hz), 28.0 (d, *J* = 2.0 Hz), 27.9 (d, *J* = 3.4 Hz), 27.8, 27.4 (d, *J* = 10.1 Hz), 26.7, 26.6 (three signals of aromatic carbon attached to boron are not observed); ^{11}B NMR (160 MHz, $CDCl_3$) δ 47.3; ^{31}P NMR (202 MHz, $CDCl_3$) δ –3.4; IR (ATR) 3039, 2920, 2849, 1604, 1581, 1490, 1459, 1447, 1390, 1376, 1264, 1220, 1086, 918, 765, 742, 669 cm^{-1}; HRMS (DART) calcd for $C_{31}H_{44}BNP$ ($[M+H]^+$) 472.32989, found 472.32950.

2.4.2.2. Experimental procedure for *trans*-chloroboration reaction

General Procedure for Table 2.1: Stock catalyst (Pd_2dba_3/Senphos **2.50**) solution (0.05 M in CH_2Cl_2, 0.08 mL, 4 μmol) was added to a 4-mL vial, which was then put under high vacuum for 15 minutes. Then Cl–BCat (23 mg, 0.15 mmol, 1.5 equiv.), the corresponding solvent (0.15 mL) and enyne **2.52** (14.2 mg, 0.100 mmol, 1.00 equiv.) were added sequentially. The resulting mixture was allowed to stir at the indicated temperature for 14 hours. At the conclusion of reaction, an aliquot from this mixture was

prepared for ^{1}H NMR analysis, and the *trans:cis* ratio was calculated based upon ^{1}H NMR.

Entry 1: The general procedure was followed, and the reaction was run at 25 °C with $PhCH_3$ as the solvent. ^{1}H NMR analysis indicated no desired product formation.

Entry 2: The general procedure was followed, and the reaction was run at 110 °C with $PhCH_3$ as the solvent. ^{1}H NMR analysis indicated the *trans*:*cis* ratio of chloroboration product was 73:27.

Entry 3: The general procedure was followed, $Pd(COD)(CH_2TMS)_2$ (1.6 mg, 4.0 μmol, 4.0 mol%), Senphos **2.50** (1.7 mg, 4.0 μmol, 4.0 mol%) were used instead of a stock catalyst solution. The reaction was run at 110 °C with $PhCH_3$ as the solvent. ^{1}H NMR analysis indicated the *trans*:*cis* ratio of chloroboration product was 66:33.

Entry 4: The general procedure was followed, and the reaction was run at 110 °C with $(CHCl_2)_2$ as the solvent. ^{1}H NMR analysis indicated the *trans*:*cis* ratio of chloroboration product was 55:45.

Entry 5: The general procedure was followed, and the reaction was run at 110 °C with $PhCF_3$ as the solvent. ^{1}H NMR analysis indicated the *trans*:*cis* ratio of chloroboration product was 77:23.

Entry 6: The general procedure was followed, and the reaction was run at 110 °C with *o*-xylene as the solvent. ^{1}H NMR analysis indicated the *trans*:*cis* ratio of chloroboration product was 87:13.

Entry 7: The general procedure was followed, and the reaction was run at 110 °C with *o*-DCB as the solvent. ^{1}H NMR analysis indicated the *trans*:*cis* ratio of chloroboration product was 88:12.

Entry 8: The general procedure was followed, and the reaction was run at 80 °C with *o*-DCB as the solvent. ^{1}H NMR analysis indicated the *trans*:*cis* ratio of chloroboration product was 82:18.

Entry 9: The general procedure was followed, and the reaction was run at 130 °C with *o*-DCB as the solvent. ^{1}H NMR analysis indicated the *trans*:*cis* ratio of chloroboration product was 97:3.

Entry 10: The general procedure was followed where Senphos **2.51** was used instead of **2.50**. The reaction was run at 130 °C with *o*-DCB as the solvent. ^{1}H NMR analysis indicated the *trans*:*cis* ratio of chloroboration product was over 98:2.

General Procedure for Scheme 2.18: Stock catalyst (Pd_2dba_3/Senphos **2.51**) solution (0.05 M in CH_2Cl_2, 0.08 mL, 4 μmol) was added to a 4-mL vial, which was put under high vacuum for 15 minutes. Then Cl–BCat (23 mg, 0.15 mmol, 1.5 equiv.), *o*-DCB (0.15 mL), an *o*-DCB solution (5.0 μL, 1.5 M) of hexamethylbenzene as the internal standard and enyne **2.52** (14.2 mg, 0.100 mmol, 1.00 equiv.) were added one by one. The resulting mixture was allowed to stir for 14 hours at 130 °C. At the conclusion of reaction, an aliquot from this mixture was prepared to determine the product *trans*:*cis* ratio. CH_2Cl_2 (2 mL) along with pinacol (118 mg, 1.00 mmol, 10.0 equiv.) were added to the reaction mixture. And after allowing the new mixture to stir for 12 hours, all volatiles were removed under reduced pressure, and the resulting crude residue was purified by silica gel chromatography. However, only the starting enyne was obtained.

General Procedure for Table 2.2: Stock catalyst (Pd_2dba_3/Senphos **2.51**) solution (0.05 M in CH_2Cl_2, 0.08 mL, 4 μmol) was added to a 4-mL vial, which was put under high vacuum for 15 minutes. Then Cl–BCat (23 mg, 0.15 mmol, 1.5 equiv.), *o*-DCB

(0.15 mL), an *o*-DCB solution (5.0 μL, 1.5 M) of hexamethylbenzene as the internal standard and enyne **2.52** (14.2 mg, 0.100 mmol, 1.00 equiv.) were added one by one. The resulting mixture was allowed to stir for 14 hours at 130 °C. At the conclusion of reaction, an aliquot from this mixture was prepared to determine the product *trans*:*cis* ratio. Then, 1,8-diaminonaphthlene (32 mg, 0.20 mmol, 2.0 equiv.) along with CH_2Cl_2 (2 mL) were added to the reaction mixture. After allowing the new mixture to stir for 12 hours, all volatiles were removed under reduced pressure, and the resulting crude residue was purified by silica gel chromatography using hexanes/EtOAc (30/1 to 20/1 gradient) as the eluent to afford the desired product as a single diastereomer.

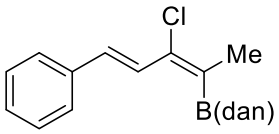

Crystals for single crystal X-ray diffraction analysis were obtained by recrystallization from hexane/CH_2Cl_2 at room temperature. 5% yield. ^{1}H NMR (600 MHz, $CDCl_3$) δ 7.41 (dt, *J* = 6.2, 1.4 Hz, 2H), 7.34 – 7.27 (m, 2H), 7.24 (td, *J* = 7.1, 1.4 Hz, 1H), 7.18 – 7.03 (m, 6H), 6.37 (dd, *J* = 7.2, 1.1 Hz, 2H), 5.71 (s, 2H), 2.13 (s, 3H); ^{13}C NMR (101 MHz, $CDCl_3$) δ 140.7, 136.9, 136.5, 136.4, 132.0, 128.9, 128.2, 127.8, 127.0, 126.0, 119.9, 118.3, 106.4, 19.9 (one signal of aromatic carbon attached to boron is not observed); ^{11}B NMR (128 MHz, $CDCl_3$) δ 29.7; IR (ATR): 3401, 3054, 1598, 1578, 1502, 1408, 1373, 1330, 1233, 1087, 819, 764, 753, 693, 654 cm^{-1}; HRMS (DART) calcd for $C_{21}H_{19}BN_2Cl$ ($[M+H]^+$) 345.13337, found 345.13429.

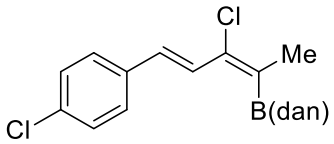

^{1}H NMR (500 MHz, $CDCl_3$) δ 7.34 – 7.29 (m, 2H), 7.25 (d, *J* = 8.7 Hz, 2H), 7.14 (dd, *J* = 8.3, 7.2 Hz, 2H), 7.09 (dd, *J* = 8.3, 1.1 Hz, 2H), 7.06 (d, *J* = 15.1 Hz, 1H), 6.99 (d, *J* = 15.1 Hz, 1H), 6.36 (dd, *J* = 7.2, 1.1 Hz, 2H), 5.70 (s, 2H), 2.12 (s, 3H); ^{13}C NMR

(101 MHz, $CDCl_3$) δ 140.64, 136.67, 136.39, 135.05, 133.84, 130.69, 129.06, 128.21, 127.81, 126.54, 119.91, 118.44, 106.42, 20.01 (one signal of aromatic carbon attached to boron is not observed); ^{11}B NMR (160 MHz, $CDCl_3$) δ 29.2; IR (ATR) 3408, 1599, 1576, 1501, 1489, 1408, 1355, 1330, 1230, 1086, 1006, 818, 809, 759, 688 665, 629 cm^{-1}; HRMS (DART) calcd for $C_{21}H_{18}BN_2Cl_2$ ($[M+H]^+$) 379.09346, found 379.09320.

2.4.2.3. Experimental procedure for *trans*-cyanoboration reaction

2.4.2.3.1. General procedure for Table 2.3

Stock catalyst (Pd_2dba_3/Senphos **2.50**) solution (0.05 M in CH_2Cl_2, 0.08 mL, 4 μmol) was added to a 4-mL vial, which was then put under high vacuum for 15 minutes. Then Cl–BCat (23 mg, 0.15 mmol, 1.5 equiv.), *o*-DCB (0.15 mL), an *o*-DCB solution (5.0 μL, 1.5 M) of hexamethylbenzene as the internal standard and enyne **2.52** (14.2 mg, 0.100 mmol, 1.00 equiv.) along with the transmetalation reagent (0.15 mmol, 1.5 equiv.) were added one by one. The resulting mixture was allowed to stir for 14 hours at 130 °C. At the conclusion of reaction, an aliquot from this mixture was taken to probe the possible products via ^1H NMR.

Entry 1: The general procedure was followed, transmetalation reagent PhCH=CHZr(Cp)$_2$Cl[64] was used. Total enyne decomposition was observed.

Entry 2: The general procedure was followed, transmetalation reagent (trimethylsiloxy)ethylene was used. Total enyne decomposition was observed.

Entry 3: The general procedure was followed, transmetalation reagent tributyl(vinyl)tin was used. Transmetalation reaction between Sn and boron was observed.

[64] Choi, J.; Martín-Gago, P.; Fu, G. C. *J. Am. Chem. Soc*. **2014**, *136*, 12161-12165.

Entry 4: The general procedure was followed, transmetalation reagent AgCN was used. 5% *trans*-cyanoboration product was observed.

Entry 5: The general procedure was followed, transmetalation reagent $Zn(CN)_2$ was used. 12% T*rans*-cyanoboration product was observed.

Entry 6: The general procedure was followed, transmetalation reagent CuCN was used. 44% T*rans*-cyanoboration product was observed.

Entry 7: The general procedure was followed, transmetalation reagent Bu_4NCN was used. No reaction occurred.

Entry 8: The general procedure was followed, transmetalation reagent Bu_3SnCN was used. Transmetalation reaction between Sn and boron was observed.

2.4.2.3.2. Synthesis of carbonaceous ligand

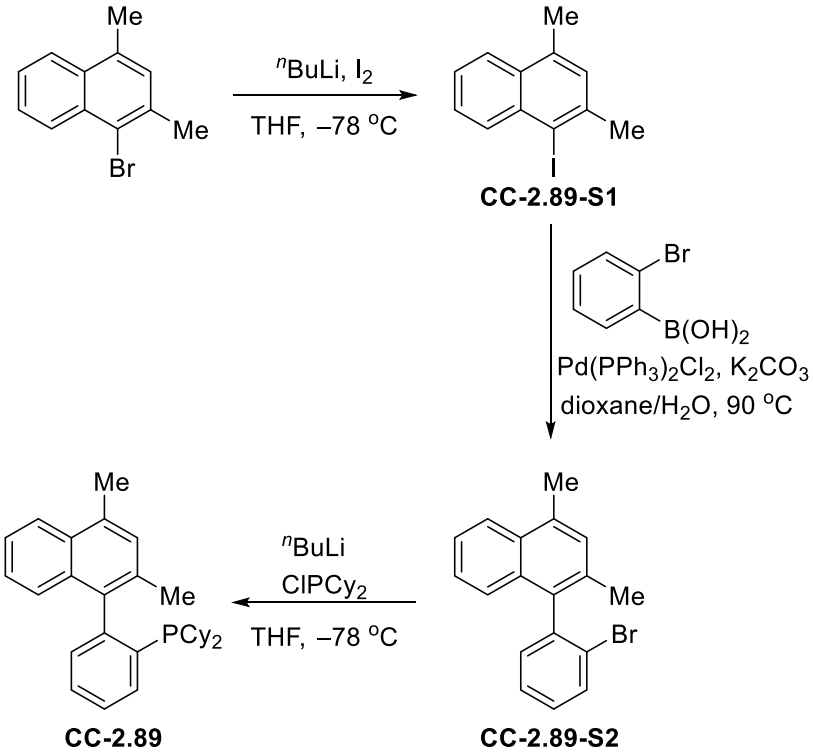

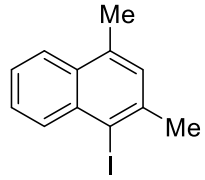

*n*Butyllithium (1.30 mL, 2.50 M in hexanes, 3.24 mmol, 1.20 equiv.) was added in a dropwise fashion into a 20-mL vial charged with a solution 1-bromo-2,4-dimethylnaphthalene (634 mg, 2.70 mmol, 1.00 equiv., synthesized according to previous literature[65].) in THF (12 mL) at –78 °C. The resulting mixture was allowed to stir for 30 minutes at the same temperature. Then a solution of I_2 (1.35 g, 5.40 mmol, 2.00 equiv.) in THF (3 mL) was added to the reaction mixture, and the resulting mixture was gradually allowed to warm to room temperature in 2 hours. At the conclusion of reaction, THF was removed, and the residue was taken up in Et_2O (15 mL) and washed with saturated $Na_2S_2O_3$ (10 mL) and H_2O (10 mL). The organic layer was then concentrated under reduced pressure, and the crude material was purified via silica gel chromatography using hexanes as the eluent to afford **CC-2.89-S1** as a colorless liquid (88% yield). ^{1}H NMR (500 MHz, $CDCl_3$) δ 8.33 – 8.24 (m, 1H), 7.92 (dd, *J* = 8.3, 1.6 Hz, 1H), 7.58 (ddd, *J* = 8.4, 6.8, 1.3 Hz, 1H), 7.52 (td, *J* = 6.8, 1.4 Hz, 1H), 7.24 (s, 1H), 2.69 (s, 3H), 2.65 (d, *J* = 2.0 Hz, 3H); ^{13}C NMR (126 MHz, $CDCl_3$) δ 140.4, 135.0, 134.6, 132.9, 131.8, 129.2, 127.4, 125.7, 124.4, 103.3, 30.3, 19.2; IR (ATR) 3060, 3007, 2917, 1600, 1510, 1475, 1432, 1387, 1379, 1049, 1026, 875, 752, 731, 709, 669, 655, 453 cm^{-1}; HRMS (DART) calcd for $C_{12}H_{11}I$ ($[M]^+$) 281.98999, found 281.99087.

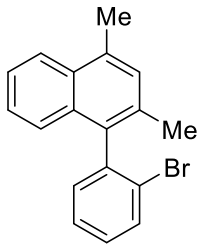

A 20-mL vial was charged with $Pd(PPh_3)_2Cl_2$ (16.5 mg, 23.5 μmol, 0.0500 equiv.), potassium carbonate (130 mg, 0.940 mmol, 2.00 equiv.) and (2-bromophenyl)boronic acid (104 mg, 0.517 mmol, 1.10

[65] Huang, S.; Kotzner, L.; De, C. K.; List, B. *J. Am. Chem. Soc*. **2015**, *137*, 3446-3449.

equiv.) under nitrogen. To this mixture 1,4-dioxane (3.5 mL), H_2O (0.5 mL) and **CC-2.89-S1** (134 mg, 0.470 mmol, 1.00 equiv.) were added, and the reaction mixture was allowed to stir at 90 °C for 3 hours. At the conclusion of reaction, Et_2O (5 mL) and H_2O (2 mL) were added to the mixture. The organic layer was separated and the aqueous layer was extracted with Et_2O (10 mL). The combined organic layers were concentrated under reduced pressure. The resulting crude material was purified via silica gel chromatography using hexanes as the eluent to afford **CC-2.89-S2** as a colorless liquid (68% yield). ^{1}H NMR (500 MHz, $CDCl_3$) δ 8.07 (dt, *J* = 8.5, 1.0 Hz, 1H), 7.81 (dd, *J* = 8.1, 1.3 Hz, 1H), 7.49 (dtd, *J* = 18.1, 7.1, 1.3 Hz, 2H), 7.41 (ddd, *J* = 8.2, 6.7, 1.3 Hz, 1H), 7.37 – 7.32 (m, 2H), 7.29 (td, *J* = 7.2, 1.4 Hz, 2H), 2.78 (d, *J* = 1.0 Hz, 3H), 2.22 (s, 3H); ^{13}C NMR (126 MHz, $CDCl_3$) δ 140.9, 135.5, 134.2, 133.2, 132.9, 132.4, 132.1, 131.1, 129.5, 129.0, 127.6, 126.1, 125.9, 125.1, 124.9, 124.2, 20.3, 19.6; IR (ATR) 2967, 2943, 2913, 2856, 1599, 1555, 1503, 1438, 1326, 1263, 1026, 961, 884, 867, 747, 639, 567, 417 cm^{-1}; HRMS (DART) calcd for $C_{18}H_{16}Br$ ($[M+H]^+$) 311.04299, found 311.04305.

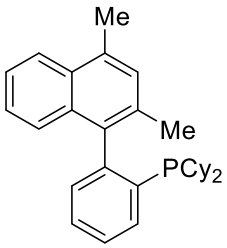

To a 20-mL vial charged with **CC-2.89-S2** (99 mg, 0.32 mmol, 1.0 equiv.) and THF (2 mL) was added *n*butyllithium (0.15 mL, 2.5 M in hexanes, 0.38 mmol, 1.2 equiv.) at –78 °C. The mixture was allowed to stir at –78 °C for 30 minutes, then a solution of chlorodicyclohexylphosphine (89 mg, 0.38 mmol, 1.2 equiv.) in THF (1 mL) was added. The resulting mixture was gradually allowed to warm to room temperature in 2 hours. THF was removed *in vacuo*, and the residue was purified via silica gel chromatography using hexanes/EtOAc (100/1) as the eluent to afford **CC-2.89** as a white solid (72% yield). ^{1}H NMR (500 MHz, $CDCl_3$) δ 7.97 (d, *J* = 8.3 Hz, 1H), 7.67 (dt, *J* = 6.6, 2.3 Hz,

1H), 7.46 – 7.42 (m, 2H), 7.40 (ddd, *J* = 8.2, 6.5, 1.5 Hz, 1H), 7.30 – 7.17 (m, 4H), 2.72 (s, 3H), 2.18 (d, *J* = 2.0 Hz, 3H), 1.91 (ddd, *J* = 15.2, 10.1, 3.2 Hz, 1H), 1.78 – 0.79 (m, 21H); ^{13}C NMR (126 MHz, $CDCl_3$) δ 147.5 (d, *J* = 31.1 Hz), 136.9 (d, *J* = 19.4 Hz), 136.7 (d, *J* = 6.2 Hz), 133.5 (d, *J* = 1.8 Hz), 133.4, 133.0 (d, *J* = 3.2 Hz), 132.7 (d, *J* = 2.0 Hz), 131.6 (d, *J* = 5.9 Hz), 131.0, 129.5, 128.6, 127.7, 126.6, 124.8, 124.4, 124.0, 34.9 (d, *J* = 15.1 Hz), 33.7 (d, *J* = 14.1 Hz), 30.4 (d, *J* = 4.8 Hz), 30.2, 30.1 (d, *J* = 11.9 Hz), 29.8 (d, *J* = 12.9 Hz), 27.6, 27.6 (d, *J* = 18.5 Hz), 27.5 (d, *J* = 4.0 Hz), 27.4 (d, *J* = 6.2 Hz), 26.7, 26.5, 21.4 (d, *J* = 4.3 Hz), 19.7; ^{31}P NMR (202 MHz, $CDCl_3$) δ –9.4; IR (ATR) 3051, 3006, 2921, 2848, 1600, 1511, 1446, 1386, 1034, 1000, 909, 875, 851, 757, 733, 669 cm^{-1}; HRMS (DART) calcd for $C_{30}H_{38}P$ ($[M+H]^+$) 429.27056, found 429.26989.

2.4.2.3.3. General procedure for Table 2.4

To a 4-mL vial charged with $Pd(COD)(CH_2TMS)_2$ (3.9 mg, 0.010 mmol, 5.0 mol%), corresponding Senphos ligand (0.010 mmol, 5.0 mol%), CuCN (29 mg, 0.32 mmol, 1.6 equiv.), Cl–BCat (55 mg, 0.36 mmol, 1.8 equiv.), and *o*-DCB (0.30 mL) was added enyne **2.52** (28.4 mg, 0.200 mmol, 1.00 equiv.) and a solution of hexamethylbenzene in *o*-DCB (5.0 μL, 3.3 M) as the internal standard. The resulting mixture was allowed to stir for 2.5 hours at 115 °C. At the conclusion of reaction, an aliquot from the reaction mixture was prepared for ^{1}H NMR analysis of *trans:cis* ratio and yield for chloroboration product against internal standard hexamethylbenzene. The rest of the mixture was passed through an acrodisc under an inert atmosphere using CH_2Cl_2 as the solvent, and 1,8-diaminonaphthlene (64 mg, 0.40 mmol, 2.0 equiv.) was added to the filtrate. After allowing the mixture to stir for 12 hours, all volatiles were removed under reduced pressure, and the *trans*:*cis* ratios and yield for cyanoboration

product were determined by ^{1}H NMR of the resulting crude material against hexamethylbenzene as the internal standard.

Entry 1: The general procedure was followed without any ligands. The yields (*trans:cis* ratios) for chloroboration product **2.53** and cyanoboration product **2.94** were 3% (75:25) and 3% (89:11).

Entry 2: The general procedure was followed with $PhPCy_2$ as the ligand. The yields (*trans:cis* ratios) for chloroboration product **2.53** and cyanoboration product **2.94** were 4% (77:23) and 13% (95:5).

Entry 3: The general procedure was followed with XPhos as the ligand. The yields (*trans:cis* ratios) for chloroboration product **2.53** and cyanoboration product **2.94** was 7% (59:41) and 10% (90:10).

Entry 4: The general procedure was followed with dppe as the ligand. The yields (*trans:cis* ratios) for chloroboration product **2.53** and cyanoboration product **2.94** were 12% (66:34) and 0.3% (not determined).

Entry 5: The general procedure was followed with Senphos **2.88** as the ligand. The yields (*trans:cis* ratios) for chloroboration product **2.53** and cyanoboration product **2.94** were 2% (69:31) and 79% (97:3).

Entry 6: The general procedure was followed with Senphos **2.89** as the ligand. The yields (*trans:cis* ratios) for chloroboration product **2.53** and cyanoboration product **2.94** were 1% (78:22) and 92% (96:4).

Entry 7: The general procedure was followed with Senphos **2.90** as the ligand. The yields (*trans:cis* ratios) for chloroboration product **2.53** and cyanoboration product **2.94** were 2% (73:27) and 69% (95:5).

Entry 8: The general procedure was followed with Senphos **2.91** as the ligand. The yields (*trans:cis* ratio) for chloroboration product **2.53** and cyanoboration product **2.94** were 5% (71:29) and 48% (95:5).

Entry 9: The general procedure was followed with Senphos **2.92** as the ligand. The yields (*trans:cis* ratios) for chloroboration product **2.53** and cyanoboration product **2.94** was 5% (71:29) and 24% (95:5).

Entry 10: The general procedure was followed with Senphos **2.93** as the ligand. The yields (*trans:cis* ratios) for chloroboration product **2.53** and cyanoboration product **2.94** was 3% (66:34) and 46% (96:4).

Entry 11: The general procedure was followed with **CC-2.89** as the ligand. The yields (*trans:cis* ratios) for chloroboration product **2.53** and cyanoboration product **2.94** was 13% (81:19) and 6% (89:11).

2.4.2.3.4. Preparation of 1,3-enynes in Table 2.5 and Table 2.6

General method of enyne syntheses by Kumada coupling:

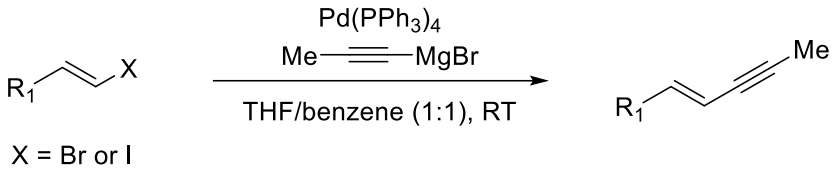

The corresponding *(E)*-styrenyl bromide[66] (to synthesize **2.95-S1**, **2.96-S1**, **2.98-S1** to **2.102-S1**, **2.106-S1**, **2.108-S1** and **2.114-S1**) or alkenyl iodide [67](to synthesize **2.109-S1** to **2.112-S1** and **2.115-S1**) precursors are known compounds. *(E)*-3-(2-

[66] (a) Liu, J.; Ren, Q.; Zhang, X.; Gong, H. *Angew. Chem. Int. Ed*. **2016**, *55*, 15544-15548; (b) Li, H.; Zhang, Z.; Shangguan, X.; Huang, S.; Chen, J.; Zhang, Y.; Wang, J. *Angew. Chem. Int. Ed*. **2014**, *53*, 11921-11925.

[67] (a) Ren, H.; Krasovskiy, A.; Knochel, P. *Org. Lett.* **2004**, *6*, 4215-4217; (b) Stille, J. K.; Simpson, J. H. *J. Am. Chem. Soc.* **1987**, *109*, 2138-2152; (c) Lehr, K.; Schulthoff, S.; Ueda, Y.; Mariz, R.; Leseurre, L.; Gabor, B.; Fürstner, A. *Chem. Eur. J*. **2015**, *21*, 219-227.

bromovinyl) thiophene was obtained using reported methods.[68] To a 20-mL vial charged with $Pd(PPh_3)_4$ (34 mg, 0.030 mmol, 0.015 equiv.), *(E)*-styrenyl bromide or alkenyl iodide (2.0 mmol, 1.0 equiv.) and benzene (5 mL) was added 1-propynyl magnesium bromide (5.2 mL, 0.50 M in THF, 2.6 mmol, 1.3 equiv.) in a dropwise fashion at room temperature under nitrogen. The mixture was allowed to stir for 14 hours at the same temperature. At the conclusion of reaction, aqueous HCl solution (5.0 mL, 1.0 M) was added slowly along with Et_2O (6 mL). The organic layer was separated, and the aqueous layer was further extracted with Et_2O (5 mL). The organic layers were then combined, and dried with Na_2SO_4. All violates were removed *in vacuo*, and the residue was purified by silica gel chromatography using hexanes as the eluent to afford the internal enynes as colorless oils. Enyne **2.114-S1** and **2.115-S1** were synthesized with the same procedure using 1-butynyl magnesium bromide and 1-ethynyl magnesium bromide, respectively. The characterization data for enynes are consistent with those reported in the literature: **2.95-S1**[69], (**2.98-S1**, **2.99-S1**, **2.101-S1**, **2.102-S1**, **2.109-S1**, **2.111-S1**, **2.114-S1**)[29], **2.115-S1**[70].

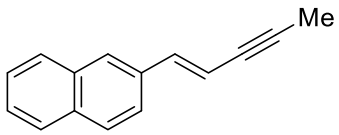

87% yield. ^{1}H NMR (600 MHz, $CDCl_3$) δ 7.86 – 7.76 (m, 3H), 7.73 (d, *J* = 1.6 Hz, 1H), 7.58 (dd, *J* = 8.6, 1.7 Hz, 1H), 7.52 – 7.42 (m, 2H), 7.06 (d, *J* = 16.1 Hz, 1H), 6.29 (dq, *J* = 16.2, 2.4, Hz, 1H), 2.07 (d, *J* = 2.4 Hz, 3H); ^{13}C NMR (151 MHz, $CDCl_3$) δ 140.3, 134.1, 133.6, 133.4, 128.4, 128.2, 127.8, 126.5, 126.5, 126.3, 122.9, 109.3, 88.8, 79.2, 4.7; IR (ATR) 3055, 3029,

[68] (a) Baladi, T.; Granzhan, A.; Piguel, S. *Eur. J. Org. Chem*. **2016**, *2016*, 2421-2434; (b) Dolby, L. J.; Wilkins, C.; Frey, T. G. *J. Org. Chem*. **1966**, *31*, 1110-1116.
[69] Park, S.; Malcolmson, S. J. *ACS Catal*. **2018**, *8*, 8468-8476.
[70] Kinoshita, H.; Ishikawa, T.; Miura, K. *Org. Lett.* **2011**, *13*, 6192-6195.

2912, 2850, 2216, 1507, 1362, 1185, 959, 867, 828, 816, 740, 486 cm^{-1}; HRMS (DART) calcd for $C_{15}H_{13}$ ($[M+H]^+$) 193.10118, found 193.10037.

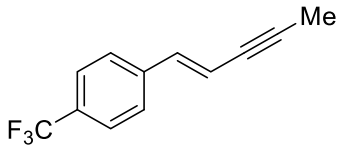

66% yield. ^1H NMR (500 MHz, $CDCl_3$) δ 7.56 (d, *J* = 8.2 Hz, 2H), 7.44 (d, *J* = 8.2 Hz, 2H), 6.87 (d, *J* = 16.2 Hz, 1H), 6.22 (dq, *J* = 16.2, 2.4 Hz, 1H), 2.03 (dd, *J* = 2.5, 0.8 Hz, 3H); ^{13}C NMR (126 MHz, $CDCl_3$) δ 140.1 (d, *J* = 1.7 Hz), 138.5, 130.0 (d, *J* = 32.5 Hz), 126.3, 125.7 (q, *J* = 3.8 Hz), 124.2 (q, *J* = 271.9 Hz), 111.8, 90.2, 78.7, 4.6; ^{19}F NMR (470 MHz, $CDCl_3$) δ –62.6; IR (ATR) 3020, 2924, 2854, 2217, 1612, 1411, 1327, 1165, 1120, 1109, 1070, 954, 860, 820, 599, 517 cm^{-1}; HRMS (DART) calcd for $C_{12}H_{10}F_3$ ($[M+H]^+$) 211.07291, found 211.07317.

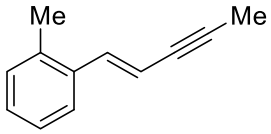

71% yield. ^1H NMR (600 MHz, $CDCl_3$) δ 7.47 (dd, *J* = 7.0, 2.1 Hz, 1H), 7.23 – 7.13 (m, 4H), 6.09 (dq, *J* = 16.1, 2.4 Hz, 1H), 2.39 (s, 3H), 2.06 (d, *J* = 2.4 Hz, 3H); ^{13}C NMR (151 MHz, $CDCl_3$) δ 138.0, 135.6, 135.6, 130.5, 128.2, 126.2, 124.9, 109.9, 88.0, 79.4, 19.8, 4.6; IR (ATR) 3014, 3019, 2949, 2913, 2849, 2217, 1482, 1458, 1436, 1377, 1048, 951, 746, 714, 608, 537, 458 cm^{-1}; HRMS (DART) calcd for $C_{12}H_{13}$ ($[M+H]^+$) 157.10118, found 157.10142.

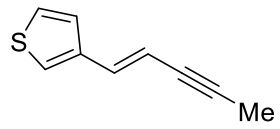

83% yield. ^1H NMR (500 MHz, $CDCl_3$) δ 7.28 – 7.25 (m, 1H), 7.20 – 7.14 (m, 2H), 6.86 (d, *J* = 16.1 Hz, 1H), 5.97 (dq, *J* = 16.2, 2.4 Hz, 1H), 2.00 (d, *J* = 2.4 Hz, 3H); ^{13}C NMR (126 MHz, $CDCl_3$) δ 139.5, 134.3, 126.4, 124.5, 122.9, 108.8, 88.3, 78.9, 4.7; IR (ATR) 3097, 3033, 2912, 2847, 2218, 1411, 1244, 1183, 947, 865, 834, 766, 623, 687, 472 cm^{-1}; HRMS (DART) calcd for C_9H_9S ($[M+H]^+$) 149.04195, found 149.04177.

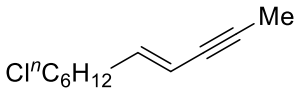

87% yield. ^{1}H NMR (500 MHz, $CDCl_3$) δ 6.07 – 5.96 (m, 1H), 5.41 (dq, *J* = 15.8, 1.9 Hz, 1H), 3.51 (t, *J* = 6.7 Hz, 2H), 2.07 (qd, *J* = 7.3, 1.5 Hz, 2H), 1.91 (d, *J* = 2.3 Hz, 3H), 1.75 (dt, *J* = 14.7, 6.8 Hz, 2H), 1.48 – 1.19 (m, 6H); ^{13}C NMR (126 MHz, $CDCl_3$) δ 143.1, 110.2, 84.2, 78.5, 45.2, 32.9, 32.7, 28.8, 28.4, 26.8, 4.3; IR (ATR) 3019, 2929, 2855, 2225, 1462, 1444, 1309, 1172, 955, 727, 651 cm^{-1}; HRMS (DART) calcd for $C_{11}H_{18}Cl$ ([M+H]$^+$) 185.10915, found 185.10880.

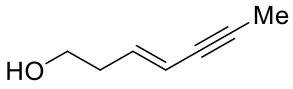

With 2.6 equiv. 1-propynyl magnesium bromide, 81% yield. ^{1}H NMR (500 MHz, $CDCl_3$) δ 5.99 (dtd, *J* = 15.5, 7.3, 0.7 Hz, 1H), 5.60 – 5.42 (m, 1H), 3.63 (t, *J* = 6.4 Hz, 2H), 2.32 (qd, *J* = 6.5, 1.4 Hz, 2H), 1.94 – 1.87 (m, 3H), 1.85 (s, br, 1H); ^{13}C NMR (126 MHz, $CDCl_3$) δ 138.8, 112.9, 85.1, 78.1, 61.7, 36.3, 4.2; IR (ATR) 3330, 2917, 2879, 2224, 1428, 1376, 1171, 1043, 954, 636, 543 cm^{-1}; HRMS (DART) calcd for $C_7H_{11}O$ ([M+H]$^+$) 111.08044, found 111.08026.

General method of enyne syntheses by terminal enyne methylation:

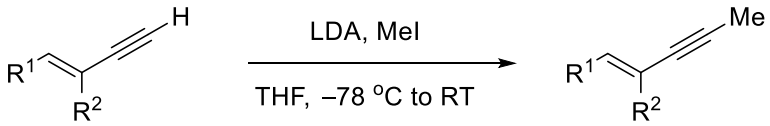

Terminal enynes precursors for synthesizing **2.97-S1**, **2.103-S1** and **2.107-S1** are known compounds.[29,71]

To a 20-mL vial charged with diisopropylamine (242 mg, 2.40 mmol, 1.20 equiv.) and THF (6 mL), *n*butyl lithium (0.88 mL, 2.5 M in hexanes, 2.2 mmol, 1.1 equiv.) was added in dropwise fashion at –78 °C. The mixture was allowed to stir at the same

[71] (a) Dateer, R. B.; Pati, K.; Liu, R. S. *Chem. Commun,* **2012**, *48*, 7200-7202; (b) Kraus, G. A.; Dong, P.; Qu, Y.; Evans, A.; Carpenter, S. *Tetrahedron Lett*. **2016**, *57*, 5185-5187.

temperature for 15 minutes. Then the terminal enyne (2.0 mmol, 1.0 equiv.) in THF (2.0 mL) was added to the LDA solution at –78 °C. After allowing the mixture to stir at –78 °C for another 20 minutes, MeI (355 mg, 2.50 mmol, 1.25 equiv.) was added at once. The resulting mixture was allowed to stir at –78 °C for 30 min and then gradually allowed to warm to room temperature in an hour. At the conclusion of reaction, THF was removed *in vacuo*, and the residue was dissolved in Et_2O (10 mL). The organic layer was further washed by H_2O (5 mL), brine (5 mL) and concentrated. The residue was purified by silica gel column chromatography using hexanes as the eluent to afford the internal enynes as colorless oils.

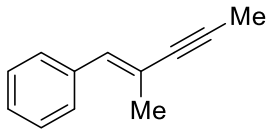

77% yield. ^{1}H NMR (600 MHz, $CDCl_3$) δ 7.39 – 7.33 (m, 2H), 7.31 – 7.27 (m, 2H), 7.25 (td, *J* = 7.3, 1.3 Hz, 1H), 6.80 (s, 1H), 2.07 (t, *J* = 1.3 Hz, 3H), 2.03 (d, *J* = 0.9 Hz, 3H); ^{13}C NMR (151 MHz, $CDCl_3$) δ 137.2, 134.7, 129.0, 128.3, 126.9, 120.6, 84.8, 83.6, 19.5, 4.4; IR (ATR) 3022, 2915, 2852, 2220, 1492, 1440, 1376, 1246, 1030, 917, 866, 762, 724, 694, 506 cm^{-1}; HRMS (DART) calcd for $C_{12}H_{13}$ ([M+H]$^+$) 157.10118, found 157.10170.

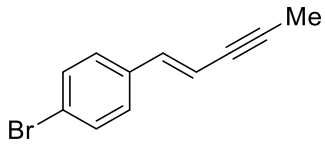

91% yield. ^{1}H NMR (500 MHz, $CDCl_3$) δ 7.46 – 7.39 (m, 2H), 7.24 – 7.16 (m, 2H), 6.78 (d, *J* = 16.2 Hz, 1H), 6.11 (dq, *J* = 16.2, 2.4 Hz, 1H), 2.01 (dd, *J* = 2.4, 0.7 Hz, 3H); ^{13}C NMR (126 MHz, $CDCl_3$) δ 138.9, 135.6, 131.9, 127.6, 122.2, 109.8, 89.2, 78.8, 4.7; IR (ATR) 3031, 2910, 2845, 2213, 1584, 1486, 1399, 1074, 1008, 962, 946, 854, 806, 786, 519 cm^{-1}; HRMS (DART) calcd for $C_{11}H_{10}Br$ ([M+H] $^+$) 220.99604, found 220.99502.

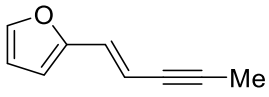

81% yield. ^{1}H NMR (500 MHz, $CDCl_3$) δ 7.34 (d, *J* = 1.6 Hz, 1H), 6.62 (d, *J* = 16.0 Hz, 1H), 6.38 (dt, *J* = 3.4, 1.6 Hz, 1H),

6.31 – 6.23 (m, 1H), 6.04 (dp, J = 16.1, 2.4 Hz, 1H), 2.01 (dd, J = 2.6, 1.6 Hz, 3H); ^{13}C NMR (126 MHz, $CDCl_3$) δ 152.5, 142.7, 127.5, 111.8, 109.2, 107.2, 89.3, 79.0, 4.7; IR (ATR) 3397, 3055, 2220, 1600, 1505, 1408, 1373, 1335, 1095, 820, 767 cm^{-1}; HRMS (DART) calcd for C_9H_9O ([M+H]$^+$) 133.06479, found 133.06543.

Synthesis of enyne **2.104-S1** by esterification:

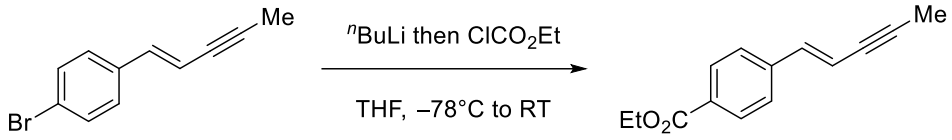

2.103-S1 **2.104-S1**

A solution of enyne **2.103-S1** (236 mg, 1.14 mmol, 1.00 equiv.) in THF (4 mL) was placed in a 20-mL vial. ^{n}Butyl lithium (0.500 mL, 2.50 M in hexanes, 1.25 mmol, 1.10 equiv.) was added to this solution in a dropwise fashion at –78 °C. After allowing the mixture to stir at the same temperature for 20 minutes, ethyl chloroformate (186 mg, 1.71 mmol, 1.50 equiv.) was added. The mixture was allowed to stir for an hour at –78 °C and then allowed to warm to room temperature in an hour. The resulting slurry was poured into H_2O (10 mL) and then diluted with Et_2O (5 mL). The organic layer was separated and violates were removed *in vacuo*. The resulting residue was purified by silica gel chromatography using hexanes/EtOAc (20/1) as the eluent to afford **2.104-S1** a white solid (47% yield). ^{1}H NMR (600 MHz, $CDCl_3$) δ 8.03 – 7.86 (m, 2H), 7.48 – 7.30 (m, 2H), 6.85 (d, J = 16.2 Hz, 1H), 6.21 (dq, J = 16.3, 2.4 Hz, 1H), 4.35 (q, J = 7.2 Hz, 2H), 2.08 – 1.89 (m, 3H), 1.37 (t, J = 7.1 Hz, 3H); ^{13}C NMR (151 MHz, $CDCl_3$) δ 166.3, 140.8, 139.0, 130.0, 129.9, 125.9, 111.6, 90.1, 78.8, 61.0, 14.4, 4.6; IR (ATR) 3035, 2983, 2912, 2212, 1711, 1607, 1411, 1363, 1279, 1266, 1178, 1127, 1105, 1026, 944, 864, 759,

694, 519 cm^{-1}; HRMS (DART) calcd for $C_{14}H_{15}O_2$ ($[M+H]^+$) 215.10666, found 215.10591.

Synthesis of enyne **2.113-S1** by ester coupling:

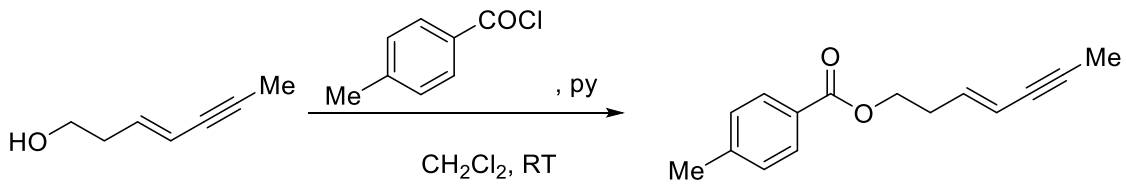

2.112-S1 **2.113-S1**

Under nitrogen, *p*-toluoyl chloride (240 mg, 1.56 mmol, 1.20 equiv.) and pyridine (123 mg, 1.56 mmol, 1.20 equiv.) were added to a 20-mL vial charged with a solution of enyne **2.122-S1** (143 mg, 1.30 mmol, 1.00 equiv.) in CH_2Cl_2 (8 mL). The resulting mixture was allowed to stir at room temperature for 14 hours. Then, the solvent was removed under reduced pressure, and the residue was purified by silica gel chromatography with hexans/EtOAc (40/1) as the eluent to afford **2.113-S1** as a white solid (68% yield). ^{1}H NMR (500 MHz, $CDCl_3$) δ 7.98 – 7.80 (m, 2H), 7.23 (d, *J* = 8.2 Hz, 2H), 6.08 (dt, *J* = 15.8, 7.1 Hz, 1H), 5.58 (dp, *J* = 15.8, 1.9 Hz, 1H), 4.32 (t, *J* = 6.6 Hz, 2H), 2.54 (qd, *J* = 6.8, 1.5 Hz, 2H), 2.40 (s, 3H), 1.92 (d, *J* = 2.3 Hz, 3H); ^{13}C NMR (126 MHz, $CDCl_3$) δ 166.6, 143.7, 138.0, 129.7, 129.1, 127.6, 112.8, 85.3, 78.1, 63.6, 32.4, 21.7, 4.3; IR (ATR) 2955, 2916, 2226, 1715, 1612, 1454, 1379, 1271, 1177, 1105, 1020, 955, 841, 753, 691 cm^{-1}; HRMS (DART) calcd for $C_{15}H_{17}O_2$ ($[M+H]^+$) 229.12231, found 229.12131.

General method of enyne syntheses by Sonogashira coupling:

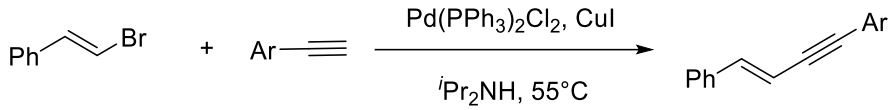

A 50-mL round bottom flask was charged with $PdCl_2(PPh_3)_2$ (84 mg, 0.12 mmol, 0.030 equiv.) and CuI (38 mg, 0.20 mol, 0.050 equiv.) under nitrogen. To this flask $^{i}Pr_2NH$ (20 mL), *(E)*-styrenyl bromide (0.73 g, 4.0 mmol, 1.0 equiv.) and the corresponding terminal alkyne (4.8 mmol, 1.2 equiv.) were added. The mixture was allowed to stir at 55 °C for 16 h. At the conclusion of reaction, H_2O (15 mL) and Et_2O (15 mL) were added to the reaction mixture, and the organic layer was separated. The aqueous layer was extracted with another portion of Et_2O (10 mL). The organic layers were combined, dried, and concentrated. The resulting crude residue was purified by silica gel chromatography using hexanes as the eluent to obtain the product as white solids. Characterization data of enyne **2.116-S1** to **2.118-S1** are consistent with reported in the literature.[72]

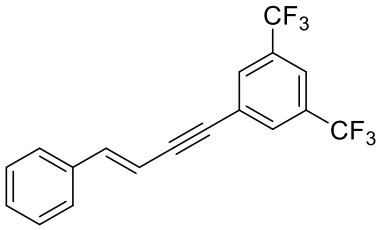

76% yield. ^{1}H NMR (600 MHz, $CDCl_3$) δ 7.91 (d, J = 1.7 Hz, 2H), 7.83 (s, 1H), 7.52 – 7.44 (m, 2H), 7.44 – 7.33 (m, 3H), 7.17 (d, J = 16.3 Hz, 1H), 6.41 (d, J = 16.2 Hz, 1H); ^{13}C NMR (151 MHz, $CDCl_3$) δ 143.6, 135.9, 132.1 (q, J = 33.8 Hz), 131.4 (q, J = 4.0 Hz), 129.4, 129.0, 126.7, 126.0, 123.2 (q, J = 272.8 Hz), 121.5 (dq, J = 7.7, 3.9 Hz), 106.9, 92.6, 88.6; ^{19}F NMR (564 MHz, $CDCl_3$) δ –65.8; IR (ATR) 3033, 2201, 1464, 1385, 1277, 1244, 1174, 1132, 1107, 1048, 953, 896, 848, 748, 684 cm^{-1}; HRMS (DART) calcd for $C_{18}H_{11}F_6$ ($[M+H]^+$) 341.07595, found 341.07569.

[72] Mokar, B. D.; Liu, R. S. *Chem. Commun*. **2014**, *50*, 8966-8969.

General method of enyne syntheses by Kumada coupling:

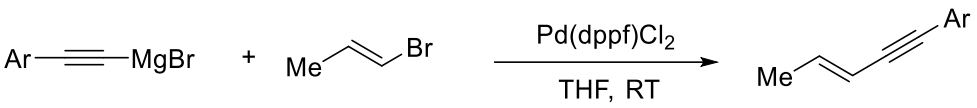

The protocol for was adapted from literature procedure.[73] Under nitrogen to a 20-mL vial charged with $Pd(dppf)Cl_2$ (44 mg, 0.060 mmol, 0.020 equiv.) and (*E*)-1-bromopropene (436 mg, 3.60 mmol, 1.20 equiv.) was added alkynyl magnesium bromide (3.0 mmol, 1.0 equiv.) in THF (12 mL) at room temperature. The mixture was allowed to stir for another 14 hours at room temperature. Then the solvent was removed *in vacuo*, and the residue was dissolved in Et_2O (10 mL). This organic solution was further washed by H_2O (10 mL) and brine (10 mL) and dried with Na_2SO_4. Volatiles were removed under reduced pressure, and the resulting crude residue was purified by silica gel column chromatography using hexane as the eluent to afford the product as colorless liquids.

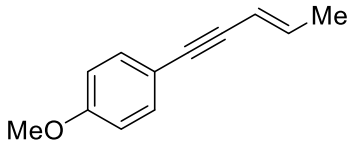

With 1-bromopropene mixture (4.6 equiv., *E*/*Z* = 26:74). Crude ^1H NMR indicates the ratio of *E*/*Z* enyne is 95:5. Purification provides pure **2.120-S1**, 56% yield. ^1H NMR (500 MHz, $CDCl_3$) δ 7.40 – 7.31 (m, 2H), 6.87 – 6.76 (m, 2H), 6.21 (dd, *J* = 15.8, 6.8 Hz, 1H), 5.70 (dq, *J* = 15.7, 1.8 Hz, 1H), 3.80 (s, 3H), 1.83 (dd, *J* = 6.8, 1.8 Hz, 3H); ^{13}C NMR (126 MHz, $CDCl_3$) δ 159.4, 139.1, 132.9, 115.9, 114.0, 111.1, 87.7, 87.0, 55.4, 18.8; IR (ATR) 3001, 2959, 2934, 2912, 2837, 1603, 1506, 1441, 1286, 1244, 1171, 1036, 950, 828, 803, 533 cm^{-1}; HRMS (DART) calcd for $C_{12}H_{13}O$ ($[M+H]^+$) 173.09609, found 173.09544.

[73] Rossi, R.; Carpita, A. *Tetrahedron Lett*. **1986**, *27*, 2529-2532.

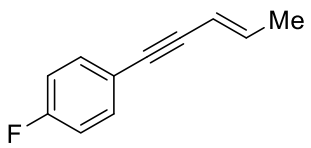

74% yield. ^{1}H NMR (500 MHz, $CDCl_3$) δ 7.43 – 7.34 (m, 2H), 7.07 – 6.90 (m, 2H), 6.24 (dqd, *J* = 14.8, 6.8, 1.2 Hz, 1H), 5.69 (dp, *J* = 15.8, 1.8 Hz, 1H), 1.84 (dt, *J* = 6.9, 1.5 Hz, 3H); ^{13}C NMR (126 MHz, $CDCl_3$) δ 162.4 (d, *J* = 248.9 Hz), 140.1, 133.4 (d, *J* = 8.2 Hz), 119.9 (d, *J* = 3.4 Hz), 115.7 (d, *J* = 22.0 Hz), 110.8, 88.0 (d, *J* = 1.4 Hz), 86.7, 18.9; ^{19}F NMR (470 MHz, $CDCl_3$) δ –111.7 (dp, *J* = 13.6, 4.8 Hz); IR (ATR) 2914, 1599, 1504, 1229, 1155, 1092, 950, 909, 831, 678, 527, 503 cm^{-1}; HRMS (DART) calcd for $C_{11}H_{10}F$ ($[M+H]^+$) 161.07610, found 161.07598.

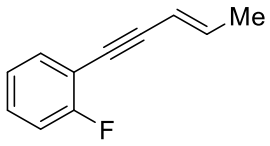

80% yield. ^{1}H NMR (500 MHz, $CDCl_3$) δ 7.41 (td, *J* = 7.5, 1.8 Hz, 1H), 7.26 (dddd, *J* = 8.1, 7.2, 5.2, 1.8 Hz, 1H), 7.15 – 6.98 (m, 2H), 6.31 (dq, *J* = 15.7, 6.8 Hz, 1H), 5.75 (dq, *J* = 15.8, 1.8 Hz, 1H), 1.85 (dd, *J* = 6.9, 1.9 Hz, 3H); ^{13}C NMR (126 MHz, $CDCl_3$) δ 162.6 (d, *J* = 250.9 Hz), 140.8, 133.4 (d, *J* = 1.4 Hz), 129.6 (d, *J* = 8.0 Hz), 124.0 (d, *J* = 3.8 Hz), 115.5 (d, *J* = 21.1 Hz), 112.4 (d, *J* = 15.8 Hz), 110.7, 93.5 (d, *J* = 3.3 Hz), 81.1, 18.9 (d, *J* = 2.2 Hz); ^{19}F NMR (470 MHz, $CDCl_3$) δ –110.4 (dt, *J* = 8.7, 6.0 Hz); IR (ATR) 3031, 2914, 2207, 1572, 1491, 1447, 1256, 1218, 1106, 951, 912, 823, 754, 577 cm^{-1}; HRMS (DART) calcd for $C_{11}H_{10}F$ ($[M+H]^+$) 161.07610, found 161.07542.

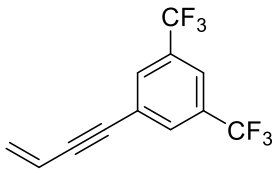

With vinyl bromide (1 M in THF), 77% yield. ^{1}H NMR (500 MHz, $CDCl_3$) δ 7.86 (d, *J* = 1.9 Hz, 2H), 7.79 (dq, *J* = 1.9, 0.9 Hz, 1H), 6.03 (dd, *J* = 17.6, 11.2 Hz, 1H), 5.84 (dd, *J* = 17.6, 1.9 Hz, 1H), 5.67 (dd, *J* = 11.2, 1.9 Hz, 1H); ^{13}C NMR (126 MHz, $CDCl_3$) δ 132.2 (q, *J* = 33.7 Hz), 131.6 (q, *J* = 4.0 Hz), 129.2 (d, *J* = 1.4 Hz), 125.8, 123.2 (q, *J* = 272.7 Hz), 121.8 (hept, *J* = 3.9 Hz), 116.5, 91.5, 86.9; ^{19}F NMR (470 MHz, $CDCl_3$) δ –63.52 (d, *J* =

11.2 Hz); IR (ATR) 1615, 1464, 1418, 1377, 1274, 1241, 1173, 1127, 1106, 1086, 979, 928, 895, 848, 712, 683, 425 cm^{-1}; HRMS (DART) calcd for $C_{12}H_6F_6$ ($[M+H]^+$) 264.03682, found 264.03737.

Synthesis of enyne **2.123-S1** by Negishi coupling:

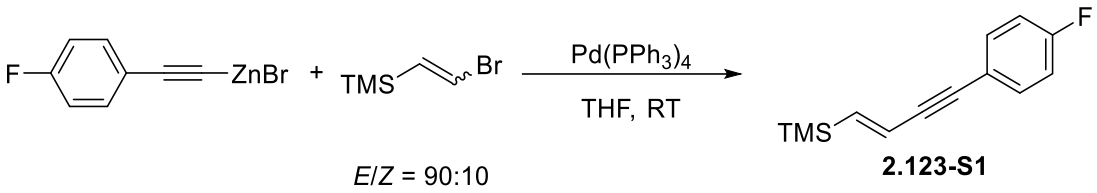

The protocol was adapted from literature procedure.[74] Under nitrogen to a 20-mL vial charged with $Pd(PPh_3)_4$ (92 mg, 0.080 mmol, 0.020 equiv.) was added a solution of ((4-fluorophenyl)ethynyl)zinc bromide (3.42 mmol, 0.850 equiv.) in THF (15 mL) followed by (2-bromovinyl)trimethylsilane (716 mg, 4.00 mmol, 1.00 equiv., E/Z = 90/10) at room temperature. The resulting mixture was allowed to stir for 14 hours at room temperature. Then the solvent was removed *in vacuo* and the residue was dissolved in Et_2O (10 mL). This organic solution was further washed by H_2O (10 mL) and concentrated. The crude product was carefully purified by silica gel chromatography using hexanes as the eluent to afford **2.123-S1** as a colorless liquid (57% yield). ^1H NMR (500 MHz, $CDCl_3$) δ 7.46 – 7.36 (m, 2H), 7.01 (t, J = 8.7 Hz, 2H), 6.54 (d, J = 19.2 Hz, 1H), 6.15 (d, J = 19.2 Hz, 1H), 0.13 (s, 9H); ^{13}C NMR (126 MHz, $CDCl_3$) δ 162.6 (d, J = 249.6 Hz), 146.1, 133.6 (d, J = 8.2 Hz), 123.3, 119.6 (d, J = 3.6 Hz), 115.7 (d, J = 22.0 Hz), 89.5 (d, J = 1.5 Hz), 88.8, –1.5; ^{19}F NMR (470 MHz, $CDCl_3$) δ –116. 3 (m); IR (ATR) 2956, 1601, 1569, 1505, 1249, 1231, 1155, 975, 863, 833, 740, 727, 694, 658, 529 cm^{-1}; HRMS (DART) calcd for $C_{13}H_{16}FSi$ ($[M+H]^+$) 219.09998, found 219.09980.

[74] Andreini, B. P.; Carpita, A.; Rossi, R. *Tetrahedron Lett*. **1988**, *29*, 2239-2242.

Synthesis of enyne **2.124-S1** by Sonogashira coupling:

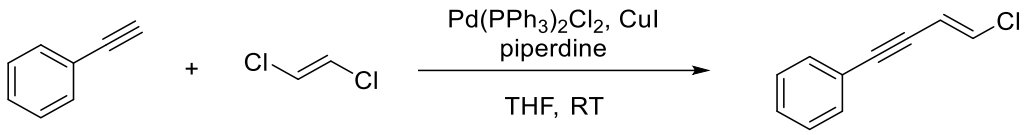

2.124-S1

Under nitrogen a 50-mL round bottom flask was charged with $PdCl_2(PPh_3)_2$ (42 mg, 0.060 mmol, 0.020 equiv.) and CuI (23 mg, 0.12 mol, 0.040 equiv.). To this flask Et_2O (6 mL), piperidine (1.02 g, 12.0 mmol, 4.00 equiv.), phenylacetylene (306 mg, 3.00 mmol, 1.00 equiv.) and *trans*-dichloroethylene (437 mg, 4.50 mmol, 1.50 equiv.) were added. The mixture was allowed to stir at room temperature for 16 h. At the conclusion of reaction H_2O (15 mL) and Et_2O (15 mL) were added, and the organic layer was separated. The aqueous layer was further washed by Et_2O (10 mL). The organic layers were combined, concentrated, and purified by silica gel chromatography using pentane as the eluent to obtain **2.134-S1** as a colorless liquid (87% yield). ^{1}H NMR (500 MHz, $CDCl_3$) δ 7.49 – 7.39 (m, 2H), 7.33 (dd, J = 5.0, 1.9 Hz, 3H), 6.63 (d, J = 13.6 Hz, 1H), 6.16 (d, J = 13.6 Hz, 1H); ^{13}C NMR (126 MHz, $CDCl_3$) δ 131.7, 130.3, 128.8, 128.5, 122.8, 114.0, 92.1, 84.5; IR (ATR) 3067, 3031, 2204, 1581, 1488, 1442, 1272, 1224, 912, 843, 752, 687, 528, 498 cm^{-1}; HRMS (DART) calcd for $C_{10}H_7Cl$ ($[M+H]^+$) 162.02308, found 162.02267.

2.4.2.3.5. General procedure for Table 2.5

To a 4-mL vial charged with $Pd(COD)(CH_2TMS)_2$ (3.9 mg, 0.010 mmol, 5.0 mol%), Senphos **2.89** or **2.93** (mol% is indicated in the corresponding entries), CuCN (29 mg, 0.32 mmol, 1.6 equiv.), Cl–BCat (55 mg, 0.36 mmol, 1.8 equiv.), and *o*-DCB (0.30 mL) was added the corresponding enyne substrate (0.20 mmol, 1.0 equiv.). The resulting

mixture was allowed to stir for 2.5 hours at the temperature indicated in the entries. At the conclusion of reaction, the mixture was passed through an acrodisc with CH_2Cl_2 under nitrogen. 1,8-Diaminonaphthlene (64 mg, 0.40 mmol, 2.0 equiv.) was then added to the filtrate and the mixture was allowed to stir for another 12 hours. Then the mixture was passed through an acrodisc and concentrated under reduced pressure. The resulting crude residue was purified by silica gel chromatography using hexanes/CH_2Cl_2 (4/1 to 1/1 gradient) as the eluent to afford the pure *trans*-selective cyanoboration products as yellow solids.

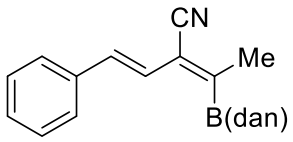

With 5 mol% Senphos **2.89** at 115 °C, 86% yield (run1: 87%, run2: 85%), 96:4. ^{1}H NMR (500 MHz, $CDCl_3$) δ 7.40 (d, *J* = 7.0 Hz, 2H), 7.31 (t, *J* = 7.2 Hz, 2H), 7.27 (d, *J* = 7.0 Hz, 1H), 7.18 – 7.09 (m, 4H), 7.03 (d, *J* = 15.9 Hz, 1H), 6.93 (d, *J* = 15.8 Hz, 1H), 6.39 (dd, *J* = 7.1, 1.3 Hz, 2H), 5.70 (s, 2H), 2.33 (s, 3H); ^{13}C NMR (101 MHz, $CDCl_3$) δ 140.1, 136.4, 135.8, 134.0, 129.0, 128.8, 127.8, 127.1, 123.9, 120.8, 120.1, 118.8, 115.6, 106.7, 22.5 (*B*-alkenyl carbon signal not observed); ^{11}B NMR (160 MHz, $CDCl_3$) δ 28.8; IR (ATR) 3397, 3055, 2220, 1600, 1505, 1408, 1373, 1335, 1095, 820, 767 cm^{-1}; HRMS (DART) calcd for $C_{22}H_{19}BN_3$ ([M+H]$^+$) 336.16665, found 336.16979.

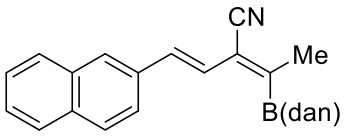

With 5 mol% Senphos **2.89** at 115 °C, 77% yield (run1: 75%, run2: 79%), 98:2. Crystals for single crystal X-ray diffraction analysis were obtained by recrystallization from hexane/CH_2Cl_2 at room temperature. ^{1}H NMR (500 MHz, $CDCl_3$) δ 7.77 (dt, *J* = 7.0, 2.6 Hz, 3H), 7.72 (d, *J* = 8.6 Hz, 1H), 7.53 (dd, *J* = 8.6, 1.7 Hz, 1H), 7.49 – 7.41 (m, 2H), 7.21 – 7.10 (m, 5H), 7.03 (d, *J* = 15.8 Hz, 1H), 6.41 (dd, *J* = 7.2, 1.3

Hz, 2H), 5.77 (s, 2H), 2.34 (s, 3H); ^{13}C NMR (126 MHz, $CDCl_3$) δ 152.5 (br), 140.2, 136.4, 134.0, 133.6, 133.5, 133.3, 128.7, 128.4, 127.9, 127.8, 127.8, 126.6, 126.6, 124.1, 123.3, 120.8, 120.1, 118.8, 115.7, 106.7, 22.6; ^{11}B NMR (160 MHz, $CDCl_3$) δ 28.9; IR (ATR) 3378, 3053, 2924, 2217, 1627, 1600, 1504, 1407, 1373, 1336, 1094, 953, 819, 765 cm^{-1}; HRMS (DART) calcd for $C_{26}H_{21}BN_3$ ($[M+H]^+$) 386.18230, found 386.18179.

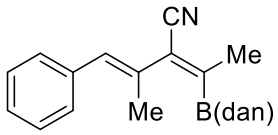

With 5 mol% Senphos **2.89** at 115 °C, 63% yield (run1: 65%, run2: 61%), >98:2. ^{1}H NMR (500 MHz, $CDCl_3$) δ 7.32 (t, *J* = 7.5 Hz, 2H), 7.27 – 7.19 (m, 3H), 7.11 (t, *J* = 7.8 Hz, 2H), 7.05 (d, *J* = 8.2 Hz, 2H), 6.86 (s, 1H), 6.32 (d, *J* = 7.2 Hz, 2H), 5.68 (s, 2H), 2.31 (s, 3H), 2.16 (d, *J* = 1.4 Hz, 3H); ^{13}C NMR (126 MHz, $CDCl_3$) δ 140.1, 136.5, 136.4, 133.0, 132.9, 129.2, 128.5, 127.7, 127.6, 125.4, 119.8, 118.6, 117.0, 106.5, 22.9, 18.1 (*B*-alkenyl carbon signal not observed); ^{11}B NMR (160 MHz, $CDCl_3$) δ 29.0; IR (ATR) 3396, 3054, 2925, 2211, 1599, 1504, 1373, 1332, 1109, 820, 765, 701 cm^{-1}; HRMS (DART) calcd for $C_{23}H_{21}BN_3$ ($[M+H]^+$) 350.18230, found 350.18304.

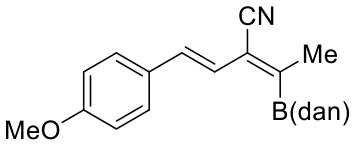

With 5 mol% Senphos **2.89** and 1.5 equiv. Cl-BCat at 115 °C, 64% yield (run1: 65%, run2: 62%), 96:4. ^{1}H NMR (600 MHz, $CDCl_3$) δ 7.35 – 7.31 (m, 2H), 7.15 (dd, *J* = 8.3, 7.2 Hz, 2H), 7.11 (dd, *J* = 8.4, 1.1 Hz, 2H), 6.96 (d, *J* = 15.8 Hz, 1H), 6.86 – 6.82 (m, 2H), 6.80 (d, *J* = 15.8 Hz, 1H), 6.39 (dd, *J* = 7.2, 1.1 Hz, 2H), 5.73 (s, 2H), 3.79 (s, 3H), 2.31 (s, 3H); ^{13}C NMR (151 MHz, $CDCl_3$) δ 160.2, 150.9 (br), 140.2, 136.4, 133.4, 128.6, 128.4, 127.8, 121.8, 120.9, 120.1, 118.7, 115.8, 114.4, 106.6, 55.4, 22.4; ^{11}B NMR (160 MHz, $CDCl_3$) δ 28.8; IR (ATR) 3358, 3053, 2932, 2219, 1598, 1508, 1407, 1373,

1333, 1247, 1173, 1032, 1095, 820, 767 cm^{-1}; HRMS (DART) calcd for $C_{23}H_{21}BN_3O$ ($[M+H]^+$) 366.17722, found 366.17843.

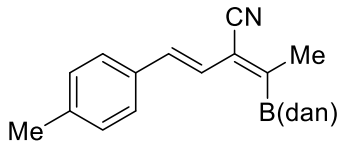

With 5 mol% Senphos **2.89** at 115 °C, 87% yield (run1: 88%, run2: 85%), 97:3. ^{1}H NMR (500 MHz, $CDCl_3$) δ 7.32 – 7.28 (m, 2H), 7.15 (dd, *J* = 8.3, 7.1 Hz, 2H), 7.13 – 7.09 (m, 4H), 7.00 (d, *J* = 15.8 Hz, 1H), 6.88 (d, *J* = 15.8 Hz, 1H), 6.38 (dd, *J* = 7.1, 1.2 Hz, 2H), 5.70 (s, 2H), 2.33 (s, 3H), 2.32 (s, 3H); ^{13}C NMR (126 MHz, $CDCl_3$) δ 140.2, 138.9, 136.4, 133.9, 133.1, 129.7, 127.8, 127.0, 122.9, 120.9, 120.1, 118.8, 115.7, 106.7, 22.4, 21.4 (*B*-alkenyl carbon signal not observed); ^{11}B NMR (160 MHz, $CDCl_3$) δ 28.6; IR (ATR) 3396, 3052, 2917, 2220, 1629, 1600, 1505, 1408, 1373, 1334, 1095, 820, 766 cm^{-1}; HRMS (DART) calcd for $C_{23}H_{21}BN_3$ ($[M+H]^+$) 350.18230, found 350.18279.

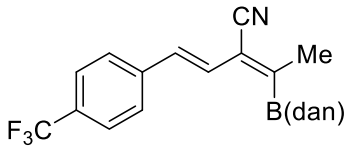

With 5 mol% Senphos **2.89** at 115 °C, 80% yield (run1: 77%, run2: 82%), >98:2. ^{1}H NMR (600 MHz, THF-d_8) δ 7.65 (d, *J* = 8.2 Hz, 2H), 7.58 (d, *J* = 8.2 Hz, 2H), 7.48 (s, 2H), 7.21 (d, *J* = 15.9 Hz, 1H), 7.06 – 6.99 (m, 3H), 6.96 (dd, *J* = 8.4, 0.9 Hz, 2H), 6.37 (dd, *J* = 7.3, 1.0 Hz, 2H), 2.34 (s, 3H); ^{13}C NMR (126 MHz, THF-d_8) δ 158.0 (br), 142.6, 141.2, 137.7, 131.6, 130.49 (q, *J* = 32.0 Hz), 128.6, 128.4, 128.2, 126.63 (q, *J* = 3.9 Hz), 125.5 (q, *J* = 272.2 Hz), 121.7, 120.2, 118.6, 115.8, 107.0, 22.9; ^{11}B NMR (160 MHz, THF-d_8) δ 29.5; ^{19}F NMR (564 MHz, THF-d_8) δ –63.4; IR (ATR) 3411, 3371, 2922, 2852, 2217, 1602, 1506, 1408, 1329, 1177, 1105, 1068, 820, 764, 690, 455 cm^{-1}; HRMS (DART) calcd for $C_{23}H_{18}BN_3F_3$ ($[M+H]^+$) 404.15404, found 404.15382.

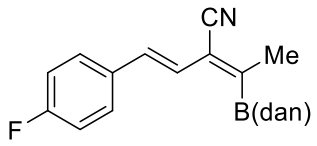

With 5 mol% Senphos **2.89** at 115 °C, 66% yield (run1: 66%, run2: 65%), 96:4. ^{1}H NMR (600 MHz, $CDCl_3$) δ

7.35 (dd, *J* = 8.6, 5.5 Hz, 2H), 7.16 (t, *J* = 7.7 Hz, 2H), 7.12 (d, *J* = 8.2 Hz, 2H), 7.01 – 6.93 (m, 3H), 6.84 (d, *J* = 15.8 Hz, 1H), 6.40 (d, *J* = 7.2 Hz, 2H), 5.74 (s, 2H), 2.33 (s, 3H); ^{13}C NMR (151 MHz, $CDCl_3$) δ 163.0 (d, *J* = 249.1 Hz), 152.7 (br), 140.1, 136.4, 132.6, 132.03 (d, *J* = 3.4 Hz), 128.7 (d, *J* = 8.1 Hz), 127.8, 123.63 (d, *J* = 2.6 Hz), 120.4, 120.1, 118.8, 116.0 (d, *J* = 21.9 Hz), 115.6, 106.7, 22.5; ^{11}B NMR (160 MHz, $CDCl_3$) δ 28.7; ^{19}F NMR (564 MHz, $CDCl_3$) δ –112.3 (tt, *J* = 8.6, 5.3 Hz); IR (ATR) 3404, 3385, 3052, 2216, 1601, 1505, 1407, 1376, 1334, 1227, 1092, 819, 763, 681 cm^{-1}; HRMS (DART) calcd for $C_{22}H_{18}BN_3F$ ($[M+H]^+$) 354.15723, found 354.15886.

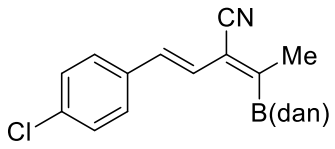

With 5 mol% Senphos **2.89** at 115 °C, 84% yield (run1: 82%, run2: 86%), >98:2. ^{1}H NMR (600 MHz, $CDCl_3$) δ 7.32 (d, *J* = 8.5 Hz, 2H), 7.27 (d, *J* = 8.4 Hz, 2H), 7.18 – 7.08 (m, 4H), 6.96 (d, *J* = 15.8 Hz, 1H), 6.89 (d, *J* = 15.8 Hz, 1H), 6.39 (d, *J* = 7.1 Hz, 2H), 5.70 (s, 2H), 2.33 (s, 3H); ^{13}C NMR (151 MHz, $CDCl_3$) δ 153.2 (br), 140.0, 136.4, 134.5, 134.3, 132.6, 129.2, 128.2, 127.8, 124.4, 120.5, 120.1, 118.9, 115.4, 106.7, 22.6; ^{11}B NMR (160 MHz, $CDCl_3$) δ 28.8; IR (ATR) 3403, 3379, 2217, 1604, 1508, 1411, 1337, 1095, 820, 765 cm^{-1}; HRMS (DART) calcd for $C_{22}H_{18}BN_3Cl$ ($[M+H]^+$) 370.12768, found 370.12759.

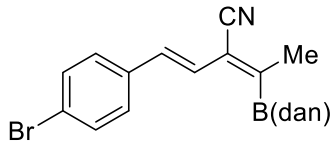

With 5 mol% Senphos **2.89** at 115 °C, 55% yield (run1: 53%, run2: 57%), 95:5. ^{1}H NMR (500 MHz, THF-d_8) δ 7.49 – 7.34 (m, 6H), 7.10 (dd, *J* = 15.9, 1.0 Hz, 1H), 7.03 (ddd, *J* = 8.3, 7.2, 1.0 Hz, 2H), 6.97 – 6.88 (m, 3H), 6.36 (dd, *J* = 7.3, 1.1 Hz, 2H), 2.31 (s, 3H); ^{13}C NMR (126 MHz, THF-d_8) δ 142.7, 137.7, 136.5, 132.9, 132.0, 129.5, 128.4, 126.8, 122.9, 121.6, 120.3, 118.5, 115.9, 107.0, 22.8 (*B*-alkenyl carbon signal not

observed); ^{11}B NMR (160 MHz, THF-d_8) δ 29.0; IR (ATR) 3403, 3374, 2216, 1603, 1506, 1408, 1376, 1335, 1094, 1072, 1007, 819, 763, 754, 686 cm^{-1}; HRMS (DART) calcd for $C_{22}H_{18}BN_3Br$ ([M+H]$^+$) 414.07717, found 414.07770.

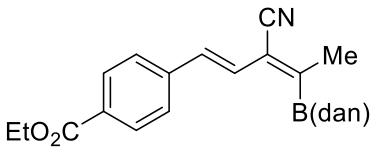

With 5 mol% Senphos **2.89** at 115 °C, 69% yield (run1: 71%, run2: 67%), >98:2. ^{1}H NMR (600 MHz, $CDCl_3$) δ 7.99 – 7.94 (m, 2H), 7.47 – 7.41 (m, 2H), 7.18 – 7.09 (m, 4H), 7.02 (d, *J* = 4.1 Hz, 2H), 6.39 (dd, *J* = 7.0, 1.2 Hz, 2H), 5.73 (s, 2H), 4.35 (q, *J* = 7.1 Hz, 2H), 2.35 (s, 3H), 1.37 (t, *J* = 7.1 Hz, 3H); ^{13}C NMR (151 MHz, $CDCl_3$) δ 166.3, 140.1, 140.0, 136.4, 132.8, 130.3, 130.2, 127.8, 126.9, 126.0, 120.5, 120.1, 119.0, 115.3, 106.8, 61.2, 22.7, 14.5 (*B*-alkenyl carbon signal not observed); ^{11}B NMR (160 MHz, $CDCl_3$) δ 28.9; IR (ATR) 3372, 2223, 1691, 1603, 1510, 1409, 1335, 1290, 1272, 1182, 1097, 765, 698 cm^{-1}; HRMS (DART) calcd for $C_{25}H_{23}BN_3O_2$ ([M+H]$^+$) 408.18778, found 408.18712.

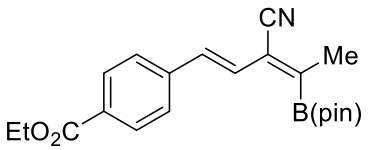

With 5 mol% Senphos **2.89** at 115 °C, pinacol (236 mg, 2.00 mmol, 10.0 equiv.) in CH_2Cl_2 (5 mL) was used rather than 1,8-diaminonaphthlene, purified by silica gel chromatography using hexanes/EtOAc (10/1) as the eluent, 56% yield (run1: 58%, run2: 53%), >98:2. Crystals for single crystal X-ray diffraction analysis were obtained by recrystallization from hexane/CH_2Cl_2 at room temperature. ^{1}H NMR (600 MHz, $CDCl_3$) δ 8.06 – 8.00 (m, 2H), 7.76 (d, *J* = 16.0 Hz, 1H), 7.51 – 7.45 (m, 2H), 7.03 (d, *J* = 16.0 Hz, 1H), 4.38 (q, *J* = 7.1 Hz, 2H), 2.25 (s, 3H), 1.40 (t, *J* = 7.1 Hz, 3H), 1.35 (s, 12H); ^{13}C NMR (151 MHz, $CDCl_3$) δ 166.4, 140.9, 133.1, 130.2 (2 signals), 127.1, 126.9, 125.7, 115.5, 84.7, 61.1, 25.0, 21.9, 14.5 (*B*-alkenyl carbon signal not observed); ^{11}B NMR (160

MHz, $CDCl_3$) δ 29.4; IR (ATR) 2979, 2929, 2221, 1712, 1605, 1361, 1269, 1141, 1102, 1019, 764, 847, 679, 627 cm^{-1}; HRMS (DART) calcd for $C_{21}H_{27}BNO_4$ ($[M+H]^+$) 368.20277, found 368.20267.

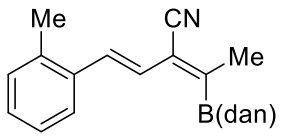

With 5 mol% Senphos **2.89** at 115 °C, 58% yield (run1: 60%, run2: 56%), 94:6. ^1H NMR (600 MHz, $CDCl_3$) δ 7.40 (d, *J* = 7.7 Hz, 1H), 7.32 – 7.23 (m, 1H), 7.20 – 7.08 (m, 7H), 6.86 (d, *J* = 15.7 Hz, 1H), 6.39 (dd, *J* = 7.2, 1.2 Hz, 2H), 5.74 (s, 2H), 2.42 (s, 3H), 2.34 (s, 3H); ^{13}C NMR (151 MHz, $CDCl_3$) δ 152.6 (br), 140.1, 136.5, 136.3, 134.8, 131.6, 130.7, 128.6, 127.8, 126.4, 125.6, 125.0, 120.9, 120.0, 118.7, 115.7, 106.7, 22.5, 19.9; ^{11}B NMR (160 MHz, $CDCl_3$) δ 28.9; IR (ATR) 3395, 3055, 2926, 2219, 1629, 1600, 1505, 1408, 1373, 1335, 1093, 957, 908, 820, 766, 732 cm^{-1}; HRMS (DART) calcd for $C_{23}H_{21}BN_3$ ($[M+H]^+$) 350.18230, found 350.18173.

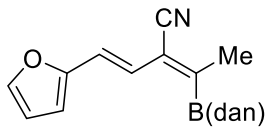

With 5 mol% Senphos **2.93** at 105 °C, 71% yield (run1: 69%, run2: 73%), 98:2. ^1H NMR (500 MHz, $CDCl_3$) δ 7.34 (d, *J* = 1.6 Hz, 1H), 7.20 – 7.05 (m, 4H), 6.91 – 6.74 (m, 2H), 6.39 (m, 4H), 5.73 (s, 2H), 2.31 (s, 3H); ^{13}C NMR (126 MHz, $CDCl_3$) δ 151.8, 143.3, 140.2, 136.3, 127.8, 122.2, 121.2, 120.4, 120.1, 118.7, 115.5, 112.1, 111.3, 106.7, 22.5 (*B*-alkenyl carbon signal not observed); ^{11}B NMR (160 MHz, $CDCl_3$) δ 28.8; IR (ATR) 3389, 3053, 2924, 2220, 1629, 1598, 1503, 1407, 1334, 1263, 1094, 1013, 820, 766, 736 cm^{-1}; HRMS (DART) calcd for $C_{20}H_{17}BN_3O$ ($[M+H]^+$) 326.14592, found 326.14575.

With 5 mol% Senphos **2.89** at 115 °C, 72% yield (run1: 70%, run2: 74%), 97:3. ^1H NMR (500 MHz, $CDCl_3$) δ 7.28 (dd, *J* = 3.1, 1.2 Hz, 1H), 7.24 (dd, *J* = 3.0, 0.6 Hz, 1H), 7.19 – 7.09 (m, 5H), 7.03 (d, *J* = 15.8 Hz, 1H), 6.77 (d, *J* = 15.8 Hz, 1H), 6.38 (dd, *J*

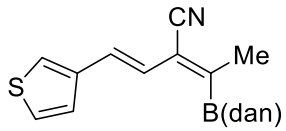

= 7.1, 1.2 Hz, 2H), 5.71 (s, 2H), 2.31 (s, 3H); ^{13}C NMR (126 MHz, $CDCl_3$) δ 140.1, 138.6, 136.4, 128.0, 127.8, 126.8, 125.0, 124.6, 123.8, 120.7, 120.1, 118.8, 115.6, 106.7, 22.4 (*B*-alkenyl carbon signal not observed); ^{11}B NMR (160 MHz, $CDCl_3$) δ 28.9; IR (ATR) 3394, 3053, 2219, 1628, 1599, 1504, 1407, 1373, 1335, 1095, 820, 766, 650 cm^{-1}; HRMS (DART) calcd for $C_{20}H_{17}BN_3S$ ([M+H]$^+$) 342.12308, found 342.12416.

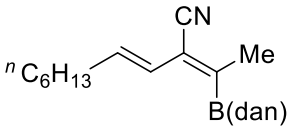

With 7 mol% Senphos **2.89** at 125 °C, 60% yield (run1: 62%, run2: 57%), 96:4. ^{1}H NMR (600 MHz, $CDCl_3$) δ 7.14 (dd, *J* = 8.3, 7.3 Hz, 2H), 7.09 (dd, *J* = 8.3, 1.0 Hz, 2H), 6.37 (dd, *J* = 7.2, 1.0 Hz, 2H), 6.24 (d, *J* = 15.4 Hz, 1H), 6.18 (dt, *J* = 15.4, 6.7 Hz, 1H), 5.69 (d, *J* = 4.4 Hz, 2H), 2.24 (s, 3H), 2.14 (q, *J* = 7.2 Hz, 2H), 1.41 (h, *J* = 6.8 Hz, 2H), 1.34 – 1.20 (m, 6H), 0.88 (t, *J* = 6.9 Hz, 3H); ^{13}C NMR (151 MHz, $CDCl_3$) δ 149.8 (br), 140.2, 137.1, 136.3, 127.7, 125.5, 120.4, 120.0, 118.6, 115.9, 106.5, 32.7, 31.7, 29.1, 29.0, 22.7, 22.0, 14.2; ^{11}B NMR (160 MHz, $CDCl_3$) δ 28.8; IR (ATR) 3367, 3054, 2954, 2853, 2218, 1598, 1505, 1406, 1372, 1361, 1333, 1095, 957, 820, 764, 664 cm^{-1}; HRMS (DART) calcd for $C_{22}H_{27}BN_3$ ([M+H]$^+$) 344.22925, found 344.22994.

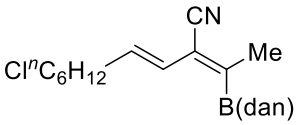

With 7 mol% Senphos **2.89** at 125 °C, 55% yield (run1: 57%, run2: 53%), 96:4. ^{1}H NMR (600 MHz, $CDCl_3$) δ 7.14 (t, *J* = 7.8 Hz, 2H), 7.09 (d, *J* = 8.3 Hz, 2H), 6.37 (d, *J* = 7.2 Hz, 2H), 6.23 (d, *J* = 15.4 Hz, 1H), 6.16 (dt, *J* = 14.9, 6.8 Hz, 1H), 5.65 (s, 2H), 3.50 (t, *J* = 6.7 Hz, 2H), 2.24 (s, 3H), 2.14 (apparent q, *J* = 7.2 Hz, 2H), 1.74 (apparent p, *J* = 7.0 Hz, 2H), 1.42 (apparent h, *J* = 7.5 Hz, 4H), 1.32 (apparent p, *J* = 7.6 Hz, 2H); ^{13}C NMR (151 MHz, $CDCl_3$) δ 140.2, 136.8, 136.4, 127.7, 125.8, 120.4, 120.0, 118.7, 115.8, 106.5, 45.2, 32.6,

32.6, 29.0, 28.5, 26.8, 22.0 (*B*-alkenyl carbon signal not observed); ^{11}B NMR (160 MHz, $CDCl_3$) δ 29.0; IR (ATR) 3393, 3054, 2927, 2854, 2218, 1628, 1598, 1504, 1406, 1373, 1333, 1095, 820, 765, 730, 665 cm^{-1}; HRMS (DART) calcd for $C_{22}H_{26}BN_3Cl$ ($[M+H]^+$) 378.19028, found 378.18893.

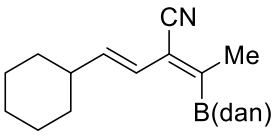

With 7 mol% Senphos **2.89** at 125 °C, 60% yield (run1: 61%, run2: 59%), 93:7. ^{1}H NMR (600 MHz, $CDCl_3$) δ 7.14 (dd, *J* = 8.3, 7.2 Hz, 2H), 7.09 (dd, *J* = 8.3, 1.0 Hz, 2H), 6.37 (dd, *J* = 7.3, 1.0 Hz, 2H), 6.20 (dd, *J* = 15.5, 1.0 Hz, 1H), 6.12 (dd, *J* = 15.5, 7.1 Hz, 1H), 5.66 (s, 2H), 2.24 (s, 3H), 2.06 (tdt, *J* = 10.9, 7.0, 3.4 Hz, 1H), 1.71 (ddq, *J* = 13.6, 7.2, 3.4 Hz, 4H), 1.64 (dtd, *J* = 12.4, 3.6, 1.7 Hz, 1H), 1.25 (m, 2H), 1.20 – 1.06 (m, 3H); ^{13}C NMR (151 MHz, $CDCl_3$) δ 149.8 (br), 142.6, 140.2, 136.4, 127.7, 123.3, 120.7, 120.0, 118.6, 115.9, 106.5, 41.1, 32.8, 26.0, 25.9, 22.1; ^{11}B NMR (160 MHz, $CDCl_3$) δ 28.7; IR (ATR) 3429, 3393, 2926, 2852, 2218, 1600, 1504, 1408, 1335, 1264, 1093, 963, 820, 732, 703 cm^{-1}; HRMS (DART) calcd for $C_{22}H_{25}BN_3$ ($[M+H]^+$) 342.21360, found 342.21457.

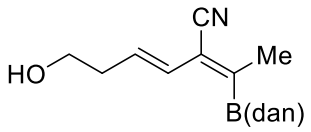

2.112-S1 was pre-treated with HBCat (29 mg, 0.24 mmol, 1.2 equiv.) in CH_2Cl_2 (1.0 mL) followed by removal of volatiles under high vacuum (150 mmTor) for 30 min at room temperature. This material was then used for the *trans*-selective cyanoboration reaction with 7 mol% Senphos **2.89** at 125 °C, 35% yield (run1: 32%, run2: 37%), 98:2. Product **2.112** appears to decompose slowly on silica gel column. ^{1}H NMR (500 MHz, $CDCl_3$) δ 7.13 (dd, *J* = 8.3, 7.2 Hz, 2H), 7.08 (dd, *J* = 8.4, 1.2 Hz, 2H), 6.39 – 6.31 (m, 3H), 6.17 (dt, *J* = 15.0, 7.1 Hz, 1H), 5.66 (s, 2H), 3.73 (t, *J* = 6.4 Hz, 2H), 2.46 – 2.35 (m, 2H), 2.25 (s, 3H), 1.39 (s, 1H); ^{13}C NMR (151 MHz, $CDCl_3$) δ 151.2 (br), 140.2, 136.3, 132.5,

128.1, 127.7, 120.1, 120.0, 118.6, 115.7, 106.6, 61.7, 35.9, 22.1; ^{11}B NMR (160 MHz, $CDCl_3$) δ 28.9; IR (ATR) 3387, 3053, 2926, 2219, 1599, 1509, 1408, 1373, 1335, 1096, 1036, 821, 768 cm^{-1}; HRMS (DART) calcd for $C_{18}H_{19}BN_3O$ ($[M+H]^+$) 304.16157, found 304.16183.

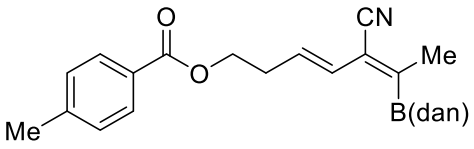

With 7 mol% Senphos **2.89** at 135 °C, 73% yield (run1: 71%, run2: 75%), 96:4. ^{1}H NMR (600 MHz, $CDCl_3$) δ 7.93 – 7.83 (m, 2H), 7.18 (d, J = 8.0 Hz, 2H), 7.15 – 7.04 (m, 4H), 6.44 – 6.36 (m, 1H), 6.32 (dd, J = 7.2, 1.1 Hz, 2H), 6.23 (dt, J = 14.9, 7.1 Hz, 1H), 5.69 (s, 2H), 4.36 (t, J = 6.5 Hz, 2H), 2.60 (q, J = 6.7 Hz, 2H), 2.39 (s, 3H), 2.24 (s, 3H); ^{13}C NMR (151 MHz, $CDCl_3$) δ 166.6, 151.6 (br), 143.8, 140.1, 136.3, 131.5, 129.7, 129.2, 128.1, 127.7, 127.4, 120.0, 120.0, 118.7, 115.6, 106.6, 63.6, 32.0, 22.2, 21.8; ^{11}B NMR (160 MHz, $CDCl_3$) δ 28.5; IR (ATR) 3367, 2957, 2219, 1702, 1599, 1508, 1407, 1373, 1335, 1274, 1178, 1096, 908, 820, 768, 754, 731 cm^{-1}; HRMS (DART) calcd for $C_{26}H_{25}BN_3O_2$ ($[M+H]^+$) 422.20343, found 422.20384.

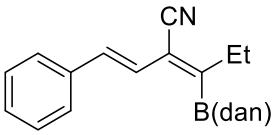

With 5 mol% Senphos **2.89** at 115 °C, 66% yield (run1: 63%, run2: 68%), 93:7. ^{1}H NMR (500 MHz, $CDCl_3$) δ 7.40 (d, J = 7.4 Hz, 2H), 7.31 (t, J = 7.3 Hz, 2H), 7.27 (d, J = 6.9 Hz, 1H), 7.17 (t, J = 7.7 Hz, 2H), 7.12 (d, J = 8.2 Hz, 2H), 7.04 (d, J = 15.9 Hz, 1H), 6.91 (d, J = 15.8 Hz, 1H), 6.40 (d, J = 7.1 Hz, 2H), 5.74 (s, 2H), 2.71 (q, J = 7.6 Hz, 2H), 1.22 (t, J = 7.6 Hz, 3H); ^{13}C NMR (126 MHz, $CDCl_3$) δ 159.2 (br), 140.1, 136.4, 135.9, 134.1, 128.9, 128.7, 127.8, 127.1, 124.1, 120.1, 119.5, 118.8, 115.5, 106.7, 30.1, 14.0; ^{11}B NMR (160 MHz, $CDCl_3$) δ 29.0; IR (ATR) 3382, 3052, 2966, 2214, 1599, 1504, 1406, 1373, 1333, 1166, 1103, 951, 818,

761, 750, 686 cm^{-1}; HRMS (DART) calcd for $C_{23}H_{21}BN_3$ ($[M+H]^+$) 350.18230, found 350.18183.

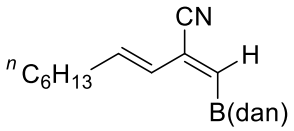

With 10 mol% Pd(COD)($CH_2TMS)_2$ and 10 mol% Senphos **2.89** at 90 °C for 40 min, 45% yield (run1: 47%, run2: 43%), 96:4. ^{1}H NMR (500 MHz, $CDCl_3$) δ 7.13 (dd, *J* = 8.3, 7.2 Hz, 2H), 7.07 (dd, *J* = 8.3, 1.0 Hz, 2H), 6.42 – 6.23 (m, 5H), 5.68 (s, 2H), 2.20 (td, *J* = 7.5, 5.9 Hz, 2H), 1.50 – 1.38 (m, 2H), 1.36 – 1.23 (m, 6H), 0.92 – 0.82 (m, 3H); ^{13}C NMR (126 MHz, $CDCl_3$) δ 141.3, 140.2, 137.7 (br), 136.4, 127.7, 126.6, 125.0, 120.1, 118.7, 117.9, 106.5, 32.9, 31.8, 29.0, 28.9, 22.7, 14.2; ^{11}B NMR (160 MHz, $CDCl_3$) δ 27.5; IR (ATR) 3387, 2923, 2853, 2223, 1629, 1598, 1502, 1406, 1373, 1331, 1165, 1143, 1047, 962, 819, 763 cm^{-1}; HRMS (DART) calcd for $C_{21}H_{25}BN_3$ ($[M+H]^+$) 330.21360, found 330.21405.

2.4.2.3.6. General procedure for Table 2.6

To a 4-mL vial charged with Pd(COD)($CH_2TMS)_2$ (3.9 mg, 0.010 mmol, 10 mol%), Senphos **2.93** (4.3 mg, 0.010 mmol, 10 mol%), CuCN (16 mg, 0.18 mmol, 1.8 equiv.), Cl–BCat (28 mg, 0.18 mmol, 1.8 equiv.) and *o*-DCB (0.10 mL) was added the corresponding enyne (0.10 mmol, 1.0 equiv.). The resulting mixture was allowed to stir for 1 hour at 105 °C. At the conclusion of reaction, the mixture was passed through an acrodisc with CH_2Cl_2 under nitrogen. 1,8-diaminonaphthlene (32 mg, 0.20 mmol, 2.0 equiv.) was then added to the filtrate, and the mixture was allowed to stir for another 12 hours. The reaction mixture was then again passed through an acrodisc and concentrated under reduced pressure. The resuting crude residue was purified by silica gel

chromatography using hexanes/CH_2Cl_2 (4/1 to 1/1 gradient) as the eluent to afford the pure *trans*-selective cyanoboration product as yellow solids.

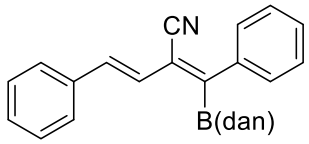

60% yield (run1: 62%, run2: 57%), 86:14. ^{1}H NMR (500 MHz, $CDCl_3$) δ 7.62 – 7.54 (d, *J* = 7.5 Hz, 2H), 7.49 – 7.38 (m, 5H), 7.32 (m, 3H), 7.24 (d, *J* = 15.4 Hz, 1H), 7.14 (m, 5H), 6.37 (d, *J* = 6.8 Hz, 2H), 5.79 (s, 2H); ^{13}C NMR (151 MHz, $CDCl_3$) δ 140.2, 138.9, 136.4, 135.7, 129.5, 129.1, 129.0, 129.0, 128.8, 127.8, 127.6, 127.3, 124.9, 120.1, 119.1, 118.9, 116.6, 106.8 (*B*-alkenyl carbon signal not observed); ^{11}B NMR (160 MHz, $CDCl_3$) δ 29.1; IR (ATR) 3396, 3055, 2219, 1628, 1599, 1504, 1407, 1373, 1336, 1149, 820, 766, 695 cm^{-1}; HRMS (DART) calcd for $C_{27}H_{21}BN_3$ ($[M+H]^+$) 398.18230, found 398.18286.

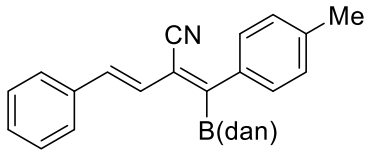

48% yield (run1: 46%, run2: 50%), 75:25. ^{1}H NMR (500 MHz, $CDCl_3$) δ 7.51 (d, *J* = 7.9 Hz, 2H), 7.45 (d, *J* = 7.0 Hz, 2H), 7.37 – 7.18 (m, 6H), 7.19 – 7.09 (m, 5H), 6.36 (dd, *J* = 7.0, 1.4 Hz, 2H), 5.79 (s, 2H), 2.40 (s, 3H); ^{13}C NMR (126 MHz, $CDCl_3$) δ 140.2, 139.8, 136.4, 136.0, 135.9, 135.3, 129.7, 129.0, 129.0, 128.9, 127.8, 127.3, 125.0, 120.1, 118.8, 118.3, 116.9, 106.8, 21.5 (*B*-alkenyl carbon signal not observed); ^{11}B NMR (160 MHz, $CDCl_3$) δ 28.8; IR (ATR) 3419, 3055, 2923, 2219, 1599, 1507, 1406, 1374, 1338, 1260, 1147, 1052, 961, 908, 819, 765, 732 cm^{-1}; HRMS (DART) calcd for $C_{28}H_{23}BN_3$ ($[M+H]^+$) 412.19795, found 412.19878.

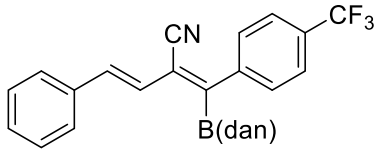

84% yield (run1: 82%, run2: 86%), 93:7. ^{1}H NMR (600 MHz, $CDCl_3$) δ 7.70 (d, *J* = 8.5 Hz, 2H), 7.67 (d, *J* = 8.3 Hz, 2H), 7.49 – 7.42 (m, 2H), 7.37 – 7.30 (m, 3H), 7.27 (d, *J* = 15.6 Hz, 1H), 7.18 – 7.12 (m, 5H), 6.38 (dd, *J* = 6.7, 1.6 Hz, 2H), 5.78

(s, 2H); ^{13}C NMR (151 MHz, $CDCl_3$) δ 152.3 (br), 142.6, 139.9, 137.0, 136.3, 135.4, 131.1 (q, J = 32.9 Hz), 129.5, 129.1, 129.1, 127.8, 127.5, 126.0 (q, J = 3.8 Hz), 124.4, 124.0 (q, J = 272.4 Hz), 120.9, 120.1, 119.1, 116.1, 106.9; ^{11}B NMR (160 MHz, $CDCl_3$) δ 29.0; ^{19}F NMR (564 MHz, $CDCl_3$) δ –62.8; IR (ATR) 3394, 3055, 2921, 2217, 1628, 1598, 1502, 1408, 1373, 1334, 1148, 907, 820, 767, 730, 692, 648 cm^{-1}; HRMS (DART) calcd for $C_{28}H_{20}BN_3F_3$ ([M+H]$^+$) 466.16969, found 466.16856.

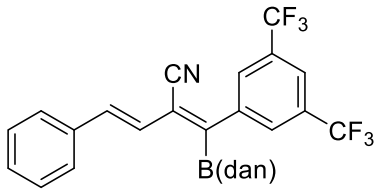

86% yield (run1: 88%, run2: 83%), >98:2. ^{1}H NMR (600 MHz, $CDCl_3$) δ 7.96 (d, J = 1.5 Hz, 2H), 7.93 (s, 1H), 7.52 – 7.45 (m, 2H), 7.39 – 7.34 (m, 3H), 7.32 (d, J = 15.8 Hz, 1H), 7.20 – 7.13 (m, 5H), 6.41 (dd, J = 5.9, 2.4 Hz, 2H), 5.79 (s, 2H); ^{13}C NMR (151 MHz, $CDCl_3$) δ 150.1 (br), 141.2, 139.7, 138.2, 136.3, 135.2, 132.5 (q, J = 33.7 Hz), 129.8, 129.2, 128.8 (d, J = 3.5 Hz), 128.7 (d, J = 4.1 Hz), 127.8, 127.6, 123.8, 123.1 (q, J = 273.0 Hz), 122.9 (p, J = 3.8 Hz), 122.7, 119.4, 115.5, 107.1; ^{11}B NMR (160 MHz, $CDCl_3$) δ 28.7; ^{19}F NMR (564 MHz, $CDCl_3$) δ –62.8; IR (ATR) 3394, 3057, 2224, 1600, 1503, 1407, 1372, 1275, 1176, 1129, 820, 736, 680 cm^{-1}; HRMS (DART) calcd for $C_{29}H_{19}BN_3F_6$ ([M+H]$^+$) 534.15707, found 534.15663.

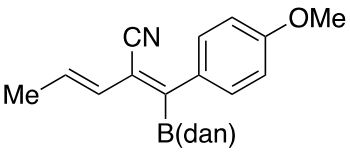

Purified by silica gel chromatography using hexane/Et_2O (5/1) as eluent, 71% yield (run1: 69%, run2: 73%), 94: 6. ^{1}H NMR (500 MHz, $CDCl_3$) δ 7.58 – 7.48 (m, 2H), 7.18 – 7.07 (m, 4H), 6.96 – 6.89 (m, 2H), 6.47 – 6.31 (m, 4H), 5.73 (s, 2H), 3.83 (s, 3H), 1.88 (dd, J = 6.3, 1.1 Hz, 3H); ^{13}C NMR (126 MHz, $CDCl_3$) δ 160.4, 151.5 (br), 140.3, 136.3, 132.9, 131.0, 130.4, 128.1, 127.7, 120.0, 118.6, 117.3, 116.8, 114.3, 106.6, 55.4, 18.4; ^{11}B NMR (160 MHz, $CDCl_3$) δ 29.0; IR (ATR) 3366, 2930, 2214, 1629, 1598,

1507, 1409, 1373, 1333, 1248, 1180, 1154, 1031, 953, 908, 821, 768, 732 cm^{-1}; HRMS (DART) calcd for $C_{23}H_{21}BN_3O$ ($[M+H]^+$) 366.17722, found 366.17607.

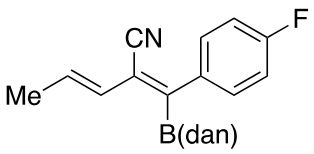

70% yield (run1: 67%, run2: 72%), 95: 5. ^1H NMR (500 MHz, $CDCl_3$) δ 7.52 (dd, *J* = 8.4, 5.3 Hz, 2H), 7.17 – 7.04 (m, 6H), 6.47 – 6.39 (m, 2H), 6.35 (dd, *J* = 7.0, 1.2 Hz, 2H), 5.70 (s, 2H), 1.90 (d, *J* = 4.9 Hz, 3H); ^{13}C NMR (151 MHz, $CDCl_3$) δ 163.1 (d, *J* = 250.1 Hz), 150.6 (br), 140.1, 136.3, 134.9 (d, *J* = 3.5 Hz), 134.3 (two signals), 130.6 (d, *J* = 8.3 Hz), 127.8, 120.0, 119.0, 118.9, 116.7, 116.0 (d, *J* = 21.8 Hz), 106.7, 18.5; ^{11}B NMR (160 MHz, $CDCl_3$) δ 29.0; ^{19}F NMR (470 MHz, $CDCl_3$) δ –111.5 (tt, *J* = 9.1, 5.2 Hz); IR (ATR) 3369, 2919, 2213,1600, 1504, 1413, 1374, 1335, 1231, 1159, 959, 820, 768 cm^{-1}; HRMS (DART) calcd for $C_{22}H_{18}BN_3F$ ($[M+H]^+$) 354.15723, found 354.15671.

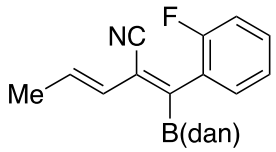

63% yield (run1: 64%, run2: 61%), 98: 2. Crystals for single crystal X-ray diffraction analysis were obtained by recrystallization from hexane/CH_2Cl_2 at –30 °C. ^1H NMR (500 MHz, THF-d_8) δ 7.51 – 7.35 (m, 3H), 7.30 (tdd, *J* = 7.3, 5.1, 1.8 Hz, 1H), 7.16 (td, *J* = 7.6, 1.1 Hz, 1H), 7.10 (ddd, *J* = 9.7, 8.4, 1.1 Hz, 1H), 6.97 (t, *J* = 7.8 Hz, 2H), 6.89 (dd, *J* = 8.3, 1.0 Hz, 2H), 6.59 (dq, *J* = 15.3, 1.6 Hz, 1H), 6.37 – 6.23 (m, 3H), 1.84 (dd, *J* = 6.8, 1.6 Hz, 3H); ^{13}C NMR (126 MHz, THF-d_8) δ 160.6 (d, *J* = 247.6 Hz), 142.6, 137.5, 133.8, 131.5 (d, *J* = 2.8 Hz), 131.1 (d, *J* = 8.2 Hz), 129.2, 128.8 (d, *J* = 14.8 Hz), 128.2, 125.1 (d, *J* = 3.5 Hz), 122.6, 121.5, 118.3, 116.6 (d, *J* = 22.0 Hz), 116.3, 106.8, 18.2 (*B*-alkenyl carbon signal not observed); ^{11}B NMR (160 MHz, THF-d_8) δ 25.4; ^{19}F NMR (470 MHz, THF-d_8) δ –110.2 (m); IR (ATR) 3060, 2977, 2923, 2218, 1638, 1555, 1447, 1394, 1360,

1334, 1266, 1229, 1139, 976, 953, 850, 801, 755 cm^{-1}; HRMS (DART) calcd for $C_{22}H_{18}BN_3F$ ($[M+H]^+$) 354.15723, found 354.15738.

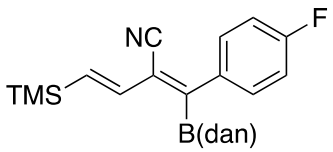

38% yield (run1: 40%, run2: 36%), 94:6. ^1H NMR (500 MHz, $CDCl_3$) δ 7.56 – 7.48 (m, 2H), 7.19 – 7.06 (m, 6H), 6.89 (d, *J* = 18.5 Hz, 1H), 6.67 (d, *J* = 18.5 Hz, 1H), 6.34 (dd, *J* = 7.0, 1.4 Hz, 2H), 5.70 (s, 2H), 0.13 (s, 9H); ^{13}C NMR (126 MHz, $CDCl_3$) δ 163.3 (d, *J* = 250.7 Hz), 153.5 (br), 140.0, 139.2, 138.6, 136.3, 134.9 (d, *J* = 3.6 Hz), 130.8 (d, *J* = 8.5 Hz), 127.8, 121.5, 120.0, 118.9, 116.5, 116.1 (d, *J* = 21.8 Hz), 106.6, -1.3; ^{11}B NMR (160 MHz, $CDCl_3$) δ 29.8; ^{19}F NMR (470 MHz, $CDCl_3$) δ –110.9 (m); IR (ATR) 3360, 3056, 2955, 2897, 2218, 1599, 1505, 1409, 1373, 1336, 1247, 1235, 1160, 1145, 839, 820, 766 cm^{-1}; HRMS (DART) calcd for $C_{24}H_{24}BN_3FSi$ ($[M+H]^+$) 412.18111, found 412.18054.

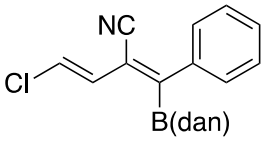

With 15 mol% Senphos **2.50**, 1.2 equiv. CuCN and 1.6 equiv. Cl-BCat at 90 °C for 25 min, obtained by using hexane/Et_2O (8/1) as the eluent, 28% yield (run1: 27%, run2: 28%), 96:4. ^1H NMR (600 MHz, $CDCl_3$) δ 7.59 – 7.49 (m, 2H), 7.49 – 7.35 (m, 3H), 7.18 – 7.04 (m, 4H), 6.89 (d, *J* = 1.1 Hz, 2H), 6.36 (dt, *J* = 6.9, 1.3 Hz, 2H), 5.71 (s, 2H); ^{13}C NMR (151 MHz, $CDCl_3$) δ 139.8, 138.1, 136.3, 130.1, 129.9, 129.1, 128.7, 127.8, 126.2, 120.1, 119.1, 115.8, 115.2, 106.9 (*B*-alkenyl carbon signal not observed); ^{11}B NMR (160 MHz, $CDCl_3$) δ 29.0; IR (ATR) 3397, 3365, 3062, 2220, 1629, 1599, 1505, 1407, 1374, 1336, 1151, 1051, 820, 766, 732, 696 cm^{-1}; HRMS (DART) calcd for $C_{21}H_{16}BN_3Cl$ ($[M+H]^+$) 356.11203, found 356.11198.

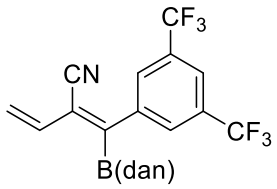

27% yield (run1: 32%, run2: 22%), 66:34. ^{1}H NMR (600 MHz, $CDCl_3$) δ 7.96 – 7.89 (m, 3H), 7.17 – 7.08 (m, 4H), 6.82 (dd, *J* = 16.9, 10.4 Hz, 1H), 6.38 (dd, *J* = 6.6, 1.7 Hz, 2H), 6.01 (d, *J* = 16.9 Hz, 1H), 5.72 (s, 2H), 5.67 (d, *J* = 10.4 Hz, 1H); ^{13}C NMR (101 MHz, $CDCl_3$) δ 140.8, 139.5, 136.3, 132.6 (q, *J* = 33.6 Hz), 132.4, 128.6, 127.8, 123.5, 123.1 (q, *J* = 271.9 Hz), 123.0 (dt, *J* = 7.8, 3.9 Hz), 122.8, 120.1, 119.4, 115.0, 107.1 (B-alkenyl carbon signal not observed); ^{11}B NMR (160 MHz, $CDCl_3$) δ 28.2; ^{19}F NMR (564 MHz, $CDCl_3$) δ –62.86 (m); IR (ATR) 3374, 3057, 2226, 1600, 1504, 1404, 1372, 1340, 1275, 1178, 1130, 906, 820, 766, 732, 704, 683, 450 cm^{-1}; HRMS (DART) calcd for $C_{23}H_{15}BN_3F_6$ ($[M+H]^+$) 458.12577, found 458.12709.

2.4.2.3.7. Illustrative *trans/cis* configuration assignment of the cyanoboration products

The *trans/cis* configuration of **2.96** and **2.105** was unambiguously determined by single crystal X-ray diffraction analysis of the corresponding major pure isolated product. The assignment of the *trans/cis* configuration of the other products shown in Table 2.5 and Table 2.6 are made by analogy based on characteristic ^{1}H NMR signature of the Me and NH(Bdan) signals: the Me signal of the *trans*-product (signal A) appears more downfield shifted than the Me signal (signal B) of the *cis* product, and the NH(Bdan) signal of the *trans*-product (signal C) appears more upfield shifted than the NH(Bdan) signal (signal D) of the *cis* product (see below spectra). A mixture of *trans/cis* products can oftentimes be obtained in small quantities during the silica gel chromatography purification process. The labeled ^{1}H NMR spectra are shown using compound **2.96** as the representative example.

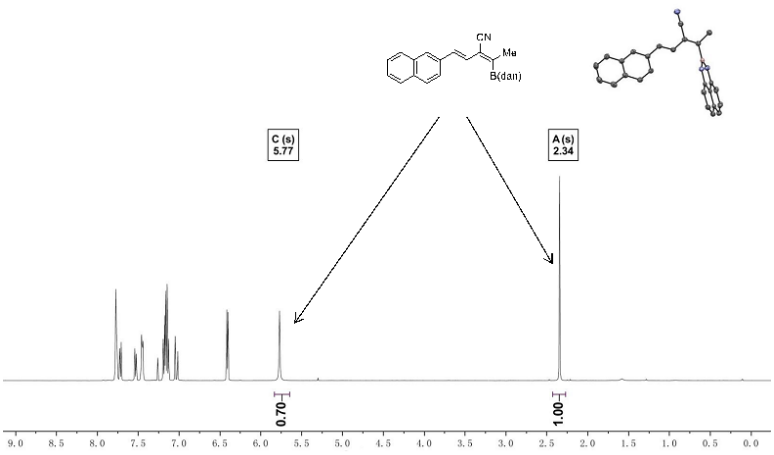

Figure 2.3. Fraction 2 of the crude mixture after column purification, pure **2.96**.

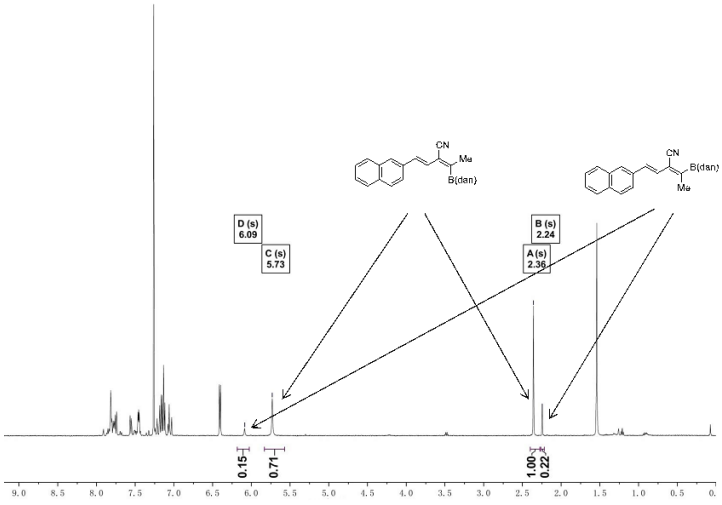

Figure 2.4. Fraction 1 of the crude mixture after column purification, *trans*-**2.96** and *cis*-**2.96** mixture.

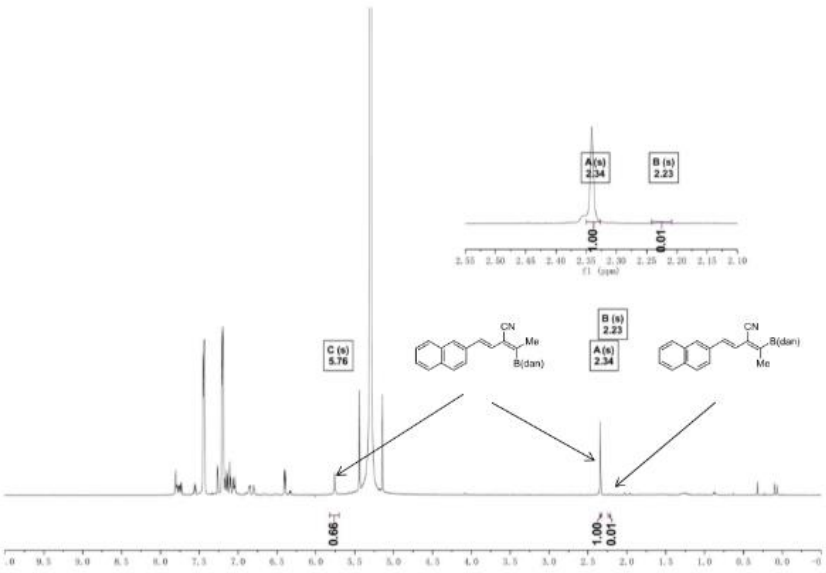

Figure 2.5. Crude mixture of *trans*-**2.96** and *cis*-**2.96** after quenching with dan.

2.4.2.3.8. Experimental procedure for derivatizations of *trans*-cyanoboration product

Reactions setup in Scheme 2.29:

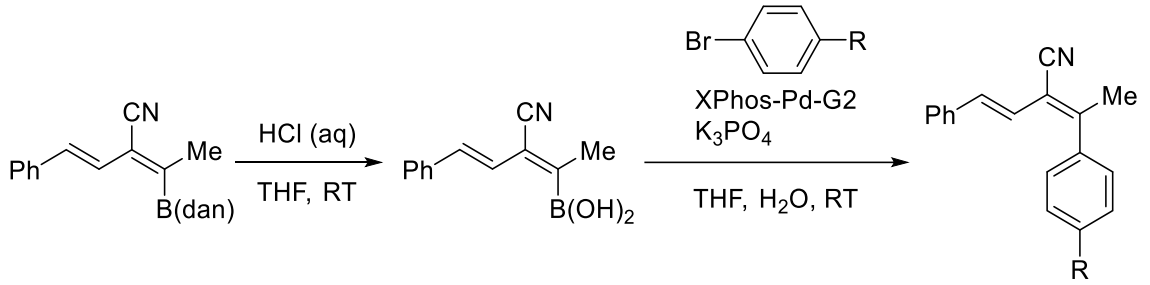

2.95 **2.131** **2.132,** R = H
2.133, R = 4-B(dan)

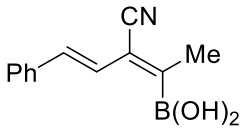

Aqueous HCl (1.4 mL, 3.0 M) was added into a 20-mL vial charged with compound **2.95** (33 mg, 0.10 mmol, 1.0 equiv.) and THF (2.8 mL). The resulting mixture was allowed to stir at room temperature for 30 minutes. At the conclusion of reaction, the mixture was diluted with Et_2O (4 mL), and the organic layer was separated. The aqueous layer was extracted with Et_2O (5 mL). The organic layers were combined and concentrated to afford 2.141 as a mixture of boronic

acid and the trimer boroxine. Boronic acid **2.131** was used for the next step without further purification (quant. yield).

Under nitrogen to a 4-mL vial charged with compound **2.131**, XPhos-Pd-G2 (4 mg, 4.0 μmol, 0.05 equiv.), THF (0.3 mL), and aqueous K_3PO_4 (0.3 mL, 0.5 M) the corresponding aryl bromide (0.15 mmol, 1.5 equiv.) was added. The resulting mixture was allowed to stir for 3 hours at room temperature. Then, H_2O (1 mL) was added, and the organic layer was separated. The aqueous layer was further extracted with Et_2O (3 mL), and the organic layers were combined and concentrated. The resulting crude material was purified by silica gel chromatography using hexanes/EtOAc (10/1) as the eluent to afford products **2.132** and **2.133**.

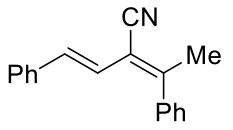

86% yield. ^{1}H NMR (500 MHz, $CDCl_3$) δ 7.48 – 7.36 (m, 3H), 7.31 – 7.16 (m, 7H), 7.01 (d, J = 16.0 Hz, 1H), 6.71 (d, J = 16.0 Hz, 1H), 2.53 (s, 3H); ^{13}C NMR (126 MHz, $CDCl_3$) δ 153.7, 139.3, 136.3, 133.2, 129.1, 128.8, 128.8, 128.4, 128.1, 126.9, 122.2, 117.0, 112.2, 25.3; IR (ATR) 3058, 2922, 2219, 1492, 1441, 1274, 1025, 960, 765, 754, 699, 693 cm^{-1}; HRMS (DART) calcd for $C_{18}H_{16}N$ ($[M+H]^+$) 246.12773, found 246.12774.

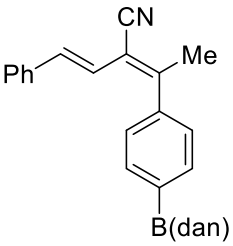

85% yield. ^{1}H NMR (500 MHz, $CDCl_3$) δ 7.72 (d, J = 7.8 Hz, 2H), 7.38 – 7.22 (m, 7H), 7.18 (t, J = 7.8 Hz, 2H), 7.10 (d, J = 8.3 Hz, 2H), 7.05 (d, J = 16.0 Hz, 1H), 6.74 (d, J = 16.0 Hz, 1H), 6.46 (d, J = 7.2 Hz, 2H), 6.09 (s, 2H), 2.56 (s, 3H); ^{13}C NMR (126 MHz, $CDCl_3$) δ 153.1, 141.0, 140.9, 136.5, 136.2, 133.6, 131.9, 128.8, 128.5, 127.9, 127.8, 127.0, 122.0, 120.0, 118.2, 116.9, 112.4, 106.3, 25.2 (*B*-aryl carbon signal not observed); ^{11}B NMR (160 MHz, $CDCl_3$) δ 29.0; IR (ATR) 3416, 3054, 2218, 1599, 1524, 1493,1408, 1374,

1332, 1088, 820, 764, 692 cm^{-1}; HRMS (DART) calcd for $C_{28}H_{23}BN_3$ ($[M+H]^+$) 412.19795, found 412.19759.

Synthesis of compound **2.134**

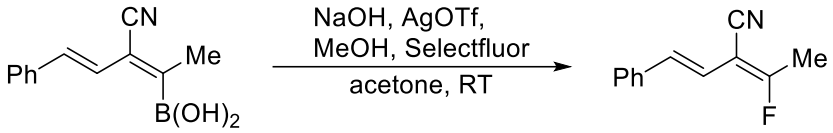

Under nitrogen to a 4-mL vial charged with a solution of NaOH (9.6 mg, 0.24 mmol, 1.2 equiv.) in MeOH (2.0 mL) was added boronic acid **2.131** (0.20 mmol, 1.0 equiv.) at room temperature. The resulting mixture was allowed to stir for 15 minutes, and then the mixture was cooled to 0 °C. AgOTf (154 mg, 0.600 mmol, 3.00 equiv.) was added in the absence of light, and the resulting mixture was allowed to stir for 30 minutes at 0°C. Then, methanol was removed *in vacuo,* and anhydrous acetone (1 mL) was added and then removed under reduced pressure to help remove methanol. After repeating for four times, 4Å Molecular sieve (100 mg), Selectfluor (85 mg, 0.24 mmol, 1.2 equiv.), and acetone (2 mL) were added to the residue. The resulting slurry was allowed to stir for 2 hours at room temperature. At the conclusion of reaction, the mixture was passed through an acrodisc and washed with acetone. The filtrate was concentrated, dissolved in Et_2O (5 mL) and further washed with H_2O (5 mL). The organic layer was dried with Na_2SO_4, and alkenyl fluoride **2.134** was obtained via silica gel chromatography using hexanes/EtOAc (15/1) as the eluent as a white solid (67% yield). ^{1}H NMR (500 MHz, $CDCl_3$) δ 7.45 (d, J = 7.2 Hz, 2H), 7.35 (t, J = 7.4 Hz, 2H), 7.33 – 7.27 (m, 1H), 6.88 (s, 2H), 2.39 (d, J = 17.0 Hz, 3H); ^{13}C NMR (101 MHz, $CDCl_3$) δ 168.7 (d, J = 280.5 Hz), 135.9 (d, J = 1.3 Hz), 132.7 (d, J = 4.2 Hz), 128.9, 128.8, 127.0, 115.6 (d, J = 3.6 Hz), 115.3 (d, J = 13.7 Hz), 98.8 (d, J = 28.6 Hz), 18.3 (d, J = 24.7 Hz); ^{19}F NMR (564 MHz, $CDCl_3$) δ –75.6 (q,

J = 17.0 Hz); IR (ATR) 3027, 2960, 2923, 2229, 1651, 1625, 1496, 1430, 1388, 1312, 1303, 1216, 1184, 1059, 1028, 953, 802, 688 cm^{-1}; HRMS (DART) calcd for $C_{12}H_{11}NF$ ($[M+H]^+$) 188.08700, found 188.08652.

Synthesis of compound **2.135**

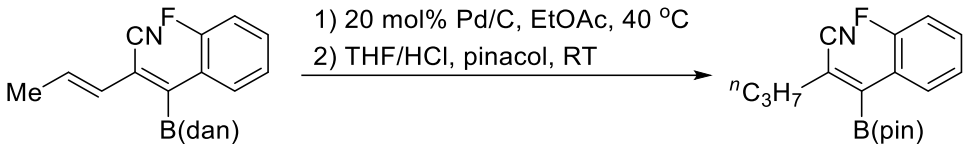

Pd/C (12 mg, 0.011 mmol, 10% wt, 0.20 equiv.), compound **2.122** (20 mg, 0.057 mmol, 1.0 equiv.), and EtOAc (0.60 mL) were added into a 4-mL vial. The vial was quickly placed under vacuum and then back filled with H_2 (1 atm) twice, and the mixture was allowed to heat at 40 °C for 3 hours under a H_2 balloon pressue. At the conclusion of reaction, the reaction mixture was passed through an acrodisc, and all volatiles were removed *in vacuo*. Pinacol (47 mg, 0.40 mmol, 7.0 equiv.) was added to this residue along with THF (1.5 mL) and aqueous HCl (0.75 mL, 4.3 M). The resulting mixture was allowed to stir for 14 hours at room temperature followed by addition of Et_2O (5 mL) and H_2O (5 mL). The organic layer was separated and the aqueous layer was further washed with Et_2O (5 mL). The combined organic layers were concentrated, and the crude material was purified via silica gel chromatography using hexanes/EtOAc (8/1) as the eluent to afford compound **2.135** as a white solid (54% yield). ^{1}H NMR (500 MHz, $CDCl_3$) δ 7.39 (td, J = 7.7, 1.8 Hz, 1H), 7.35 – 7.29 (m, 1H), 7.17 (td, J = 7.6, 1.1 Hz, 1H), 7.06 (ddd, J = 9.6, 8.3, 1.1 Hz, 1H), 2.68 – 2.61 (m, 2H), 1.71 (h, J = 7.4 Hz, 2H), 1.28 (s, 12H), 1.01 (t, J = 7.4 Hz, 3H); ^{13}C NMR (126 MHz, $CDCl_3$) δ 159.6 (d, J = 246.5 Hz), 130.4, 130.4 (d, J = 10.6 Hz), 128.0, 127.5 (d, J = 15.1 Hz), 124.4 (d, J = 3.4 Hz),

118.4, 115.5 (d, J = 21.9 Hz), 84.7, 36.0, 24.8, 22.3, 13.4 (*B*-alkenyl carbon signal not observed); ^{11}B NMR (160 MHz, $CDCl_3$) δ 29.9; ^{19}F NMR (470 MHz, $CDCl_3$) δ –112.8 (m); IR (ATR) 2963, 2929, 2873, 2213, 1486, 1450, 1357, 1327, 1268, 1140, 1081, 971, 846, 753 cm^{-1}; HRMS (DART) calcd for $C_{18}H_{24}BNO_2F$ ($[M+H]^+$) 316.18786, found 316.18866.

Reaction setup in Scheme 2.32

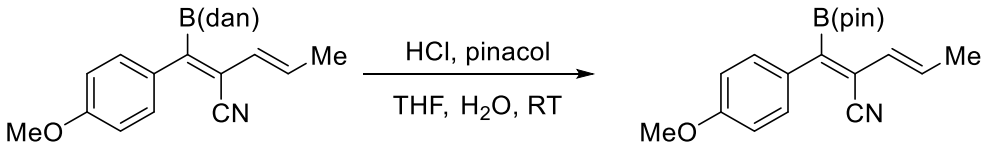

2.120-S1

To a 20-mL vial charged with compound **2.120** (146 mg, 0.400 mmol, 1.00 equiv.), pinacol (236 mg, 2.00 mmol, 5.00 equiv.) and THF (8 mL) was added followed by aqueous HCl (6.0 mL, 4.3 M). The resulting mixture was allowed to stir at room temperature for 20 hours. At the conclusion of reaction, Et_2O (4 mL) was added to the mixture, and the organic layer was separated. The aqueous layer was further extracted with additional Et_2O (5 mL).The combined organic layers were concentrated under reduce pressure, and the resulting crude material was further purified by silica gel chromatography using hexanes/EtOAc (5/1) as the eluent to afford **2.120-S1** as a white solid (84% yield). ^{1}H NMR (500 MHz, $CDCl_3$) δ 7.40 – 7.34 (m, 2H), 6.94 – 6.86 (m, 2H), 6.69 (dq, J = 15.4, 1.6 Hz, 1H), 6.38 (dq, J = 15.3, 6.8 Hz, 1H), 3.82 (s, 3H), 1.90 (dd, J = 6.8, 1.7 Hz, 3H), 1.33 (s, 12H); ^{13}C NMR (126 MHz, $CDCl_3$) δ 159.9, 133.7, 131.4, 130.1, 127.9, 121.9, 116.9, 113.9, 84.8, 55.4, 24.9, 18.6 (*B*-alkenyl carbon signal not observed); ^{11}B NMR (160 MHz, $CDCl_3$) δ 30.0; IR (ATR) 2978, 2934, 2838, 2218,

1604, 1509, 1357, 1328, 1291, 1250, 1178, 1137, 1032, 972, 849, 832, 732 cm^{-1}; HRMS (DART) calcd for $C_{19}H_{25}BNO_3$ ($[M+H]^+$) 326.19220, found 326.19142.

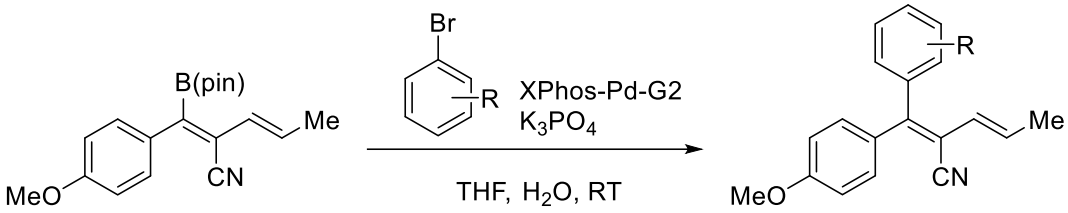

2.139 R = 4-OMe
2.140 R = 4-F
2.141 R = 3-OMe

Under nitrogen to a 20-mL vial charged with compound **2.120-S1** (109 mg, 0.330 mmol, 1.00 equiv.) and XPhos-Pd-G2 (13 mg, 0.016 mmol, 0.050 equiv.) was added THF (2.7 mL), aqueous K_3PO_4 (0.9 mL, 0.6 M) and the corresponding aryl bromide (0.50 mmol, 1.5 equiv.). The resulting mixture was allowed to stir for 15 hours at room temperature. Then, H_2O (1 mL) was added and the organic layer was separated. The aqueous layer was further extracted with Et_2O (3 mL), and the organic layers were combined and concentrated. This crude material was purified by silica gel chromatography using hexanes/EtOAc (15/1) as the eluent to afford 8a-8c as white solids.

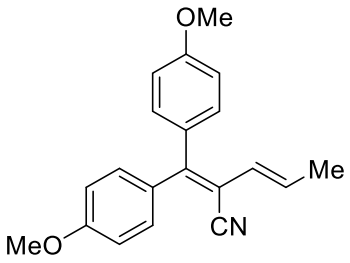

With 4-bromo-anisole, 88% yield. ^1H NMR (500 MHz, $CDCl_3$) δ 7.33 – 7.28 (m, 2H), 7.13 – 7.07 (m, 2H), 6.93 – 6.85 (m, 4H), 6.32 (dq, *J* = 15.4, 6.6 Hz, 1H), 6.21 (dq, *J* = 15.4, 1.5 Hz, 1H), 3.85 (s, 3H), 3.84 (s, 3H), 1.82 (dd, *J* = 6.7, 1.5 Hz, 3H); ^{13}C NMR (126 MHz, $CDCl_3$) δ 160.7, 160.3, 153.3, 132.7, 132.1, 131.7, 131.4, 131.3, 126.6, 118.8, 113.8, 113.7, 108.8, 55.4, 55.4, 18.4; IR (ATR) 3005, 2930, 2838, 2214, 1602, 1573, 1506, 1461, 1442, 1302, 1282, 1247, 1172, 1029,

960, 829, 737, 603, 572 cm^{-1}; HRMS (DART) calcd for $C_{20}H_{20}NO_2$ ($[M+H]^+$) 306.14886, found 306.14963.

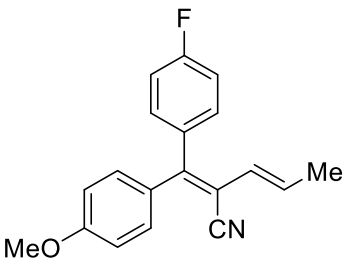

With 4-bromo-fluorobenzene, 80% yield. ^1H NMR (500 MHz, $CDCl_3$) δ 7.35 – 7.27 (m, 2H), 7.15 (ddt, *J* = 8.2, 5.1, 2.5 Hz, 2H), 7.12 – 7.04 (m, 2H), 6.92 – 6.84 (m, 2H), 6.35 (dq, *J* = 15.4, 6.8 Hz, 1H), 6.10 (dq, *J* = 15.4, 1.6 Hz, 1H), 3.83 (s, 3H), 1.82 (dd, *J* = 6.8, 1.6 Hz, 3H); ^{13}C NMR (126 MHz, $CDCl_3$) δ 163.1 (d, *J* = 249.9 Hz), 160.9, 152.2, 135.2 (d, *J* = 3.4 Hz), 132.5, 132.4, 132.2, 131.6, 126.2, 118.4, 115.6 (d, *J* = 21.5 Hz), 113.9, 110.0, 55.5, 18.5; ^{19}F NMR (470 MHz, $CDCl_3$) δ –111.6 (ddd, *J* = 13.5, 8.4, 5.1 Hz); IR (ATR) 2960, 2926, 2850, 2216, 1602, 1575, 1505, 1461, 1444, 1289, 1251, 1228, 1173, 1158, 1095,1028, 960 831, 804, 736, 566 cm^{-1}; HRMS (DART) calcd for $C_{19}H_{16}NOF$ ($[M+H]^+$) 293.12104, found 293.11995.

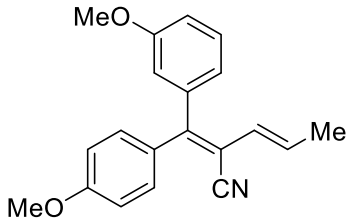

With 3-bromo-anisole, 90% yield. ^1H NMR (600 MHz, $CDCl_3$) δ 7.35 – 7.24 (m, 3H), 6.93 (dd, *J* = 8.4, 2.5 Hz, 1H), 6.91 – 6.84 (m, 2H), 6.76 (dt, *J* = 7.6, 1.2 Hz, 1H), 6.68 (dd, *J* = 2.7, 1.5 Hz, 1H), 6.38 – 6.25 (m, 1H), 6.15 (dq, *J* = 15.4, 1.5 Hz, 1H), 3.83 (d, *J* = 0.9 Hz, 3H), 3.78 (d, *J* = 0.9 Hz, 3H), 1.81 (dt, *J* = 6.8, 1.2 Hz, 3H); ^{13}C NMR (151 MHz, $CDCl_3$) δ 160.7, 159.6, 153.2, 140.5, 132.2, 132.0, 131.5, 129.5, 126.4, 122.8, 118.5, 115.9, 114.5, 113.8, 109.9, 55.5, 55.5, 18.5; IR (ATR) 3004, 2935, 2913, 2837, 2216, 1604, 1576, 1509, 1462, 1446, 1287, 1253, 1178, 1034, 961, 837, 802, 787, 700 cm^{-1}; HRMS (DART) calcd for $C_{20}H_{20}NO_2$ ($[M+H]^+$) 306.14886, found 306.14950.

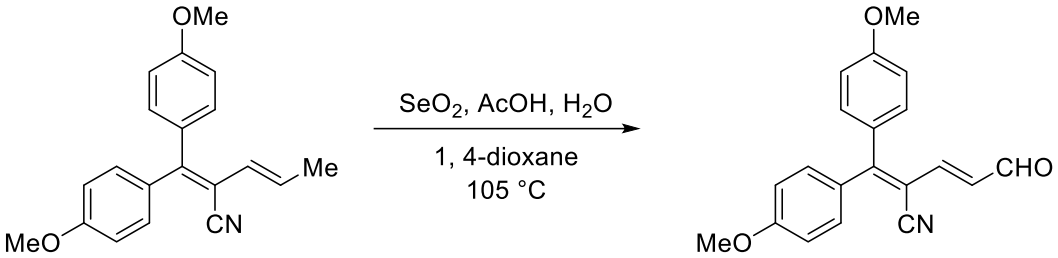

2.142-S1

SeO_2 (162 mg, 1.45 mmol, 5.00 equiv.) and compound **2.139** (89 mg, 0.29 mmol, 1.0 equiv.) were placed in a 20-mL vial. To this vial 1,4-dioxane (1.8 mL), H_2O (0.10 mL) and AcOH (0.050 mL) were added successively. The resulting mixture was allowed to stir at 105 °C for 12 hours. Then, another portion of SeO_2 (64 mg, 0.58 mmol, 2.0 equiv.) was added, and the mixture was allowed to stir for another 12 hours at 105 °C. At the conclusion of reaction, the reaction mixture was passed through celite, and the filtrate was concentrated. This crude residue was purified by silica gel chromatography using hexanes/EtOAc (4/1) as the eluent to afford product **2.142-S1** as a yellow solid (77% yield). ^{1}H NMR (500 MHz, $CDCl_3$) δ 9.55 (d, J = 7.5 Hz, 1H), 7.46 – 7.36 (m, 2H), 7.25 (d, J = 15.5 Hz, 1H), 7.18 – 7.12 (m, 2H), 7.00 – 6.95 (m, 2H), 6.95 – 6.91 (m, 2H), 6.67 (dd, J = 15.5, 7.5 Hz, 1H), 3.89 (s, 3H), 3.87 (s, 3H); ^{13}C NMR (126 MHz, $CDCl_3$) δ 192.6, 164.5, 162.4, 162.0, 147.1, 133.1, 132.9, 131.3, 131.0 (two signals), 130.1, 114.2, 114.0, 105.7, 55.6, 55.6; IR (ATR) 3007, 2934, 2839, 2730, 2214, 1672, 1593, 1573, 1501, 1253, 1171, 1116, 1027, 835, 732 cm^{-1}; HRMS (DART) calcd for $C_{20}H_{18}NO_3$ ($[M+H]^+$) 320.12812, found 320.12696.

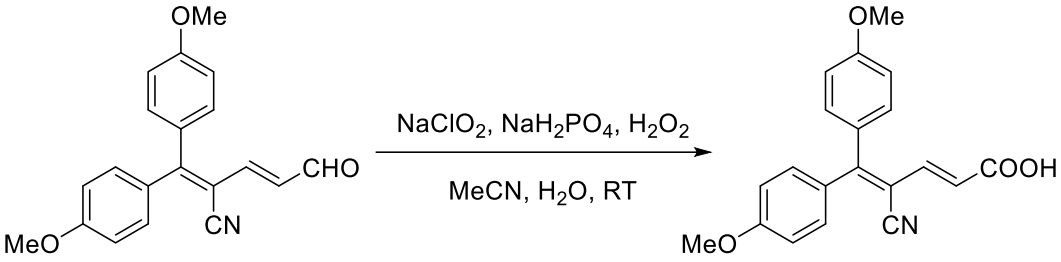

H_2O (0.50 mL), MeCN (0.13 mL) and aqueous H_2O_2 (35% v/v, 0.25 mmol, 25 μL, 2.0 equiv.) were added to a 4-mL vial charged with compound **2.142-S1** (40.4 mg, 0.125 mmol, 1.00 equiv.) and NaH_2PO_4 (7.8 mg, 0.065 mmol, 0.52 equiv.). The mixture was cooled to 0 °C and then a pre-cooled solution (0 °C) of $NaClO_2$ (35 mg, 0.31 mmol, 2.5 equiv.) in H_2O (0.31 mL) was added in a dropwise fashion. The mixture was allowed to stir for 30 min and then allowed to warm to room temperature. At the conclusion of reaction, Et_2O (5 mL) and H_2O (3 mL) were added to this mixture. The organic layer was separated, and the concentrated organic layer was purified by silica gel chromatography using hexanes/EtOAc (1/1) as the eluent to afford product **2.142** as a yellow solid (69% yield). ^{1}H NMR (500 MHz, CDCl3) δ 11.79 (s, br, 1H), 7.53 (d, J = 15.4 Hz, 1H), 7.41 – 7.35 (m, 2H), 7.14 – 7.07 (m, 2H), 6.98 – 6.88 (m, 4H), 6.42 (d, J = 15.5 Hz, 1H), 3.88 (s, 3H), 3.86 (s, 3H); ^{13}C NMR (126 MHz, $CDCl_3$) δ 171.8, 164.0, 162.2, 161.9, 142.4, 133.2, 132.8, 131.6, 130.3, 120.6, 117.8, 114.2, 114.0, 105.5, 55.6, 55.6; IR (ATR) 2934, 2839, 2213, 1685, 1598, 1508, 1286, 1255, 1210, 1173, 1029, 836, 732 cm^{-1}; HRMS (DART) calcd for $C_{20}H_{18}NO_4$ ([M+H]$^+$) 336.12303, found 336.12345.

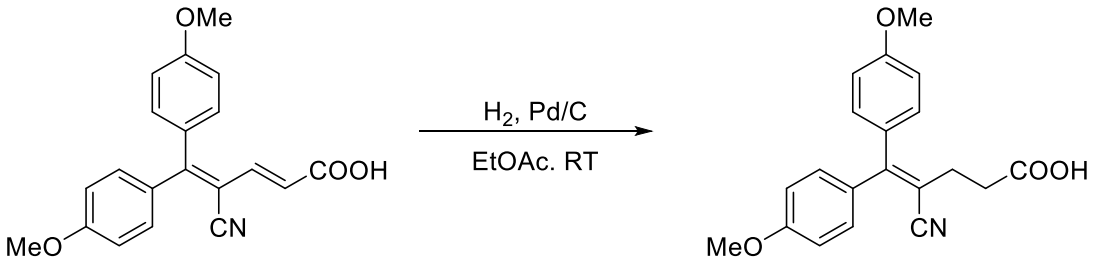

A 4-mL vial was charged with compound **2.142** (10.2 mg, 0.0300 mmol, 1.00 equiv.), Pd/C (3.1 mg, 3.0 μmol, 10% wt, 0.10 equiv.) and EtOAc (0.4 mL). The vial was quickly placed under vacuum and then and back filled with H_2 (1 atm) twice. The resulting mixture was allowed to stir at room temperature for 2 hours under a H_2 balloon pressure. At the conclusion of reaction, all violates were removed *in vacuo*, and the residue was purified by silica gel chromatography using EtOAc as the eluent to afford Satigrel as a white solid (91% yield, 97:3 hydrogenation selectivity (Satigrel *vs.* fully hydrogenated byproduct).[75] ^{1}H NMR (600 MHz, $CDCl_3$) δ 7.27 (d, J = 8.8 Hz, 2H), 7.07 – 7.01 (m, 2H), 6.92 – 6.83 (m, 4H), 3.83 (s, 3H), 3.82 (s, 3H), 2.71 (apparent, s, 4H) (COOH signal not observed); ^{13}C NMR (151 MHz, $CDCl_3$) δ 173.6 (br), 160.7, 160.3, 158.2, 132.4, 131.3, 131.1, 131.0, 120.0, 114.0, 113.8, 107.0, 55.5, 55.5, 32.8, 27.4; IR (ATR) 2931, 2839, 2204, 1709, 1605, 1509, 1283, 1249, 1174, 1030, 833 cm^{-1}; HRMS (DART) calcd for $C_{20}H_{20}NO_4$ ($[M+H]^+$) 338.13868, found 338.13898.

2.4.2.4. Experiemntal procedure for reaction mechanism investigation

In a 4-mL vial charged with Cl–BCat (46.2 mg, 0.300 mmol, 1.00 equiv.) and *o*-DCB (0.3 mL) was added TMSCN (30 mg, 0.30 mmol, 1.0 equiv.). The resulting mixture was allowed to stir at room temperature for 4 hours to afford a deep red solution, and ^{11}B NMR indicated the full consumption of Cl–BCat (^{11}B NMR, δ 24.2 ppm). To another 4-mL vial charged with Pd(COD)($CH_2TMS)_2$ (3.9 mg, 0.010 mmol, 5.0 mol%), Senphos **2.89** (4.2 mg, 0.010 mmol, 5.0 mol%) and *o*-DCB (0.15 mL) was added enyne **2.52** (28.4 mg, 0.200 mmol, 1.00 equiv.) along with a solution of hexamethylbenzene in *o*-DCB (5.0

[75] Yamagishi, Y.; Akasaka, K.; Suzuki, T.; Miyamoto, M.; Nakamoto, K.; Okano, K.; Abe, S.; Ikuta, H.; Hayashi, K.; Yoshimura, H.; Fujimori, T.; Harada, K.; Yamatsu, I. Diphenyl-methane Derivative, Pharmaceutical Composition and Use. European Patent EP0238973B1, March 17, 1987.

μL, 3.3 M) as the internal standard and the previous generated BCat–CN solution (0.15 mL). The resulting mixture was allowed to stir for 2.5 hours at 115 °C. At the conclusion of reaction, an aliquot of the reaction mixture was prepared for ^{1}H NMR analysis indicating a 51% enyne **2.52** conversion against internal standard hexamethylbenzene. The rest of the mixture was passed through an acrodisc under an inert atmosphere using CH_2Cl_2 as the solvent, and 1,8-diaminonaphthlene (64 mg, 0.40 mmol, 2.0 equiv.) was added to the filtrate. After allowing the mixture to stir for another 12 hours, all volatiles were removed under reduced pressure, and the ^{1}H NMR analysis of the resulting crude material against hexamethylbenzene indicates a 17% yield of the *trans*-cyanoboration product with a *trans*:*cis* ratio of 94:6.

2.4.3. X-ray crystallographic data

Crystal data and structure refinement for compound **2.58**.

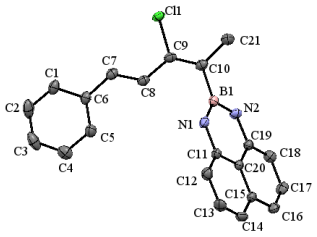

Identification code	C21H18BClN2	
Empirical formula	C21 H18 B Cl N2	
Formula weight	344.63	
Temperature	100(2) K	
Wavelength	0.71073 Å	
Crystal system	Triclinic	
Space group	P-1	
Unit cell dimensions	a = 8.7796(13) Å	α = 64.295(2)°.
	b = 10.6561(15) Å	β = 73.190(2)°.
	c = 10.7226(15) Å	γ = 78.931(2)°.
Volume	862.7(2) Å^3	
Z	2	
Density (calculated)	1.327 Mg/m^3	
Absorption coefficient	0.226 mm^{-1}	
F(000)	360	
Crystal size	0.330 x 0.240 x 0.070 mm^3	
Theta range for data collection	2.127 to 28.342°.	
Index ranges	-11<=h<=11, -14<=k<=14, -14<=l<=14	
Reflections collected	15116	
Independent reflections	4282 [R(int) = 0.0288]	
Completeness to theta = 25.242°	99.8 %	
Absorption correction	Semi-empirical from equivalents	
Max. and min. transmission	0.7457 and 0.6527	
Refinement method	Full-matrix least-squares on F^2	
Data / restraints / parameters	4282 / 2 / 233	
Goodness-of-fit on F^2	1.023	
Final R indices [I>2sigma(I)]	R1 = 0.0498, wR2 = 0.1269	
R indices (all data)	R1 = 0.0676, wR2 = 0.1387	
Extinction coefficient	n/a	
Largest diff. peak and hole	0.552 and -0.243 e.Å^{-3}	

Crystal data and structure refinement for compound **2.96**.

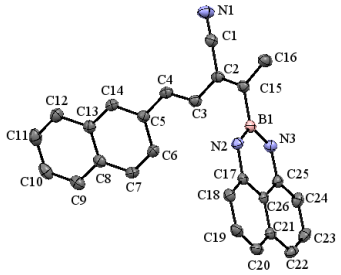

Identification code	C26H20BN3
Empirical formula	C26 H20 B N3
Formula weight	385.26
Temperature	123(2) K
Wavelength	1.54178 Å
Crystal system	Tetragonal
Space group	$P4_2/n$
Unit cell dimensions	a = 23.0525(5) Å α = 90°. b = 23.0525(5) Å β = 90°. c = 7.6338(2) Å γ = 90°.
Volume	4056.7(2) $Å^3$
Z	8
Density (calculated)	1.262 Mg/m^3
Absorption coefficient	0.574 mm^{-1}
F(000)	1616
Crystal size	0.560 x 0.220 x 0.160 mm^3
Theta range for data collection	2.711 to 66.840°.
Index ranges	-27<=h<=22, -27<=k<=27, -9<=l<=9
Reflections collected	22309
Independent reflections	3569 [R(int) = 0.0276]
Completeness to theta = 66.840°	99.2 %
Absorption correction	Semi-empirical from equivalents
Max. and min. transmission	0.7528 and 0.6580
Refinement method	Full-matrix least-squares on F^2
Data / restraints / parameters	3569 / 2 / 278
Goodness-of-fit on F^2	1.060
Final R indices [I>2sigma(I)]	R1 = 0.0338, wR2 = 0.0869
R indices (all data)	R1 = 0.0345, wR2 = 0.0874
Extinction coefficient	n/a
Largest diff. peak and hole	0.206 and -0.156 e.$Å^{-3}$

Crystal data and structure refinement for compound **2.105**.

Identification code	C21H26BNO4
Empirical formula	C21 H26 B N O4
Formula weight	367.24
Temperature	123(2) K
Wavelength	1.54178 Å
Crystal system	Orthorhombic
Space group	Fdd2
Unit cell dimensions	a = 31.1427(6) Å α = 90°. b = 37.9695(8) Å β = 90°. c = 13.9845(3) Å γ = 90°.
Volume	16536.3(6) Å^3
Z	32
Density (calculated)	1.180 Mg/m^3
Absorption coefficient	0.645 mm^{-1}
F(000)	6272
Crystal size	0.580 x 0.280 x 0.150 mm^3
Theta range for data collection	3.655 to 66.608°.
Index ranges	-37<=h<=36, -41<=k<=45, -16<=l<=16
Reflections collected	30171
Independent reflections	7254 [R(int) = 0.0267]
Completeness to theta = 66.608°	99.7 %
Absorption correction	Semi-empirical from equivalents
Max. and min. transmission	0.7528 and 0.6531
Refinement method	Full-matrix least-squares on F^2
Data / restraints / parameters	7254 / 571 / 575
Goodness-of-fit on F^2	1.035
Final R indices [I>2sigma(I)]	R1 = 0.0369, wR2 = 0.1073
R indices (all data)	R1 = 0.0383, wR2 = 0.1091
Extinction coefficient	n/a
Largest diff. peak and hole	0.258 and -0.215 e.Å^{-3}

Crystal data and structure refinement for compound **2.122**.

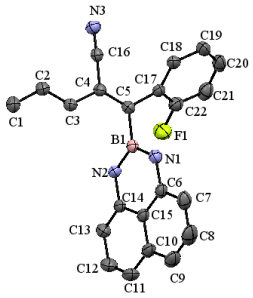

Identification code	C22H17BFN3	
Empirical formula	C22 H17 B F N3	
Formula weight	353.19	
Temperature	173(2) K	
Wavelength	1.54178 Å	
Crystal system	Monoclinic	
Space group	$P2_1/n$	
Unit cell dimensions	a = 8.7227(4) Å	α = 90°.
	b = 7.3770(3) Å	β = 98.3760(10)°.
	c = 28.3779(11) Å	γ = 90°.
Volume	1806.57(13) $Å^3$	
Z	4	
Density (calculated)	1.299 Mg/m^3	
Absorption coefficient	0.675 mm^{-1}	
F(000)	736	
Crystal size	0.420 x 0.280 x 0.260 mm^3	
Theta range for data collection	3.148 to 66.424°.	
Index ranges	-10<=h<=10, -8<=k<=8, -33<=l<=32	
Reflections collected	19722	
Independent reflections	3171 [R(int) = 0.0228]	
Completeness to theta = 66.424°	99.4 %	
Absorption correction	Semi-empirical from equivalents	
Max. and min. transmission	0.7528 and 0.6787	
Refinement method	Full-matrix least-squares on F^2	
Data / restraints / parameters	3171 / 2 / 251	
Goodness-of-fit on F^2	1.036	
Final R indices [I>2sigma(I)]	R1 = 0.0438, wR2 = 0.1190	
R indices (all data)	R1 = 0.0477, wR2 = 0.1236	
Extinction coefficient	n/a	
Largest diff. peak and hole	0.733 and -0.331 $e.Å^{-3}$	

2.4.4. NMR Spectra of New Compounds

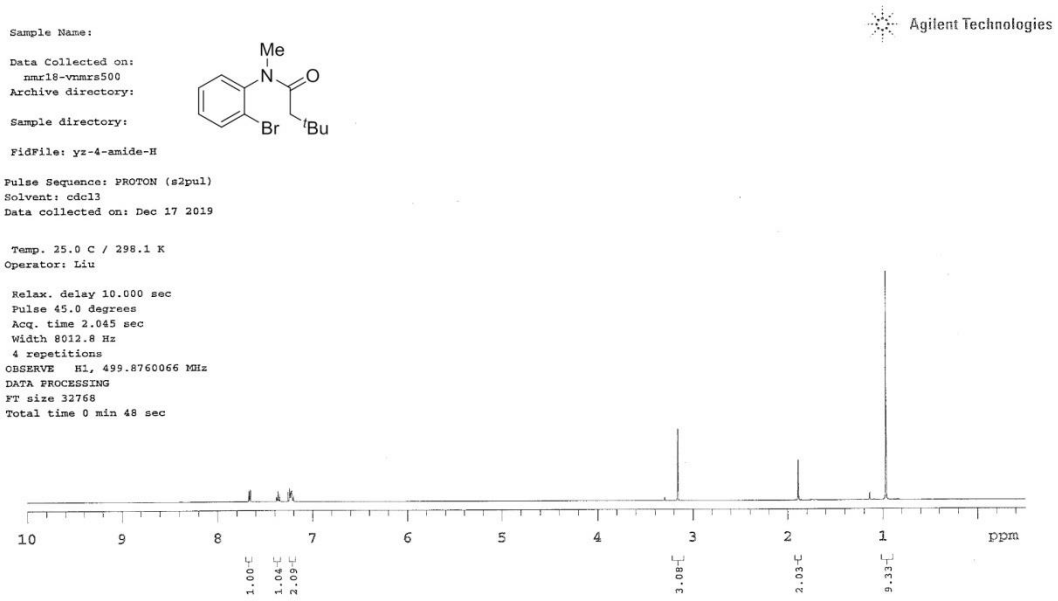

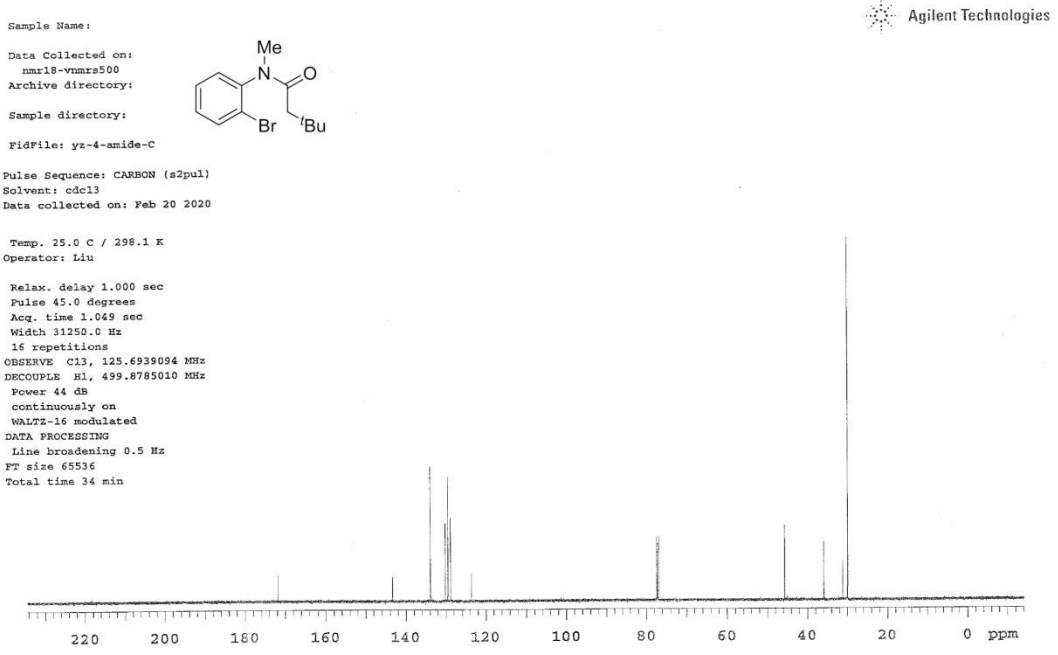

Sample Name:

Data Collected on:
nmr19-vnmrs600
Archive directory:

Sample directory:

FidFile: PROTON

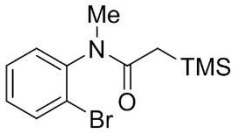

Pulse Sequence: PROTON (s2pul)
Solvent: cdcl3
Data collected on: Dec 26 2019

Temp. 25.0 C / 298.1 K
Operator: Liu

Relax. delay 10.000 sec
Pulse 45.0 degrees
Acq. time 1.704 sec
Width 9615.4 Hz
4 repetitions
OBSERVE H1, 599.6806832 MHz
DATA PROCESSING
FT size 32768
Total time 0 min 47 sec

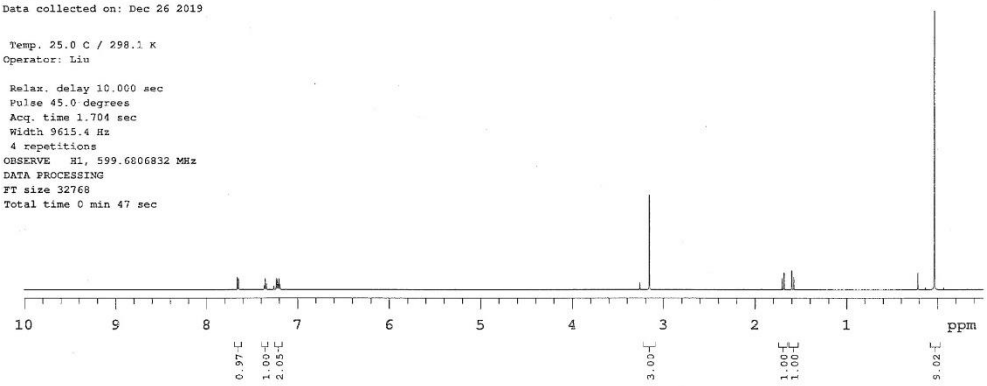

Sample Name:

Data Collected on:
nmr19-vnmrs600
Archive directory:

Sample directory:

FidFile: CARBON

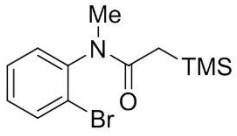

Pulse Sequence: CARBON (s2pul)
Solvent: cdcl3
Data collected on: Dec 26 2019

Temp. 25.0 C / 298.1 K
Operator: Liu

Relax. delay 1.000 sec
Pulse 45.0 degrees
Acq. time 0.865 sec
Width 37878.8 Hz
40 repetitions
OBSERVE C13, 150.7898097 MHz
DECOUPLE H1, 599.6836825 MHz
Power 45 dB
continuously on
WALTZ-16 modulated
DATA PROCESSING
Line broadening 0.5 Hz
FT size 65536
Total time 3 min 7 sec

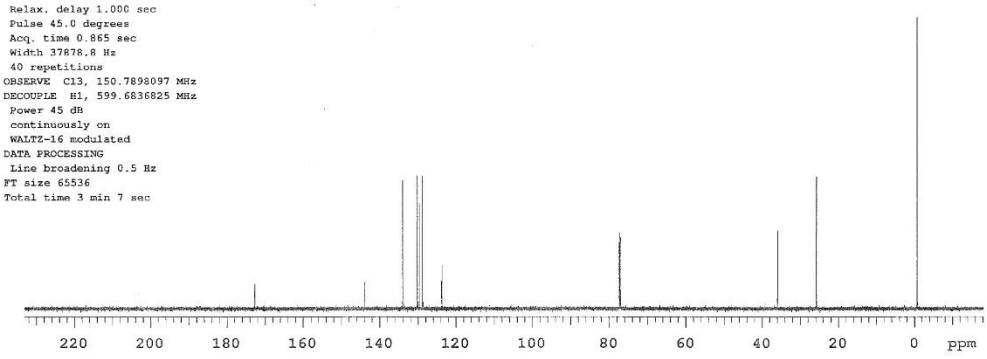

Sample Name:

Data Collected on:
nmr19-vnmrs600
Archive directory:

Sample directory:

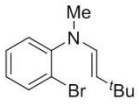

FidFile: PROTON

Pulse Sequence: PROTON (s2pul)
Solvent: cdcl3
Data collected on: Dec 19 2019

Temp. 25.0 C / 298.1 K
Operator: Liu

Relax. delay 10.000 sec
Pulse 45.0 degrees
Acq. time 1.704 sec
Width 9615.4 Hz
5 repetitions
OBSERVE H1, 599.6806841 MHz
DATA PROCESSING
FT size 32768
Total time 1 min 57 sec

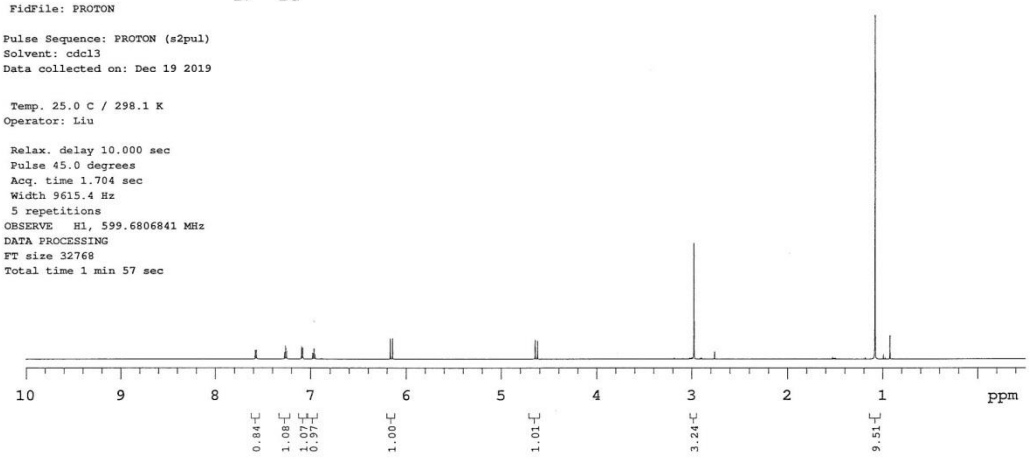

Sample Name:

Data Collected on:
nmr19-vnmrs600
Archive directory:

Sample directory:

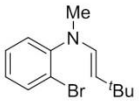

FidFile: CARBON

Pulse Sequence: CARBON (s2pul)
Solvent: cdcl3
Data collected on: Dec 19 2019

Temp. 25.0 C / 298.1 K
Operator: Liu

Relax. delay 1.000 sec
Pulse 45.0 degrees
Acq. time 0.865 sec
Width 37878.8 Hz
208 repetitions
OBSERVE C13, 150.7898050 MHz
DECOUPLE H1, 599.6836825 MHz
Power 45 dB
continuously on
WALTZ-16 modulated
DATA PROCESSING
Line broadening 0.5 Hz
FT size 65536
Total time 31 min

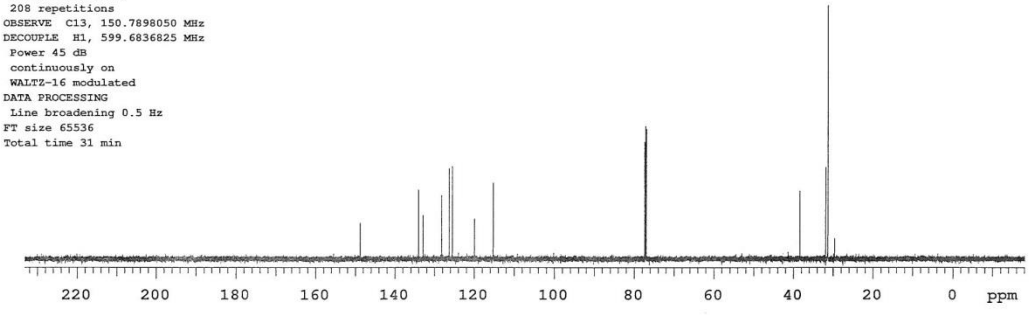

Sample Name:

Data Collected on:
nmr19-vnmrs600
Archive directory:

Sample directory:

FidFile: PROTON

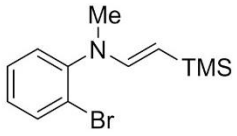

Pulse Sequence: PROTON (s2pul)
Solvent: cdcl3
Data collected on: Dec 27 2019

Temp. 25.0 C / 298.1 K
Operator: Liu

Relax. delay 10.000 sec
Pulse 45.0 degrees
Acq. time 1.704 sec
Width 9615.4 Hz
4 repetitions
OBSERVE H1, 599.6806832 MHz
DATA PROCESSING
FT size 32768
Total time 0 min 47 sec

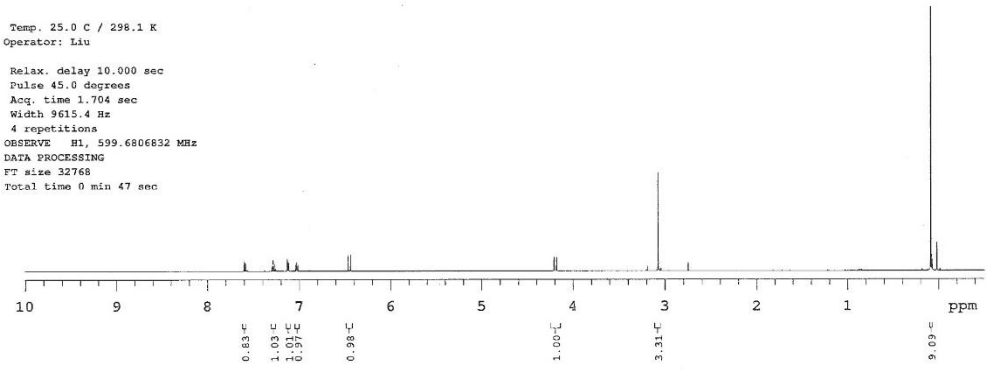

Sample Name:

Data Collected on:
nmr19-vnmrs600
Archive directory:

Sample directory:

FidFile: CARBON

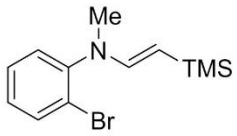

Pulse Sequence: CARBON (s2pul)
Solvent: cdcl3
Data collected on: Dec 27 2019

Temp. 25.0 C / 298.1 K
Operator: Liu

Relax. delay 1.000 sec
Pulse 45.0 degrees
Acq. time 0.865 sec
Width 37878.8 Hz
56 repetitions
OBSERVE C13, 150.7898050 MHz
DECOUPLE H1, 599.6836825 MHz
Power 45 dB
continuously on
WALTZ-16 modulated
DATA PROCESSING
Line broadening 0.5 Hz
FT size 65536
Total time 31 min

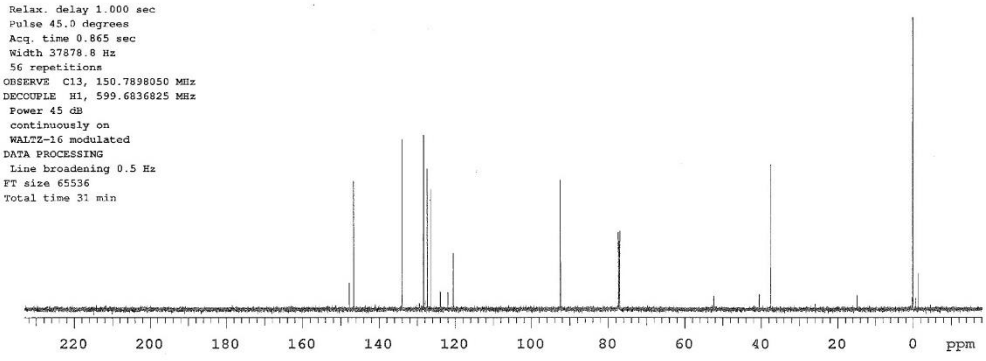

Parameter	Value
1 Solvent	cdcl3
2 Temperature	25.0
3 Relaxation Delay	1.0000
4 Nucleus	1H

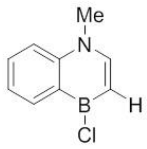

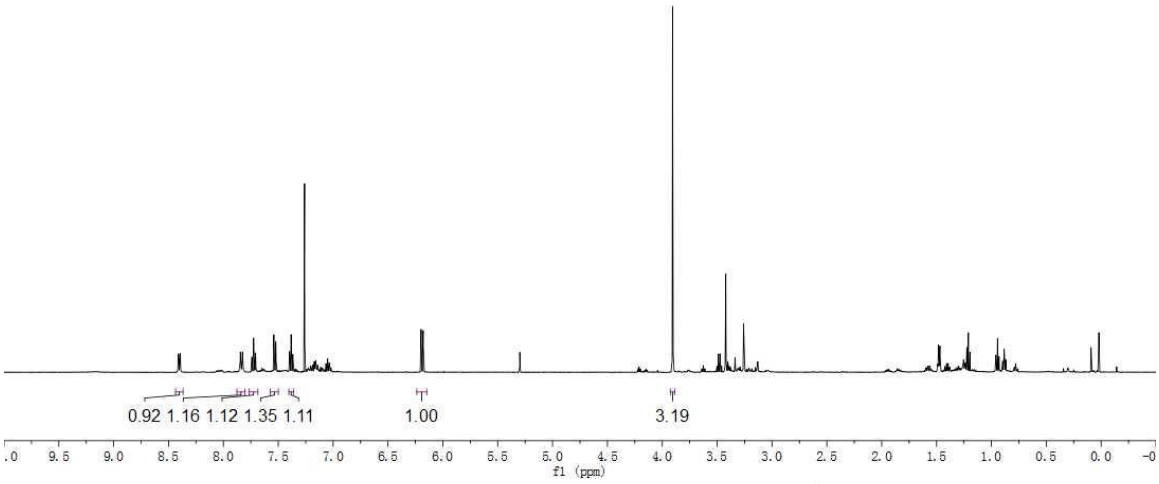

Sample Name:

Data Collected on:
nmr18-vnmrs500
Archive directory:

Sample directory:

FidFile: PROTON

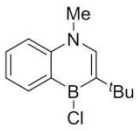

Agilent Technologies

Pulse Sequence: PROTON (s2pul)
Solvent: cdcl3
Data collected on: Dec 23 2019

Temp. 25.0 C / 298.1 K
Operator: Liu

Relax. delay 10.000 sec
Pulse 45.0 degrees
Acq. time 2.045 sec
Width 8012.8 Hz
4 repetitions
OBSERVE H1, 499.8760066 MHz
DATA PROCESSING
FT size 32768
Total time 0 min 48 sec

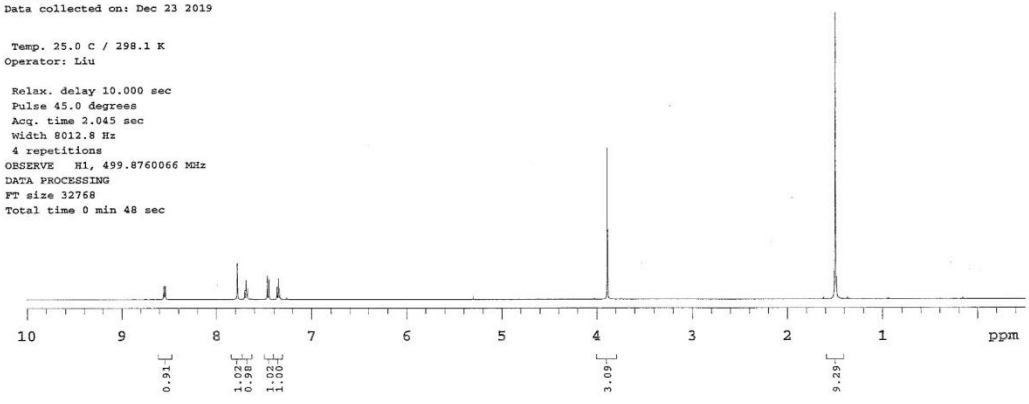

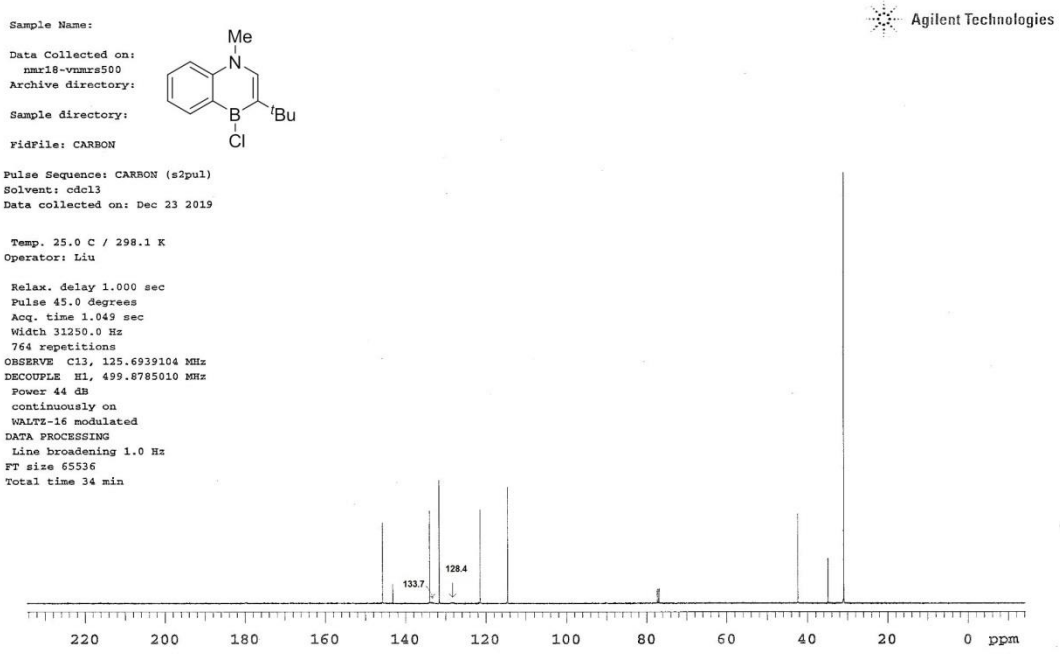
Agilent Technologies
Sample Name:
Data Collected on:
nmr18-vnmrs500
Archive directory:
Sample directory:
FidFile: CARBON
Me
N
B
Cl
tBu
Pulse Sequence: CARBON (s2pul)
Solvent: cdcl3
Data collected on: Dec 23 2019
Temp. 25.0 C / 298.1 K
Operator: Liu
Relax. delay 1.000 sec
Pulse 45.0 degrees
Acq. time 1.049 sec
Width 31250.0 Hz
764 repetitions
OBSERVE C13, 125.6939104 MHz
DECOUPLE H1, 499.8785010 MHz
Power 44 dB
continuously on
WALTZ-16 modulated
DATA PROCESSING
Line broadening 1.0 Hz
FT size 65536
Total time 34 min
133.7
128.4
220
200
180
160
140
120
100
80
60
40
20
0
ppm

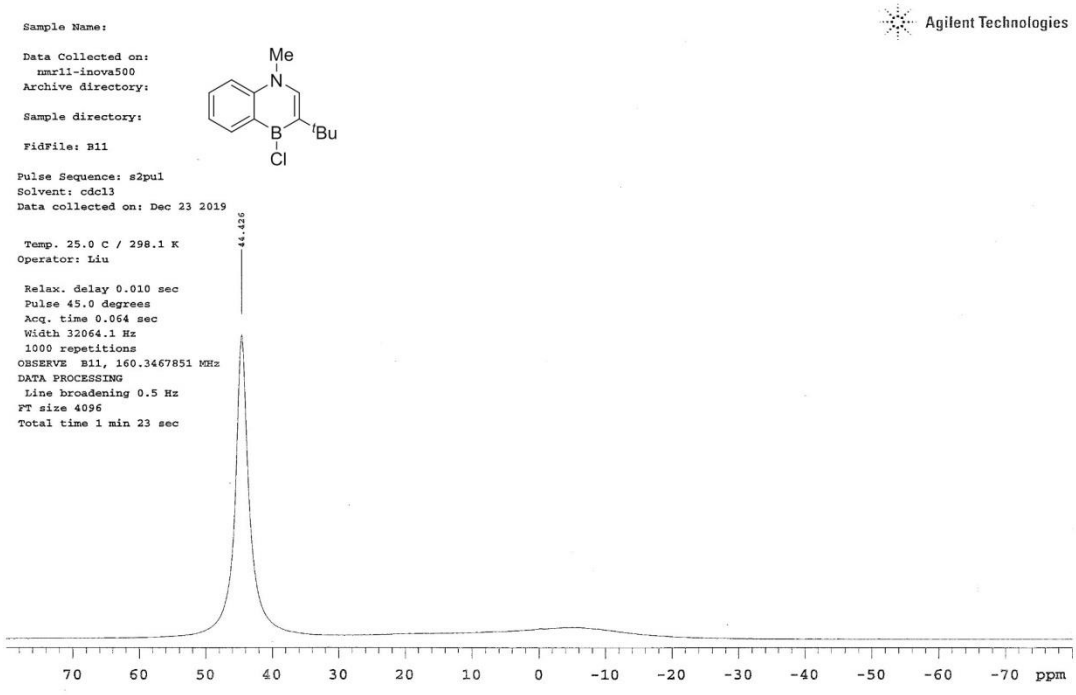
Agilent Technologies
Sample Name:
Data Collected on:
nmr11-inova500
Archive directory:
Sample directory:
FidFile: B11
Me
N
B
Cl
tBu
Pulse Sequence: s2pul
Solvent: cdcl3
Data collected on: Dec 23 2019
Temp. 25.0 C / 298.1 K
Operator: Liu
Relax. delay 0.010 sec
Pulse 45.0 degrees
Acq. time 0.064 sec
Width 32064.1 Hz
1000 repetitions
OBSERVE B11, 160.3467851 MHz
DATA PROCESSING
Line broadening 0.5 Hz
FT size 4096
Total time 1 min 23 sec
44.426
70
60
50
40
30
20
10
0
-10
-20
-30
-40
-50
-60
-70
ppm

Parameter	Value
1 Solvent	cdcl3
2 Temperature	25.0
3 Relaxation Delay	10.0000
4 Nucleus	1H

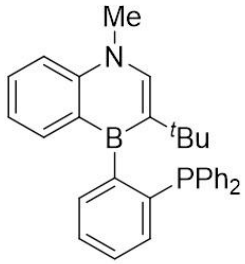

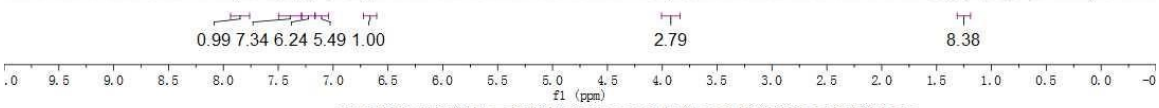

Parameter	Value
1 Solvent	cdcl3
2 Temperature	25.0
3 Relaxation Delay	1.0000
4 Nucleus	13C

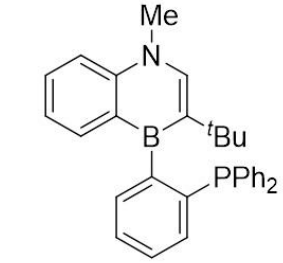

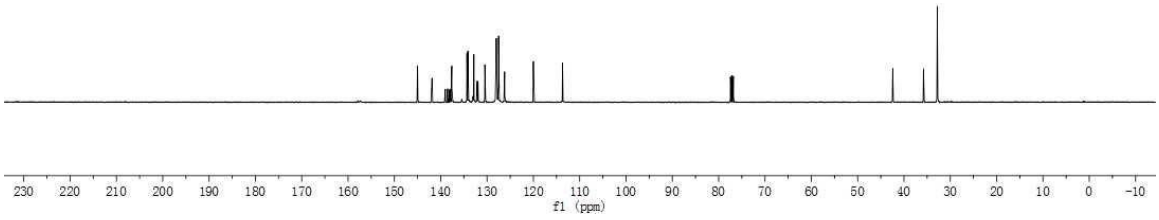

Parameter	Value
1 Solvent	cdcl3
2 Temperature	25.0
3 Relaxation Delay	0.0100
4 Nucleus	11B

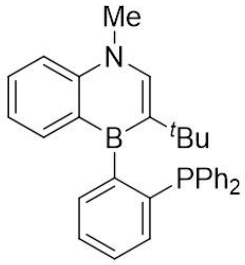

A(s)
46.6

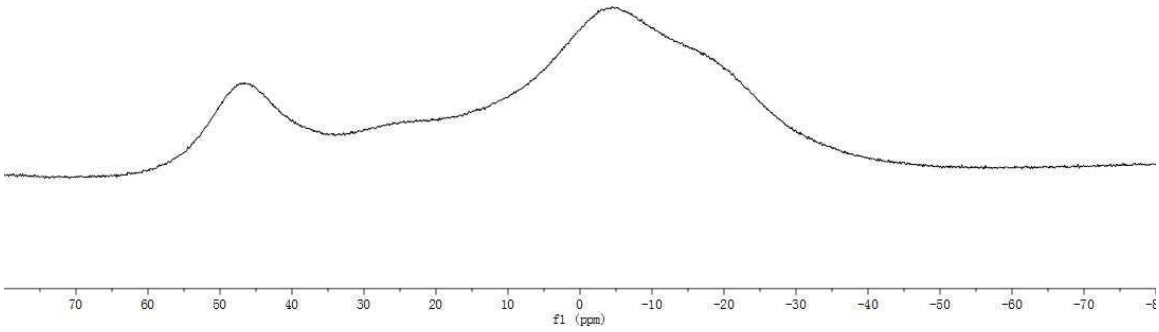

Parameter	Value
1 Solvent	cdcl3
2 Temperature	25.0
3 Relaxation Delay	1.0000
4 Nucleus	31P

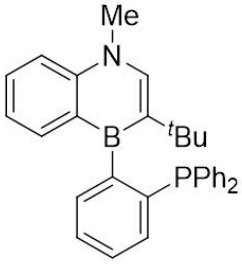

A(s)
-10.2

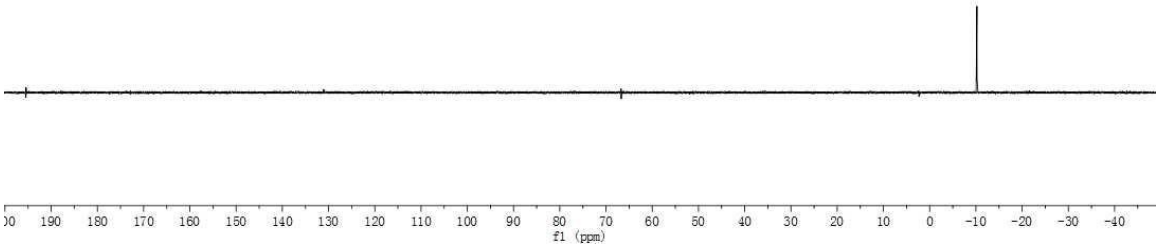

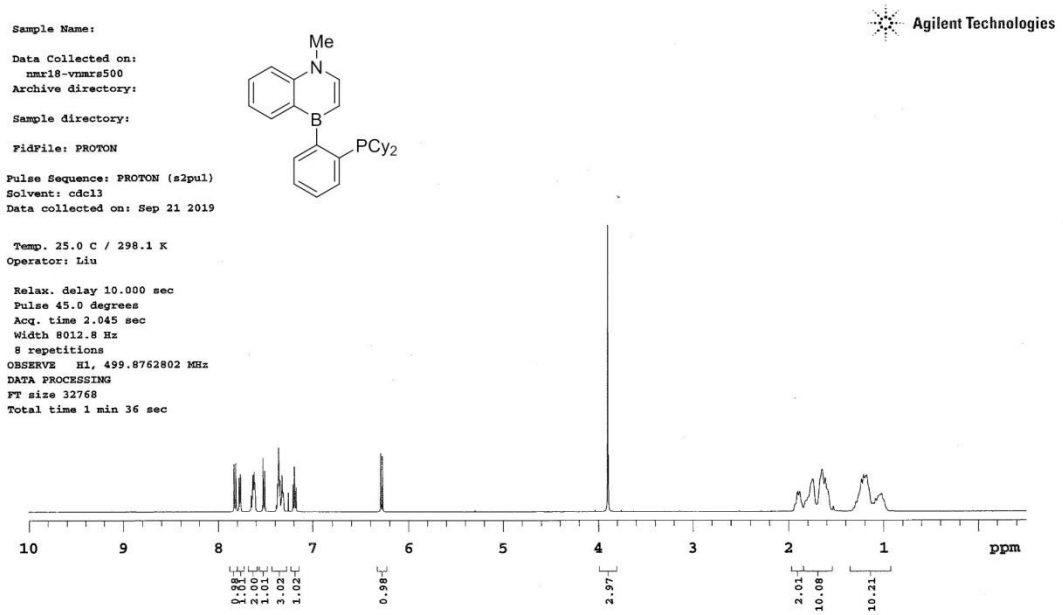
Agilent Technologies
Sample Name:
Data Collected on:
nmr18-vnmrs500
Archive directory:
Sample directory:
FidFile: PROTON
Pulse Sequence: PROTON (s2pul)
Solvent: cdcl3
Data collected on: Sep 21 2019
Temp. 25.0 C / 298.1 K
Operator: Liu
Relax. delay 10.000 sec
Pulse 45.0 degrees
Acq. time 2.045 sec
Width 8012.8 Hz
8 repetitions
OBSERVE H1, 499.8762802 MHz
DATA PROCESSING
FT size 32768
Total time 1 min 36 sec
Me
N
B
PCy2
10
9
8
7
6
5
4
3
2
1
ppm
0.98
1.01
2.00
1.01
3.02
1.02
0.98
2.97
2.01
10.08
10.21

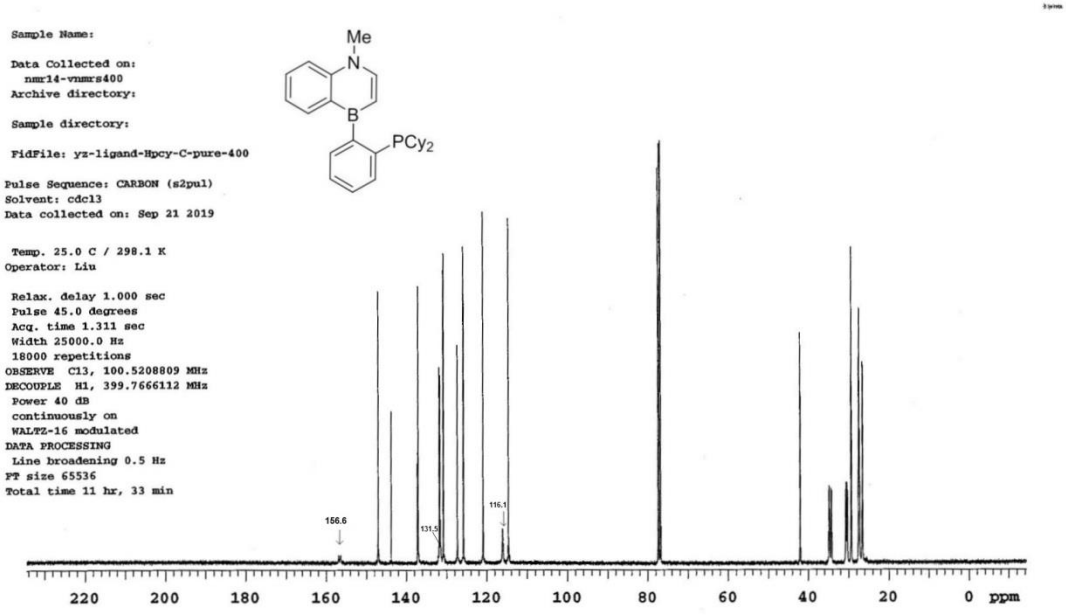
Sample Name:
Data Collected on:
nmr14-vnmrs400
Archive directory:
Sample directory:
FidFile: yz-ligand-Hpcy-C-pure-400
Pulse Sequence: CARBON (s2pul)
Solvent: cdcl3
Data collected on: Sep 21 2019
Temp. 25.0 C / 298.1 K
Operator: Liu
Relax. delay 1.000 sec
Pulse 45.0 degrees
Acq. time 1.311 sec
Width 25000.0 Hz
18000 repetitions
OBSERVE C13, 100.5208809 MHz
DECOUPLE H1, 399.7666112 MHz
Power 40 dB
continuously on
WALTZ-16 modulated
DATA PROCESSING
Line broadening 0.5 Hz
FT size 65536
Total time 11 hr, 33 min
Me
N
B
PCy2
156.6
131.5
116.1
220
200
180
160
140
120
100
80
60
40
20
0
ppm

Agilent Technologies

Sample Name:

Data Collected on:
nmr11-inova500
Archive directory:

Sample directory:

FidFile: B11

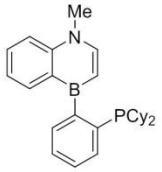

Pulse Sequence: s2pul
Solvent: cdcl3
Data collected on: Sep 20 2019

Temp. 25.0 C / 298.1 K
Operator: Liu

Relax. delay 0.010 sec
Pulse 45.0 degrees
Acq. time 0.064 sec
Width 32064.1 Hz
1804 repetitions
OBSERVE B11, 160.3466755 MHz
DATA PROCESSING
Line broadening 0.5 Hz
FT size 4096
Total time 13 min

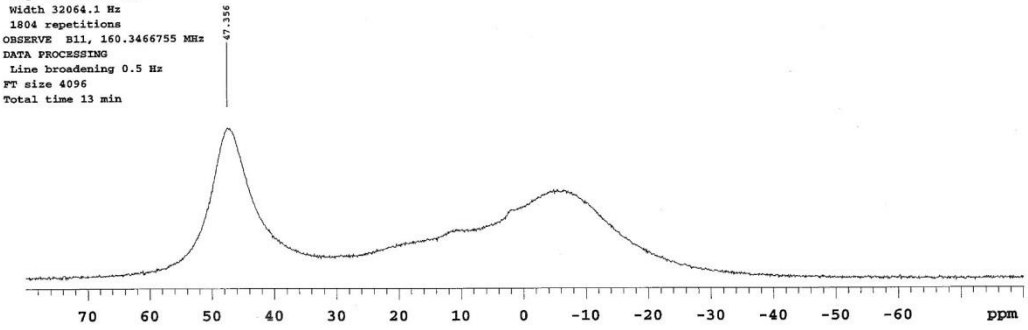

STANDARD PHOSPHORUS PARAMETERS

Agilent Technologies

Sample Name:

Data Collected on:
nmr18-vnmrs500
Archive directory:

Sample directory:

FidFile: PHOSPHORUS

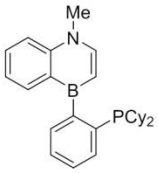

Pulse Sequence: PHOSPHORUS (s2pul)
Solvent: cdcl3
Data collected on: Sep 20 2019

Temp. 25.0 C / 298.1 K
Operator: Liu

Relax. delay 1.000 sec
Pulse 45.0 degrees
Acq. time 0.655 sec
Width 50000.0 Hz
20 repetitions
OBSERVE P31, 202.3535033 MHz
DECOUPLE H1, 499.8787746 MHz
Power 45 dB
on during acquisition
off during delay
WALTZ-16 modulated
DATA PROCESSING
Line broadening 0.5 Hz
FT size 65536
Total time 0 min 33 sec

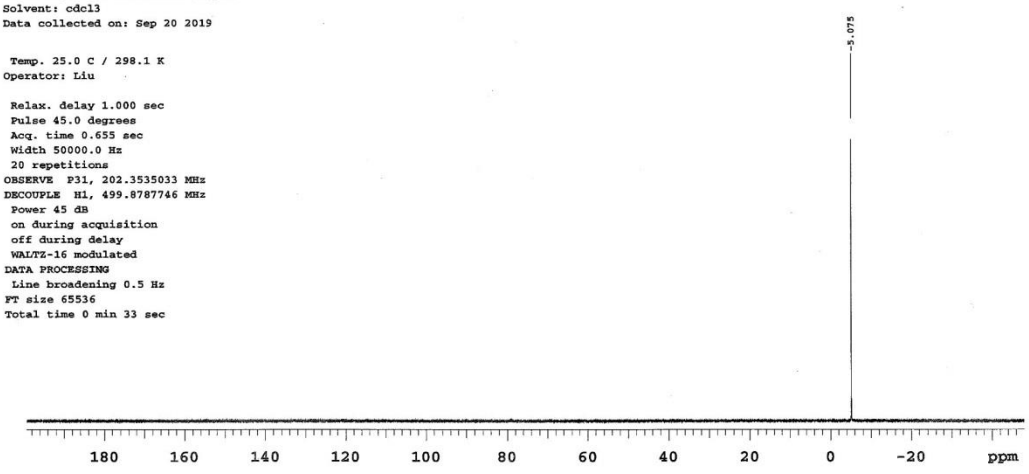

Me

Sample Name:

Data Collected on:
nmr18-vnmrs500
Archive directory:

Sample directory:

FidFile: PROTON

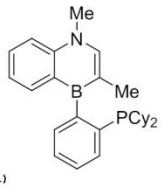

Agilent Technologies

Pulse Sequence: PROTON (s2pul)
Solvent: cdcl3
Data collected on: Aug 17 2019

Temp. 25.0 C / 298.1 K
Operator: Liu

Relax. delay 10.000 sec
Pulse 45.0 degrees
Acq. time 2.045 sec
Width 8012.8 Hz
5 repetitions
OBSERVE H1, 499.8762780 MHz
DATA PROCESSING
FT size 32768
Total time 1 min 36 sec

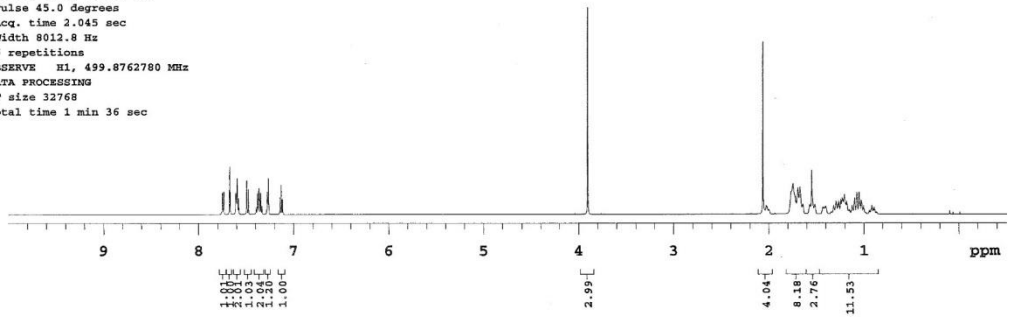

Sample Name:

Data Collected on:
nmr18-vnmrs500
Archive directory:

Sample directory:

FidFile: yz-ligand-Mepcy-C

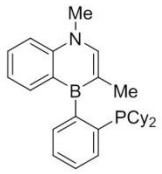

Pulse Sequence: CARBON (s2pul)
Solvent: cdcl3
Data collected on: Aug 17 2019

Temp. 25.0 C / 298.1 K
Operator: Liu

Relax. delay 1.000 sec
Pulse 45.0 degrees
Acq. time 1.049 sec
Width 31250.0 Hz
560 repetitions
OBSERVE C13, 125.6939734 MHz
DECOUPLE H1, 499.8787746 MHz
Power 45 dB
continuously on
WALTZ-16 modulated
DATA PROCESSING
Line broadening 0.5 Hz
FT size 65536
Total time 34 min

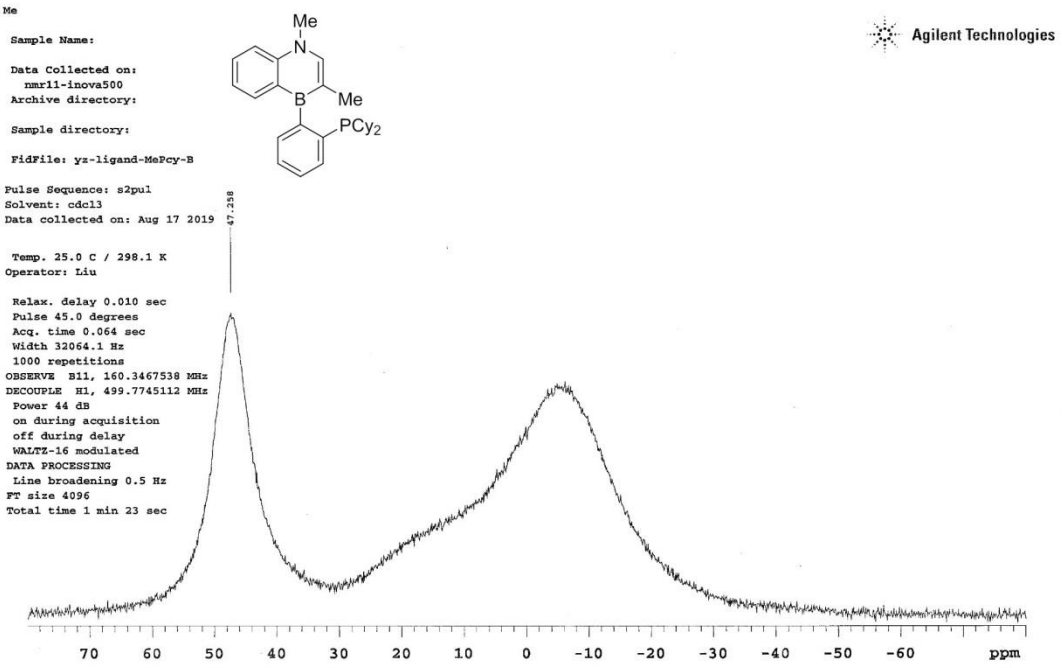
Me
Sample Name:
Data Collected on:
nmr11-inova500
Archive directory:
Sample directory:
FidFile: yz-ligand-MePcy-B
Pulse Sequence: s2pul
Solvent: cdcl3
Data collected on: Aug 17 2019
Temp. 25.0 C / 298.1 K
Operator: Liu
Relax. delay 0.010 sec
Pulse 45.0 degrees
Acq. time 0.064 sec
Width 32064.1 Hz
1000 repetitions
OBSERVE B11, 160.3467538 MHz
DECOUPLE H1, 499.7745112 MHz
Power 44 dB
on during acquisition
off during delay
WALTZ-16 modulated
DATA PROCESSING
Line broadening 0.5 Hz
FT size 4096
Total time 1 min 23 sec
47.258
Me
N
B
Me
PCy2
Agilent Technologies
70 60 50 40 30 20 10 0 -10 -20 -30 -40 -50 -60 ppm

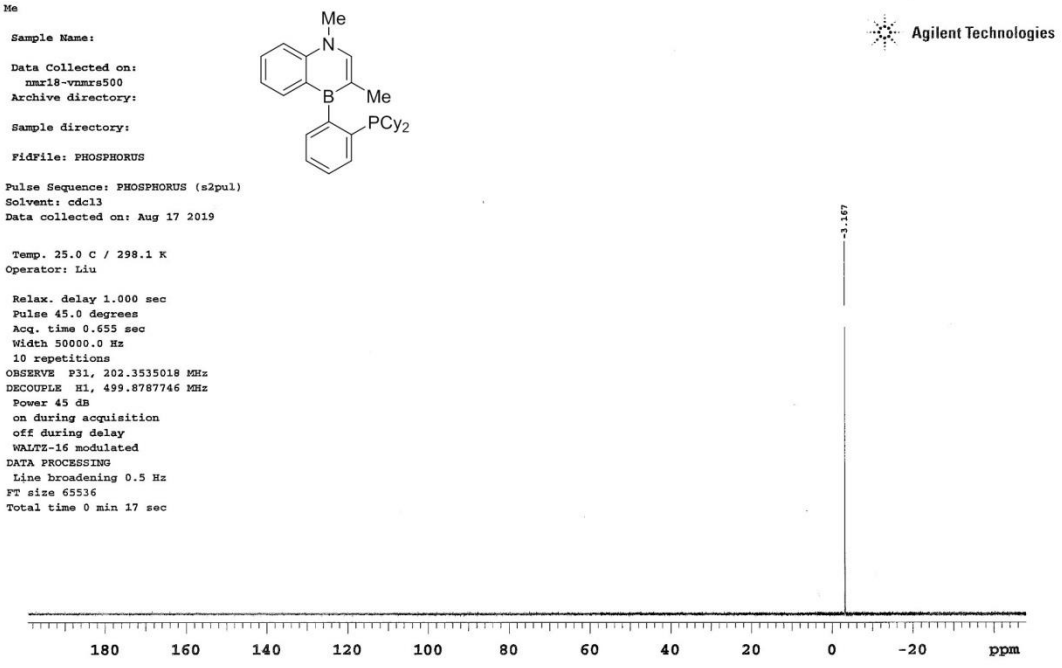
Me
Sample Name:
Data Collected on:
nmr18-vnmrs500
Archive directory:
Sample directory:
FidFile: PHOSPHORUS
Pulse Sequence: PHOSPHORUS (s2pul)
Solvent: cdcl3
Data collected on: Aug 17 2019
Temp. 25.0 C / 298.1 K
Operator: Liu
Relax. delay 1.000 sec
Pulse 45.0 degrees
Acq. time 0.655 sec
Width 50000.0 Hz
10 repetitions
OBSERVE P31, 202.3535018 MHz
DECOUPLE H1, 499.8787746 MHz
Power 45 dB
on during acquisition
off during delay
WALTZ-16 modulated
DATA PROCESSING
Line broadening 0.5 Hz
FT size 65536
Total time 0 min 17 sec
-3.167
Me
N
B
Me
PCy2
Agilent Technologies
180 160 140 120 100 80 60 40 20 0 -20 ppm

Et

Sample Name:

Data Collected on:
nmr18-vnmrs500
Archive directory:

Sample directory:

FidFile: yz-ligand-Etpcy-H

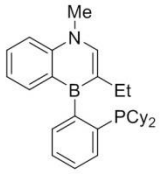

Pulse Sequence: PROTON (s2pul)
Solvent: cdcl3
Data collected on: Aug 17 2019

Temp. 25.0 C / 298.1 K
Operator: Liu

Relax. delay 10.000 sec
Pulse 45.0 degrees
Acq. time 2.045 sec
Width 8012.8 Hz
8 repetitions
OBSERVE H1, 499.8762807 MHz
DATA PROCESSING
FT size 32768
Total time 2 min 0 sec

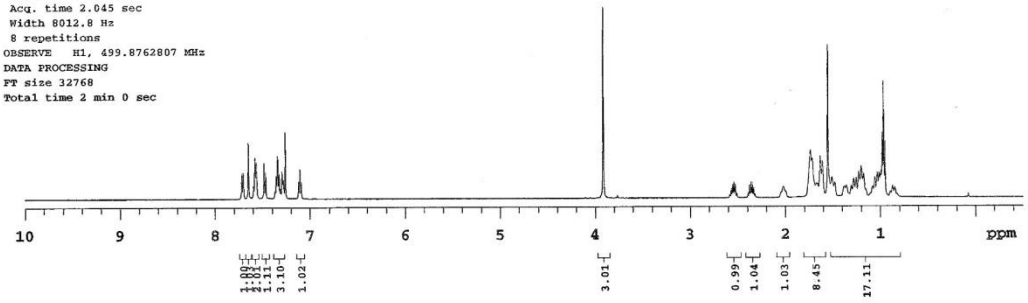

Agilent Technologies

Sample Name:

Data Collected on:
nmr14-vnmrs400
Archive directory:

Sample directory:

FidFile: CARBON

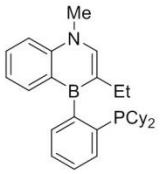

Pulse Sequence: CARBON (s2pul)
Solvent: cdcl3
Data collected on: Aug 17 2019

Temp. 25.0 C / 298.1 K
Operator: Liu

Relax. delay 1.000 sec
Pulse 45.0 degrees
Acq. time 1.311 sec
Width 25000.0 Hz
4256 repetitions
OBSERVE C13, 100.5208748 MHz
DECOUPLE H1, 399.7666112 MHz
Power 40 dB
continuously on
WALTZ-16 modulated
DATA PROCESSING
Line broadening 0.5 Hz
FT size 65536
Total time 6 hr, 25 min

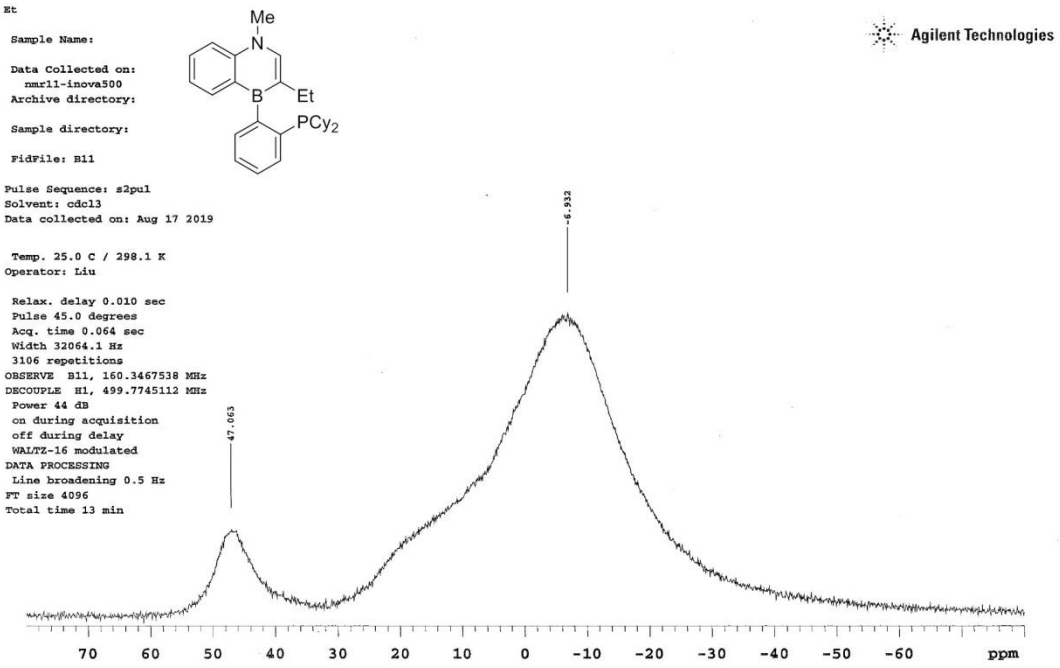
Et
Sample Name:
Data Collected on:
nmr11-inova500
Archive directory:
Sample directory:
FidFile: B11
Me
N
B
Et
PCy2
Agilent Technologies
Pulse Sequence: s2pul
Solvent: cdcl3
Data collected on: Aug 17 2019
Temp. 25.0 C / 298.1 K
Operator: Liu
Relax. delay 0.010 sec
Pulse 45.0 degrees
Acq. time 0.064 sec
Width 32064.1 Hz
3106 repetitions
OBSERVE B11, 160.3467538 MHz
DECOUPLE H1, 499.7745112 MHz
Power 44 dB
on during acquisition
off during delay
WALTZ-16 modulated
DATA PROCESSING
Line broadening 0.5 Hz
FT size 4096
Total time 13 min
47.063
6.932
70 60 50 40 30 20 10 0 -10 -20 -30 -40 -50 -60 ppm

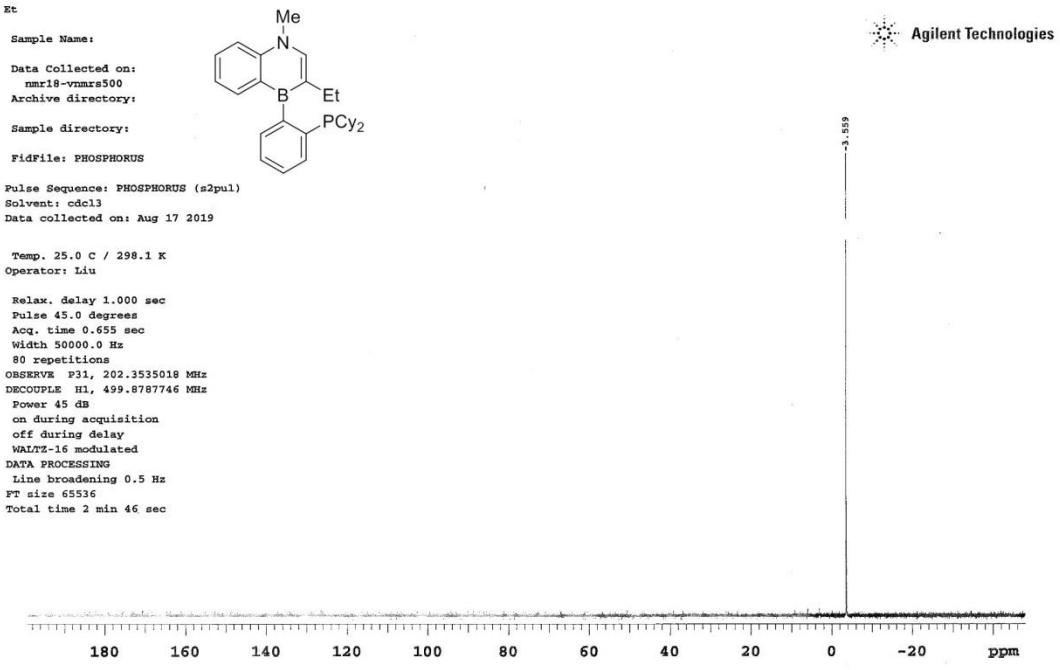
Et
Sample Name:
Data Collected on:
nmr18-vnmrs500
Archive directory:
Sample directory:
FidFile: PHOSPHORUS
Me
N
B
Et
PCy2
Agilent Technologies
Pulse Sequence: PHOSPHORUS (s2pul)
Solvent: cdcl3
Data collected on: Aug 17 2019
Temp. 25.0 C / 298.1 K
Operator: Liu
Relax. delay 1.000 sec
Pulse 45.0 degrees
Acq. time 0.655 sec
Width 50000.0 Hz
80 repetitions
OBSERVE P31, 202.3535018 MHz
DECOUPLE H1, 499.8787746 MHz
Power 45 dB
on during acquisition
off during delay
WALTZ-16 modulated
DATA PROCESSING
Line broadening 0.5 Hz
FT size 65536
Total time 2 min 46 sec
3.559
180 160 140 120 100 80 60 40 20 0 -20 ppm

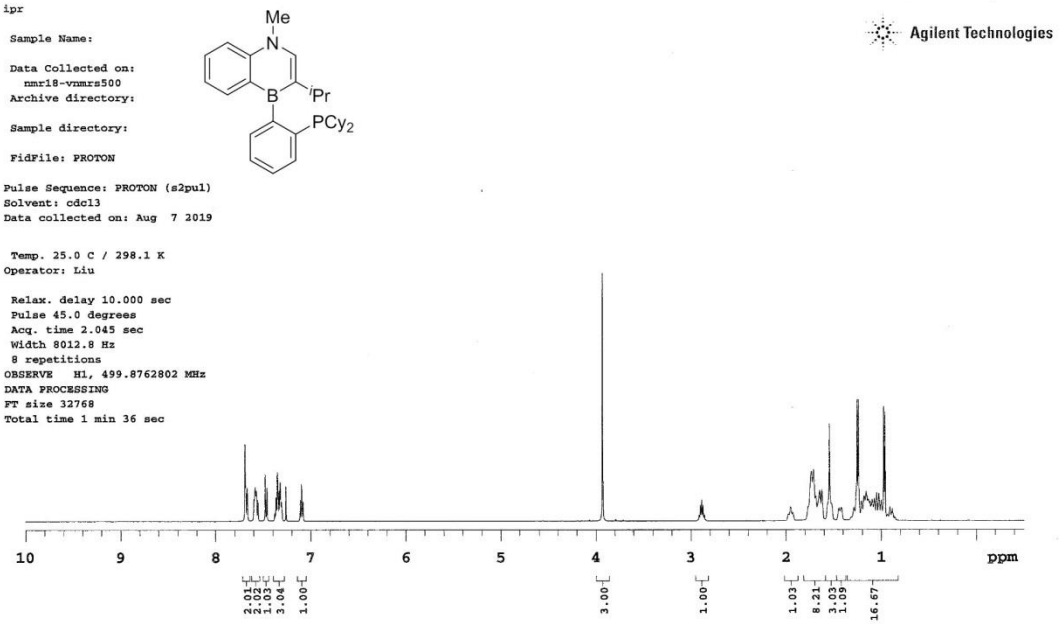
ipr
Sample Name:
Data Collected on:
nmr18-vnmrs500
Archive directory:
Sample directory:
FidFile: PROTON
Pulse Sequence: PROTON (s2pul)
Solvent: cdcl3
Data collected on: Aug 7 2019
Temp. 25.0 C / 298.1 K
Operator: Liu
Relax. delay 10.000 sec
Pulse 45.0 degrees
Acq. time 2.045 sec
Width 8012.8 Hz
8 repetitions
OBSERVE H1, 499.8762802 MHz
DATA PROCESSING
FT size 32768
Total time 1 min 36 sec
Me
N
B
iPr
PCy2
Agilent Technologies
10
9
8
7
6
5
4
3
2
1
ppm
2.01
2.02
1.03
3.04
1.00
3.00
1.00
1.03
8.21
3.03
1.09
16.67

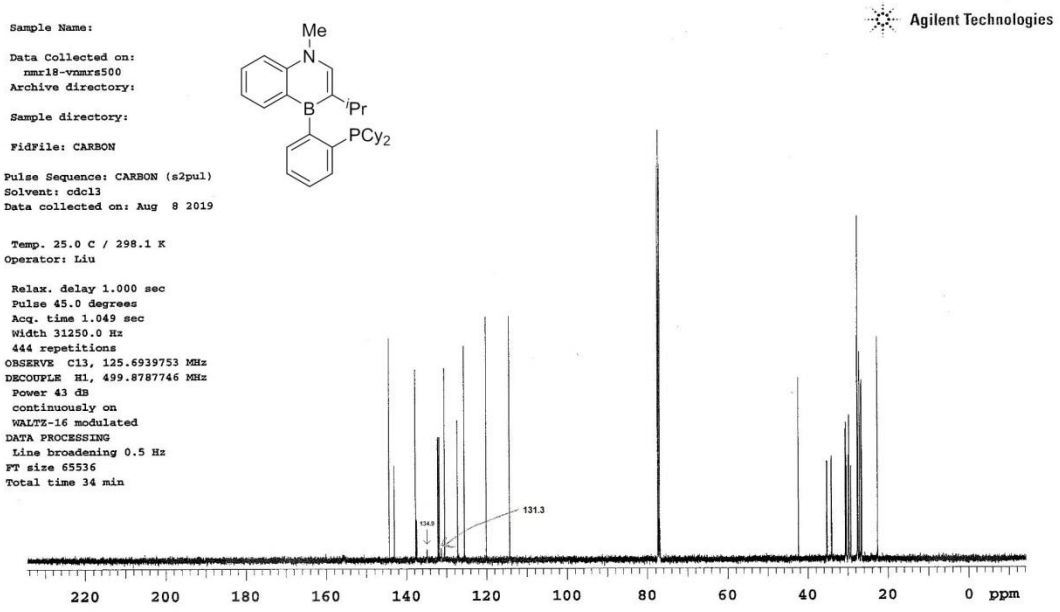
Sample Name:
Data Collected on:
nmr18-vnmrs500
Archive directory:
Sample directory:
FidFile: CARBON
Pulse Sequence: CARBON (s2pul)
Solvent: cdcl3
Data collected on: Aug 8 2019
Temp. 25.0 C / 298.1 K
Operator: Liu
Relax. delay 1.000 sec
Pulse 45.0 degrees
Acq. time 1.049 sec
Width 31250.0 Hz
444 repetitions
OBSERVE C13, 125.6939753 MHz
DECOUPLE H1, 499.8787746 MHz
Power 43 dB
continuously on
WALTZ-16 modulated
DATA PROCESSING
Line broadening 0.5 Hz
FT size 65536
Total time 34 min
Me
N
B
iPr
PCy2
Agilent Technologies
134.9
131.3
220
200
180
160
140
120
100
80
60
40
20
0
ppm

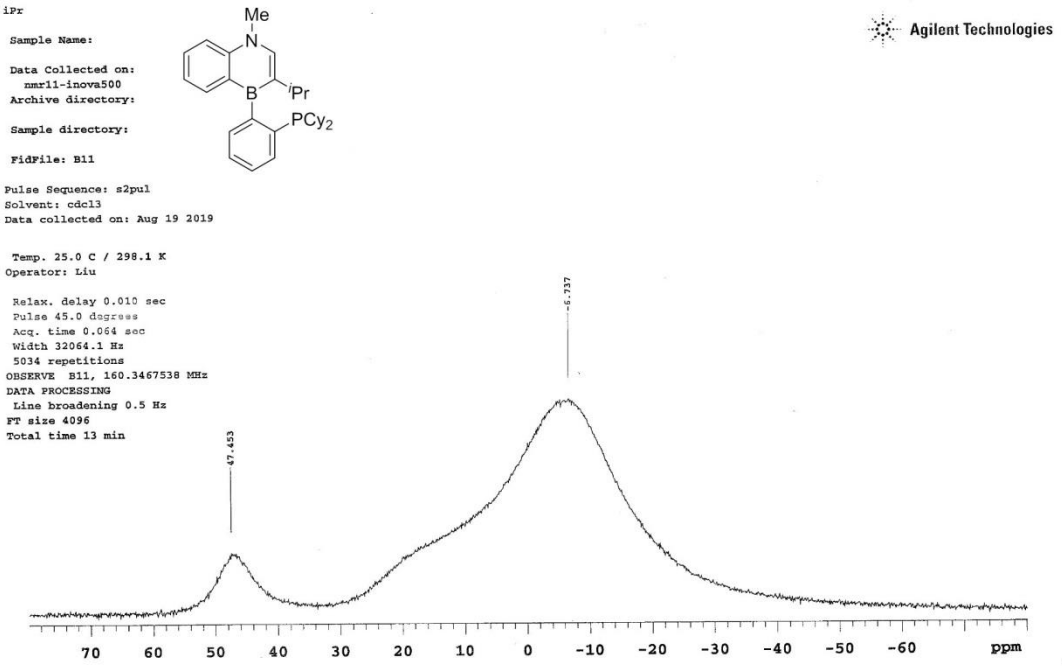
iPr
Sample Name:
Data Collected on:
nmr11-inova500
Archive directory:
Sample directory:
FidFile: B11
Pulse Sequence: s2pul
Solvent: cdcl3
Data collected on: Aug 19 2019
Temp. 25.0 C / 298.1 K
Operator: Liu
Relax. delay 0.010 sec
Pulse 45.0 degrees
Acq. time 0.064 sec
Width 32064.1 Hz
5034 repetitions
OBSERVE B11, 160.3467538 MHz
DATA PROCESSING
Line broadening 0.5 Hz
FT size 4096
Total time 13 min
Me
N
B
iPr
PCy2
Agilent Technologies
47.453
6.337
70 60 50 40 30 20 10 0 -10 -20 -30 -40 -50 -60 ppm

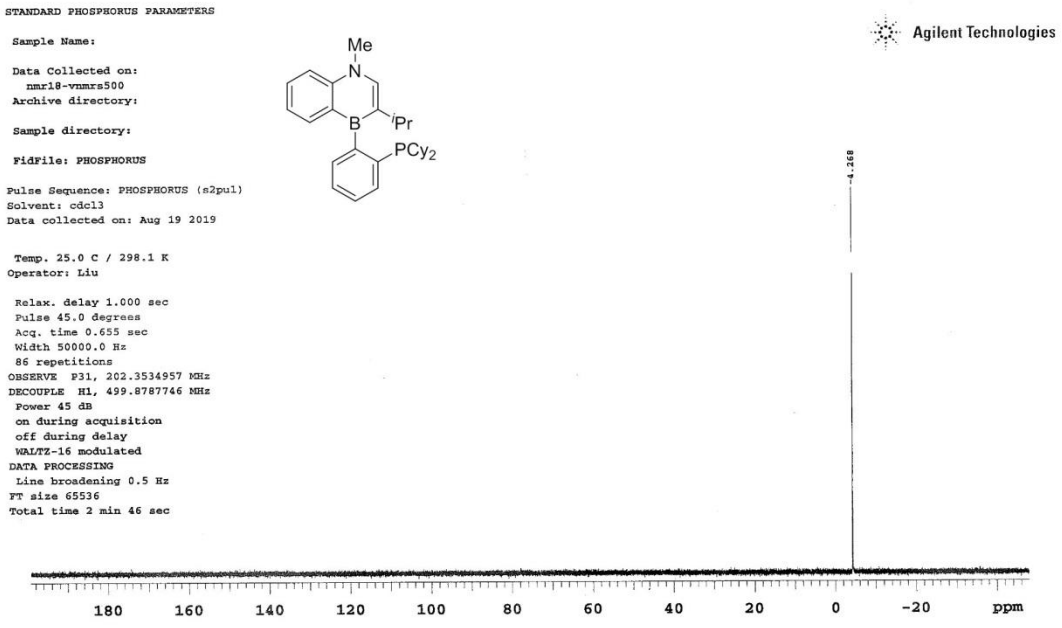
STANDARD PHOSPHORUS PARAMETERS
Sample Name:
Data Collected on:
nmr18-vnmrs500
Archive directory:
Sample directory:
FidFile: PHOSPHORUS
Pulse Sequence: PHOSPHORUS (s2pul)
Solvent: cdcl3
Data collected on: Aug 19 2019
Temp. 25.0 C / 298.1 K
Operator: Liu
Relax. delay 1.000 sec
Pulse 45.0 degrees
Acq. time 0.655 sec
Width 50000.0 Hz
86 repetitions
OBSERVE P31, 202.3534957 MHz
DECOUPLE H1, 499.8787746 MHz
Power 45 dB
on during acquisition
off during delay
WALTZ-16 modulated
DATA PROCESSING
Line broadening 0.5 Hz
FT size 65536
Total time 2 min 46 sec
Me
N
B
iPr
PCy2
Agilent Technologies
4.268
180 160 140 120 100 80 60 40 20 0 -20 ppm

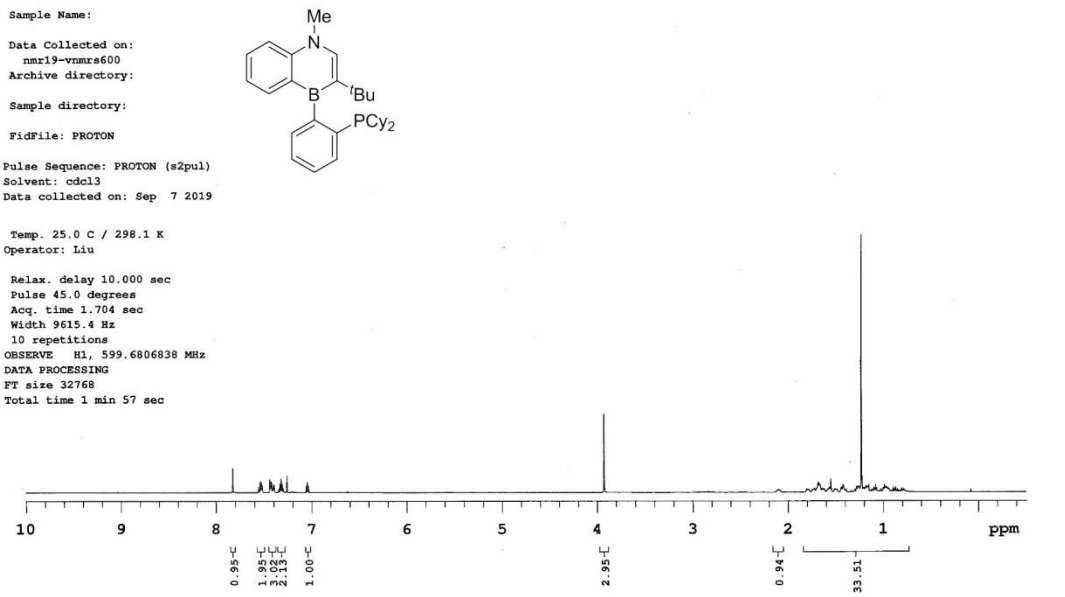
Sample Name:
Data Collected on:
nmr19-vnmrs600
Archive directory:
Sample directory:
FidFile: PROTON
Pulse Sequence: PROTON (s2pul)
Solvent: cdcl3
Data collected on: Sep 7 2019
Temp. 25.0 C / 298.1 K
Operator: Liu
Relax. delay 10.000 sec
Pulse 45.0 degrees
Acq. time 1.704 sec
Width 9615.4 Hz
10 repetitions
OBSERVE H1, 599.6806838 MHz
DATA PROCESSING
FT size 32768
Total time 1 min 57 sec
Me
N
B
tBu
PCy2
10
9
8
7
6
5
4
3
2
1
ppm
0.95
1.95
3.02
2.13
1.00
2.95
0.94
33.51

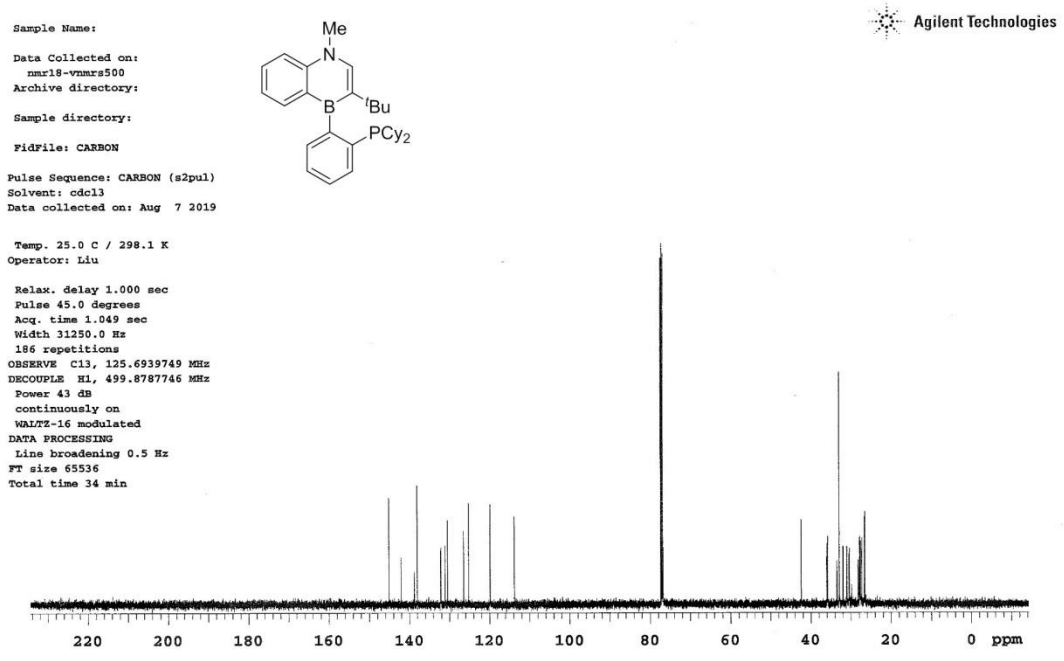
Agilent Technologies
Sample Name:
Data Collected on:
nmr18-vnmrs500
Archive directory:
Sample directory:
FidFile: CARBON
Pulse Sequence: CARBON (s2pul)
Solvent: cdcl3
Data collected on: Aug 7 2019
Temp. 25.0 C / 298.1 K
Operator: Liu
Relax. delay 1.000 sec
Pulse 45.0 degrees
Acq. time 1.049 sec
Width 31250.0 Hz
186 repetitions
OBSERVE C13, 125.6939749 MHz
DECOUPLE H1, 499.8787746 MHz
Power 43 dB
continuously on
WALTZ-16 modulated
DATA PROCESSING
Line broadening 0.5 Hz
FT size 65536
Total time 34 min
Me
N
B
tBu
PCy2
220
200
180
160
140
120
100
80
60
40
20
0 ppm

STANDARD PROTON PARAMETERS

Sample Name:

Data Collected on:
nmr11-inova500
Archive directory:

Sample directory:

FidFile: B11

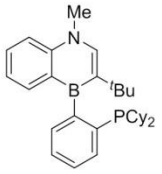

Agilent Technologies

Pulse Sequence: s2pul
Solvent: cdcl3
Data collected on: Sep 7 2019

Temp. 25.0 C / 298.1 K
Operator: Liu

Relax. delay 0.010 sec
Pulse 45.0 degrees
Acq. time 0.064 sec
Width 32064.1 Hz
1018 repetitions
OBSERVE B11, 160.3467695 MHz
DATA PROCESSING
Line broadening 0.5 Hz
FT size 4096
Total time 2 min 46 sec

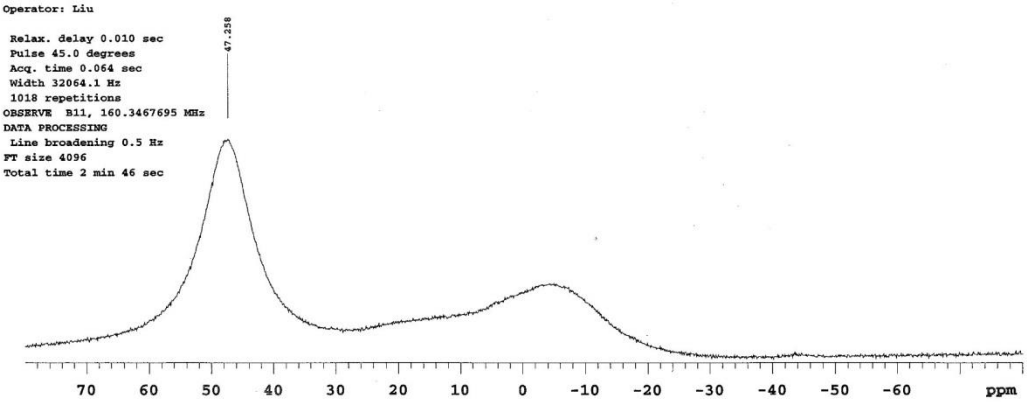

STANDARD PHOSPHORUS PARAMETERS

Sample Name:

Data Collected on:
nmr18-vnmrs500
Archive directory:

Sample directory:

FidFile: PHOSPHORUS

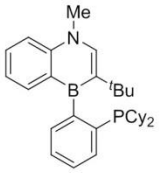

Agilent Technologies

Pulse Sequence: PHOSPHORUS (s2pul)
Solvent: cdcl3
Data collected on: Sep 7 2019

Temp. 25.0 C / 298.1 K
Operator: Liu

Relax. delay 1.000 sec
Pulse 45.0 degrees
Acq. time 0.655 sec
Width 50000.0 Hz
Single scan
OBSERVE P31, 202.3535079 MHz
DECOUPLE H1, 499.8787746 MHz
Power 45 dB
on during acquisition
off during delay
WALTZ-16 modulated
DATA PROCESSING
Line broadening 0.5 Hz
FT size 65536
Total time 0 min 2 sec

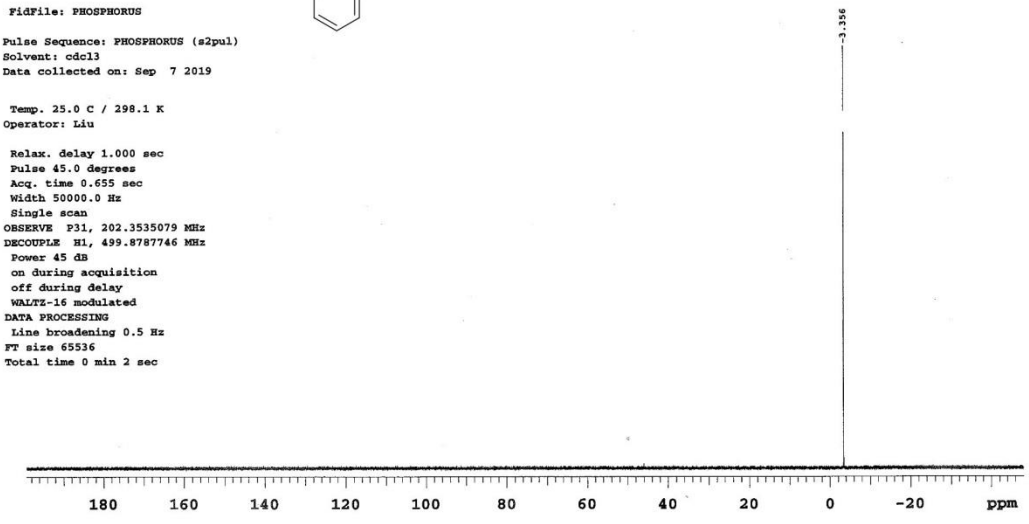

Parameter	Value
1 Solvent	cdcl3
2 Temperature	25.0
3 Relaxation Delay	10.0000
4 Nucleus	1H

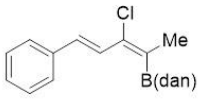

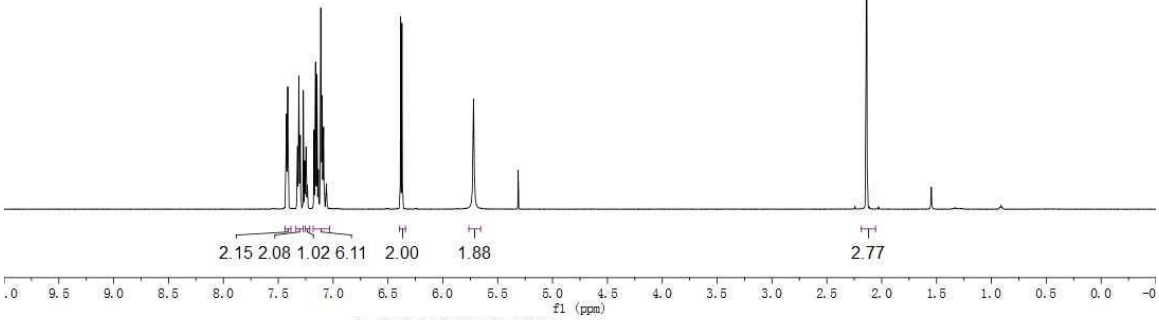

Parameter	Value
1 Solvent	cdcl3
2 Temperature	25.0
3 Relaxation Delay	1.0000
4 Nucleus	13C

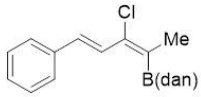

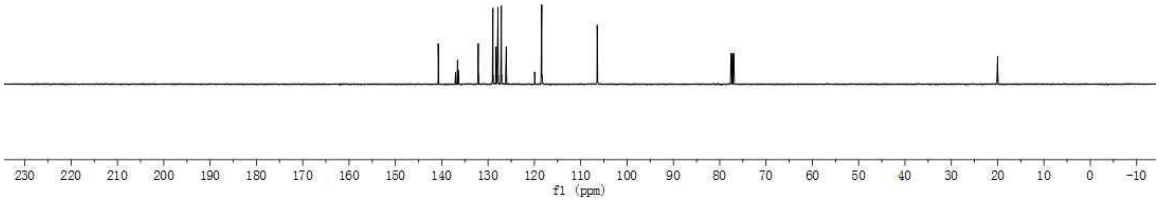

Parameter	Value
1 Solvent	cdcl3
2 Temperature	25.0
3 Relaxation Delay	0.0100
4 Nucleus	11B

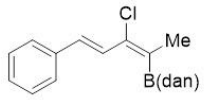

A(s)
29.7

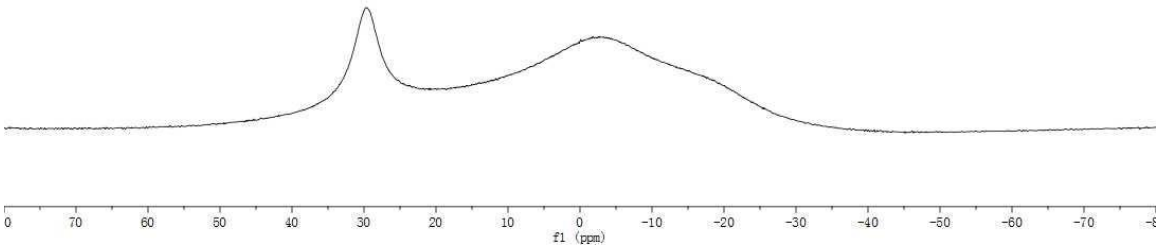

Parameter	Value
1 Solvent	cdcl3
2 Temperature	25.0
3 Relaxation Delay	10.0000
4 Nucleus	1H

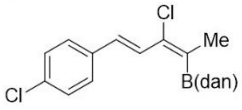

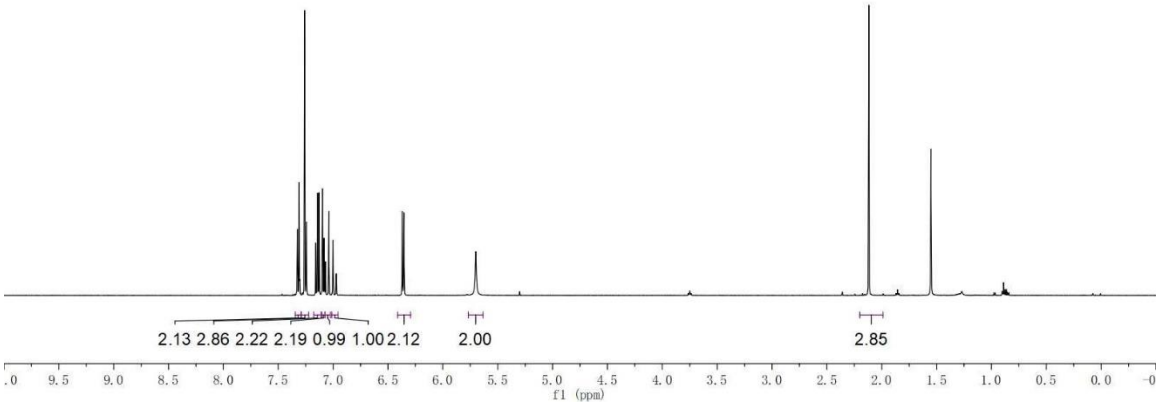

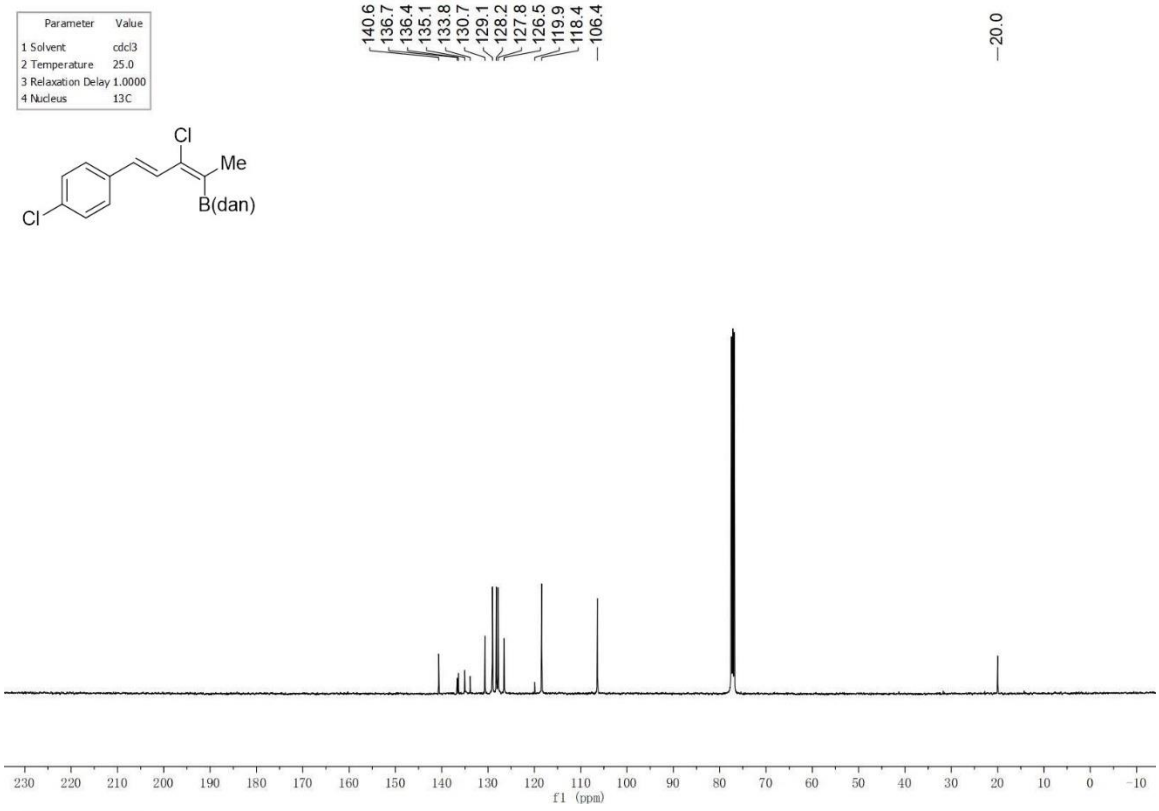
Parameter Value
1 Solvent cdcl3
2 Temperature 25.0
3 Relaxation Delay 1.0000
4 Nucleus 13C
Cl
Me
B(dan)
Cl
140.6
136.7
136.4
135.1
133.8
130.7
129.1
128.2
127.8
126.5
119.9
118.4
106.4
20.0
f1 (ppm)

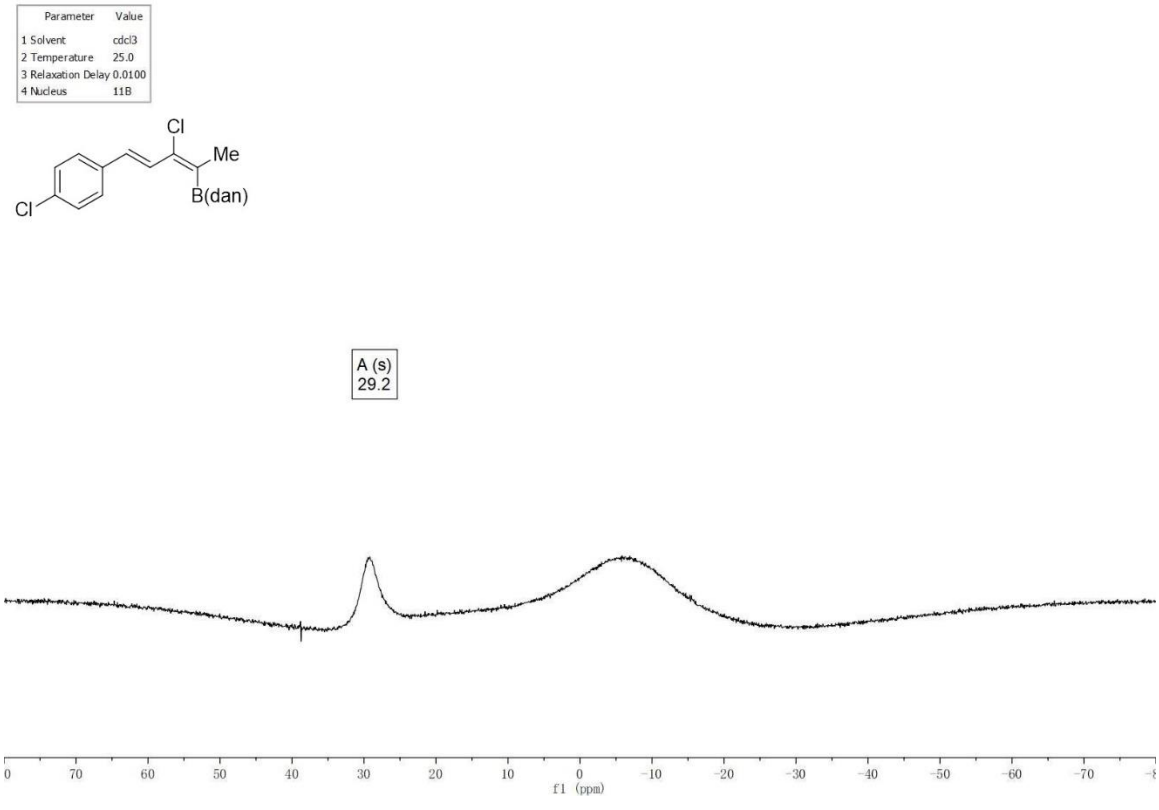
Parameter Value
1 Solvent cdcl3
2 Temperature 25.0
3 Relaxation Delay 0.0100
4 Nucleus 11B
Cl
Me
B(dan)
Cl
A (s)
29.2
f1 (ppm)

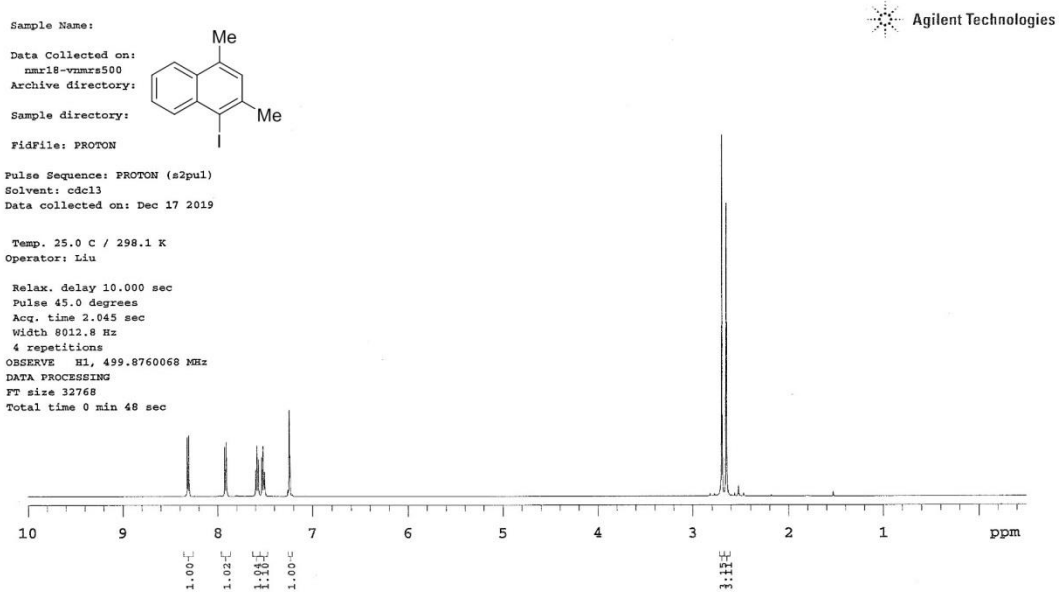
Agilent Technologies
Sample Name:
Data Collected on:
nmr18-vnmrs500
Archive directory:
Sample directory:
FidFile: PROTON
Me
Me
I
Pulse Sequence: PROTON (s2pul)
Solvent: cdcl3
Data collected on: Dec 17 2019
Temp. 25.0 C / 298.1 K
Operator: Liu
Relax. delay 10.000 sec
Pulse 45.0 degrees
Acq. time 2.045 sec
Width 8012.8 Hz
4 repetitions
OBSERVE H1, 499.8760068 MHz
DATA PROCESSING
FT size 32768
Total time 0 min 48 sec
10
9
8
7
6
5
4
3
2
1
ppm
1.00
1.02
1.10
1.00
3.15

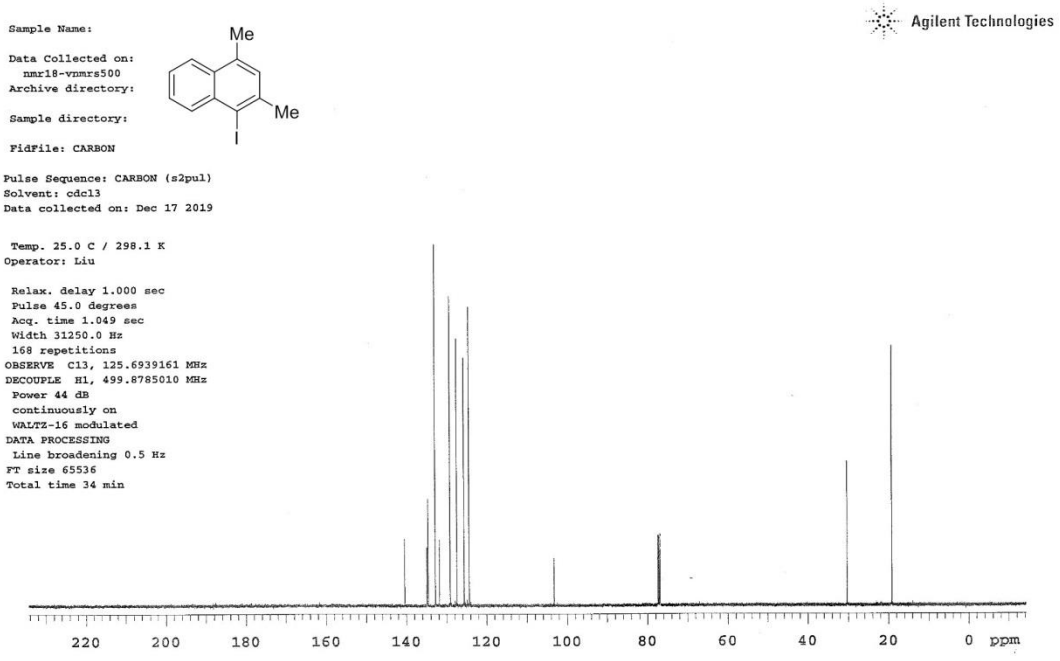
Agilent Technologies
Sample Name:
Data Collected on:
nmr18-vnmrs500
Archive directory:
Sample directory:
FidFile: CARBON
Me
Me
I
Pulse Sequence: CARBON (s2pul)
Solvent: cdcl3
Data collected on: Dec 17 2019
Temp. 25.0 C / 298.1 K
Operator: Liu
Relax. delay 1.000 sec
Pulse 45.0 degrees
Acq. time 1.049 sec
Width 31250.0 Hz
168 repetitions
OBSERVE C13, 125.6939161 MHz
DECOUPLE H1, 499.8785010 MHz
Power 44 dB
continuously on
WALTZ-16 modulated
DATA PROCESSING
Line broadening 0.5 Hz
FT size 65536
Total time 34 min
220
200
180
160
140
120
100
80
60
40
20
0
ppm

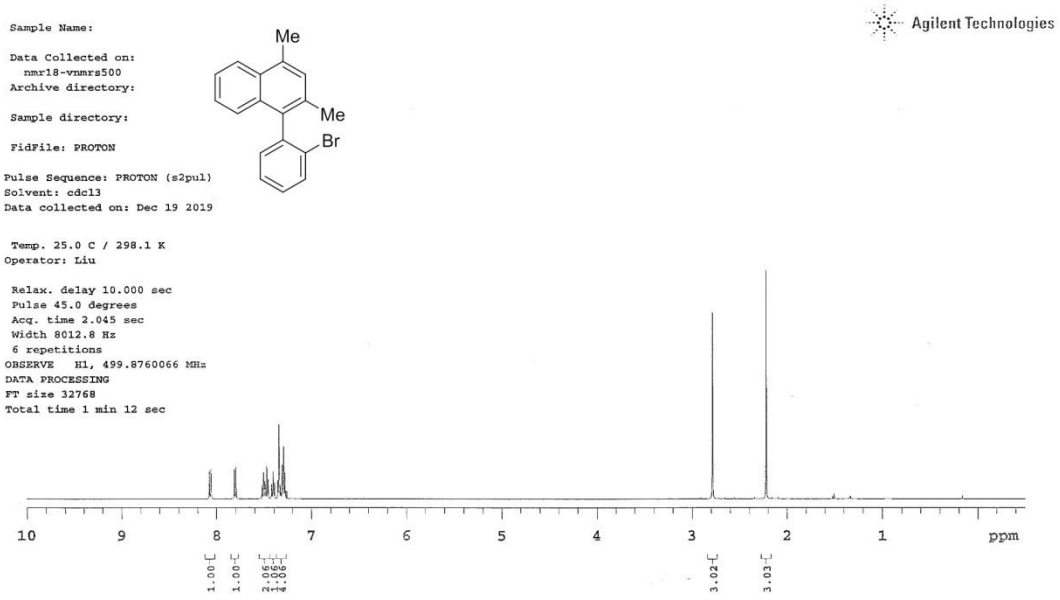
Agilent Technologies
Sample Name:
Data Collected on:
nmr18-vnmrs500
Archive directory:
Sample directory:
FidFile: PROTON
Me
Me
Br
Pulse Sequence: PROTON (s2pul)
Solvent: cdcl3
Data collected on: Dec 19 2019
Temp. 25.0 C / 298.1 K
Operator: Liu
Relax. delay 10.000 sec
Pulse 45.0 degrees
Acq. time 2.045 sec
Width 8012.8 Hz
6 repetitions
OBSERVE H1, 499.8760066 MHz
DATA PROCESSING
FT size 32768
Total time 1 min 12 sec
10
9
8
7
6
5
4
3
2
1
ppm
1.00
1.00
2.06
4.00
3.02
3.03

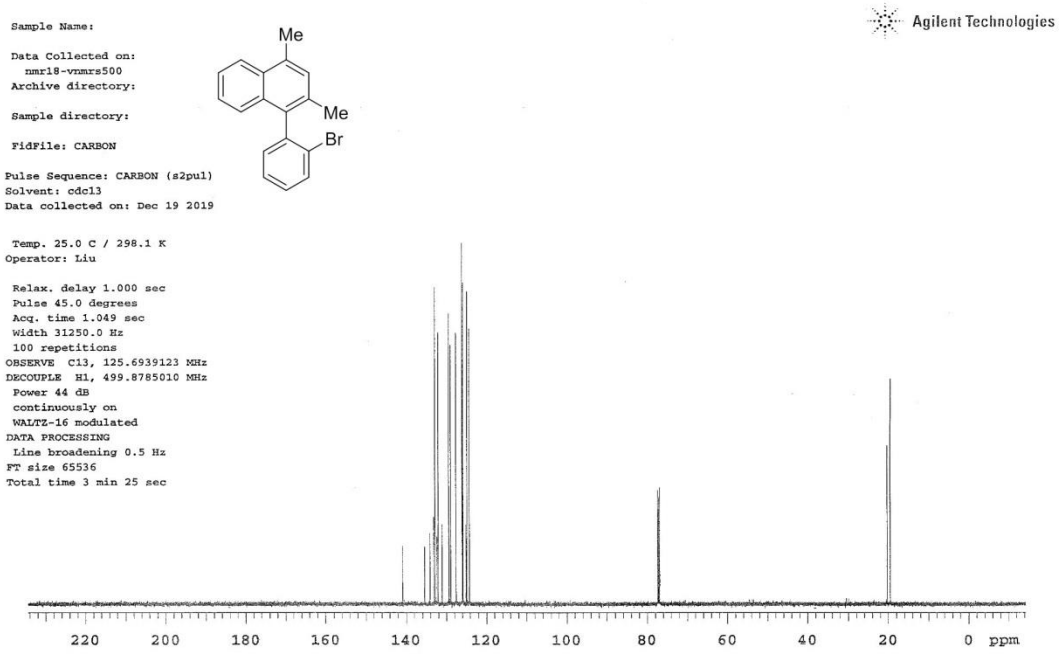
Agilent Technologies
Sample Name:
Data Collected on:
nmr18-vnmrs500
Archive directory:
Sample directory:
FidFile: CARBON
Me
Me
Br
Pulse Sequence: CARBON (s2pul)
Solvent: cdcl3
Data collected on: Dec 19 2019
Temp. 25.0 C / 298.1 K
Operator: Liu
Relax. delay 1.000 sec
Pulse 45.0 degrees
Acq. time 1.049 sec
Width 31250.0 Hz
100 repetitions
OBSERVE C13, 125.6939123 MHz
DECOUPLE H1, 499.8785010 MHz
Power 44 dB
continuously on
WALTZ-16 modulated
DATA PROCESSING
Line broadening 0.5 Hz
FT size 65536
Total time 3 min 25 sec
220
200
180
160
140
120
100
80
60
40
20
0
ppm

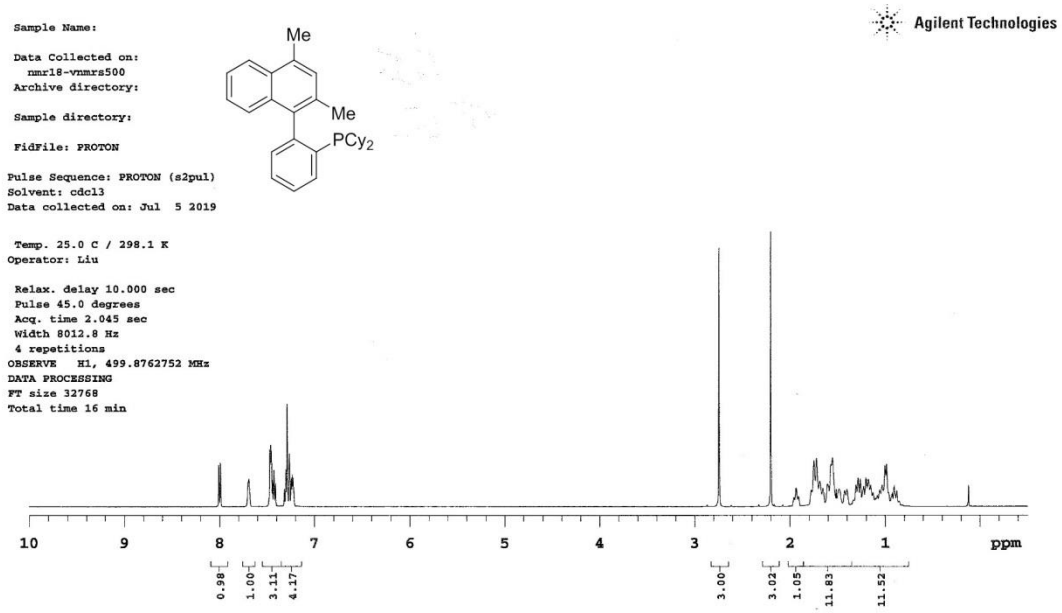
Agilent Technologies
Sample Name:
Data Collected on:
nmr18-vnmrs500
Archive directory:
Sample directory:
FidFile: PROTON
Me
Me
PCy2
Pulse Sequence: PROTON (s2pul)
Solvent: cdcl3
Data collected on: Jul 5 2019
Temp. 25.0 C / 298.1 K
Operator: Liu
Relax. delay 10.000 sec
Pulse 45.0 degrees
Acq. time 2.045 sec
Width 8012.8 Hz
4 repetitions
OBSERVE H1, 499.8762752 MHz
DATA PROCESSING
FT size 32768
Total time 16 min
10
9
8
7
6
5
4
3
2
1
ppm
0.98
1.00
3.11
4.17
3.00
3.02
1.05
11.83
11.52

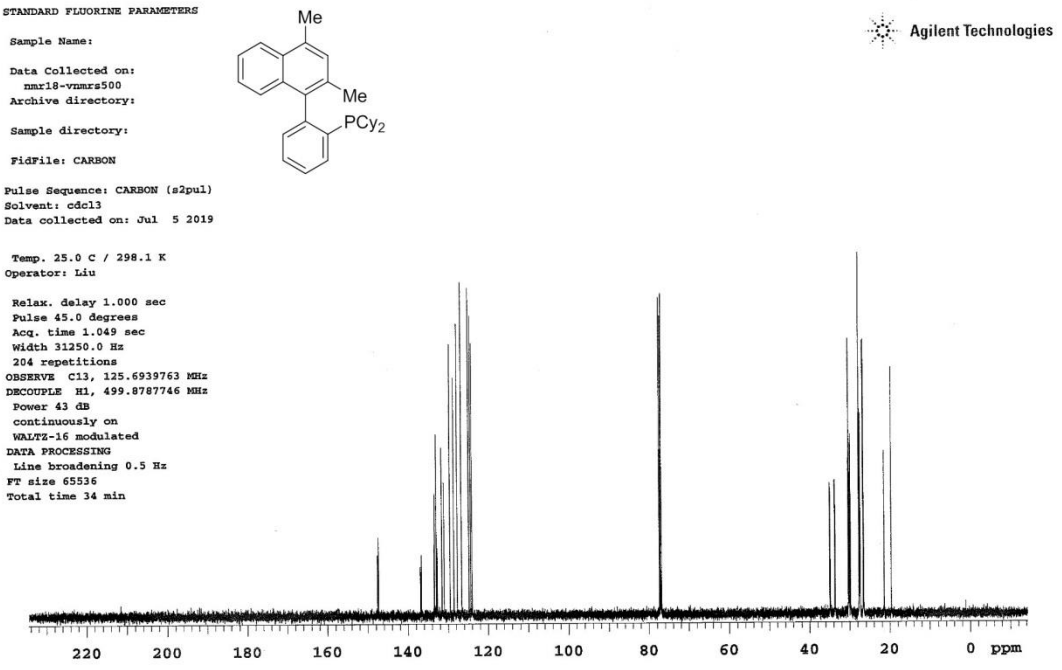
Agilent Technologies
STANDARD FLUORINE PARAMETERS
Sample Name:
Data Collected on:
nmr18-vnmrs500
Archive directory:
Sample directory:
FidFile: CARBON
Me
Me
PCy2
Pulse Sequence: CARBON (s2pul)
Solvent: cdcl3
Data collected on: Jul 5 2019
Temp. 25.0 C / 298.1 K
Operator: Liu
Relax. delay 1.000 sec
Pulse 45.0 degrees
Acq. time 1.049 sec
Width 31250.0 Hz
204 repetitions
OBSERVE C13, 125.6939763 MHz
DECOUPLE H1, 499.8787746 MHz
Power 43 dB
continuously on
WALTZ-16 modulated
DATA PROCESSING
Line broadening 0.5 Hz
FT size 65536
Total time 34 min
220
200
180
160
140
120
100
80
60
40
20
0
ppm

Sample Name:

Data Collected on:
nmr18-vnmrs500
Archive directory:

Sample directory:

FidFile: PHOSPHORUS

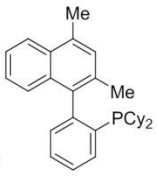

Pulse Sequence: PHOSPHORUS (s2pul)
Solvent: cdcl3
Data collected on: Jul 5 2019

Temp. 25.0 C / 298.1 K
Operator: Liu

Relax. delay 1.000 sec
Pulse 45.0 degrees
Acq. time 0.655 sec
Width 50000.0 Hz
7 repetitions
OBSERVE P31, 202.3535033 MHz
DECOUPLE H1, 499.8787746 MHz
Power 43 dB
on during acquisition
off during delay
WALTZ-16 modulated
DATA PROCESSING
Line broadening 0.5 Hz
FT size 65536
Total time 0 min 12 sec

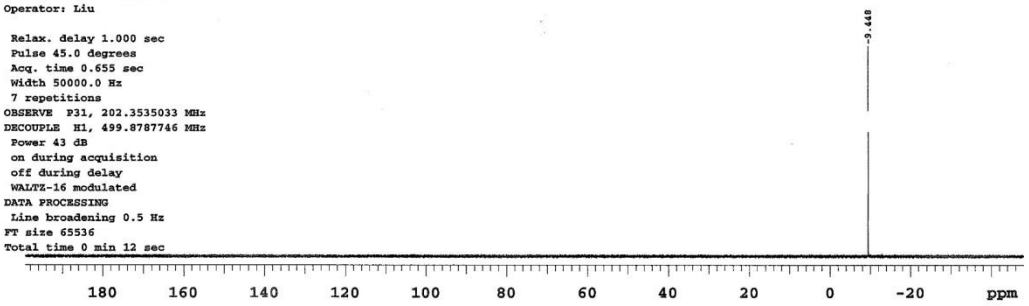

Sample Name:

Data Collected on:
nmr19-vnmrs600
Archive directory:

Sample directory:

FidFile: PROTON

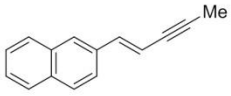

Pulse Sequence: PROTON (s2pul)
Solvent: cdcl3
Data collected on: Oct 19 2019

Temp. 25.0 C / 298.1 K
Operator: Liu

Relax. delay 10.000 sec
Pulse 45.0 degrees
Acq. time 1.704 sec
Width 9615.4 Hz
8 repetitions
OBSERVE H1, 599.6806832 MHz
DATA PROCESSING
FT size 32768
Total time 1 min 34 sec

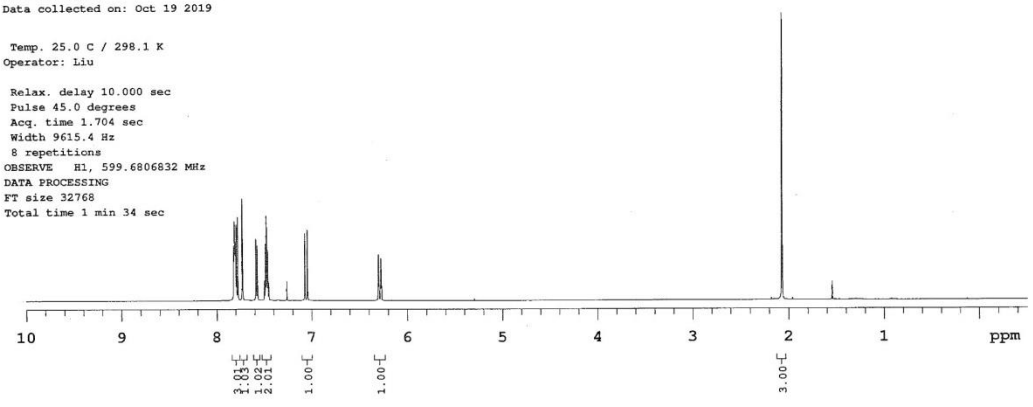

Sample Name:

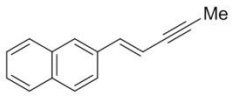

Data Collected on:
nmr19-vnmrs600
Archive directory:

Sample directory:

FidFile: CARBON

Pulse Sequence: CARBON (s2pul)
Solvent: cdcl3
Data collected on: Oct 19 2019

Temp. 25.0 C / 298.1 K
Operator: Liu

Relax. delay 1.000 sec
Pulse 45.0 degrees
Acq. time 0.865 sec
Width 37878.8 Hz
140 repetitions
OBSERVE C13, 150.7898143 MHz
DECOUPLE H1, 599.6836825 MHz
Power 46 dB
continuously on
WALTZ-16 modulated
DATA PROCESSING
Line broadening 0.5 Hz
FT size 65536
Total time 31 min

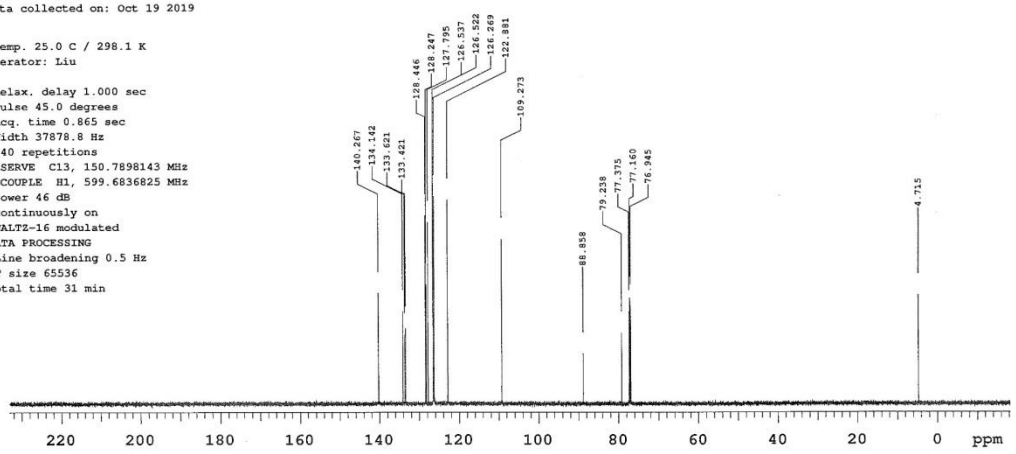

Agilent Technologies

Sample Name:

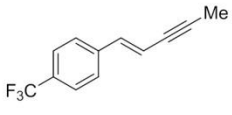

Data Collected on:
nmr18-vnmrs500
Archive directory:

Sample directory:

FidFile: PROTON

Pulse Sequence: PROTON (s2pul)
Solvent: cdcl3
Data collected on: Oct 21 2019

Temp. 25.0 C / 298.1 K
Operator: Liu

Relax. delay 10.000 sec
Pulse 45.0 degrees
Acq. time 2.045 sec
Width 8012.8 Hz
6 repetitions
OBSERVE H1, 499.8762807 MHz
DATA PROCESSING
FT size 32768
Total time 1 min 36 sec

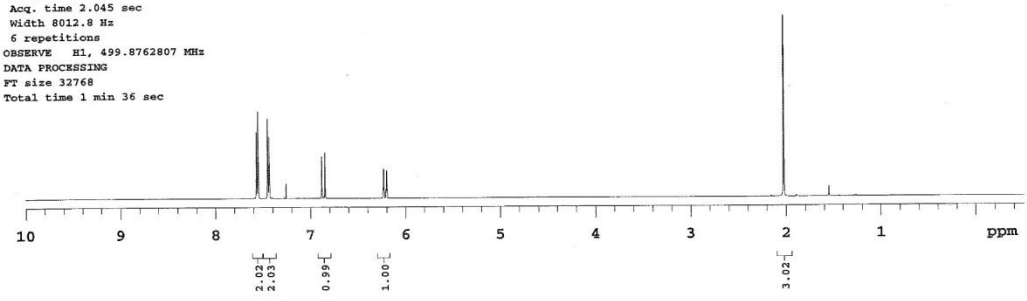

Agilent Technologies

Sample Name:

Data Collected on:
nmr18-vnmrs500
Archive directory:

Sample directory:

FidFile: CARBON

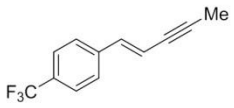

Pulse Sequence: CARBON (s2pul)
Solvent: cdcl3
Data collected on: Oct 21 2019

Temp. 25.0 C / 298.1 K
Operator: Liu

Relax. delay 1.000 sec
Pulse 45.0 degrees
Acq. time 1.049 sec
Width 31250.0 Hz
300 repetitions
OBSERVE C13, 125.6939696 MHz
DECOUPLE H1, 499.8787746 MHz
Power 45 dB
continuously on
WALTZ-16 modulated
DATA PROCESSING
Line broadening 0.5 Hz
FT size 65536
Total time 34 min

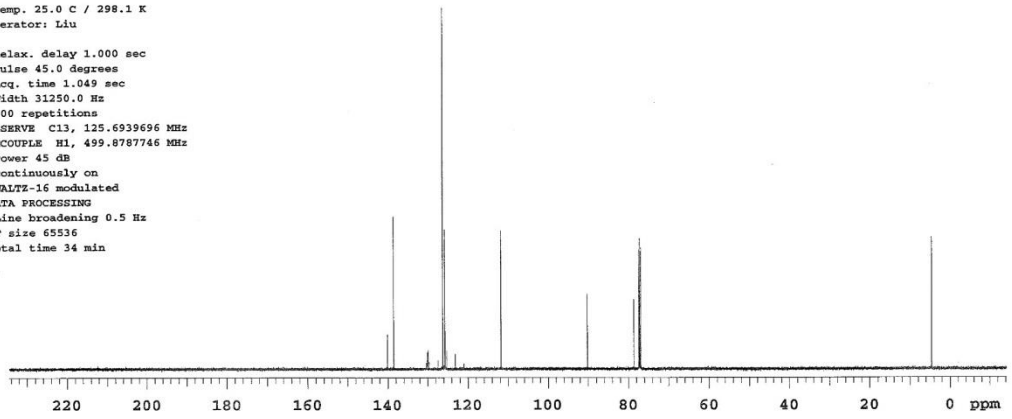

STANDARD FLUORINE PARAMETERS

Agilent Technologies

Sample Name:

Data Collected on:
nmr18-vnmrs500
Archive directory:

Sample directory:

FidFile: FLUORINE

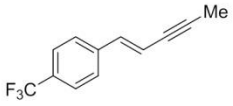

Pulse Sequence: FLUORINE (s2pul)
Solvent: cdcl3
Data collected on: Oct 21 2019

Temp. 25.0 C / 298.1 K
Operator: Liu

Relax. delay 1.000 sec
Pulse 30.0 degrees
Acq. time 0.603 sec
Width 108.7 kHz
10 repetitions
OBSERVE F19, 470.3536374 MHz
DATA PROCESSING
FT size 131072
Total time 0 min 16 sec

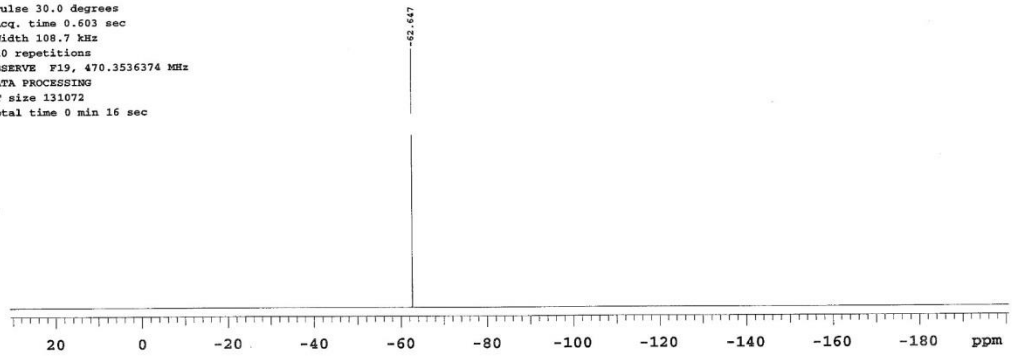

Sample Name:

Data Collected on:
nmr19-vnmrs600
Archive directory:

Sample directory:

FidFile: PROTON

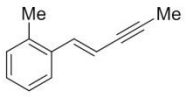

Pulse Sequence: PROTON (s2pul)
Solvent: cdcl3
Data collected on: Jan 2 2020

Temp. 25.0 C / 298.1 K
Operator: Liu

Relax. delay 10.000 sec
Pulse 45.0 degrees
Acq. time 1.704 sec
Width 9615.4 Hz
4 repetitions
OBSERVE H1, 599.6806832 MHz
DATA PROCESSING
FT size 32768
Total time 0 min 47 sec

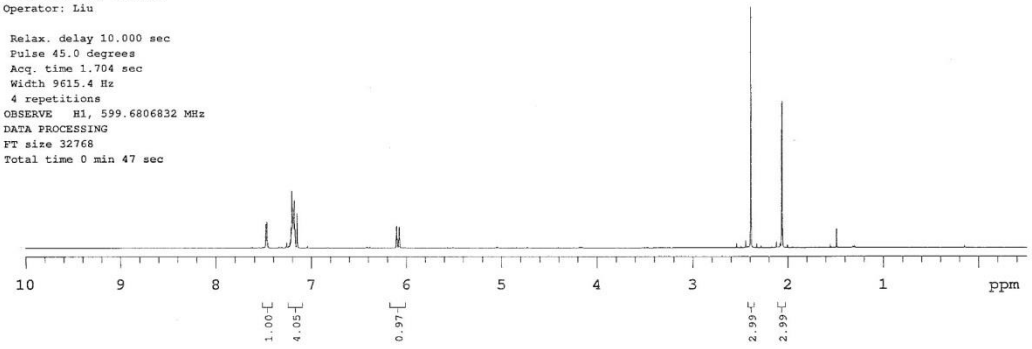

Sample Name:

Data Collected on:
nmr19-vnmrs600
Archive directory:

Sample directory:

FidFile: CARBON

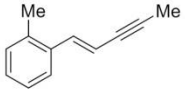

Pulse Sequence: CARBON (s2pul)
Solvent: cdcl3
Data collected on: Jan 2 2020

Temp. 25.0 C / 298.1 K
Operator: Liu

Relax. delay 1.000 sec
Pulse 45.0 degrees
Acq. time 0.865 sec
Width 37878.8 Hz
16 repetitions
OBSERVE C13, 150.7898189 MHz
DECOUPLE H1, 599.6836825 MHz
Power 45 dB
continuously on
WALTZ-16 modulated
DATA PROCESSING
Line broadening 0.5 Hz
FT size 65536
Total time 3 min 7 sec

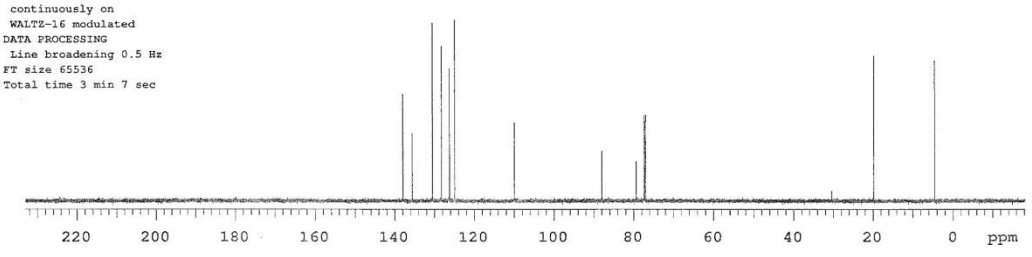

Agilent Technologies

Sample Name:

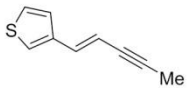

Data Collected on:
nmr18-vnmrs500
Archive directory:

Sample directory:

FidFile: PROTON

Pulse Sequence: PROTON (s2pul)
Solvent: cdcl3
Data collected on: Oct 23 2019

Temp. 25.0 C / 298.1 K
Operator: Liu

Relax. delay 10.000 sec
Pulse 45.0 degrees
Acq. time 2.045 sec
Width 8012.8 Hz
4 repetitions
OBSERVE H1, 499.8762802 MHz
DATA PROCESSING
FT size 32768
Total time 0 min 48 sec

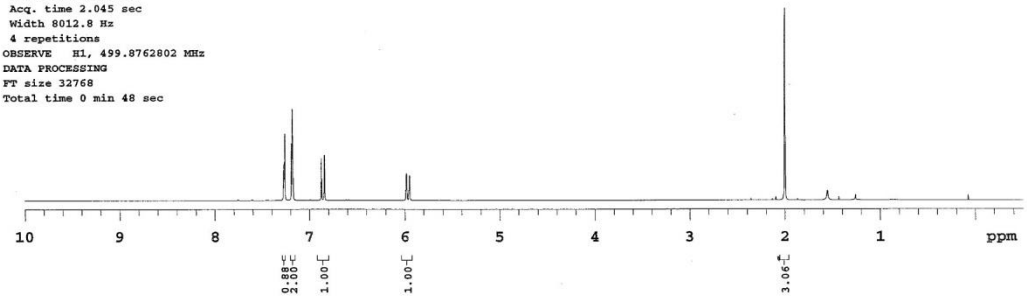

Agilent Technologies

Sample Name:

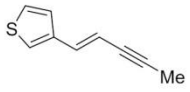

Data Collected on:
nmr18-vnmrs500
Archive directory:

Sample directory:

FidFile: CARBON

Pulse Sequence: CARBON (s2pul)
Solvent: cdcl3
Data collected on: Oct 23 2019

Temp. 25.0 C / 298.1 K
Operator: Liu

Relax. delay 1.000 sec
Pulse 45.0 degrees
Acq. time 1.049 sec
Width 31250.0 Hz
202 repetitions
OBSERVE C13, 125.6939715 MHz
DECOUPLE H1, 499.8787746 MHz
Power 45 dB
continuously on
WALTZ-16 modulated
DATA PROCESSING
Line broadening 0.5 Hz
FT size 65536
Total time 34 min

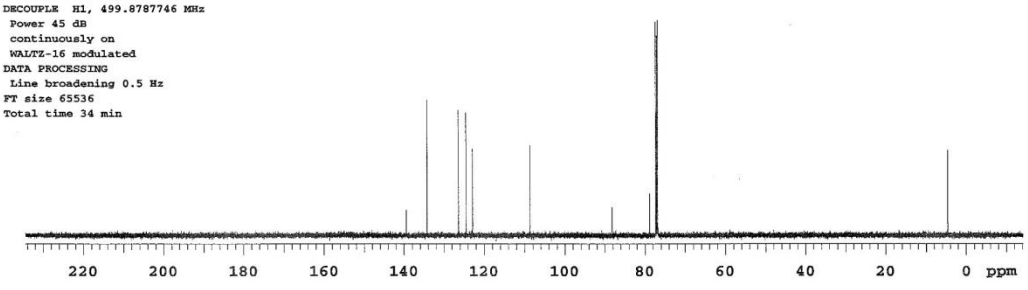

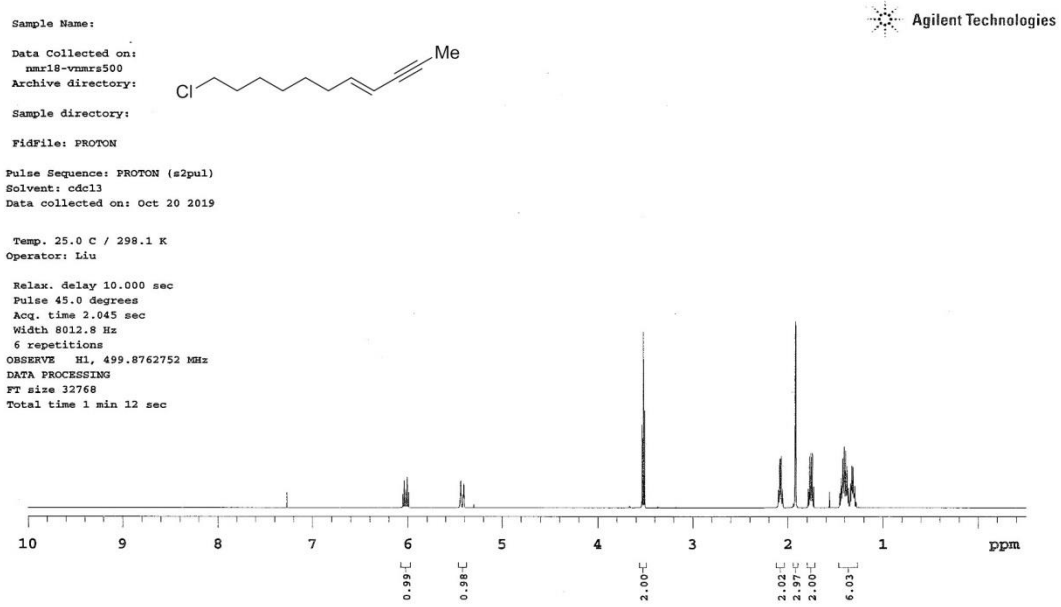
Agilent Technologies
Sample Name:
Data Collected on:
nmr18-vnmrs500
Archive directory:
Sample directory:
FidFile: PROTON
Me
Cl
Pulse Sequence: PROTON (s2pul)
Solvent: cdcl3
Data collected on: Oct 20 2019
Temp. 25.0 C / 298.1 K
Operator: Liu
Relax. delay 10.000 sec
Pulse 45.0 degrees
Acq. time 2.045 sec
Width 8012.8 Hz
6 repetitions
OBSERVE H1, 499.8762752 MHz
DATA PROCESSING
FT size 32768
Total time 1 min 12 sec
10
9
8
7
6
5
4
3
2
1
ppm
0.99
0.98
2.00
2.02
2.97
2.00
6.03

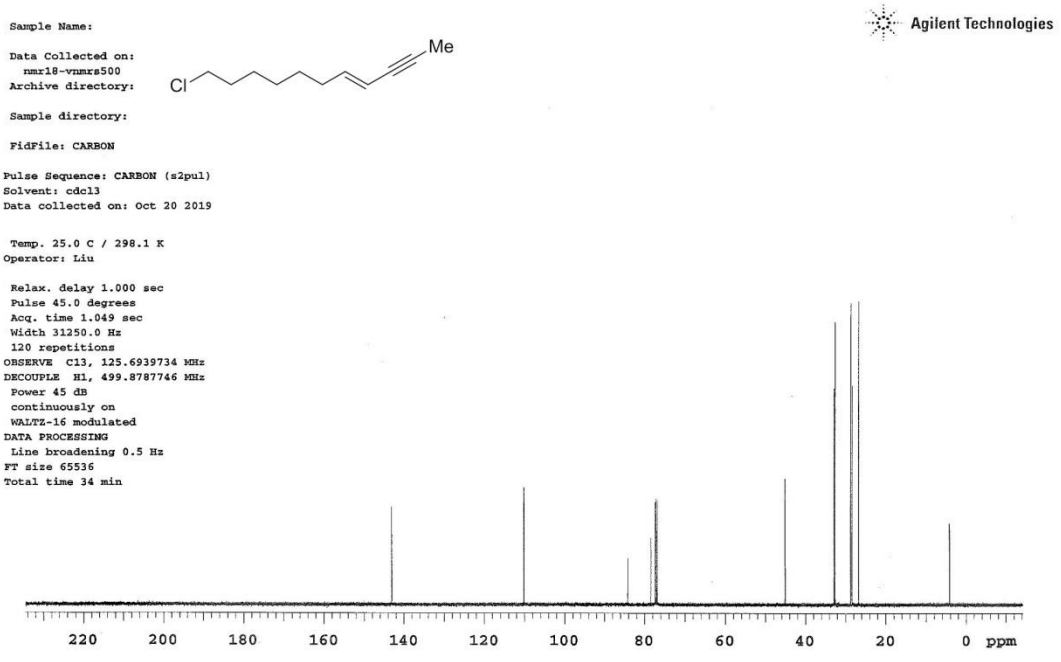
Agilent Technologies
Sample Name:
Data Collected on:
nmr18-vnmrs500
Archive directory:
Sample directory:
FidFile: CARBON
Me
Cl
Pulse Sequence: CARBON (s2pul)
Solvent: cdcl3
Data collected on: Oct 20 2019
Temp. 25.0 C / 298.1 K
Operator: Liu
Relax. delay 1.000 sec
Pulse 45.0 degrees
Acq. time 1.049 sec
Width 31250.0 Hz
120 repetitions
OBSERVE C13, 125.6939734 MHz
DECOUPLE H1, 499.8787746 MHz
Power 45 dB
continuously on
WALTZ-16 modulated
DATA PROCESSING
Line broadening 0.5 Hz
FT size 65536
Total time 34 min
220
200
180
160
140
120
100
80
60
40
20
0 ppm

Agilent Technologies

Sample Name:

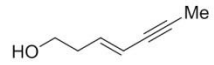

Data Collected on:
nmr18-vnmrs500
Archive directory:

Sample directory:

FidFile: PROTON

Pulse Sequence: PROTON (s2pul)
Solvent: cdcl3
Data collected on: Oct 24 2019

Temp. 25.0 C / 298.1 K
Operator: Liu

Relax. delay 10.000 sec
Pulse 45.0 degrees
Acq. time 2.045 sec
Width 8012.8 Hz
8 repetitions
OBSERVE H1, 499.8762802 MHz
DATA PROCESSING
FT size 32768
Total time 1 min 36 sec

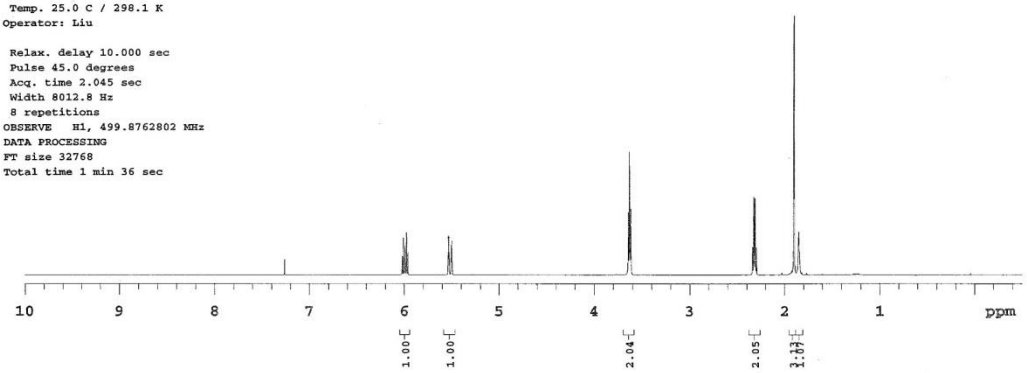

Agilent Technologies

Sample Name:

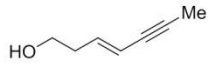

Data Collected on:
nmr18-vnmrs500
Archive directory:

Sample directory:

FidFile: CARBON

Pulse Sequence: CARBON (s2pul)
Solvent: cdcl3
Data collected on: Oct 24 2019

Temp. 25.0 C / 298.1 K
Operator: Liu

Relax. delay 1.000 sec
Pulse 45.0 degrees
Acq. time 1.049 sec
Width 31250.0 Hz
124 repetitions
OBSERVE C13, 125.6939753 MHz
DECOUPLE H1, 499.8787746 MHz
Power 45 dB
continuously on
WALTZ-16 modulated
DATA PROCESSING
Line broadening 0.5 Hz
FT size 65536
Total time 34 min

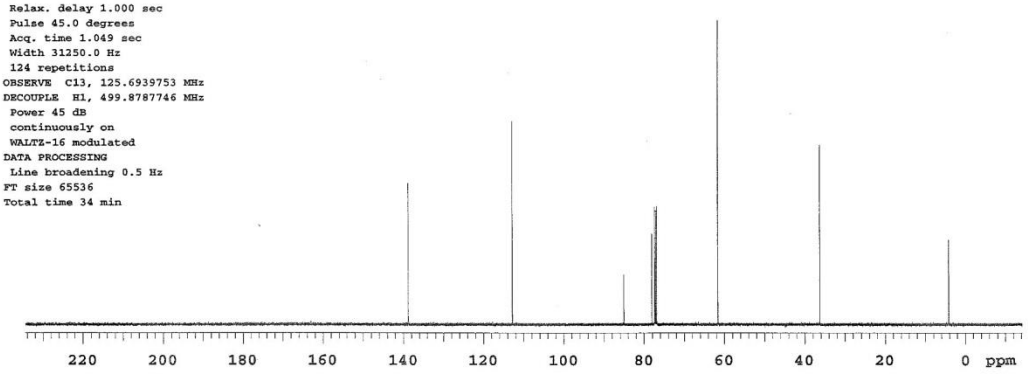

Sample Name:

Data Collected on:
nmr19-vnmrs600
Archive directory:

Sample directory:

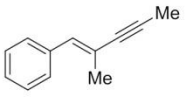

FidFile: PROTON

Pulse Sequence: PROTON (s2pul)
Solvent: cdcl3
Data collected on: Nov 7 2019

Temp. 25.0 C / 298.1 K
Operator: Liu

Relax. delay 10.000 sec
Pulse 45.0 degrees
Acq. time 1.704 sec
Width 9615.4 Hz
4 repetitions
OBSERVE H1, 599.6806910 MHz
DATA PROCESSING
FT size 32768
Total time 0 min 47 sec

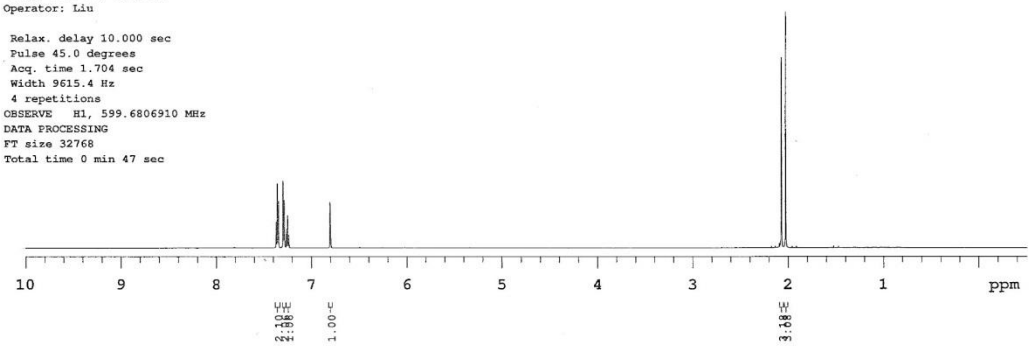

Sample Name:

Data Collected on:
nmr19-vnmrs600
Archive directory:

Sample directory:

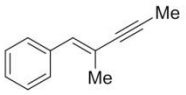

FidFile: CARBON

Pulse Sequence: CARBON (s2pul)
Solvent: d2o
Data collected on: Nov 7 2019

Temp. 25.0 C / 298.1 K
Operator: Liu

Relax. delay 1.000 sec
Pulse 45.0 degrees
Acq. time 0.865 sec
Width 37878.8 Hz
26 repetitions
OBSERVE C13, 150.7898204 MHz
DECOUPLE H1, 599.6852237 MHz
Power 46 dB
continuously on
WALTZ-16 modulated
DATA PROCESSING
Line broadening 0.5 Hz
FT size 65536
Total time 0 min 56 sec

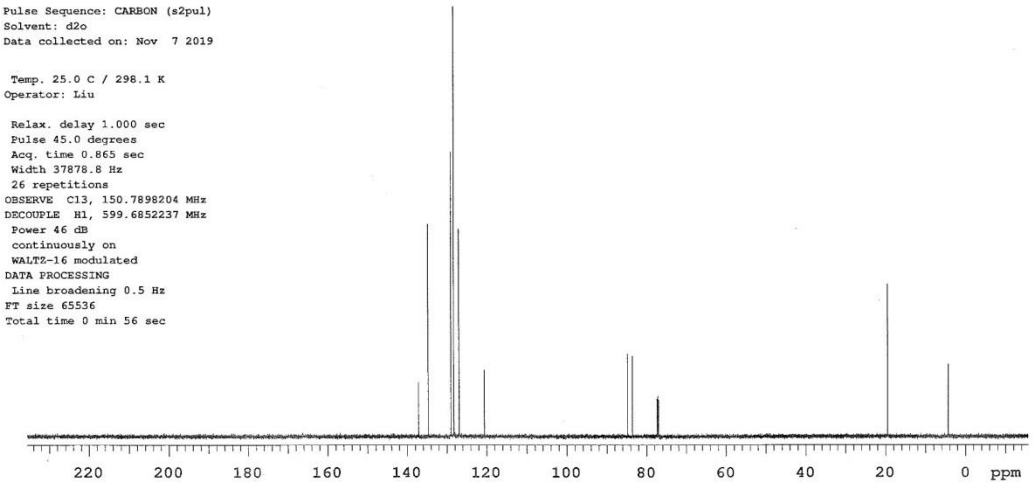

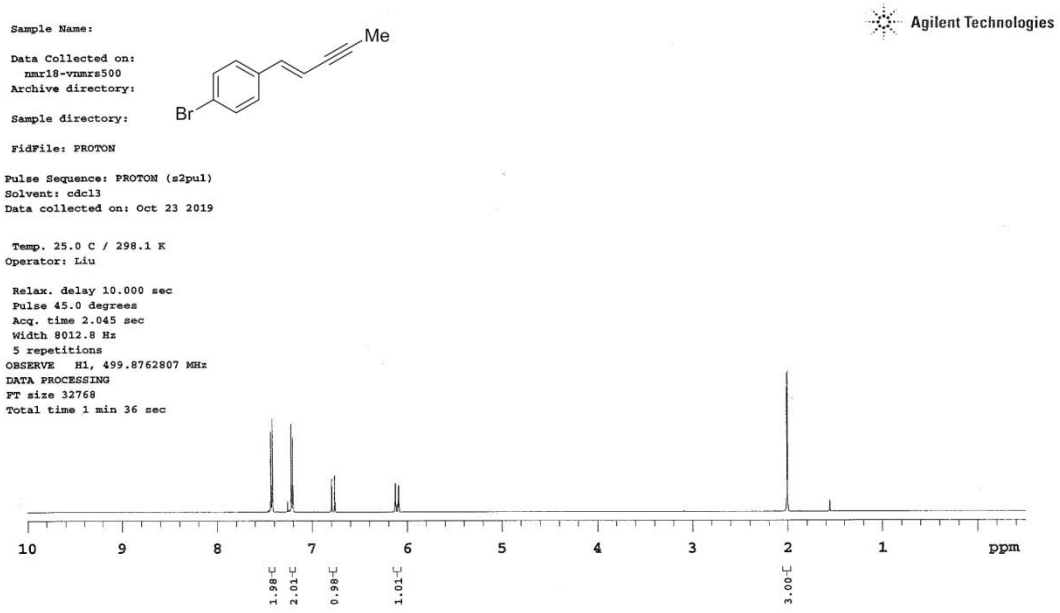
Agilent Technologies
Sample Name:
Data Collected on:
nmr18-vnmrs500
Archive directory:
Sample directory:
FidFile: PROTON
Me
Br
Pulse Sequence: PROTON (s2pul)
Solvent: cdcl3
Data collected on: Oct 23 2019
Temp. 25.0 C / 298.1 K
Operator: Liu
Relax. delay 10.000 sec
Pulse 45.0 degrees
Acq. time 2.045 sec
Width 8012.8 Hz
5 repetitions
OBSERVE H1, 499.8762807 MHz
DATA PROCESSING
FT size 32768
Total time 1 min 36 sec
10
9
8
7
6
5
4
3
2
1
ppm
1.98
2.01
0.98
1.01
3.00

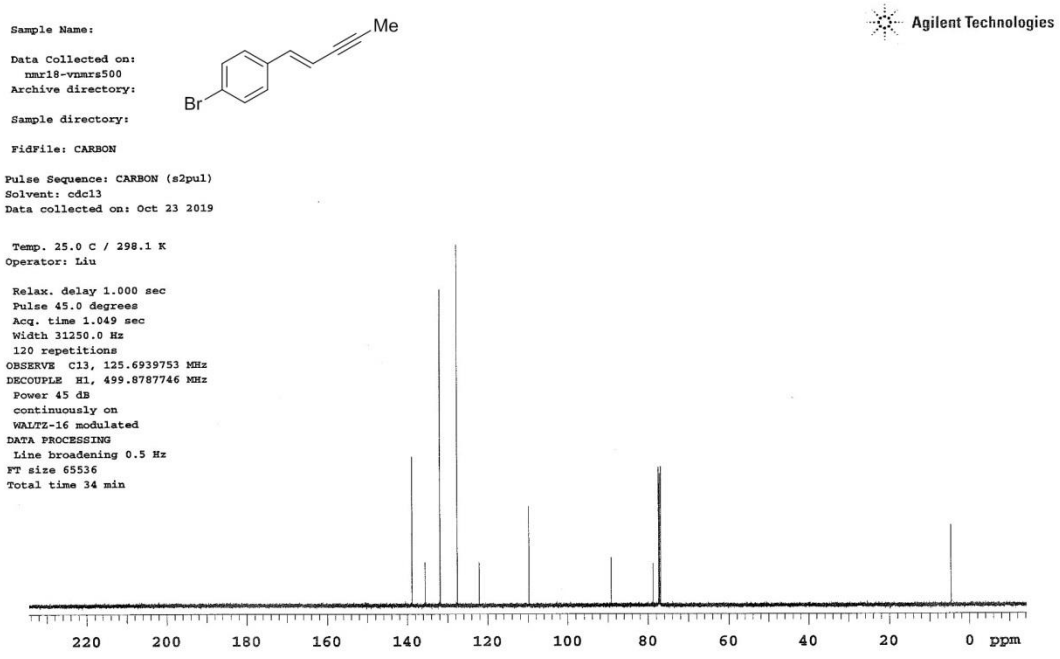
Agilent Technologies
Sample Name:
Data Collected on:
nmr18-vnmrs500
Archive directory:
Sample directory:
FidFile: CARBON
Me
Br
Pulse Sequence: CARBON (s2pul)
Solvent: cdcl3
Data collected on: Oct 23 2019
Temp. 25.0 C / 298.1 K
Operator: Liu
Relax. delay 1.000 sec
Pulse 45.0 degrees
Acq. time 1.049 sec
Width 31250.0 Hz
120 repetitions
OBSERVE C13, 125.6939753 MHz
DECOUPLE H1, 499.8787746 MHz
Power 45 dB
continuously on
WALTZ-16 modulated
DATA PROCESSING
Line broadening 0.5 Hz
FT size 65536
Total time 34 min
220
200
180
160
140
120
100
80
60
40
20
0 ppm

2-furan

Sample Name:

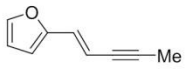

Data Collected on:
nmr18-vnmrs500
Archive directory:

Sample directory:

FidFile: PROTON

Pulse Sequence: PROTON (s2pul)
Solvent: cdcl3
Data collected on: Jun 26 2019

Temp. 25.0 C / 298.1 K
Operator: Liu

Relax. delay 10.000 sec
Pulse 45.0 degrees
Acq. time 2.045 sec
Width 8012.8 Hz
6 repetitions
OBSERVE H1, 499.8762752 MHz
DATA PROCESSING
FT size 32768
Total time 8 min 2 sec

Agilent Technologies

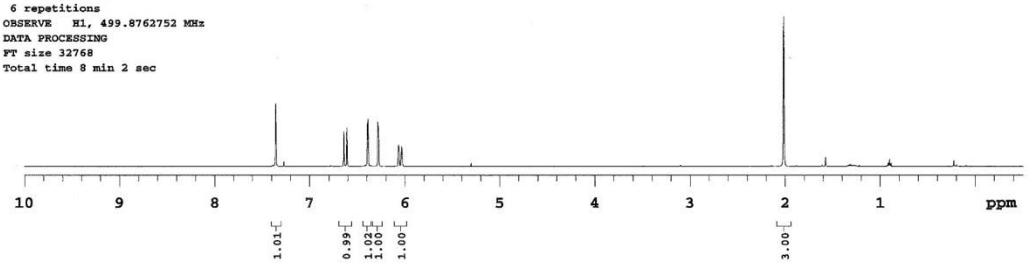

2-furan

Sample Name:

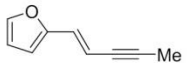

Data Collected on:
nmr18-vnmrs500
Archive directory:

Sample directory:

FidFile: CARBON

Pulse Sequence: CARBON (s2pul)
Solvent: cdcl3
Data collected on: Jun 26 2019

Temp. 25.0 C / 298.1 K
Operator: Liu

Relax. delay 1.000 sec
Pulse 45.0 degrees
Acq. time 1.049 sec
Width 31250.0 Hz
40 repetitions
OBSERVE C13, 125.6939753 MHz
DECOUPLE H1, 499.8787746 MHz
Power 43 dB
continuously on
WALTZ-16 modulated
DATA PROCESSING
Line broadening 0.5 Hz
FT size 65536
Total time 5 hr, 41 min

Agilent Technologies

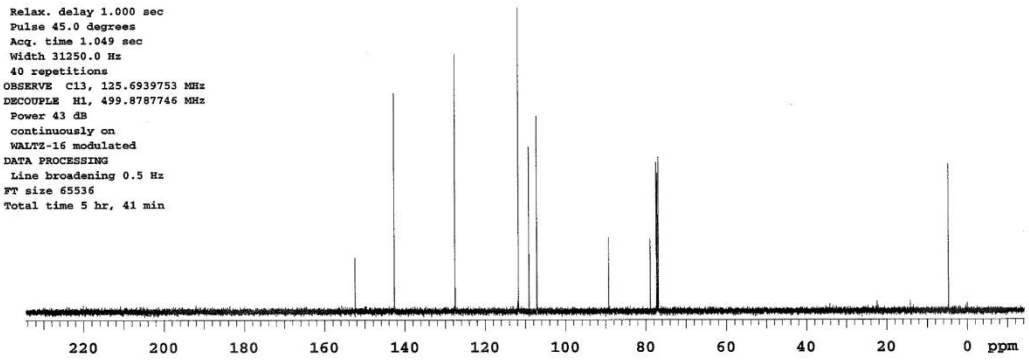

Sample Name:

Data Collected on:
nmr19-vnmrs600
Archive directory:

Sample directory:

FidFile: PROTON

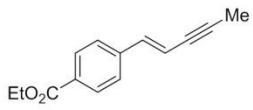

Pulse Sequence: PROTON (s2pul)
Solvent: cdcl3
Data collected on: Oct 22 2019

Temp. 25.0 C / 298.1 K
Operator: Liu

Relax. delay 10.000 sec
Pulse 45.0 degrees
Acq. time 1.704 sec
Width 9615.4 Hz
2 repetitions
OBSERVE H1, 599.6806841 MHz
DATA PROCESSING
FT size 32768
Total time 0 min 59 sec

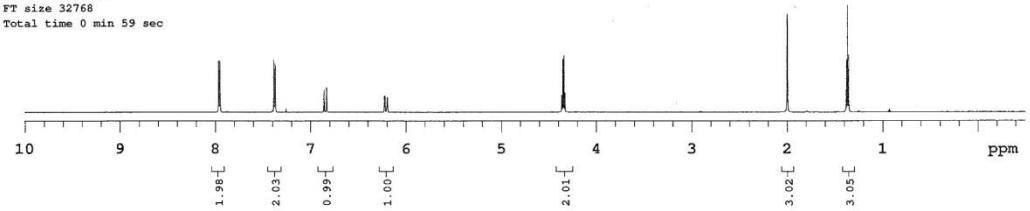

Sample Name:

Data Collected on:
nmr19-vnmrs600
Archive directory:

Sample directory:

FidFile: CARBON

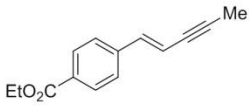

Pulse Sequence: CARBON (s2pul)
Solvent: cdcl3
Data collected on: Oct 22 2019

Temp. 25.0 C / 298.1 K
Operator: Liu

Relax. delay 1.000 sec
Pulse 45.0 degrees
Acq. time 0.865 sec
Width 37878.8 Hz
40 repetitions
OBSERVE C13, 150.7898154 MHz
DECOUPLE H1, 599.6836825 MHz
Power 46 dB
continuously on
WALTZ-16 modulated
DATA PROCESSING
Line broadening 0.5 Hz
FT size 65536
Total time 31 min

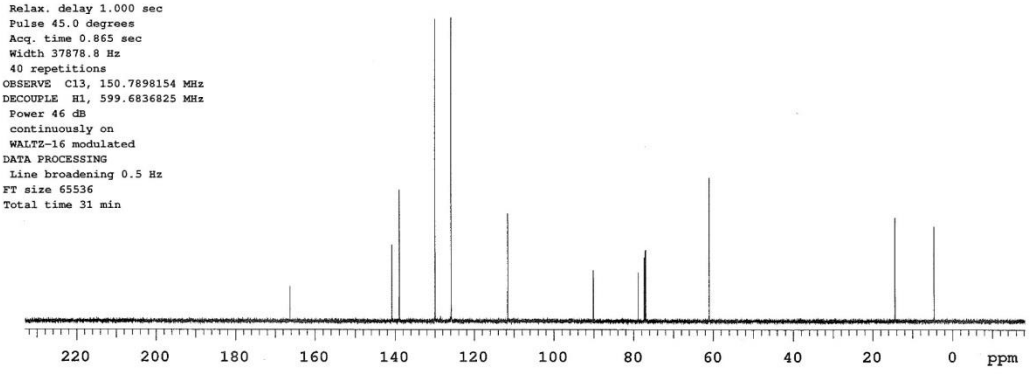

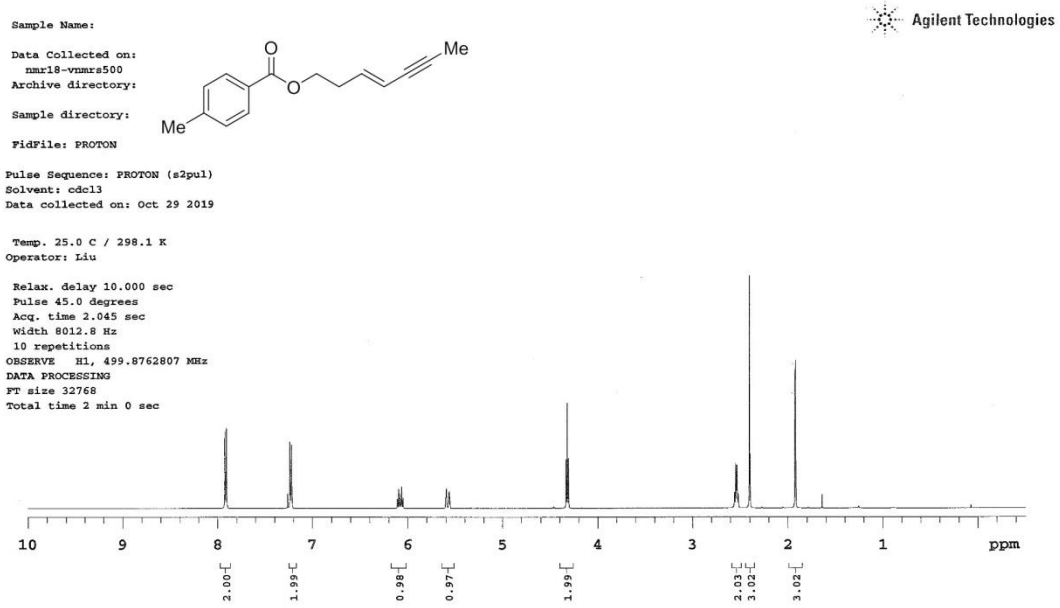
Agilent Technologies
Sample Name:
Data Collected on:
nmr18-vnmrs500
Archive directory:
Sample directory:
FidFile: PROTON
Me
O
O
Me
Pulse Sequence: PROTON (s2pul)
Solvent: cdcl3
Data collected on: Oct 29 2019
Temp. 25.0 C / 298.1 K
Operator: Liu
Relax. delay 10.000 sec
Pulse 45.0 degrees
Acq. time 2.045 sec
Width 8012.8 Hz
10 repetitions
OBSERVE H1, 499.8762807 MHz
DATA PROCESSING
FT size 32768
Total time 2 min 0 sec
10 9 8 7 6 5 4 3 2 1 ppm
2.00 1.99 0.98 0.97 1.99 2.03 3.02 3.02

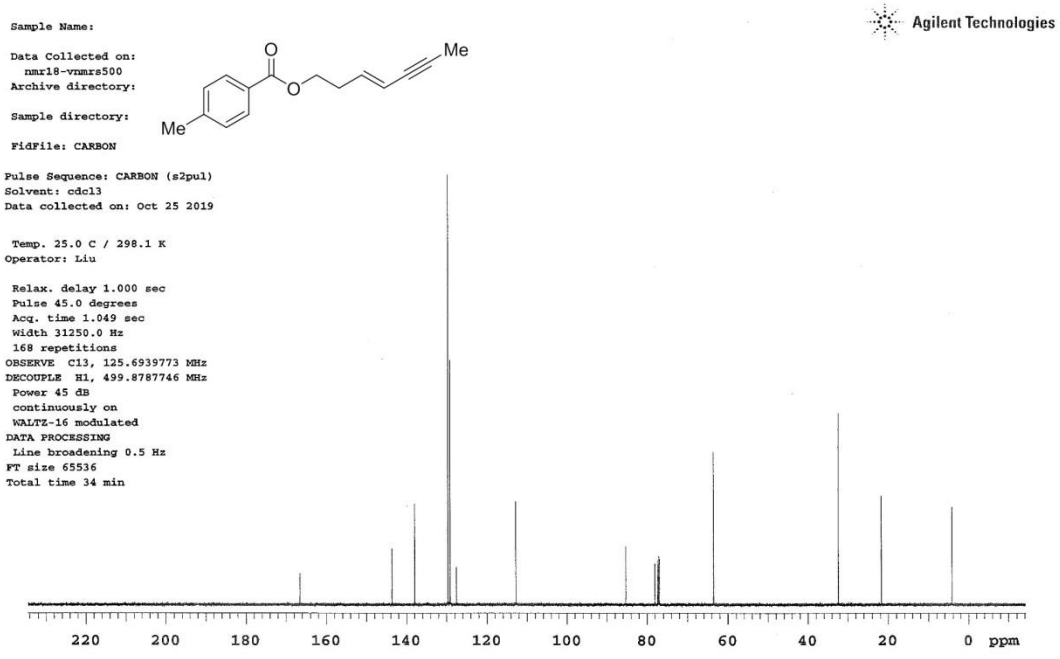
Agilent Technologies
Sample Name:
Data Collected on:
nmr18-vnmrs500
Archive directory:
Sample directory:
FidFile: CARBON
Me
O
O
Me
Pulse Sequence: CARBON (s2pul)
Solvent: cdcl3
Data collected on: Oct 25 2019
Temp. 25.0 C / 298.1 K
Operator: Liu
Relax. delay 1.000 sec
Pulse 45.0 degrees
Acq. time 1.049 sec
Width 31250.0 Hz
168 repetitions
OBSERVE C13, 125.6939773 MHz
DECOUPLE H1, 499.8787746 MHz
Power 45 dB
continuously on
WALTZ-16 modulated
DATA PROCESSING
Line broadening 0.5 Hz
FT size 65536
Total time 34 min
220 200 180 160 140 120 100 80 60 40 20 0 ppm

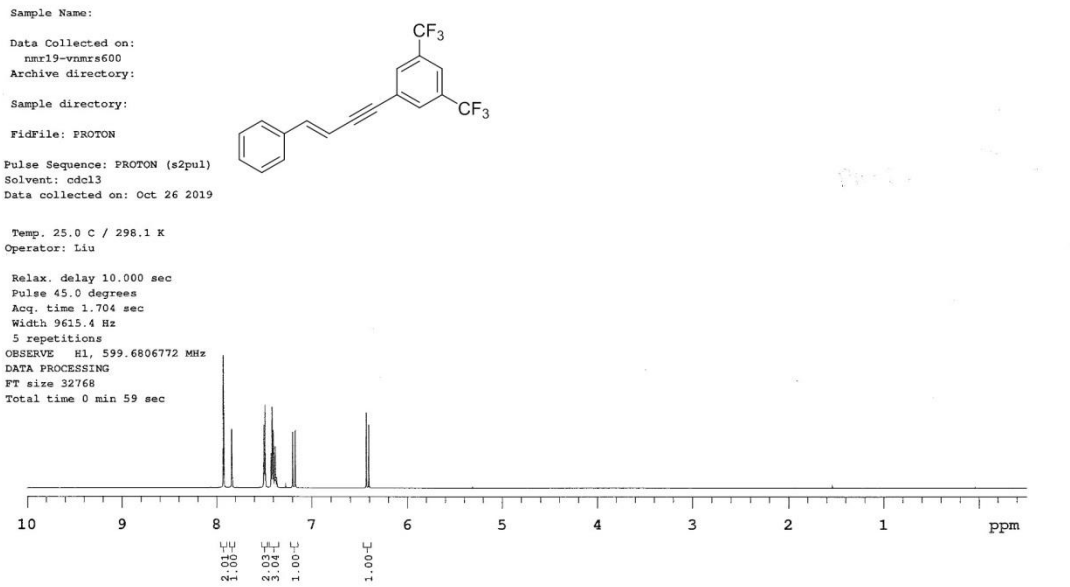
Sample Name:
Data Collected on:
nmr19-vnmrs600
Archive directory:
Sample directory:
FidFile: PROTON
Pulse Sequence: PROTON (s2pul)
Solvent: cdcl3
Data collected on: Oct 26 2019
Temp. 25.0 C / 298.1 K
Operator: Liu
Relax. delay 10.000 sec
Pulse 45.0 degrees
Acq. time 1.704 sec
Width 9615.4 Hz
5 repetitions
OBSERVE H1, 599.6806772 MHz
DATA PROCESSING
FT size 32768
Total time 0 min 59 sec
CF3
CF3
10
9
8
7
6
5
4
3
2
1
ppm
2.01
1.00
2.03
3.04
1.00
1.00

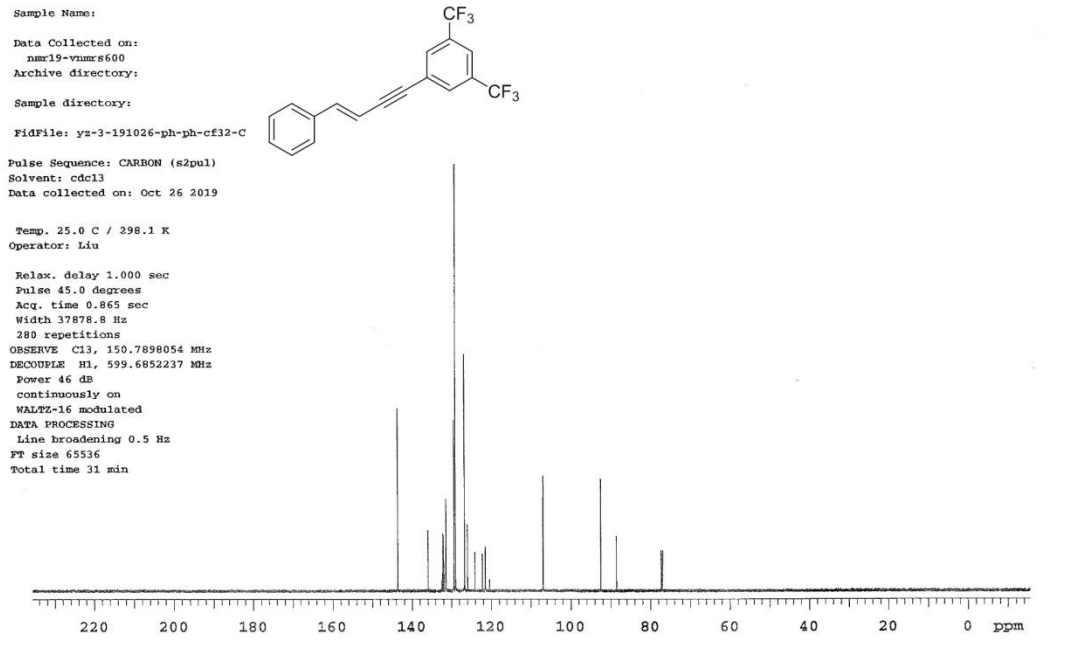
Sample Name:
Data Collected on:
nmr19-vnmrs600
Archive directory:
Sample directory:
FidFile: yz-3-191026-ph-ph-cf32-C
Pulse Sequence: CARBON (s2pul)
Solvent: cdcl3
Data collected on: Oct 26 2019
Temp. 25.0 C / 298.1 K
Operator: Liu
Relax. delay 1.000 sec
Pulse 45.0 degrees
Acq. time 0.865 sec
Width 37878.8 Hz
280 repetitions
OBSERVE C13, 150.7898054 MHz
DECOUPLE H1, 599.6852237 MHz
Power 46 dB
continuously on
WALTZ-16 modulated
DATA PROCESSING
Line broadening 0.5 Hz
FT size 65536
Total time 31 min
CF3
CF3
220
200
180
160
140
120
100
80
60
40
20
0
ppm

STANDARD FLUORINE PARAMETERS

Sample Name:

Data Collected on:
nmr19-vnmrs600
Archive directory:

Sample directory:

FidFile: yz-3-191026-ph-ph-cf32-F

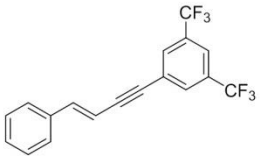

Pulse Sequence: FLUORINE (s2pul)
Solvent: cdcl3
Data collected on: Oct 26 2019

Temp. 25.0 C / 298.1 K
Operator: Liu

Relax. delay 1.000 sec
Pulse 30.0 degrees
Acq. time 0.996 sec
Width 131.6 kHz
10 repetitions
OBSERVE F19, 564.2650590 MHz
DATA PROCESSING
FT size 262144
Total time 0 min 20 sec

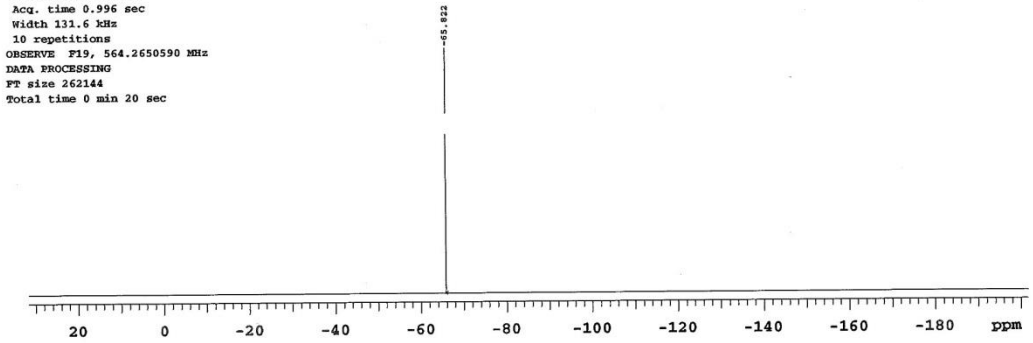

Agilent Technologies

Sample Name:

Data Collected on:
nmr18-vnmrs500
Archive directory:

Sample directory:

FidFile: PROTON

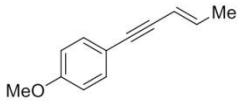

Pulse Sequence: PROTON (s2pul)
Solvent: cdcl3
Data collected on: Sep 28 2019

Temp. 25.0 C / 298.1 K
Operator: Liu

Relax. delay 10.000 sec
Pulse 45.0 degrees
Acq. time 2.045 sec
Width 8012.8 Hz
6 repetitions
OBSERVE H1, 499.8762807 MHz
DATA PROCESSING
FT size 32768
Total time 1 min 12 sec

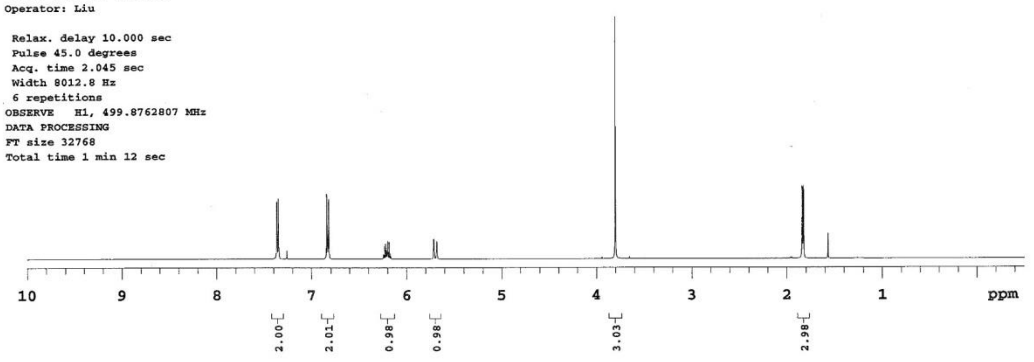

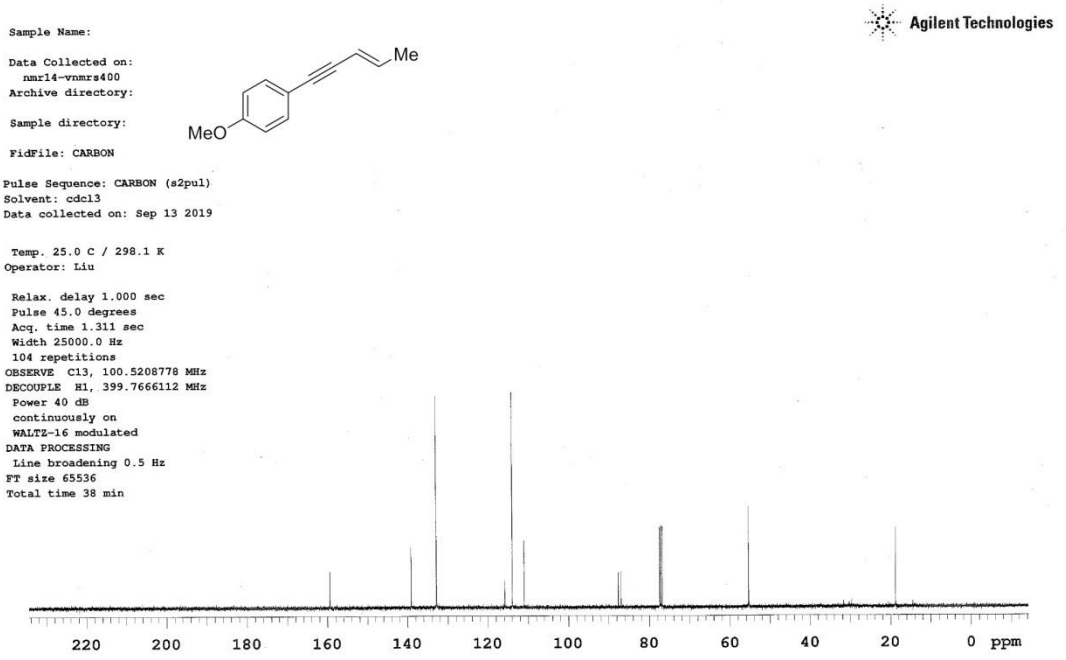
Agilent Technologies
Sample Name:
Data Collected on:
nmr14-vnmrs400
Archive directory:
Sample directory:
FidFile: CARBON
Me
MeO
Pulse Sequence: CARBON (s2pul)
Solvent: cdcl3
Data collected on: Sep 13 2019
Temp. 25.0 C / 298.1 K
Operator: Liu
Relax. delay 1.000 sec
Pulse 45.0 degrees
Acq. time 1.311 sec
Width 25000.0 Hz
104 repetitions
OBSERVE C13, 100.5208778 MHz
DECOUPLE H1, 399.7666112 MHz
Power 40 dB
continuously on
WALTZ-16 modulated
DATA PROCESSING
Line broadening 0.5 Hz
FT size 65536
Total time 38 min
220
200
180
160
140
120
100
80
60
40
20
0
ppm

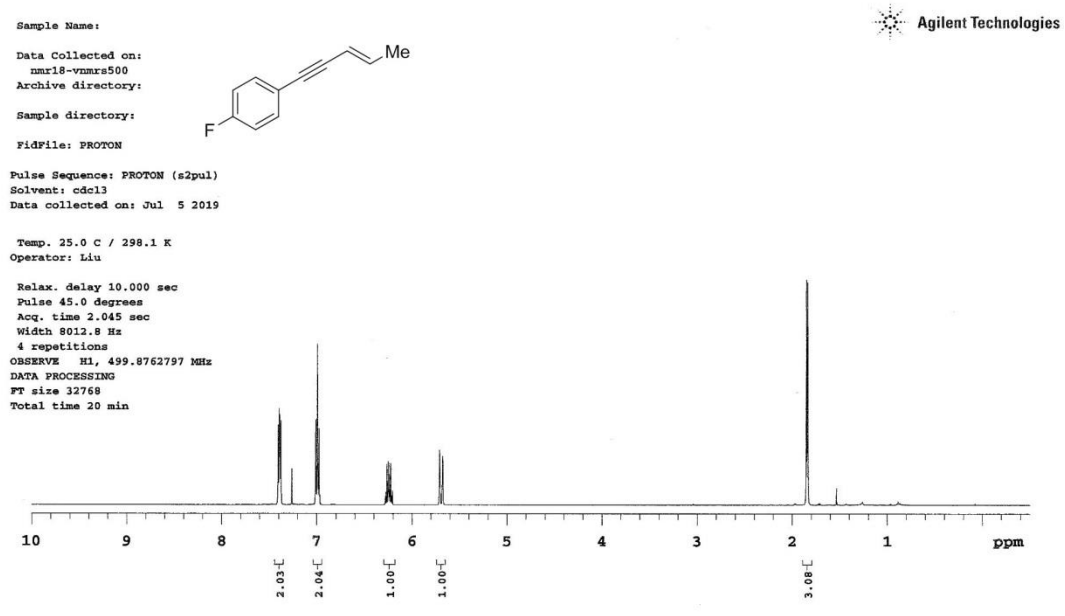
Agilent Technologies
Sample Name:
Data Collected on:
nmr18-vnmrs500
Archive directory:
Sample directory:
FidFile: PROTON
Me
F
Pulse Sequence: PROTON (s2pul)
Solvent: cdcl3
Data collected on: Jul 5 2019
Temp. 25.0 C / 298.1 K
Operator: Liu
Relax. delay 10.000 sec
Pulse 45.0 degrees
Acq. time 2.045 sec
Width 8012.8 Hz
4 repetitions
OBSERVE H1, 499.8762797 MHz
DATA PROCESSING
FT size 32768
Total time 20 min
10
9
8
7
6
5
4
3
2
1
ppm
2.03
2.04
1.00
1.00
3.08

Agilent Technologies

Sample Name:

Data Collected on:
nmr18-vnmrs500
Archive directory:

Sample directory:

FidFile: CARBON

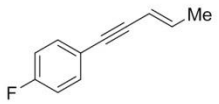

Pulse Sequence: CARBON (s2pul)
Solvent: cdcl3
Data collected on: Jul 5 2019

Temp. 25.0 C / 298.1 K
Operator: Liu

Relax. delay 1.000 sec
Pulse 45.0 degrees
Acq. time 1.049 sec
Width 31250.0 Hz
300 repetitions
OBSERVE C13, 125.6939696 MHz
DECOUPLE H1, 499.8787746 MHz
Power 43 dB
continuously on
WALTZ-16 modulated
DATA PROCESSING
Line broadening 0.5 Hz
FT size 65536
Total time 34 min

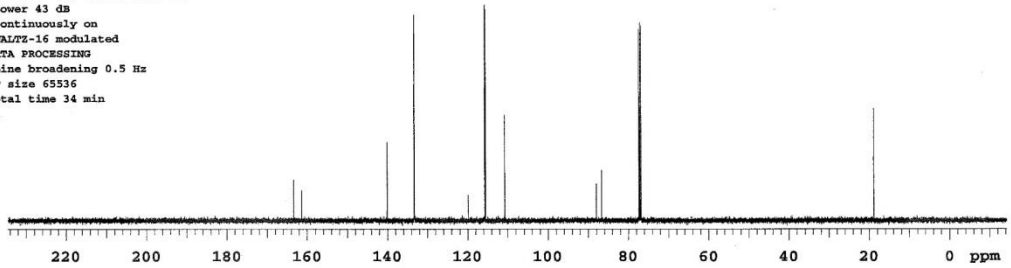

STANDARD FLUORINE PARAMETERS

Agilent Technologies

Sample Name:

Data Collected on:
nmr18-vnmrs500
Archive directory:

Sample directory:

FidFile: FLUORINE

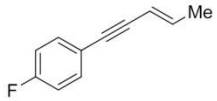

Pulse Sequence: FLUORINE (s2pul)
Solvent: cdcl3
Data collected on: Jul 5 2019

Temp. 25.0 C / 298.1 K
Operator: Liu

Relax. delay 1.000 sec
Pulse 30.0 degrees
Acq. time 0.603 sec
Width 108.7 kHz
24 repetitions
OBSERVE F19, 470.3536374 MHz
DATA PROCESSING
FT size 131072
Total time 2 min 40 sec

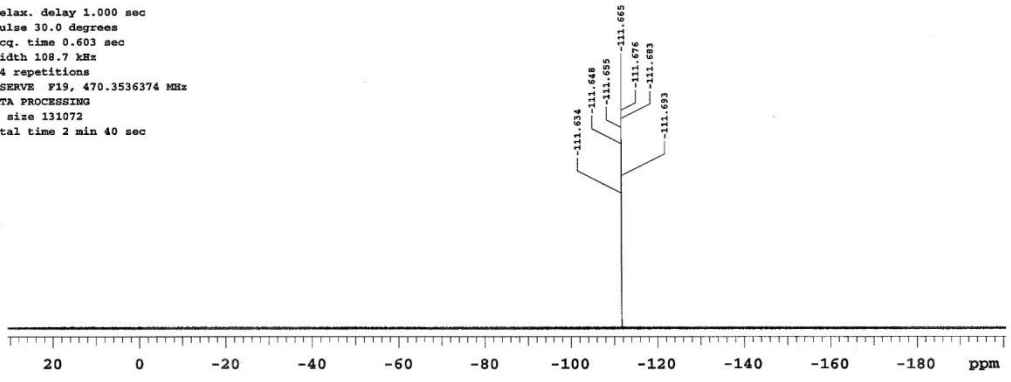

Agilent Technologies

Sample Name:

Data Collected on:
nmr18-vnmrs500
Archive directory:

Sample directory:

FidFile: PROTON

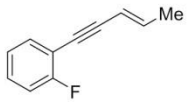

Pulse Sequence: PROTON (s2pul)
Solvent: cdcl3
Data collected on: Oct 21 2019

Temp. 25.0 C / 298.1 K
Operator: Liu

Relax. delay 10.000 sec
Pulse 45.0 degrees
Acq. time 2.045 sec
Width 8012.8 Hz
3 repetitions
OBSERVE H1, 499.8762782 MHz
DATA PROCESSING
FT size 32768
Total time 2 min 0 sec

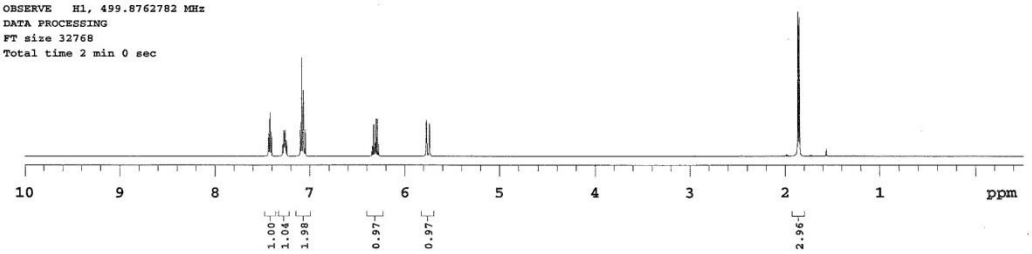

Agilent Technologies

Sample Name:

Data Collected on:
nmr18-vnmrs500
Archive directory:

Sample directory:

FidFile: CARBON

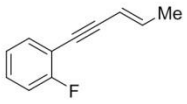

Pulse Sequence: CARBON (s2pul)
Solvent: cdcl3
Data collected on: Oct 21 2019

Temp. 25.0 C / 298.1 K
Operator: Liu

Relax. delay 1.000 sec
Pulse 45.0 degrees
Acq. time 1.049 sec
Width 31250.0 Hz
162 repetitions
OBSERVE C13, 125.6939753 MHz
DECOUPLE H1, 499.8787746 MHz
Power 45 dB
continuously on
WALTZ-16 modulated
DATA PROCESSING
Line broadening 0.5 Hz
FT size 65536
Total time 34 min

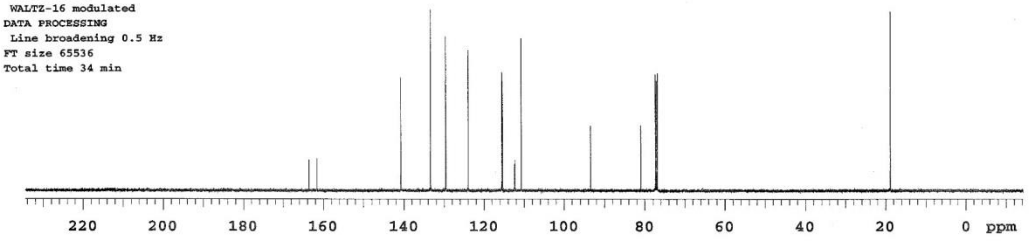

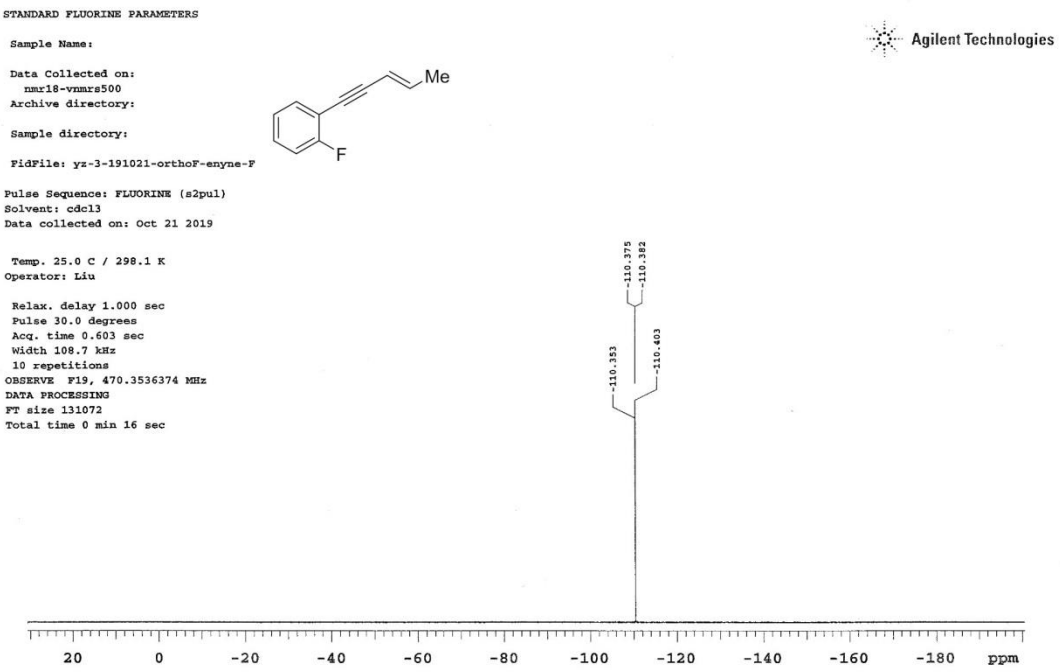
STANDARD FLUORINE PARAMETERS
Sample Name:
Data Collected on:
nmr18-vnmrs500
Archive directory:
Sample directory:
FidFile: yz-3-191021-orthoF-enyne-F
Pulse Sequence: FLUORINE (s2pul)
Solvent: cdcl3
Data collected on: Oct 21 2019
Temp. 25.0 C / 298.1 K
Operator: Liu
Relax. delay 1.000 sec
Pulse 30.0 degrees
Acq. time 0.603 sec
Width 108.7 kHz
10 repetitions
OBSERVE F19, 470.3536374 MHz
DATA PROCESSING
FT size 131072
Total time 0 min 16 sec
Agilent Technologies
Me
F
-110.375
-110.382
-110.353
-110.403
20
0
-20
-40
-60
-80
-100
-120
-140
-160
-180
ppm

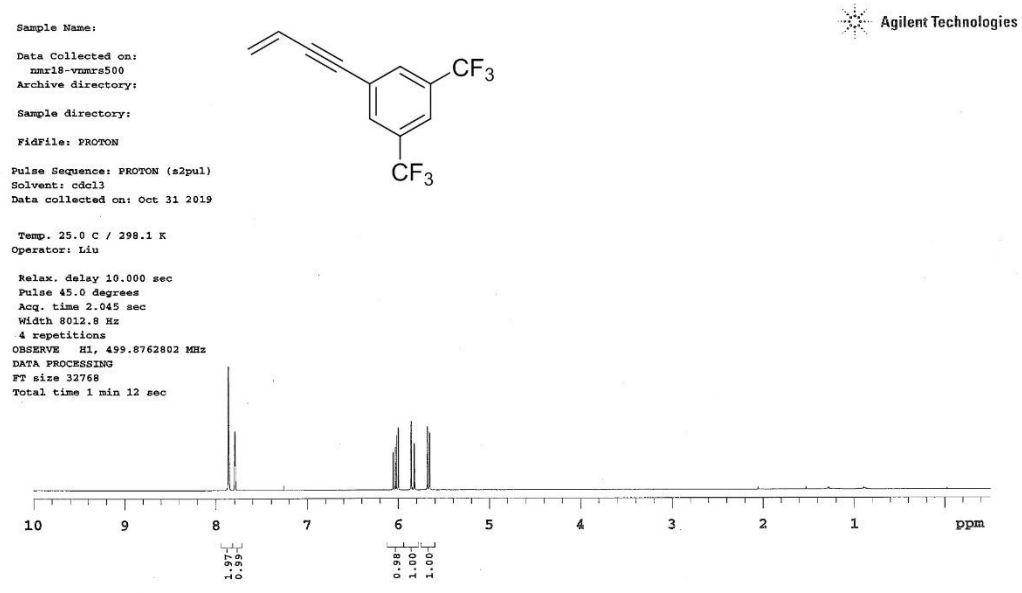
Sample Name:
Data Collected on:
nmr18-vnmrs500
Archive directory:
Sample directory:
FidFile: PROTON
Pulse Sequence: PROTON (s2pul)
Solvent: cdcl3
Data collected on: Oct 31 2019
Temp. 25.0 C / 298.1 K
Operator: Liu
Relax. delay 10.000 sec
Pulse 45.0 degrees
Acq. time 2.045 sec
Width 8012.8 Hz
4 repetitions
OBSERVE H1, 499.8762802 MHz
DATA PROCESSING
FT size 32768
Total time 1 min 12 sec
Agilent Technologies
CF3
CF3
10
9
8
7
6
5
4
3
2
1
ppm
1.97
0.99
0.98
1.00
1.00

Agilent Technologies

Sample Name:

Data Collected on:
nmr18-vnmrs500
Archive directory:

Sample directory:

FidFile: CARBON

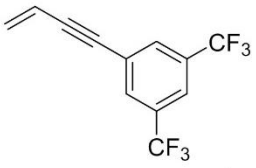

Pulse Sequence: CARBON (s2pul)
Solvent: cdcl3
Data collected on: Oct 31 2019

Temp. 25.0 C / 298.1 K
Operator: Liu

Relax. delay 1.000 sec
Pulse 45.0 degrees
Acq. time 1.049 sec
Width 31250.0 Hz
200 repetitions
OBSERVE C13, 125.6939545 MHz
DECOUPLE H1, 499.8787746 MHz
Power 45 dB
continuously on
WALTZ-16 modulated
DATA PROCESSING
Line broadening 0.5 Hz
FT size 65536
Total time 34 min

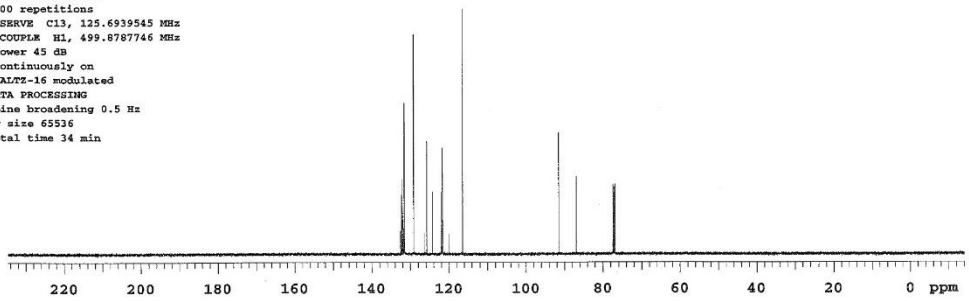

STANDARD FLUORINE PARAMETERS

Agilent Technologies

Sample Name:

Data Collected on:
nmr18-vnmrs500
Archive directory:

Sample directory:

FidFile: FLUORINE

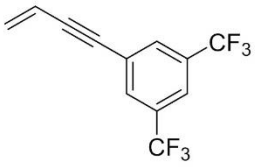

Pulse Sequence: FLUORINE (s2pul)
Solvent: cdcl3
Data collected on: Oct 31 2019

Temp. 25.0 C / 298.1 K
Operator: Liu

Relax. delay 1.000 sec
Pulse 30.0 degrees
Acq. time 0.603 sec
Width 108.7 kHz
10 repetitions
OBSERVE F19, 470.3536374 MHz
DATA PROCESSING
FT size 131072
Total time 0 min 16 sec

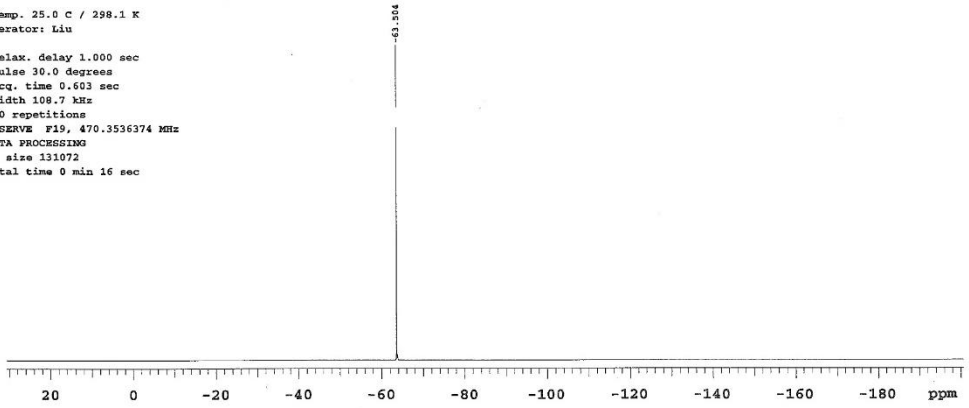

Agilent Technologies

Sample Name:

Data Collected on:
nmr18-vnmrs500
Archive directory:

Sample directory:

FidFile: PROTON

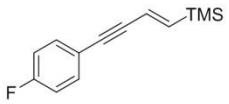

Pulse Sequence: PROTON (s2pul)
Solvent: cdcl3
Data collected on: Nov 1 2019

Temp. 25.0 C / 298.1 K
Operator: Liu

Relax. delay 10.000 sec
Pulse 45.0 degrees
Acq. time 2.045 sec
Width 8012.8 Hz
5 repetitions
OBSERVE H1, 499.8762807 MHz
DATA PROCESSING
FT size 32768
Total time 1 min 0 sec

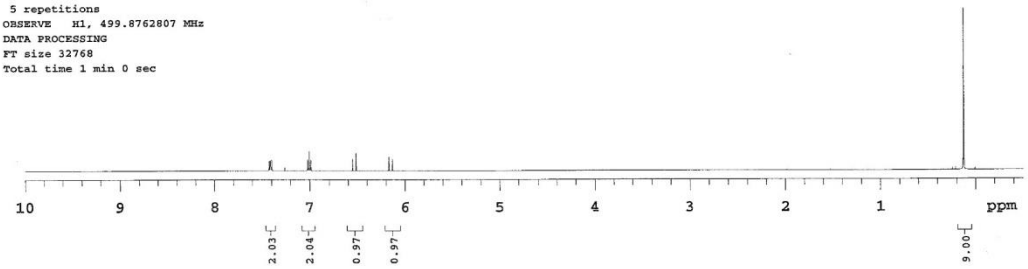

Agilent Technologies

Sample Name:

Data Collected on:
nmr18-vnmrs500
Archive directory:

Sample directory:

FidFile: CARBON

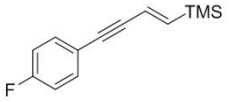

Pulse Sequence: CARBON (s2pul)
Solvent: cdcl3
Data collected on: Nov 1 2019

Temp. 25.0 C / 298.1 K
Operator: Liu

Relax. delay 1.000 sec
Pulse 45.0 degrees
Acq. time 1.049 sec
Width 31250.0 Hz
204 repetitions
OBSERVE C13, 125.6939697 MHz
DECOUPLE H1, 499.8787746 MHz
Power 45 dB
continuously on
WALTZ-16 modulated
DATA PROCESSING
Line broadening 0.5 Hz
FT size 65536
Total time 17 min

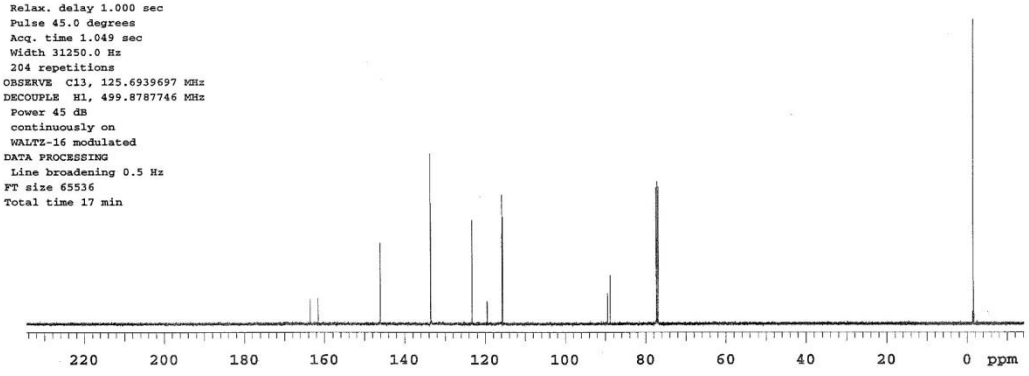

STANDARD FLUORINE PARAMETERS

Sample Name:

Data Collected on:
nmr18-vnmrs500
Archive directory:

Sample directory:

FidFile: FLUORINE

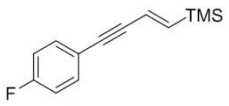

Agilent Technologies

Pulse Sequence: FLUORINE (s2pul)
Solvent: cd3cn
Data collected on: Nov 1 2019

Temp. 25.0 C / 298.1 K
Operator: Liu

Relax. delay 1.000 sec
Pulse 30.0 degrees
Acq. time 0.603 sec
Width 108.7 kHz
10 repetitions
OBSERVE F19, 470.3561256 MHz
DATA PROCESSING
FT size 131072
Total time 0 min 16 sec

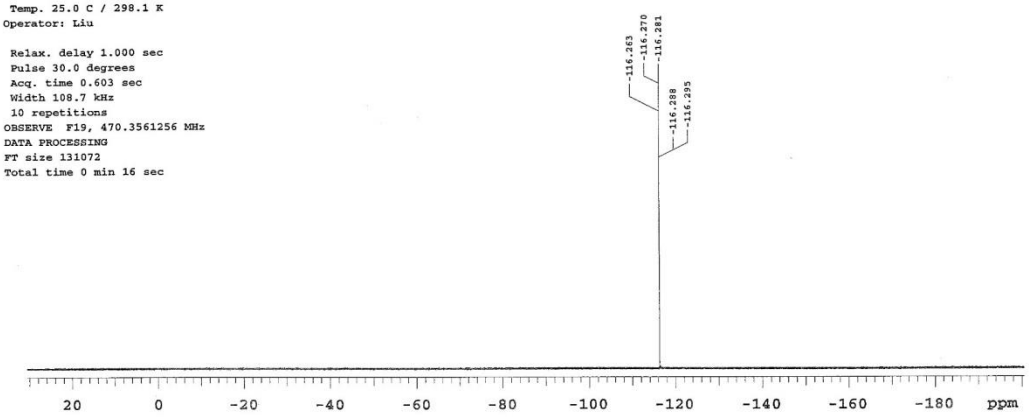

STANDARD PROTON PARAMETERS

Sample Name:

Data Collected on:
nmr18-vnmrs500
Archive directory:

Sample directory:

FidFile: PROTON

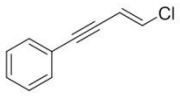

Agilent Technologies

Pulse Sequence: PROTON (s2pul)
Solvent: cdcl3
Data collected on: Mar 17 2020

Temp. 25.0 C / 298.1 K
Operator: Liu

Relax. delay 10.000 sec
Pulse 45.0 degrees
Acq. time 2.045 sec
Width 8012.8 Hz
6 repetitions
OBSERVE H1, 499.8760066 MHz
DATA PROCESSING
FT size 32768
Total time 1 min 12 sec

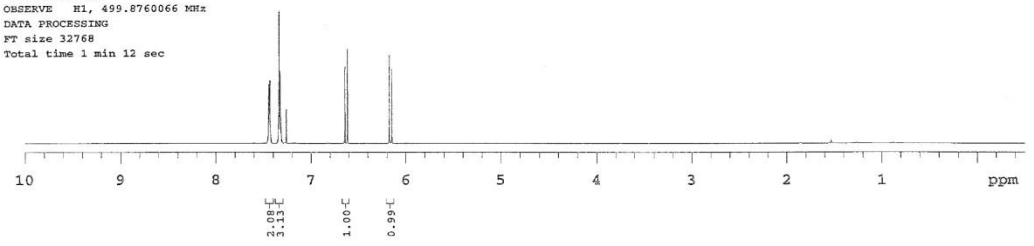

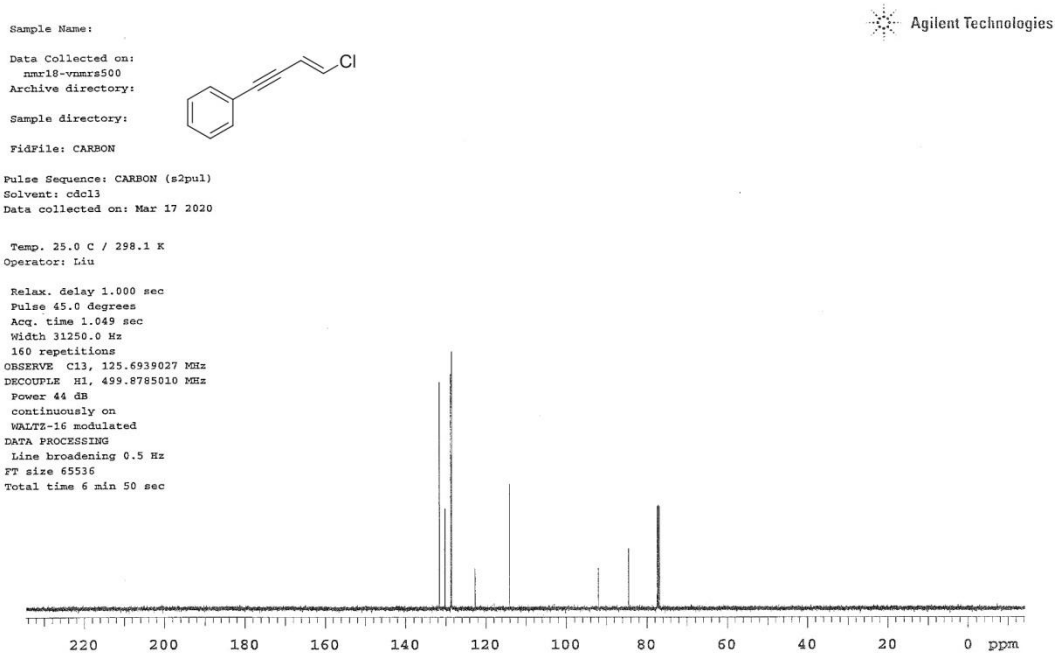
Agilent Technologies
Sample Name:
Data Collected on:
nmr18-vnmrs500
Archive directory:
Sample directory:
FidFile: CARBON
Cl
Pulse Sequence: CARBON (s2pul)
Solvent: cdcl3
Data collected on: Mar 17 2020
Temp. 25.0 C / 298.1 K
Operator: Liu
Relax. delay 1.000 sec
Pulse 45.0 degrees
Acq. time 1.049 sec
Width 31250.0 Hz
160 repetitions
OBSERVE C13, 125.6939027 MHz
DECOUPLE H1, 499.8785010 MHz
Power 44 dB
continuously on
WALTZ-16 modulated
DATA PROCESSING
Line broadening 0.5 Hz
FT size 65536
Total time 6 min 50 sec
220
200
180
160
140
120
100
80
60
40
20
0
ppm

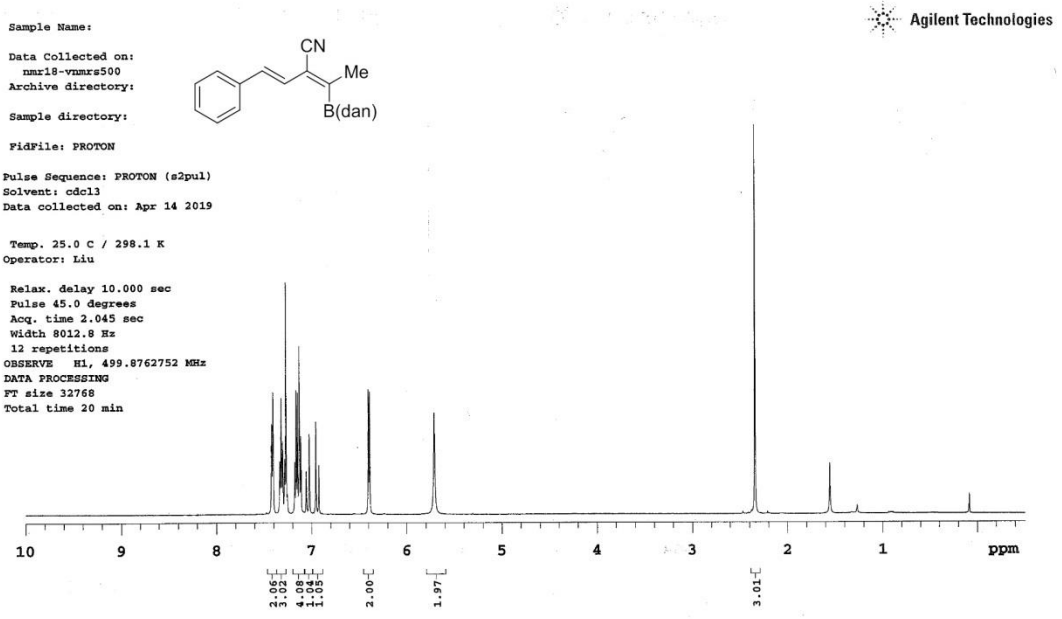
Agilent Technologies
Sample Name:
Data Collected on:
nmr18-vnmrs500
Archive directory:
Sample directory:
FidFile: PROTON
CN
Me
B(dan)
Pulse Sequence: PROTON (s2pul)
Solvent: cdcl3
Data collected on: Apr 14 2019
Temp. 25.0 C / 298.1 K
Operator: Liu
Relax. delay 10.000 sec
Pulse 45.0 degrees
Acq. time 2.045 sec
Width 8012.8 Hz
12 repetitions
OBSERVE H1, 499.8762752 MHz
DATA PROCESSING
FT size 32768
Total time 20 min
10
9
8
7
6
5
4
3
2
1
ppm
2.06
3.02
4.08
1.04
1.05
2.00
1.97
3.01

H

Sample Name:

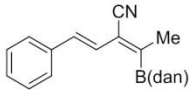

Data Collected on:
nmr14-vnmrs400
Archive directory:

Sample directory:

FidFile: yz-3-190417-H-C

Pulse Sequence: CARBON (s2pul)
Solvent: cdcl3
Data collected on: Apr 17 2019

Temp. 25.0 C / 298.1 K
Operator: Liu

Relax. delay 1.000 sec
Pulse 45.0 degrees
Acq. time 1.311 sec
Width 25000.0 Hz
16000 repetitions
OBSERVE C13, 100.5208755 MHz
DECOUPLE H1, 399.7666112 MHz
Power 40 dB
continuously on
WALTZ-16 modulated
DATA PROCESSING
Line broadening 0.5 Hz
FT size 65536
Total time 10 hr, 16 min

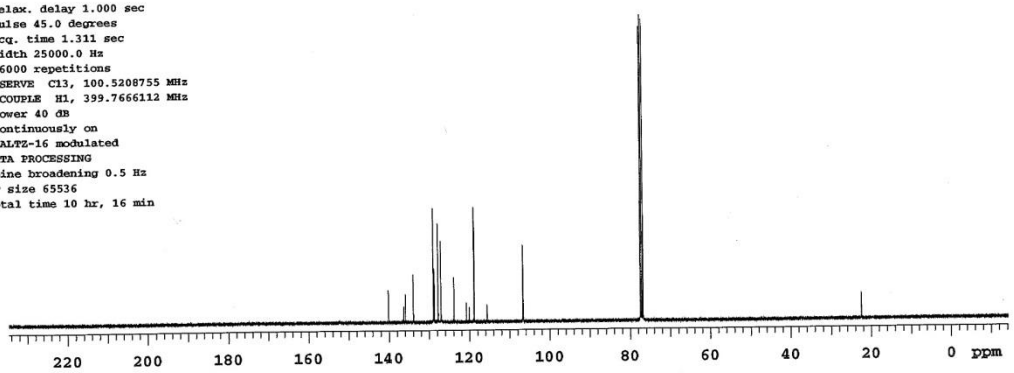

Agilent Technologies

Sample Name:

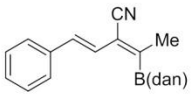

Data Collected on:
nmr11-inova500
Archive directory:

Sample directory:

FidFile: B11

Pulse Sequence: s2pul
Solvent: cdcl3
Data collected on: Apr 18 2019

Temp. 25.0 C / 298.1 K
Operator: Liu

Relax. delay 0.010 sec
Pulse 45.0 degrees
Acq. time 0.064 sec
Width 32064.1 Hz
2010 repetitions
OBSERVE B11, 160.3467851 MHz
DECOUPLE H1, 499.7745112 MHz
Power 44 dB
on during acquisition
off during delay
WALTZ-16 modulated
DATA PROCESSING
Line broadening 0.5 Hz
FT size 4096
Total time 13 min

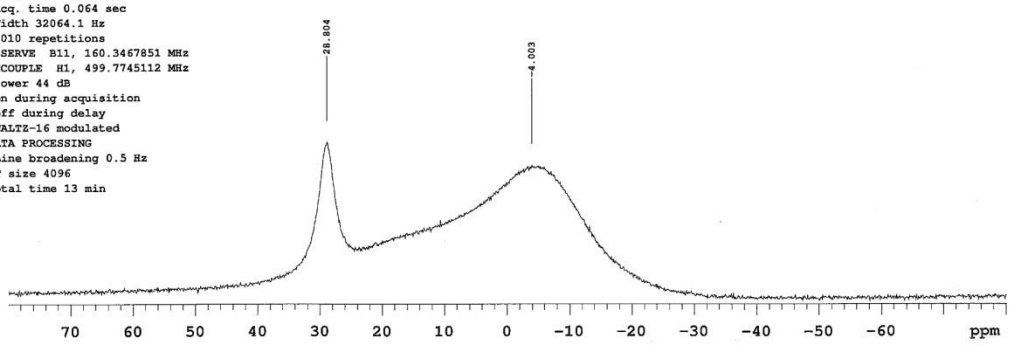

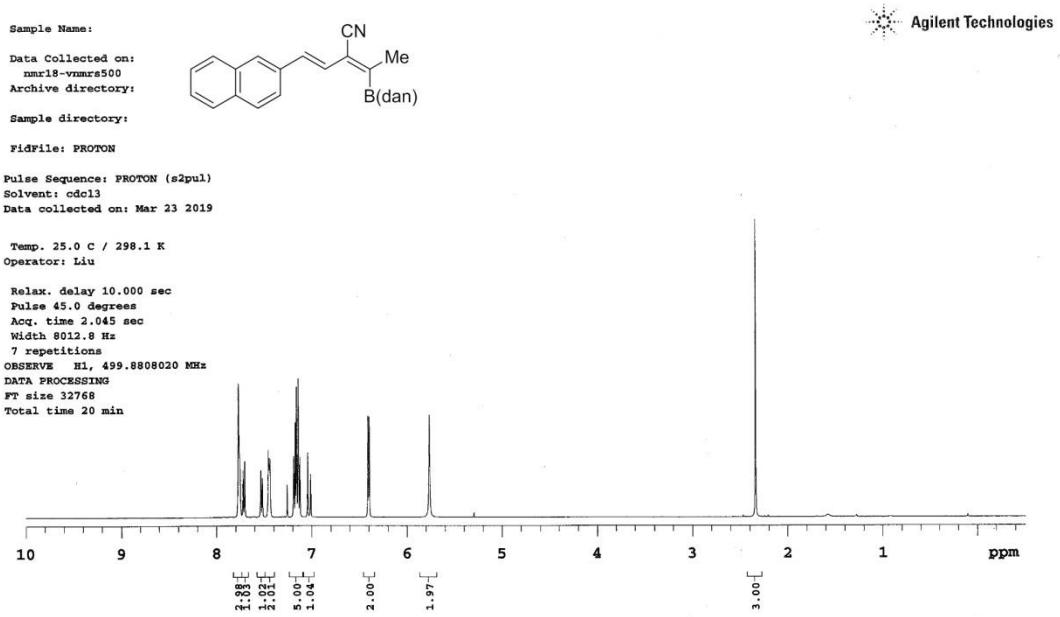
Agilent Technologies
Sample Name:
Data Collected on:
nmr18-vnmrs500
Archive directory:
Sample directory:
FidFile: PROTON
Pulse Sequence: PROTON (s2pul)
Solvent: cdcl3
Data collected on: Mar 23 2019
Temp. 25.0 C / 298.1 K
Operator: Liu
Relax. delay 10.000 sec
Pulse 45.0 degrees
Acq. time 2.045 sec
Width 8012.8 Hz
7 repetitions
OBSERVE H1, 499.8808020 MHz
DATA PROCESSING
FT size 32768
Total time 20 min
CN
Me
B(dan)
10
9
8
7
6
5
4
3
2
1
ppm
2.08
1.83
1.02
1.01
5.00
1.04
2.00
1.97
3.00

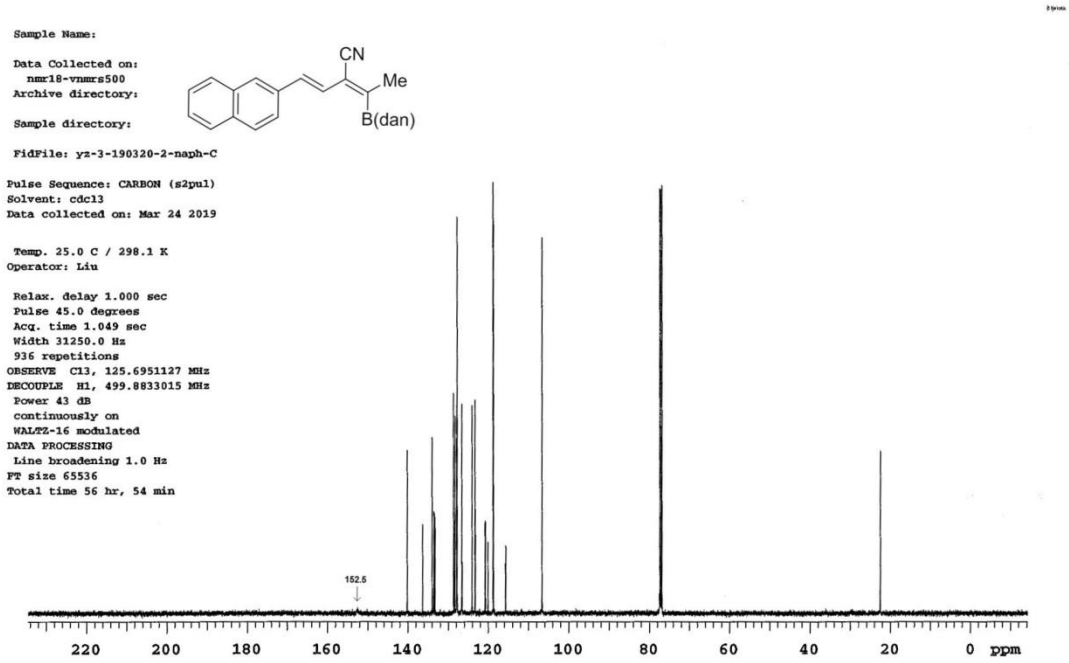
Sample Name:
Data Collected on:
nmr18-vnmrs500
Archive directory:
Sample directory:
FidFile: yz-3-190320-2-naph-C
Pulse Sequence: CARBON (s2pul)
Solvent: cdcl3
Data collected on: Mar 24 2019
Temp. 25.0 C / 298.1 K
Operator: Liu
Relax. delay 1.000 sec
Pulse 45.0 degrees
Acq. time 1.049 sec
Width 31250.0 Hz
936 repetitions
OBSERVE C13, 125.6951127 MHz
DECOUPLE H1, 499.8833015 MHz
Power 43 dB
continuously on
WALTZ-16 modulated
DATA PROCESSING
Line broadening 1.0 Hz
FT size 65536
Total time 56 hr, 54 min
CN
Me
B(dan)
152.5
220
200
180
160
140
120
100
80
60
40
20
0
ppm

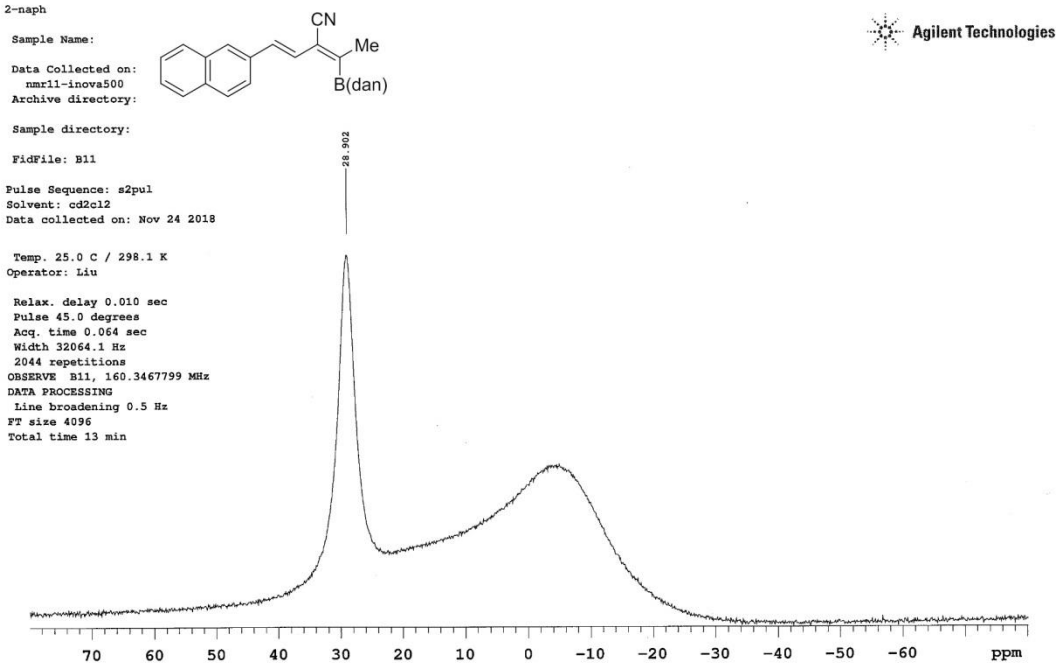
2-naph
Sample Name:
Data Collected on:
nmr11-inova500
Archive directory:
Sample directory:
FidFile: B11
Pulse Sequence: s2pul
Solvent: cd2cl2
Data collected on: Nov 24 2018
Temp. 25.0 C / 298.1 K
Operator: Liu
Relax. delay 0.010 sec
Pulse 45.0 degrees
Acq. time 0.064 sec
Width 32064.1 Hz
2044 repetitions
OBSERVE B11, 160.3467799 MHz
DATA PROCESSING
Line broadening 0.5 Hz
FT size 4096
Total time 13 min
CN
Me
B(dan)
28.902
70 60 50 40 30 20 10 0 -10 -20 -30 -40 -50 -60 ppm

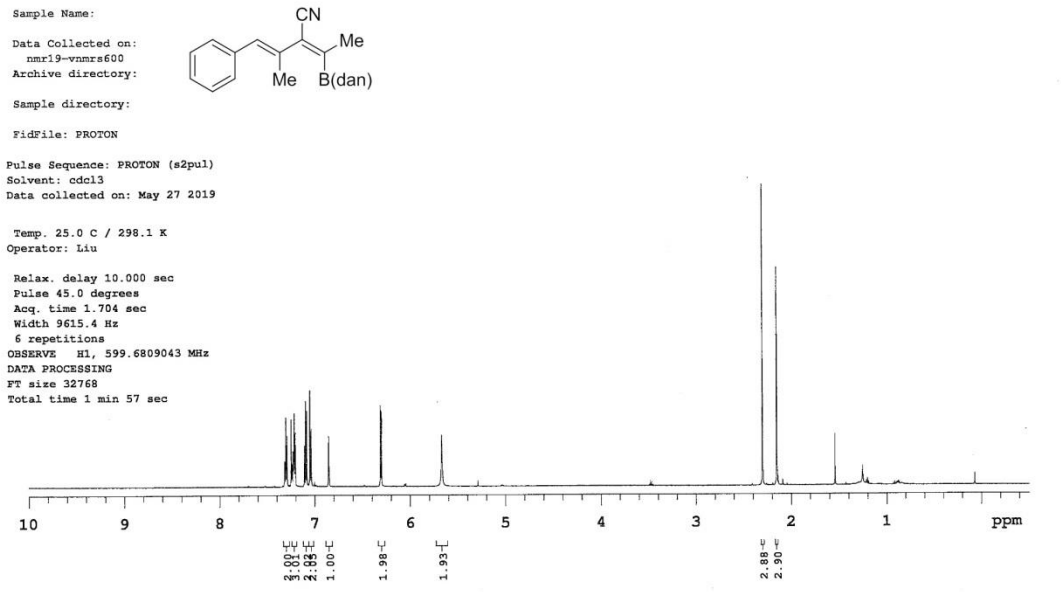
Sample Name:
Data Collected on:
nmr19-vnmrs600
Archive directory:
Sample directory:
FidFile: PROTON
Pulse Sequence: PROTON (s2pul)
Solvent: cdcl3
Data collected on: May 27 2019
Temp. 25.0 C / 298.1 K
Operator: Liu
Relax. delay 10.000 sec
Pulse 45.0 degrees
Acq. time 1.704 sec
Width 9615.4 Hz
6 repetitions
OBSERVE H1, 599.6809043 MHz
DATA PROCESSING
FT size 32768
Total time 1 min 57 sec
CN
Me
Me
B(dan)
10 9 8 7 6 5 4 3 2 1 ppm
3.01
3.01
2.05
1.00
1.98
1.93
2.88
2.90

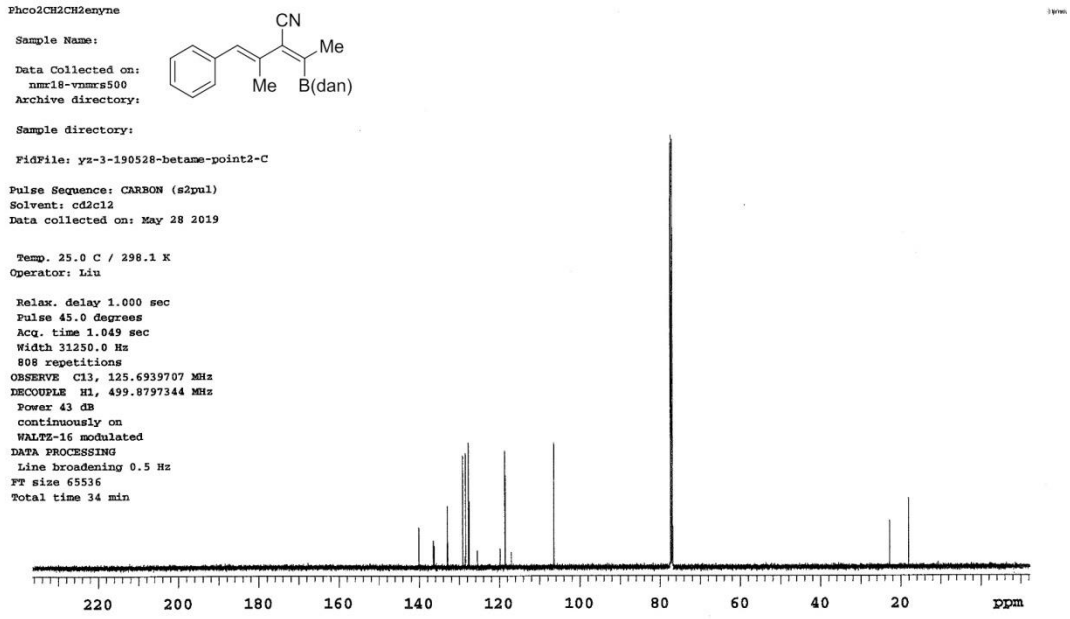
Phco2CH2CH2enyne
Sample Name:
Data Collected on:
nmr18-vnmrs500
Archive directory:
Sample directory:
FidFile: yz-3-190528-betame-point2-C
Pulse Sequence: CARBON (s2pul)
Solvent: cd2cl2
Data collected on: May 28 2019
Temp. 25.0 C / 298.1 K
Operator: Liu
Relax. delay 1.000 sec
Pulse 45.0 degrees
Acq. time 1.049 sec
Width 31250.0 Hz
808 repetitions
OBSERVE C13, 125.6939707 MHz
DECOUPLE H1, 499.8797344 MHz
Power 43 dB
continuously on
WALTZ-16 modulated
DATA PROCESSING
Line broadening 0.5 Hz
FT size 65536
Total time 34 min
CN
Me
Me
B(dan)
220
200
180
160
140
120
100
80
60
40
20
ppm

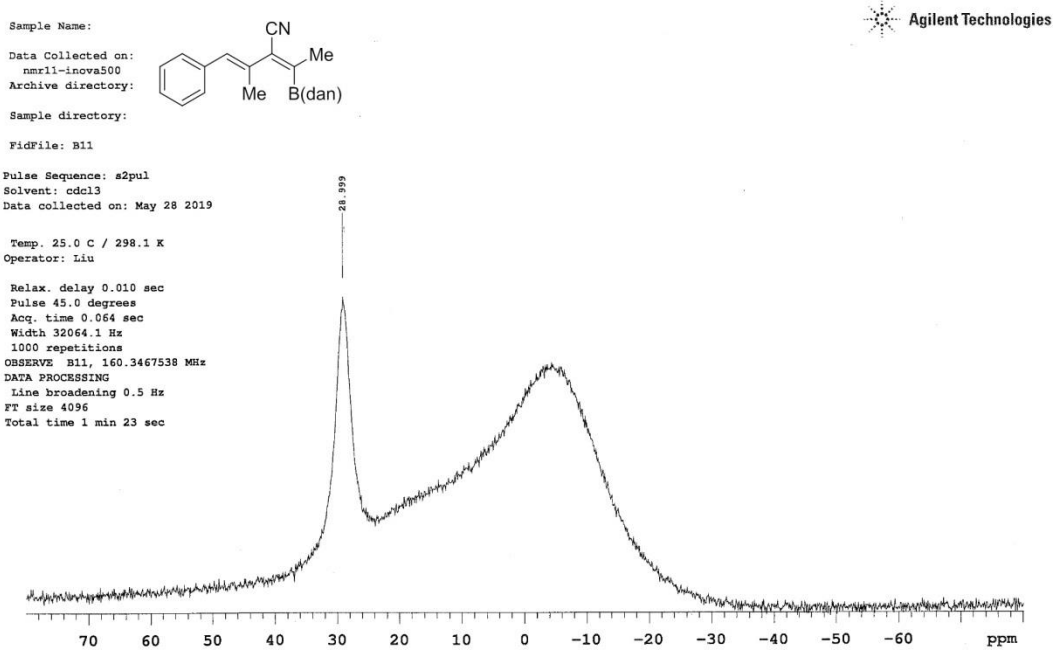
Agilent Technologies
Sample Name:
Data Collected on:
nmr11-inova500
Archive directory:
Sample directory:
FidFile: B11
Pulse Sequence: s2pul
Solvent: cdcl3
Data collected on: May 28 2019
Temp. 25.0 C / 298.1 K
Operator: Liu
Relax. delay 0.010 sec
Pulse 45.0 degrees
Acq. time 0.064 sec
Width 32064.1 Hz
1000 repetitions
OBSERVE B11, 160.3467538 MHz
DATA PROCESSING
Line broadening 0.5 Hz
FT size 4096
Total time 1 min 23 sec
28.999
CN
Me
Me
B(dan)
70
60
50
40
30
20
10
0
-10
-20
-30
-40
-50
-60
ppm

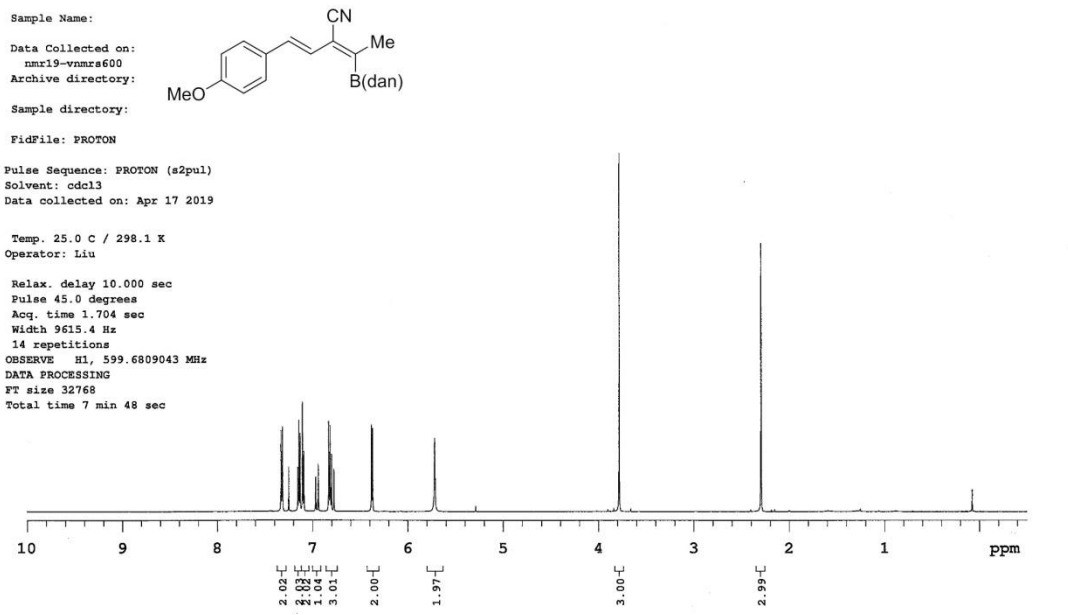
Sample Name:
Data Collected on:
nmr19-vnmrs600
Archive directory:
Sample directory:
FidFile: PROTON
Pulse Sequence: PROTON (s2pul)
Solvent: cdcl3
Data collected on: Apr 17 2019
Temp. 25.0 C / 298.1 K
Operator: Liu
Relax. delay 10.000 sec
Pulse 45.0 degrees
Acq. time 1.704 sec
Width 9615.4 Hz
14 repetitions
OBSERVE H1, 599.6809043 MHz
DATA PROCESSING
FT size 32768
Total time 7 min 48 sec
CN
Me
B(dan)
MeO
10
9
8
7
6
5
4
3
2
1
ppm
2.02
2.03
1.04
3.01
2.00
1.97
3.00
2.99

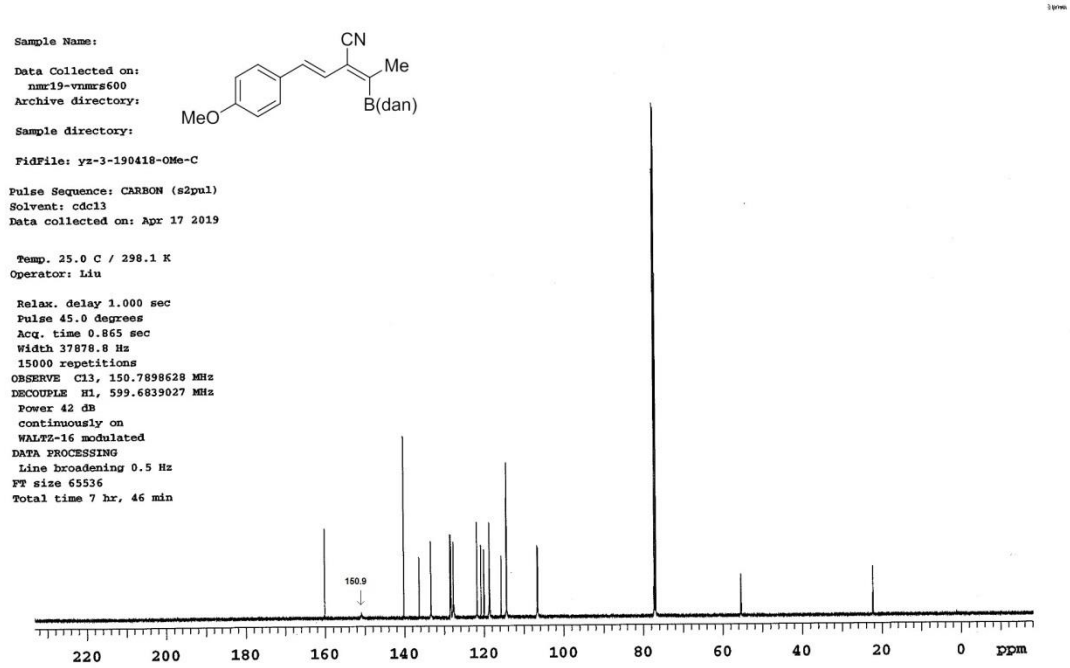
Sample Name:
Data Collected on:
nmr19-vnmrs600
Archive directory:
Sample directory:
FidFile: yz-3-190418-OMe-C
Pulse Sequence: CARBON (s2pul)
Solvent: cdcl3
Data collected on: Apr 17 2019
Temp. 25.0 C / 298.1 K
Operator: Liu
Relax. delay 1.000 sec
Pulse 45.0 degrees
Acq. time 0.865 sec
Width 37878.8 Hz
15000 repetitions
OBSERVE C13, 150.7898628 MHz
DECOUPLE H1, 599.6839027 MHz
Power 42 dB
continuously on
WALTZ-16 modulated
DATA PROCESSING
Line broadening 0.5 Hz
FT size 65536
Total time 7 hr, 46 min
CN
Me
B(dan)
MeO
150.9
220
200
180
160
140
120
100
80
60
40
20
0
ppm

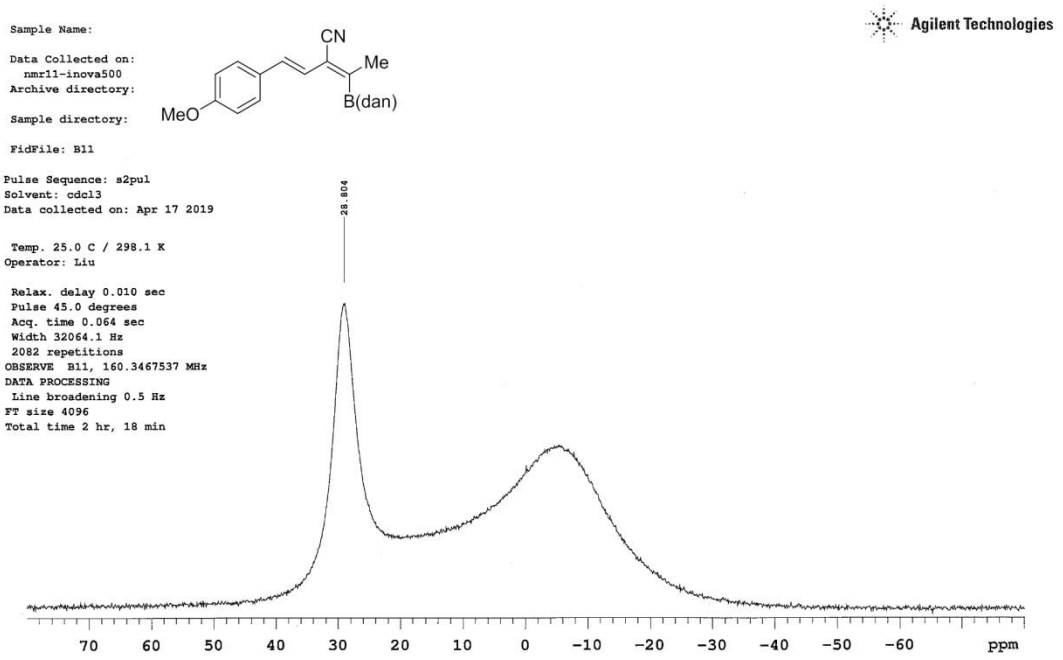
Agilent Technologies
Sample Name:
Data Collected on:
nmr11-inova500
Archive directory:
Sample directory:
FidFile: B11
CN
Me
B(dan)
MeO
Pulse Sequence: s2pul
Solvent: cdcl3
Data collected on: Apr 17 2019
Temp. 25.0 C / 298.1 K
Operator: Liu
Relax. delay 0.010 sec
Pulse 45.0 degrees
Acq. time 0.064 sec
Width 32064.1 Hz
2082 repetitions
OBSERVE B11, 160.3467537 MHz
DATA PROCESSING
Line broadening 0.5 Hz
FT size 4096
Total time 2 hr, 18 min
28.804
70 60 50 40 30 20 10 0 -10 -20 -30 -40 -50 -60 ppm

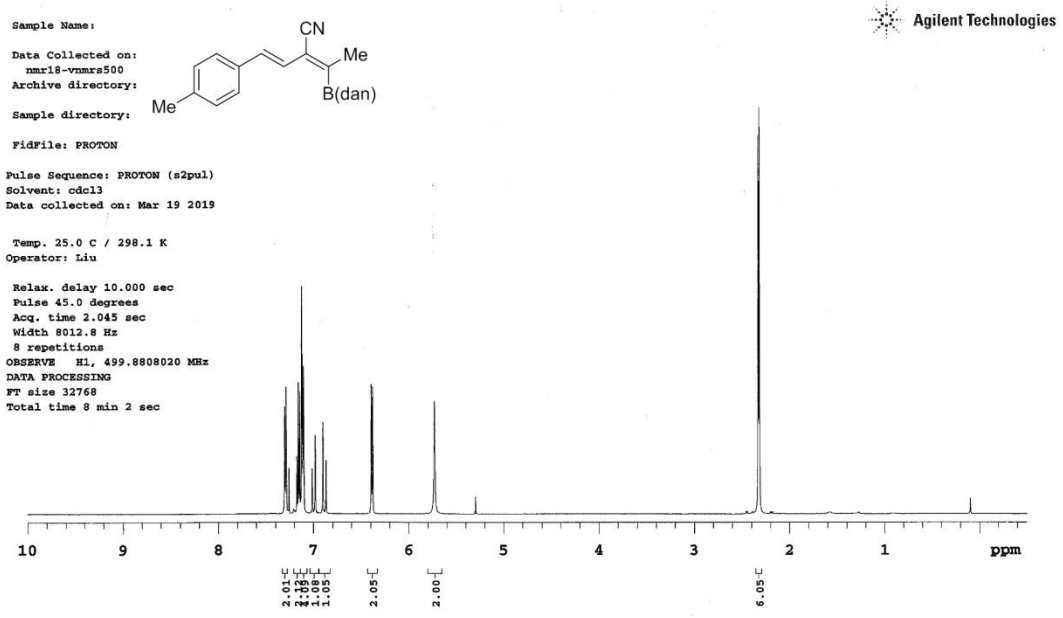
Agilent Technologies
Sample Name:
Data Collected on:
nmr18-vnmrs500
Archive directory:
Sample directory:
FidFile: PROTON
CN
Me
B(dan)
Me
Pulse Sequence: PROTON (s2pul)
Solvent: cdcl3
Data collected on: Mar 19 2019
Temp. 25.0 C / 298.1 K
Operator: Liu
Relax. delay 10.000 sec
Pulse 45.0 degrees
Acq. time 2.045 sec
Width 8012.8 Hz
8 repetitions
OBSERVE H1, 499.8808020 MHz
DATA PROCESSING
FT size 32768
Total time 8 min 2 sec
10 9 8 7 6 5 4 3 2 1 ppm
2.01
2.09
1.08
1.05
2.05
2.00
6.05

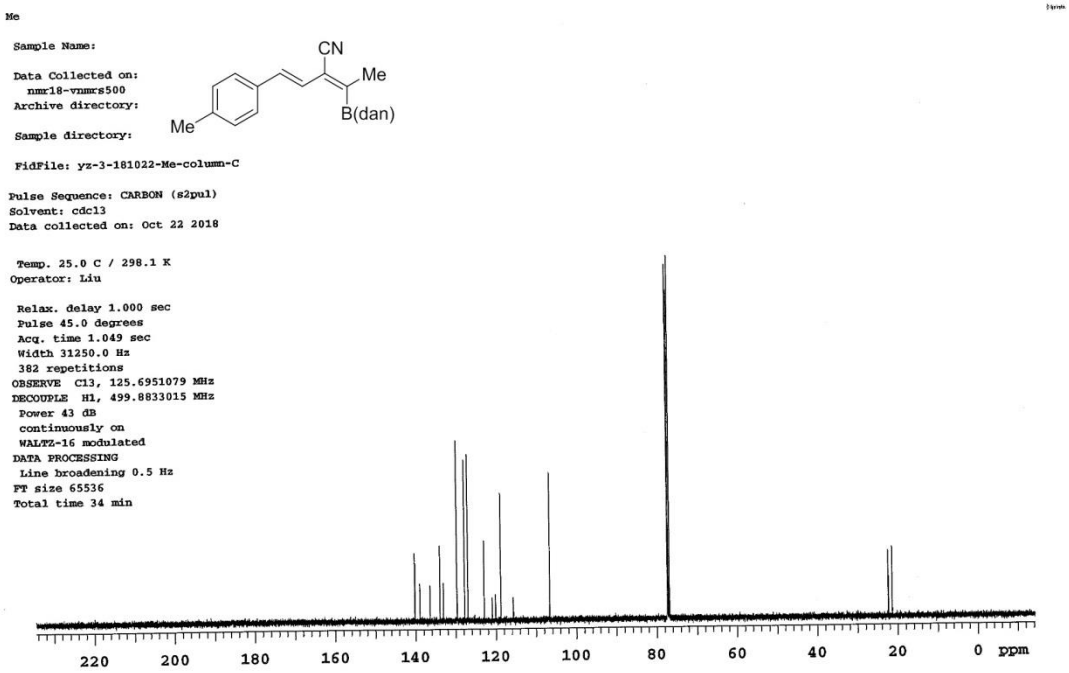
Me
Sample Name:
Data Collected on:
nmr18-vnmrs500
Archive directory:
Sample directory:
FidFile: yz-3-181022-Me-column-C
Pulse Sequence: CARBON (s2pul)
Solvent: cdcl3
Data collected on: Oct 22 2018
Temp. 25.0 C / 298.1 K
Operator: Liu
Relax. delay 1.000 sec
Pulse 45.0 degrees
Acq. time 1.049 sec
Width 31250.0 Hz
382 repetitions
OBSERVE C13, 125.6951079 MHz
DECOUPLE H1, 499.8833015 MHz
Power 43 dB
continuously on
WALTZ-16 modulated
DATA PROCESSING
Line broadening 0.5 Hz
FT size 65536
Total time 34 min
CN
Me
Me
B(dan)
220
200
180
160
140
120
100
80
60
40
20
0
ppm

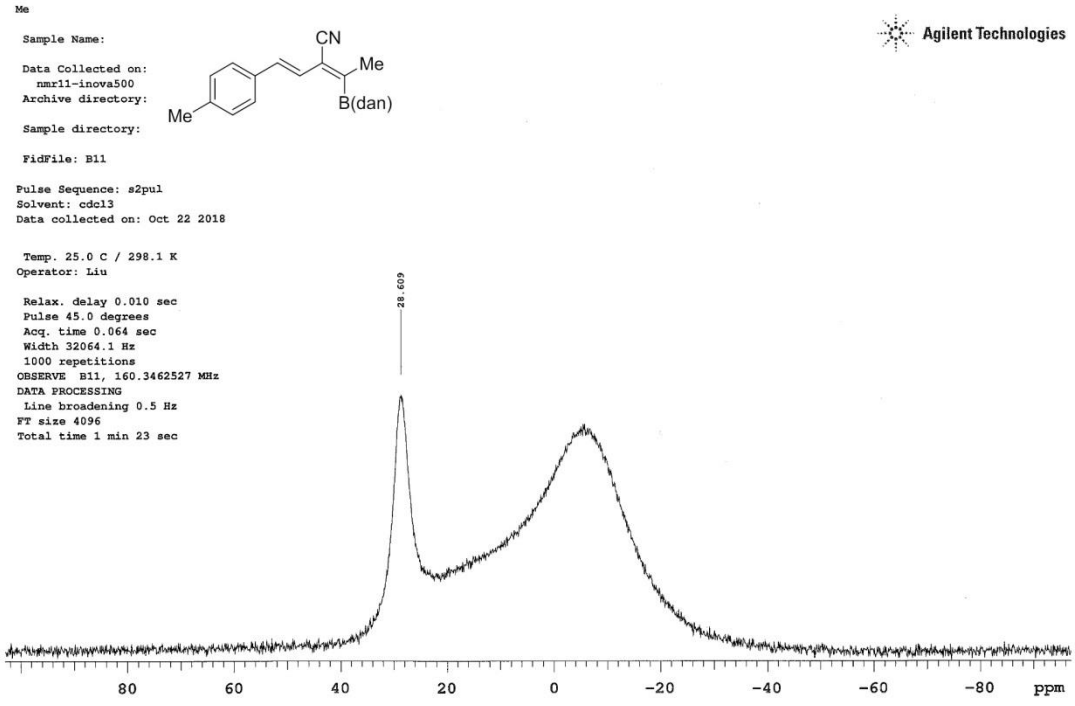
Me
Sample Name:
Data Collected on:
nmr11-inova500
Archive directory:
Sample directory:
FidFile: B11
Pulse Sequence: s2pul
Solvent: cdcl3
Data collected on: Oct 22 2018
Temp. 25.0 C / 298.1 K
Operator: Liu
Relax. delay 0.010 sec
Pulse 45.0 degrees
Acq. time 0.064 sec
Width 32064.1 Hz
1000 repetitions
OBSERVE B11, 160.3462527 MHz
DATA PROCESSING
Line broadening 0.5 Hz
FT size 4096
Total time 1 min 23 sec
28.609
CN
Me
Me
B(dan)
Agilent Technologies
80
60
40
20
0
-20
-40
-60
-80
ppm

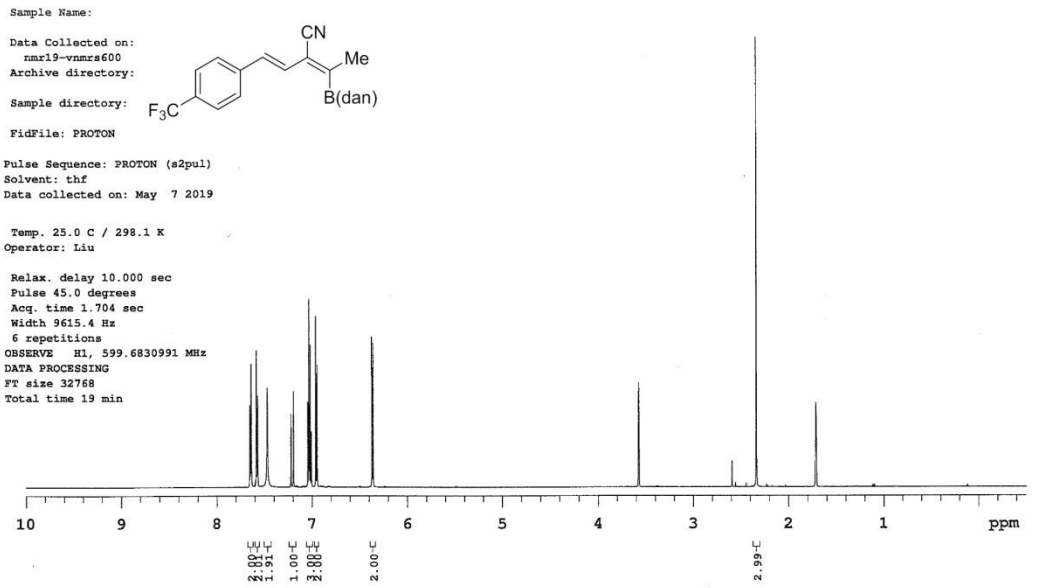
Sample Name:
Data Collected on:
nmr19-vnmrs600
Archive directory:
Sample directory:
FidFile: PROTON
Pulse Sequence: PROTON (s2pul)
Solvent: thf
Data collected on: May 7 2019
Temp. 25.0 C / 298.1 K
Operator: Liu
Relax. delay 10.000 sec
Pulse 45.0 degrees
Acq. time 1.704 sec
Width 9615.4 Hz
6 repetitions
OBSERVE H1, 599.6830991 MHz
DATA PROCESSING
FT size 32768
Total time 19 min
CN
Me
B(dan)
F3C
10
9
8
7
6
5
4
3
2
1
ppm
2.00
1.91
1.00
2.00
2.99

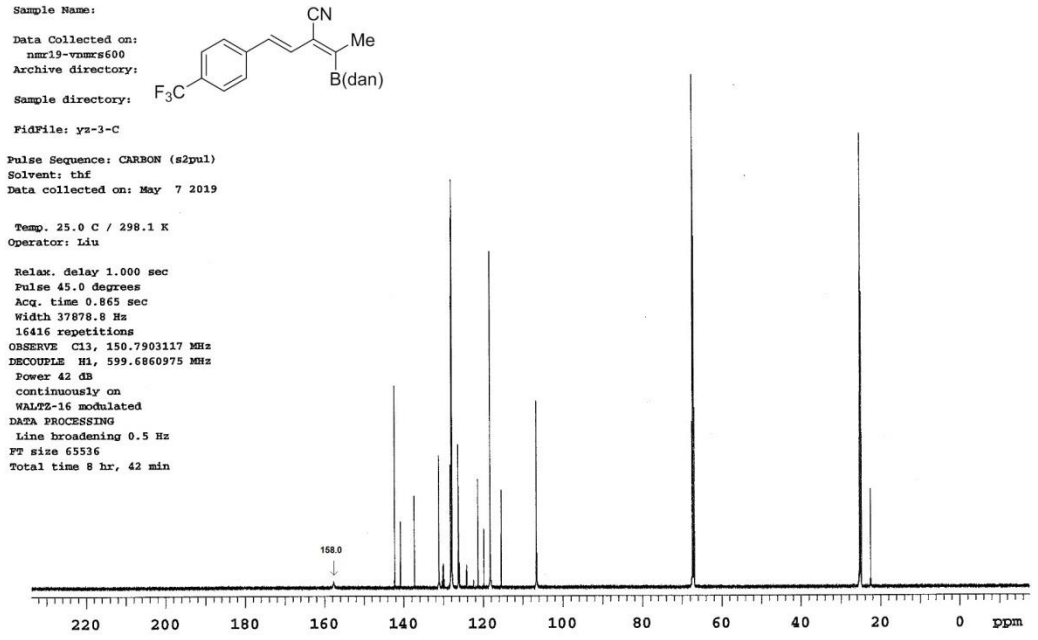
Sample Name:
Data Collected on:
nmr19-vnmrs600
Archive directory:
Sample directory:
FidFile: yz-3-C
Pulse Sequence: CARBON (s2pul)
Solvent: thf
Data collected on: May 7 2019
Temp. 25.0 C / 298.1 K
Operator: Liu
Relax. delay 1.000 sec
Pulse 45.0 degrees
Acq. time 0.865 sec
Width 37878.8 Hz
16416 repetitions
OBSERVE C13, 150.7903117 MHz
DECOUPLE H1, 599.6860975 MHz
Power 42 dB
continuously on
WALTZ-16 modulated
DATA PROCESSING
Line broadening 0.5 Hz
FT size 65536
Total time 8 hr, 42 min
CN
Me
B(dan)
F3C
158.0
220
200
180
160
140
120
100
80
60
40
20
0
ppm

Agilent Technologies

Sample Name:

Data Collected on:
nmr11-inova500
Archive directory:

Sample directory:

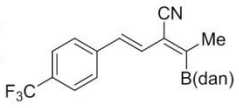

FidFile: B11

Pulse Sequence: s2pul
Solvent: thf
Data collected on: May 7 2019

Temp. 25.0 C / 298.1 K
Operator: Liu

Relax. delay 0.010 sec
Pulse 45.0 degrees
Acq. time 0.064 sec
Width 32064.1 Hz
1036 repetitions
OBSERVE B11, 160.3467145 MHz
DATA PROCESSING
Line broadening 0.5 Hz
FT size 4096
Total time 13 min

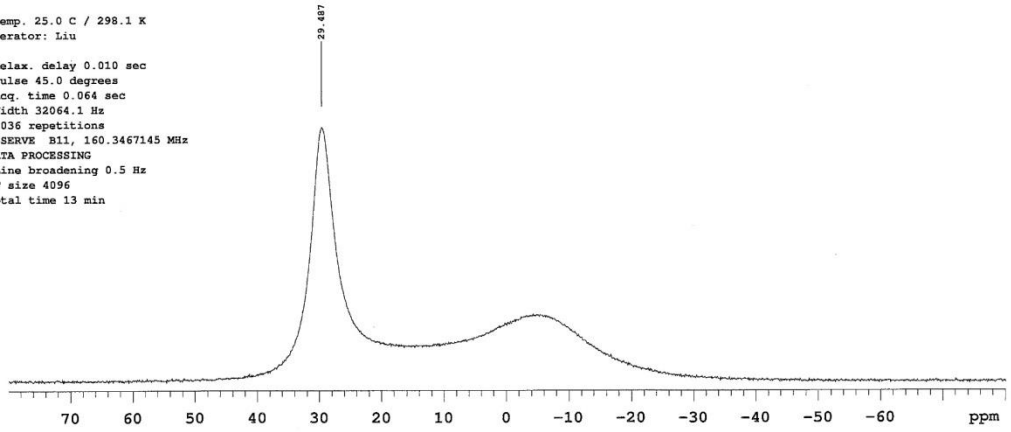

STANDARD FLUORINE PARAMETERS

Sample Name:

Data Collected on:
nmr19-vnmrs600
Archive directory:

Sample directory:

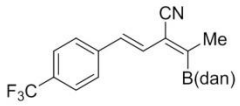

FidFile: FLUORINE

Pulse Sequence: FLUORINE (s2pul)
Solvent: thf
Data collected on: May 7 2019

Temp. 25.0 C / 298.1 K
Operator: Liu

Relax. delay 1.000 sec
Pulse 30.0 degrees
Acq. time 0.996 sec
Width 131.6 kHz
12 repetitions
OBSERVE F19, 564.2658812 MHz
DATA PROCESSING
FT size 262144
Total time 3 min 20 sec

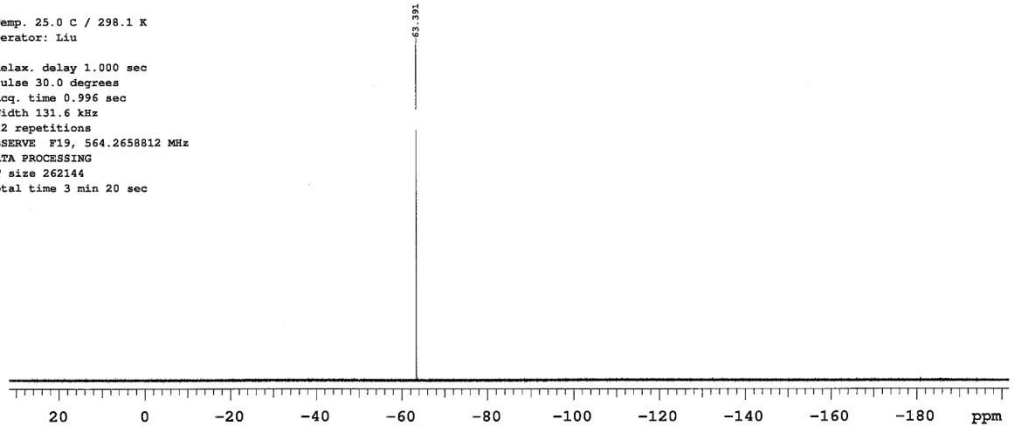

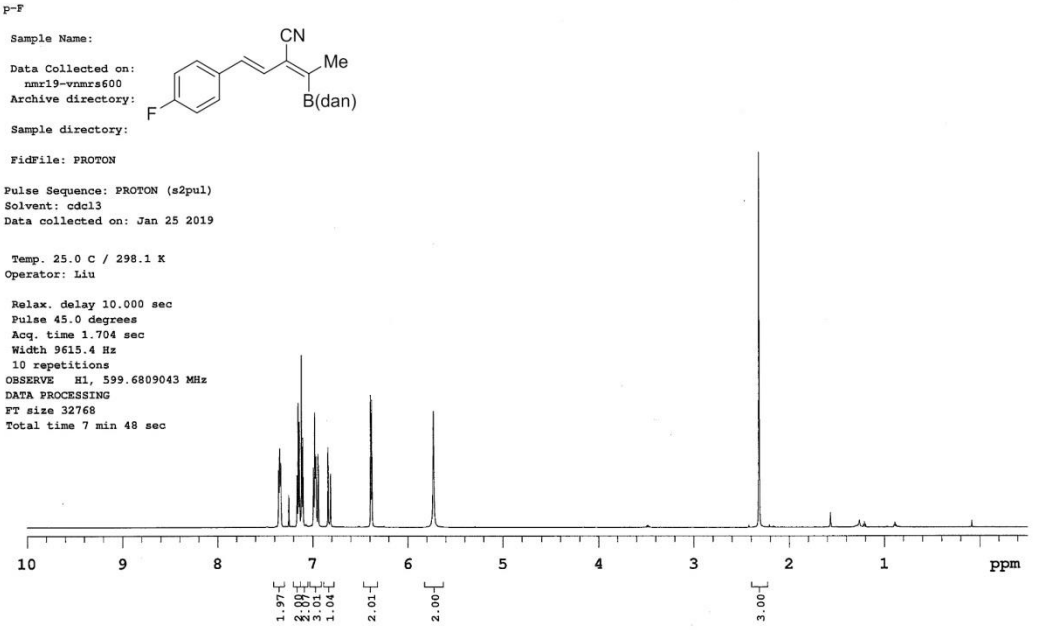
p-F
Sample Name:
Data Collected on:
nmr19-vnmrs600
Archive directory:
Sample directory:
FidFile: PROTON
Pulse Sequence: PROTON (s2pul)
Solvent: cdcl3
Data collected on: Jan 25 2019
Temp. 25.0 C / 298.1 K
Operator: Liu
Relax. delay 10.000 sec
Pulse 45.0 degrees
Acq. time 1.704 sec
Width 9615.4 Hz
10 repetitions
OBSERVE H1, 599.6809043 MHz
DATA PROCESSING
FT size 32768
Total time 7 min 48 sec
CN
Me
B(dan)
F
10
9
8
7
6
5
4
3
2
1
ppm
1.97
2.09
3.01
1.04
2.01
2.00
3.00

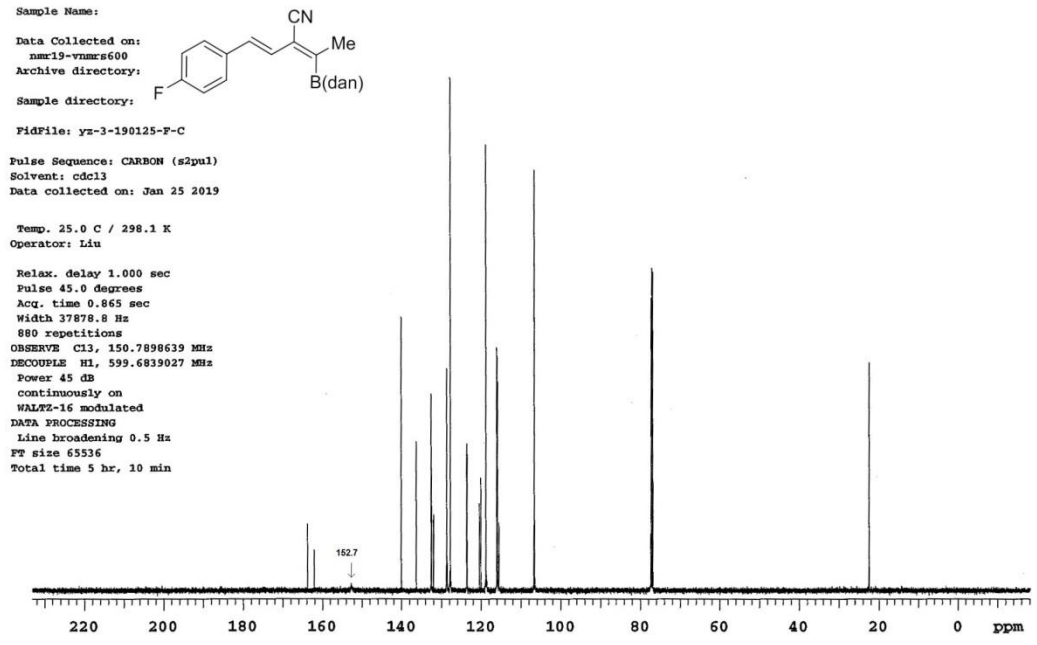
Sample Name:
Data Collected on:
nmr19-vnmrs600
Archive directory:
Sample directory:
FidFile: yz-3-190125-F-C
Pulse Sequence: CARBON (s2pul)
Solvent: cdcl3
Data collected on: Jan 25 2019
Temp. 25.0 C / 298.1 K
Operator: Liu
Relax. delay 1.000 sec
Pulse 45.0 degrees
Acq. time 0.865 sec
Width 37878.8 Hz
880 repetitions
OBSERVE C13, 150.7898639 MHz
DECOUPLE H1, 599.6839027 MHz
Power 45 dB
continuously on
WALTZ-16 modulated
DATA PROCESSING
Line broadening 0.5 Hz
FT size 65536
Total time 5 hr, 10 min
CN
Me
B(dan)
F
152.7
220
200
180
160
140
120
100
80
60
40
20
0
ppm

p-F

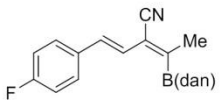

Agilent Technologies

Sample Name:

Data Collected on:
nmr11-inova500
Archive directory:

Sample directory:

FidFile: B11

Pulse Sequence: s2pul
Solvent: cdcl3
Data collected on: Jan 25 2019

Temp. 25.0 C / 298.1 K
Operator: Liu

Relax. delay 0.010 sec
Pulse 45.0 degrees
Acq. time 0.064 sec
Width 32064.1 Hz
1132 repetitions
OBSERVE B11, 160.3469104 MHz
DATA PROCESSING
Line broadening 0.5 Hz
FT size 4096
Total time 13 min

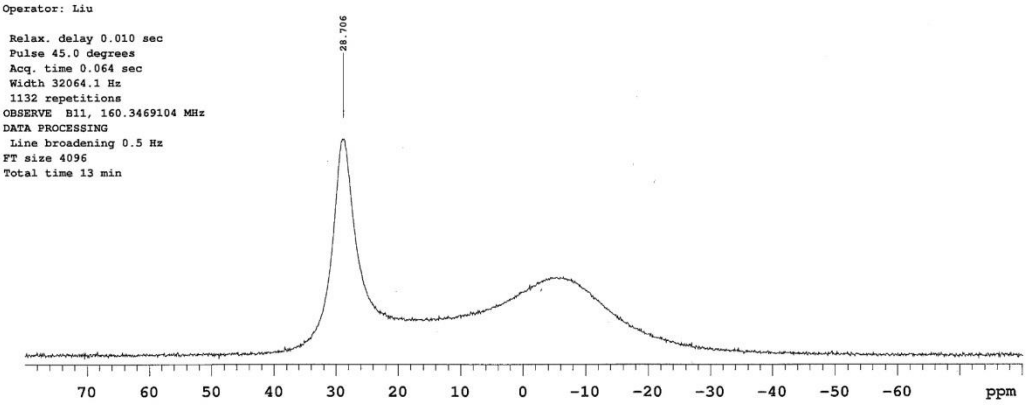

p-F

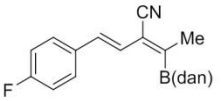

Sample Name:

Data Collected on:
nmr19-vnmrs600
Archive directory:

Sample directory:

FidFile: yz-3-190123-F-F

Pulse Sequence: FLUORINE (s2pul)
Solvent: cdcl3
Data collected on: Jan 23 2019

Temp. 25.0 C / 298.1 K
Operator: Liu

Relax. delay 1.000 sec
Pulse 30.0 degrees
Acq. time 0.996 sec
Width 131.6 kHz
16 repetitions
OBSERVE F19, 564.2638160 MHz
DATA PROCESSING
FT size 262144
Total time 33 min

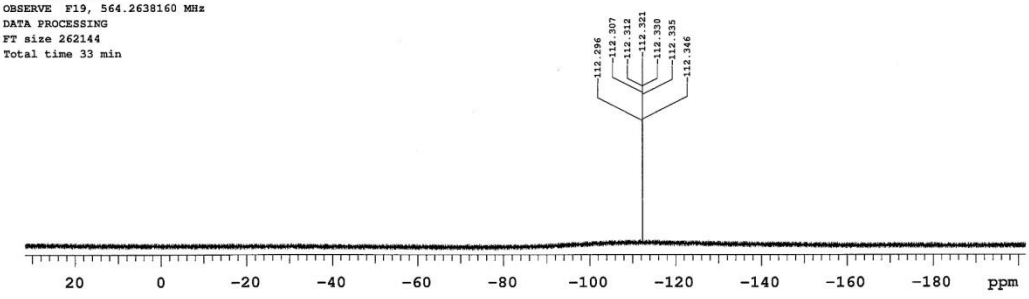

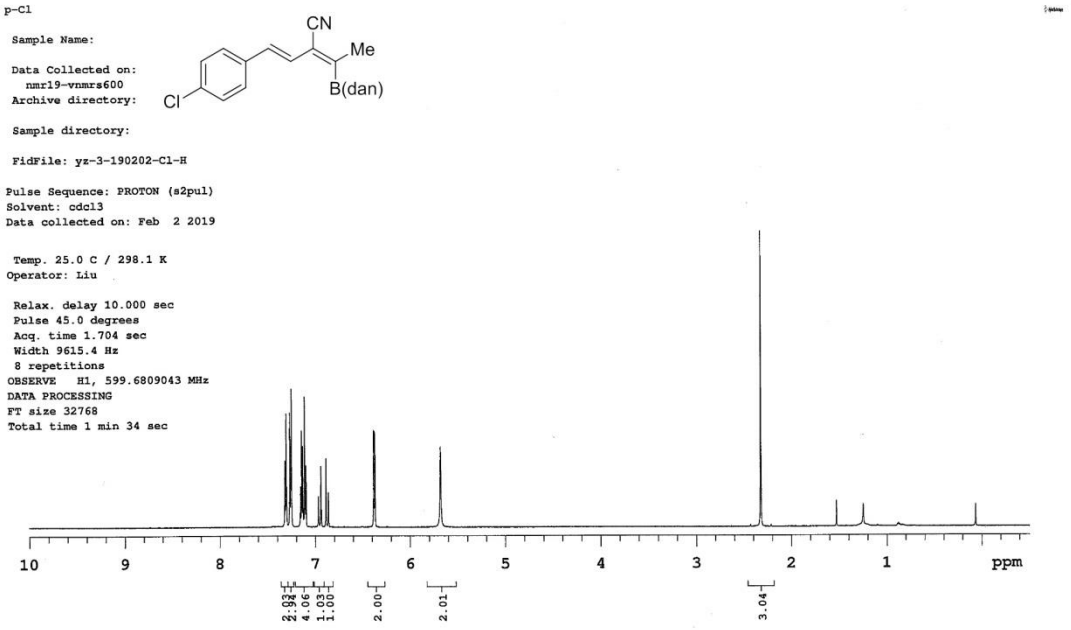
p-Cl
Sample Name:
Data Collected on:
nmr19-vnmrs600
Archive directory:
Sample directory:
FidFile: yz-3-190202-Cl-H
Pulse Sequence: PROTON (s2pul)
Solvent: cdcl3
Data collected on: Feb 2 2019
Temp. 25.0 C / 298.1 K
Operator: Liu
Relax. delay 10.000 sec
Pulse 45.0 degrees
Acq. time 1.704 sec
Width 9615.4 Hz
8 repetitions
OBSERVE H1, 599.6809043 MHz
DATA PROCESSING
FT size 32768
Total time 1 min 34 sec
CN
Me
B(dan)
Cl
10
9
8
7
6
5
4
3
2
1
ppm
2.03
2.94
4.06
1.03
1.00
2.00
2.01
3.04

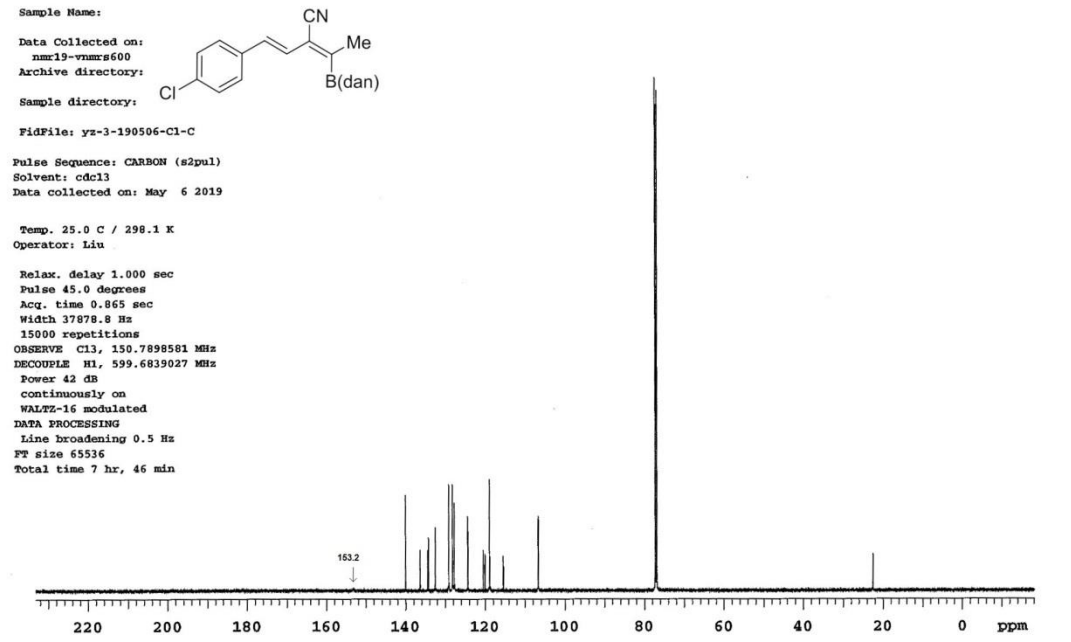
Sample Name:
Data Collected on:
nmr19-vnmrs600
Archive directory:
Sample directory:
FidFile: yz-3-190506-Cl-C
Pulse Sequence: CARBON (s2pul)
Solvent: cdcl3
Data collected on: May 6 2019
Temp. 25.0 C / 298.1 K
Operator: Liu
Relax. delay 1.000 sec
Pulse 45.0 degrees
Acq. time 0.865 sec
Width 37878.8 Hz
15000 repetitions
OBSERVE C13, 150.7898581 MHz
DECOUPLE H1, 599.6839027 MHz
Power 42 dB
continuously on
WALTZ-16 modulated
DATA PROCESSING
Line broadening 0.5 Hz
FT size 65536
Total time 7 hr, 46 min
CN
Me
B(dan)
Cl
153.2
220
200
180
160
140
120
100
80
60
40
20
0
ppm

p-Cl

Sample Name:

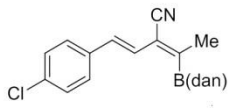

Data Collected on:
nmr11-inova500
Archive directory:

Sample directory:

FidFile: B11

Pulse Sequence: s2pul
Solvent: cdcl3
Data collected on: Feb 4 2019

Temp. 25.0 C / 298.1 K
Operator: Liu

Relax. delay 0.010 sec
Pulse 45.0 degrees
Acq. time 0.064 sec
Width 32064.1 Hz
2948 repetitions
OBSERVE B11, 160.3466442 MHz
DATA PROCESSING
Line broadening 0.5 Hz
FT size 4096
Total time 2 hr, 18 min

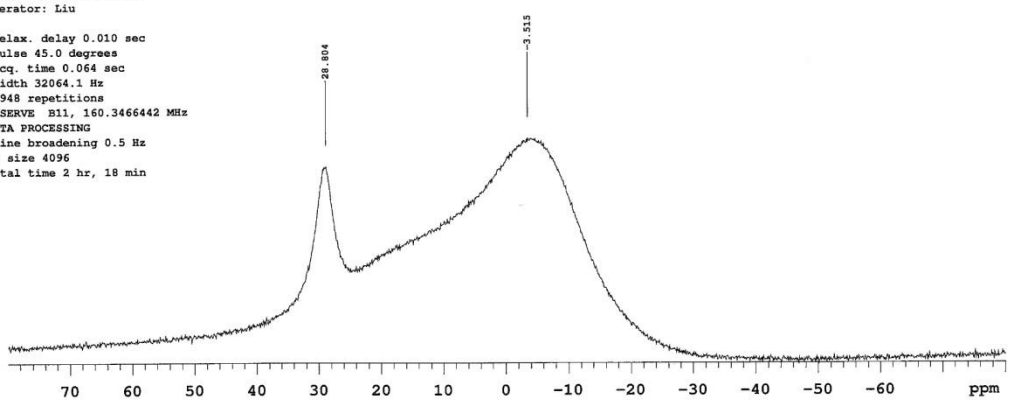

Agilent Technologies

Sample Name:

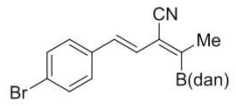

Data Collected on:
nmr18-vnmrs500
Archive directory:

Sample directory:

FidFile: PROTON

Pulse Sequence: PROTON (s2pul)
Solvent: thf
Data collected on: Jun 9 2019

Temp. 25.0 C / 298.1 K
Operator: Liu

Relax. delay 10.000 sec
Pulse 45.0 degrees
Acq. time 2.045 sec
Width 8012.8 Hz
8 repetitions
OBSERVE H1, 499.8790445 MHz
DATA PROCESSING
FT size 32768
Total time 1 min 36 sec

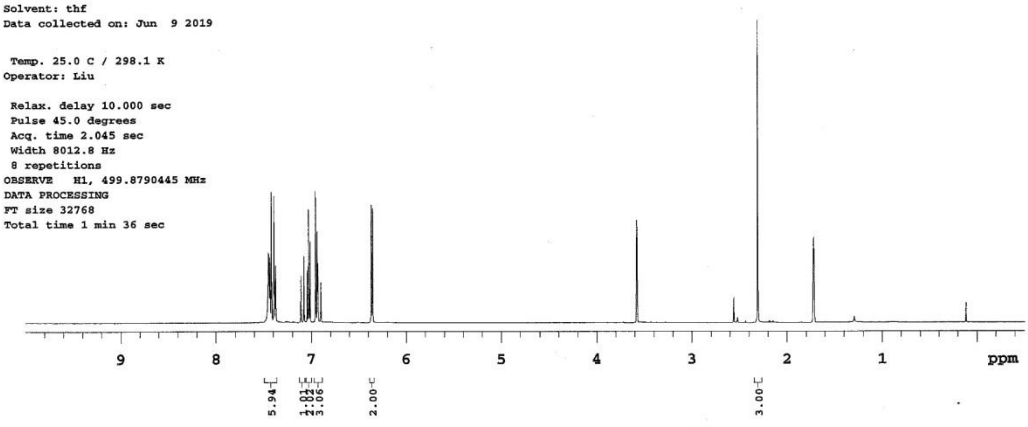

Agilent Technologies

Sample Name:

Data Collected on:
nmr18-vnmrs500
Archive directory:

Sample directory:

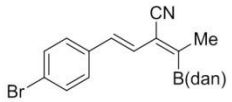

FidFile: yz-3-190609-pbr-thf-C

Pulse Sequence: CARBON (s2pul)
Solvent: thf
Data collected on: Jun 9 2019

Temp. 25.0 C / 298.1 K
Operator: Liu

Relax. delay 1.000 sec
Pulse 45.0 degrees
Acq. time 1.049 sec
Width 31250.0 Hz
404 repetitions
OBSERVE C13, 125.6945602 MHz
DECOUPLE H1, 499.8806042 MHz
Power 43 dB
continuously on
WALTZ-16 modulated
DATA PROCESSING
Line broadening 0.5 Hz
FT size 65536
Total time 5 hr, 41 min

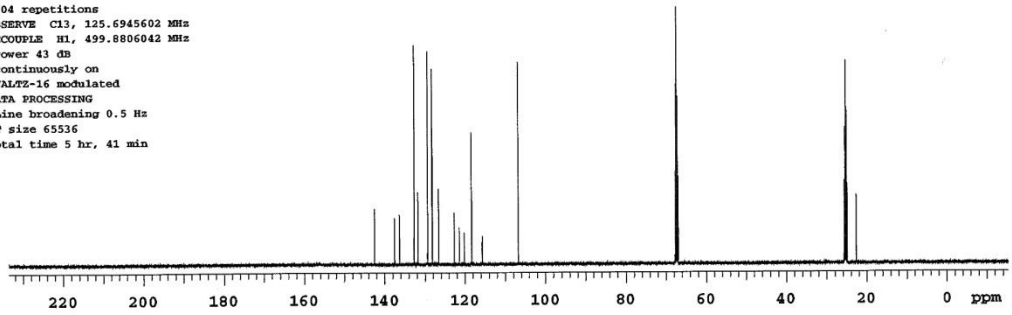

Agilent Technologies

Sample Name:

Data Collected on:
nmr11-inova500
Archive directory:

Sample directory:

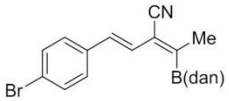

FidFile: B11

Pulse Sequence: s2pul
Solvent: thf
Data collected on: Jun 9 2019

Temp. 25.0 C / 298.1 K
Operator: Liu

Relax. delay 0.010 sec
Pulse 45.0 degrees
Acq. time 0.064 sec
Width 32064.1 Hz
1000 repetitions
OBSERVE B11, 160.3466205 MHz
DATA PROCESSING
Line broadening 0.5 Hz
FT size 4096
Total time 1 min 23 sec

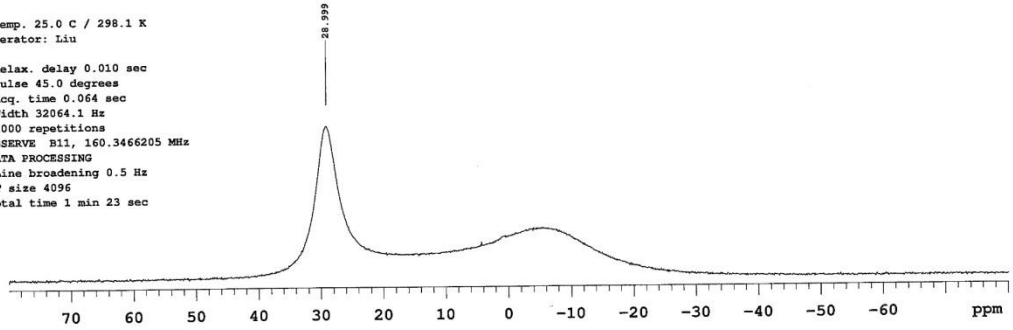

Sample Name:

Data Collected on:
nmr19-vnmrs600
Archive directory:

Sample directory:

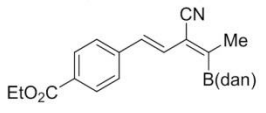

FidFile: PROTON

Pulse Sequence: PROTON (s2pul)
Solvent: cdcl3
Data collected on: May 30 2019

Temp. 25.0 C / 298.1 K
Operator: Liu

Relax. delay 10.000 sec
Pulse 45.0 degrees
Acq. time 1.704 sec
Width 9615.4 Hz
8 repetitions
OBSERVE H1, 599.6809043 MHz
DATA PROCESSING
FT size 32768
Total time 1 min 34 sec

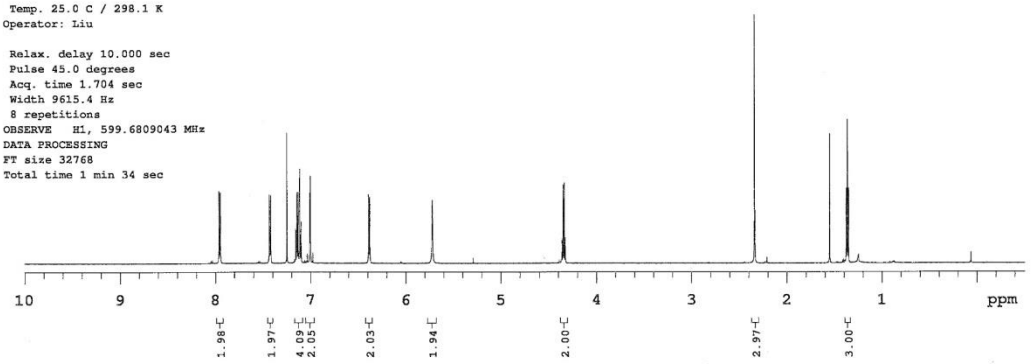

Sample Name:

Data Collected on:
nmr19-vnmrs600
Archive directory:

Sample directory:

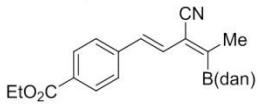

FidFile: CARBON

Pulse Sequence: CARBON (s2pul)
Solvent: cdcl3
Data collected on: May 30 2019

Temp. 25.0 C / 298.1 K
Operator: Liu

Relax. delay 1.000 sec
Pulse 45.0 degrees
Acq. time 0.865 sec
Width 37878.8 Hz
5020 repetitions
OBSERVE C13, 150.7898593 MHz
DECOUPLE H1, 599.6839027 MHz
Power 42 dB
continuously on
WALTZ-16 modulated
DATA PROCESSING
Line broadening 0.5 Hz
FT size 65536
Total time 5 hr, 10 min

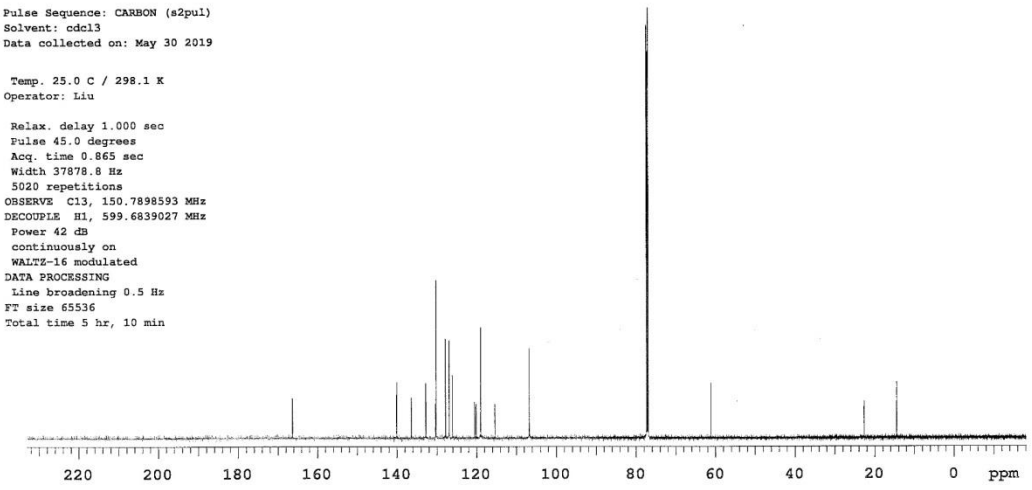

Agilent Technologies

Sample Name:

Data Collected on:
nmr11-inova500
Archive directory:

Sample directory:

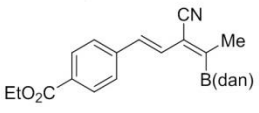

FidFile: B11

Pulse Sequence: s2pul
Solvent: cdcl3
Data collected on: May 31 2019

Temp. 25.0 C / 298.1 K
Operator: Liu

Relax. delay 0.010 sec
Pulse 45.0 degrees
Acq. time 0.064 sec
Width 32064.1 Hz
3646 repetitions
OBSERVE B11, 160.3467538 MHz
DATA PROCESSING
Line broadening 0.5 Hz
FT size 4096
Total time 13 min

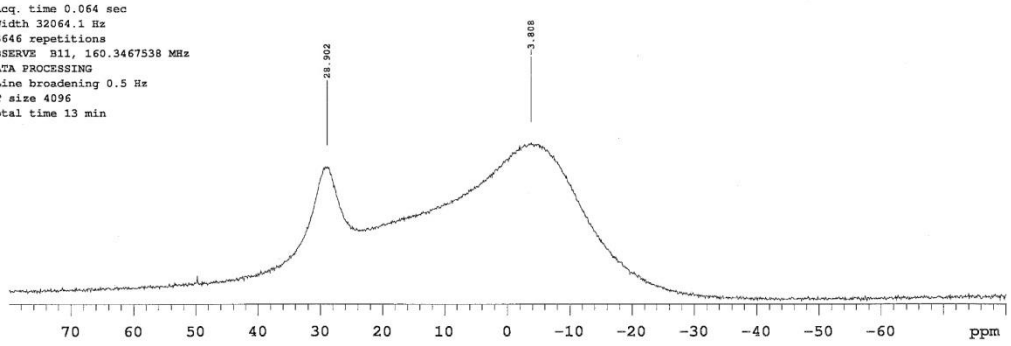

Sample Name:

Data Collected on:
nmr19-vnmrs600
Archive directory:

Sample directory:

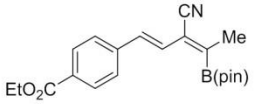

FidFile: PROTON

Pulse Sequence: PROTON (s2pul)
Solvent: cdcl3
Data collected on: Jun 1 2019

Temp. 25.0 C / 298.1 K
Operator: Liu

Relax. delay 10.000 sec
Pulse 45.0 degrees
Acq. time 1.704 sec
Width 9615.4 Hz
8 repetitions
OBSERVE H1, 599.6809043 MHz
DATA PROCESSING
FT size 32768
Total time 1 min 34 sec

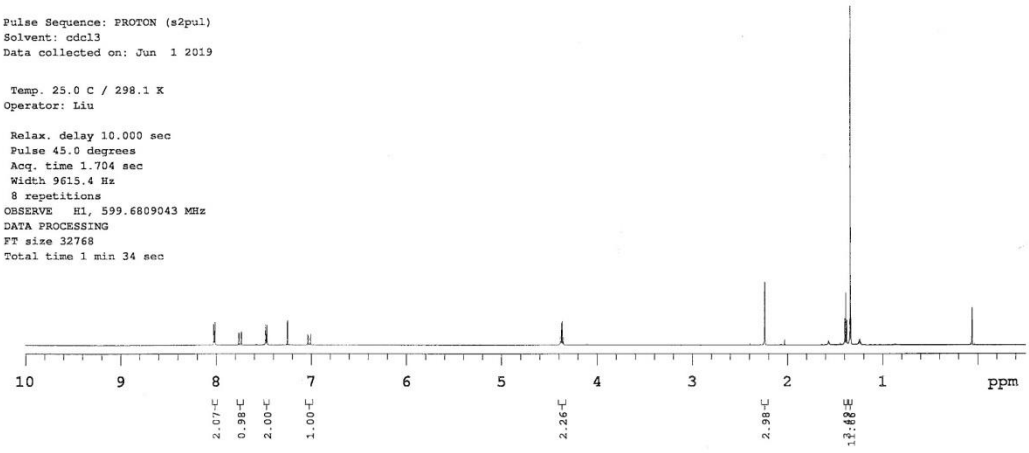

Sample Name:

Data Collected on:
nmr19-vnmrs600
Archive directory:

Sample directory:

FidFile: CARBON

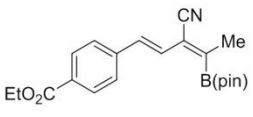

Pulse Sequence: CARBON (s2pul)
Solvent: cdcl3
Data collected on: Jun 1 2019

Temp. 25.0 C / 298.1 K
Operator: Liu

Relax. delay 1.000 sec
Pulse 45.0 degrees
Acq. time 0.865 sec
Width 37878.8 Hz
4092 repetitions
OBSERVE C13, 150.7898581 MHz
DECOUPLE H1, 599.6839027 MHz
Power 42 dB
continuously on
WALTZ-16 modulated
DATA PROCESSING
Line broadening 0.5 Hz
FT size 65536
Total time 5 hr, 10 min

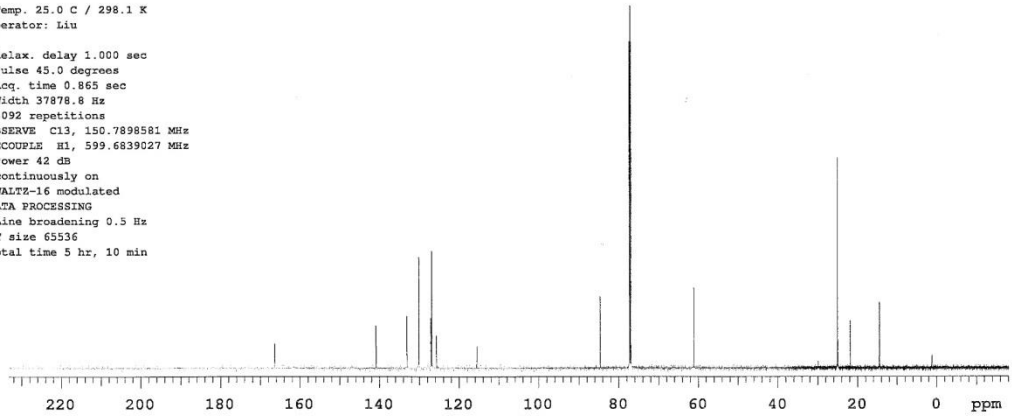

Agilent Technologies

Sample Name:

Data Collected on:
nmr11-inova500
Archive directory:

Sample directory:

FidFile: B11

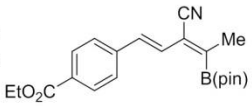

Pulse Sequence: s2pul
Solvent: cdcl3
Data collected on: Jun 2 2019

Temp. 25.0 C / 298.1 K
Operator: Liu

Relax. delay 0.010 sec
Pulse 45.0 degrees
Acq. time 0.064 sec
Width 32064.1 Hz
1000 repetitions
OBSERVE B11, 160.3464720 MHz
DATA PROCESSING
Line broadening 0.5 Hz
FT size 4096
Total time 1 min 23 sec

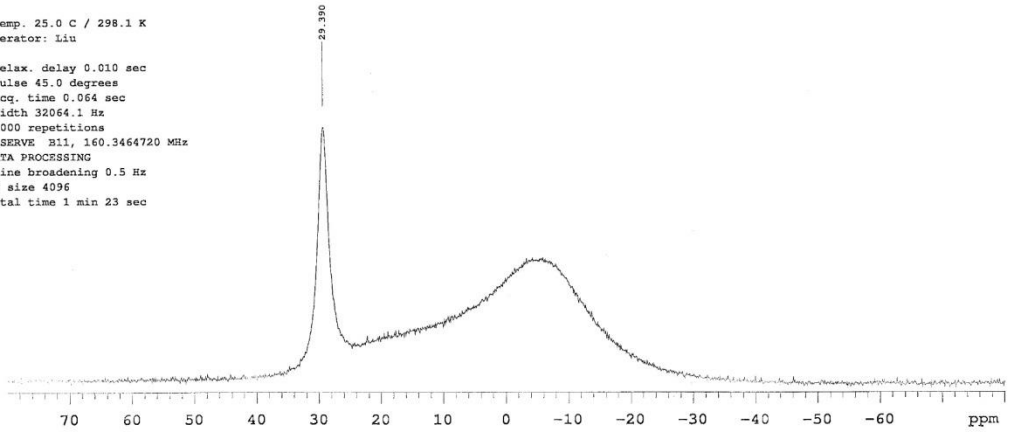

Agilent Technologies

Sample Name:

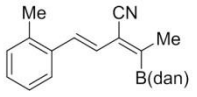

Data Collected on:
nmr18-vnmrs500
Archive directory:

Sample directory:

FidFile: PROTON

Pulse Sequence: PROTON (s2pul)
Solvent: cdcl3
Data collected on: Feb 6 2020

Temp. 25.0 C / 298.1 K
Operator: Liu

Relax. delay 10.000 sec
Pulse 45.0 degrees
Acq. time 2.045 sec
Width 8012.8 Hz
6 repetitions
OBSERVE H1, 499.8760066 MHz
DATA PROCESSING
FT size 32768
Total time 1 min 12 sec

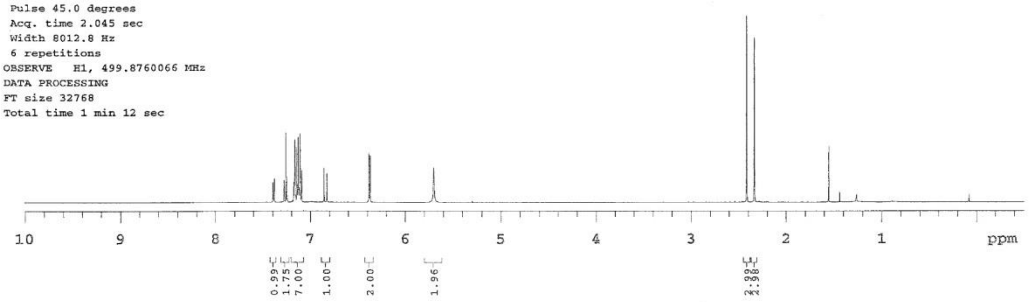

Sample Name:

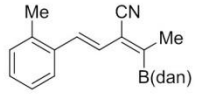

Data Collected on:
nmr19-vnmrs600
Archive directory:

Sample directory:

FidFile: CARBON

Pulse Sequence: CARBON (s2pul)
Solvent: cdcl3
Data collected on: Jan 3 2020

Temp. 25.0 C / 298.1 K
Operator: Liu

Relax. delay 1.000 sec
Pulse 45.0 degrees
Acq. time 0.865 sec
Width 37878.8 Hz
304 repetitions
OBSERVE C13, 150.7898132 MHz
DECOUPLE H1, 599.6836825 MHz
Power 45 dB
continuously on
WALTZ-16 modulated
DATA PROCESSING
Line broadening 0.5 Hz
FT size 65536
Total time 31 min

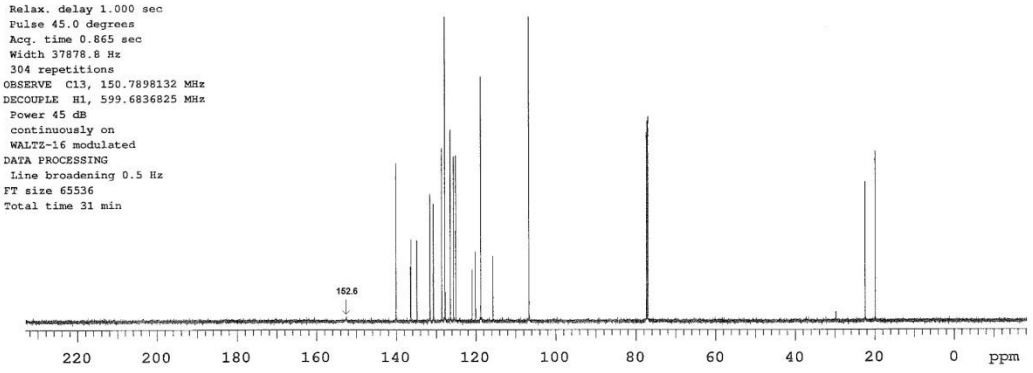

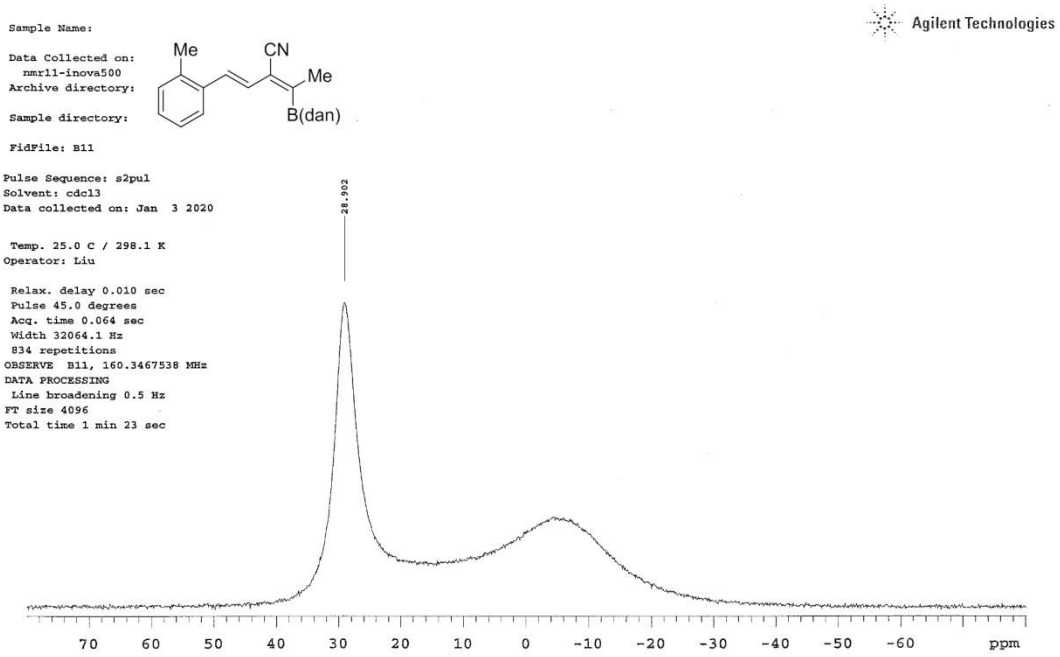
Agilent Technologies
Sample Name:
Data Collected on:
nmr11-inova500
Archive directory:
Sample directory:
FidFile: B11
Me
CN
Me
B(dan)
Pulse Sequence: s2pul
Solvent: cdcl3
Data collected on: Jan 3 2020
Temp. 25.0 C / 298.1 K
Operator: Liu
Relax. delay 0.010 sec
Pulse 45.0 degrees
Acq. time 0.064 sec
Width 32064.1 Hz
834 repetitions
OBSERVE B11, 160.3467538 MHz
DATA PROCESSING
Line broadening 0.5 Hz
FT size 4096
Total time 1 min 23 sec
28.902
70 60 50 40 30 20 10 0 -10 -20 -30 -40 -50 -60 ppm

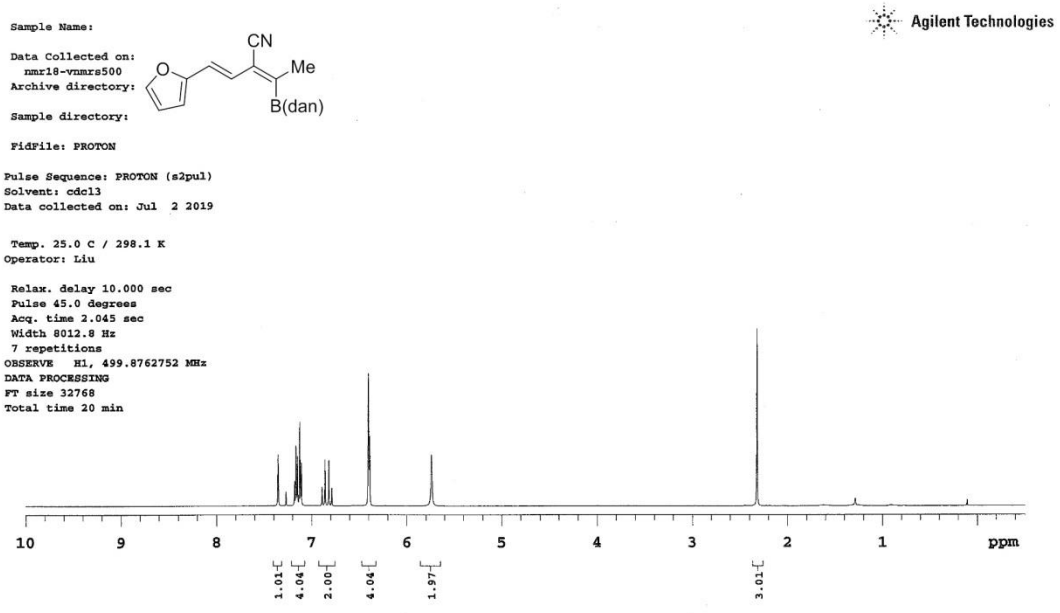
Agilent Technologies
Sample Name:
Data Collected on:
nmr18-vnmrs500
Archive directory:
Sample directory:
FidFile: PROTON
CN
Me
O
B(dan)
Pulse Sequence: PROTON (s2pul)
Solvent: cdcl3
Data collected on: Jul 2 2019
Temp. 25.0 C / 298.1 K
Operator: Liu
Relax. delay 10.000 sec
Pulse 45.0 degrees
Acq. time 2.045 sec
Width 8012.8 Hz
7 repetitions
OBSERVE H1, 499.8762752 MHz
DATA PROCESSING
FT size 32768
Total time 20 min
10 9 8 7 6 5 4 3 2 1 ppm
1.01
4.04
2.00
4.04
1.97
3.01

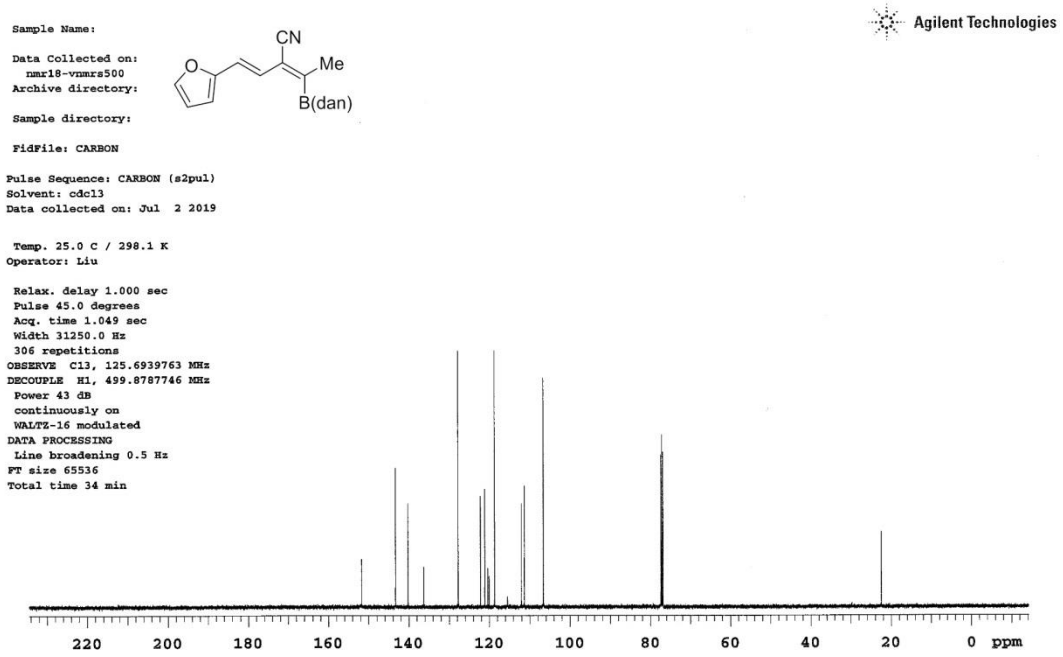
Agilent Technologies
Sample Name:
Data Collected on:
nmr18-vnmrs500
Archive directory:
Sample directory:
FidFile: CARBON
Pulse Sequence: CARBON (s2pul)
Solvent: cdcl3
Data collected on: Jul 2 2019
Temp. 25.0 C / 298.1 K
Operator: Liu
Relax. delay 1.000 sec
Pulse 45.0 degrees
Acq. time 1.049 sec
Width 31250.0 Hz
306 repetitions
OBSERVE C13, 125.6939763 MHz
DECOUPLE H1, 499.8787746 MHz
Power 43 dB
continuously on
WALTZ-16 modulated
DATA PROCESSING
Line broadening 0.5 Hz
FT size 65536
Total time 34 min
CN
Me
B(dan)
O
220 200 180 160 140 120 100 80 60 40 20 0 ppm

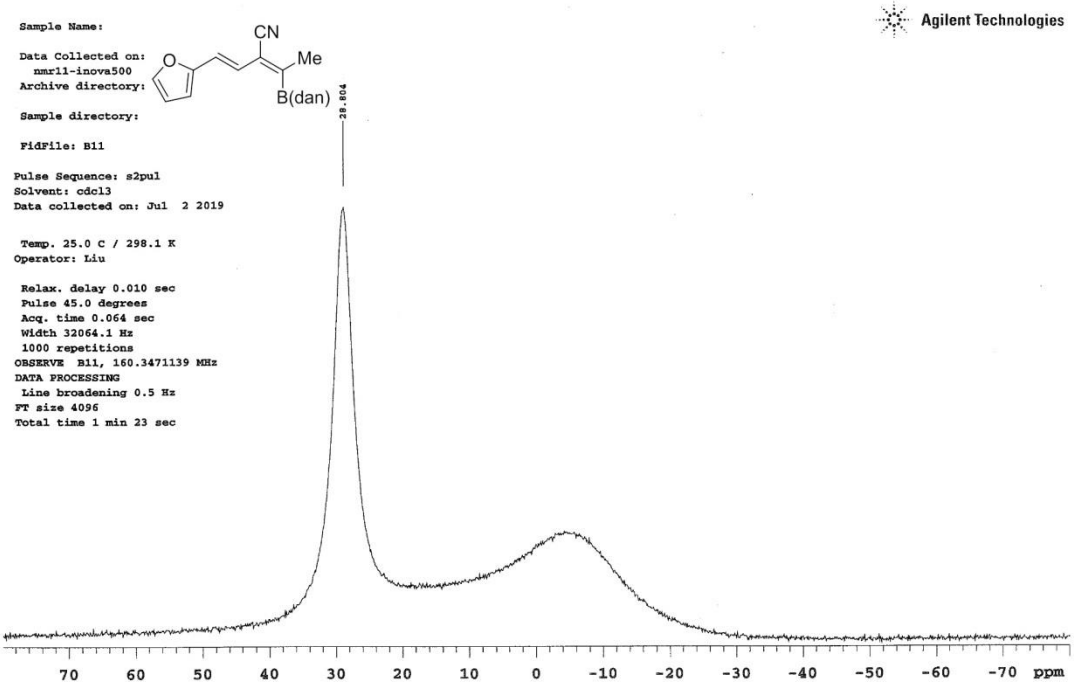
Agilent Technologies
Sample Name:
Data Collected on:
nmr11-inova500
Archive directory:
Sample directory:
FidFile: B11
Pulse Sequence: s2pul
Solvent: cdcl3
Data collected on: Jul 2 2019
Temp. 25.0 C / 298.1 K
Operator: Liu
Relax. delay 0.010 sec
Pulse 45.0 degrees
Acq. time 0.064 sec
Width 32064.1 Hz
1000 repetitions
OBSERVE B11, 160.3471139 MHz
DATA PROCESSING
Line broadening 0.5 Hz
FT size 4096
Total time 1 min 23 sec
CN
Me
B(dan)
O
28.804
70 60 50 40 30 20 10 0 -10 -20 -30 -40 -50 -60 -70 ppm

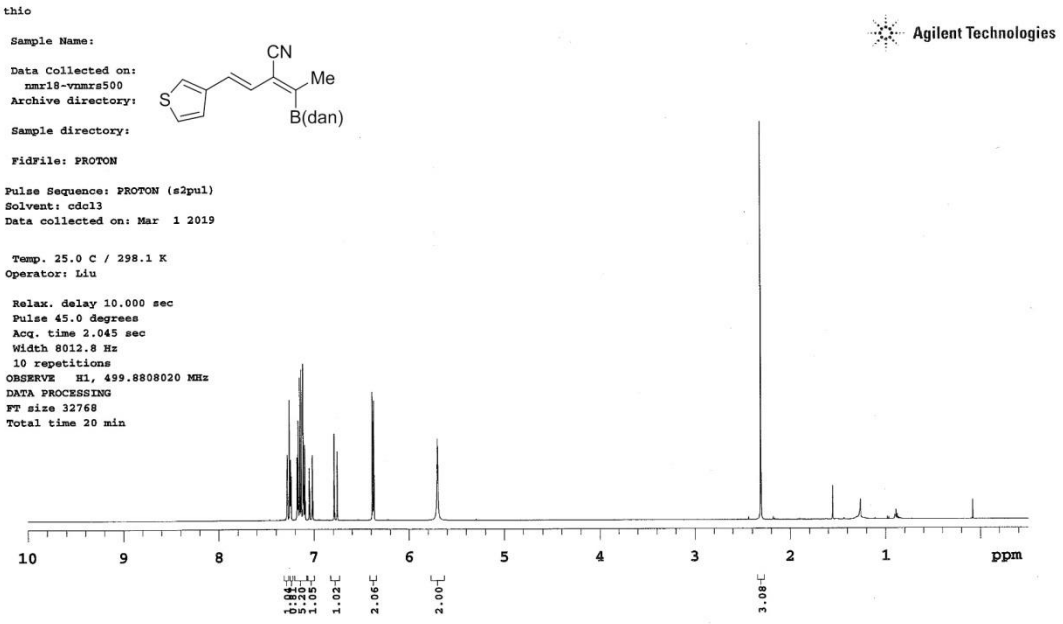
thio
Sample Name:
Data Collected on:
nmr18-vnmrs500
Archive directory:
Sample directory:
FidFile: PROTON
Pulse Sequence: PROTON (s2pul)
Solvent: cdcl3
Data collected on: Mar 1 2019
Temp. 25.0 C / 298.1 K
Operator: Liu
Relax. delay 10.000 sec
Pulse 45.0 degrees
Acq. time 2.045 sec
Width 8012.8 Hz
10 repetitions
OBSERVE H1, 499.8808020 MHz
DATA PROCESSING
FT size 32768
Total time 20 min
CN
Me
S
B(dan)
Agilent Technologies
10
9
8
7
6
5
4
3
2
1
ppm
0.84
5.20
1.05
1.02
2.06
2.00
3.08

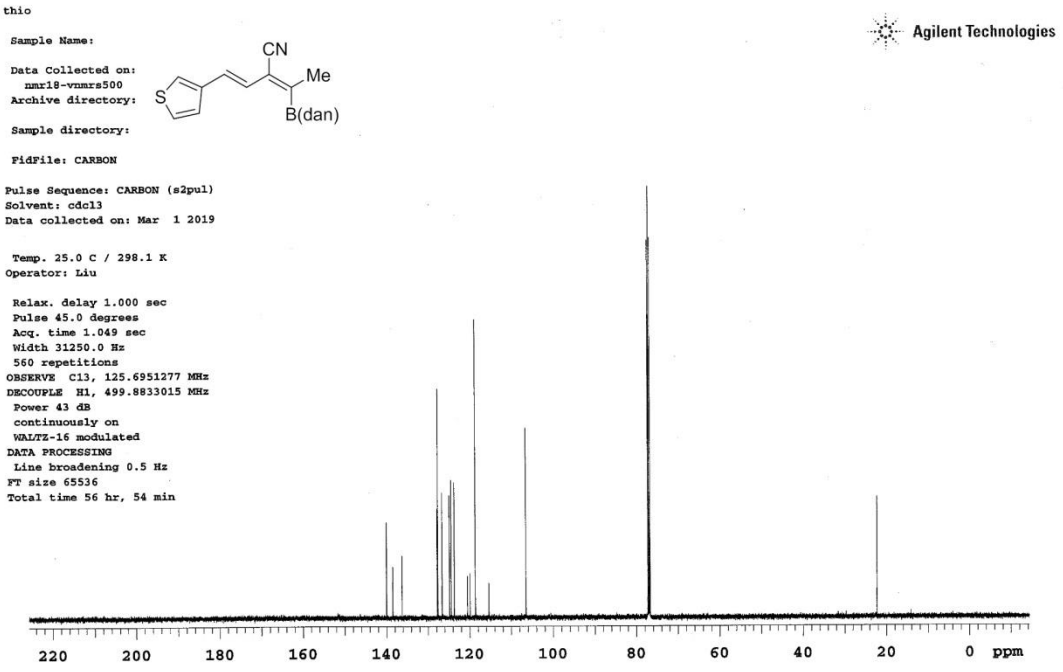
thio
Sample Name:
Data Collected on:
nmr18-vnmrs500
Archive directory:
Sample directory:
FidFile: CARBON
Pulse Sequence: CARBON (s2pul)
Solvent: cdcl3
Data collected on: Mar 1 2019
Temp. 25.0 C / 298.1 K
Operator: Liu
Relax. delay 1.000 sec
Pulse 45.0 degrees
Acq. time 1.049 sec
Width 31250.0 Hz
560 repetitions
OBSERVE C13, 125.6951277 MHz
DECOUPLE H1, 499.8833015 MHz
Power 43 dB
continuously on
WALTZ-16 modulated
DATA PROCESSING
Line broadening 0.5 Hz
FT size 65536
Total time 56 hr, 54 min
CN
Me
S
B(dan)
Agilent Technologies
220
200
180
160
140
120
100
80
60
40
20
0
ppm

thio

Agilent Technologies

Sample Name:

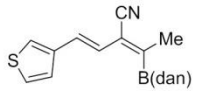

Data Collected on:
nmr11-inova500
Archive directory:

Sample directory:

FidFile: yz-3-190228-thio-B

Pulse Sequence: s2pul
Solvent: cdcl3
Data collected on: Feb 28 2019

Temp. 25.0 C / 298.1 K
Operator: Liu

Relax. delay 0.010 sec
Pulse 45.0 degrees
Acq. time 0.064 sec
Width 32064.1 Hz
1230 repetitions
OBSERVE B11, 160.3466912 MHz
DATA PROCESSING
Line broadening 0.5 Hz
FT size 4096
Total time 13 min

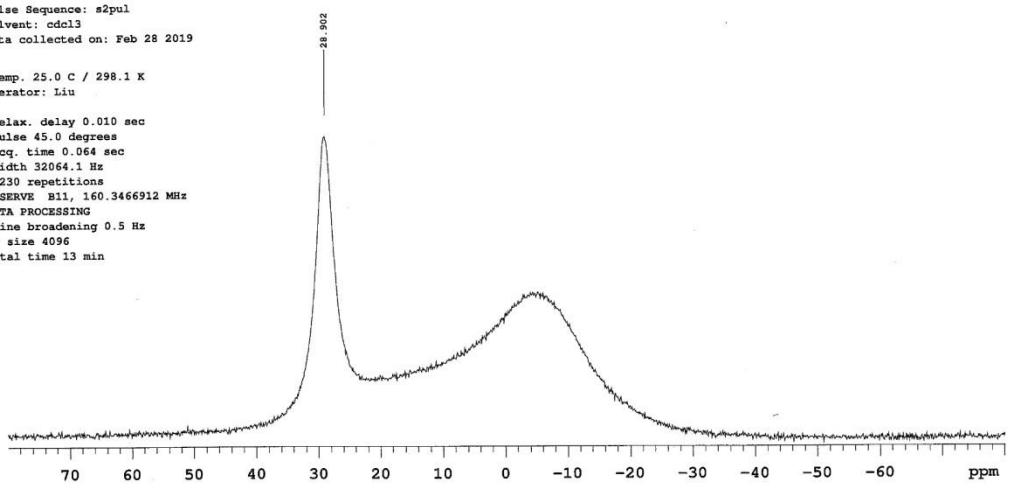

Sample Name:

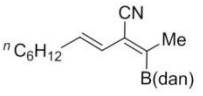

Data Collected on:
nmr19-vnmrs600
Archive directory:

Sample directory:

FidFile: PROTON

Pulse Sequence: PROTON (s2pul)
Solvent: cdcl3
Data collected on: Jun 6 2019

Temp. 25.0 C / 298.1 K
Operator: Liu

Relax. delay 10.000 sec
Pulse 45.0 degrees
Acq. time 1.704 sec
Width 9615.4 Hz
8 repetitions
OBSERVE H1, 599.6809043 MHz
DATA PROCESSING
FT size 32768
Total time 1 min 34 sec

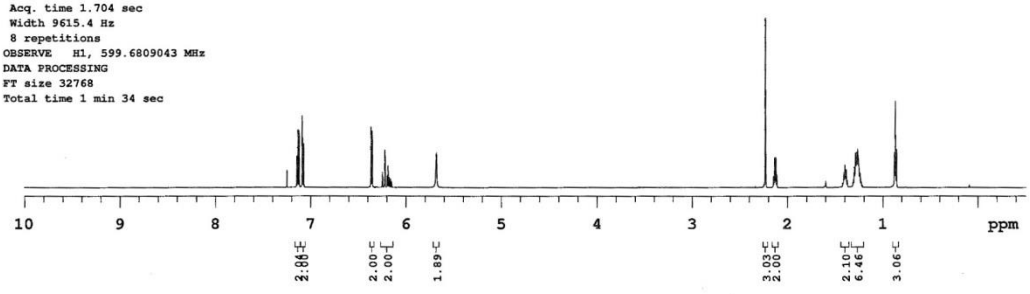

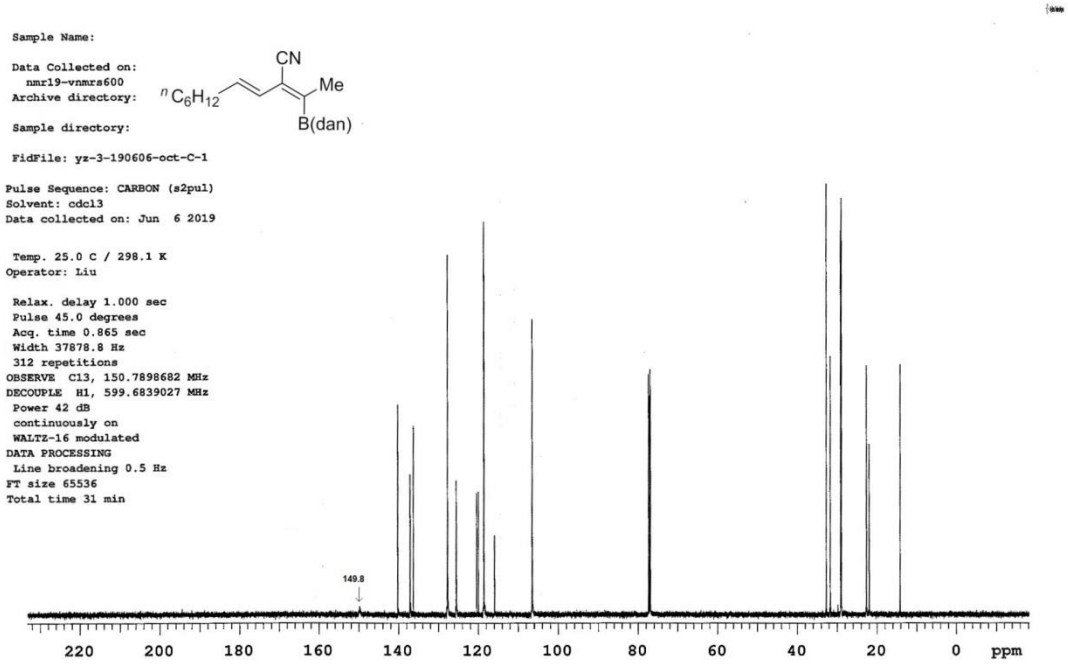
Sample Name:
Data Collected on:
nmr19-vnmrs600
Archive directory:
Sample directory:
FidFile: yz-3-190606-oct-C-1
Pulse Sequence: CARBON (s2pul)
Solvent: cdcl3
Data collected on: Jun 6 2019
Temp. 25.0 C / 298.1 K
Operator: Liu
Relax. delay 1.000 sec
Pulse 45.0 degrees
Acq. time 0.865 sec
Width 37878.8 Hz
312 repetitions
OBSERVE C13, 150.7898682 MHz
DECOUPLE H1, 599.6839027 MHz
Power 42 dB
continuously on
WALTZ-16 modulated
DATA PROCESSING
Line broadening 0.5 Hz
FT size 65536
Total time 31 min
CN
Me
B(dan)
149.8
220
200
180
160
140
120
100
80
60
40
20
0
ppm

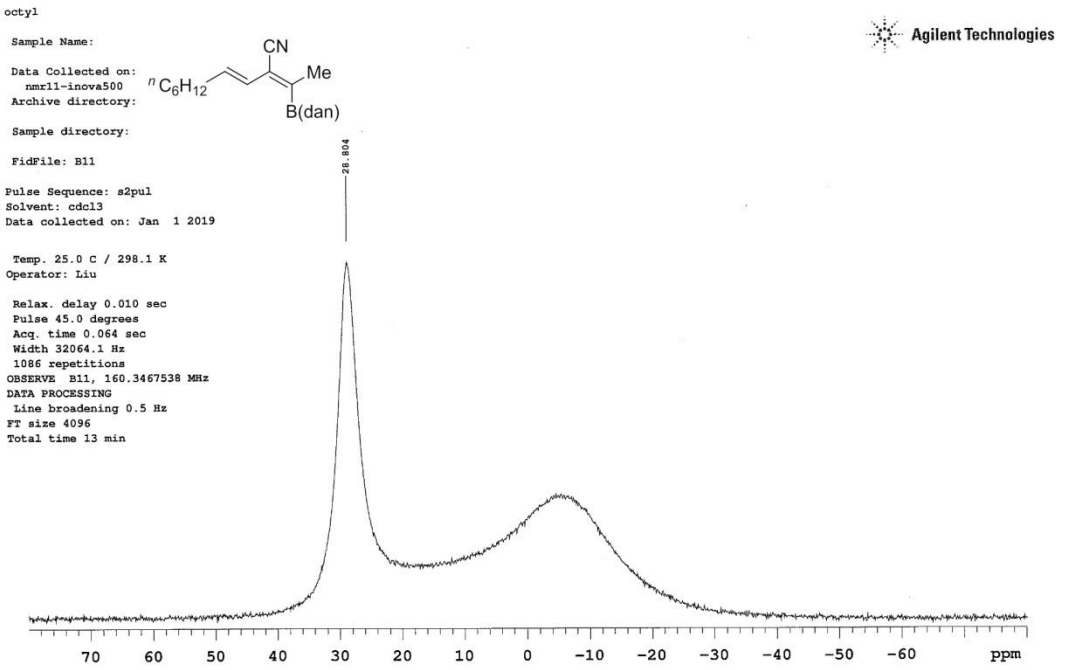
octyl
Agilent Technologies
Sample Name:
Data Collected on:
nmr11-inova500
Archive directory:
Sample directory:
FidFile: B11
Pulse Sequence: s2pul
Solvent: cdcl3
Data collected on: Jan 1 2019
Temp. 25.0 C / 298.1 K
Operator: Liu
Relax. delay 0.010 sec
Pulse 45.0 degrees
Acq. time 0.064 sec
Width 32064.1 Hz
1086 repetitions
OBSERVE B11, 160.3467538 MHz
DATA PROCESSING
Line broadening 0.5 Hz
FT size 4096
Total time 13 min
CN
Me
B(dan)
28.804
70
60
50
40
30
20
10
0
-10
-20
-30
-40
-50
-60
ppm

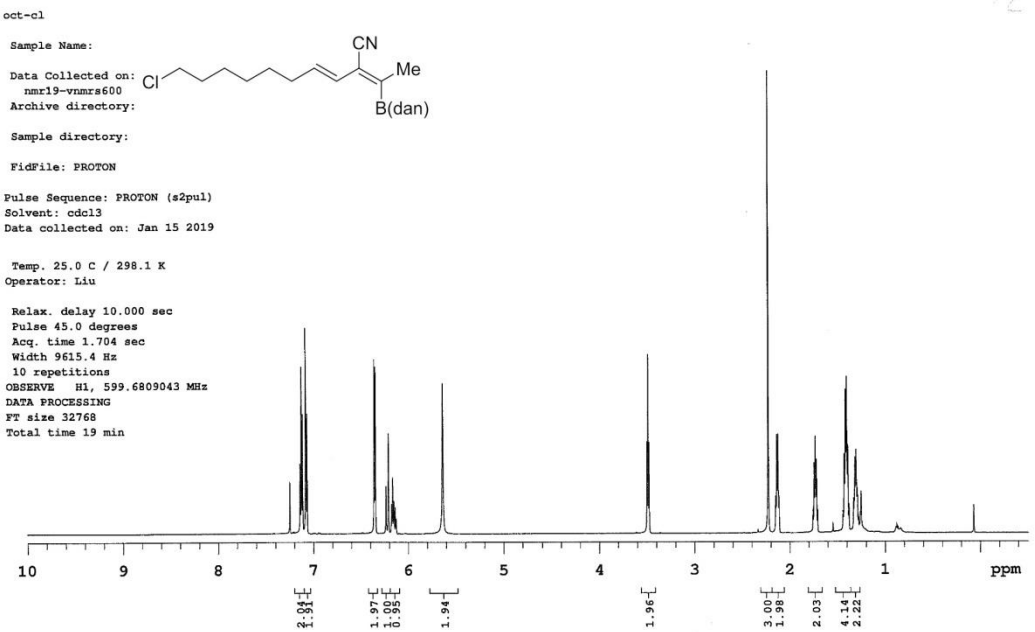
oct-cl
Sample Name:
Data Collected on:
nmr19-vnmrs600
Archive directory:
Sample directory:
FidFile: PROTON
Pulse Sequence: PROTON (s2pul)
Solvent: cdcl3
Data collected on: Jan 15 2019
Temp. 25.0 C / 298.1 K
Operator: Liu
Relax. delay 10.000 sec
Pulse 45.0 degrees
Acq. time 1.704 sec
Width 9615.4 Hz
10 repetitions
OBSERVE H1, 599.6809043 MHz
DATA PROCESSING
FT size 32768
Total time 19 min
CN
Me
Cl
B(dan)
10
9
8
7
6
5
4
3
2
1
ppm
2.04
2.01
1.97
1.00
0.95
1.94
1.96
3.00
1.98
2.03
4.14
2.22

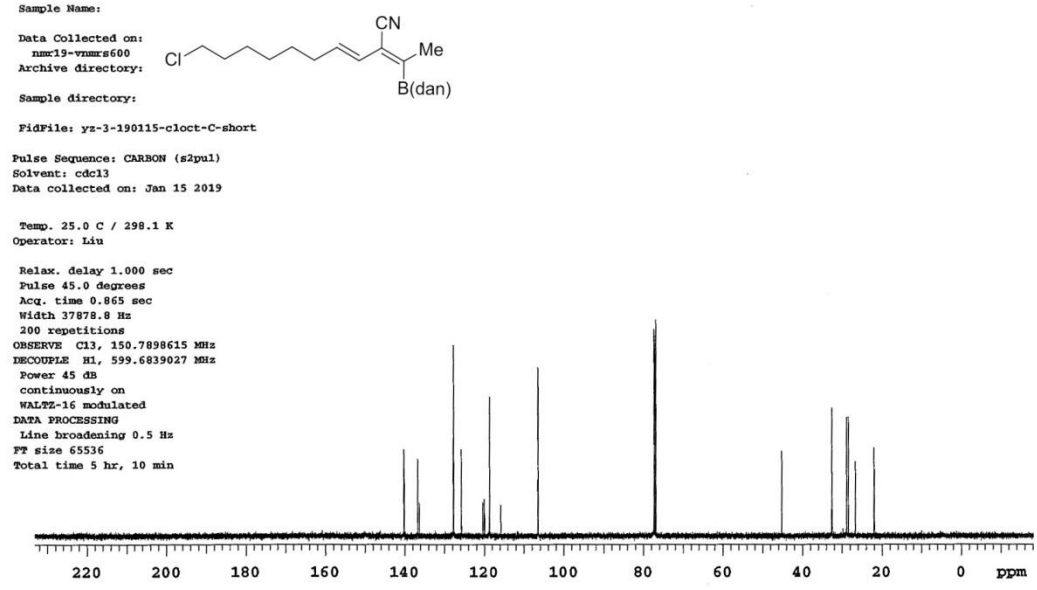
Sample Name:
Data Collected on:
nmr19-vnmrs600
Archive directory:
Sample directory:
FidFile: yz-3-190115-cloct-C-short
Pulse Sequence: CARBON (s2pul)
Solvent: cdcl3
Data collected on: Jan 15 2019
Temp. 25.0 C / 298.1 K
Operator: Liu
Relax. delay 1.000 sec
Pulse 45.0 degrees
Acq. time 0.865 sec
Width 37878.8 Hz
200 repetitions
OBSERVE C13, 150.7898615 MHz
DECOUPLE H1, 599.6839027 MHz
Power 45 dB
continuously on
WALTZ-16 modulated
DATA PROCESSING
Line broadening 0.5 Hz
FT size 65536
Total time 5 hr, 10 min
CN
Me
Cl
B(dan)
220
200
180
160
140
120
100
80
60
40
20
0
ppm

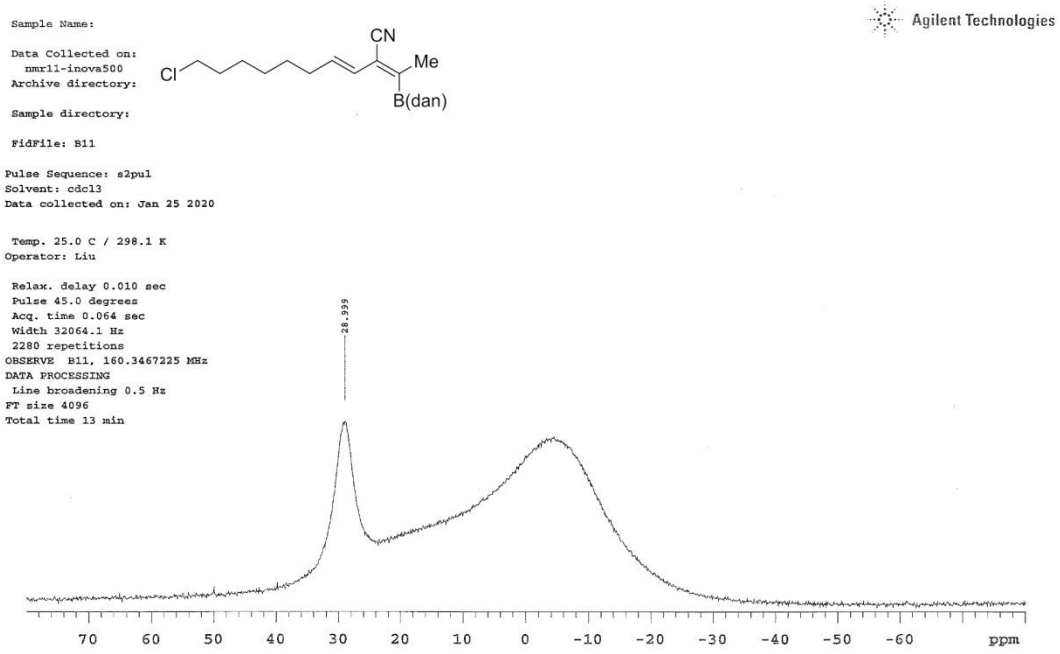
Agilent Technologies
Sample Name:
Data Collected on:
nmr11-inova500
Archive directory:
Sample directory:
FidFile: B11
Pulse Sequence: s2pul
Solvent: cdcl3
Data collected on: Jan 25 2020
Temp. 25.0 C / 298.1 K
Operator: Liu
Relax. delay 0.010 sec
Pulse 45.0 degrees
Acq. time 0.064 sec
Width 32064.1 Hz
2280 repetitions
OBSERVE B11, 160.3467225 MHz
DATA PROCESSING
Line broadening 0.5 Hz
FT size 4096
Total time 13 min
CN
Me
Cl
B(dan)
28.999
70 60 50 40 30 20 10 0 -10 -20 -30 -40 -50 -60 ppm

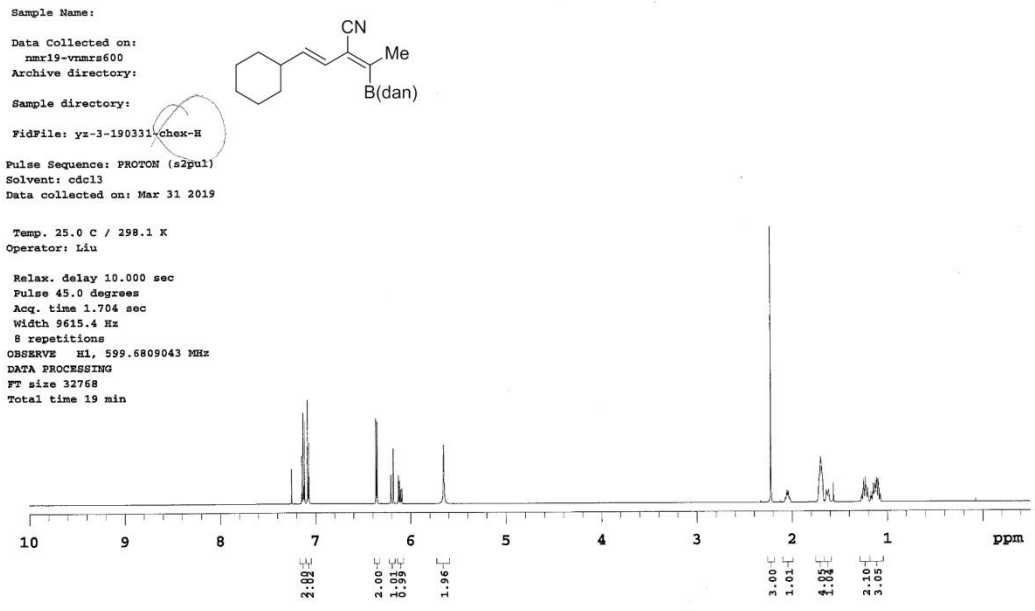
Sample Name:
Data Collected on:
nmr19-vnmrs600
Archive directory:
Sample directory:
FidFile: yz-3-190331-chex-H
Pulse Sequence: PROTON (s2pul)
Solvent: cdcl3
Data collected on: Mar 31 2019
Temp. 25.0 C / 298.1 K
Operator: Liu
Relax. delay 10.000 sec
Pulse 45.0 degrees
Acq. time 1.704 sec
Width 9615.4 Hz
8 repetitions
OBSERVE H1, 599.6809043 MHz
DATA PROCESSING
FT size 32768
Total time 19 min
CN
Me
B(dan)
10 9 8 7 6 5 4 3 2 1 ppm
2.02
2.00
1.99
0.99
1.96
3.00
1.01
4.05
1.04
2.10
3.05

Sample Name:

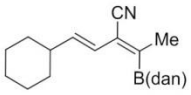

Data Collected on:
nmr19-vnmrs600
Archive directory:

Sample directory:

FidFile: yz-3-190331-chex-c

Pulse Sequence: CARBON (s2pul)
Solvent: cdcl3
Data collected on: Mar 31 2019

Temp. 25.0 C / 298.1 K
Operator: Liu

Relax. delay 1.000 sec
Pulse 45.0 degrees
Acq. time 0.865 sec
Width 37878.8 Hz
23176 repetitions
OBSERVE C13, 150.7898628 MHz
DECOUPLE H1, 599.6839027 MHz
Power 42 dB
continuously on
WALTZ-16 modulated
DATA PROCESSING
Line broadening 3.0 Hz
FT size 65536
Total time 12 hr, 57 min

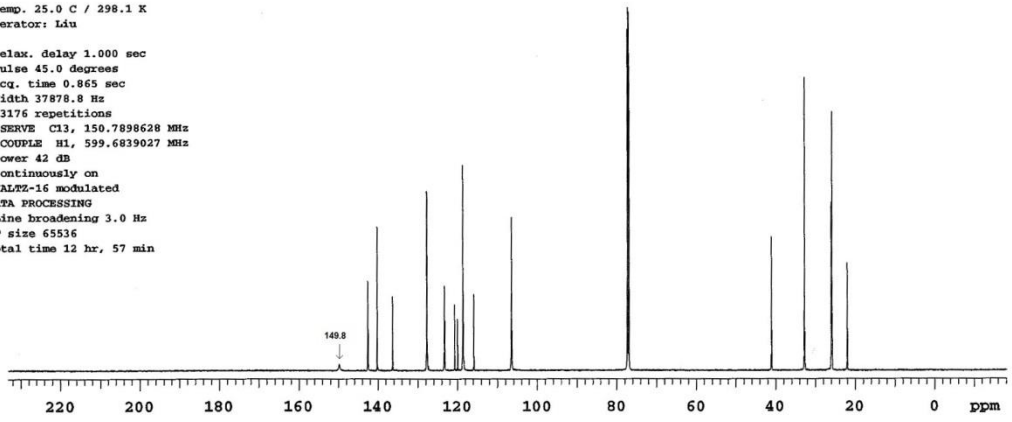

Agilent Technologies

Sample Name:

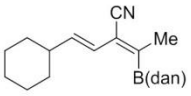

Data Collected on:
nmr11-inova500
Archive directory:

Sample directory:

FidFile: B11

Pulse Sequence: s2pul
Solvent: cdcl3
Data collected on: Apr 1 2019

Temp. 25.0 C / 298.1 K
Operator: Liu

Relax. delay 0.010 sec
Pulse 45.0 degrees
Acq. time 0.064 sec
Width 32064.1 Hz
2008 repetitions
OBSERVE B11, 160.3466755 MHz
DATA PROCESSING
Line broadening 0.5 Hz
FT size 4096
Total time 13 min

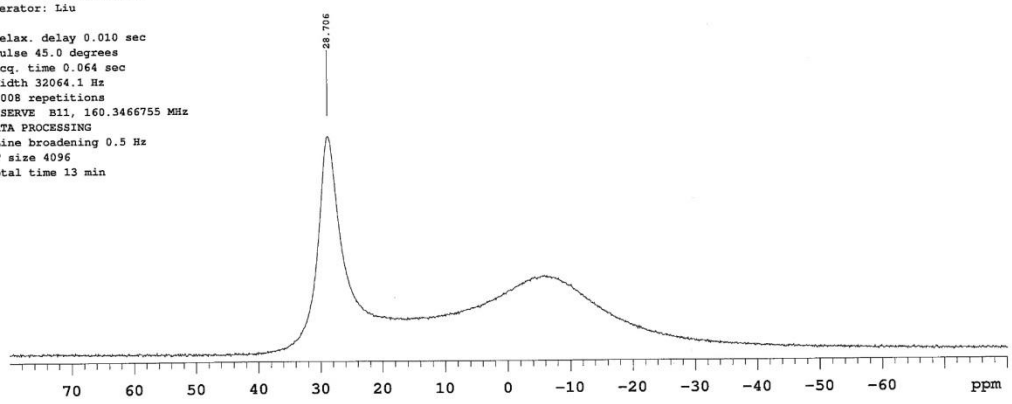

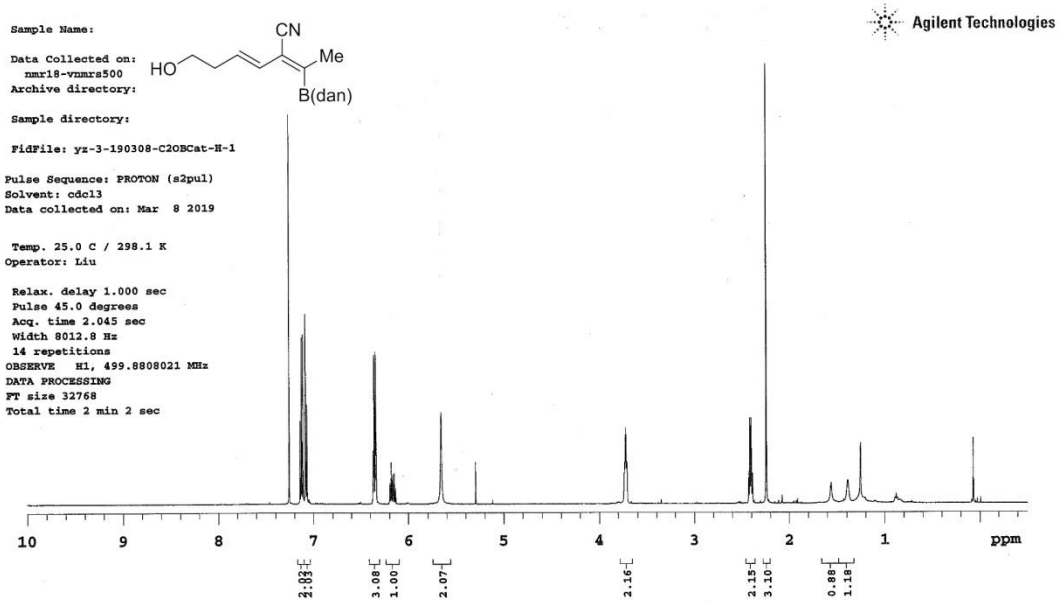
Agilent Technologies
Sample Name:
Data Collected on:
nmr18-vnmrs500
Archive directory:
Sample directory:
FidFile: yz-3-190308-C2OBCat-H-1
Pulse Sequence: PROTON (s2pul)
Solvent: cdcl3
Data collected on: Mar 8 2019
Temp. 25.0 C / 298.1 K
Operator: Liu
Relax. delay 1.000 sec
Pulse 45.0 degrees
Acq. time 2.045 sec
Width 8012.8 Hz
14 repetitions
OBSERVE H1, 499.8808021 MHz
DATA PROCESSING
FT size 32768
Total time 2 min 2 sec
CN
Me
HO
B(dan)
10
9
8
7
6
5
4
3
2
1
ppm
2.03
3.08
1.00
2.07
2.16
2.15
3.10
0.88
1.18

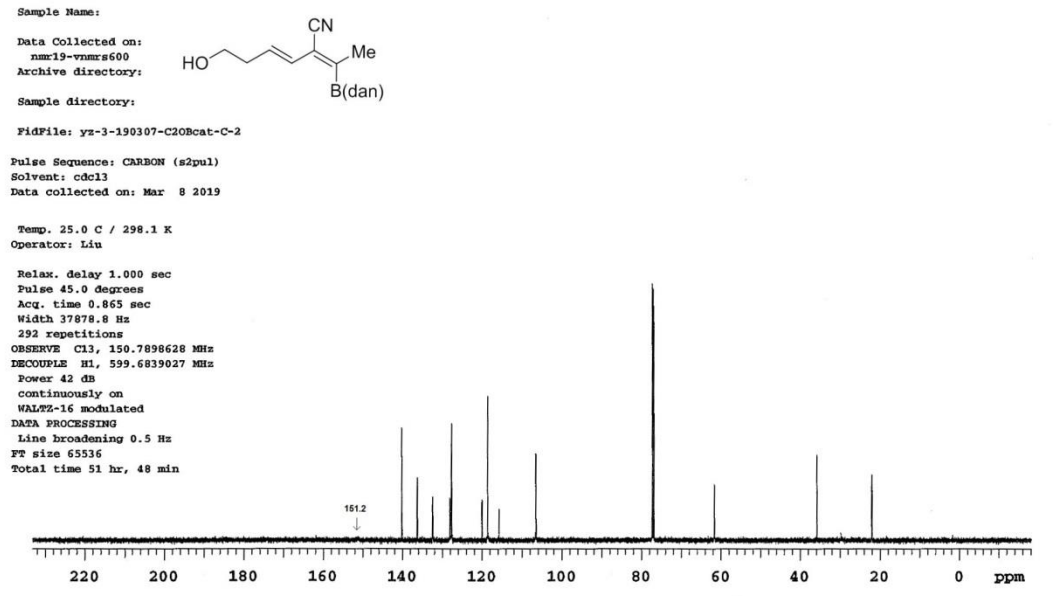
Sample Name:
Data Collected on:
nmr19-vnmrs600
Archive directory:
Sample directory:
FidFile: yz-3-190307-C2OBcat-C-2
Pulse Sequence: CARBON (s2pul)
Solvent: cdcl3
Data collected on: Mar 8 2019
Temp. 25.0 C / 298.1 K
Operator: Liu
Relax. delay 1.000 sec
Pulse 45.0 degrees
Acq. time 0.865 sec
Width 37878.8 Hz
292 repetitions
OBSERVE C13, 150.7898628 MHz
DECOUPLE H1, 599.6839027 MHz
Power 42 dB
continuously on
WALTZ-16 modulated
DATA PROCESSING
Line broadening 0.5 Hz
FT size 65536
Total time 51 hr, 48 min
CN
Me
HO
B(dan)
151.2
220
200
180
160
140
120
100
80
60
40
20
0
ppm

Agilent Technologies

Sample Name:

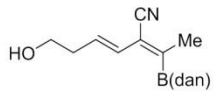

Data Collected on:
nmr11-inova500
Archive directory:

Sample directory:

FidFile: B11

Pulse Sequence: s2pul
Solvent: cdcl3
Data collected on: Mar 8 2019

Temp. 25.0 C / 298.1 K
Operator: Liu

Relax. delay 0.010 sec
Pulse 45.0 degrees
Acq. time 0.064 sec
Width 32064.1 Hz
1022 repetitions
OBSERVE B11, 160.3467382 MHz
DATA PROCESSING
Line broadening 0.5 Hz
FT size 4096
Total time 2 hr, 18 min

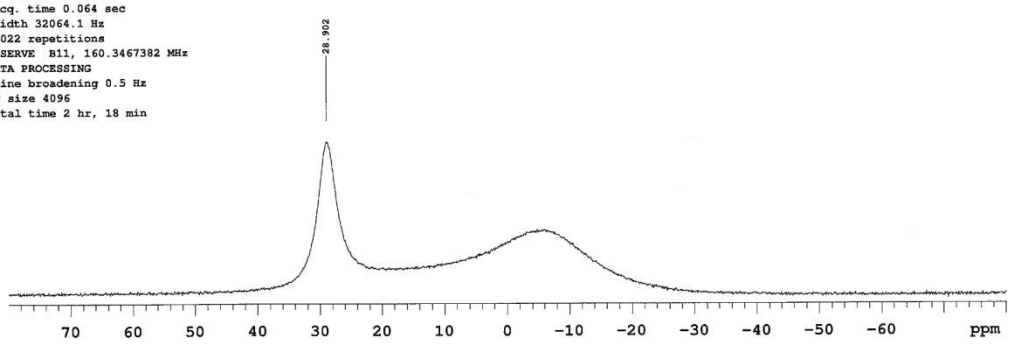

Sample Name:

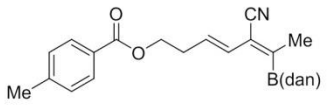

Data Collected on:
nmr19-vnmrs600
Archive directory:

Sample directory:

FidFile: PROTON

Pulse Sequence: PROTON (s2pul)
Solvent: cdcl3
Data collected on: Jun 14 2019

Temp. 25.0 C / 298.1 K
Operator: Liu

Relax. delay 10.000 sec
Pulse 45.0 degrees
Acq. time 1.704 sec
Width 9615.4 Hz
8 repetitions
OBSERVE H1, 599.6809043 MHz
DATA PROCESSING
FT size 32768
Total time 1 min 34 sec

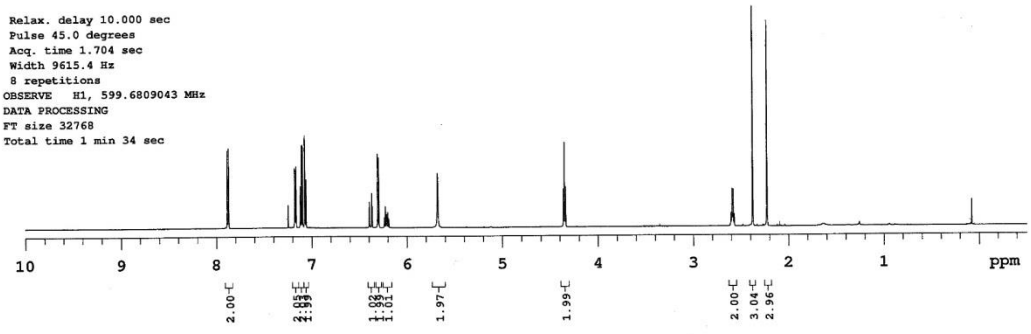

Sample Name:

Data Collected on:
nmr19-vnmrs600
Archive directory:

Sample directory:

FidFile: yz-3-190614-phco2-C

Pulse Sequence: CARBON (s2pul)
Solvent: cdcl3
Data collected on: Jun 14 2019

Temp. 25.0 C / 298.1 K
Operator: Liu

Relax. delay 1.000 sec
Pulse 45.0 degrees
Acq. time 0.865 sec
Width 37878.8 Hz
1960 repetitions
OBSERVE C13, 150.7898662 MHz
DECOUPLE H1, 599.6839027 MHz
Power 42 dB
continuously on
WALTZ-16 modulated
DATA PROCESSING
Line broadening 0.5 Hz
FT size 65536
Total time 5 hr, 10 min

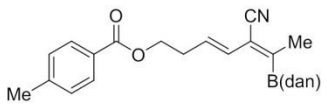

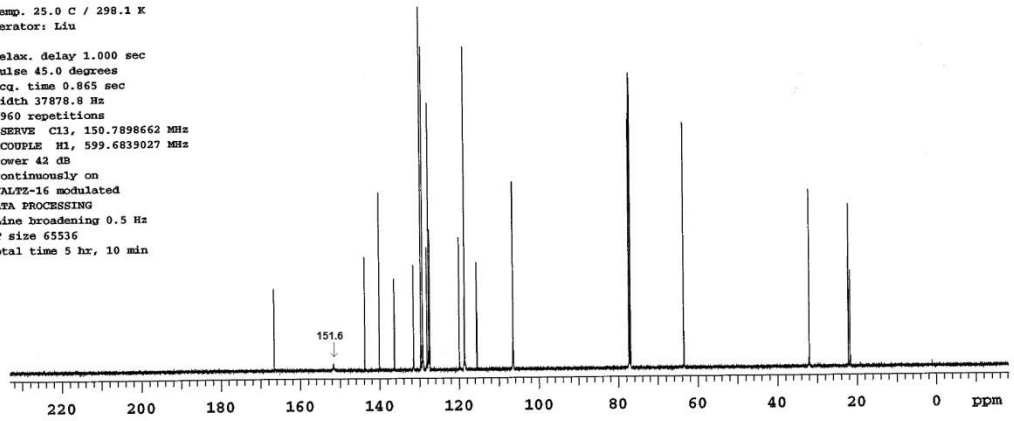

Agilent Technologies

Sample Name:

Data Collected on:
nmr11-inova500
Archive directory:

Sample directory:

FidFile: B11

Pulse Sequence: s2pul
Solvent: cdcl3
Data collected on: Jun 12 2019

Temp. 25.0 C / 298.1 K
Operator: Liu

Relax. delay 0.010 sec
Pulse 45.0 degrees
Acq. time 0.064 sec
Width 32064.1 Hz
1244 repetitions
OBSERVE B11, 160.3470826 MHz
DATA PROCESSING
Line broadening 0.5 Hz
FT size 4096
Total time 13 min

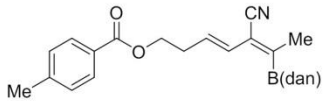

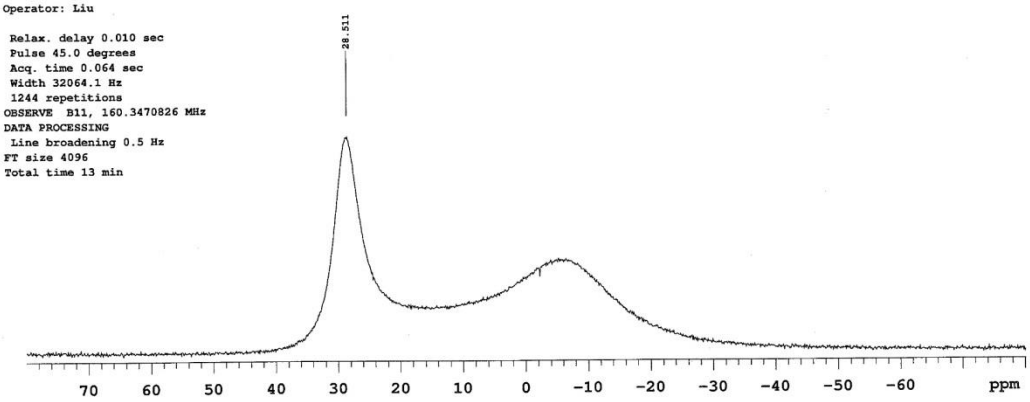

Sample Name:

Data Collected on:
nmr18-vnmrs500
Archive directory:

Sample directory:

FidFile: yz-3-190509-Et-H

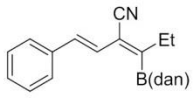

Pulse Sequence: PROTON (s2pul)
Solvent: cdcl3
Data collected on: May 9 2019

Temp. 25.0 C / 298.1 K
Operator: Liu

Relax. delay 10.000 sec
Pulse 45.0 degrees
Acq. time 2.045 sec
Width 8012.8 Hz
8 repetitions
OBSERVE H1, 499.8762752 MHz
DATA PROCESSING
FT size 32768
Total time 20 min

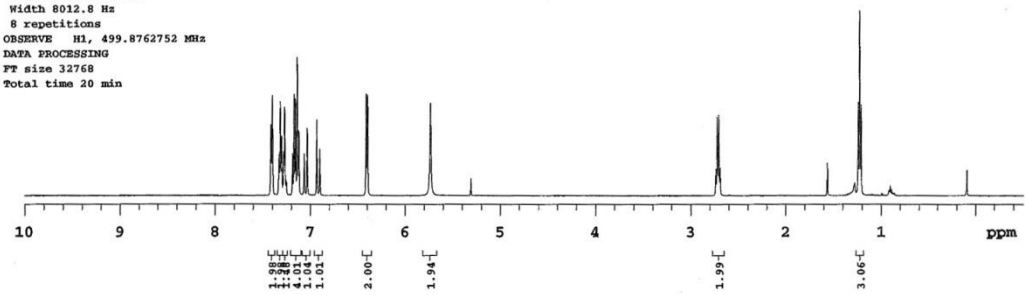

Agilent Technologies

Sample Name:

Data Collected on:
nmr18-vnmrs500
Archive directory:

Sample directory:

FidFile: CARBON

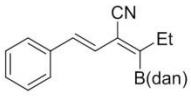

Pulse Sequence: CARBON (s2pul)
Solvent: cdcl3
Data collected on: May 5 2019

Temp. 25.0 C / 298.1 K
Operator: Liu

Relax. delay 1.000 sec
Pulse 45.0 degrees
Acq. time 1.049 sec
Width 31250.0 Hz
1102 repetitions
OBSERVE C13, 125.6939894 MHz
DECOUPLE H1, 499.8787746 MHz
Power 43 dB
continuously on
WALTZ-16 modulated
DATA PROCESSING
Line broadening 0.5 Hz
FT size 65536
Total time 22 hr, 45 min

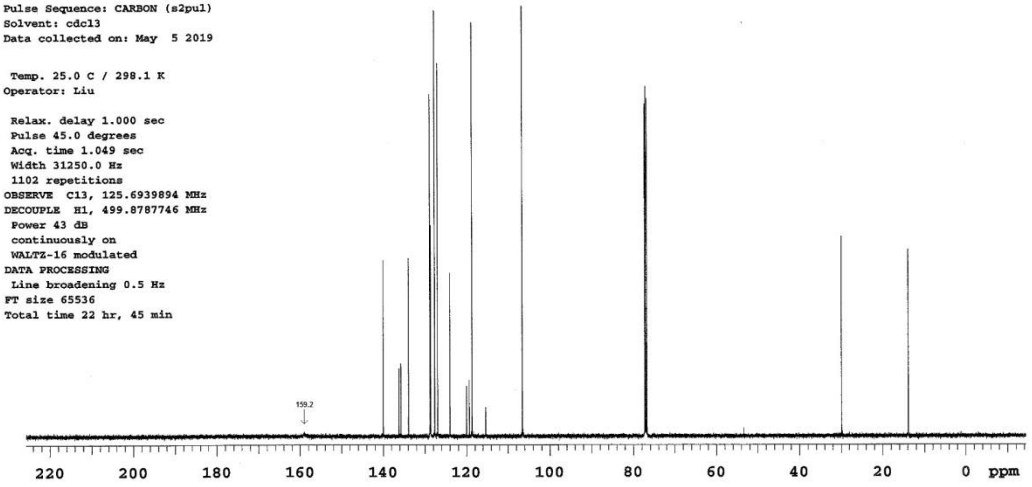

Agilent Technologies

Sample Name:

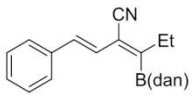

Data Collected on:
nmr11-inova500
Archive directory:

Sample directory:

FidFile: B11

Pulse Sequence: s2pul
Solvent: cdcl3
Data collected on: May 5 2019

Temp. 25.0 C / 298.1 K
Operator: Liu

Relax. delay 0.010 sec
Pulse 45.0 degrees
Acq. time 0.064 sec
Width 32064.1 Hz
1350 repetitions
OBSERVE B11, 160.3467538 MHz
DATA PROCESSING
Line broadening 0.5 Hz
FT size 4096
Total time 2 hr, 18 min

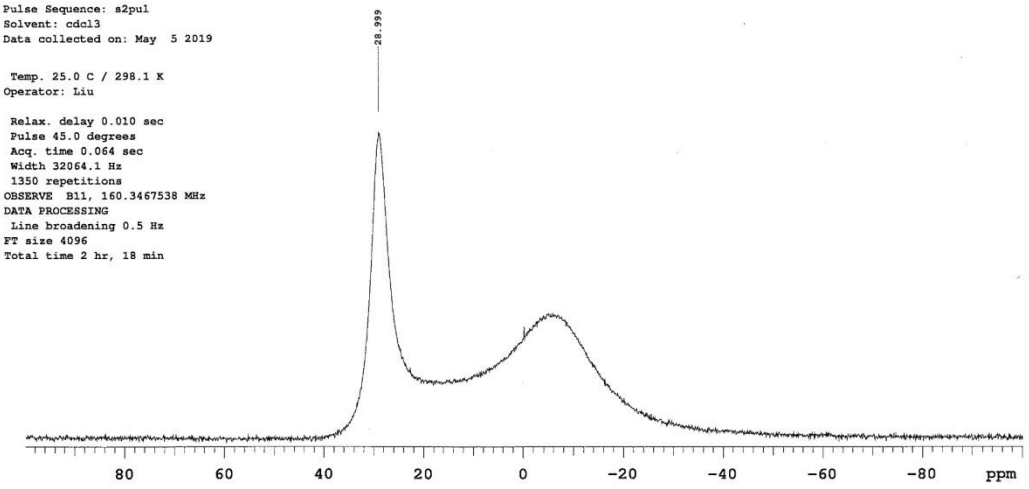

Agilent Technologies

Sample Name:

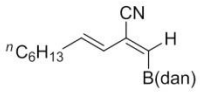

Data Collected on:
nmr18-vnmrs500
Archive directory:

Sample directory:

FidFile: PROTON

Pulse Sequence: PROTON (s2pul)
Solvent: cdcl3
Data collected on: Mar 17 2020

Temp. 25.0 C / 298.1 K
Operator: Liu

Relax. delay 10.000 sec
Pulse 45.0 degrees
Acq. time 2.045 sec
Width 8012.8 Hz
7 repetitions
OBSERVE H1, 499.8760066 MHz
DATA PROCESSING
FT size 32768
Total time 2 min 0 sec

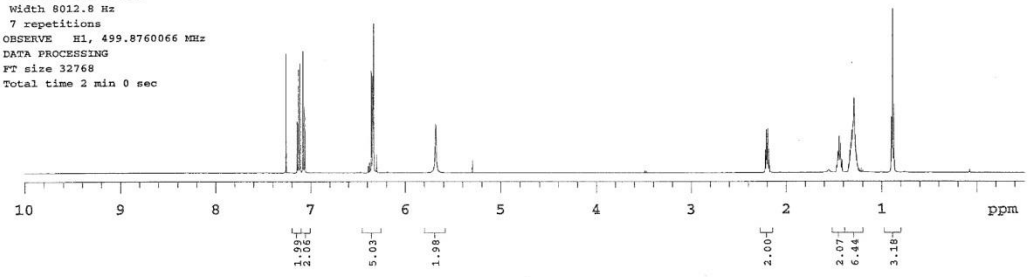

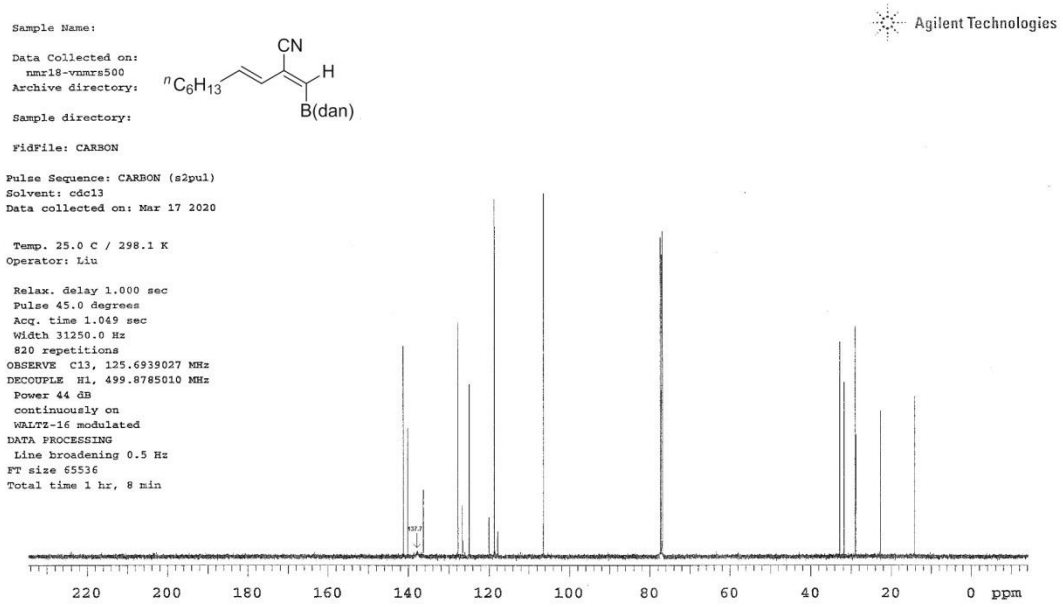
Agilent Technologies
Sample Name:
Data Collected on:
nmr18-vnmrs500
Archive directory:
Sample directory:
FidFile: CARBON
CN
H
$^{n}C_6H_{13}$
B(dan)
Pulse Sequence: CARBON (s2pul)
Solvent: cdcl3
Data collected on: Mar 17 2020
Temp. 25.0 C / 298.1 K
Operator: Liu
Relax. delay 1.000 sec
Pulse 45.0 degrees
Acq. time 1.049 sec
Width 31250.0 Hz
820 repetitions
OBSERVE C13, 125.6939027 MHz
DECOUPLE H1, 499.8785010 MHz
Power 44 dB
continuously on
WALTZ-16 modulated
DATA PROCESSING
Line broadening 0.5 Hz
FT size 65536
Total time 1 hr, 8 min
137.7
220 200 180 160 140 120 100 80 60 40 20 0 ppm

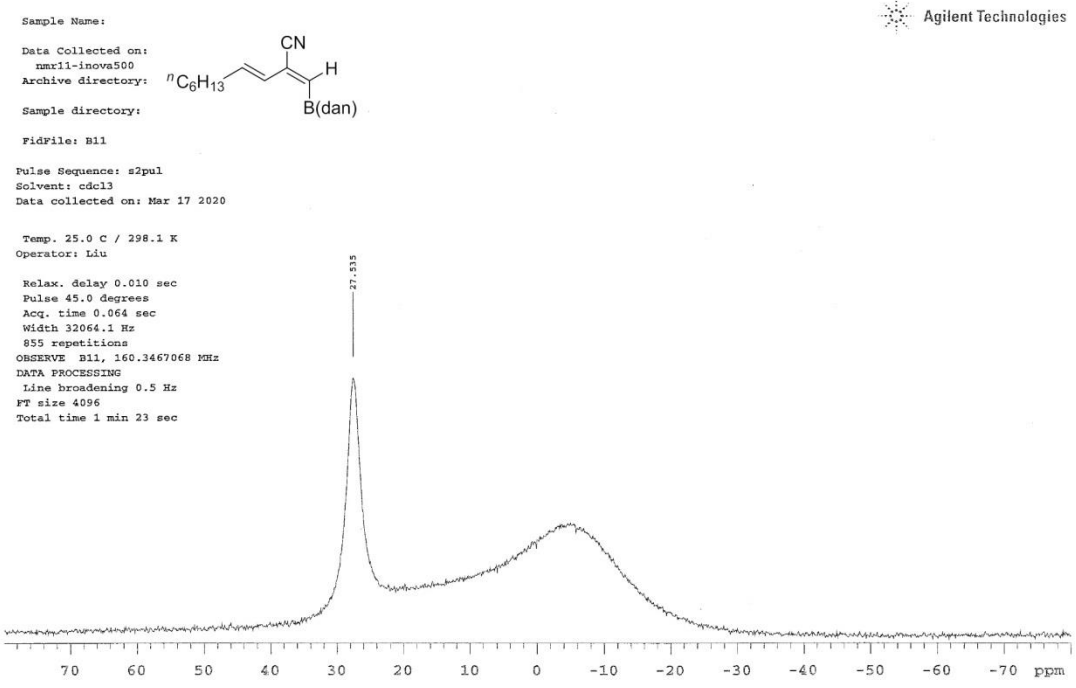
Agilent Technologies
Sample Name:
Data Collected on:
nmr11-inova500
Archive directory:
Sample directory:
FidFile: B11
CN
H
$^{n}C_6H_{13}$
B(dan)
Pulse Sequence: s2pul
Solvent: cdcl3
Data collected on: Mar 17 2020
Temp. 25.0 C / 298.1 K
Operator: Liu
Relax. delay 0.010 sec
Pulse 45.0 degrees
Acq. time 0.064 sec
Width 32064.1 Hz
855 repetitions
OBSERVE B11, 160.3467068 MHz
DATA PROCESSING
Line broadening 0.5 Hz
FT size 4096
Total time 1 min 23 sec
27.535
70 60 50 40 30 20 10 0 -10 -20 -30 -40 -50 -60 -70 ppm

Agilent Technologies

Sample Name:

Data Collected on:
nmr18-vnmrs500
Archive directory:

Sample directory:

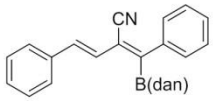

FidFile: PROTON

Pulse Sequence: PROTON (s2pul)
Solvent: cdcl3
Data collected on: Feb 3 2020

Temp. 25.0 C / 298.1 K
Operator: Liu

Relax. delay 10.000 sec
Pulse 45.0 degrees
Acq. time 2.045 sec
Width 8012.8 Hz
10 repetitions
OBSERVE H1, 499.8760042 MHz
DATA PROCESSING
FT size 32768
Total time 2 min 0 sec

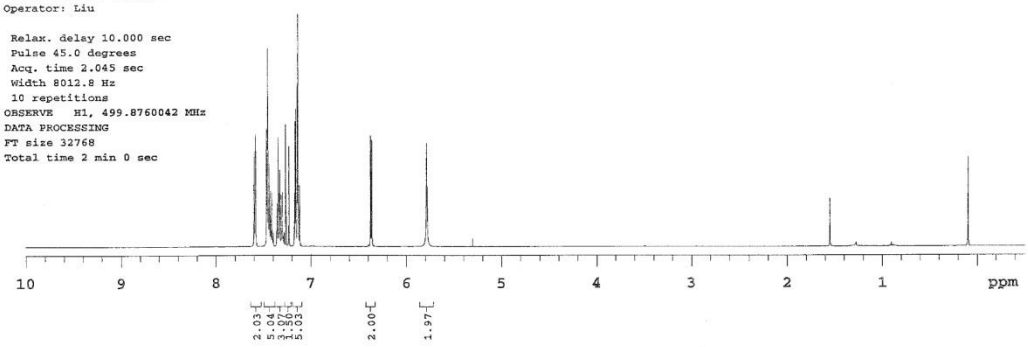

Sample Name:

Data Collected on:
nmr19-vnmrs600
Archive directory:

Sample directory:

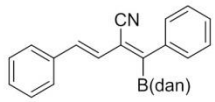

FidFile: CARBON

Pulse Sequence: CARBON (s2pul)
Solvent: cdcl3
Data collected on: May 22 2019

Temp. 25.0 C / 298.1 K
Operator: Liu

Relax. delay 1.000 sec
Pulse 45.0 degrees
Acq. time 0.865 sec
Width 37878.8 Hz
824 repetitions
OBSERVE C13, 150.7898628 MHz
DECOUPLE H1, 599.6839027 MHz
Power 42 dB
continuously on
WALTZ-16 modulated
DATA PROCESSING
Line broadening 0.5 Hz
FT size 65536
Total time 2 hr, 4 min

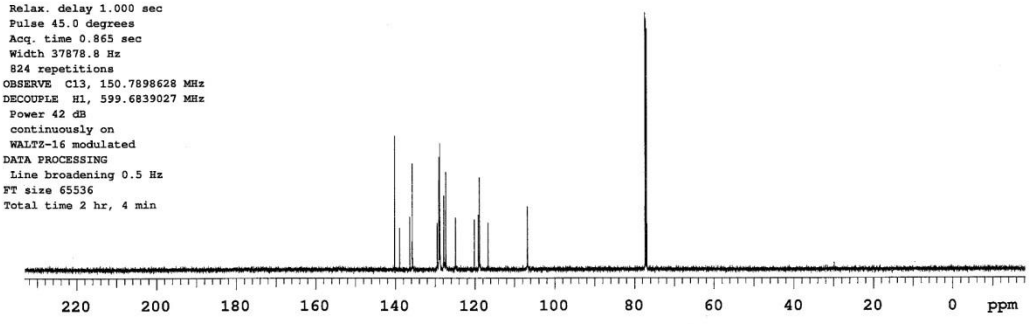

Agilent Technologies

Sample Name:

Data Collected on:
nmr11-inova500
Archive directory:

Sample directory:

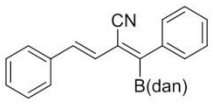

FidFile: B11

Pulse Sequence: s2pul
Solvent: cdcl3
Data collected on: May 22 2019

Temp. 25.0 C / 298.1 K
Operator: Liu

Relax. delay 0.010 sec
Pulse 45.0 degrees
Acq. time 0.064 sec
Width 32064.1 Hz
1000 repetitions
OBSERVE B11, 160.3467538 MHz
DATA PROCESSING
Line broadening 0.5 Hz
FT size 4096
Total time 1 min 23 sec

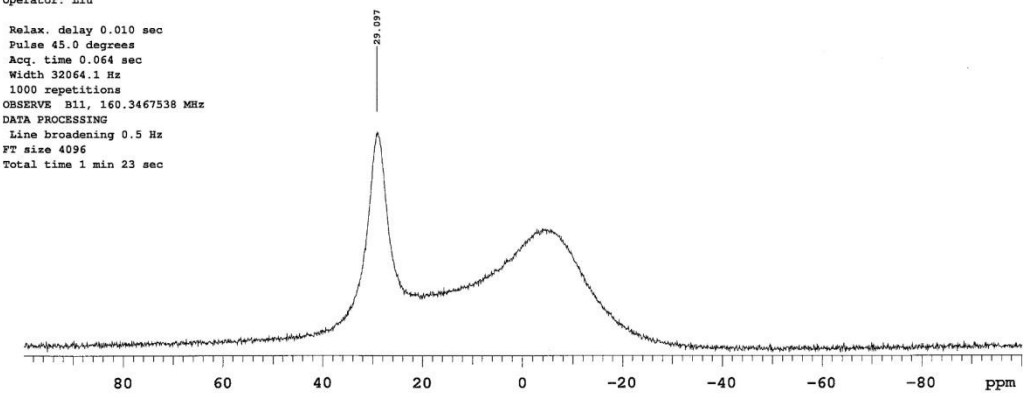

Agilent Technologies

Sample Name:

Data Collected on:
nmr18-vnmrs500
Archive directory:

Sample directory:

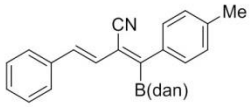

FidFile: PROTON

Pulse Sequence: PROTON (s2pul)
Solvent: cdcl3
Data collected on: Feb 23 2020

Temp. 25.0 C / 298.1 K
Operator: Liu

Relax. delay 10.000 sec
Pulse 45.0 degrees
Acq. time 2.045 sec
Width 8012.8 Hz
6 repetitions
OBSERVE H1, 499.8760059 MHz
DATA PROCESSING
FT size 32768
Total time 1 min 12 sec

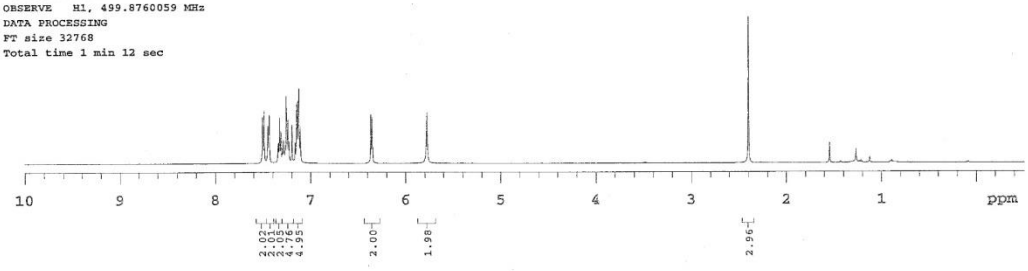

Sample Name:

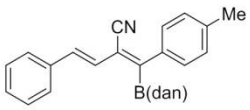

Data Collected on:
nmr18-vnmrs500
Archive directory:

Sample directory:

FidFile: CARBON

Pulse Sequence: CARBON (s2pul)
Solvent: cdcl3
Data collected on: May 26 2019

Temp. 25.0 C / 298.1 K
Operator: Liu

Relax. delay 1.000 sec
Pulse 45.0 degrees
Acq. time 1.049 sec
Width 31250.0 Hz
800 repetitions
OBSERVE C13, 125.6939658 MHz
DECOUPLE H1, 499.8787746 MHz
Power 43 dB
continuously on
WALTZ-16 modulated
DATA PROCESSING
Line broadening 0.5 Hz
FT size 65536
Total time 1 hr, 42 min

Agilent Technologies

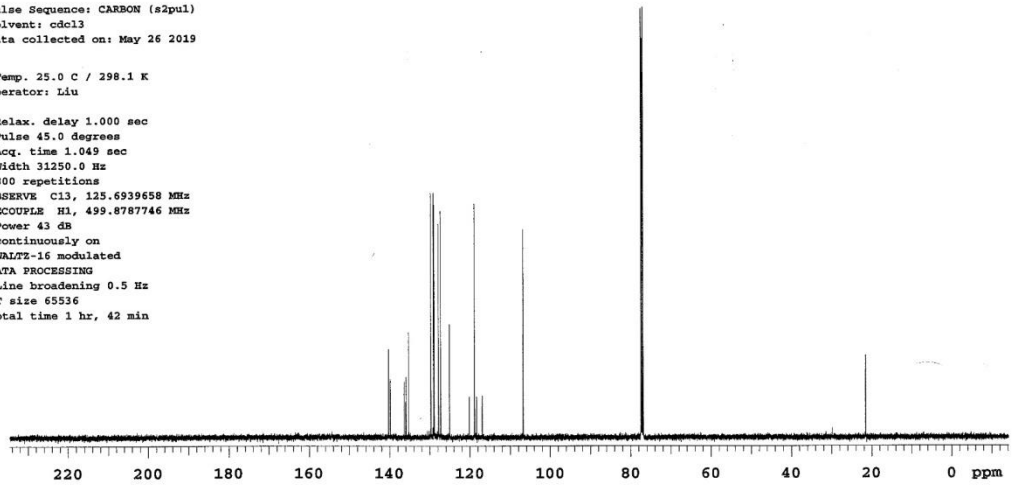

STANDARD PROTON PARAMETERS

Sample Name:

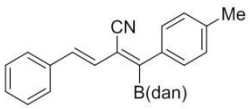

Data Collected on:
nmr11-inova500
Archive directory:

Sample directory:

FidFile: B11

Pulse Sequence: s2pul
Solvent: cdcl3
Data collected on: May 26 2019

Temp. 25.0 C / 298.1 K
Operator: Liu

Relax. delay 0.010 sec
Pulse 45.0 degrees
Acq. time 0.064 sec
Width 32064.1 Hz
1000 repetitions
OBSERVE B11, 160.3467695 MHz
DATA PROCESSING
Line broadening 0.5 Hz
FT size 4096
Total time 1 min 23 sec

Agilent Technologies

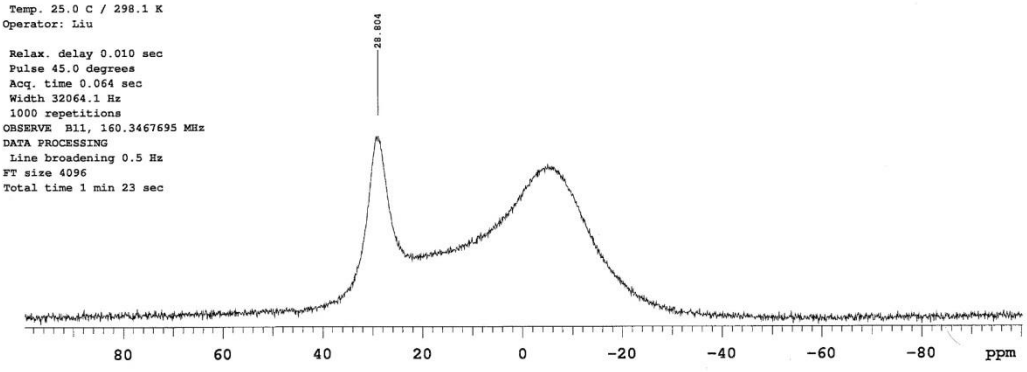

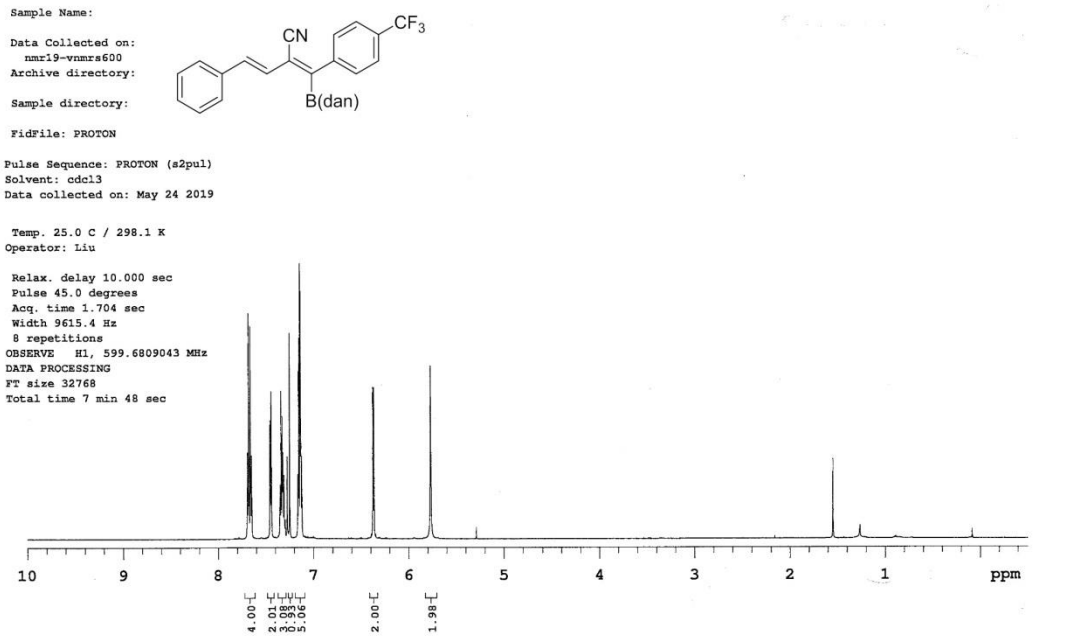
Sample Name:
Data Collected on:
nmr19-vnmrs600
Archive directory:
Sample directory:
FidFile: PROTON
CN
CF3
B(dan)
Pulse Sequence: PROTON (s2pul)
Solvent: cdcl3
Data collected on: May 24 2019
Temp. 25.0 C / 298.1 K
Operator: Liu
Relax. delay 10.000 sec
Pulse 45.0 degrees
Acq. time 1.704 sec
Width 9615.4 Hz
8 repetitions
OBSERVE H1, 599.6809043 MHz
DATA PROCESSING
FT size 32768
Total time 7 min 48 sec
10
9
8
7
6
5
4
3
2
1
ppm
4.00
2.01
3.93
5.06
2.00
1.98

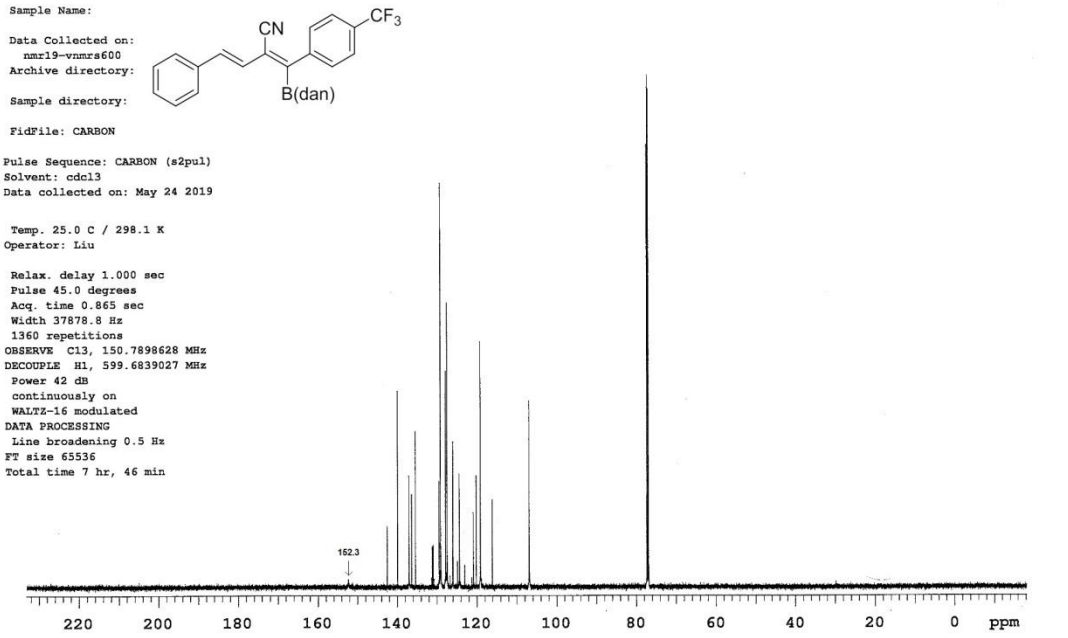
Sample Name:
Data Collected on:
nmr19-vnmrs600
Archive directory:
Sample directory:
FidFile: CARBON
CN
CF3
B(dan)
Pulse Sequence: CARBON (s2pul)
Solvent: cdcl3
Data collected on: May 24 2019
Temp. 25.0 C / 298.1 K
Operator: Liu
Relax. delay 1.000 sec
Pulse 45.0 degrees
Acq. time 0.865 sec
Width 37878.8 Hz
1360 repetitions
OBSERVE C13, 150.7898628 MHz
DECOUPLE H1, 599.6839027 MHz
Power 42 dB
continuously on
WALTZ-16 modulated
DATA PROCESSING
Line broadening 0.5 Hz
FT size 65536
Total time 7 hr, 46 min
162.3
220
200
180
160
140
120
100
80
60
40
20
0
ppm

Agilent Technologies

Sample Name:

Data Collected on:
nmr11-inova500
Archive directory:

Sample directory:

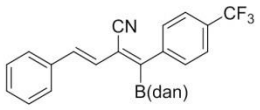

FidFile: B11

Pulse Sequence: s2pul
Solvent: cdcl3
Data collected on: May 24 2019

Temp. 25.0 C / 298.1 K
Operator: Liu

Relax. delay 0.010 sec
Pulse 45.0 degrees
Acq. time 0.064 sec
Width 32064.1 Hz
1000 repetitions
OBSERVE B11, 160.3467538 MHz
DATA PROCESSING
Line broadening 0.5 Hz
FT size 4096
Total time 1 min 23 sec

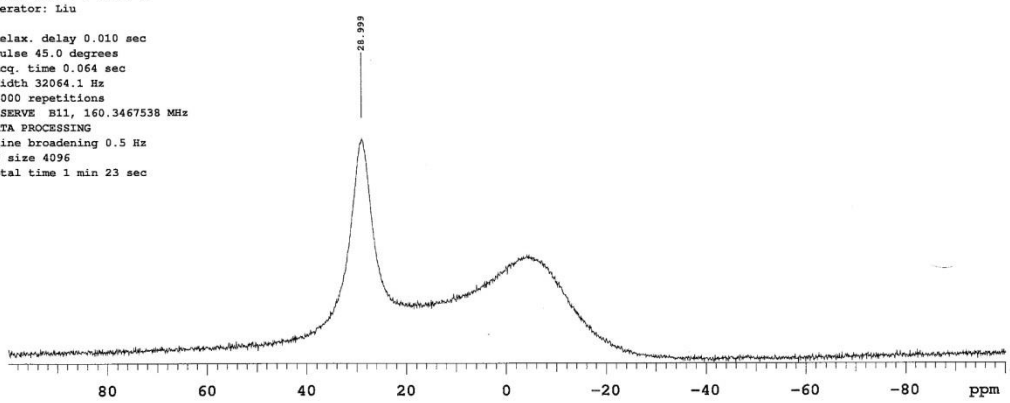

STANDARD FLUORINE PARAMETERS

Sample Name:

Data Collected on:
nmr19-vnmrs600
Archive directory:

Sample directory:

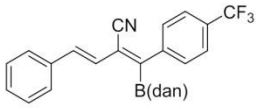

FidFile: FLUORINE

Pulse Sequence: FLUORINE (s2pul)
Solvent: cdcl3
Data collected on: May 24 2019

Temp. 25.0 C / 298.1 K
Operator: Liu

Relax. delay 1.000 sec
Pulse 30.0 degrees
Acq. time 0.996 sec
Width 131.6 kHz
10 repetitions
OBSERVE F19, 564.2638160 MHz
DATA PROCESSING
FT size 262144
Total time 0 min 20 sec

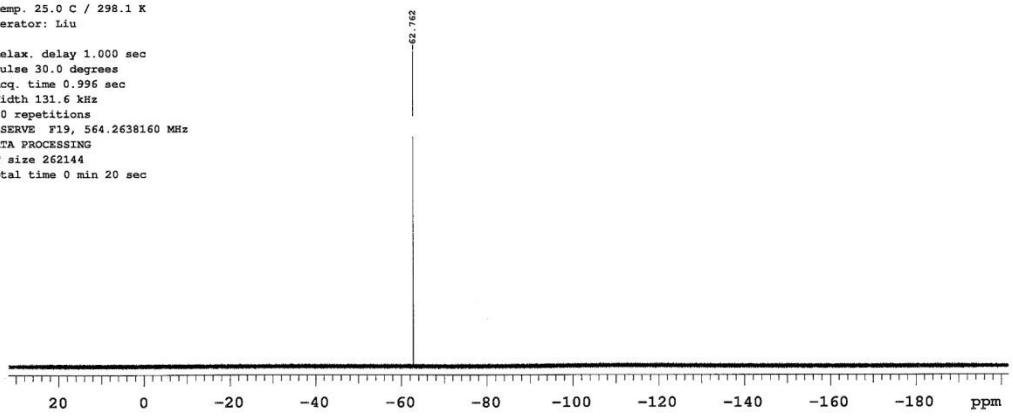

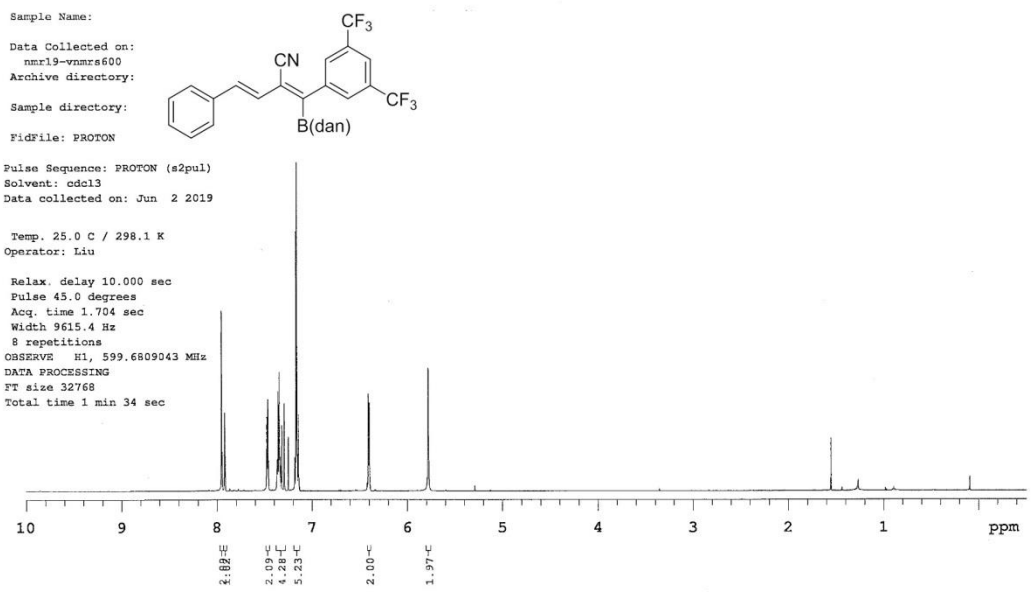
Sample Name:
Data Collected on:
nmr19-vnmrs600
Archive directory:
Sample directory:
FidFile: PROTON
CF3
CN
CF3
B(dan)
Pulse Sequence: PROTON (s2pul)
Solvent: cdcl3
Data collected on: Jun 2 2019
Temp. 25.0 C / 298.1 K
Operator: Liu
Relax. delay 10.000 sec
Pulse 45.0 degrees
Acq. time 1.704 sec
Width 9615.4 Hz
8 repetitions
OBSERVE H1, 599.6809043 MHz
DATA PROCESSING
FT size 32768
Total time 1 min 34 sec
10
9
8
7
6
5
4
3
2
1
ppm
2.02
2.09
4.28
5.23
2.00
1.97

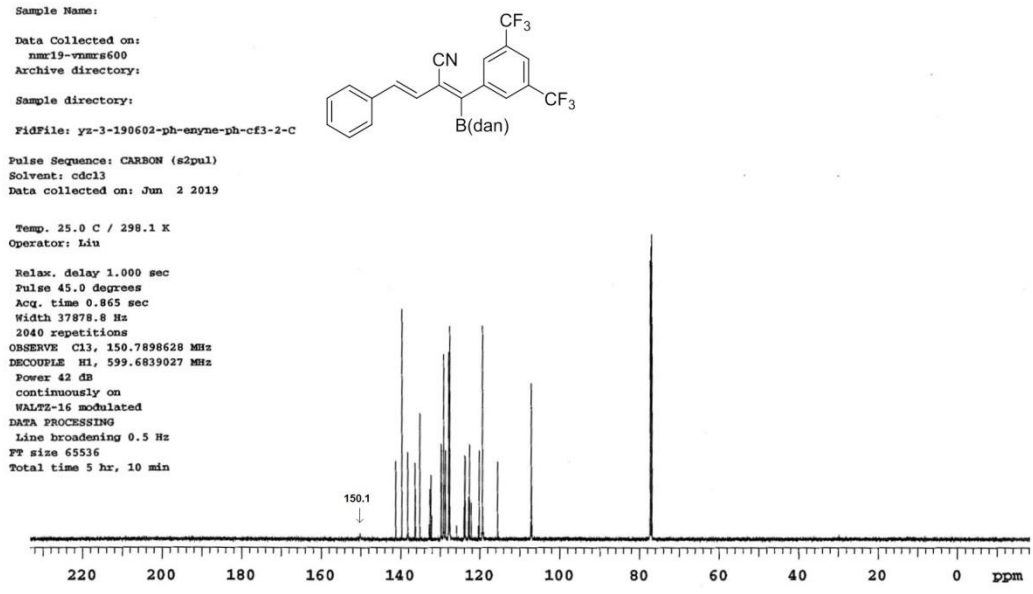
Sample Name:
Data Collected on:
nmr19-vnmrs600
Archive directory:
Sample directory:
FidFile: yz-3-190602-ph-enyne-ph-cf3-2-C
CF3
CN
CF3
B(dan)
Pulse Sequence: CARBON (s2pul)
Solvent: cdcl3
Data collected on: Jun 2 2019
Temp. 25.0 C / 298.1 K
Operator: Liu
Relax. delay 1.000 sec
Pulse 45.0 degrees
Acq. time 0.865 sec
Width 37878.8 Hz
2040 repetitions
OBSERVE C13, 150.7898628 MHz
DECOUPLE H1, 599.6839027 MHz
Power 42 dB
continuously on
WALTZ-16 modulated
DATA PROCESSING
Line broadening 0.5 Hz
FT size 65536
Total time 5 hr, 10 min
150.1
220
200
180
160
140
120
100
80
60
40
20
0
ppm

Agilent Technologies

Sample Name:

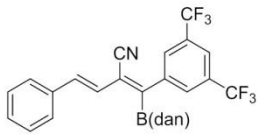

Data Collected on:
nmr11-inova500
Archive directory:

Sample directory:

FidFile: B11

Pulse Sequence: s2pul
Solvent: cdcl3
Data collected on: Jun 2 2019

Temp. 25.0 C / 298.1 K
Operator: Liu

Relax. delay 0.010 sec
Pulse 45.0 degrees
Acq. time 0.064 sec
Width 32064.1 Hz
1000 repetitions
OBSERVE B11, 160.3464720 MHz
DATA PROCESSING
Line broadening 0.5 Hz
FT size 4096
Total time 1 min 23 sec

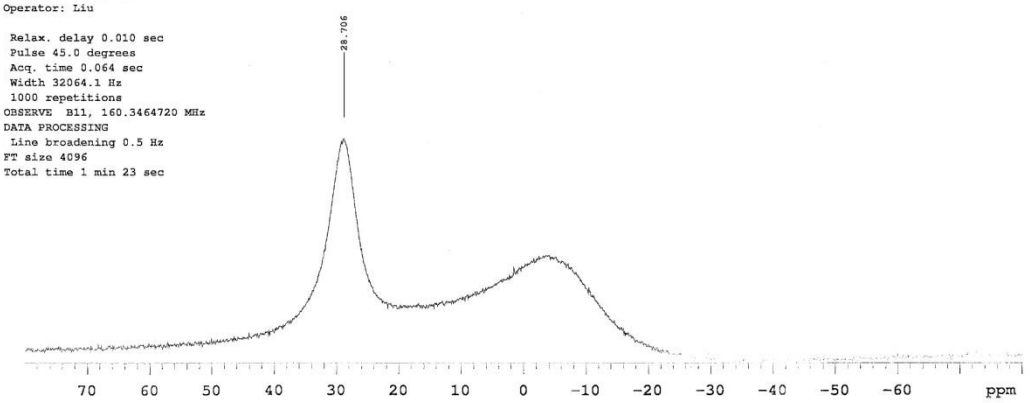

STANDARD FLUORINE PARAMETERS

Sample Name:

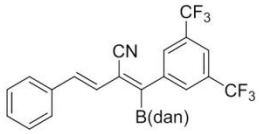

Data Collected on:
nmr19-vnmrs600
Archive directory:

Sample directory:

FidFile: FLUORINE

Pulse Sequence: FLUORINE (s2pul)
Solvent: cdcl3
Data collected on: Jun 2 2019

Temp. 25.0 C / 298.1 K
Operator: Liu

Relax. delay 1.000 sec
Pulse 30.0 degrees
Acq. time 0.996 sec
Width 131.6 kHz
20 repetitions
OBSERVE F19, 564.2638160 MHz
DATA PROCESSING
FT size 262144
Total time 0 min 40 sec

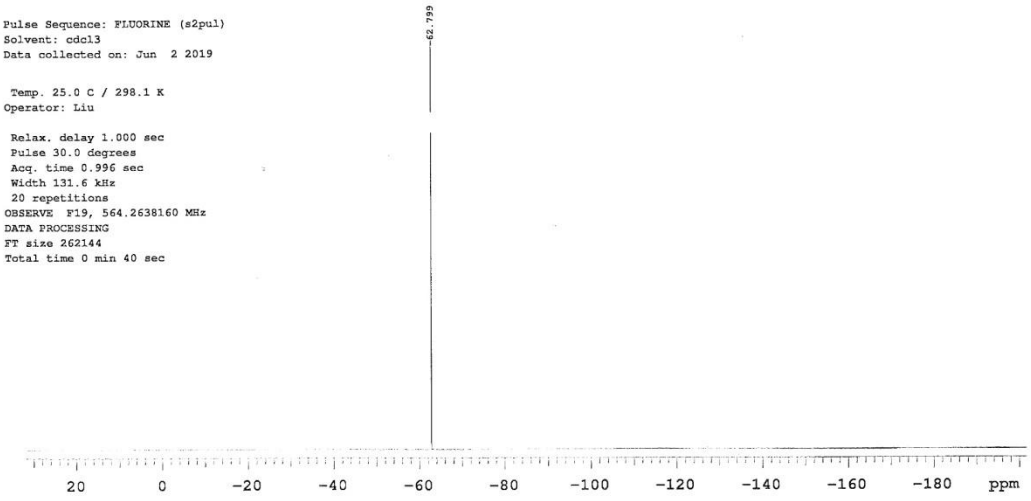

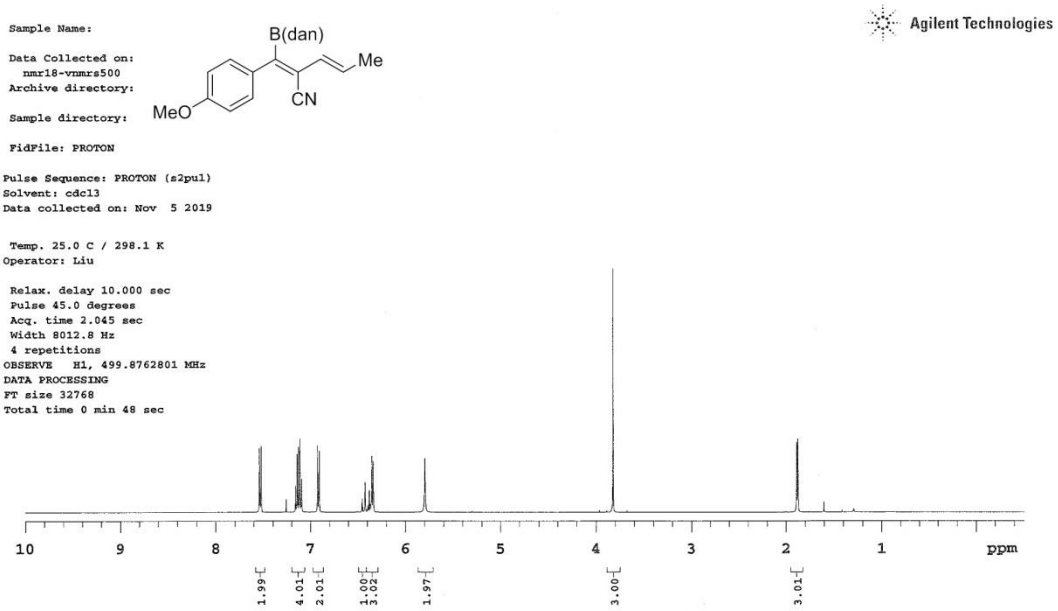
Agilent Technologies
Sample Name:
B(dan)
Me
CN
MeO
Data Collected on:
nmr18-vnmrs500
Archive directory:
Sample directory:
FidFile: PROTON
Pulse Sequence: PROTON (s2pul)
Solvent: cdcl3
Data collected on: Nov 5 2019
Temp. 25.0 C / 298.1 K
Operator: Liu
Relax. delay 10.000 sec
Pulse 45.0 degrees
Acq. time 2.045 sec
Width 8012.8 Hz
4 repetitions
OBSERVE H1, 499.8762801 MHz
DATA PROCESSING
FT size 32768
Total time 0 min 48 sec
10
9
8
7
6
5
4
3
2
1
ppm
1.99
4.01
2.01
1.00
3.02
1.97
3.00
3.01

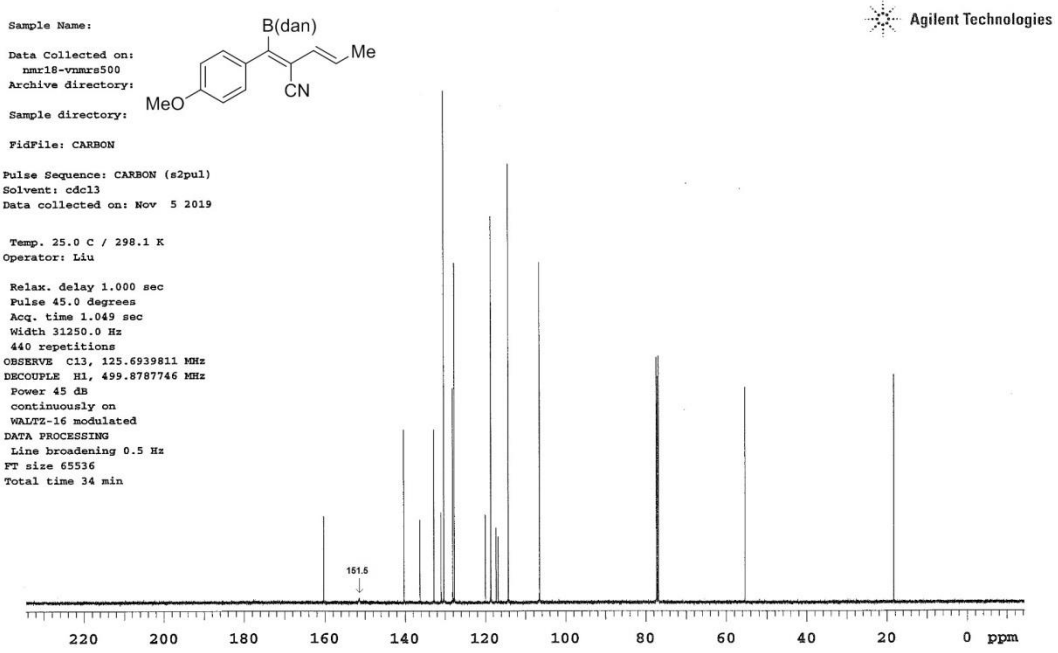
Agilent Technologies
Sample Name:
B(dan)
Me
CN
MeO
Data Collected on:
nmr18-vnmrs500
Archive directory:
Sample directory:
FidFile: CARBON
Pulse Sequence: CARBON (s2pul)
Solvent: cdcl3
Data collected on: Nov 5 2019
Temp. 25.0 C / 298.1 K
Operator: Liu
Relax. delay 1.000 sec
Pulse 45.0 degrees
Acq. time 1.049 sec
Width 31250.0 Hz
440 repetitions
OBSERVE C13, 125.6939811 MHz
DECOUPLE H1, 499.8787746 MHz
Power 45 dB
continuously on
WALTZ-16 modulated
DATA PROCESSING
Line broadening 0.5 Hz
FT size 65536
Total time 34 min
151.5
220
200
180
160
140
120
100
80
60
40
20
0 ppm

Agilent Technologies

Sample Name:

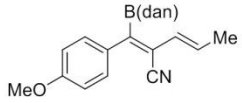

Data Collected on:
nmr11-inova500
Archive directory:

Sample directory:

FidFile: B11

Pulse Sequence: s2pul
Solvent: cdcl3
Data collected on: Sep 19 2019

Temp. 25.0 C / 298.1 K
Operator: Liu

Relax. delay 0.010 sec
Pulse 45.0 degrees
Acq. time 0.064 sec
Width 32064.1 Hz
1000 repetitions
OBSERVE B11, 160.3466912 MHz
DATA PROCESSING
Line broadening 0.5 Hz
FT size 4096
Total time 1 min 23 sec

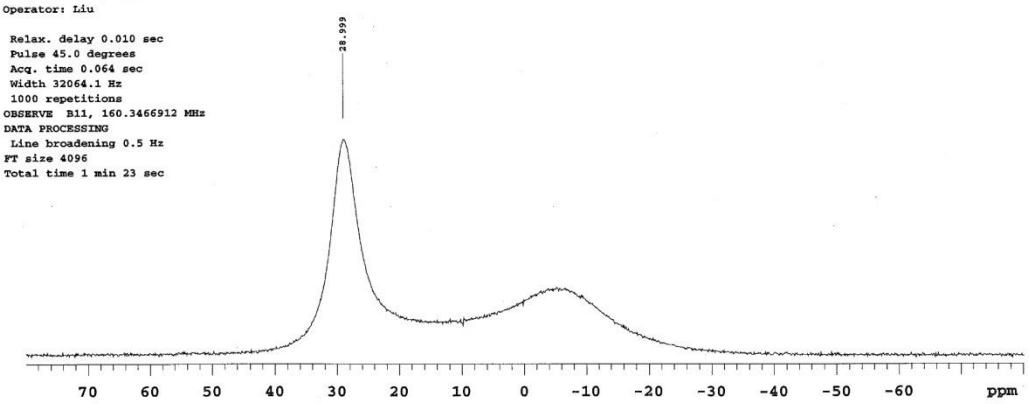

Agilent Technologies

Sample Name:

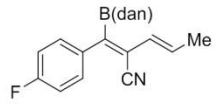

Data Collected on:
nmr18-vnmrs500
Archive directory:

Sample directory:

FidFile: PROTON

Pulse Sequence: PROTON (s2pul)
Solvent: cdcl3
Data collected on: Jul 16 2019

Temp. 25.0 C / 298.1 K
Operator: Liu

Relax. delay 10.000 sec
Pulse 45.0 degrees
Acq. time 2.045 sec
Width 8012.8 Hz
6 repetitions
OBSERVE H1, 499.8762802 MHz
DATA PROCESSING
FT size 32768
Total time 20 min

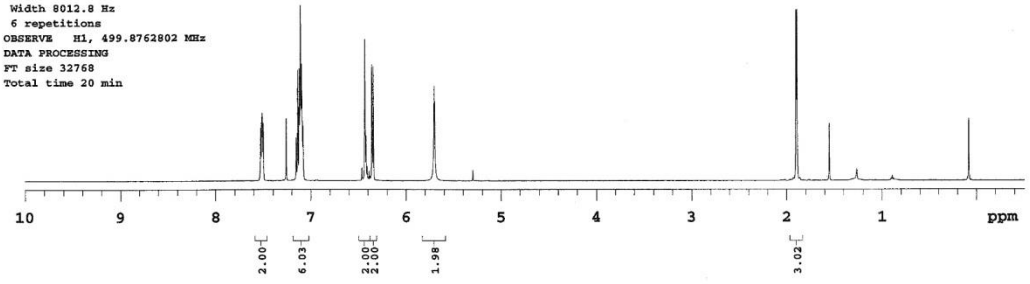

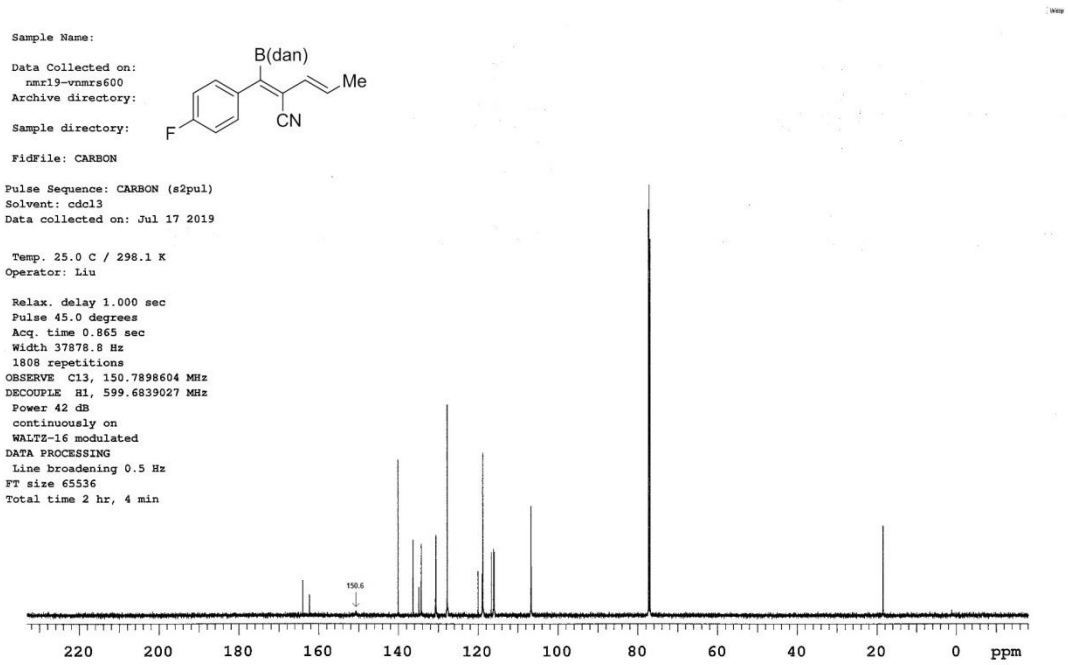
Sample Name:
Data Collected on:
nmr19-vnmrs600
Archive directory:
Sample directory:
FidFile: CARBON
B(dan)
Me
CN
F
Pulse Sequence: CARBON (s2pul)
Solvent: cdcl3
Data collected on: Jul 17 2019
Temp. 25.0 C / 298.1 K
Operator: Liu
Relax. delay 1.000 sec
Pulse 45.0 degrees
Acq. time 0.865 sec
Width 37878.8 Hz
1808 repetitions
OBSERVE C13, 150.7898604 MHz
DECOUPLE H1, 599.6839027 MHz
Power 42 dB
continuously on
WALTZ-16 modulated
DATA PROCESSING
Line broadening 0.5 Hz
FT size 65536
Total time 2 hr, 4 min
150.6
220
200
180
160
140
120
100
80
60
40
20
0
ppm

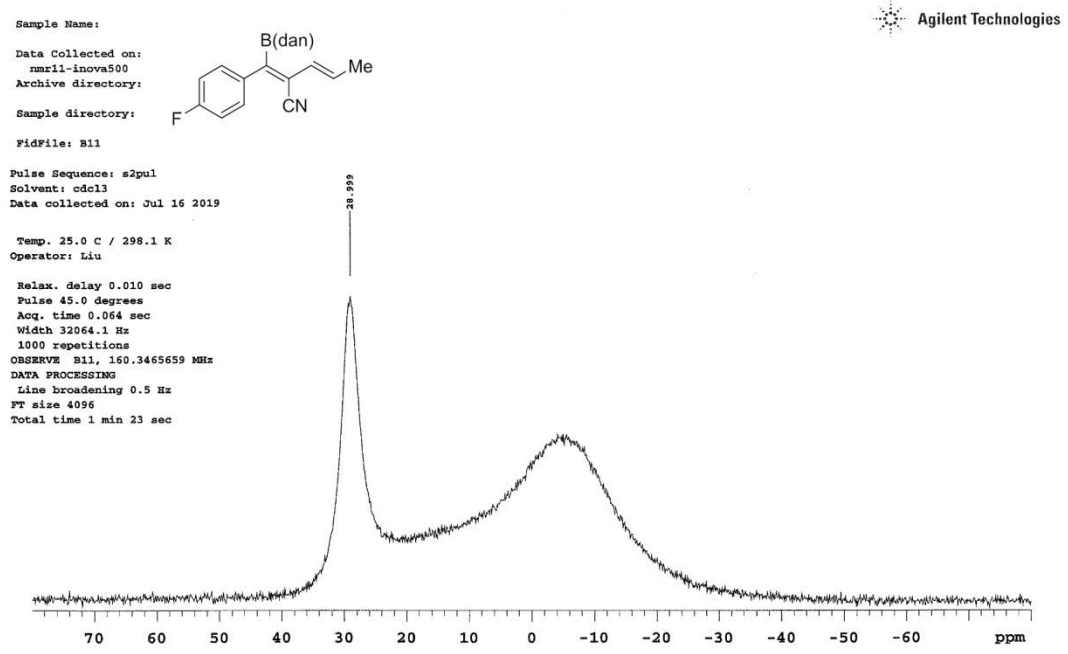
Agilent Technologies
Sample Name:
Data Collected on:
nmr11-inova500
Archive directory:
Sample directory:
FidFile: B11
B(dan)
Me
CN
F
Pulse Sequence: s2pul
Solvent: cdcl3
Data collected on: Jul 16 2019
Temp. 25.0 C / 298.1 K
Operator: Liu
Relax. delay 0.010 sec
Pulse 45.0 degrees
Acq. time 0.064 sec
Width 32064.1 Hz
1000 repetitions
OBSERVE B11, 160.3465659 MHz
DATA PROCESSING
Line broadening 0.5 Hz
FT size 4096
Total time 1 min 23 sec
28.999
70
60
50
40
30
20
10
0
-10
-20
-30
-40
-50
-60
ppm

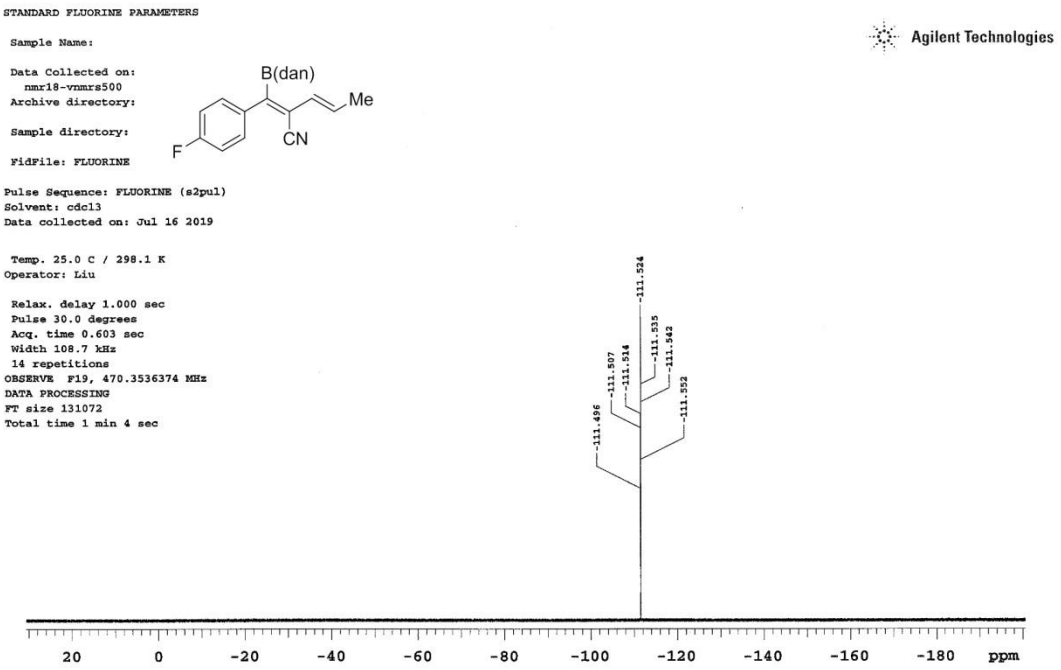
STANDARD FLUORINE PARAMETERS
Sample Name:
Data Collected on:
nmr18-vnmrs500
Archive directory:
Sample directory:
FidFile: FLUORINE
B(dan)
Me
CN
F
Pulse Sequence: FLUORINE (s2pul)
Solvent: cdcl3
Data collected on: Jul 16 2019
Temp. 25.0 C / 298.1 K
Operator: Liu
Relax. delay 1.000 sec
Pulse 30.0 degrees
Acq. time 0.603 sec
Width 108.7 kHz
14 repetitions
OBSERVE F19, 470.3536374 MHz
DATA PROCESSING
FT size 131072
Total time 1 min 4 sec
-111.524
-111.535
-111.542
-111.552
-111.507
-111.514
-111.496
20
0
-20
-40
-60
-80
-100
-120
-140
-160
-180
ppm

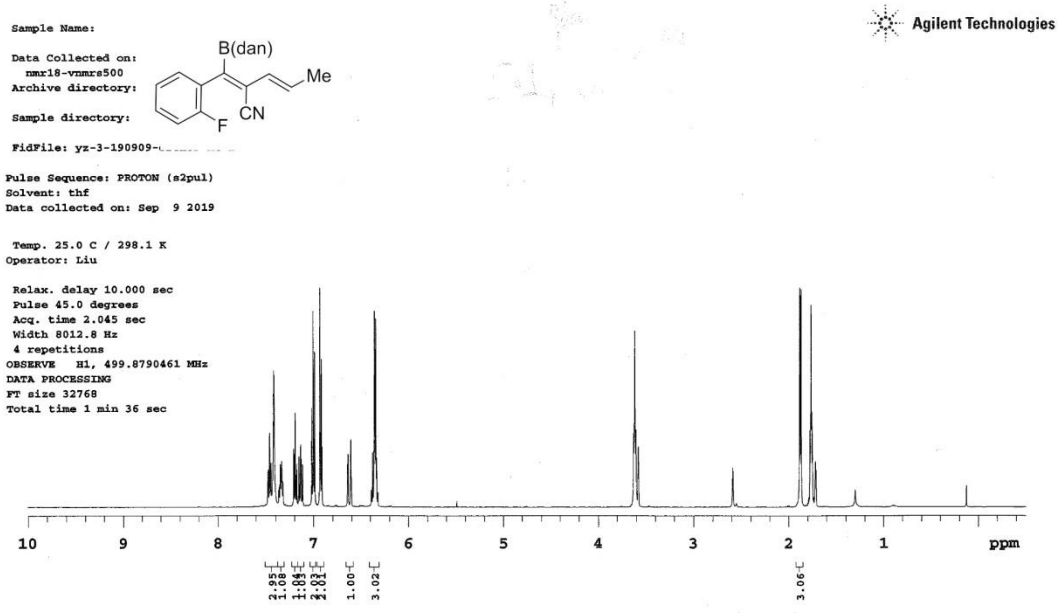
Sample Name:
Data Collected on:
nmr18-vnmrs500
Archive directory:
Sample directory:
FidFile: yz-3-190909-
B(dan)
Me
CN
F
Pulse Sequence: PROTON (s2pul)
Solvent: thf
Data collected on: Sep 9 2019
Temp. 25.0 C / 298.1 K
Operator: Liu
Relax. delay 10.000 sec
Pulse 45.0 degrees
Acq. time 2.045 sec
Width 8012.8 Hz
4 repetitions
OBSERVE H1, 499.8790461 MHz
DATA PROCESSING
FT size 32768
Total time 1 min 36 sec
10
9
8
7
6
5
4
3
2
1
ppm
2.05
1.08
1.05
2.03
1.00
3.02
3.06

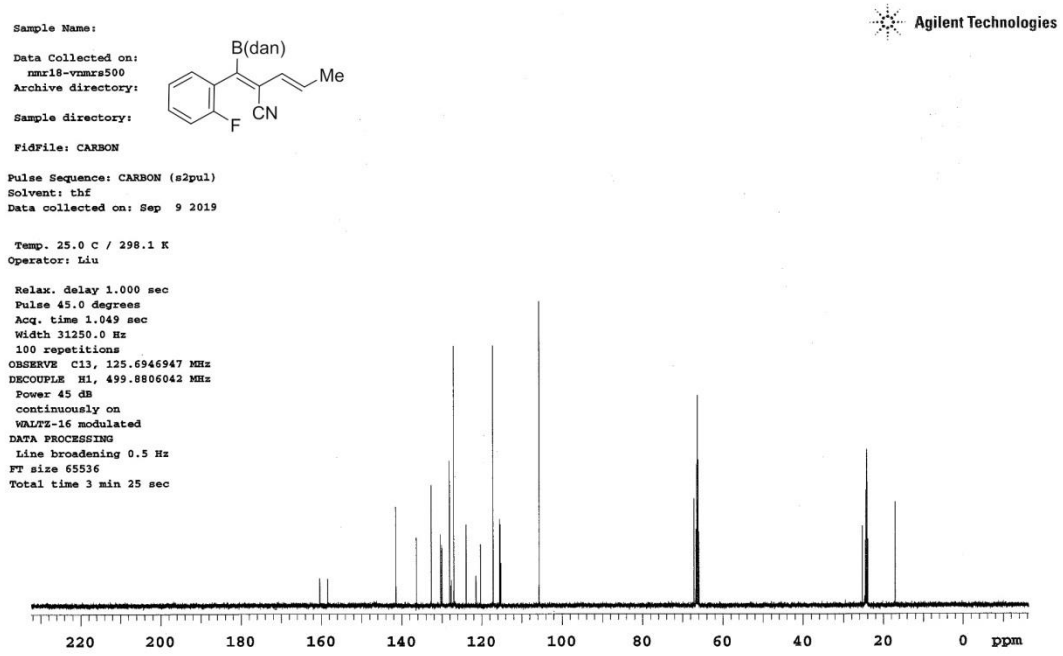
Agilent Technologies
Sample Name:
Data Collected on:
nmr18-vnmrs500
Archive directory:
Sample directory:
FidFile: CARBON
B(dan)
Me
CN
F
Pulse Sequence: CARBON (s2pul)
Solvent: thf
Data collected on: Sep 9 2019
Temp. 25.0 C / 298.1 K
Operator: Liu
Relax. delay 1.000 sec
Pulse 45.0 degrees
Acq. time 1.049 sec
Width 31250.0 Hz
100 repetitions
OBSERVE C13, 125.6946947 MHz
DECOUPLE H1, 499.8806042 MHz
Power 45 dB
continuously on
WALTZ-16 modulated
DATA PROCESSING
Line broadening 0.5 Hz
FT size 65536
Total time 3 min 25 sec
220 200 180 160 140 120 100 80 60 40 20 0 ppm

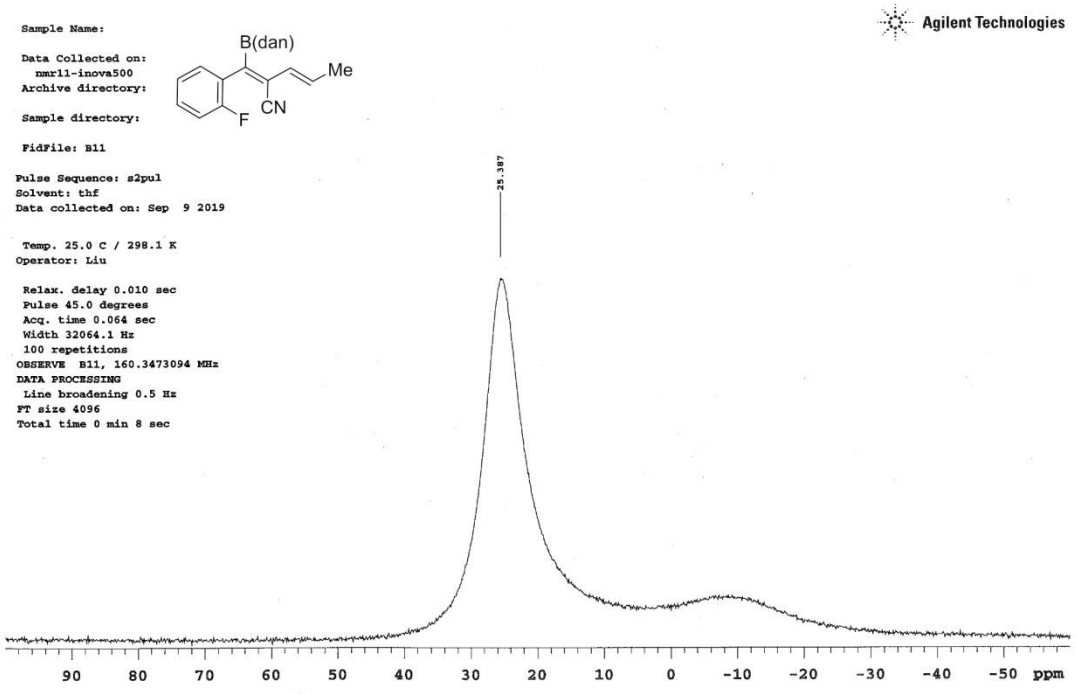
Agilent Technologies
Sample Name:
Data Collected on:
nmr11-inova500
Archive directory:
Sample directory:
FidFile: B11
B(dan)
Me
CN
F
25.387
Pulse Sequence: s2pul
Solvent: thf
Data collected on: Sep 9 2019
Temp. 25.0 C / 298.1 K
Operator: Liu
Relax. delay 0.010 sec
Pulse 45.0 degrees
Acq. time 0.064 sec
Width 32064.1 Hz
100 repetitions
OBSERVE B11, 160.3473094 MHz
DATA PROCESSING
Line broadening 0.5 Hz
FT size 4096
Total time 0 min 8 sec
90 80 70 60 50 40 30 20 10 0 -10 -20 -30 -40 -50 ppm

STANDARD FLUORINE PARAMETERS

Sample Name:

Data Collected on:
nmr18-vnmrs500
Archive directory:

Sample directory:

FidFile: FLUORINE

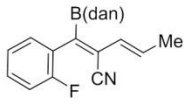

Pulse Sequence: FLUORINE (s2pul)
Solvent: thf
Data collected on: Sep 9 2019

Temp. 25.0 C / 298.1 K
Operator: Liu

Relax. delay 1.000 sec
Pulse 30.0 degrees
Acq. time 0.603 sec
Width 108.7 kHz
4 repetitions
OBSERVE F19, 470.3553589 MHz
DATA PROCESSING
FT size 131072
Total time 0 min 6 sec

Agilent Technologies

Sample Name:

Data Collected on
nmr18-vnmrs500
Archive directory

Sample directory:

FidFile: PROTON

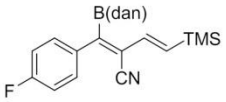

Pulse Sequence: PROTON (s2pul)
Solvent: cdcl3
Data collected on: Sep 3 2019

Temp. 25.0 C / 298.1 K
Operator: Liu

Relax. delay 10.000 sec
Pulse 45.0 degrees
Acq. time 2.045 sec
Width 8012.8 Hz
6 repetitions
OBSERVE H1, 499.8762806 MHz
DATA PROCESSING
FT size 32768
Total time 2 min 0 sec

Agilent Technologies

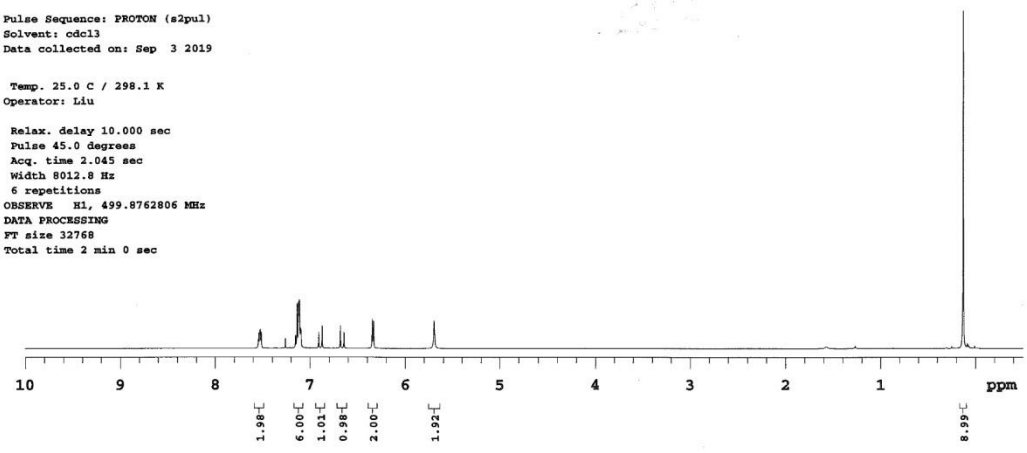

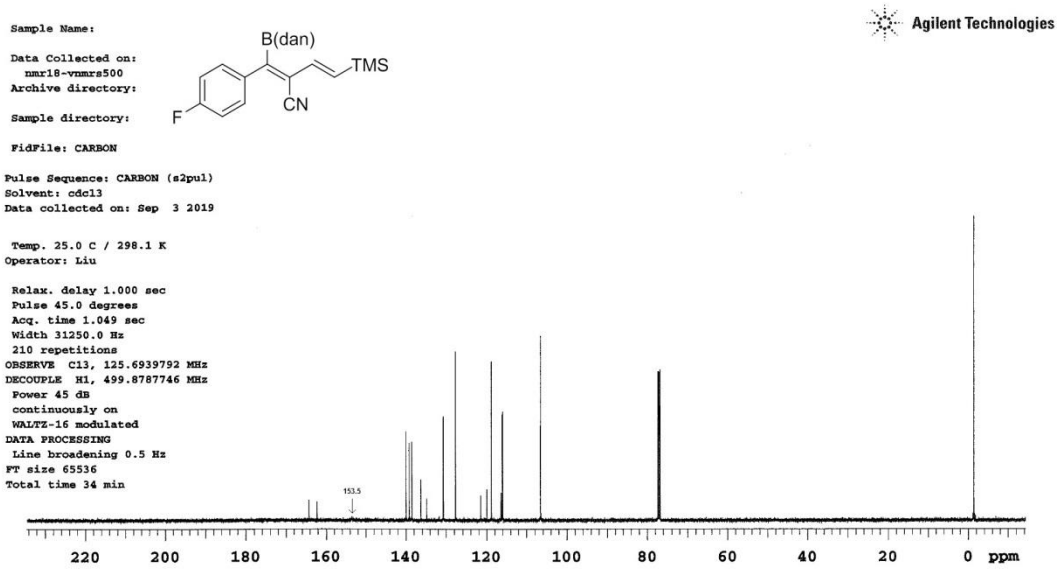
Agilent Technologies
Sample Name:
Data Collected on:
nmr18-vnmrs500
Archive directory:
Sample directory:
FidFile: CARBON
B(dan)
TMS
CN
F
Pulse Sequence: CARBON (s2pul)
Solvent: cdcl3
Data collected on: Sep 3 2019
Temp. 25.0 C / 298.1 K
Operator: Liu
Relax. delay 1.000 sec
Pulse 45.0 degrees
Acq. time 1.049 sec
Width 31250.0 Hz
210 repetitions
OBSERVE C13, 125.6939792 MHz
DECOUPLE H1, 499.8787746 MHz
Power 45 dB
continuously on
WALTZ-16 modulated
DATA PROCESSING
Line broadening 0.5 Hz
FT size 65536
Total time 34 min
153.5
220 200 180 160 140 120 100 80 60 40 20 0 ppm

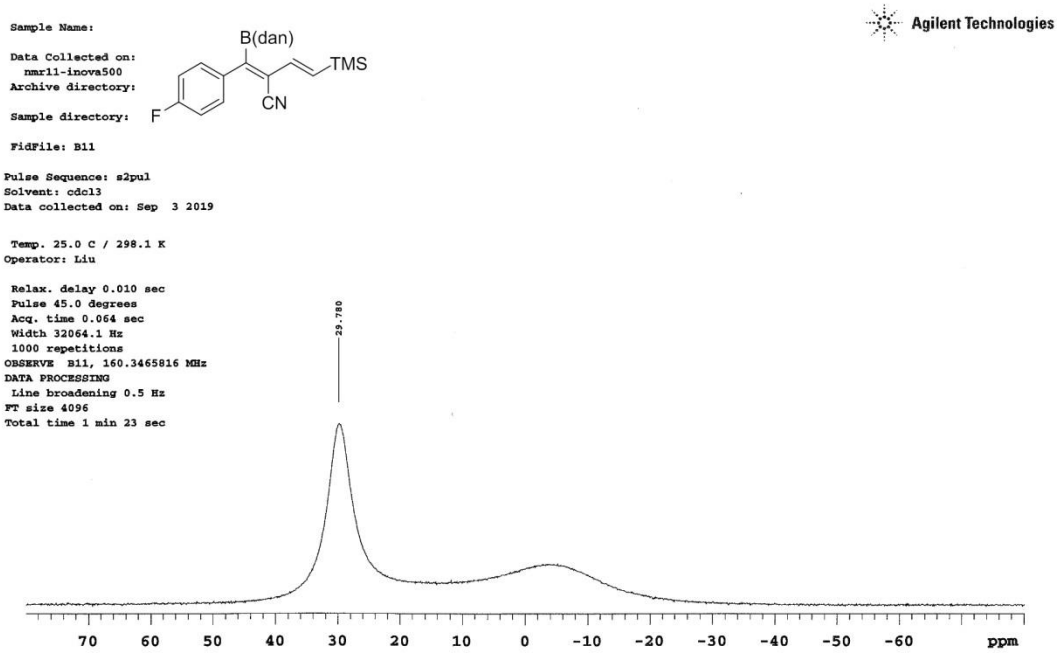
Agilent Technologies
Sample Name:
Data Collected on:
nmr11-inova500
Archive directory:
Sample directory:
FidFile: B11
B(dan)
TMS
CN
F
Pulse Sequence: s2pul
Solvent: cdcl3
Data collected on: Sep 3 2019
Temp. 25.0 C / 298.1 K
Operator: Liu
Relax. delay 0.010 sec
Pulse 45.0 degrees
Acq. time 0.064 sec
Width 32064.1 Hz
1000 repetitions
OBSERVE B11, 160.3465816 MHz
DATA PROCESSING
Line broadening 0.5 Hz
FT size 4096
Total time 1 min 23 sec
29.780
70 60 50 40 30 20 10 0 -10 -20 -30 -40 -50 -60 ppm

STANDARD FLUORINE PARAMETERS

Sample Name:

Data Collected on:
nmr18-vnmrs500
Archive directory:

Sample directory:

FidFile: yz-3-190223-p-F-tms-F

Pulse Sequence: FLUORINE (s2pul)
Solvent: cdcl3
Data collected on: Feb 23 2020

Temp. 25.0 C / 298.1 K
Operator: Liu

Relax. delay 1.000 sec
Pulse 30.0 degrees
Acq. time 0.603 sec
Width 108.7 kHz
20 repetitions
OBSERVE F19, 470.3533800 MHz
DATA PROCESSING
FT size 131072
Total time 0 min 32 sec

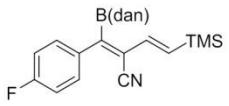

Agilent Technologies

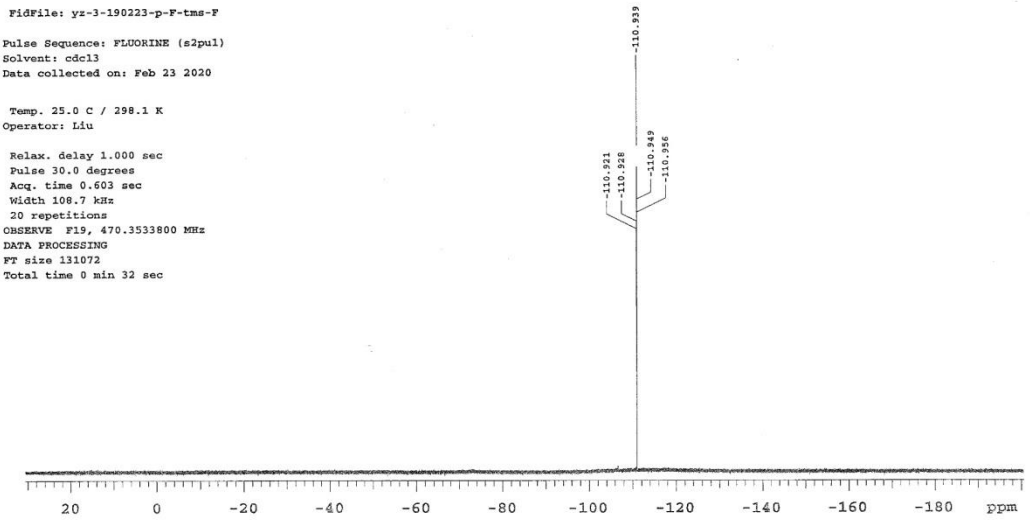

Sample Name:

Data Collected on:
nmr19-vnmrs600
Archive directory:

Sample directory:

FidFile: PROTON

Pulse Sequence: PROTON (s2pul)
Solvent: cdcl3
Data collected on: Mar 19 2020

Temp. 25.0 C / 298.1 K
Operator: Liu

Relax. delay 10.000 sec
Pulse 45.0 degrees
Acq. time 1.704 sec
Width 9615.4 Hz
10 repetitions
OBSERVE H1, 599.6806838 MHz
DATA PROCESSING
FT size 32768
Total time 1 min 57 sec

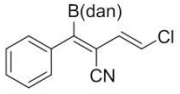

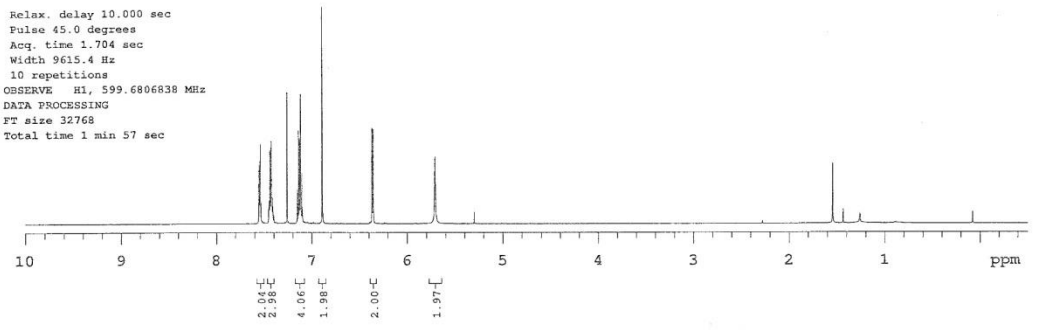

Sample Name:

Data Collected on:
nmr19-vnmrs600
Archive directory:

Sample directory:

FidFile: CARBON

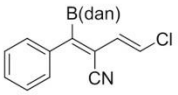

Pulse Sequence: CARBON (s2pul)
Solvent: cdcl3
Data collected on: Mar 18 2020

Temp. 25.0 C / 298.1 K
Operator: Liu

Relax. delay 1.000 sec
Pulse 45.0 degrees
Acq. time 0.865 sec
Width 37878.8 Hz
460 repetitions
OBSERVE C13, 150.7898050 MHz
DECOUPLE H1, 599.6836825 MHz
Power 45 dB
continuously on
WALTZ-16 modulated
DATA PROCESSING
Line broadening 0.5 Hz
FT size 65536
Total time 31 min

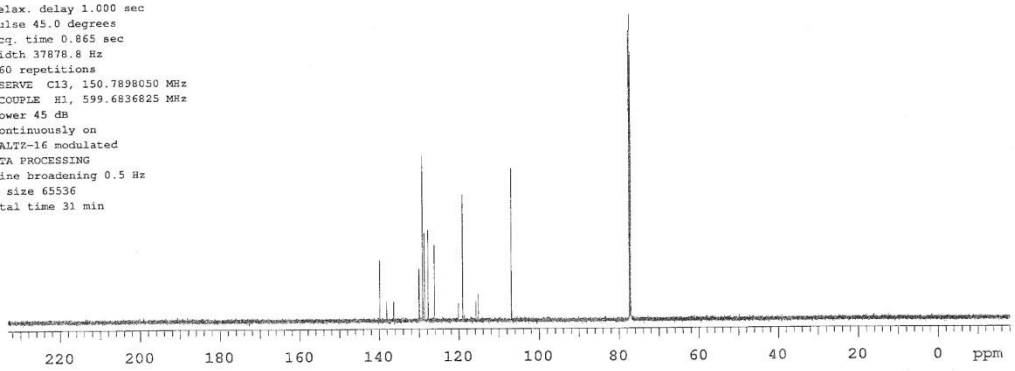

Agilent Technologies

Sample Name:

Data Collected on:
nmr11-inova500
Archive directory:

Sample directory:

FidFile: B11

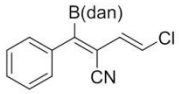

Pulse Sequence: s2pul
Solvent: cdcl3
Data collected on: Mar 19 2020

Temp. 25.0 C / 298.1 K
Operator: Liu

Relax. delay 0.010 sec
Pulse 45.0 degrees
Acq. time 0.064 sec
Width 32064.1 Hz
3000 repetitions
OBSERVE B11, 160.3466912 MHz
DATA PROCESSING
Line broadening 0.5 Hz
FT size 4096
Total time 4 min 8 sec

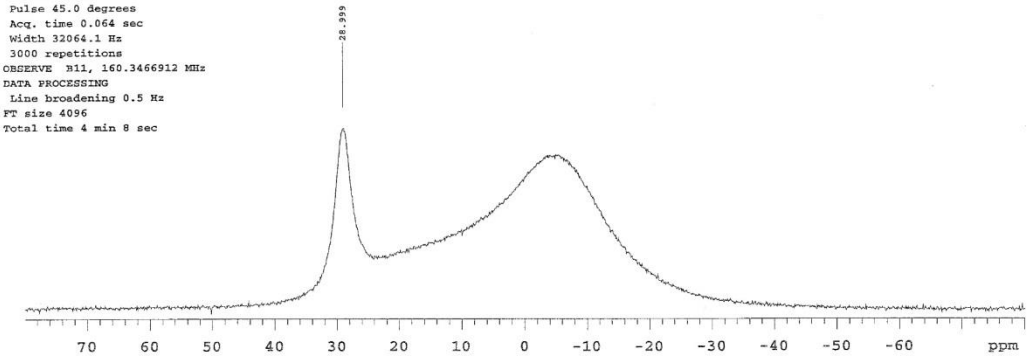

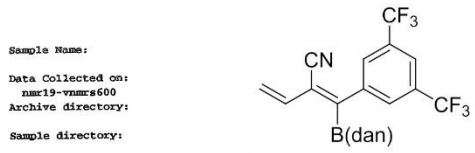

Sample Name:

Data Collected on:
nmr19-vnmrs600
Archive directory:

Sample directory:

FidFile: yz-3-190629-biscf3-terminal-H

Pulse Sequence: PROTON (s2pul)
Solvent: cdcl3
Data collected on: Jun 29 2019

Temp. 25.0 C / 298.1 K
Operator: Liu

Relax. delay 10.000 sec
Pulse 45.0 degrees
Acq. time 1.704 sec
Width 9615.4 Hz
4 repetitions
OBSERVE H1, 599.6809043 MHz
DATA PROCESSING
FT size 32768
Total time 1 min 34 sec

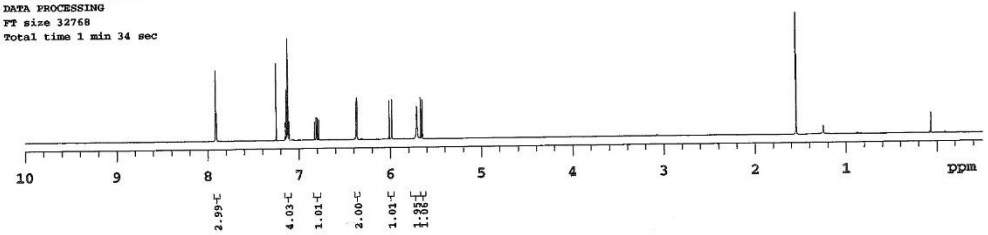

Agilent Technologies

Sample Name:

Data Collected on:
nmr14-vnmrs400
Archive directory:

Sample directory:

FidFile: CARBON

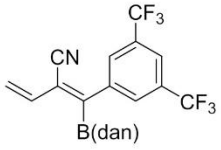

Pulse Sequence: CARBON (s2pul)
Solvent: cdcl3
Data collected on: Jun 21 2019

Temp. 25.0 C / 298.1 K
Operator: Liu

Relax. delay 1.000 sec
Pulse 45.0 degrees
Acq. time 1.311 sec
Width 25000.0 Hz
4612 repetitions
OBSERVE C13, 100.5208755 MHz
DECOUPLE H1, 399.7666112 MHz
Power 40 dB
continuously on
WALTZ-16 modulated
DATA PROCESSING
Line broadening 0.5 Hz
FT size 65536
Total time 6 hr, 25 min

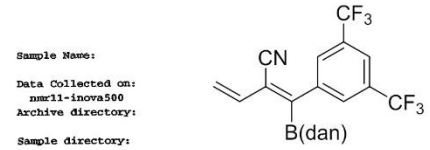

Sample Name:

Data Collected on:
nmr11-inova500
Archive directory:

Sample directory:

FidFile: yz-3-190629-biscf3-terminal-B

Pulse Sequence: s2pul
Solvent: cdcl3
Data collected on: Jun 29 2019

Temp. 25.0 C / 298.1 K
Operator: Liu

Relax. delay 0.010 sec
Pulse 45.0 degrees
Acq. time 0.064 sec
Width 32064.1 Hz
2032 repetitions
OBSERVE B11, 160.3470983 MHz
DATA PROCESSING
Line broadening 0.5 Hz
FT size 4096
Total time 12 min

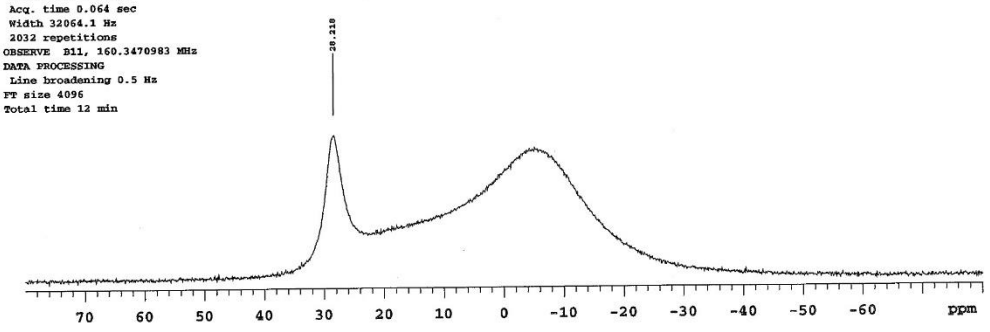

STANDARD FLUORINE PARAMETERS

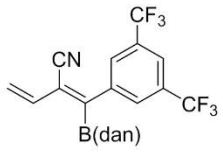

Sample Name:

Data Collected on:
nmr19-vnmrs600
Archive directory:

Sample directory:

FidFile: FLUORINE

Pulse Sequence: FLUORINE (s2pul)
Solvent: cdcl3
Data collected on: Jun 26 2019

Temp. 25.0 C / 298.1 K
Operator: Liu

Relax. delay 1.000 sec
Pulse 30.0 degrees
Acq. time 0.996 sec
Width 131.6 kHz
10 repetitions
OBSERVE F19, 564.2638160 MHz
DATA PROCESSING
FT size 262144
Total time 0 min 40 sec

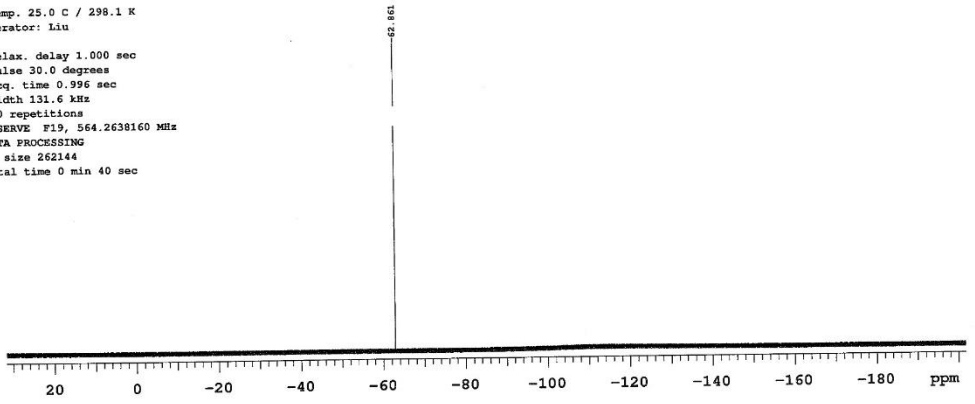

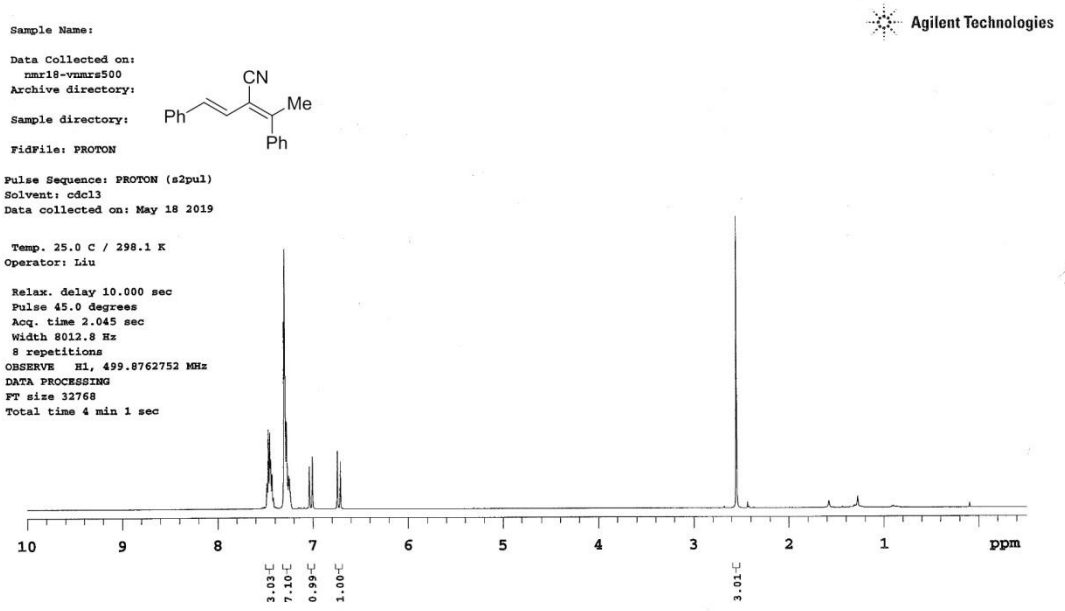
Agilent Technologies
Sample Name:
Data Collected on:
nmr18-vnmrs500
Archive directory:
Sample directory:
FidFile: PROTON
CN
Me
Ph
Ph
Pulse Sequence: PROTON (s2pul)
Solvent: cdcl3
Data collected on: May 18 2019
Temp. 25.0 C / 298.1 K
Operator: Liu
Relax. delay 10.000 sec
Pulse 45.0 degrees
Acq. time 2.045 sec
Width 8012.8 Hz
8 repetitions
OBSERVE H1, 499.8762752 MHz
DATA PROCESSING
FT size 32768
Total time 4 min 1 sec
10
9
8
7
6
5
4
3
2
1
ppm
3.03
7.10
0.99
1.00
3.01

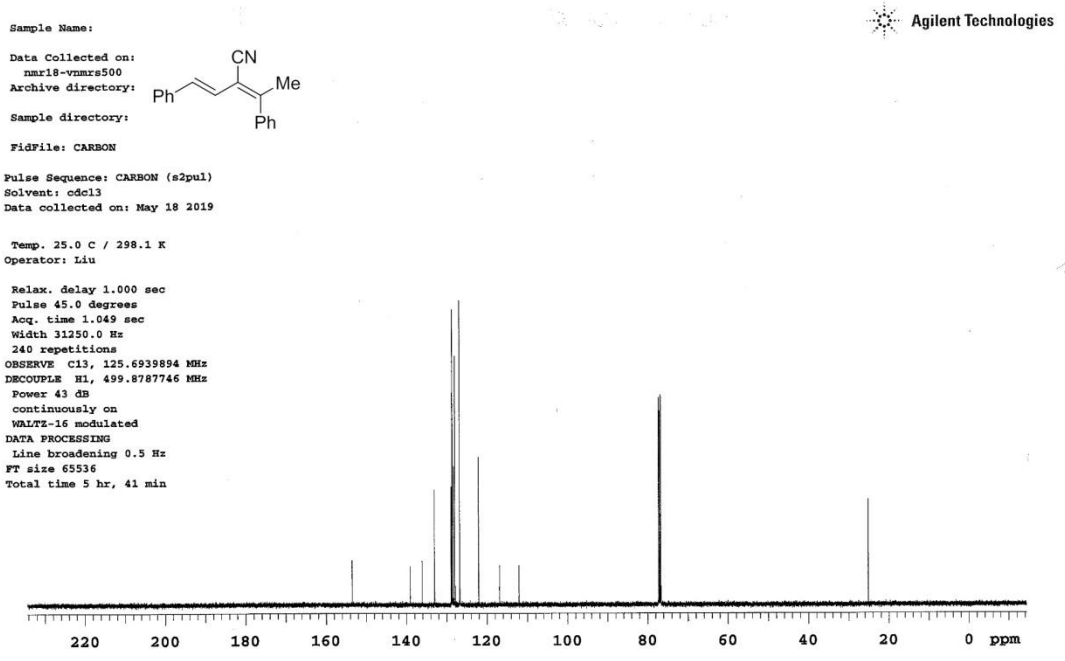
Agilent Technologies
Sample Name:
Data Collected on:
nmr18-vnmrs500
Archive directory:
Sample directory:
FidFile: CARBON
CN
Me
Ph
Ph
Pulse Sequence: CARBON (s2pul)
Solvent: cdcl3
Data collected on: May 18 2019
Temp. 25.0 C / 298.1 K
Operator: Liu
Relax. delay 1.000 sec
Pulse 45.0 degrees
Acq. time 1.049 sec
Width 31250.0 Hz
240 repetitions
OBSERVE C13, 125.6939894 MHz
DECOUPLE H1, 499.8787746 MHz
Power 43 dB
continuously on
WALTZ-16 modulated
DATA PROCESSING
Line broadening 0.5 Hz
FT size 65536
Total time 5 hr, 41 min
220
200
180
160
140
120
100
80
60
40
20
0
ppm

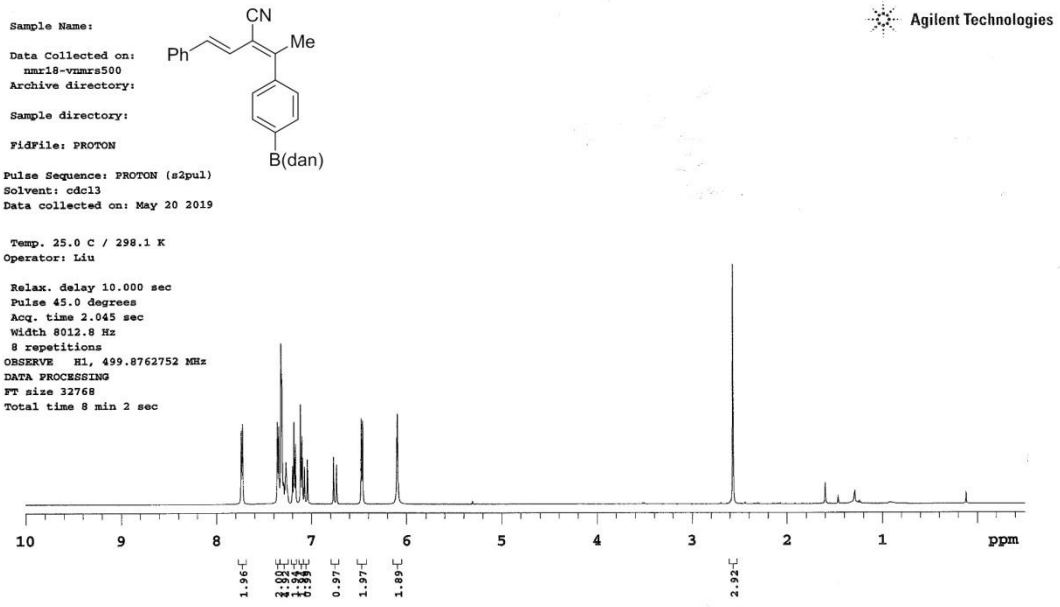
Agilent Technologies
Sample Name:
Data Collected on:
nmr18-vnmrs500
Archive directory:
Sample directory:
FidFile: PROTON
CN
Me
Ph
B(dan)
Pulse Sequence: PROTON (s2pul)
Solvent: cdcl3
Data collected on: May 20 2019
Temp. 25.0 C / 298.1 K
Operator: Liu
Relax. delay 10.000 sec
Pulse 45.0 degrees
Acq. time 2.045 sec
Width 8012.8 Hz
8 repetitions
OBSERVE H1, 499.8762752 MHz
DATA PROCESSING
FT size 32768
Total time 8 min 2 sec
10
9
8
7
6
5
4
3
2
1
ppm
1.96
2.00
0.97
1.97
1.89
2.92

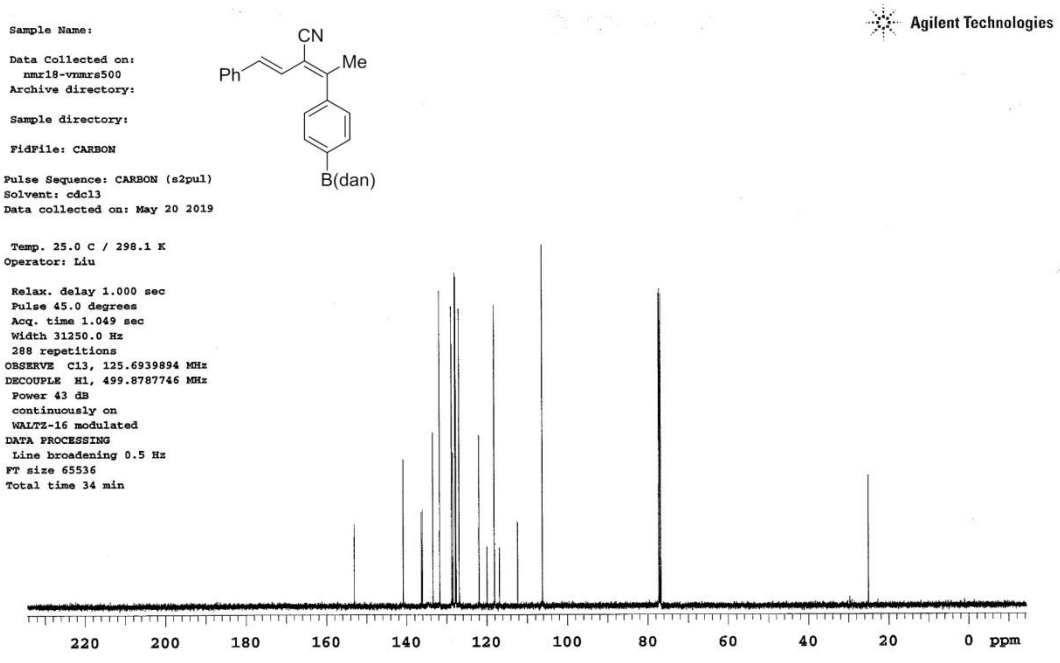
Agilent Technologies
Sample Name:
Data Collected on:
nmr18-vnmrs500
Archive directory:
Sample directory:
FidFile: CARBON
CN
Me
Ph
B(dan)
Pulse Sequence: CARBON (s2pul)
Solvent: cdcl3
Data collected on: May 20 2019
Temp. 25.0 C / 298.1 K
Operator: Liu
Relax. delay 1.000 sec
Pulse 45.0 degrees
Acq. time 1.049 sec
Width 31250.0 Hz
288 repetitions
OBSERVE C13, 125.6939894 MHz
DECOUPLE H1, 499.8787746 MHz
Power 43 dB
continuously on
WALTZ-16 modulated
DATA PROCESSING
Line broadening 0.5 Hz
FT size 65536
Total time 34 min
220
200
180
160
140
120
100
80
60
40
20
0
ppm

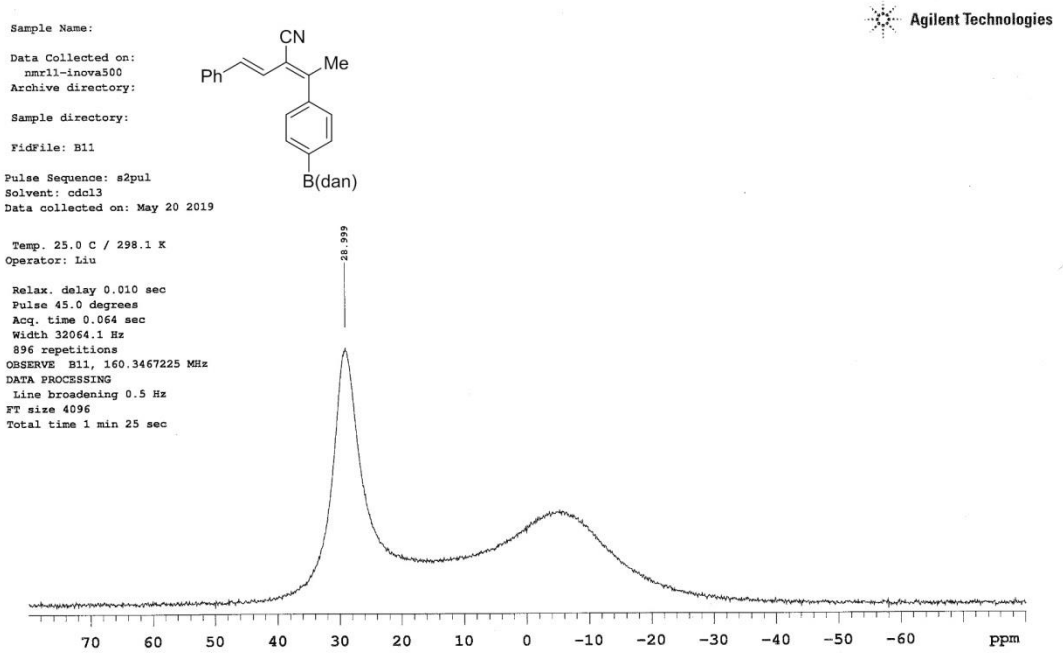
Agilent Technologies
Sample Name:
Data Collected on:
nmr11-inova500
Archive directory:
Sample directory:
FidFile: B11
Pulse Sequence: s2pul
Solvent: cdcl3
Data collected on: May 20 2019
Temp. 25.0 C / 298.1 K
Operator: Liu
Relax. delay 0.010 sec
Pulse 45.0 degrees
Acq. time 0.064 sec
Width 32064.1 Hz
896 repetitions
OBSERVE B11, 160.3467225 MHz
DATA PROCESSING
Line broadening 0.5 Hz
FT size 4096
Total time 1 min 25 sec
CN
Me
Ph
B(dan)
28.999
70 60 50 40 30 20 10 0 -10 -20 -30 -40 -50 -60 ppm

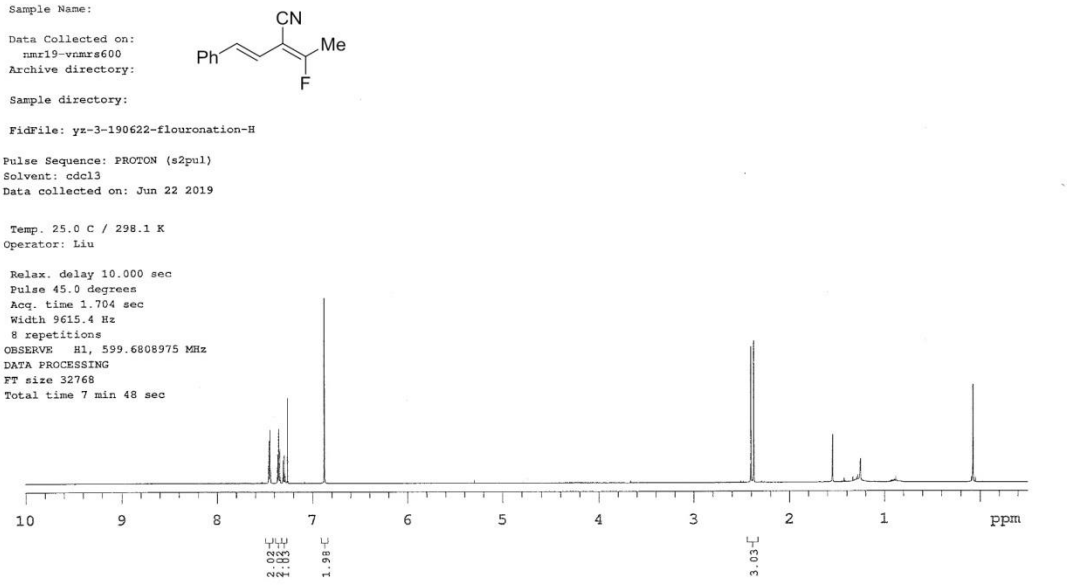
Sample Name:
Data Collected on:
nmr19-vnmrs600
Archive directory:
Sample directory:
FidFile: yz-3-190622-flouronation-H
Pulse Sequence: PROTON (s2pul)
Solvent: cdcl3
Data collected on: Jun 22 2019
Temp. 25.0 C / 298.1 K
Operator: Liu
Relax. delay 10.000 sec
Pulse 45.0 degrees
Acq. time 1.704 sec
Width 9615.4 Hz
8 repetitions
OBSERVE H1, 599.6808975 MHz
DATA PROCESSING
FT size 32768
Total time 7 min 48 sec
CN
Me
Ph
F
10 9 8 7 6 5 4 3 2 1 ppm
2.02
1.03
1.98
3.03

Sample Name:

Data Collected on:
nmr14-vnmrs400
Archive directory:

Sample directory:

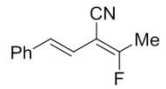

FidFile: yz-3-190622-fluorination-C

Pulse Sequence: CARBON (s2pul)
Solvent: cdcl3
Data collected on: Jun 21 2019

Temp. 25.0 C / 298.1 K
Operator: Liu

Relax. delay 1.000 sec
Pulse 45.0 degrees
Acq. time 1.311 sec
Width 25000.0 Hz
8000 repetitions
OBSERVE C13, 100.5208755 MHz
DECOUPLE H1, 399.7666112 MHz
Power 40 dB
continuously on
WALTZ-16 modulated
DATA PROCESSING
Line broadening 0.5 Hz
FT size 65536
Total time 5 hr, 8 min

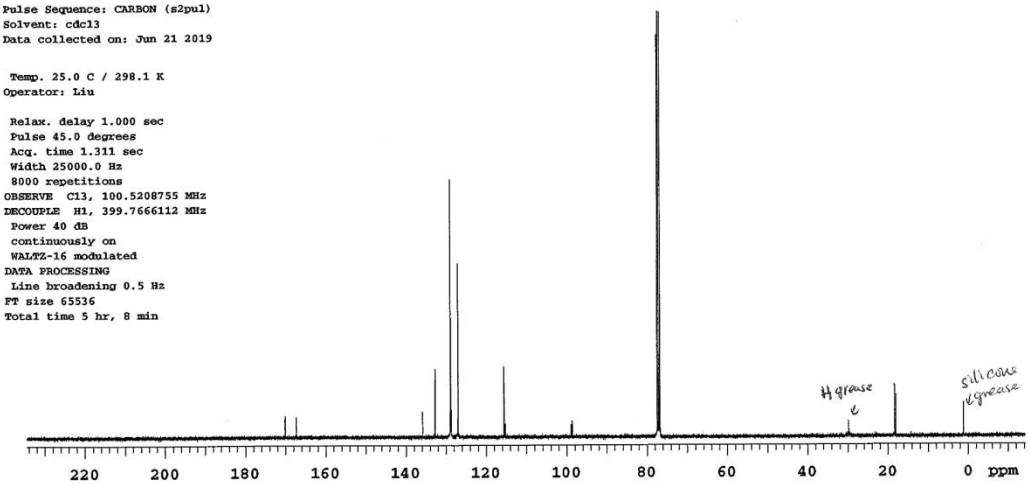

STANDARD FLUORINE PARAMETERS

Sample Name:

Data Collected on:
nmr19-vnmrs600
Archive directory:

Sample directory:

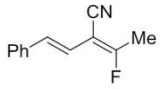

FidFile: FLUORINE

Pulse Sequence: FLUORINE (s2pul)
Solvent: cdcl3
Data collected on: Jun 22 2019

Temp. 25.0 C / 298.1 K
Operator: Liu

Relax. delay 1.000 sec
Pulse 30.0 degrees
Acq. time 0.996 sec
Width 131.6 kHz
20 repetitions
OBSERVE F19, 564.2638160 MHz
DATA PROCESSING
FT size 262144
Total time 3 min 20 sec

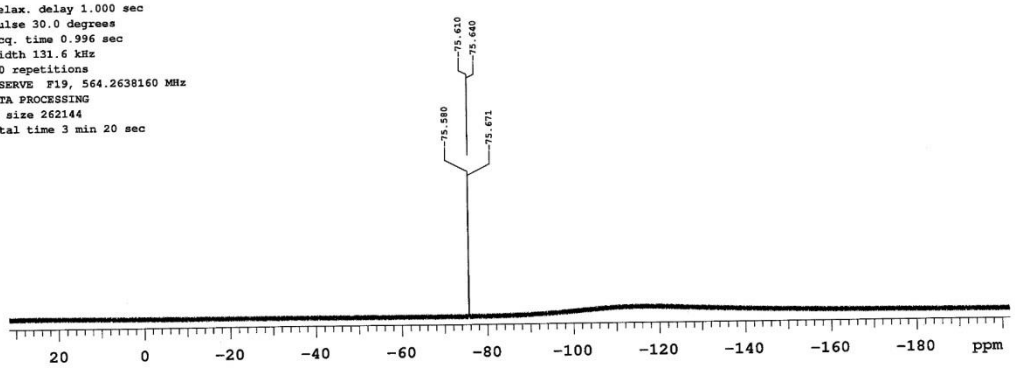

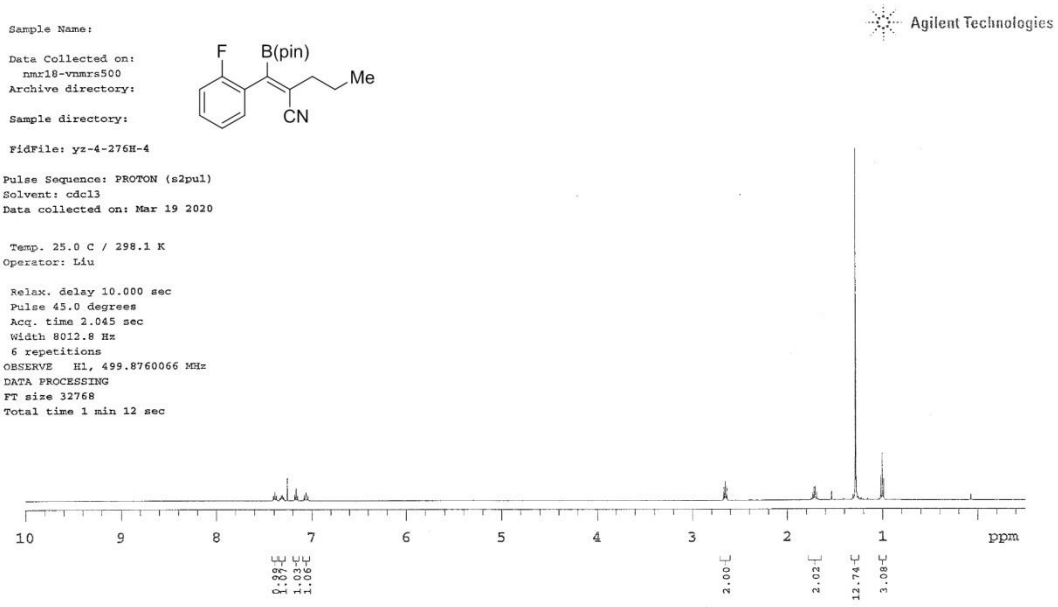
Agilent Technologies
Sample Name:
Data Collected on:
nmr18-vnmrs500
Archive directory:
Sample directory:
FidFile: yz-4-276H-4
Pulse Sequence: PROTON (s2pul)
Solvent: cdcl3
Data collected on: Mar 19 2020
Temp. 25.0 C / 298.1 K
Operator: Liu
Relax. delay 10.000 sec
Pulse 45.0 degrees
Acq. time 2.045 sec
Width 8012.8 Hz
6 repetitions
OBSERVE H1, 499.8760066 MHz
DATA PROCESSING
FT size 32768
Total time 1 min 12 sec
F
B(pin)
Me
CN
10
9
8
7
6
5
4
3
2
1
ppm
1.88
1.03
1.06
2.00
2.02
12.74
3.08

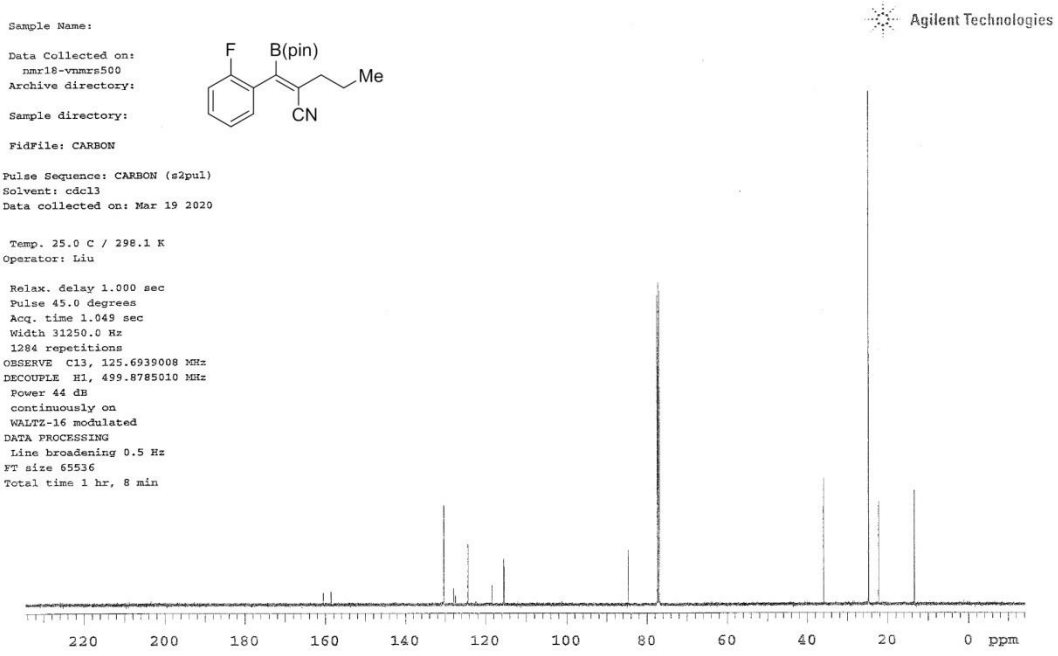
Agilent Technologies
Sample Name:
Data Collected on:
nmr18-vnmrs500
Archive directory:
Sample directory:
FidFile: CARBON
Pulse Sequence: CARBON (s2pul)
Solvent: cdcl3
Data collected on: Mar 19 2020
Temp. 25.0 C / 298.1 K
Operator: Liu
Relax. delay 1.000 sec
Pulse 45.0 degrees
Acq. time 1.049 sec
Width 31250.0 Hz
1284 repetitions
OBSERVE C13, 125.6939008 MHz
DECOUPLE H1, 499.8785010 MHz
Power 44 dB
continuously on
WALTZ-16 modulated
DATA PROCESSING
Line broadening 0.5 Hz
FT size 65536
Total time 1 hr, 8 min
F
B(pin)
Me
CN
220
200
180
160
140
120
100
80
60
40
20
0
ppm

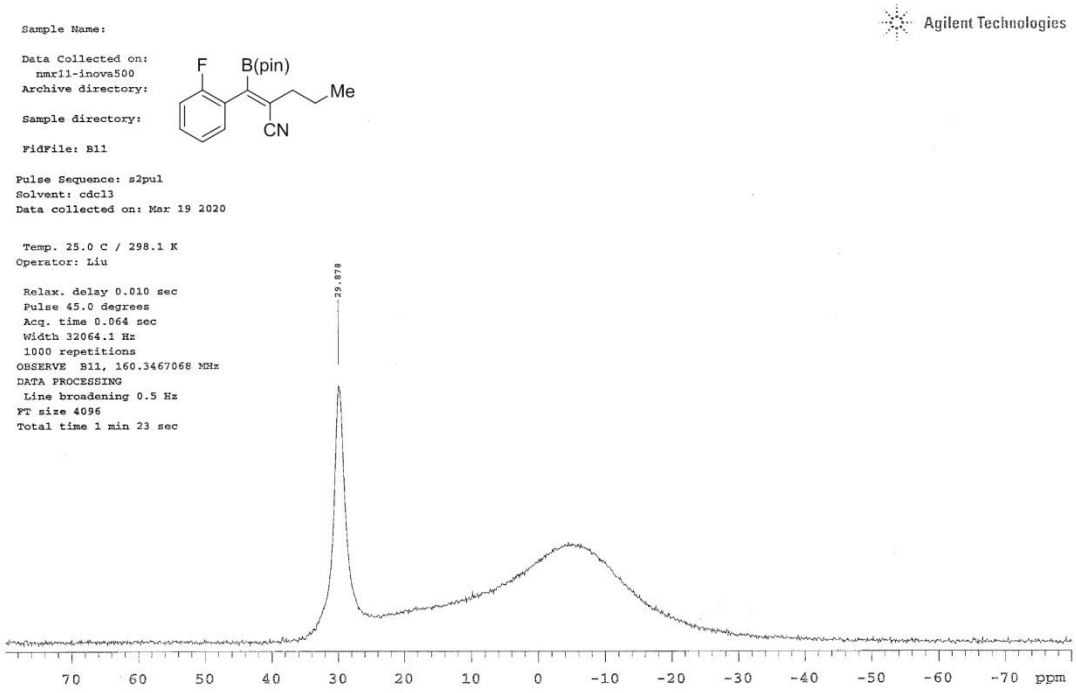
Agilent Technologies
Sample Name:
Data Collected on:
nmr11-inova500
Archive directory:
Sample directory:
FidFile: B11
F
B(pin)
Me
CN
Pulse Sequence: s2pul
Solvent: cdcl3
Data collected on: Mar 19 2020
Temp. 25.0 C / 298.1 K
Operator: Liu
Relax. delay 0.010 sec
Pulse 45.0 degrees
Acq. time 0.064 sec
Width 32064.1 Hz
1000 repetitions
OBSERVE B11, 160.3467068 MHz
DATA PROCESSING
Line broadening 0.5 Hz
FT size 4096
Total time 1 min 23 sec
29.878
70 60 50 40 30 20 10 0 -10 -20 -30 -40 -50 -60 -70 ppm

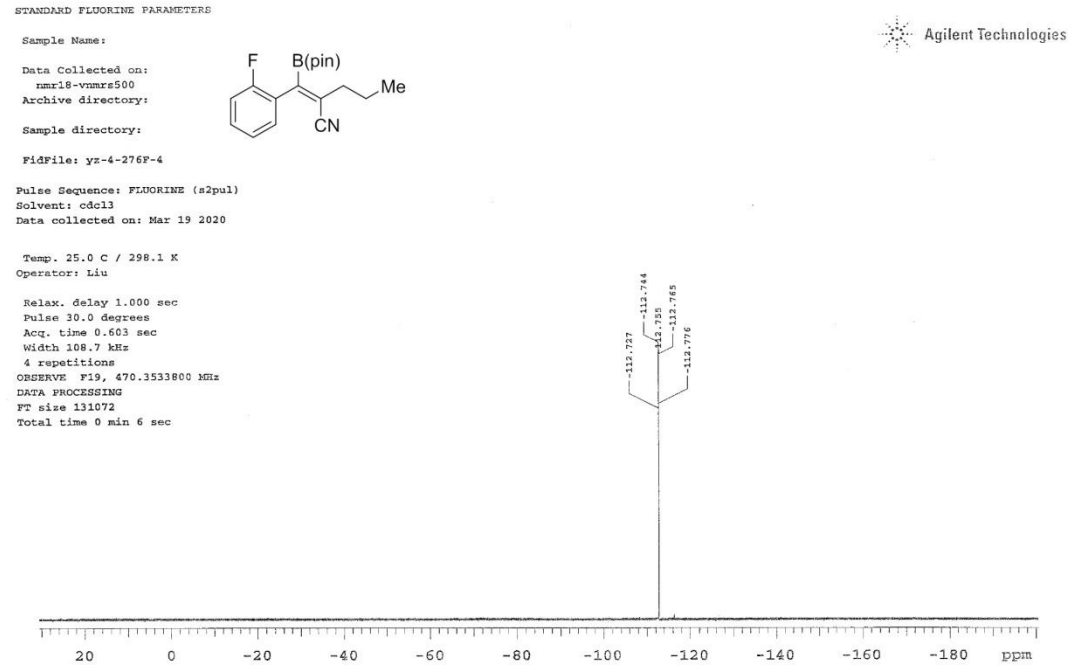
STANDARD FLUORINE PARAMETERS
Agilent Technologies
Sample Name:
Data Collected on:
nmr18-vnmrs500
Archive directory:
Sample directory:
FidFile: yz-4-276F-4
F
B(pin)
Me
CN
Pulse Sequence: FLUORINE (s2pul)
Solvent: cdcl3
Data collected on: Mar 19 2020
Temp. 25.0 C / 298.1 K
Operator: Liu
Relax. delay 1.000 sec
Pulse 30.0 degrees
Acq. time 0.603 sec
Width 108.7 kHz
4 repetitions
OBSERVE F19, 470.3533800 MHz
DATA PROCESSING
FT size 131072
Total time 0 min 6 sec
-112.727
-112.744
-112.755
-112.765
-112.776
20 0 -20 -40 -60 -80 -100 -120 -140 -160 -180 ppm

Sample Name:

Data Collected on:
nmr19-vnmrs600
Archive directory:

Sample directory:

FidFile: PROTON

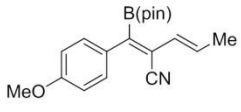

Pulse Sequence: PROTON (s2pul)
Solvent: cdcl3
Data collected on: Nov 6 2019

Temp. 25.0 C / 298.1 K
Operator: Liu

Relax. delay 10.000 sec
Pulse 45.0 degrees
Acq. time 1.704 sec
Width 9615.4 Hz
4 repetitions
OBSERVE H1, 599.6806832 MHz
DATA PROCESSING
FT size 32768
Total time 0 min 47 sec

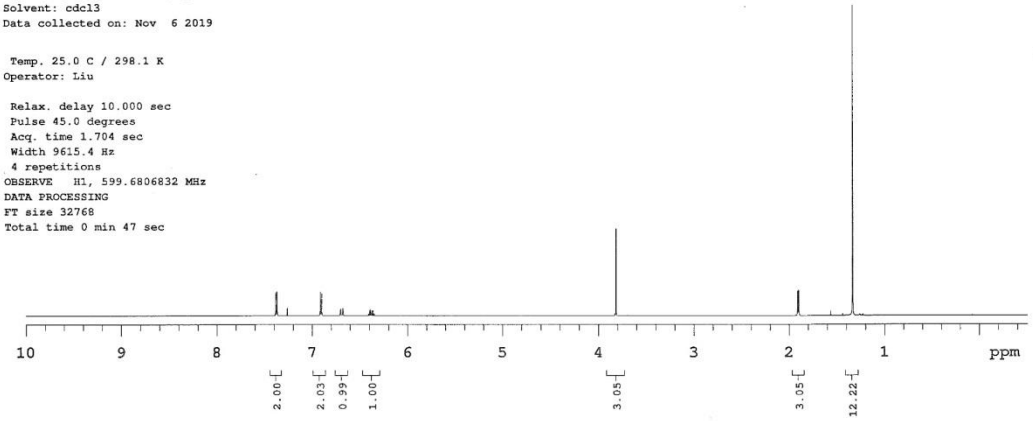

Sample Name:

Data Collected on:
nmr19-vnmrs600
Archive directory:

Sample directory:

FidFile: CARBON

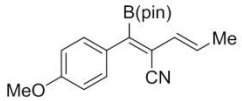

Pulse Sequence: CARBON (s2pul)
Solvent: cdcl3
Data collected on: Nov 6 2019

Temp. 25.0 C / 298.1 K
Operator: Liu

Relax. delay 1.000 sec
Pulse 45.0 degrees
Acq. time 0.865 sec
Width 37878.8 Hz
400 repetitions
OBSERVE C13, 150.7898074 MHz
DECOUPLE H1, 599.6836825 MHz
Power 46 dB
continuously on
WALTZ-16 modulated
DATA PROCESSING
Line broadening 0.5 Hz
FT size 65536
Total time 31 min

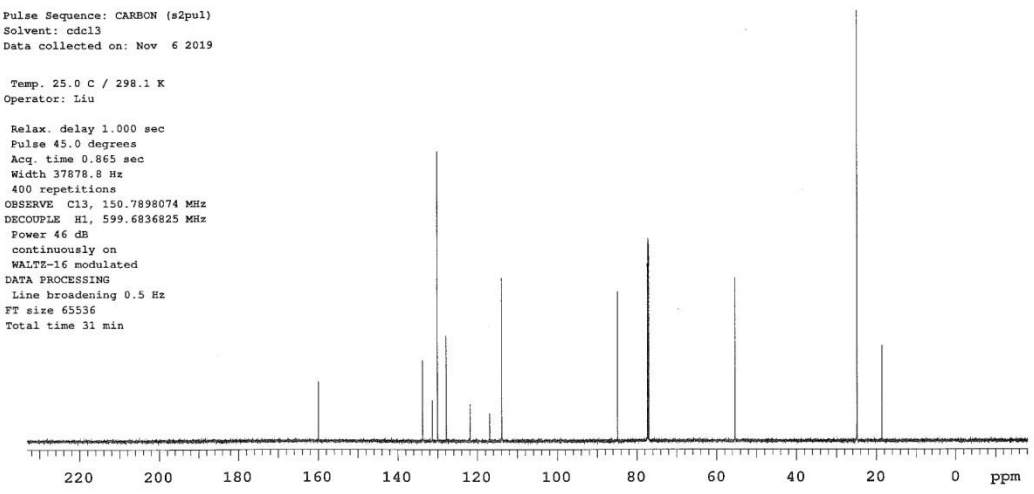

Agilent Technologies

Sample Name:

Data Collected on:
nmr11-inova500
Archive directory:

Sample directory:

FidFile: B11

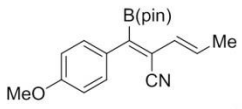

Pulse Sequence: s2pul
Solvent: cdcl3
Data collected on: Sep 21 2019

Temp. 25.0 C / 298.1 K
Operator: Liu

Relax. delay 0.010 sec
Pulse 45.0 degrees
Acq. time 0.064 sec
Width 32064.1 Hz
1000 repetitions
OBSERVE B11, 160.3466912 MHz
DATA PROCESSING
Line broadening 0.5 Hz
FT size 4096
Total time 1 min 23 sec

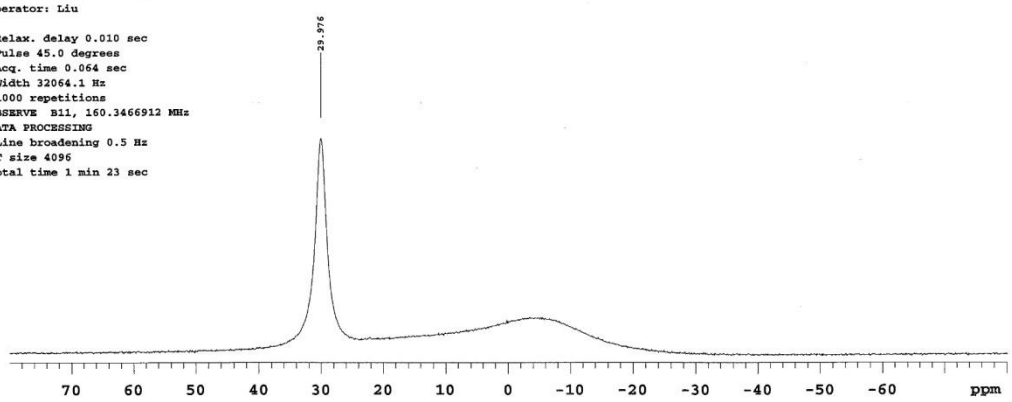

Agilent Technologies

Sample Name:

Data Collected on:
nmr18-vnmrs500
Archive directory:

Sample directory:

FidFile: PROTON

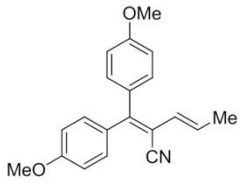

Pulse Sequence: PROTON (s2pul)
Solvent: cdcl3
Data collected on: Oct 2 2019

Temp. 25.0 C / 298.1 K
Operator: Liu

Relax. delay 10.000 sec
Pulse 45.0 degrees
Acq. time 2.045 sec
Width 8012.8 Hz
8 repetitions
OBSERVE H1, 499.8762802 MHz
DATA PROCESSING
FT size 32768
Total time 1 min 36 sec

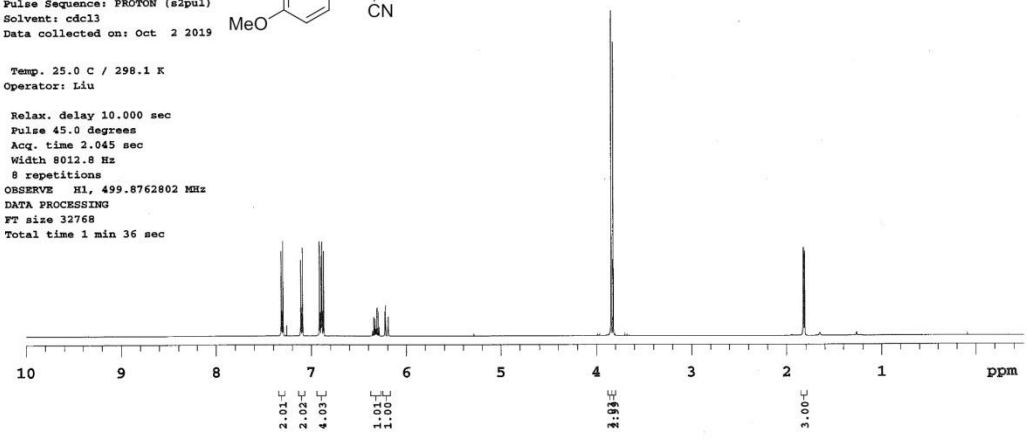

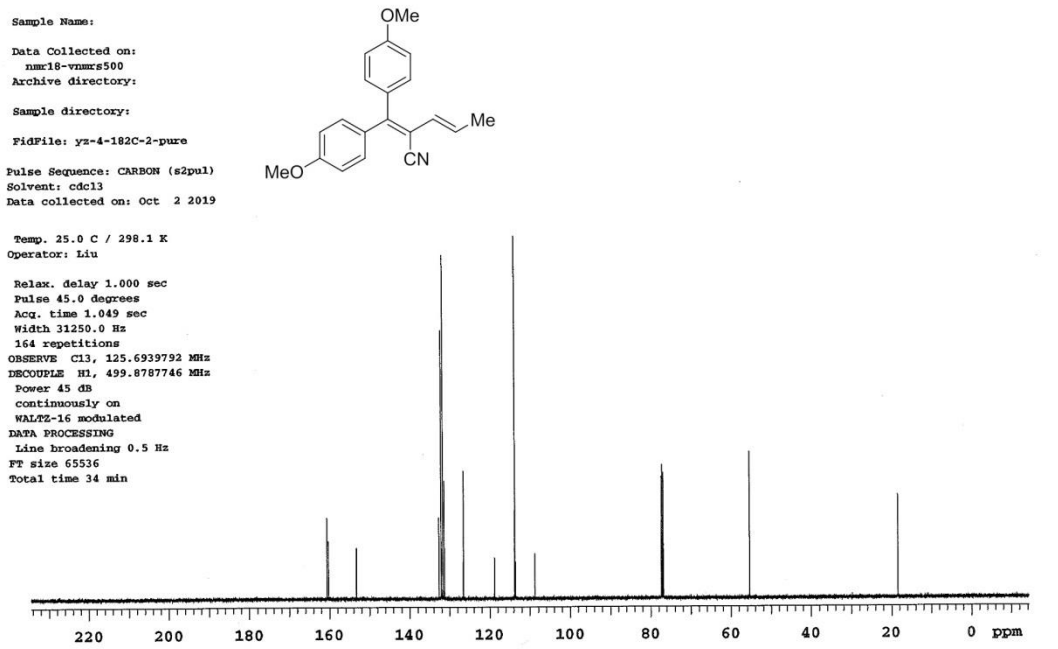
Sample Name:
Data Collected on:
nmr18-vnmrs500
Archive directory:
Sample directory:
FidFile: yz-4-182C-2-pure
Pulse Sequence: CARBON (s2pul)
Solvent: cdcl3
Data collected on: Oct 2 2019
Temp. 25.0 C / 298.1 K
Operator: Liu
Relax. delay 1.000 sec
Pulse 45.0 degrees
Acq. time 1.049 sec
Width 31250.0 Hz
164 repetitions
OBSERVE C13, 125.6939792 MHz
DECOUPLE H1, 499.8787746 MHz
Power 45 dB
continuously on
WALTZ-16 modulated
DATA PROCESSING
Line broadening 0.5 Hz
FT size 65536
Total time 34 min
OMe
Me
CN
MeO
220
200
180
160
140
120
100
80
60
40
20
0
ppm

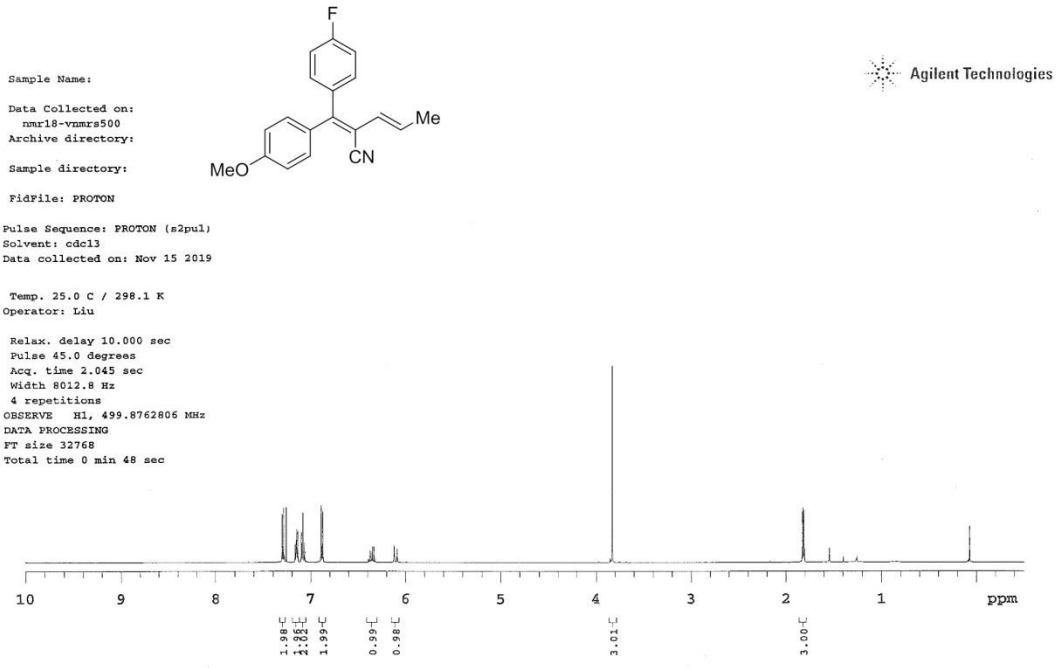
Sample Name:
Data Collected on:
nmr18-vnmrs500
Archive directory:
Sample directory:
FidFile: PROTON
Pulse Sequence: PROTON (s2pul)
Solvent: cdcl3
Data collected on: Nov 15 2019
Temp. 25.0 C / 298.1 K
Operator: Liu
Relax. delay 10.000 sec
Pulse 45.0 degrees
Acq. time 2.045 sec
Width 8012.8 Hz
4 repetitions
OBSERVE H1, 499.8762806 MHz
DATA PROCESSING
FT size 32768
Total time 0 min 48 sec
F
Me
CN
MeO
Agilent Technologies
10
9
8
7
6
5
4
3
2
1
ppm
1.98
1.82
1.99
0.99
0.98
3.01
3.00

Sample Name:

Data Collected on:
nmr18-vnmrs500
Archive directory:

Sample directory:

FidFile: CARBON

Pulse Sequence: CARBON (s2pul)
Solvent: cdcl3
Data collected on: Nov 15 2019

Temp. 25.0 C / 298.1 K
Operator: Liu

Relax. delay 1.000 sec
Pulse 45.0 degrees
Acq. time 1.049 sec
Width 31250.0 Hz
824 repetitions
OBSERVE C13, 125.6939696 MHz
DECOUPLE H1, 499.8787746 MHz
Power 45 dB
continuously on
WALTZ-16 modulated
DATA PROCESSING
Line broadening 0.5 Hz
FT size 65536
Total time 34 min

Agilent Technologies

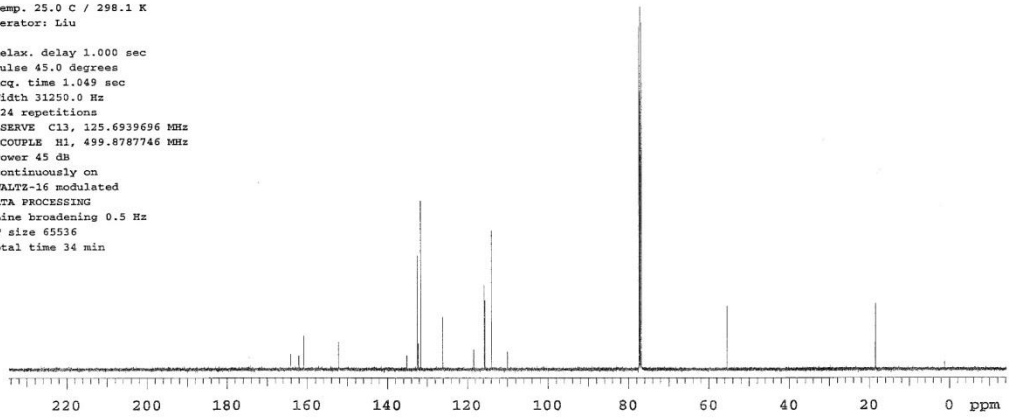

STANDARD FLUORINE PARAMETERS

Sample Name:

Data Collected on:
nmr18-vnmrs500
Archive directory:

Sample directory:

FidFile: FLUORINE

Pulse Sequence: FLUORINE (s2pul)
Solvent: cdcl3
Data collected on: Nov 15 2019

Temp. 25.0 C / 298.1 K
Operator: Liu

Relax. delay 1.000 sec
Pulse 30.0 degrees
Acq. time 0.603 sec
Width 108.7 kHz
20 repetitions
OBSERVE F19, 470.3536374 MHz
DATA PROCESSING
FT size 131072
Total time 0 min 32 sec

Agilent Technologies

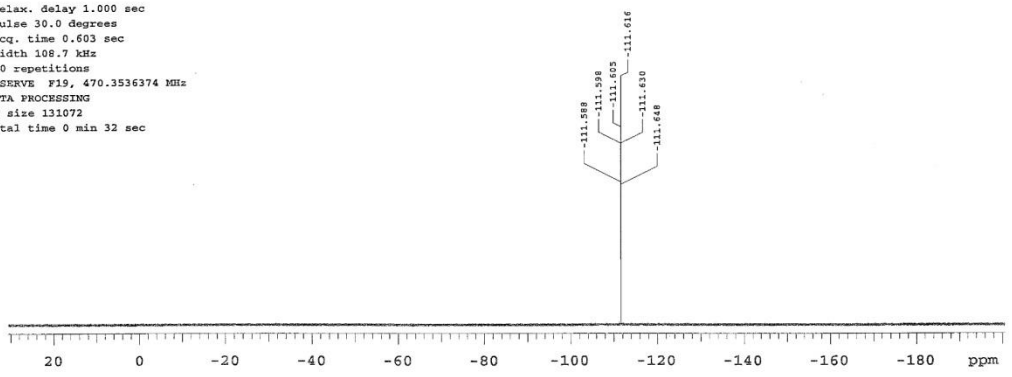

Sample Name:

Data Collected on:
nmr19-vnmrs600
Archive directory:

Sample directory:

FidFile: yz-4-242H-1

Pulse Sequence: PROTON (s2pul)
Solvent: cdcl3
Data collected on: Jan 3 2020

Temp. 25.0 C / 298.1 K
Operator: Liu

Relax. delay 10.000 sec
Pulse 45.0 degrees
Acq. time 1.704 sec
Width 9615.4 Hz
6 repetitions
OBSERVE H1, 599.6806841 MHz
DATA PROCESSING
FT size 32768
Total time 1 min 57 sec

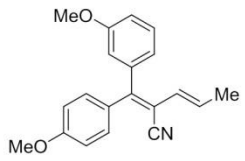

8c

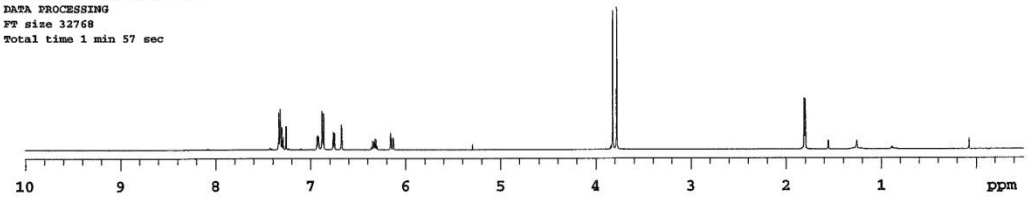

Sample Name:

Data Collected on:
nmr19-vnmrs600
Archive directory:

Sample directory:

FidFile: CARBON

Pulse Sequence: CARBON (s2pul)
Solvent: cdcl3
Data collected on: Jan 3 2020

Temp. 25.0 C / 298.1 K
Operator: Liu

Relax. delay 1.000 sec
Pulse 45.0 degrees
Acq. time 0.865 sec
Width 37878.8 Hz
240 repetitions
OBSERVE C13, 150.7898050 MHz
DECOUPLE H1, 599.6836825 MHz
Power 45 dB
continuously on
WALTZ-16 modulated
DATA PROCESSING
Line broadening 0.5 Hz
FT size 65536
Total time 31 min

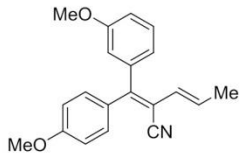

8c

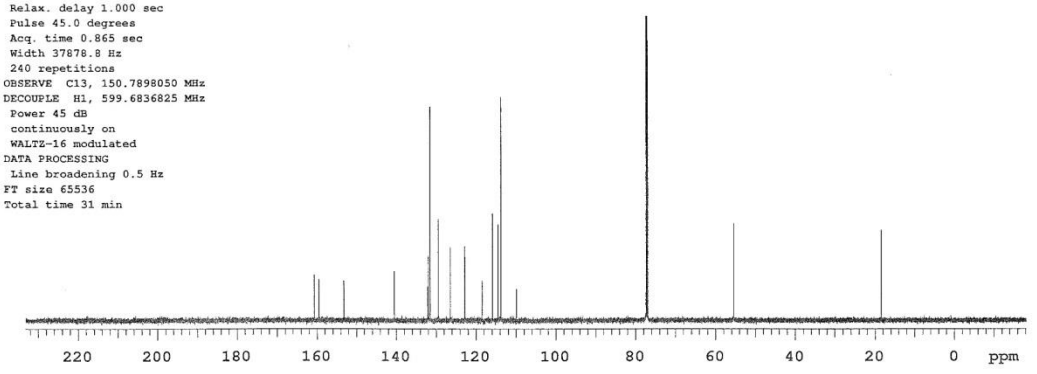

Agilent Technologies

Sample Name:

Data Collected on:
nmr18-vnmrs500
Archive directory:

Sample directory:

FidFile: PROTON

Pulse Sequence: PROTON (s2pul)
Solvent: cdcl3
Data collected on: Oct 4 2019

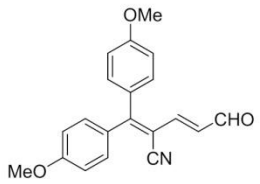

Temp. 25.0 C / 298.1 K
Operator: Liu

Relax. delay 10.000 sec
Pulse 45.0 degrees
Acq. time 2.045 sec
Width 8012.8 Hz
4 repetitions
OBSERVE H1, 499.8762807 MHz
DATA PROCESSING
FT size 32768
Total time 0 min 48 sec

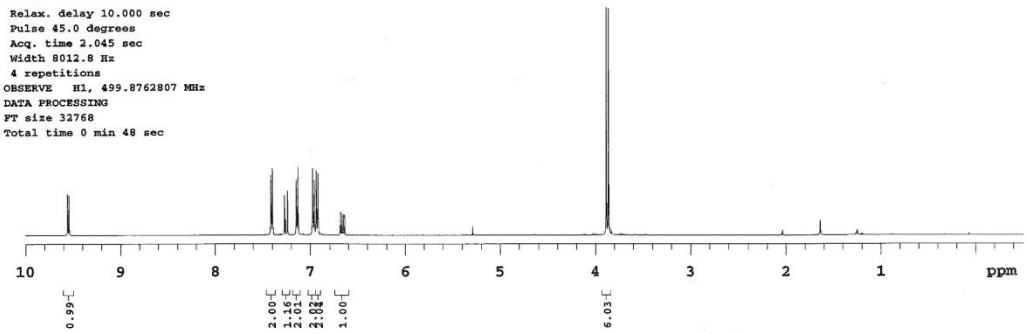

Sample Name:

Data Collected on:
nmr18-vnmrs500
Archive directory:

Sample directory:

FidFile: yz-4-182C-3

Pulse Sequence: CARBON (s2pul)
Solvent: cdcl3
Data collected on: Oct 4 2019

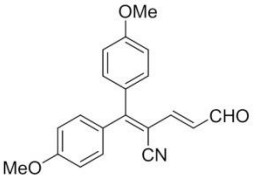

Temp. 25.0 C / 298.1 K
Operator: Liu

Relax. delay 1.000 sec
Pulse 45.0 degrees
Acq. time 1.049 sec
Width 31250.0 Hz
124 repetitions
OBSERVE C13, 125.6939811 MHz
DECOUPLE H1, 499.8787746 MHz
Power 45 dB
continuously on
WALTZ-16 modulated
DATA PROCESSING
Line broadening 0.5 Hz
FT size 65536
Total time 34 min

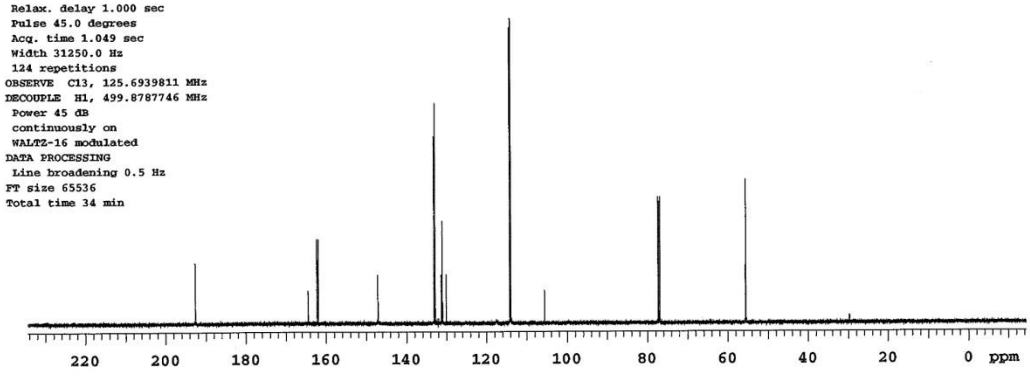

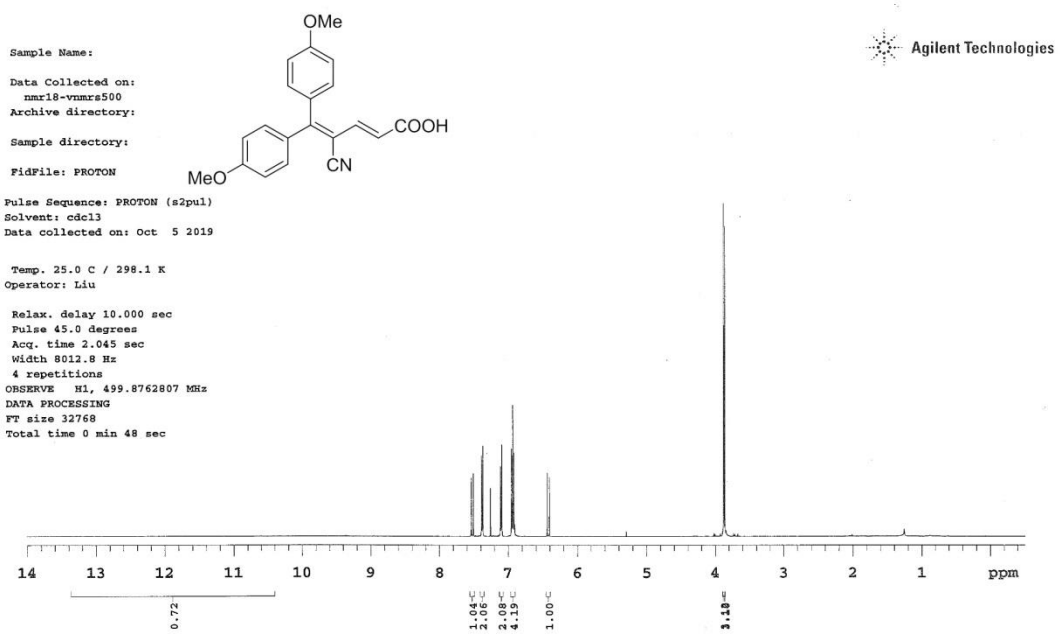
Sample Name:
Data Collected on:
nmr18-vnmrs500
Archive directory:
Sample directory:
FidFile: PROTON
OMe
COOH
CN
MeO
Agilent Technologies
Pulse Sequence: PROTON (s2pul)
Solvent: cdcl3
Data collected on: Oct 5 2019
Temp. 25.0 C / 298.1 K
Operator: Liu
Relax. delay 10.000 sec
Pulse 45.0 degrees
Acq. time 2.045 sec
Width 8012.8 Hz
4 repetitions
OBSERVE H1, 499.8762807 MHz
DATA PROCESSING
FT size 32768
Total time 0 min 48 sec
14 13 12 11 10 9 8 7 6 5 4 3 2 1 ppm
0.72
1.04
2.06
2.08
4.19
1.00
3.18

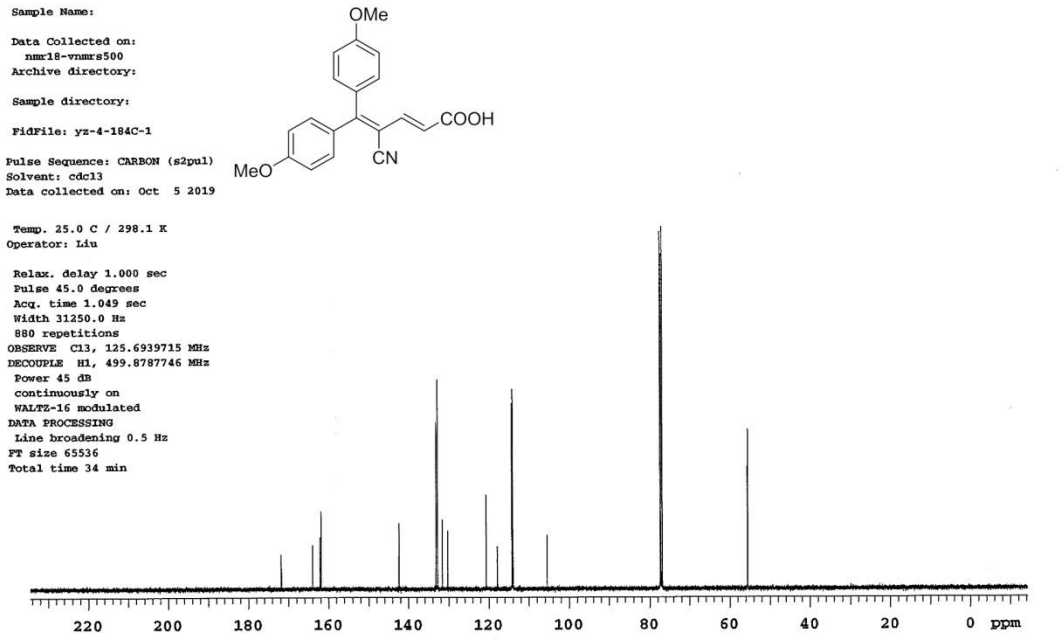
Sample Name:
Data Collected on:
nmr18-vnmrs500
Archive directory:
Sample directory:
FidFile: yz-4-184C-1
OMe
COOH
CN
MeO
Pulse Sequence: CARBON (s2pul)
Solvent: cdcl3
Data collected on: Oct 5 2019
Temp. 25.0 C / 298.1 K
Operator: Liu
Relax. delay 1.000 sec
Pulse 45.0 degrees
Acq. time 1.049 sec
Width 31250.0 Hz
880 repetitions
OBSERVE C13, 125.6939715 MHz
DECOUPLE H1, 499.8787746 MHz
Power 45 dB
continuously on
WALTZ-16 modulated
DATA PROCESSING
Line broadening 0.5 Hz
FT size 65536
Total time 34 min
220 200 180 160 140 120 100 80 60 40 20 0 ppm

Sample Name:

Data Collected on:
nmr19-vnmrs600
Archive directory:

Sample directory:

FidFile: yz-4-198-2-H

Pulse Sequence: PROTON (s2pul)
Solvent: cdcl3
Data collected on: Oct 30 2019

Temp. 25.0 C / 298.1 K
Operator: Liu

Relax. delay 10.000 sec
Pulse 45.0 degrees
Acq. time 1.704 sec
Width 9615.4 Hz
4 repetitions
OBSERVE H1, 599.6806838 MHz
DATA PROCESSING
FT size 32768
Total time 0 min 47 sec

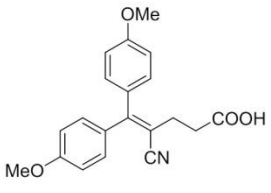

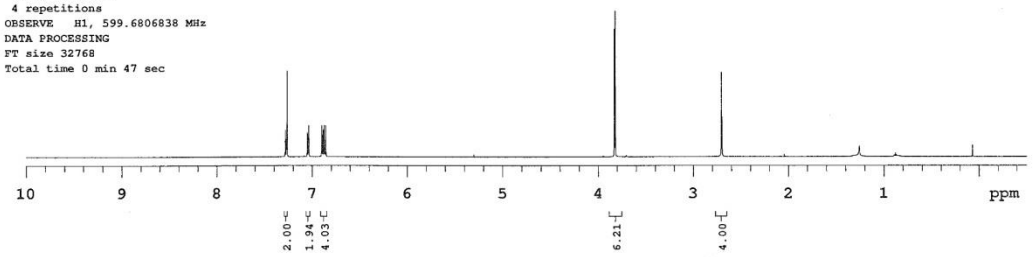

Sample Name:

Data Collected on:
nmr19-vnmrs600
Archive directory:

Sample directory:

FidFile: yz-198-2-C

Pulse Sequence: CARBON (s2pul)
Solvent: cdcl3
Data collected on: Oct 30 2019

Temp. 25.0 C / 298.1 K
Operator: Liu

Relax. delay 1.000 sec
Pulse 45.0 degrees
Acq. time 0.865 sec
Width 37878.8 Hz
10000 repetitions
OBSERVE C13, 150.7898054 MHz
DECOUPLE H1, 599.6836825 MHz
Power 46 dB
continuously on
WALTZ-16 modulated
DATA PROCESSING
Line broadening 0.5 Hz
FT size 65536
Total time 5 hr, 10 min

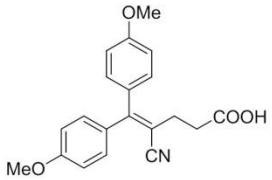

line broadening = 0.5

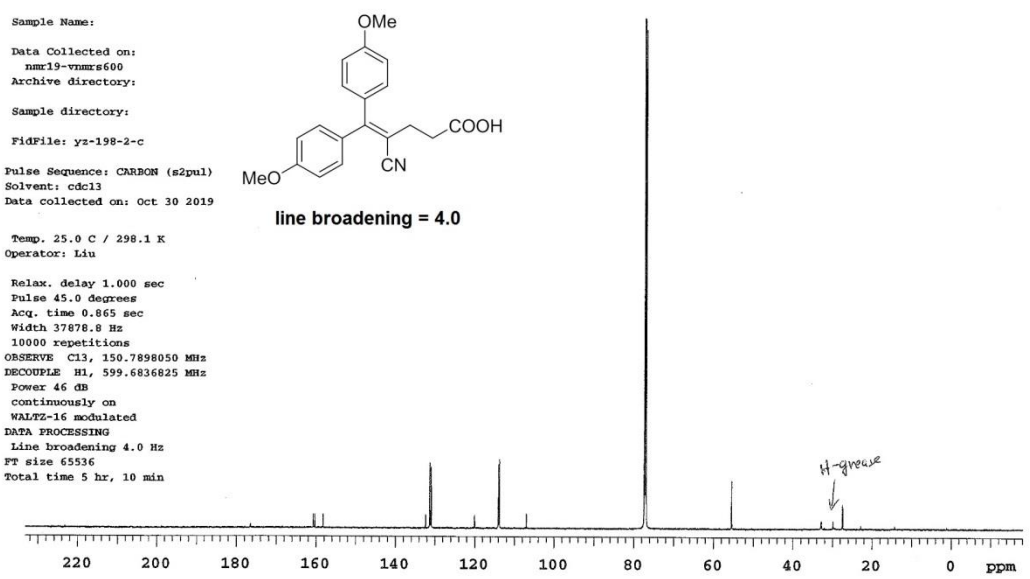

	Parameter	Value
1	Solvent	odcb
2	Temperature	25.0
3	Relaxation Delay	0.0100
4	Nucleus	11B

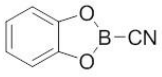

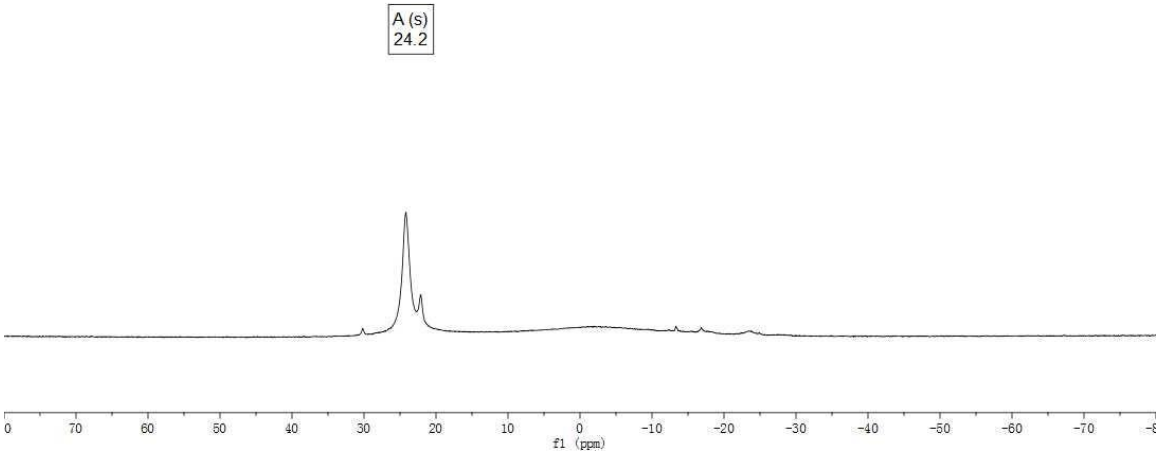

Chapter Three. Evaluation of Palladium-Azaborine Coordination Dynamics in Pd/Senphos Complexes

3.1. Background

Alkenes are one of the most common ligand classes in organometallic compounds,[1] and its history can be traced back to the very first organometallic compound, the Zeise's salt.[2] Consequently, borataalkene, the isoelectronic and isostructural analogue of alkene (Figure 3.1, right), would provide an opportunity to expand the available ligand chemical space.[3]

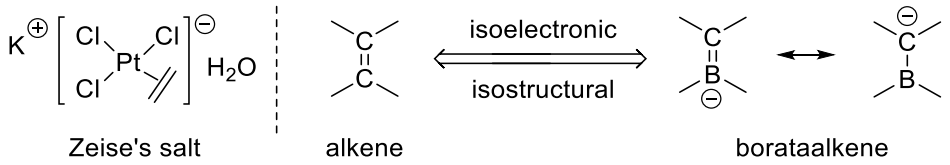

Figure 3.1. Structure of Zeise's salt and borataalkene.

3.1.1. Metal complexes containing borataalkene ligand

Borataalkenes are typically generated *in situ* from α-deprotonation of mono-boryl alkanes and can engage in subsequent transformations for synthetic applications, (e.g.

[1] (a) Crabtree, R. H. *The Organometallic Chemistry of the Transition Metals*, 5th ed.; Wiley, Hoboken, NJ, 2009; (b) Elschenbroich, C. *Organometallics*, 3rd ed.; Wiley-VCH, Weinheim, 2006; (c) Albano, V. G.; Natile, G.; Panunzi, A. *Coord. Chem. Rev*. **1994**, *133*, 67-114; (d) Fairlamb, I. J. S. *Org. Biomol. Chem.* **2008**, *6*, 3645-3656.

[2] (a) W. C. Zeise, *Overs. K. Dan. Vidensk. Selsk. Forth*. **1825-26**, 13; (b) Zeise, W. C. *Ann. Phys. Chem*. **1831**, *21*, 497-541.

[3] For reviews, see: (a) Emslie, D. J. H.; Cowie, B. E.; Kolpin, K. B. *Dalton Trans*. **2012**, *41*, 1101-1117; (b) Goettel, J. T.; Braunschweig, H. *Coord. Chem. Rev*. **2019**, *380*, 184-299.

boron-Wittig reactions).[4,5] On the other hand, the application of borataalkene ligand in organometallic chemistry remains underdeveloped. Unlike alkenes, which usually coordinate to the transition metals in a symmetrical η^2-C,C fashion,[6] borataalkenes bind to transition metals unsymmetrically with diverse coordination modes such as η^2-B,C[7-15], η^1-B[15-16] and η^1-C[17-19]. These variations originate from the highly biased borataalkene electronic structure (Figure 3.2), where the HOMO (highest occupied molecular orbital) is largely contributed by the filled carbon p-orbital and the LUMO (lowest unoccupied molecular orbital) is largely contributed by the empty boron p-orbital. Therefore, the electron richness of the metal plays a role in the coordination of borataalkene and the correct coordination mode assignment relies on single crystal X-ray diffraction analysis.[3a]

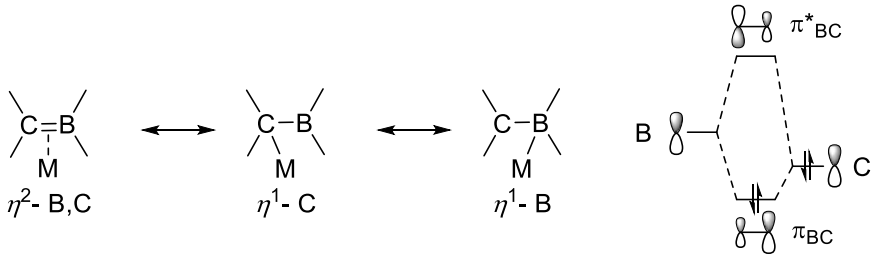

Figure 3.2. Illustration of metal borataalkene interactions.

---

[4] (a) Cainelli, G.; Dal Bello, G.; Zubiani, G. *Tetrahedron Lett.* **1966**, *36*, 4315-4318; (b) Rathke, M. W.; Kow, R. *J. Am. Chem. Soc.* **1972**, *96*, 6854-6856; (c) Olmstead, M. M.; Power, P. P.; Weese, K. J.; Doedens, R. J. *J. Am. Chem. Soc.* **1987**, *109*, 2541-2542; (d) Klusik, H.; Berndt, A. *Angew. Chem. Int. Ed. Engl.* **1983**, *22*, 877-878; (e) Kow, R.; Rathke, M. W. *J. Am. Chem. Soc*. **1973**, *95*, 2715-2716; (f) Ramsey, B. G.; Isabelle, L. M. *J. Org. Chem.* **1981**, *46*, 179-182; (g) Kohrt, S.; Dachwitz, S.; Daniliuc, C. G.; Kehr, G.; Erker, G. *Dalton Trans*. **2015**, *44*, 21032-21040; (h) Cuenca, A. B.; Fernández, E. *Chem. Soc. Rev.* **2021**, *50*, 72-86.

[5] For other syntheses methods, see: (a) Yu, J.; Kehr, G.; Daniliuc C. G.; Erker, G. *Eur. J. Inorg. Chem*. **2013**, 3312-3315; (b) Hoefelmeyer, J. D.; Solé, S.; Gabbaï, F. P. *Dalton Trans.* **2004**, 1254-1258; (c) Möbus, J.; Kehr, G.; Daniliuc, C. G.; Fröhlich, R.; Erker, G. *Dalton Trans.* **2014**, *43*, 632-638; (d) Wang, L.; Jian, Z.; Daniliuc, C. G.; Kehr, G.; Erker, G. *Dalton Trans*. **2018**, *47*, 10853-10856; (e) Chiu, C.; Gabbaï, F. P. *Angew. Chem. Int. Ed.* **2007**, *46*, 6878-6881.

[6] (a) Weding, N.; Hapke, M. *Chem. Soc. Rev.* **2011**, *40*, 4525-4514; (b) Franke, R.; Selent, D.; Börner, A. *Chem. Rev.* **2012**, *112*, 5675-5732; (c) Obligacion, J. V.; Chirik, P. J. *Nat. Rev. Chem.* **2018**, *2*, 15-34. For rare exceptions, see: (d) Stoebenau, E. J.; Jordan, R. F. *J. Am. Chem. Soc.* **2006**, *128*, 8162-8175; (e) Sauriol, F.; Wong, E.; Leung, A. M. H.; Donaghue, I. E.; Baird, M. C.; Wondimagegn, T.; Ziegler, T. *Angew. Chem. Int. Ed.* **2009**, *48*, 3342-3345. For reviews of alkene bound main group metals, see: (f) Harder, S. *Chem. Rev.* **2010**, *110*, 3852-3876; (g) Hill, M. S.; Liptrot, D. J.; Weetman, C. *Chem. Soc. Rev*. **2016**, *45*, 972-988.

Piers and co-workers reported a η^2-B,C borataalkene ligated tantalum system.[7] Hydroboration of tantalocene methylidene methyl **3.2** with Piers borane **3.1** delivers the four-membered tantalum complex **3.3** at –78 °C. As the temperature rises above –20 °C, it gradually reductively eliminates to the singlet η^2-B,C bound complex **3.4**, which is in equilibrium with the triplet η^1-C bound complex **3.4'**. Due to their different spin states, complex **3.4** and **3.4'** show distinct reactivity patterns where complex **3.4** selectively undergoes oxidative cyclization reaction with 2-butyne to furnish the five-membered tantalum complex **3.5**, and complex **3.4'** selectively undergoes ligand association with CO or ^{t}butyl isonitrile to provide the new η^2-B,C bound complex **3.6**.

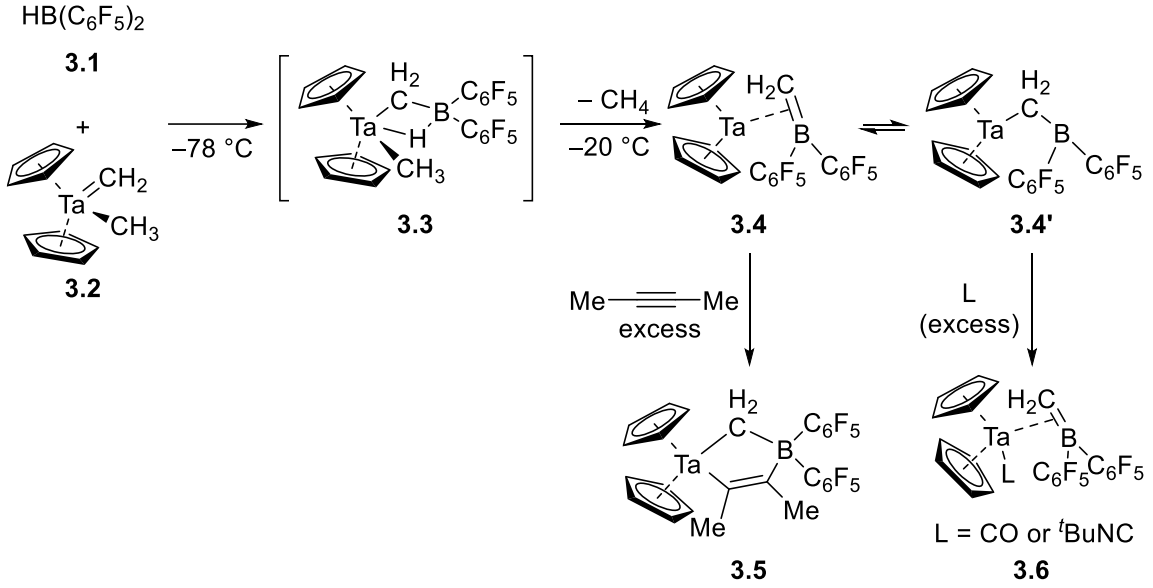

Scheme 3.1. Piers's synthesis of Ta(II) η^2-B,C borataalkene complexes.

[7] (a) Cook, K. S.; Piers, W. E.; Rettig, S. J. *Organometallics* **1999**, *18*, 1575-1577; (b) Cook, K. S.; Piers, W. E.; Woo, T. K.; McDonald, R. *Organometallics* **2001**, *20*, 3927-3937; (c) Cook, K. S.; Piers, W. E.; McDonald, R. *J. Am. Chem. Soc.* **2002**, *124*, 5411-5418; (d) Cook, K. S.; Piers, W. E.; Hayes, P. G.; Parvez, M. *Organometallics* **2002**, *21*, 2422-2425.

The Szymczak group synthesized an η^2-B,C borataalkene bound Ru complex (Scheme 3.2).[8] In the way of designing new bifunctional ruthenium complexes, they discovered that the *NNN*-isoindoline pincer ligated ruthenium dimer **3.7** undergoes dehydrogenation reaction with 9-BBN (9-borabicyclo[3.3.1]nonane) to afford the η^2-B,C bound Ru complex **3.8**. Under CO and H_2 atmosphere, complex **3.8** acts as an efficient catalyst in alkyne hydrogenation reaction, where dihydrogen can be activated by the 9-BBN group to give complex **3.9**.

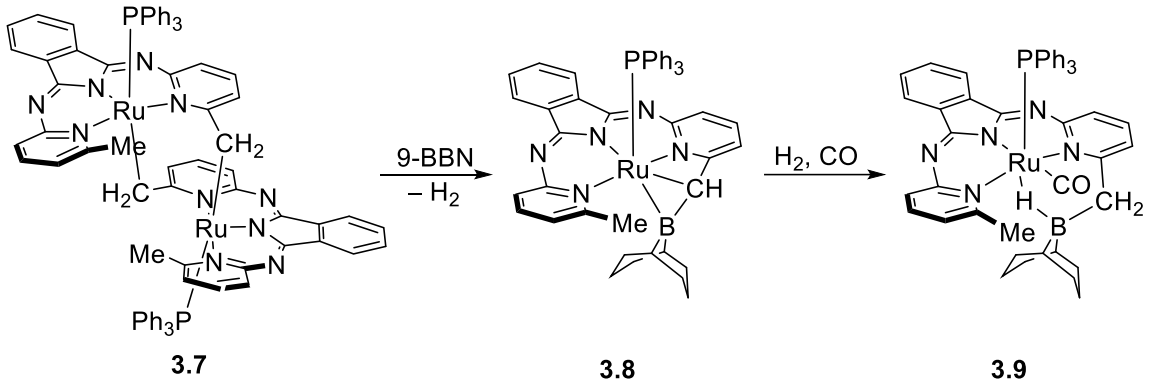

3.7 **3.8** **3.9**

Scheme 3.2. Szymczak's synthesis of Ru(II) η^2-B,C borataalkene complex.

Owen and co-workers successfully synthesized a rhodium complex with η^2-B,C coordination.[9] Complexation reaction of borane-bound 2-mercaptopyridine lithium salt **3.10** with $[Rh(nbd)Cl]_2$ (nbd: 2,5-norbornadiene) provides complex **3.11** with two bridging hydrides. Further treatment of two equivalents of PPh_3 triggers rearrangements to deliver the η^2-B,C bound complex **3.12** as follows: The coordination of the first equivalent PPh_3 converts nbd to a mono-dentate ligand followed by β-migratory insertion to afford complex **3.14**. And the coordination of the second equivalent PPh_3 induces a migration of the

[8] Tseng, K.-N. T.; Kampf, J. W.; Szymczak, N. K. *J. Am. Chem. Soc.* **2016**, *138*, 10378-10381.
[9] Iannetelli, A.; Da Costa, R. C.; Guwy, A. J.; Tizzard, G. J.; Coles, S. J.; Owen, G. R. *Organometallics* **2020**, *39*, 1976-1988.

norbornenyl group with subsequent rhodium hydride β-migratory insertion to afford intermediate **3.16**. Finally, a β-alkyl elimination occurs to furnish complex **3.12**.

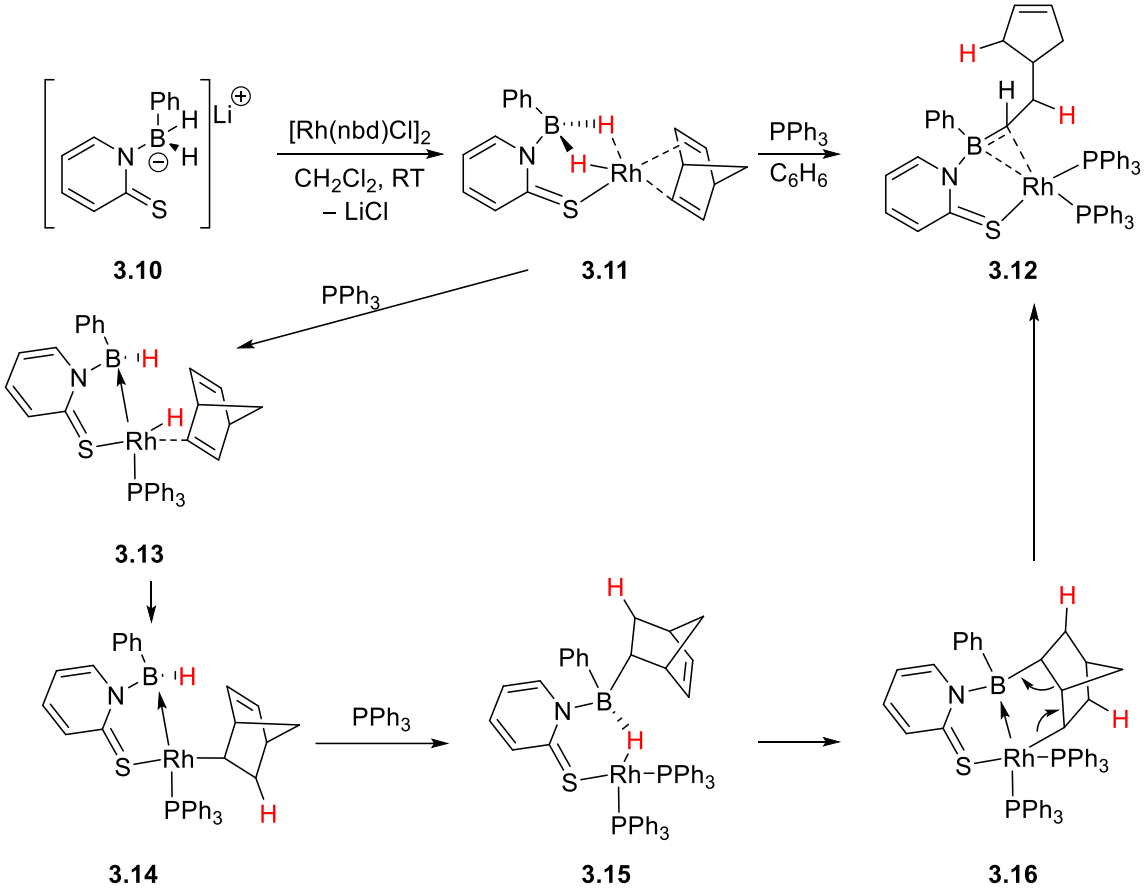

Scheme 3.3. Owen's synthesis of Rh(I) η^2-B,C borataalkene complex.

Another rhodium-based example is reported by the Erker group.[10] Deprotonation of FLP (frustrated Lewis pair) **3.17** with a bulky base LiTMP (lithium tetramethylpiperidide) yields η^1-C bound lithium complex **3.18** (Scheme 3.4). Subsequent complexation with rhodium precursors affords the phosphine supported complexes **3.19**, featuring a η^2-B,C borataalkene coordination.

[10] Watanabe, K.; Ueno, A.; Tao, X.; Škoch, K.; Jie, X.; Vagin, S.; Rieger, B.; Daniliuc, C. G.; Letzel, M. C.; Kehr, G.; Erker, G. *Chem. Sci.* **2020**, *11*, 7349-7355.

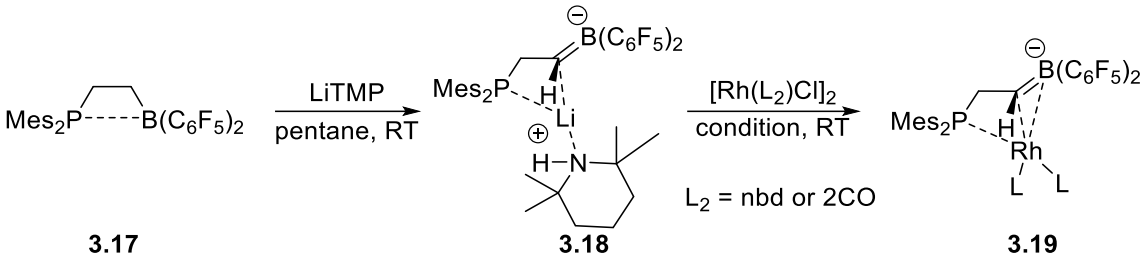

3.17 **3.18** **3.19**

Scheme 3.4. Erker's synthesis of Rh(I) η^2-B,C borataalkene complexes.

The Ozerov group observed a metal η^2-B,C borataalkene coordination in iridium alkenylidene bridging complexes (Scheme 3.5).[11] In the presence of excess alkene, PBP pincer iridium complex **3.20** undergoes ligand exchange followed by a terminal $C_{alkenyl}$–H activation to afford iridium hydride **3.22**. Subsequent α-migration of alkenyl group followed by β-hydride migratory insertion results in iridium-borataalkene complex **3.21**.

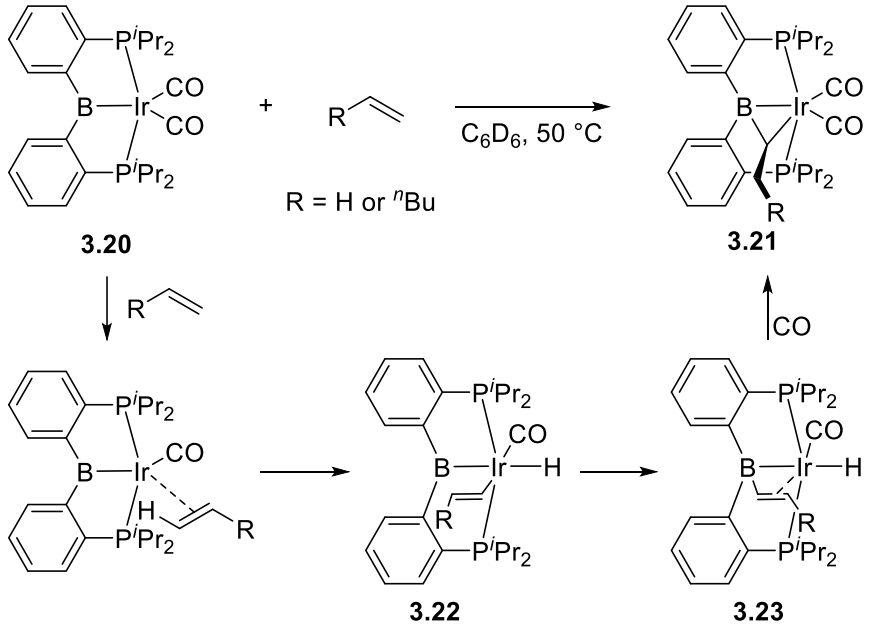

Scheme 3.5. Ozerov's synthesis of Ir(I) η^2-B,C borataalkene complexes.

[11] Cao, Y.; Shih, W.-C.; Bhuvanesh, N.; Ozerov, O. V. *Chem. Sci*. **2020**, *11*, 10998-11002.

Various metal η^2-B,C bound azaborataallenes ($R^1_2N{=}B{=}CR^2_2$) complexes are reported by Nöth[12] and Braunschweig.[13] The molybdenum borylene transfer reaction (Scheme 3.6, eq. 1) and complexation reaction of amino-9-fluorenylideneborane **3.26** with a series of first-row transition metal carbonyl complexes and (Scheme 3.6, eq. 2) both result in complexes where the metals selectively coordinate to the C=B bond rather than other double bonds.

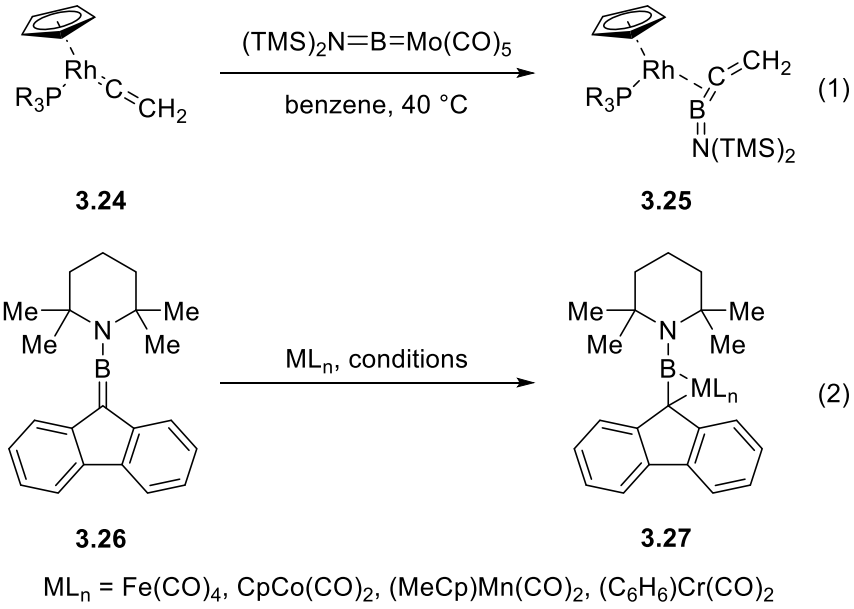

Scheme 3.6. Metal azaborataallene complexes with η^2-B,C coordination.

Martin and coworkers discovered the dual reactivity patterns of 9-borataphenanthrene towards metal complexes.[14] When treated with $Au(PPh_3)Cl$, 9-borataphenanthrene anion **3.28** exhibits its borataalkene character, leading to a η^2-B,C

[12] (a) Helm, S.; Nöth, H. *Angew. Chem. Int. Ed.* **1988**, *27*, 1331-1337; (b) Channareddy, S.; Linti, G.; Nöth, H. *Angew. Chem. Int. Ed*. **1990**, *29*, 199-201; (c) Helm, S. W.; Linti, G.; Nöth, H.; Channareddy, S.; Hofmann, P. *Chem. Ber.* **1991**, *125*, 73-86.

[13] Braunschweig, H.; Ye, Q.; Damme, A.; Kupfer, T.; Radacki, K.; Wolf, J. *Angew. Chem. Int. Ed.* **2011**, *50*, 9462-9466.

[14] Bartholome, T. A.; Kaur, A.; Wilson, D. J. D.; Dutton, J. L.; Martin, C. D. *Angew. Chem. Int. Ed.* **2020**, *59*, 11470-11476.

bound gold complex **3.29** (Scheme 3.7) whereas when treated with $Cr(MeCN)_3(CO)_3$, compound **3.28** displays the boratabenzene character, leading to a η^6 coordinated chromium complex.

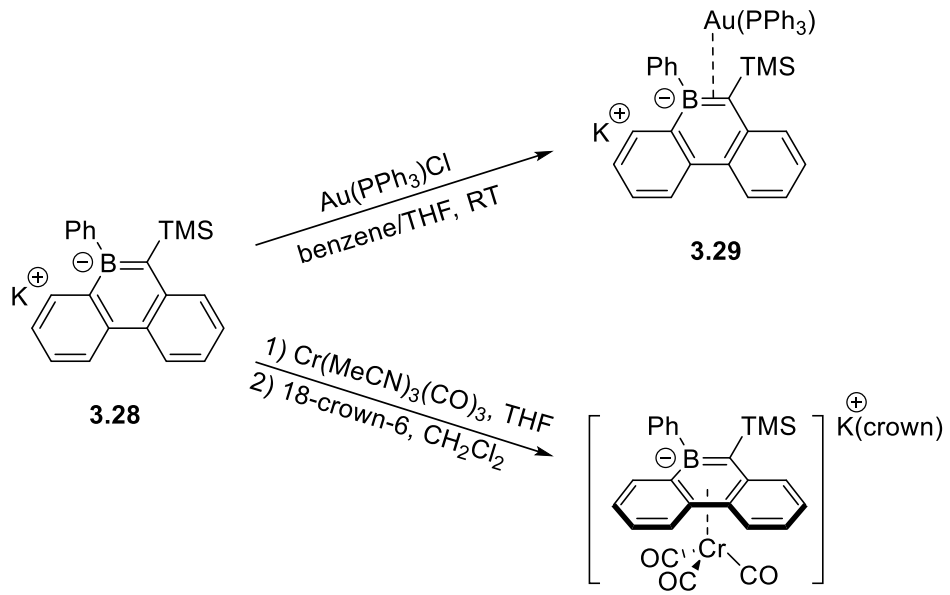

Scheme 3.7. Martin's synthesis of Au(I) η^2-B,C borataalkene complex.

The Crimmin group reported a study of the CAAC (cyclic (alkyl)(amino)carbene) stabilized lithium boryl ligand that reacted with various metals complexes.[15] Solid-state data along with the calculations indicate as the coinage metal becomes heavier, its coordination to ligand **3.30** slips from η^2-B,C to η^1-B fashion. Additionally, $ZnCl_2$, which possesses low-energy d-electrons that is less available for binding, coordinates to ligand **3.30** in a completely η^1-B mode, highlighting the necessity of the d-electron back-donation to engage the η^2-B,C coordination.

[15] Phillips, N. A.; Kong, R. Y.; White, A. J. P.; Crimmin, M. R. *Angew. Chem. Int. Ed.* **2021**, *60*, 12013-12019.

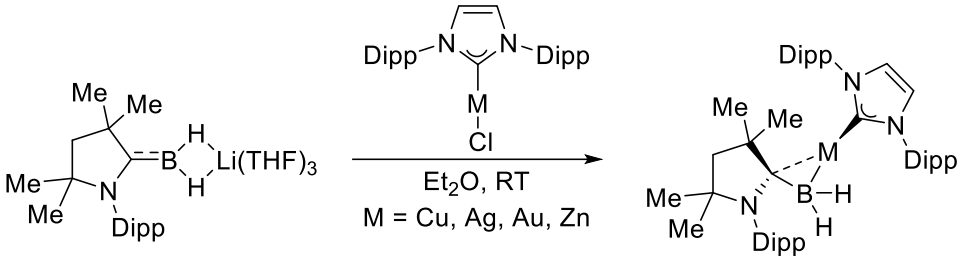

3.30

dipp = 2,6-isopropylphenyl

3.31

Scheme 3.8. Coordination slippage among Group 11 borataalkene complexes.

A gold(I) complex with η^1-B coordination is described by Bertrand group.[16] They discovered the hydride in CAAC stabilized borohydride **3.32** is acidic enough to be deprotonated by KHMDS (potassium bis(trimethylsilyl) amide) to afford a unique boryl anion **3.33** which has a strong borataalkene character. Further complexion with Me_3PAuCl results in η^1-B coordinated complex **3.34**.

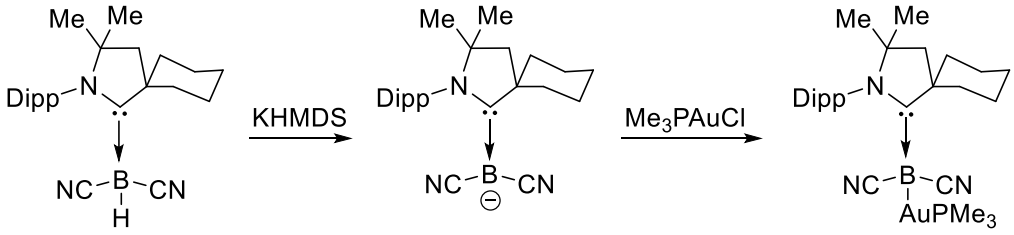

3.32 **3.33** **3.34**

Scheme 3.9. Bertrand's synthesis of Au(I) η^1-B borataalkene complex.

As discussed in Piers's tantalum-based example (Scheme 3.1), borataalkene can also serve as an η^1-C bound ligand, and several Ti(IV) complexes fall into this category

[16] (a) Ruiz, D. A.; Ung, G.; Melaimi, M.; Bertrand, G. *Angew. Chem. Int. Ed.* **2013**, *52*, 7590-7592; (b) Arrowsmith, M.; Auerhammer, D.; Bertermann, R.; Braunschweig, H.; Celik, M. A.; Erdmannsdörfer, J.; Krummenacher, I.; Kupfer, T. *Angew. Chem. Int. Ed.* **2017**, *56*, 11263-11267.

(Scheme 3.10).[17] Starting from ligand-supported dimethyl titanium(IV), $B(C_6F_5)_3$ is capable of abstracting a methyl group to form the loosely coordinated zwitterionic **3.35**. As a thermally unstable complex, it undergoes α-abstraction to release methane followed by pentafluorophenyl group migration to afford complex **3.36**. The η^1-C coordination mode in complex **3.36** is confirmed by X-ray crystallography analysis.

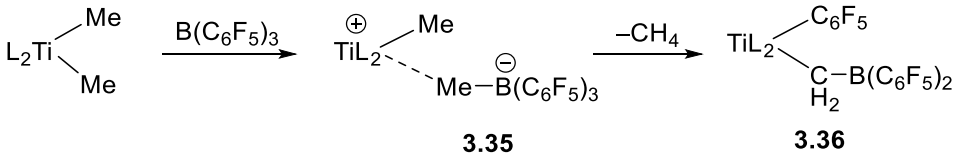

3.35 **3.36**

Scheme 3.10. Synthesis of Ti(IV) η^1-C borataalkene complexes.

The Sadighi group reported a copper η^1-C bound borataalkene complex (Scheme 3.11).[18] NHC (*N*-heterocyclic carbene) stabilized copper boryl **3.37** undergoes β-migratory insertion with styrene to provide copper β-boryl complex **3.38**. Upon heating, complex **3.38** is converted to the α-borylalkyl complex **3.40** through a β-hydride elimination and alkene reinsertion process. Although the η^2-B,C coordination in complex **3.40** is characterized by X-ray crystallography, such binding mode is absent in the solution state via ^{11}B NMR.

[17] (a) Thorn, M. G.; Vilardo, J. S.; Fanwick, P. E.; Rothwell, I. P. *Chem. Commun*. **1998**, 2427-2428; (b) Fenwick, A. E.; K. Phomphrai,M. G. Thorn, J. S. Vilardo, C. A. Trefun, B. Hanna, P. E. Fanwick ,I. P. Rothwell *Organometallics* **2004**, *23*, 2146-2156; (c) Amo, V.; Andrés, R.; de Jesús, E.; de la Mata, F. J.; Flores, J. C.; Gómez, R.; Gómez-Sal, M. P.; Turner, J. F. C. *Organometallics* **2005**, *24*, 2331-2338; (d) Gómez, R.; Gómez-Sal, P.; del Real, P. A.; Royo, P. *J. Organomet. Chem.* **1999**, *588*, 22-27; (e) Zhang, S.; Piers, W. E.; Gao, X.; Parvez, M. *J. Am. Chem. Soc*. **2000**, *122*, 5499-5509; (f) Scollard, J. D.; McConville, D. H.; Rettig, S. J. *Organometallics* **1997**, *16*, 1810-1812.

[18] Laitar, D. S.; Tsui, E. T.; Sadighi, J. P. *Organometallics* **2006**, *25*, 2405-2408.

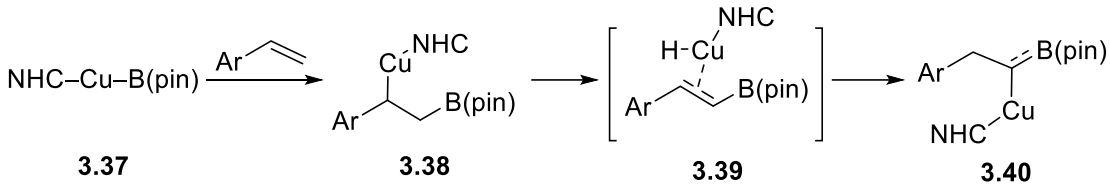

3.37 **3.38** **3.39** **3.40**

Scheme 3.11. Sadighi's synthesis of Cu(I) η^1-C borataalkene complexes.

A series of η^1-C bound borataalkene complexes with Group 6 metals are reported (Scheme 3.12).[19] Hydroboration reaction of metal carbyne species **3.41** occurs in either 1,2 or 2,1-addition fashion to provide hydridocarbene **3.42** or borylcarbene **3.42'**, respectively. α-Migratory insertion of hydride or boryl group ultimately delivers complex **3.43**, where the metal forms a η^2-aryl interaction in addition to the η^1-C coordination.

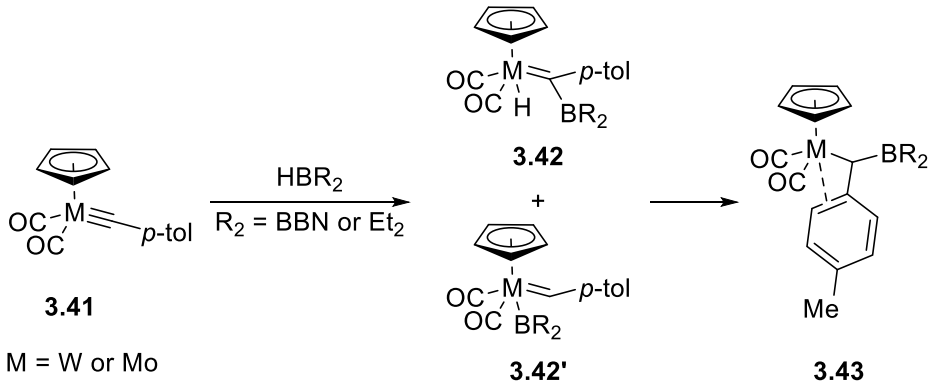

3.41

M = W or Mo

3.42 **3.42'** **3.43**

Scheme 3.12. Synthesis of Group 6 η^1-C borataalkene complexes.

3.1.2. Metal complexes containing borylferrocence or ambiphilic ligands

The metal η^2-B,C coordination does not only exist in complexes with borataalkene ligands, but also in complexes with C_{aryl}–B moiety containing ligands such as

[19] (a) Wadepohl, H.; Elliott, G. P.; Pritzkow, H.; Stone, F. G. A.; Wolf, A. *J. Organomet. Chem.* **1994**, *482*, 243-251; (b) Barratt, D.; Davies, S. J.; Elliott, G. P.; Howard, J. A. K.; Lewis, D. B.; Stone, F. G. A. *J. Organomet. Chem.* **1987**, *325*, 185-201; (c) Carriedo, G. A.; Elliott, G. P.; Howard, J. A. K.; Lewis, D. B.; Stone, F. G. A. *J. Chem. Soc., Chem. Commun*. **1984**, 1585-1586; (d) Wadepohl, H.; Arnold, U.; Kohl, U.; Pritzkow, H.; Wolf, A. *J. Chem. Soc., Dalton Trans*. **2000**, 3554-3565.

borylferrocence and boron containing ambiphilic ligands. Scheme 3.13 shows the syntheses of various mono- and bis-borylferrocences **3.44** and **3.45**.[20] X-ray diffraction analyses indicate the Cp (cyclopentadienyl) rings are not coplanar with the boron groups, and the resulting bent angle increases as the boron group becomes more acidic. Additionally, the Cp rings are slightly deformed. These observations are further validated by DFT (density functional theory) calculations that it is the combination of p orbitals from both the Cp ring and the boron interact with the iron center rather than a separate Fe–B interaction in additional to the Fe–C interaction.[20c]

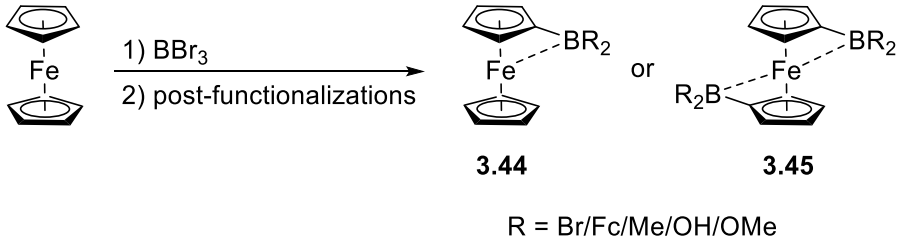

Scheme 3.13. Iron(II) η^2-B,C$_{ipso}$ interactions in borylferrocenes.

Pioneered by Bourissou,[21] ambiphilic ligands are multi-dentate ligands containing both Lewis base(s), such as phosphines, and Lewis acid(s), such as Group 13 elements. To date, a variety of transition metals have been reported to form the η^1-B coordination (Figure

[20] (a) Renk, T.; Ruf, W.; Siebert, W. *J. Organomet. Chem*. **1976**, *120*, 1-25; (b) Appel, A.; Jäkle, F.; Priermeier, T.; Schmid, R.; Wagner, M. *Organometallics*, **1996**, *15*, 1188-1194; (c) Scheibitz, M.; Bolte, M.; Bats, J. W.; Lerner, H.-W.; Nowik, I.; Herber, R. H.; Krapp, A.; Lein, M.; Holthausen, M. C.; Wagner, M. *Chem. Eur. J*. **2005**, *11*, 584-603.

[21] Bontemps, S.; Gornitzka, H.; Bouhadir, G.; Miqueu, K.; Bourissou, D. *Angew. Chem. Int. Ed.* **2006**, *45*, 1611-1614.

3.3) with boron-containing ambiphilic ligands.[22] And in some cases such coordination is augmented by an aryl η^1-C_{ipso} or η^2-C_{ipso},C_{ortho} coordination without significantly perturbing the ring aromaticity. These coordination arrangements can be considered as formal η^2-B,C binding.[3a]

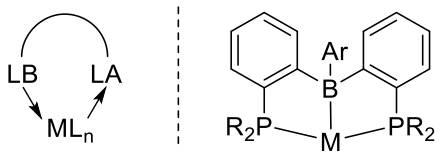

Figure 3.3. Illustration of the metal boron-containing ambiphilic ligand interaction.

A collection of η^2-B,C_{ipso} or η^3-B,C_{ipso},C_{ortho} ambiphilic ligands bound to Fe,[23] Co,[24] Rh,[25] Ni,[26] Pd,[27] Pt[28] and Cu[29] complexes are shown in Scheme 3.14. Among them, iron shows great coordination diversity. For example, in complex **3.46** the ligand displays an η^2-B,C coordination to Fe(I) whereas in complex **3.48** it shows an η^7 coordination to Fe(0).

---

[22] For reviews, see: (a) Amgoune, A.; Bourissou, D. *Chem. Commun*. **2011**, *47*, 859-871; (b) Tiddens, M. R.; Moret, M.-E. Metal-Ligand Cooperation at Phosphine-Based Acceptor Pincer Ligands. In *Topics in Organometallic Chemistry*; Springer, Berlin, Heidelberg, 2020; (c) Bennett, M. A.; Bhargava, S. K.; Mirzadeh, N.; Privér, S. H. *Coord. Chem. Rev*. **2018**, *370*, 69-128; (d) Vogt, M.; Langer, R. *Eur. J. Inorg. Chem*. **2020**, *2020*, 3885-3898; (e) Bouhadir, G.; Bourissou, D. *Chem. Soc. Rev.* **2016**, *45*, 1065-1079; (f) You, D.; Gabbaï, F. P. *Trends in Chemistry* **2019**, *1*, 485-496; (g) Kameo, H.; Nakazawa, H. *Chem. Asian J.* **2013**, *8*, 1720-1734.

[23] (a) Suess, D. L. M.; Peters, J. C. *J. Am. Chem. Soc*. **2013**, *135*, 4938-4941; (b) Moret, M.-E.; Peters, J. C. *Angew. Chem. Int. Ed.* **2011**, *50*, 2063-2067; (c) Suess, D. L. M.; Peters, J. C. *J. Am. Chem. Soc.* **2013**, *135*, 4938-4941.

[24] Nesbit, M. A.; Suess, D. L. M.; Peters, J. C. *Organometallics* **2015**, *34*, 4741-4752.

[25] (a) Cowie, B. E.; Emslie, D. J. H.; Jenkins, H. A.; Britten, J. F. *Inorg. Chem*. **2010**, *49*, 4060-4072; (b) Shih, W.-C.; Gu, W.; MacInnis, M. C.; Timpa, S. D.; Bhuvanesh, N.; Zhou, J.; Ozerov, O. V. *J. Am. Chem. Soc.* **2016**, *138*, 2086-2089; (c) Shih, W.-C.; Gu, W.; MacInnis, M. C.; Herbert, D. E.; Ozerov, O. V. *Organometallics* **2017**, *36*, 1718-1726.

[26] (a) Harman, W. H.; Peters, J. C. *J. Am. Chem. Soc.* **2012**, *134*, 5080-5082; (b) MacMillan, S. N.; Harmanb, W. H.; Peters, J. C. *Chem. Sci*. **2014**, *5*, 590-597.

[27] (a) Malacea, R.; Chahdoura, F.; Devillard, M.; Saffon, N.; Gómez, M.; Bourissou, D. *Adv. Synth. Catal.* **2013**, *355*, 2274-2284; (b) Schindler, T.; Lux, M.; Peters, M.; Scharf, L. T.; Osseili, H.; Maron, L.; Tauchert, M. E. *Organometallics* **2015**, *34*, 1978-1984; (c) Kameo, H.; Yamamoto, J.; Asada, A.; Nakazawa, H.; Matsuzaka, H.; Bourissou, D. *Angew. Chem. Int. Ed.* **2019**, *58*, 18783-18787.

[28] Cowie, B. E.; Emslie, D. J. H. *Chem. Eur. J*. **2014**, *20*, 16899-16912.

[29] Sircoglou, M.; Bontemps, S.; Mercy, M.; Miqueu, K.; Ladeira, S.; Saffon, N.; Maron, L.; Bouhadir, G.; Bourissou, D. *Inorg. Chem.* **2010**, *49*, 3983-3990.

Moreover, the solid-state structure of complex **3.47** exhibits both η^2 and η^3 coordinations while in solution only the η^2-coordination is observed, highlighting the dynamic nature of these ligands.[23a]

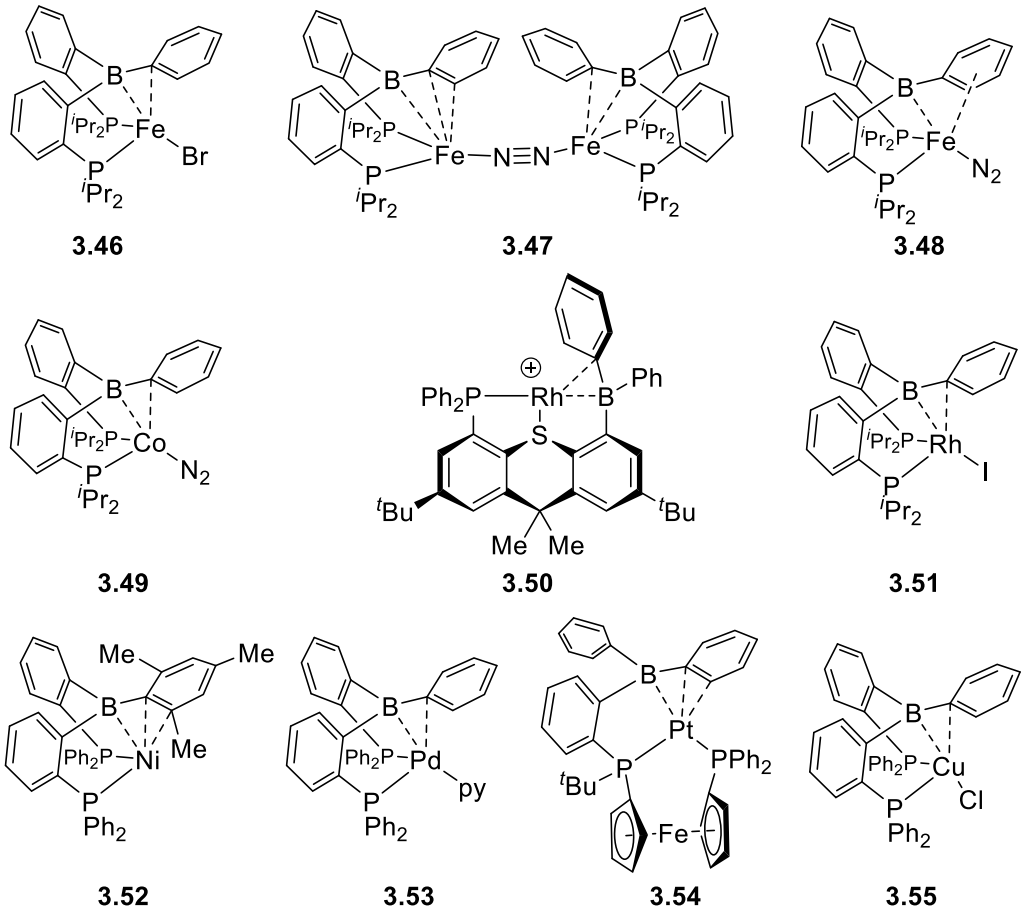

Scheme 3.14. Collection of η^n bound complexes with ambiphilic ligands.

These ambiphilic ligands can be non-innocent ligands, where the electrophilic boron group is capable of stabilizing, for example, a hydride.[30] Facile E–H (E = H, O, S, Si, C) activations occur with Ni or Co complexes (Scheme 3.15).[24,26] Nickel complex **3.52** activates dihydrogen to furnish nickel complex **3.56** which reduces alkenes to alkanes.

[30] Devillard, M.; Bouhadir, G.; Bourissou, D. *Angew. Chem. Int. Ed*. **2015**, *54*, 730-732.

Palladium complex **3.57** reacts with a naked hydride to deliver monomeric anionic Pd(0) complex **3.58** that can mediate the dechlorination of PhCl.[27b]

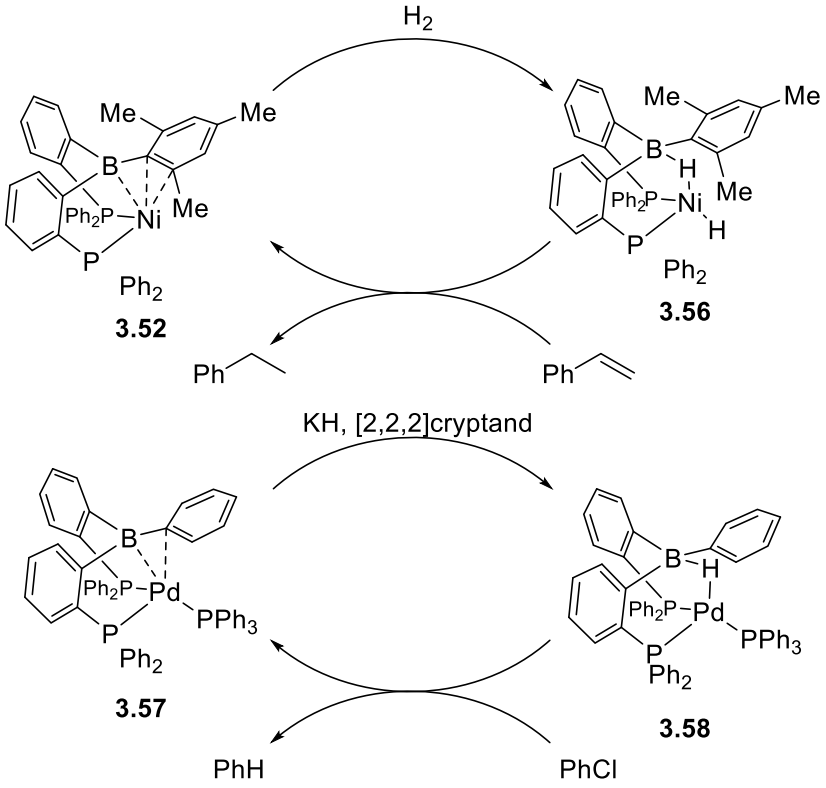

Scheme 3.15. Complexes with non-innocent ambiphilic ligands.

3.1.3. Palladium η^n-arene interactions with biaryl monophosphine ligands

Biaryl monophosphine bound palladium complexes are widely used in the construction of C–C and C–N bonds.[31] In the corresponding catalytic cycles, such ligand is proposed to stabilize Pd(0)[31a] or Pd(II)[32] intermediates via Pd η^n-arene interactions.[33]

Pd η^n-arene interactions are first discovered in MOP and MAP bound Pd(II) complexes back in 1990s (MOP: 2-(diphenylphosphino)-2′-methoxy-1,1′-binaphthyl; MAP:2-(diphenylphosphino)-2′-dimethylamino-1,1′-binaphthyl).[34] X-ray crystallography analyses indicate such interaction is stronger with a cationic palladium center (Scheme 3.16, complex **3.59** *vs.* **3.60**), highlighting the back-donation by aryl π-electrons to the electron deficient palladium center.

---

[31] (a) Surry, D. S.; Buchwald, S. L. *Angew. Chem. Int. Ed.* **2008**, *47*, 6338-6361; (b) Surry, D. S.; Buchwald, S. L. *Chem. Sci.* **2011**, *2*, 27-50; (c) Ingoglia, B. T.; Wagen, C. C.; Buchwald, S. L. *Tetrahedron* **2019**, *75*, 4199-4211; (d) Buskes, M. J.; Blanco, M. *Molecules* **2020**, *25*, 3493-3514.

[32] Arrechea, P. L.; Buchwald, S. L. *J. Am. Chem. Soc*. **2016**, *138*, 12486-12493.

[33] For Pd-arene interactions in other systems, see: (a) Falvello, L. R.; Forniés, J.; Navarro, R.; Sicilia, V.; Tomás, M. *Angew. Chem. Int. Ed. Engl.* **1990**, *29*, 891-893; (b) Li, C.-S.; Jou, D.-C.; Cheng, C.-H. *Organometallics* **1993**, *12*, 3945-3954; (c) Cámpora, J.; López, J. A.; Palma, P.; Valerga, P.; Spillner, E.; Carmona, E. *Angew. Chem. Int. Ed.* **1999**, *38*, 147-151; (d) Catellani, M.; Mealli, C.; Motti, E.; Paoli, P.; Perez-Carreño, E.; Pregosin, P. S. *J. Am. Chem. Soc*. **2002**, *124*, 4336-4346; (e) Vignolle, J.; Gornitzka, H.; Donnadieu, B.; Bourissou, D.; Bertrand, G. *Angew. Chem. Int. Ed.* **2008**, *47*, 2271-2274; (f) Maestri, G.; Motti, E.; Della, Ca', N.; Malacria, M.; Derat, E.; Catellani, M. *J. Am. Chem. Soc*. **2011**, *133*, 8574-8585; (g) Murahashi, T.; Takase, K.; Oka, M.; Ogoshi, S. *J. Am. Chem. Soc.* **2011**, *133*, 14908-14911; (h) Li, Y.; Wang, W. H.; He, K. H.; Shi, Z. J. *Organometallics*, **2012**, *31*, 4397-4400; (i) Yamamoto, K.; Kimura, S.; Murahashi, T. *Angew. Chem. Int. Ed*. **2016**, *55*, 5322-5326; (j) Tan, C.; Qasim, M.; Pang, W.; Chen, C. *Polym. Chem*. **2020**, *11*, 411-416.

[34] (a) Hayashi, T.; Iwamura, H.; Naito, M.; Matsumoto, Y.; Uozumi, Y.; Miki, M.; Yanagi, K. *J. Am. Chem. Soc*. **1994**, *116*, 775-776; (b) Kocovsky, P.; Vyskocil, S.; Cisarova, I.; Sejbal, J.; Tislerova, I.; Smrcina, M.; Lloyd Jones, G. C.; Stephen, S. C.; Butts, C. P.; Murray, M.; Langer, V. *J. Am. Chem. Soc*. **1999**, *121*, 7714-7715; (c) Hayashi, T. *Acc. Chem. Res.* **2000**, *33*, 354-362; (d) Lloyd-Jones, G. C. *Chem. Eur. J*. **2000**, *6*, 4348-4347; (d) Faller, J. W.; Sarantopoulos, N. *Organometallics* **2004**, *23*, 2008-2014; (e) Dotta, P.; Kumar, P. G. A.; Pregosin, P. S.; Albinati, A.; Rizzato, S. *Organometallics* **2004**, *23*, 4247-4254; (f) Ficks, A.; Hiney, R. M.; Harrington, R. W.; Gilheany, D. G.; Higham, L. J. *Dalton Trans*. **2012**, *41*, 3515-3522.

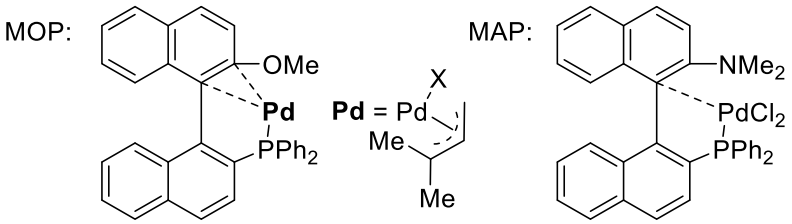

3.59 X = Cl
3.60 X = OTf

3.61

Scheme 3.16. Early examples of arene bound Pd(II) complexes.

In the course of developing efficient Suzuki-Miyaura cross-coupling systems, several effective Buchwald ligand bound Pd(0) catalysts have been identified (Scheme 3.17, complex **3.62** to **3.64**) to reveal Pd(0) η^n-arene interactions (all structural information are obtained from single crystal X-ray diffraction analysis).[35] For instance, in complex **3.62** the Pd–C_{ipso} distance is well below the sum of their Van der Waals radii. Plus, the palladium oxidation state remains zero and the lengths of the two flanking C_{ortho}–O bonds in the complex are identical to the ones in free ligand, which are all consistent with a true η^1 binding.[35b] Similar coordination mode is also observed in the palladium oxidative insertion products (e.g., Scheme 3.17, complex **3.65**).[36] Unlike the Pd(II) examples in Scheme 3.16

[35] (a) Walker, S. D.; Barder, T. E.; Martinelli, J. R.; Buchwald, S. L. *Angew. Chem. Int. Ed.* **2004**, *43*, 1871-1876; (b) Barder, T. E.; Walker, S. D.; Martinelli, J. R.; Buchwald, S. L. *J. Am. Chem. Soc.* **2005**, *127*, 4685-4696; (c) Reid, S. M.; Boyle, R. C.; Mague, J. T.; Fink, M. J. *J. Am. Chem. Soc*. **2003**, *125*, 7816-7817; (d) Christmann, U.; Vilar, R.; White, A. J. P.; Williams, D. J. *Chem. Commun*. **2004**, 1294-1295; (e) Yin, J. J.; Rainka, M. P.; Zhang, X. X.; Buchwald, S. L. *J. Am. Chem. Soc.* **2002**, *124*, 1162-1163; (f) Christmann, U.; Pantazis, D. A.; Benet-Buchholz, J.; McGrady, J. E.; Maseras, F.; Vilar, R. *J. Am. Chem. Soc*. **2006**, *128*, 6376-6390.

[36] (a) Yamashita, M.; Takamiya, I.; Jin, K.; Nozaki, K. *J. Organomet. Chem*. **2006**, *691*, 3189-3195; (b) Fors, B. P.; Watson, D. A.; Biscoe, M. R.; Buchwald, S. L. *J. Am. Chem. Soc.* **2008**, *130*, 13552-13554; (c) Milner, P. J.; Maimone, T. J.; Su, M.; Chen, J.; Müller, P.; Buchwald, S. L. *J. Am. Chem. Soc.* **2012**, *134*, 19922-19934; (d) Su, M.; Buchwald, S. L. *Angew. Chem. Int. Ed*. **2012**, *51*, 4710-4713; (e) Milner, P. J.; Yang, Y.; Buchwald, S. L. *Organometallics* **2015**, *34*, 4775-4780; (f) Sather, A. C.; Lee, H. G.; De La Rosa, V. Y.; Yang, Y.; Müller, P.; Buchwald, S. L. *J. Am. Chem. Soc.* **2015**, *137*, 41, 13433-13438; (g) Gioria, E.; Pozo, J. D.; Martínez-Ilarduya, J. M.; Espinet, P. *Angew. Chem. Int. Ed*. **2016**, *55,* 13276-13280; (h) Olsen, E.; Arrechea, P.; Buchwald, S. *Angew. Chem. Int. Ed*. **2017**, *56*, 10569-10572; (i) Ingoglia, B. T.; Buchwald, S. L. *Org. Lett.* **2017**, *19*, 2853-2856.

where the electron rich oxygen or nitrogen group does not coordinate to palladium, the Pd(II) center in Buchwald ligand bound Pd(II) complexes can bind the proximal oxygen (complex **3.66**-*O*-bound). Although the η^1-*C*- and *O*-bound complexes are in fast equilibrium, experiments demonstrate that the reductive elimination preferentially occurs with complex **3.66**-*C*-bound.[32,36b,36g]

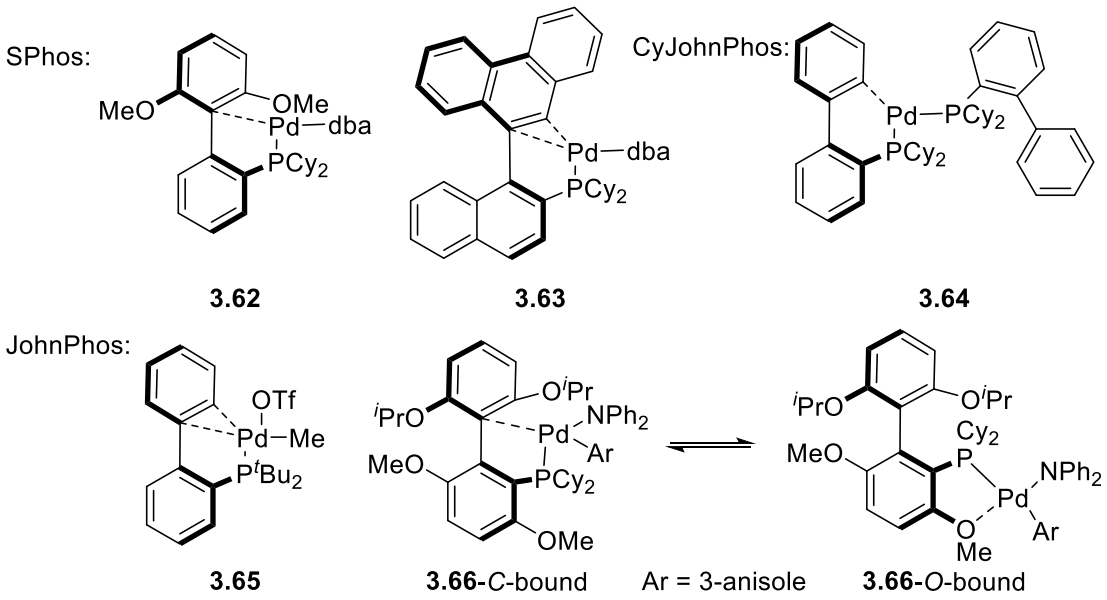

Scheme 3.17. Representative examples of Pd η^n-arene interactions containing Buchwald ligands.

Obtaining useful information regarding the Pd η^n-arene interactions seems difficult experimentally,[37] therefore, *in silico* simulations are conducted to evaluate the C(2)–P bond rotational energy barrier.[38,39] By varying the C(1)–C(2)–P–Pd dihedral angle in various Buchwald ligands **3.67**-**3.70** bound Pd(0) and Pd(II) complexes, PES (potential energy

[37] (a) Phan, N. T. S.; Van Der Sluys, M.; Jones, C. W. *Adv. Synth. Catal*. **2006**, *348*, 609-679; (b) Christman, W. E.; Morrow, T. J.; Arulsamy, N.; Hulley, E. B. *Organometallics* **2018**, *37*, 2706-2715.
[38] (a) Barder, T. E.; Biscoe, M. R.; Buchwald, S. L. *Organometallics* **2007**, *26*, 2183-2192; (b) Barder, T. E.; Buchwald, S. L. *J. Am. Chem. Soc.* **2007**, *129*, 12003-12010.
[39] Kim, S.-T.; Kim, S.; Baik, M.-H. *Chem. Sci.* **2020**, 11, 1017-1025.

surface) maps are generated where the lowest local minima is always the rotamer with Pd η^1-C_{ipso} arene interaction (proximal) and the highest energy conformer represents the overall rotational barrier. The data are summarized in Table 3.1. For Pd(0) complexes, a more sterically demanding ligand leads to higher rotational barrier (entry 1 *vs.* 2). For Pd(II) complexes, increasing the steric bulkiness of the biaryl ring (entry 3 *vs.* 4) or having a more rigid phosphine substituent (entry 4 *vs.* 5) leads to a higher barrier. The influence of the palladium oxidation state is revealed from the comparison of entry 2 (Pd(0)) *vs.* entry 3 (Pd(II)) where the Pd(II) complex shows a lower barrier than the Pd(0) counterpart,[40] suggesting the arene motif in Buchwald ligands is a better π-acceptor than a π-donor towards palladium.

Table 3.1. Summary of the calculated overall rotational barrier of Buchwald ligands bound Pd(0) and Pd(II) complexes.

entry	**Pd**	ligand	rotational barrier (kcal/mol)
1	Pd(0)	**3.67**	14.0[a]
2	Pd(0)	**3.68**	21.1[a]
3	Ph–Pd(II)–Cl	**3.68**	13.1[b]
4	Ph–Pd(II)–Cl	**3.69**	21.1[b]
5	Ph–Pd(II)–Cl	**3.70**	17.5[b]

[a] Calculated with B3LYP/6-311++G(2d,2p)/LANL2DZ method. [b] Calculated with B3LYP-D3/cc-pVTZ(-f)/LACV3P method.

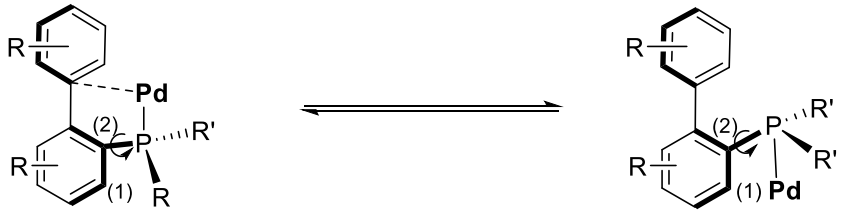

[40] Since the calculations are done with different basis sets, systematic errors may be applied.

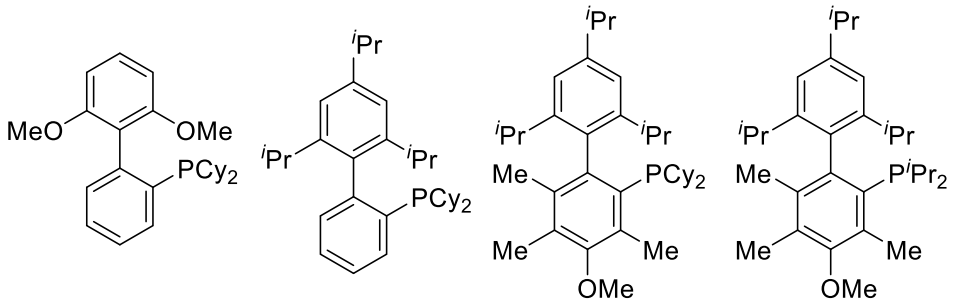

3.67 **3.68** **3.69** **3.70**

3.2. Evaluation of solid-state structures of Pd/Senphos complexes

Pd/Senphos catalytic system shows its versatility in a series of site-, regio- and *trans*-selective X-boration (X = H, Cl or CN) reactions of (*E*)-1,3-enynes (Scheme 3.18).[41,42] And the use of carbonaceous analogs of Senphos ligands, as well as various mono- and bi-dentate ligands are demonstrated to be inferior to the Senphos ligand class under otherwise identical reaction conditions.[41a,c]

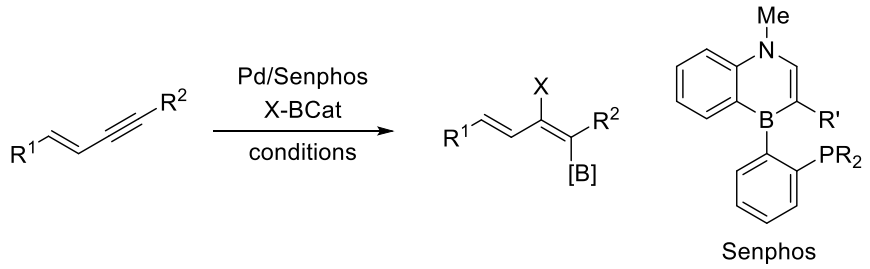

Scheme 3.18. Pd/Senphos catalyzed 1,3-enyne X-boration reactions.

Evidenced by X-ray crystallography analysis and NMR study, monobenzofused 1,4-Senphos bound Pd(0) complex **3.71** and Pd(II) complex **3.72** share an unusual κ^2-P-η^2-B,C coordination to palladium (Figure 3.4).[41b] And the overall neutral azaborine ring serves

[41] (a) Xu, S.; Haeffner, F.; Li, B.; Zakharov, L. N.; Liu, S.-Y. *Angew. Chem. Int. Ed.* **2014**, *53*, 6795-6799; (b) Xu, S.; Zhang, Y.; Li, B.; Liu, S.-Y. *J. Am. Chem. Soc.* **2016**, *138*, 14566-14569; (c) Zhang, Y.; Li, B.; Liu, S.-Y. *Angew. Chem. Int. Ed.* **2020**, *59*, 15928-15932.

[42] For *trans*-chloroboration reaction of 1,3-enynes, see Chapter 2.

as a masked borataalkene equivalent (i.e., minimum/borataalkene), distinguishing itself from the borataalkene precedents where the it is negatively charged (chapter 3.1.1).

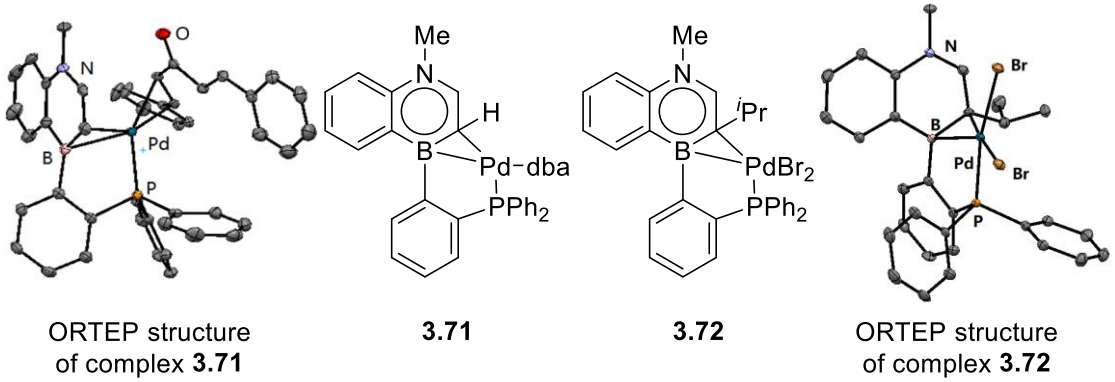

Figure 3.4. ORTEP structures of η^2-B,C coordination mode in monobenzofused 1,4-Senphos bound palladium complexes.

To systematically examine the coordination behavior of azaborines, we synthesized *B*–*o*-diphenyl-phosphinophenyl substituted monocyclic 1,2-, 1,3- and 1,4-azaborines **3.73** to **3.75**, respectively. Due to their structural similarity to monobenzofused 1,4-Senphos, they are named as 1,2-Senphos, 1,3-Senphos, and 1,4-Senphos in the following sections.

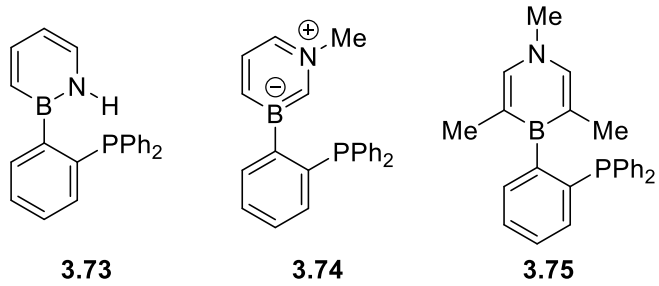

Figure 3.5. Structures of 1,2-, 1,3- and 1,4-Senphos ligands.

3.2.1. Unique η^n-B,C,(C) coordination mode in Pd/Senphos complexes

With various Senphos ligands in hand, we further complexed them with Pd_2dba_3 (dba: dibenzylideneacetone) and PdX_2 (X = Cl or Br), respectively. All resulting

Pd/Senphos complexes are crystallographically characterized (Figure 3.6), showing the existence of η^2-B,C borataalkene coordination to the palladium (Table 3.2)[43] with an exception from complex **3.76** where the azaborine ring binds to the palladium in an η^3-B,C,C borataallyl[3,11,44] fashion.[45] For 1,3-Senphos ligand **3.74** bound Pd(0) complex, two constitutional isomers **3.78** and **3.78'** (Figure 3.6) are obtained from one single crystal, highlighting the similar electron property of the C(4) and C(2) position in 1,3-Senphos ligand **3.74**. For consistency purpose, complex **3.78'** will not be discussed below.

[43] A typical Pd–C_{arene} interaction has a bond length between 2.233(3) Å and 2.676(6) Å, see ref. 27, 34, 35, and (a) Son, J.-H.; Pudenz, M. A.; Hoefelmeyer, J. D. *Dalton Trans.* **2010**, *39*, 11081-11090. And a typical Pd–B interaction in borataalkene and borataallyl bound palladium complexes has a bond length between 2.193(4) Å and 2.395(4) Å, see ref. 27, 44. Therefore, the Pd–C and Pd–B bond lengths in Pd/Senphos complexes are consistent with η^2-B,C coordination.

[44] For borataallyl bound metal complexes, see: (a) Jiang, F.; Shapiro, P. J.; Fahs, F.; Twamley, B. *Angew. Chem. Int. Ed.* **2003**, *42*, 2651-2653; (b) Emslie, D. J. H.; Harrington, L. E.; Jenkins, H. A.; Robertson, C. M.; Britten, J. F. *Organometallics* **2008**, *27*, 5317-5325; (c) Kolpin, K. B.; Emslie, D. J. H. *Angew. Chem. Int. Ed.* **2010**, *49*, 2716-2719; (d) Zhao, X.; Otten, E.; Song, D.; Stephan, D. W. *Chem. Eur. J.* **2010**, *16*, 2040-2044; (e) Roy, D. K.; De, A.; Pa, S.; Varghese, B.; Ghosh, S. *Chem. Eur. J.* **2015**, *21*, 13732-13738; (f) Saha, K.; Joseph, B.; Ramalakshmi, R.; Anju, R. S.; Varghese, B.; Ghosh, S. *Chem. Eur. J.* **2016**, *22*, 7871-7878; (g) Roy, D. K.; Yuvaraj, K.; Jagan, R.; Ghosh, S. *J. Organomet. Chem*. **2016**, *811*, 8-13; (h) Hui, Z.; Watanabe, T.; Tobita, H. *Organometallics* **2017**, *36*, 4816-4824; (I) Gomosta, S.; Saha, K.; Kaur, U.; Pathak, K.; Roisnel, T.; Phukan, A. K.; Ghosh, S. *Inorg. Chem*. **2019**, *58*, 9992-9997.

[45] In complex **3.76**, the Pd–C(4) bond has a length of 2.698(4) Å, which is well below the sum of the palladium (1.63 Å) and carbon (1.70 Å) Van der Waals radii (3.33 Å), whereas in complex **3.77**, the Pd–C(4) distance is 3.044(2) Å, indicating a very weak interaction. See: (a) Bondi, A. *J. Phys. Chem.* **1964**, *68*, 441-451; (b) Mantina, M.; Chamberlin, A. C.; Valero, R.; Cramer, C. J.; Truhlar, D. G. *J. Phys. Chem. A* **2009**, *113*, 5806-5812.

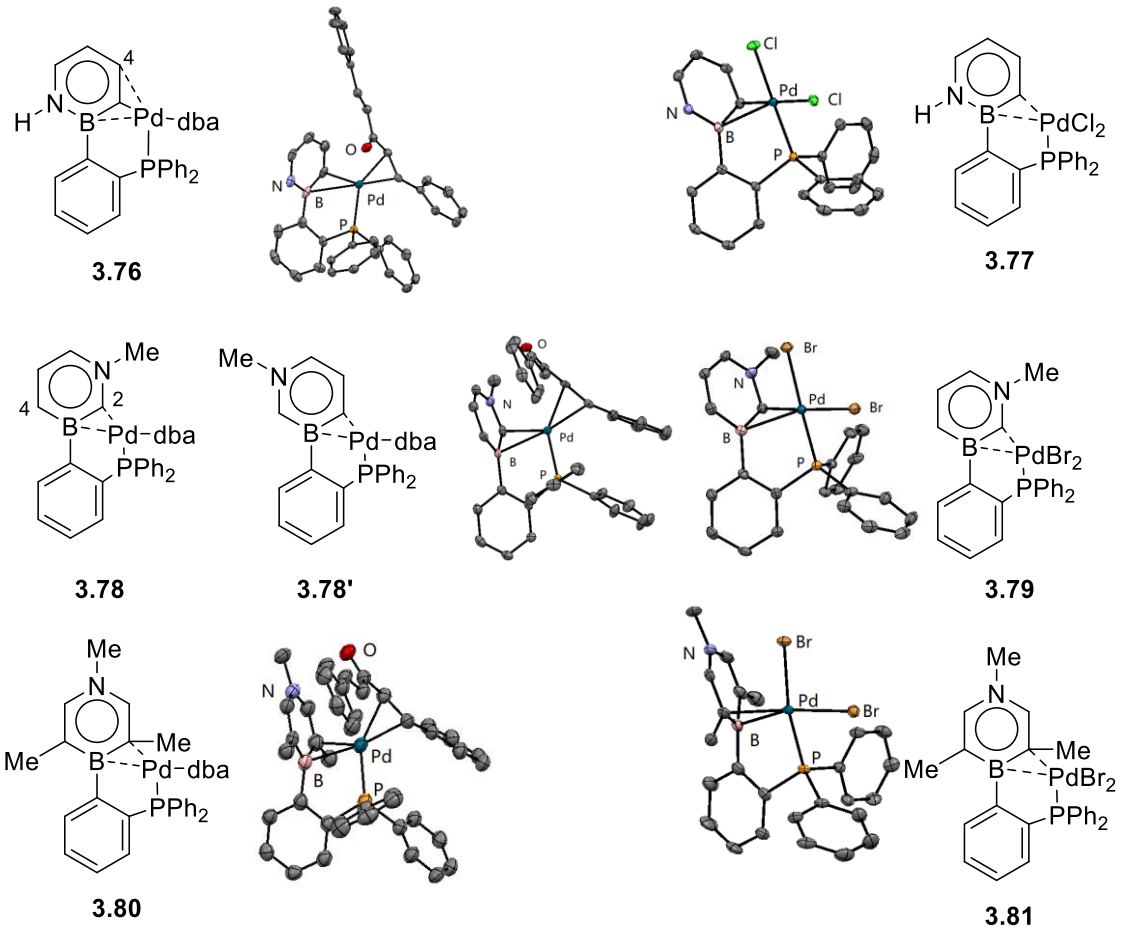

Figure 3.6. ORTEP structures of 1,2-, 1,3- and 1,4-Senphos bound palladium complexes.

The Pd–B and Pd–C_{ortho} bond lengths in Pd/Senphos complex **3.76-3.81** are summarized in Table 3.2. When considering the palladium borataalkene interactions, an electron rich palladium such as Pd(0) would favor back-donation to the empty π^*_{BC} orbital (Figure 3.2) and an electron deficient palladium such as Pd(II) would interact with the π_{BC} orbital more through electron donation from Senphos. Among 1,2-, 1,3- and 1,4-Senphos ligands, as the distance between nitrogen and boron becomes longer, it appears that the electrons on nitrogen have less tendency to contribute to the boron p orbital. Thus the interaction between an electron rich Pd(0) and the boron appears to be stronger (Table 3.2, Pd(0)–B bond becomes shorter) along the series of 1,2-, 1,3- and 1,4-Senphos. Conversely,

the Pd(0)–C_{ortho} distance becomes shorter the more the palladium is being pushed away from the boron atom. On the other hand, only slight variations in Pd(II)–B and Pd(II)–C_{ortho} bond lengths are observed along 1,2-, 1,3- and 1,4-Senphos, indicating very similar bonding interaction. Moreover, with a given Senphos, the Pd(II)–C_{ortho} bond is always shorter than the Pd(0)–C_{ortho} bond, highlighting the importance of electron donation from ligand to the metal in electron deficient Pd(II) complexes.

Table 3.2. Summary of Pd–B and Pd–C_{ortho} lengths (Å) in Pd/Senphos complexes.

ligand / bond	1,2-Senphos **3.73**	1,3-Senphos **3.74**	1,4-Senphos **3.75**
Pd(0)–B	2.730(5)	2.382(15)	2.336(6)
Pd(0)–C_{ortho}	2.271(4)	2.309(6)	2.369(6)
Pd(II)–B	2.430(2)	2.456(8)	2.483(5)
Pd(II)–C_{ortho}	2.250(2)	2.235(7)	2.270(5)

3.2.2. Azaborine intra-ring structures in Pd/Senphos complexes

Unlike the ambiphilic ligands (chapter 3.1.2), the Senphos coordination to palladium perturbs the azaborine aromaticity, leading to a change in azaborine intra-ring structure. For the purpose of intra-ring structure comparison, a small corresponding azaborine molecule (compound **3.83**, **3.85** and **3.87**, **Table 3.3** to **Table 3.5**, circled) is used as a reference to compare with Pd(0) and Pd(II)/Senphos complexes.

For 1,2-Senphos, NRT (natural resonance theory) calculation of parental 1,2-azaborine shows two most possible resonance structures aminoborane **3.82** and iminium/borataalkene **3.82'** where the former one prevails with a relative weight of 93%.[46] This is consistent with the bond lengths pattern in reference compound **3.83**[47] where bonds

[46] Baranac-Stojanović, M. *Chem. Eur. J.* **2014**, *20*, 16558-16565.
[47] Marwitz, A. J. V.; Lamm, A. N.; Zakharov, L. N.; Vasiliu, M.; Dixon, D. A.; Liu, S.-Y. *Chem. Sci.* **2012**, *3*, 825-829,

C(3)–C(4) and C(5)–C(6) has more double bond character and bond C(4)–C(5) has more single bond character (Table 3.3). Although a similar situation is observed in Pd(0) complex **3.76**, this trend is reversed in Pd(II) complex **3.77** where bond C(4)–C(5) has more double bond character. Comparing complex **3.76** with complex **3.77**, a clear bond length change is observed in all 1,2-azaborine intra-ring bonds (except bond B(2)–C(3)), indicating a resonance shift of from aminoborane to iminium/borataalkene structure.

Table 3.3. Bond lengths (Å) summary for 1,2-Senphos compounds.

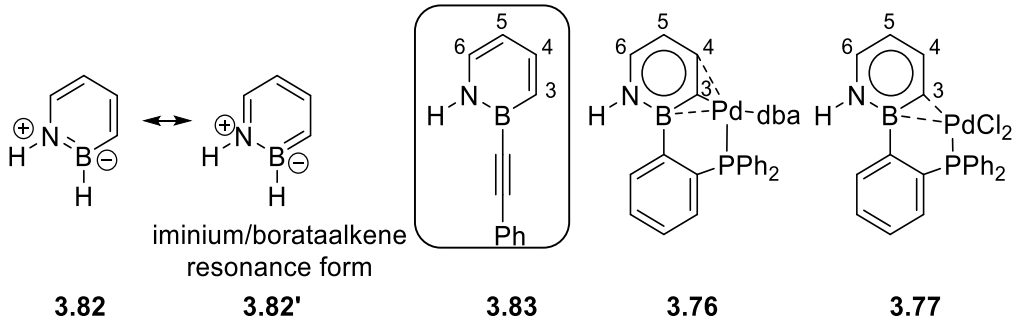

3.82 **3.82'** **3.83** **3.76** **3.77**

	N(1)–B(1)	B(2)–C(3)	C(3)–C(4)	C(4)–C(5)	C(5)–C(6)	C(6)–N(1)
3.83	1.427(5)	1.488(6)	1.368(5)	1.417(5)	1.352(6)	1.380(5)
3.76	1.438(7)	1.518(6)	1.394(9)	1.413(8)	1.361(6)	1.354(8)
3.77	1.461(3)	1.516(3)	1.418(3)	1.370(3)	1.394(3)	1.331(3)

For 1,3-Senphos, NRT calculation of parental 1,3-azaborine shows the two most possible resonance structures **3.84** and **3.84'** contribute equally,[46] which is well illustrated by the almost equal C(4)–C(5) and C(5)–C(6) bond distances in reference compound **3.85** (Table 3.4).[48] With palladium coordination, in particular for Pd(II) complex, a lengthening in bonds B(3)–C(4) and C(5)–C(6) and a shortening in bonds C(4)–C(5) and C(6)–N(1) are observed, indicating a resonance structure shift from **3.84** to **3.84'**.

[48] Xu, S.; Mikulas, T. C.; Zakharov, L. N.; Dixon, D. A.; Liu, S.-Y. *Angew. Chem. Int. Ed*. **2013**, *52*, 7527-7531.

Table 3.4. Bond lengths (Å) summary for 1,3-Senphos compounds.

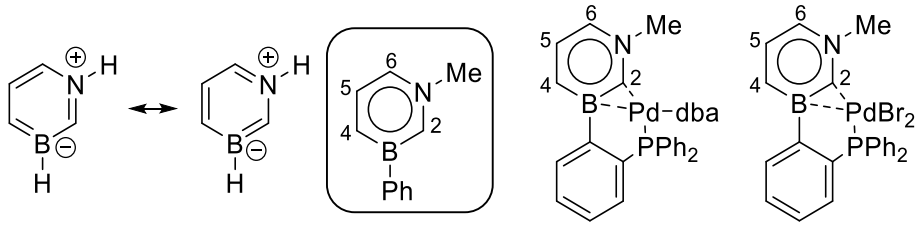

3.84 **3.84'** **3.85** **3.78** **3.79**

	N(1)–C(2)	C(2)–B(3)	B(3)–C(4)	C(4)–C(5)	C(5)–C(6)	C(6)–N(1)
3.85	1.348(3)	1.508(3)	1.505(4)	1.380(3)	1.375(3)	1.356(3)
3.78	1.359(10)	1.502(11)	1.530(10)	1.381(9)	1.376(11)	1.354(12)
3.79	1.391(9)	1.510(10)	1.546(10)	1.347(10)	1.412(10)	1.302(9)

Parental 1,4-azaborine has one localized form **3.86** and one delocalized form **3.86'** (or two equally populated resonance forms), and the reference compound **3.87**[49] has the C_{2v} geometry. The 1,4-Senphos η^2-B,C coordination breaks such symmetry (Table 3.5), and in complex **3.80** and **3.81**, N(1)–C(2) and C(5)–C(6) distances indicate more double bond character, gradually favoring the delocalized resonance form **3.86'**. Such resonance shift (in particular for the transition from Pd(0) to Pd(II)) is less dramatic compared to 1,2- and 1,3-Senphos bound palladium complexes, highlighting a resonance limit on 1,4-azaborine core.

[49] Liu, X.; Zhang, Y.; Li, B.; Zakharov, L. N.; Vasiliu, M.; Dixon, D. A.; Liu, S.-Y. *Angew. Chem. Int. Ed.* **2016**, *55*, 8333-8337.

Table 3.5. Bond lengths (Å) summary for 1,4-Senphos compounds.

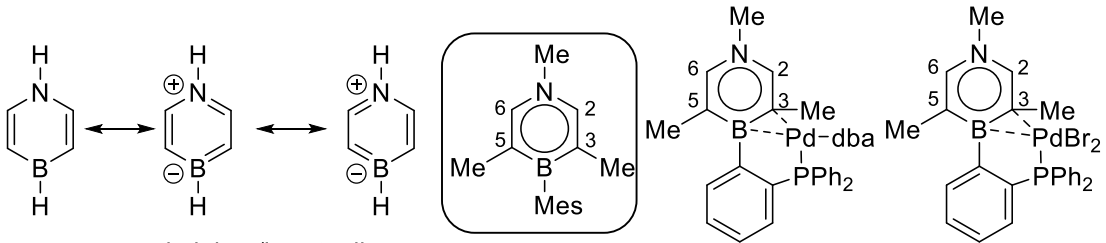

3.86 **3.86'** **3.87** **3.80** **3.81**

	N(1)–C(2)	C(2)–C(3)	C(3)–B(4)	B(4)–C(5)	C(5)–C(6)	C(6)–N(1)
3.87	1.368(2)	1.364	1.514(2)	1.512(2)	1.369(2)	1.368(2)
3.80	1.334(7)	1.390(8)	1.531(8)	1.542(9)	1.364(8)	1.368(7)
3.81	1.335(6)	1.408(6)	1.526(7)	1.547(6)	1.356(7)	1.379(7)

Overall, the Senphos coordination to palladium perturbs the azaborine aromaticity. As the palladium center becomes more electron deficient, the resonance structure of Senphos ligand favors the borataalkene structure more.

3.2.3. *Trans* influence of Senphos ligands in Pd(II) complexes

In organometallics, *trans* influence refers to the elongation of a metal-ligand bond that originates from the ligand *trans* to it.[50] And it has been intensively studied in the square

[50] (a) Pidcock, A.; Richards, R. E.; Venanzi, L. M. *J. Chem. Soc. A* **1966**, 1707-1710; (b) Appleton, T. G.; Clark, H. C.; Manzer, L. E. *Coord. Chem. Rev.* **1973**, *10*, 335-422; (c) Cross, R. J. *Adv. Inorg. Chem*. **1989**, *34*, 219-292; (d) Rigamonti, L.; Manassero, C.; Rusconi, M.; Manassero, M.; Pasini, A. *Dalton Trans.* **2009**, 1206-1213; (e) Rigamonti, L.; Rusconi, M.; Manassero, C.; Manassero, M.; Pasini, A. *Inorg. Chim. Acta* **2010**, *363*, 3498-3505; (f) Rigamonti, L.; Forni, A.; Manassero, M.; Manassero, C.; Pasini, A. *Inorg. Chem*. **2010**, *49*, 123-135.

planar Pt(II) complexes.[51] Similar rules are also applicable to square planar Pd(II) complexes.[52] With the pseudo-square planar geometry (the boron atom is located above/below the square plane containing C, Pd, 2Br and P atoms) in Pd(II)/Senphos complexes **3.77, 3.79** and **3.81**, we studied the *trans* influence of the borataalkene motif in 1,2-, 1,3- and 1,4-Senphos ligands. And the palladium halogen bond lengths are summarized in Table 3.6. In every complex, the Pd–X^1 bond (*trans* to P atom) is always longer than the Pd–X^2 bond (*trans* to borataalkene), indicating the phosphine group has a stronger *trans* influence than the borataalkene in Senphos. On the another hand, the Pd–X^2 bonds exhibit similar bond lengths as the ones *trans* to Pd–$C\pi_{sp}^2$ bonds in other palladium complexes.[53,54,35f] Since alkene predominantly acts as π-donor towards electron deficient

[51] For selective reports, see: (a) Hartley, F. R. *Chem. Soc. Rev.* **1973**, *2*, 163-179; (b) Manojlovic-Muir, L. J.; Muir, K. W. *Inorg. Chim. Acta* **1974**, *10*, 47-49; (c) Burdett, J. K.; Albright, T. A. *Inorg. Chem*. **1979**, *18*, 2112-2120; (d) Kerrison, S. J. S.; Sadler, P. J. *J. Chem. Soc., Dalton Trans*. **1982**, 2363-2369; (e) Wendt, O. F.; Elding, L. I. *J. Chem. Soc., Dalton Trans*. **1997**, 4725-4732; (f) Kuznik, N.; Wendt, O. F. *J. Chem. Soc., Dalton Trans*. **2002**, 3074-3078; (g) Zhu, J.; Lin, Z.; Marder, T. B. *Inorg. Chem*. **2005**, *44*, 9384-9390; (h) Braunschweig, H.; Brenner, P.; Müller, A.; Radacki, K.; Rais, D.; Uttinger, K. *Chem. Eur. J.* **2007**, *13*, 7171-7176; (i) Pinter, B.; Van Speybroeck, V.; Waroquier, M.; Geerlings, P.; De Proft, F. *Phys. Chem. Chem. Phys.* **2013**, *15*, 17354-17365; (j) Tsipis, A. C. *J. Comput. Chem*. **2019**, *40*, 2550-2562.

[52] For selective reports, see: (a) Clark, D. T.; Adams, D. B.; Briggs, D. *J. Chem. Soc. D*, **1971**, 602-604; (b) Motschi, H.; Pregosin, P. S.; Venanzi, L. M. *Helv. Chim. Acta* **1979**, *62*, 667-677; (c) Anderson, O. P.; Packard, A. B. *Inorg. Chem*. **1979**, *18*, 1129-1132; (d) Oskarsson, Å.; Norén, B.; Svensson, C.; Elding, L. I. *Acta Cryst.* **1990**, *B46*, 748-752; (e) Abu-Surrah, A. S.; Lappalainen, K.; Repo, T.; Klinga, M.; Leskelä, M.; Hodali, H. A. *Polyhedron* **2000**, *19*, 1601-1605; (f) Yamashita, M.; Vicario, J. V. C.; Hartwig, J. F. *J. Am. Chem. Soc*. **2003**, *125*, 16347-16360; (g) Sajith, P. K.; Suresh, C. H. *Inorg. Chem*. **2011**, *50*, 8085-8093; (h) Rezabal, E.; Ugalde, J. M.; Frenking, G. *J. Phys. Chem. A* **2017**, *121*, 7709-7716.

[53] A Pd–Cl bond *trans* to an alkene has a length between 2.2950(8) Å and 2.3240(6) Å, and a Pd–Cl bond *trans* to an aryl has a length between 2.308(1) Å and 2.3205(6) Å, see: (a) Bettucci, L.; Bianchini, C.; Oberhauser, W.; Vogt, M.; Grutzmacher, H. *Dalton Trans.* **2010**, *39*, 6509-6517; (b) Massard, A.; Rampazzi, V.; Perrier, A.; Bodio, E.; Picquet, M.; Richard, P.; Hierso, J.-C.; Le Gendre, P. *Organometallics* **2012**, *31*, 947-958; (c) Gioria, E.; Martínez-Ilarduya, J. M.; García-Cuadrado, D.; Miguel, J. A.; Genov, M.; Espinet, P. *Organometallics* **2013**, *32*, 4255-4261; (d) Horak, K. T.; Agapie, T. *J. Am. Chem. Soc*. **2016**, *138*, 3443-3452; (e) Monti, A.; Rama, R. J.; Gómez, B.; Maya, C.; Alvarez, E.; Carmona, E.; Nicasio, M.C. *Inorg. Chim. Acta* **2021**, *518*, 120214.

[54] A Pd–Br bond *trans* to an alkene has a length between 2.4253(8) Å and 2.4601(4) Å, and a Pd–Br bond *trans* to an aryl has a length of 2.4727 Å, see: ref. 35f and (a) Stepnicka, P.; Cisarova, I. *Collect. Czechoslov. Chem. Commun*. **1996**, *61*, 1335-1341; (b) Yen, S. K.; Hoh, L. L.; Huynh, H. V.; Hor, T. S. A. *Dalton Transactions* **2007**, 3952-3958; (c) Kim, N.-H.; Ha, K. *Acta Cryst*. **2009**, *E65*, m727.

palladium center,[1d] the π-electron donating ability of borataalkene in Senphos ligands towards Pd(II) can be regarded as in the same range as normal aryl and alkenes (e.g., reference complexes **3.88**-Cl[53a] and complex **3.88**-Br[35f]). When evaluating the *trans*-influence using the corresponded Pd–X^1 distance as an internal reference, 1,4-Senphos has the weakest π-electron donation ability and 1,2-Senphos has the strongest ability with 1,3-Senphos in the middle.[55] The data also support that the borataalkene has a stronger *trans*-influence than an alkene (complex **3.77** *vs.* complex **3.88**-Cl) but a weaker *trans*-influence than an electron-rich aryl (complex **3.79** and **3.81** *vs.* complex **3.88**-Br).

[55] In terms of the Pd–X^2/Pd–X^1 ratios, both counter anions (Cl or Br) reflect similar numbers where Cl is usually 0.3% bigger than Br. For pairs of complexes with same ligand but different counter anion (Cl and Br), see: pair 1: (a) Tsoureas, N.; Danopoulos, A. A.; Tulloch, A. A. D.; Light, M. E. *Organometallics* **2003**, *22*, 4750-4758; (b) Lee, H. M.; Chiu, P. L. *Acta Cryst.* **2004**, *E60*, m1473-m1474; pair 2: (c) Coleman, K. S.; Green, M. L.; Pascu, S. I.; Rees, N. H.; Cowley, A. R.; Rees, L. H. *J. Chem. Soc., Dalton Trans.* **2001**, 3384-3395; pair 3: (d) Liu, S.; Peloso, R.; Braunstein, P. *Dalton Trans.* **2010**, *39*, 2563-2572; pair 4: (e) Sabounchei, S. J.; Hashemi, A.; Yousefi, A.; Derakhshandeh, P. G.; Karamian, R.; Asadbegy, M.; Van Hecke, K. *Polyhedron*, **2017**, *135*, 1-9; (f) Sabounchei, S. J.; Badpa, K.; Hashemi, A.; Moniriyan, F.; Gable, R. W. *Appl. Organomet. Chem*. **2019**, *33*, e4882; pair 5: (g) Blacker, A. J.; Clarke, M. L.; Loft, M. S.; Mahon, M. F.; Humphries, M. E.; Williams, J. M. J. *Chem. Eur. J.* **2000**, *6*, 353-360; (h) Cabrera, A.; Sharma, P.; Pérez-Flores, F. J.; Velasco, L.; Arias, J. L.; Rubio-Pérez, L. *Catal. Sci. Technol.* **2014**, *4*, 2626-2630.

Table 3.6. Summary of palladium-halogen bonds (Å) in Pd(II) complexes.

	complex **3.77** (X = Cl)	complex **3.79** (X = Br)	complex **3.81** (X = Br)	complex **3.88**-Cl (X = Cl)	complex **3.88**-Br (X = Br)
Pd–X^1 (Å)	2.3495(6)	2.4731(8)	2.5108(4)	2.353(1)	2.4870(3)
Pd–X^2 (Å)	2.3280(6)	2.4338(9)	2.4562(5)	2.319(1)	2.4728(4)
$\frac{Pd–X^2}{Pd–X^1}$ (%)	99.08(4)	98.41(5)	97.83(3)	98.56(1)	99.43(2)

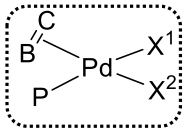

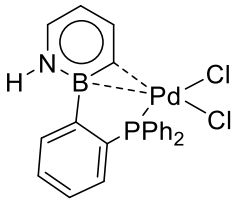

3.77

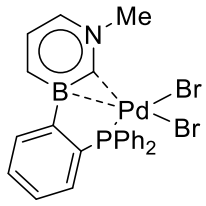

3.79

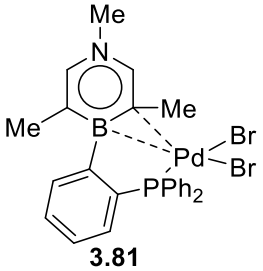

3.81

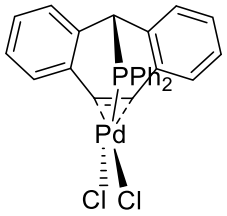

3.88-Cl

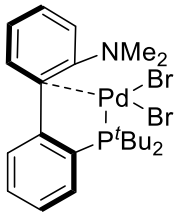

3.88-Br

3.3. Evaluation of rotational energy barriers in Pd/Senphos complexes

The solid-state structures show the coordination behavior of Senphos ligands toward the palladium, but they cannot describe how strong these interactions are, especially in the solution state where reactions occur. Therefore, it would be informative to have a quantitative systematic evaluation of the Pd/Senphos interaction in solution.

The Hoefelmeyer group studied the rotational energy barrier of the *B*–mesityl group in 8-(dimesitylboryl)quinoline chelated metal (Cu(I) or Ag(I)) complexes.[43a] In the ^{1}H NMR spectra of complex **3.89**, the authors observed the broadening of both mesityl *ortho*-methyl and *meta*-H signals, indicating a dynamic η^3-B,C,C coordination to the metal (Scheme 3.19). With these broadening ^{1}H NMR signals as markers, the rotational energy

barriers of complexes **3.89** are measured via VT (variable temperature) ^{1}H NMR to be 15.1(1) (X = Cu) and 15.2(3) kcal/mol (X = Ag).

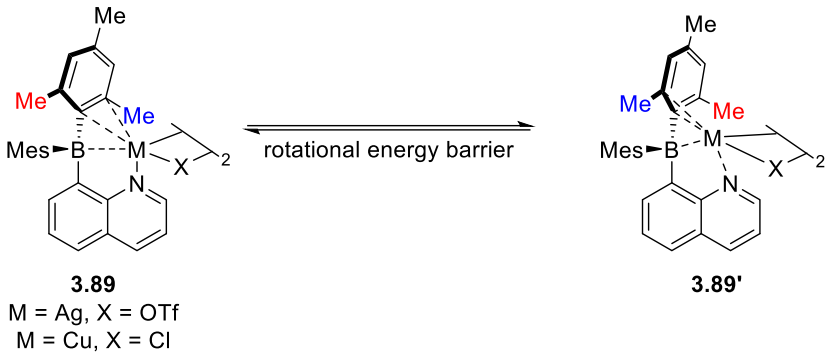

3.89
M = Ag, X = OTf
M = Cu, X = Cl

3.89'

Scheme 3.19. Hoefelmeyer's system for rotational energy barrier measurement.

We designed a new set of Pd/Senphos complexes **3.93-3.98**[56] from Senphos ligands **3.90-3.92** which have the *B*–*o*-di-*p*-tolylphosphinophenyl substituents. And we envisioned that the two *p*-tolyl-methyl groups in palladium complexes would act as stereochemical indicators to reveal the intramolecular coordination dynamics through VT-^{1}H NMR study.

[56] These complexes are proposed to have similar coordination mode compared to their non-methylated analogs, *B*–*o*-di-phenylphosphinophenyl substituted complexes **3.76-3.81**.

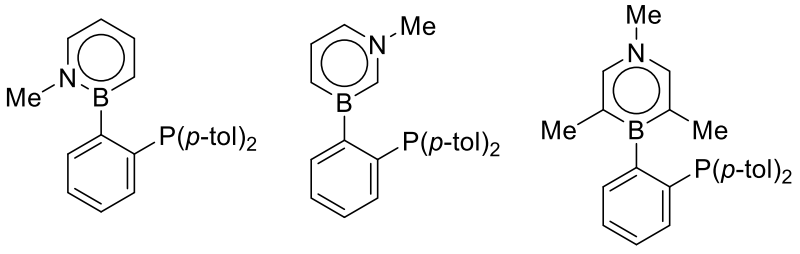

3.90 **3.91** **3.92**

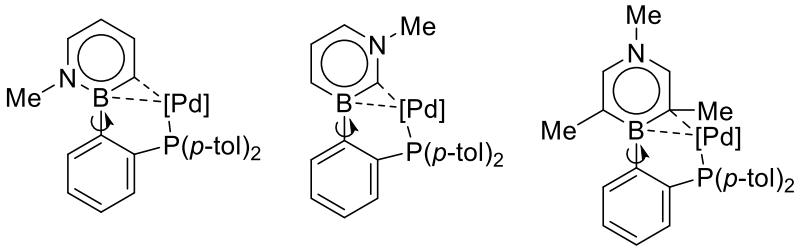

	1,2-Senphos	1,3-Senphos	1,4-Senphos
[Pd] = Pd(0)•dba	**3.93**	**3.95**	**3.97**
[Pd] = $Pd(II)Br_2$	**3.94**	**3.96**	**3.98**

Figure 3.7. Structures of 1,2-, 1,3- and 1,4-Senphos ligands and the corresponding palladium complexes.

At low temperature, the Senphos η^n coordination dynamics is slow on the NMR time scale,[57] thus the two *p*-tolyl-methyl groups in the planar-chiral structure are diastereotopic and non-exchangeable (leading to two distinct methyl signals in ^{1}H NMR). On the other hand, at high temperature, the Senphos η^n coordination is dynamic on the NMR time scale, thus allowing the two diastereotopic methyl groups to exchange (leading to one methyl signal representing two *p*-tolyl-methyl groups in ^{1}H NMR). The 'transition' temperature from two signals to one signal is the coalescence temperature (T_c, in K), which in conjunction with the chemical frequency difference ($\Delta\nu$, in Hz) of the two *p*-tolyl-methyl

[57] Bryant, R. G. *J. Chem. Educ.* **1983**, *60*, 933-935.

group signals at low temperature can reveal the rotational energy barrier $\Delta G^{\neq}$ (eqs 1 and 2) in various complexes.[58]

$$k = \frac{\kappa k_B T_c}{h} e^{-\frac{\Delta G^{\neq}}{RT}} \quad \text{(eq. 1)}$$

$$k = \frac{\pi}{\sqrt{2}} \Delta\nu \quad \text{(eq. 2)}$$

3.3.1. Pd complexes containing 1,2-Senphos ligand

For Pd(0)/1,2-Senphos complex **3.93** at room temperature in MeCN-*d*3, the two *p*-tolyl-methyl groups display one broad signal. However, raising the temperature to 50 or 70 °C leads to two sharp signals. We speculate that the broad single peak observed at room temperature results from the complicated dynamics associated with the dba ligand. Since the coalescence temperature is not reached even at 70 °C, with a chemical frequency difference of the two *p*-tolyl methyl groups is 108.4 Hz, the rotational energy barrier is estimated to be higher than 16.7 kcal/mol.

[58] (a) Friebolin, H. In Basic One- and Two-imensional NMR Spectroscopy, 5th Ed.; Wiley-VCH, Weinheim, 2011; (b) Gutowsky, H. S.; Holm, C. H. *J. Chem. Phys.* **1956**, *25*, 1228-1234; (c) Gasparro, F. P.; Kolodny, N. H. *J. Chem. Educ*. **1977**, *54*, 258-261; (d) Morris, K. F.; Erickson, L. E. *J. Chem. Educ*. **1996**, *73*, 471-473.

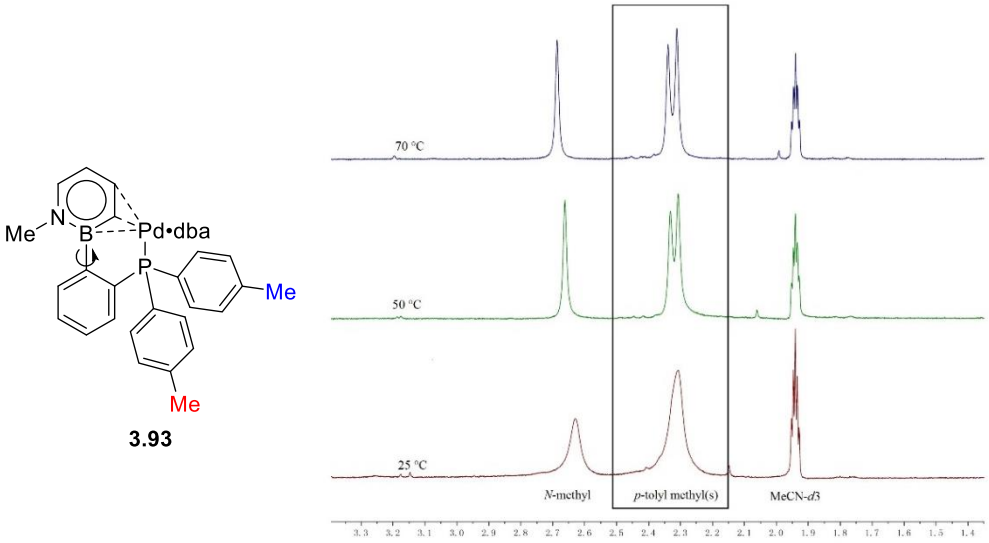

Figure 3.8. VT-^{1}H NMR spectrum of Pd(0)/1,2-Senphos complex **3.93** in MeCN-*d*3.

For Pd(II)/1,2-Senphos complex **3.94**, the chemical frequency difference of the two *p*-tolyl-methyl groups is 17.8 Hz and the coalescence temperature is determined to be 328 K. Therefore, the rotational energy barrier is estimated to be 16.9(1) kcal/mol.[59]

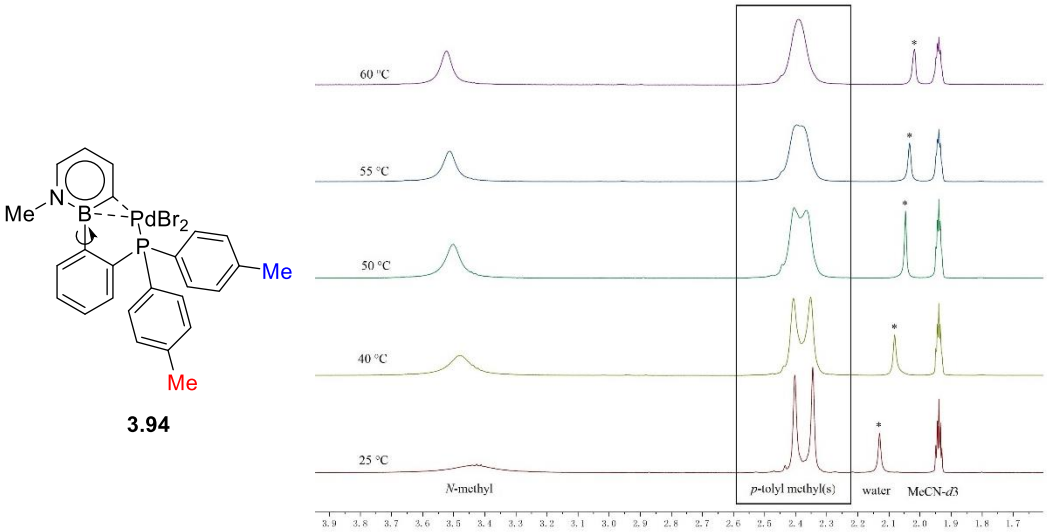

Figure 3.9. VT-^{1}H NMR spectrum of Pd(II)/1,2-Senphos complex **3.94** in MeCN-*d*3.

[59] At –35 ºC, two N–Me signals are observed, and we speculate one represents the η^3-B,C,C coordination and the other is η^2-B,C coordination. As the temperature raises to 25 ºC, they coalesce to one N–Me signal.

3.3.2. Pd complexes containing 1,3-Senphos ligand

The complexation between 1,3-Senphos **3.91** and Pd_2dba_3 results in two constitutional isomers. At –40 ºC, two distinctive *N*–Me ^{1}H NMR signals at 3.99 ppm and 2.98 ppm were observed.[60] Accordingly, they give four diastereotopic *p*-tolyl-methyl signals.[61] The chemical frequency differences of these methyl groups are 47.2 Hz and 96.3 Hz, and both coalescence temperatures are determined to be 288 K. Therefore, the energy barriers are estimated to be 14.2(3) and 13.8(2) kcal/mol for complex **3.95** and **3.95'**, respectively.

[60] Based on the solid-state structures, in complex **3.78** where Pd(0) coordinates to the C(2) position, the C(6) –N(1) distance is 1.318(10) Å, and in complex **3.78'** where Pd(0) coordinates to the C(4) position, the N(1)–C(2) distance is 1.359(10) Å. Therefore, the nitrogen in complex **3.78** has more iminium character and the N–Me peak would be downfield shifted compared to complex **3.78'**. We applied this observation for complex **3.95** and **3.95'** and concluded in the ^{1}H NMR the N–Me peak at 3.99 ppm represents complex **3.95** and the N–Me peak at 2.98 ppm represents complex **3.95'**.

[61] During the VT-^{1}H NMR experiments, when the temperature is below the coalescence temperature, the N–Me peak in complex **3.95** is usually sharper than the one in complex **3.95'**, and we concluded the two sharper *p*-tolyl methyl peaks (2.36 and 2.25 ppm) correspond to complex **3.95** and the two broader *p*-tolyl methyl peaks (2.48 and 2.23 ppm) correspond to complex **3.95'**.

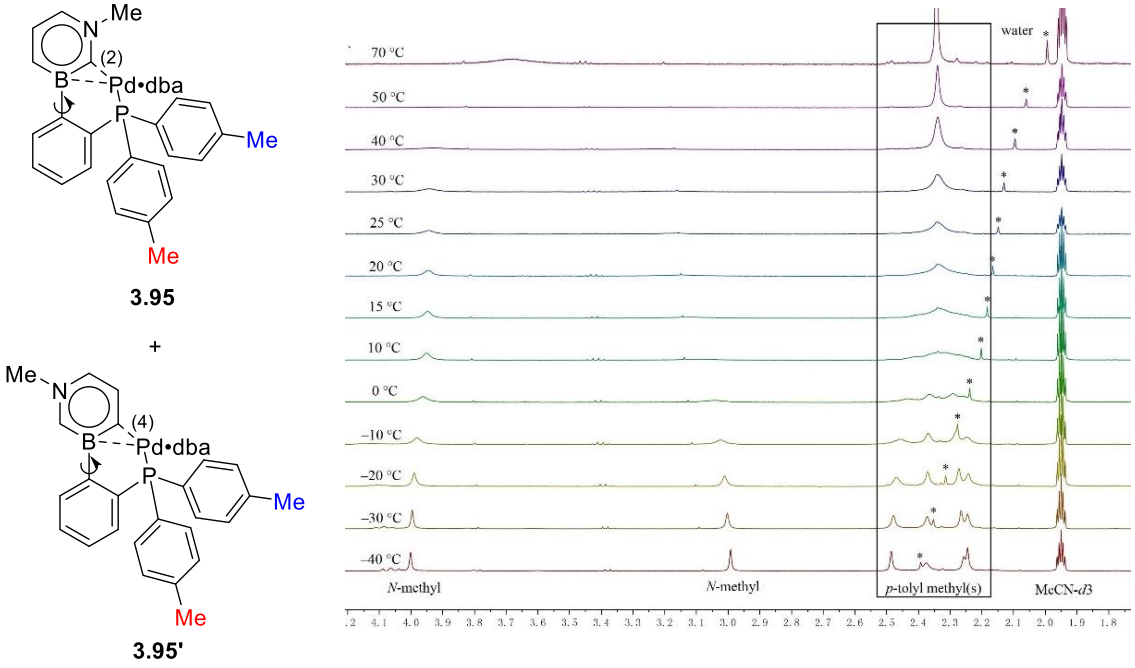

Figure 3.10. VT-^{1}H NMR spectrum of Pd(0)/1,3-Senphos complex **3.95** and **3.95'** in MeCN-*d*3.

The coordination of 1,3-Senphos **3.91** with $PdBr_2$ yields complex **3.96**. The chemical frequency difference of the two *p*-tolyl-methyl groups is 51.2 Hz and the coalescence temperature is determined to be 273 K. Therefore, the energy barrier is estimated to be 13.4(1) kcal/mol.

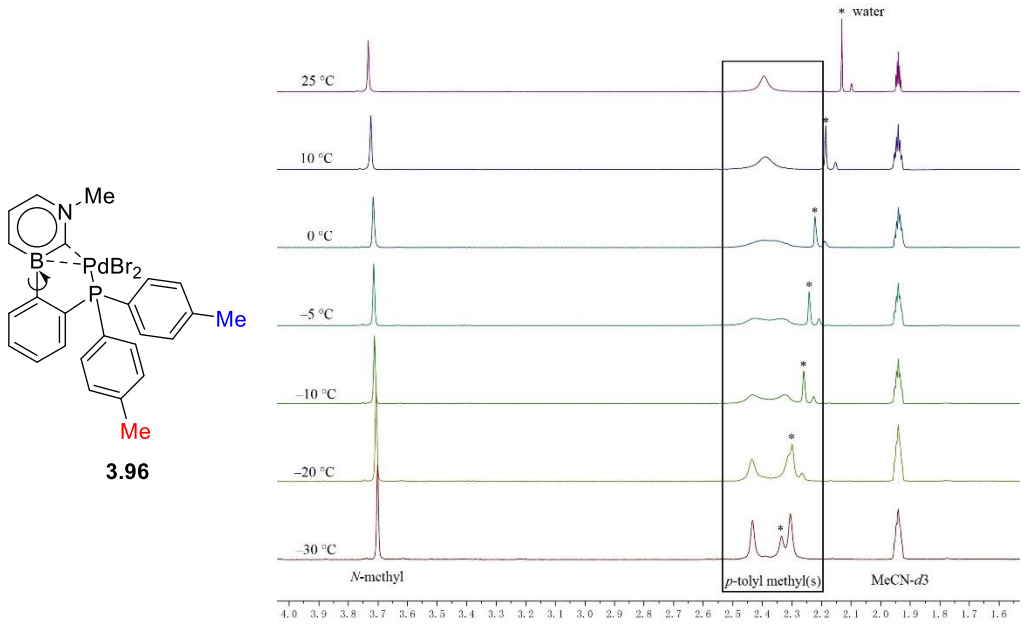

Figure 3.11. VT-^{1}H NMR spectrum of Pd(II)/1,3-Senphos complex **3.96** in MeCN-*d*3.

With the ambient coalescence temperature of complex **3.96** in MeCN-*d*3, we further investigated the solvent influence of the rotational barrier. Two additional solvents, namely 1,4-dioxane-*d*8 and THF-*d*8, are examined. As shown in Figure 3.12, the chemical frequency difference of the two *p*-tolyl-methyl groups in 1,4-dioxane-*d*8 is 54.8 Hz and the coalescence temperature is determined to be 328 K which leads to an energy barrier of 16.1(2) kcal/mol. Due to the boiling point limitation of THF-*d*8 (b.p. 66 °C), the coalescence of the two *p*-tolyl-methyl peaks in complex **3.96** cannot be reached (Figure 3.13). Instead, based on their partial coalescence at 55 °C, the coalescence temperature is extrapolated to be 65 °C. Hence, with a 71.2 Hz difference in the chemical frequency of the two *p*-tolyl-methyl groups, the rotational energy barrier in THF is calculated to be 16.5(1) kcal/mol. Overall, the solvent indeed influences the rotational energy barrier of

complex **3.96**, with 13.4 kcal/mol in MeCN, 16.1(2) kcal/mol in 1,4-dioxane and 16.5(1) kcal/mol in THF.[62]

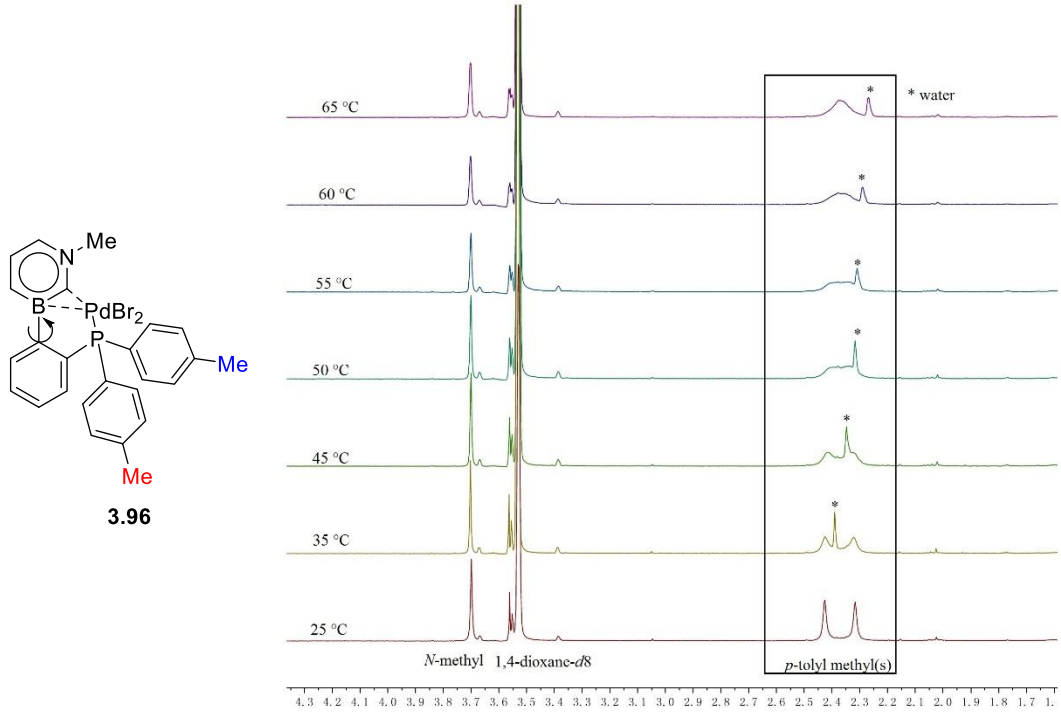

Figure 3.12. VT-^{1}H NMR spectrum of Pd(II)/1,3-Senphos complex **3.96** in 1,4-dioxane-*d*8.

[62] The origin of the solvent influence is currently unknown. The dielectric constant (ε) for MeCN, 1,4-dioxane and THF is 37.5, 2.25 and 7.58, respectively. For solvent coordinating ability, see: Alvarze, S. *Chem. Eur. J.* **2020**, *26*, 4350-4377.

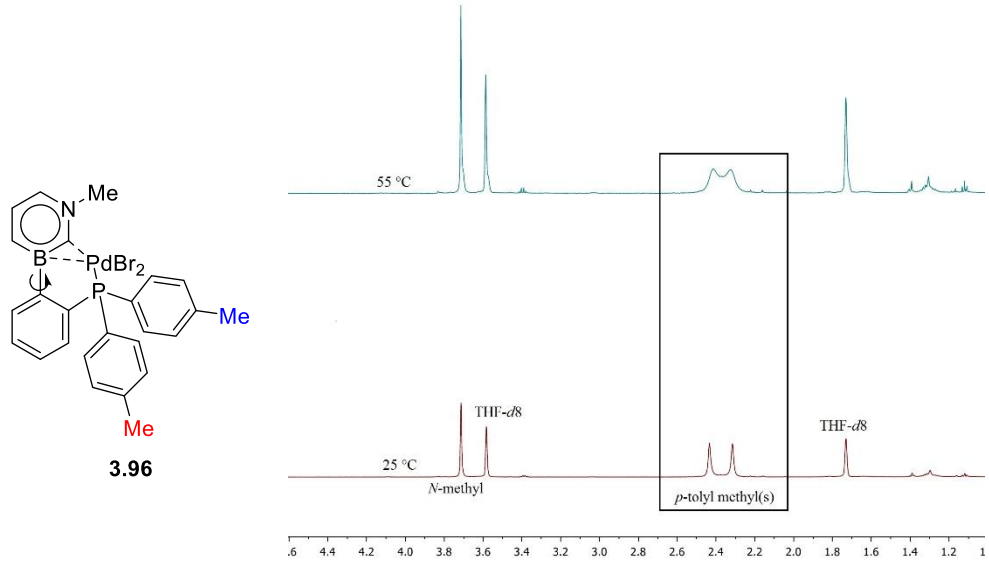

Figure 3.13. VT-^{1}H NMR spectrum of Pd(II)/1,3-Senphos complex **3.96** in THF-*d*8.

3.3.3. Pd complexes containing 1,4-Senphos ligand

For Pd(0)/1,4-Senphos complex **3.97**, another set of ^{1}H NMR signals, i.e., the two flanking methyl groups on azaborine ring, can also serve as stereochemical handles. For consistency, this new marker is not considered in the rotational barrier calculations (but they show very similar dynamics comparing to the *p*-tolyl-methyl groups). A dynamic pathway where the palladium shifts between the two possible η^2-B,C coordination sites is not typically observed.[43a,63] The chemical frequency difference in the two *p*-tolyl-methyl groups for complex **3.97** is 101.5 Hz and the coalescence temperature is determined to be 298 K. Therefore, the rotational energy barrier is calculated to be 13.9(1) kcal/mol.

[63] Li, C.-S.; Jou, D.-C.; Cheng, C.-H. *Organometallics* **1993**, *12*, 3945-3954.

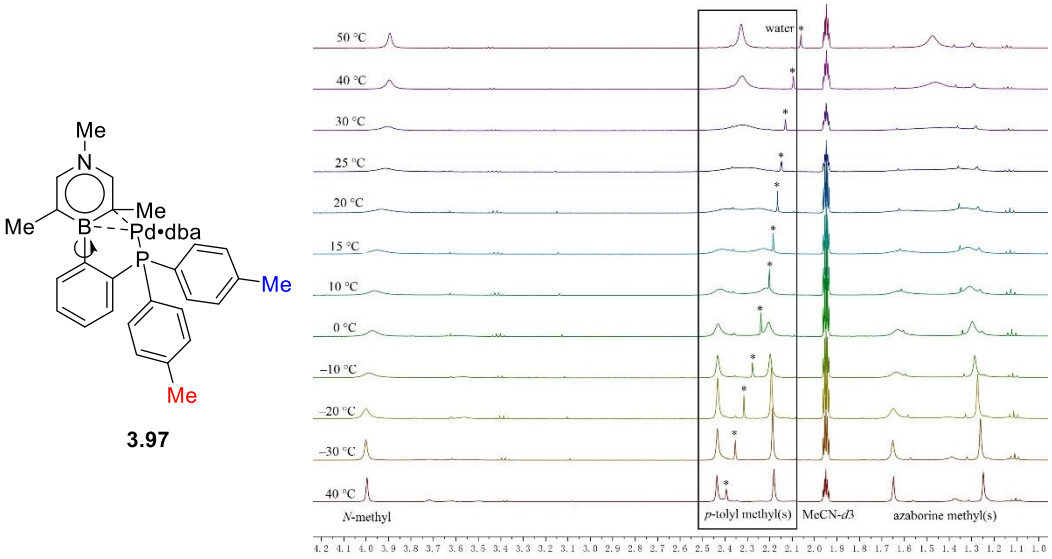

Figure 3.14. VT-^{1}H NMR spectrum of Pd(0)-1,4-Senphos complex **3.97** in MeCN-*d*3.

Unlike the other two Pd(II) complexes, the two *p*-tolyl-methyl groups in Pd(II)/1,4-Senphos complex **3.98** undergo fast exchange even at –40 °C. Due to the freezing point of the solvent MeCN-*d*3, lowering temperature below –40 °C is not feasible. Therefore, an exact energy value cannot be determined, and the rotational energy barrier is estimated to be less than 11.3 kcal/mol.[64]

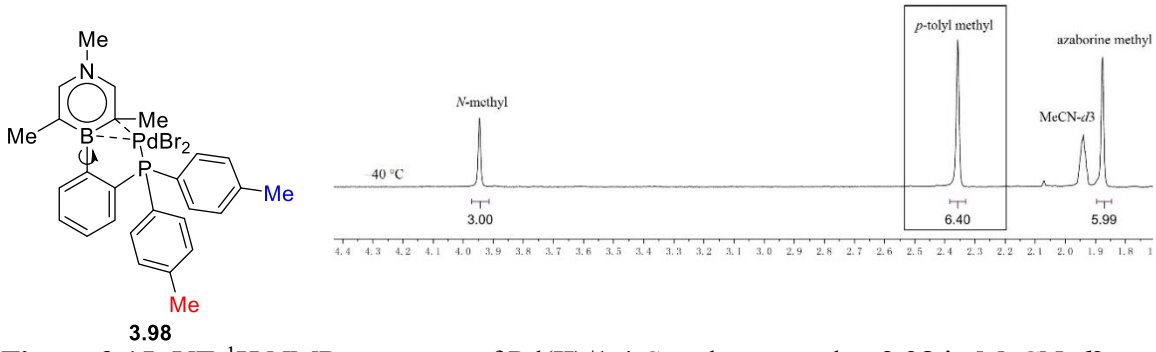

Figure 3.15. VT-^{1}H NMR spectrum of Pd(II)/1,4-Senphos complex **3.98** in MeCN-*d*3.

[64] The chemical frequency difference is set to 50 Hz, a similar value to complex **3.96**. And the coalescence temperature is set to 233K.

3.3.4. Pd complexes containing carbonaceous Senphos ligand

With the success in determining the rotational energy barriers of a series of Pd/Senphos complexes, we next evaluated the rotational energy barrier of the palladium complexes of the corresponding carbonaceous ligand. As summarized in chapter 3.1.3, the η^1-C or η^2-C,C biaryl phosphine bound palladium complexes have been mainly studied via X-ray crystallography and *in silico* simulations, and the rotational energy barrier has not been examined experimentally. For the purpose of a direct comparison, we synthesized ligand **3.99**, the carbonaceous analogue of 1,3-Senphos **3.91**,[65] followed by complexation with Pd_2dba_3 or $PdBr_2$ to yield complexes **3.100** and **3.101**.[66] At –40 °C in MeCN-*d*3, both complex **3.100** and **3.101** show a single signal representing the two *p*-tolyl-methyl groups, indicating fast dynamics even at –40 °C.[67] The results in Figure 3.16 are consistent with very weak κ^2-type bonding between carbonaceous ligand **3.99** and palladium in MeCN-*d*3.

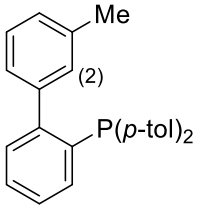

3.99

[65] The carbonaceous analogue of 1,2-Senphos **3.90** shows two diastereotopic *p*-tolyl-methyl signals in ^{1}H NMR at room temperature, indicating its axial chirality nature. Under the same conditions, such phenomenon is absent in compound **3.99** and only a single signal representing the two *p*-tolyl-methyl groups is observed.

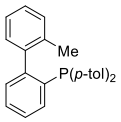

[66] The complexation between $PdBr_2$ and ligand **3.99** in solvent Et_2O generates what we tentatively assign as a mono-nuclear palladium complex **3.101** along with 5% di-nuclear palladium complex by ^{31}P NMR. However, due to the very low solubility of this mono-nuclear palladium complex **3.101** and high solubility of the di-nuclear palladium complex in CD_3CN, the VT-^{1}H NMR experiment is conducted with a 1:1 mixture of the two complexes where signals corresponding to complex **3.101** is labeled with asterisk (*). The VT-^{1}H NMR experiment of the isolated complex **3.101** is less clean than the mentioned mixture. For controlling the generation of mono- and di-nuclear palladium complexes, see: (a) Schmid, T. E.; Jones, D. C.; Songis, O.; Diebolt, O.; Furst, M. R. L.; Slawin, A. M. Z.; Cazin, C. S. J. *Dalton Trans*. **2013**, *42*, 7345-7353; (b) Vuoti, S.; Haukka, M.; Pursiainen, J. *J. Organomet. Chem*. **2007**, *692*, 5044-5052; (c) Zhang, Z.; Cordier, M.; Dixneuf, P. H.; Soulé, J.-F. *Org. Lett*. **2020**, *22*, 5936-5940.

[67] Both complexes are confirmed with κ^2-type bonding by the broadening or upfield shifted of the C(2) proton.

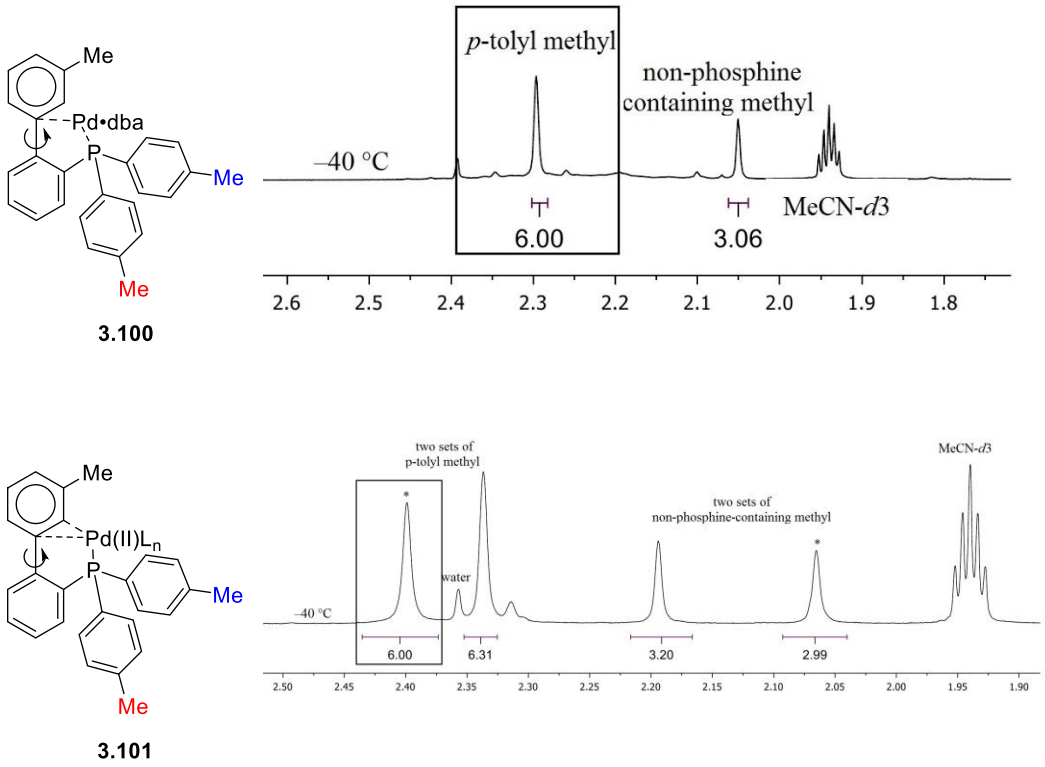

Figure 3.16. VT-^{1}H NMR spectrum of carbonaceous ligand **3.99** bound palladium complexes in MeCN-*d*3.

3.3.5. Summary

The rotational energy barriers measured by VT-^{1}H NMR experiments for Senphos or carbonaceous ligand bound palladium complexes are summarized in Table 3.7, and these rotational barriers are postulated to represent the binding energy of the η^n-coordination to the palladium. Most of the complexes have a rotational energy barrier less than 15 kcal/mol, indicating they have reasonable rotation dynamics at room temperature. Therefore, the η^n ligated Senphos ligands can be classified as hemilabile ligands.[68] In Table 3.7 two general

[68] (a) Jeffrey, J. C.; Rauchfuss, T. B. *Inorg. Chem*. **1979**, *18*, 2658-2666; for reviews, see: (b) Bader, A.; Lindner, E. *Coord. Chem. Rev*. **1991**, *108*, 27-110; (c) Slone, C. S.; Weinberger, D. A.; Mirkin, C. A. *Prog. Inorg. Chem*. **1999**, *48*, 233-250; (d) Braunstein, P.; Naud, F. *Angew. Chem. Int. Ed.* **2001**, *40*, 680-699; (e) McPherson, J. N.; Das, B.; Colbran, S. B. *Coord. Chem. Rev*. **2018**, *375*, 285-332.

trends can be observed: First, with a given Senphos ligand, the Pd(0) complex has a stronger binding than the corresponding Pd(II) complex. Presumably the borataalkene motif in Senphos acts generally as a better electron acceptor rather than an electron donor towards palladium. The change in binding ability as a function of the oxidation state of palladium would facilitate the opening of a coordination site during the transformation from a Pd(0)/Senphos complex to Pd(II)/Senphos complex (e.g., oxidative addition). The Senphos ligand could possibly convert from a bi-dentate to a mono-dentate ligand upon oxidative addition. Second, for Pd(0) complexes, ligand binding affinity is as follows: 1,2-Senphos > 1,3-Senphos ≈ 1,4-Senphos > CC-Senphos, and for Pd(II) complexes, the ligand binding affinity is as follows: 1,2-Senphos > 1,3-Senphos > 1,4-Senphos. This tunable nature of Senphos ligands may guide reaction design in future Pd/Senphos catalyzed reactions.

Table 3.7. Summary of energy barriers (kcal/mol) in various Pd/Senphos complexes in MeCN-*d*3.

ligand / metal	1,2-Senphos	1,3-Senphos	1,4-Senphos	CC-Senphos
Pd(0)	>16.7	14.2(3)	14.2(1)	<11.3
Pd(II)	16.9(1)	13.4(1)	<11.3	<11.3

3.3.6. Evaluation of various Senphos and carbonaceous ligands in *trans*-hydroboration reaction

With HBCat as the boron source, α-branched enyne **3.102** as the substrate and MeCN as the solvent, we evaluated the effects of different Senphos ligands in palladium catalyzed *trans*-hydroboration reaction. As shown in Table 3.8, the choice of Senphos ligands moderately influences both the *trans*-hydroboration reactivity and selectivity

(entries 1-3) where 1,4-Senphos **3.75** leads to the formation of product **3.103** with the highest yield and diastereoselectivity followed by 1,2-Senphos and 1,3-Senphos (entries 1-3). Monobenzofused 1,4-Senphos **3.105** performs similar to 1,4-Senphos **3.75** (entries 3-4). Although carbonaceous ligand **3.99** possesses a weaker κ^2-type bonding with palladium than 1,3-Senphos **3.74**, it still serves as a better ligand in the *trans*-hydroboration reaction (entry 2 *vs.* 5). Therefore, we conclude that the diastereoselectivity of the *trans*-hydroboration reaction is governed by more complicated factors than simply the nature of the η^n-binding of the various ligands to the palladium metal.

Table 3.8. Evaluation of various Senphos and carbonaceous ligands in palladium-catalyzed enyne *trans*-hydroboration reaction.[a]

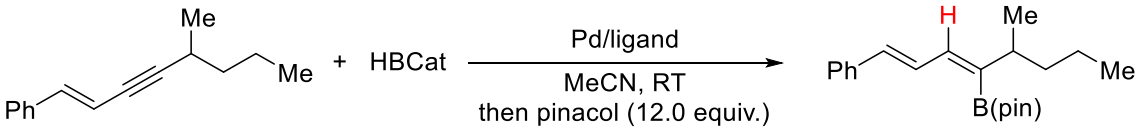

3.102 **3.103**

entry	ligand	yield (*trans*:*cis*)[b]
1	**3.104**	74% (78:22)
2	**3.74**	53% (57:43)
3	**3.75**	80% (82:18)
4[c]	**3.105**	71% (82:18)
5	**3.99**	54% (68:32)

[a] Reaction was setup with 1.0 equiv. enyne **3.102**, 1.5 equiv. HBCat and 4 mol% Pd(0)/Senphos complex in MeCN (1.25 M). [b] The yield and diastereomeric ratio were determined by ^{1}H NMR of crude mixture after silica gel plug with 1,3,5-trimethoxybenzene as the internal standard. [c] The internal standard is hexamethylbenzene.

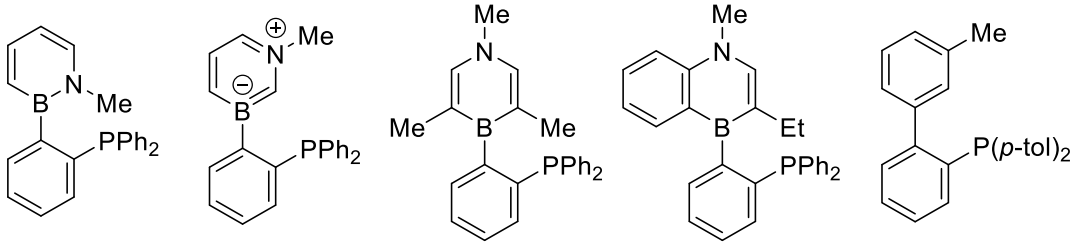

3.104 **3.74** **3.75** **3.105** **3.99**

3.4. Conclusion

A series of 1,2-, 1,3- and 1,4-Senphos ligated Pd(0) or Pd(II) complexes were evaluated based on solid-state structures and variable-temperature NMR measurements. For B–*o*-diphenylphosphinophenyl substituted Senphos ligands, their η^2-B,C or η^3-B,C,C coordination to palladium are validated by the corresponded solid-state structures, and such coordination, especially to Pd(II), promotes the azaborine intra-ring structure have more iminium/borataalkene character. Furthermore, we also investigated the *trans*-influence of the borataalkene motif in various Senphos ligands. For B–*o*-di-*p*-tolylphosphinophenyl substituted Senphos ligands, the rotational energy barriers in a series of Senphos or carbonaceous ligand bound palladium complexes were determined via VT-^{1}H NMR technique, and the results indicate that Senphos ligands are hemilabile binding ligands that generally bind to palladium more strongly than the carbonaceous ligand. The moderate ligand influence in the palladium-catalyzed *trans*-hydroboration reaction suggests additional influencing contributors beyond η^n-binding strength among 1,2-, 1,3-, 1,4-Senphos and carbonaceous analogue ligands.

3.5. Experimental section

3.5.1. General information

^{1}H, ^{13}C, ^{31}P and ^{19}F spectra were recorded on Varian 400, 500 or 600 MHz spectrometers and ^{11}B spectra were on Inova 500 MHz spectrometers at ambient temperature. ^{1}H NMR spectra were reported with the solvent resonance as internal standard. ^{13}C NMR spectra were reported with the solvent resonance as internal standard. ^{11}B NMR spectra were reported with BF_3•Et_2O (δ 0 ppm) as externally reference. ^{31}P NMR spectra were reported with H_3PO_4 (δ 0 ppm) as externally reference. IR spectra were recorded on

a Bruker FTIR Alpha (ATR mode) spectrometer. High-resolution mass spectroscopy data were obtained at the Mass Spectroscopy Facilities at Chemistry Department of Boston College with DART ion source in positive ion mode.

All oxygen- and moisture-sensitive manipulations were carried out under N_2 atmosphere with standard Schlenk techniques or in N_2 glovebox.

Solvents used under N_2 atmosphere (pentane, THF, benzene, Et_2O, MeCN and CH_2Cl_2) were purified by passing through a neutral alumina column under argon. MeCN-*d*3 and $CDCl_3$ were dried with 5Å molecular sieves. All other chemicals and solvents were purchased and used as received.

3.5.2. Experimental procedures

3.5.2.1. Experimental procedure for synthesizing Senphos and carbonaceous ligands

Synthesis of Senphos ligand **3.73**

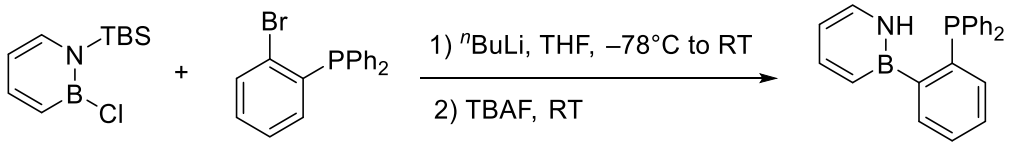

To a 20-mL vial charged with (2-bromophenyl)diphenylphosphine (171 mg, 0.500 mmol, 1.00 equiv.) and THF (5.0 mL) was added ^{n}BuLi (2.5 M in hexanes, 0.20 mL, 0.50 mmol, 1.0 equiv.) at −78 °C, and the resulting mixture was allowed to stir at the same temperature for 0.5 h. Then, a THF (2 mL) solution of *N*–TBS-*B*–Cl substituted 1,2-azaborine[69] (114 mg, 0.500 mmol, 1.00 equiv.) was introduced at once, and the new mixture was allowed to stir at −78 ºC for 1.5 h and was gradually allowed to warm to room

[69] Marwitz, A. J. V.; Matus, M. H.; Zakharov, L. N.; Dixon, D. A.; Liu, S.-Y. *Angew. Chem. Int. Ed*. **2009**, *48*, 973-977.

temperature in another 2 h. TBAF (1.0 M in THF, 0.75 mL, 0.75 mmol, 1.5 equiv.) was added to the mixture, which was then allowed to stir for 1h. At the conclusion of reaction, H_2O (10 mL) along with Et_2O (10 mL) were poured into the mixture, and the organic layer was separated and the aqueous layer was further washed with Et_2O (10 mL). The organic layers were combined and concentrated under reduced pressure. The resulting crude residue was purified by silica gel chromatography using hexanes/EtOAc (30/1) as the eluent to afford ligand **3.73** as a white solid (147 mg, 87%). ^{1}H NMR (500 MHz, $CDCl_3$) δ 8.35 (br, s, 1H), 7.65 (dd, *J* = 11.2, 6.5 Hz, 1H), 7.61 (dd, *J* = 7.6, 3.2 Hz, 1H), 7.37 (t, *J* = 7.4 Hz, 1H), 7.35 – 7.18 (m, 12H), 7.02 (dd, *J* = 7.7, 4.6 Hz, 1H), 6.89 (d, *J* = 11.2 Hz, 1H), 6.33 (td, *J* = 6.5, 1.5 Hz, 1H); ^{13}C NMR (101 MHz, $CDCl_3$) δ 143.9, 140.3 (d, *J* = 9.9 Hz), 137.9 (d, *J* = 10.9 Hz), 134.4 (d, *J* = 11.7 Hz), 134.0 (d, *J* = 19.1 Hz), 133.3, 133.2, 128.6 (d, *J* = 1.5 Hz), 128.6, 128.3, 128.2, 110.8 (two signals of aromatic carbons attached to boron are not observed); ^{11}B NMR (160 MHz, $CDCl_3$) δ 34.7; ^{31}P NMR (202.3 MHz, $CDCl_3$) δ −8.3; IR (ATR): 3382, 3068, 3050, 1611, 1536, 1449, 1432, 1416, 1222, 1087, 977, 834, 741, 728, 695, 526, 502, 472 cm^{-1}; HRMS (DART) calcd for $C_{22}H_{19}BNP$ ($[M+H]^+$) 340.14262, found 340.14102.

Synthesis of Senphos ligands **3.74**, **3.75**, **3.90** to **3.92** and **3.104**

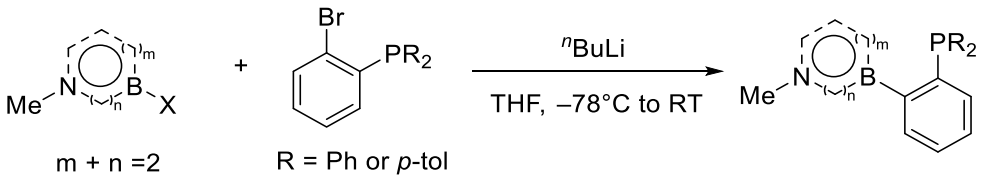

To a 20-mL vial charged with (2-bromophenyl)diarylphosphine (0.500 mmol, 1.00 equiv.) and THF (5.0 mL) was added ^{n}BuLi (2.5 M in hexanes, 0.20 mL, 0.50 mmol, 1.0 equiv.) at −78 °C. After allowing the mixture to stir at the same temperature for 0.5 h, a

THF (2 mL) solution of *N*–Me-*B*–X substituted azaborine[70] (0.5 mmol, 1 equiv.) was introduced at once, and the new mixture was allowed to stir at −78 ºC for 1.5 h and then was allowed to gradually warm to room temperature in another 2 h. At the conclusion of reaction, all violates were removed *in vacuo*, and the residue was purified by silica gel chromatography using pentane/Et_2O as the eluent to afford the desired ligands as white solids.

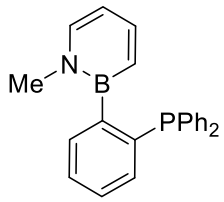

59% yield. ^{1}H NMR (500 MHz, $CDCl_3$) δ 7.51 (ddd, *J* = 10.9, 6.5, 1.2 Hz, 1H), 7.43 – 7.34 (m, 2H), 7.34 – 7.21 (m, 11H), 7.20 – 7.12 (m, 2H), 6.61 (dd, *J* = 10.9, 1.5 Hz, 1H), 6.36 (td, *J* = 6.6, 1.6 Hz, 1H), 3.24 (s, 3H); ^{13}C NMR (126 MHz, $CDCl_3$) δ 141.6, 140.2 (d, *J* = 6.7 Hz), 138.1, 138.0, 134.1 (d, *J* = 19.5 Hz), 133.6 (d, *J* = 18.8 Hz), 132.9, 132.0 (d, *J* = 13.4 Hz), 131.6 (br), 128.4 (br), 128.0, 127.6, 111.3, 42.2 (d, *J* = 2.7 Hz) (one signal of aromatic carbon attached to boron is not observed); ^{11}B NMR (160 MHz, $CDCl_3$) δ 36.3; ^{31}P NMR (162 MHz, $CDCl_3$) δ –9.2, IR (ATR) cm^{-1}; HRMS (DART) calcd for $C_{23}H_{22}BNP$ ($[M+H]^+$) 354.15774, found 354.15782.

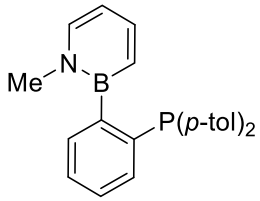

66% yield. ^{1}H NMR (400 MHz, $CDCl_3$) δ 7.53 (dd, *J* = 10.9, 6.5 Hz, 1H), 7.44 – 7.31 (m, 3H), 7.35 – 7.27 (m, 1H), 7.25 – 7.04 (m, 9H), 6.65 (dd, *J* = 10.9, 1.5 Hz, 1H), 6.37 (td, *J* = 6.6, 1.5 Hz, 1H), 3.27 (s, 3H), 2.37 (s, 6H); ^{13}C NMR (101 MHz, Chloroform-*d*) δ 141.6, 140.7 (d, *J* = 6.7 Hz), 139.2, 138.1 (br, d, *J* = 19.9 Hz), 134.8 (d, *J* = 10.7 Hz),

[70] For review, see: Giustra, Z. X.; Liu, S.-Y. *J. Am. Chem. Soc.* **2018**, *140*, 1184-1194. For 1,2-azaborine, X = Cl, see: (a) Thiedemann, B.; Gliese, P. J.; Hoffmann, J.; Lawrence, P. G.; Sönnichsen, F. D.; Staubitz, A. *Chem. Commun*. **2017**, *53*, 7258-7261; for 1,3-azaborine, X = OPiv, see ref. 48; for 1,4-azaborine, X = OMe, see ref. 49.

134.0 (br, d, J = 20.0 Hz), 133.6 (br, d, J = 19.0 Hz), 132.7, 131.9 (d, J = 13.5 Hz), 129.1 (br, d, J = 6.7 Hz), 127.8, 127.5, 111.2, 42.2 (d, J = 2.7 Hz), 21.4 (one signal of aromatic carbon attached to boron is not observed); ^{11}B NMR (160 MHz, $CDCl_3$) δ 36.0; ^{31}P NMR (202 MHz, $CDCl_3$) δ –10.4; IR (ATR): 3065, 3034, 3012, 2919, 1607, 1515, 1496, 1451, 1413, 1398, 1308, 1213, 1186, 1091, 978, 806, 741, 691, 507 cm^{-1}; HRMS (DART) calcd for $C_{25}H_{26}BNP$ ($[M+H]^+$) 382.18904, found 382.18726.

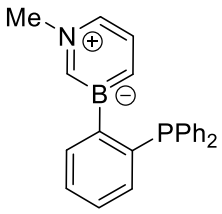

42% yield. ^{1}H NMR (600 MHz, CD_2Cl_2) δ 7.51 (ddd, J = 7.4, 3.7, 1.4 Hz, 1H), 7.47 (dd, J = 10.6, 2.5 Hz, 1H), 7.39 (dd, J = 10.6, 5.5 Hz, 1H), 7.32 – 7.30 (m, 7H), 7.27 – 7.25 (m, 5H), 7.17 (td, J = 7.6, 1.5 Hz, 1H), 7.12 (d, J = 5.6 Hz, 1H), 6.98 (dd, J = 7.7, 4.2 Hz, 1H), 3.89 (s, 3H); ^{13}C NMR (151 MHz, CD_2Cl_2) δ 148.1 (br), 144.6 (br), 140.1 (d, J = 8.5 Hz), 139.8 (d, J = 13.3 Hz), 134.9 (d, J = 11.4 Hz), 134.3 (d, J = 19.4 Hz), 133.5, 130.5, 128.8 (d, J = 6.6 Hz), 128.6, 128.2, 127.1, 125.7, 50.4; (one signal of aromatic carbon attached to boron is not observed); ^{11}B NMR (160 MHz, CD_2Cl_2) δ 34.3; ^{31}P NMR (202 MHz, CD_2Cl_2) δ –8.7; IR (ATR): 3046, 2998, 1584, 1516, 1476, 1461, 1441, 1434, 1318, 1221, 1166, 1089, 1026, 940, 828, 744, 697, 507 cm^{-1}; HRMS (DART) calcd for $C_{23}H_{22}BNP$ ($[M+H]^+$) 354.15774, found 354.15742.

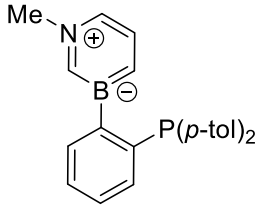

61% yield. ^{1}H NMR (600 MHz, $CDCl_3$) δ 7.52 (ddd, J = 7.4, 3.6, 1.4 Hz, 1H), 7.48 (ddd, J = 10.6, 2.7, 1.0 Hz, 1H), 7.38 (dd, J = 10.6, 5.6 Hz, 1H), 7.30 (tt, J = 7.3, 1.1 Hz, 1H), 7.22 (t, J = 2.3 Hz, 1H), 7.19 – 7.13 (m, 5H), 7.10 (dd, J = 8.1, 1.5 Hz, 4H), 7.06 (dt, J = 5.6, 1.3 Hz, 1H), 6.99 (ddd, J = 7.9, 4.3, 1.2 Hz, 1H), 3.87 (s, 3H), 2.33 (s, 6H); ^{13}C NMR (151 MHz, $CDCl_3$) δ 153.1 (br), 147.6 (br), 144.6 (br), 140.2 (d, J = 7.6 Hz), 137.9, 135.9

(d, J = 11.3 Hz), 134.4 (d, J = 11.3 Hz), 134.0 (d, J = 19.1 Hz), 133.0, 130.4, 129.2, 127.5, 126.7, 125.1, 49.9, 21.4; ^{11}B NMR (192 MHz, $CDCl_3$) δ 34.8; ^{31}P NMR (243 MHz, $CDCl_3$) δ –10.2; ATR (IR): 3035, 3011, 2946, 2919, 1495, 1459, 1441, 1318, 1263, 1221, 1185, 1166, 1090, 1019, 940, 806, 750, 734, 510 cm^{-1}; HRMS (DART) calcd for $C_{25}H_{26}BNP$ ($[M+H]^+$) 382.18904, found 382.18946.

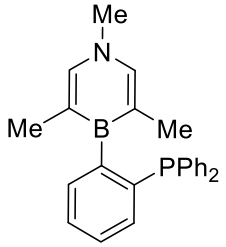

54% yield. ^{1}H NMR (600 MHz, $CDCl_3$) δ 7.37 (tt, J = 7.2, 1.4 Hz, 1H), 7.32 – 7.23 (m, 14H), 7.20 (ddd, J = 7.9, 4.2, 1.4 Hz, 1H), 3.68 (s, 3H), 1.84 (s, 6H); ^{13}C NMR (151 MHz, $CDCl_3$) δ 155.9 (br, d, J = 51.4 Hz), 140.3, 139.0 (d, J = 12.2 Hz), 138.1 (d, J = 3.5 Hz), 133.6 (d, J = 18.6 Hz), 133.1 (d, J = 1.3 Hz), 130.7 (d, J = 15.7 Hz), 130.2 (br), 128.2 (d, J = 6.4 Hz), 128.2, 128.0, 126.2, 44.3, 19.2 (d, J = 2.8 Hz); ^{11}B NMR (192 MHz, $CDCl_3$) δ 43.4; ^{31}P NMR (243 MHz, $CDCl_3$) δ – 9.3; IR (ATR): 3050, 2001, 2934, 2850, 1606, 1478, 1433, 1383, 1270, 1256, 1166, 938, 743, 696, 502 cm^{-1}; HRMS (DART) calcd for $C_{25}H_{26}BNP$ ($[M+H]^+$) 382.18904, found 382.18947.

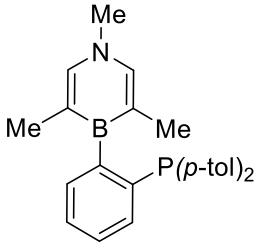

68% yield. ^{1}H NMR (400 MHz, $CDCl_3$) δ 7.34 (ddt, J = 7.9, 6.8, 1.7 Hz, 1H), 7.26 (s, 2H), 7.25 – 7.12 (m, 7H), 7.13 – 7.06 (m, 4H), 3.68 (s, 3H), 2.34 (s, 6H), 1.82 (s, 6H); ^{13}C NMR (101 MHz, $CDCl_3$) δ 140.3, 138.7 (d, J = 3.4 Hz), 137.7, 135.8 (d, J = 11.1 Hz), 133.6 (d, J = 18.7 Hz), 133.0 (d, J = 1.4 Hz), 130.6 (d, J = 15.8 Hz), 130.2 (br), 129.0 (d, J = 6.6 Hz), 128.0 (d, J = 1.2 Hz), 126.2 (d, J = 1.2 Hz), 44.4, 21.4, 19.2 (d, J = 2.7 Hz) (one signal of aromatic carbon attached to boron is not observed); ^{11}B NMR (192 MHz, $CDCl_3$) δ 43.3; ^{31}P NMR (243 MHz, $CDCl_3$) δ –10.9; IR (ATR): 3032, 3011, 2935, 1607,

1496, 1452, 1425, 1269, 1255, 1167, 1091, 1019, 938, 806, 752, 690, 517 cm^{-1}; HRMS (DART) calcd for $C_{27}H_{30}BNP$ ($[M+H]^+$) 410.22034, found 410.22065.

Synthesis of ligand **3.99**

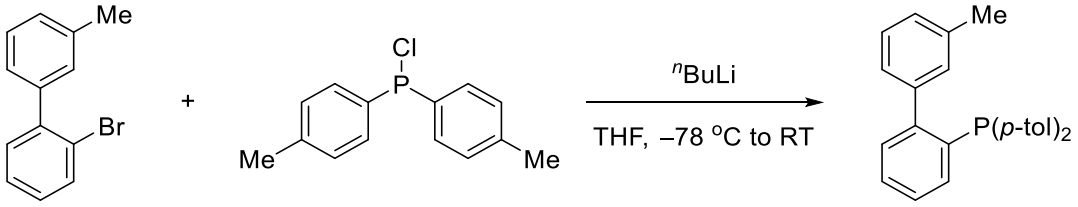

To a 20-mL vial charged with 2-bromo-3'-methyl-1,1'-biphenyl[71](247 mg, 1.00 mmol, 1.00 equiv.) and THF (3 mL) was added *n*BuLi (0.40 mL, 2.5 M in hexanes, 1.0 mmol, 1.0 equiv) at –78°C. The resulting mixture was allowed to stir at the same temperature for 15 minutes, then a THF (1 mL) solution of di-*p*-tolyl phosphine chloride (248 mg, 1.0 mmol, 1.0 equiv.) was added, and the resulting mixture was gradually allowed to warm to room temperature in 2 hours. At the conclusion of reaction, THF was removed *in vacuo*, and the residue was purified via silica gel chromatography using hexanes/EtOAc (50/1) as the eluent to afford a white solid, which was then recrystallized from EtOAc/MeOH at –30°C to provide the pure product (53% yield). ^{1}H NMR (400 MHz, $CDCl_3$) δ 7.40 – 7.22 (m, 4H), 7.20 – 7.06 (m, 10H), 7.00 (d, J = 7.5 Hz, 1H), 6.90 (s, 1H), 2.35 (s, 6H), 2.23 (s, 3H); ^{13}C NMR (101 MHz, $CDCl_3$) δ 148.5, 148.2, 141.8 (d, J = 6.4 Hz), 138.3, 137.0, 136.6 (d, J = 14.4 Hz), 134.7 (d, J = 10.4 Hz), 134.1, 134.0 (d, J = 20.1 Hz), 130.8 (d, J = 3.5 Hz), 130.0 (d, J = 4.9 Hz), 129.3 (d, J = 7.0 Hz), 128.5, 127.9, 127.4 (d, J = 26.4 Hz), 126.8 (d, J = 3.8 Hz), 21.5, 21.4; ^{31}P NMR (162 MHz, $CDCl_3$) δ –14.7; IR (ATR): 3013, 2918, 2862, 1599, 1584, 1496, 1457, 1186, 1091, 1019, 908, 805, 788,

[71] Xu, S.; Chen, R.; Fu, Z.; Zhou, Q.; Zhang, Y.; Wang, J. *ACS Catal.* **2017**, *7*, 1993-1997.

758, 730, 704, 626, 508, 491, 425 cm^{-1}; HRMS (DART) calcd for $C_{27}H_{26}P$ ($[M+H]^+$) 381.17666, found 381.17794.

3.5.2.2. Experimental procedure for synthesizing Pd(0) complexes

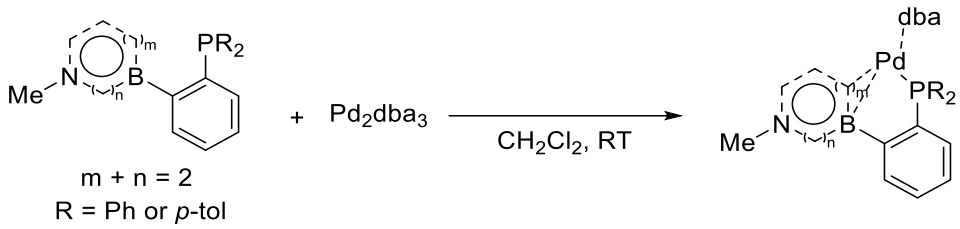

Pd(0) complexes **3.76**, **3.78**, **3.80**, **3.93**, **3.95**, **3.97** and **3.100** were synthesized as follows: In a 4-mL vial charged with Senphos ligand or CC-Senphos (0.020 mmol, 1.0 equiv.) was added Pd_2dba_3 (9.2 mg, 0.010 mmol, 0.50 equiv.) and CH_2Cl_2 (0.5 mL), and the resulting mixture was allowed to stir at room temperature for 14 hours, at which time point the mixture was analyzed by ^{31}P NMR to confirm the full conversion of the starting ligand. If not, an extra portion of Pd_2dba_3 (0.9 mg, 0.001 mmol, 0.05 equiv.) was added[72] and the mixture was allowed to stir at room temperature for 4 hours. At the conclusion of reaction, all volatiles were removed under vacuum, and the resulting residue was used without further purifications. For complexes **3.93**, **3.95** and **3.97**, the corresponded residues were dissolved in MeCN-*d*3 and used in VT-^1H NMR experiment. For complexes **3.76**, **3.78**, **3.80**, suitable crystals for single crystal X-ray diffraction analysis were obtained by recrystallization from pentane/CH_2Cl_2 or pentane/benzene at –30 °C. Due to the conformational dynamics, the ^1H and ^{13}C NMR signals of complexes **3.76**, **3.78**, **3.80**, **3.93**, **3.95**, **3.97** and **3.100** are too broad, especially in the aromatic region, to be identified.

[72] Commercially available Pd_2dba_3 usually vary in the quality, see: Zalesskiy, S. S.; Ananikov, V. P. *Organometallics* **2012**, *31*, 2302-2309. The Pd_2dba_3 in this chapter was purchased from Strem and used as received.

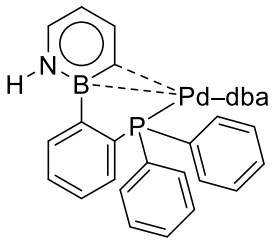

^{11}B NMR (160 MHz, CD_2Cl_2) δ 33.9; ^{31}P NMR (162 MHz, CD_2Cl_2) δ 24.3.

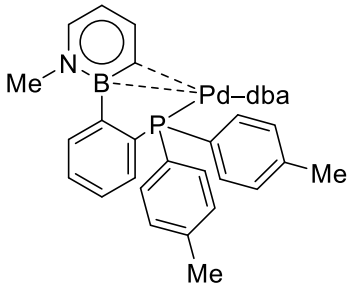

^{1}H NMR (400 MHz, CD_3CN) δ 4.77 (br, s, 1H), 2.63 (br, s, 3H), 2.43 – 2.21 (br, s, 6H); ^{13}C NMR (101 MHz, CD_3CN) δ 142.2 (br), 140.8, 140.1 (br), 134.6 (br), 133.2 (d, J = 14.8 Hz), 132.3 (br), 130.0, 130.0, 129.4 (br), 129.0 (d, J = 5.0 Hz), 127.8 (br), 41.4, 21.4; ^{11}B NMR (160 MHz, CD_3CN) δ 34.7; ^{31}P NMR (162 MHz, CD_3CN) δ 26.0.

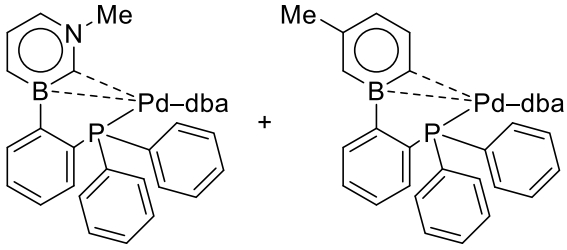

^{1}H NMR (400 MHz, CD_3CN) δ 3.94 (br, s, 3H), 3.17 (br, s, 2H); ^{13}C NMR (101 MHz, CD_3CN) δ 50.1, 48.8; ^{11}B NMR (160 MHz, CD_3CN) δ 24.7; ^{31}P NMR (202 MHz, CD_3CN) δ 30.0 – 28.2 (m).

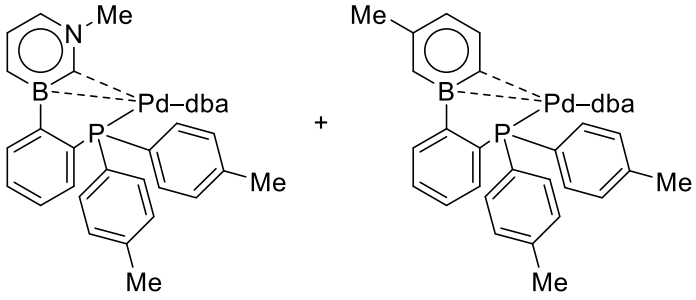

^{1}H NMR (400 MHz, CD_3CN) δ 3.94 (s, 2H), 3.17 (s, 1H), 2.33 (s, 6H); ^{13}C NMR (101 MHz, CD_3CN) δ 21.3; ^{11}B NMR (160 MHz, CD_3CN) δ 24.0; ^{31}P NMR (162 MHz, CD_3CN) δ 30.6 – 26.7 (m).

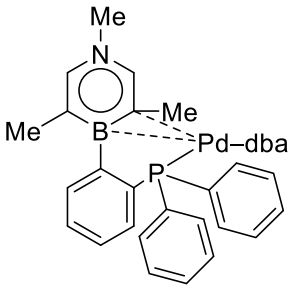

^{1}H NMR (400 MHz, CD_3CN) δ 5.03 (s, 1H), 4.47 (s, 1H), 3.91 (br, s, 3H), 1.46 (br, s, 6H); ^{13}C NMR (101 MHz, CD_3CN) δ 45.6, 20.4; ^{11}B NMR (160 MHz, CD_3CN) δ 32.0; ^{31}P NMR (162 MHz, CD_3CN) δ 28.7.

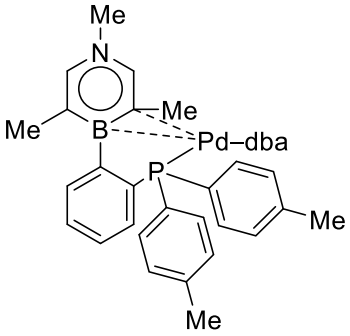

^{1}H NMR (400 MHz, CD_3CN) δ 3.90 (br, s, 3H), 2.31 (br, s, 6H), 1.74 – 1.19 (br, s, 6H); ^{13}C NMR (101 MHz, CD_3CN) δ 45.5, 21.3, 20.4; ^{11}B NMR (160 MHz, CD_3CN) δ 31.5; ^{31}P NMR (162 MHz, CD_3CN) δ 27.7.

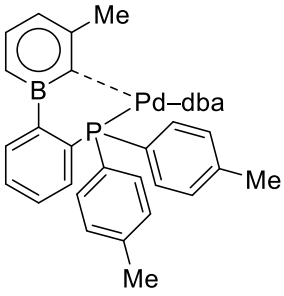

^{1}H NMR (400 MHz, CD_3CN) δ 2.33 (s, 6H), 2.10 (s, 3H); ^{31}P NMR (162 MHz, CD_3CN) δ 27.9.

3.5.2.3. Experimental procedure for synthesizing Pd(II) complexes

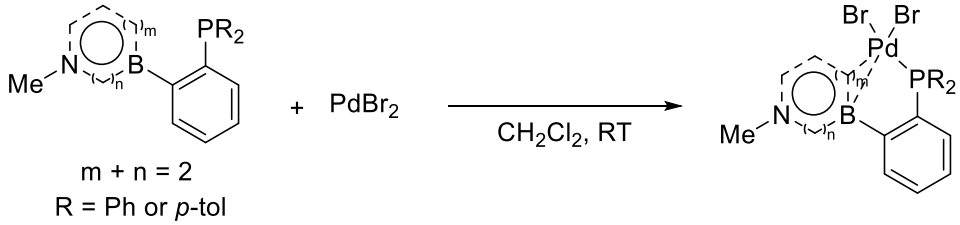

m + n = 2
R = Ph or *p*-tol

Pd(II) complexes **3.77**, **3.79**, **3.81**, **3.94**, **3.96** and **3.98** were synthesized as follows: In a 4-mL vial charged with Senphos ligand (0.020 mmol, 1.0 equiv.) was added $PdBr_2$ (5.4 mg, 0.020 mmol, 1.0 equiv.) or $PdCl_2(MeCN)_2$ (5.3 mg, 0.020 mmol, 1.0 equiv., for complex **3.77** only) and CH_2Cl_2 (0.5 mL), and the resulting mixture was allowed to stir at room temperature for 14 hours. At the conclusion of reaction, all volatiles were removed *in vacuo*, and the residue was used without further purifications. For complexes **3.94**, **3.96** and **3.98**, the corresponded residues were dissolved in MeCN-*d*3 and used in VT-^{1}H NMR experiment. For complexes **3.77**, **3.79**, **3.81**, suitable crystals for single crystal X-ray diffraction analysis were obtained by recrystallization from pentane/CH_2Cl_2 at –30 °C.

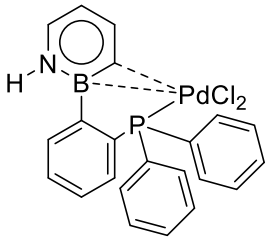

With CH_2Cl_2 (0.3 mL). 68% yield. Due to the very low solubility of the complex in $CDCl_3$, ^{13}C spectrum is not feasible. ^{1}H NMR (400 MHz, $CDCl_3$) δ 10.88 (br, s, 1H), 8.31 (br, s, 2H), 7.84 – 7.39 (m, 12H), 7.33 – 7.20 (m, 1H), 7.07 (t, J = 9.1 Hz, 2H), 5.56 (br, s, 1H); ^{11}B NMR (160 MHz, CD_2Cl_2) δ 31.4; ^{31}P NMR (202 MHz, $CDCl_3$) δ 40.7.

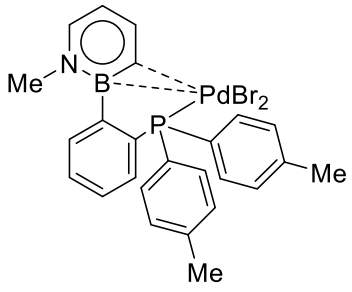

97% yield. Due to conformational dynamics the ^{1}H and ^{13}C NMR signals are broad. ^{1}H NMR (500 MHz, CD_3CN) δ 7.85 (br, s, 1H), 7.77 – 7.60 (m, 3H), 7.52 – 7.45 (m, 4H), 7.43 – 7.24 (m, 4H), 7.17 (d, J = 7.8 Hz, 2H), 6.87 – 6.62 (br, s, 1H), 6.70 – 6.30 (br, s, 1H), 3.44 (br, s, 3H), 2.40 (s, 3H), 2.35 (s, 3H); ^{13}C NMR (126 MHz, CD_3CN) δ 148.9 (br), 143.6, 143.3 (br), 142.8 (br), 136.5(br), 136.1 (br), 135.6 (d, J = 10.2 Hz), 134.4 (d, J = 16.0 Hz), 133.8 (br), 131.4 (br), 130.2 (br), 129.4 (d, J = 12.2 Hz), 129.1 (d, J = 11.3 Hz), 128.4 (br), 127.8 (br), 127.3 (br), 44.0, 21.5, 21.4 (six signals of aromatic carbons are not observed due to dynamics and their

attachments to boron); ^{11}B NMR (160 MHz, CD_3CN) δ 34.3; ^{31}P NMR (202 MHz, CD_3CN) δ 33.9.

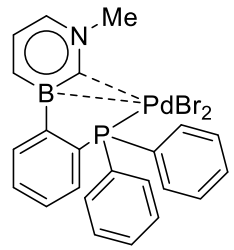

96% yield. ^{1}H NMR (400 MHz, CD_3CN) δ 8.44 (d, *J* = 11.2 Hz, 1H), 8.30 (d, *J* = 5.1 Hz, 1H), 8.02 – 7.37 (m, 13H), 7.30 (t, *J* = 7.6 Hz, 1H), 7.13 (t, *J* = 8.5 Hz, 1H), 6.28 – 6.17 (m, 1H), 3.74 (s, 3H); ^{13}C NMR (151 MHz, CD_3CN) δ 158.4 (br), 145.2, 136.0, 135.6, 135.2, 134.5, 134.4 (d, *J* = 10.3 Hz), 134.3 (d, *J* = 2.6 Hz), 132.8 (d, *J* = 2.9 Hz), 130 (br), 129.0 (d, *J* = 8.0 Hz), 110.5 (br), 50.8. (two signals of aromatic carbons are not observed due to dynamics and their attachments to boron); ^{11}B NMR (160 MHz, CD_3CN) δ 29.3. ^{31}P NMR (162 MHz, CD_3CN) δ 38.2.

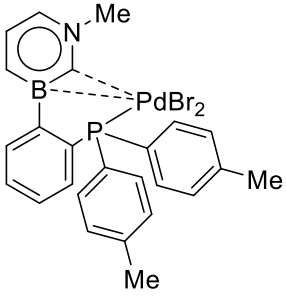

Quant. yield. ^{1}H NMR (600 MHz, CD_3CN) δ 8.40 (d, *J* = 11.2 Hz, 1H), 8.27 (d, *J* = 4.8 Hz, 1H), 8.03 – 7.65 (br, s, 2H), 7.56 (dd, *J* = 11.2, 5.2 Hz, 1H), 7.50 – 7.47 (m, 1H), 7.39 (d, *J* = 7.7 Hz, 1H), 7.45 – 7.21 (br, s, 6H), 7.26 (tdd, *J* = 7.6, 2.7, 1.3 Hz, 1H), 7.11 – 7.07 (m, 1H), 6.19 (s, 1H), 3.72 (s, 3H), 2.38 (s, 6H); ^{13}C NMR (151 MHz, CD_3CN) δ 158.3, 153.7 (br), 145.1, 136.1, 135.9, 135.7, 134.4 (d, *J* = 10.3 Hz), 134.3, 134.1 (d, *J* = 2.7 Hz), 132.6 (d, *J* = 2.6 Hz), 130.3 (br), 128.9 (d, *J* = 7.9 Hz), 110.9, 50.9, 21.5 (one signals of aromatic carbons are not observed due to dynamics and their attachment to boron); ^{11}B NMR (160 MHz, CD_3CN) δ 28.9; ^{31}P NMR (202 MHz, CD_3CN) δ 37.5.

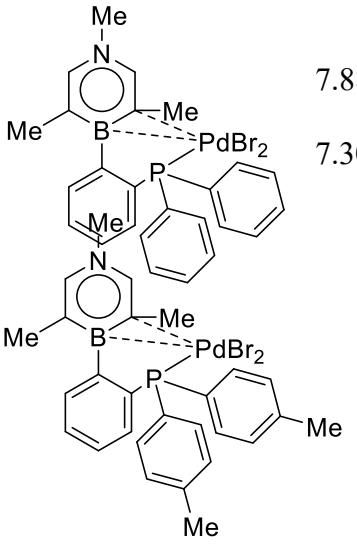

95% yield. ^{1}H NMR (400 MHz, CD_3CN) δ 8.17 (s, 2H), 7.88 – 7.77 (m, 4H), 7.60 – 7.51 (m, 2H), 7.51 – 7.43 (m, 5H), 7.30 (td, *J* = 7.6, 3.2 Hz, 1H), 7.23 (t, *J* = 8.2 Hz, 1H), 7.17 (d, *J* = 7.5 Hz, 1H), 3.98 (s, 3H), 1.88 (s, 6H); ^{13}C NMR (101 MHz, CD_3CN) δ 157.0, 135.2 (d, *J* = 10.1 Hz), 132.6 (d, *J* = 10.5 Hz), 132.3 (br), 131.9 (d, *J* = 22.5 Hz), 129.3 (d, *J* = 11.6 Hz), 128.6 (d, *J* = 8.3 Hz), 47.1, 20.4 (five signals of aromatic carbons are not observed due to dynamics and their attachment to boron); ^{11}B NMR (160 MHz, CD_3CN) δ 34.6; ^{31}P NMR (202 MHz, CD_3CN) δ 35.9.

95% yield. ^{1}H NMR (600 MHz, CD_3CN) δ 8.15 (s, 2H), 7.71 – 7.68 (m, 4H), 7.44 (dt, *J* = 7.6, 4.7 Hz, 1H), 7.30 – 7.29 (m, 5H), 7.22 (t, *J* = 8.3 Hz, 1H), 7.15 (d, *J* = 7.5 Hz, 1H), 3.98 (s, 3H), 2.38 (s, 6H), 1.89 (s, 6H); ^{13}C NMR (151 MHz, CD_3CN) δ 156.9, 151.7 (br), 143.0, 141.4 (br, d, *J* = 50.1 Hz), 135.2 (d, *J* = 10.5 Hz), 132.4 (d, *J* = 12.7 Hz), 131.9 (d, *J* = 22.6 Hz), 129.9 (d, *J* = 11.9 Hz), 129.6 (br), 128.5 (d, *J* = 7.6 Hz), 47.1, 21.5, 20.4 (two signals of aromatic carbons are not observed due to dynamics and their attachment to boron); ^{11}B NMR (160 MHz, CD_3CN) δ 34.8; ^{31}P NMR (202 MHz, CD_3CN) δ 35.4.

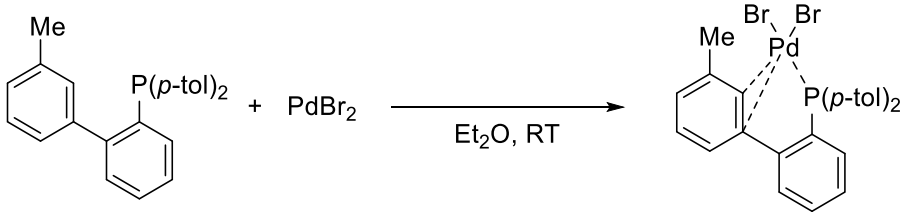

In a 4-mL vial charged with CC-Senphos ligand **3.99** (3.8 mg, 0.010 mmol, 1.0 equiv.) was added $PdBr_2$ (2.7 mg, 0.010 mmol, 1.0 equiv.) and Et_2O (0.4 mL), and the resulting mixture was allowed to stir at room temperature for 14 hours. At the conclusion

of reaction, all volatiles were removed *in vacuo*, and the residue was used without further purifications (83% yield). ^{1}H NMR (600 MHz, $CDCl_3$) δ 7.82 (d, *J* = 7.5 Hz, 1H), 7.60 (dt, *J* = 7.8, 5.4 Hz, 4H), 7.37 (q, *J* = 6.3 Hz, 1H), 7.30 (t, *J* = 7.4 Hz, 1H), 7.18 (t, *J* = 7.7 Hz, 1H), 7.12 – 6.98 (m, 7H), 6.21 (s, 1H), 2.38 (s, 6H), 2.08 (s, 3H); ^{13}C NMR (151 MHz, $CDCl_3$) δ 146.0 (t, *J* = 5.3 Hz), 141.8, 140.2, 137.1, 136.2 (t, *J* = 6.4 Hz), 133.8 (t, *J* = 4.5 Hz), 132.9 (t, *J* = 24.9 Hz), 131.9 (t, *J* = 3.9 Hz), 130.4, 129.6, 128.6 (t, *J* = 5.5 Hz), 127.4 (d, *J* = 6.8 Hz), 127.3, 127.1, 126.9, 125.8 (t, *J* = 4.6 Hz), 21.6, 21.5; ^{31}P NMR (243 MHz, $CDCl_3$) δ 21.7.

3.5.2.4. Experimental procedure for Table 3.8

To a 4-mL vial charged with enyne **3.102** (0.100 mmol, 19.8 mg, 1.00 equiv.) and catalyst solution (Pd_2dba_3/Senphos, 0.05 M in CH_2Cl_2, 0.08 mL, 0.004 mmol, 4 mol%) was put under high vacuum for 15 minutes, and then trimethoxybenzene (internal standard, 1 mg) in MeCN (0.08 mL) was added along with HBCat (18 mg, 0.15 mmol, 1.5 equiv.). And the resulting mixture was allowed to stir for 6 hours at room temperature. Then, a pinacol solution (1.20 mmol, 142 mg, 12.0 equiv. in 0.5 mL CH_2Cl_2) was added and the new mixture was allowed to stir for another 12 hours. At the conclusion of reaction, the crude mixture was passed through a silica gel plug using hexanes/EtOAc (5/1) as the eluent, and the product yield and *trans:cis* ratio were obtained through ^{1}H NMR against the internal standard.

Entry 1: The general procedure was followed with Pd(0)/Senphos **3.104** complex solution. ^{1}H NMR analysis indicated the product yield is 74% with a *trans:cis* ratio of 78:22.

Entry 2: The general procedure was followed with Pd(0)/Senphos **3.74** complex solution. ^{1}H NMR analysis indicated the product yield is 53% with a *trans:cis* ratio of 57:43.

Entry 3: The general procedure was followed with Pd(0)/Senphos **3.75** complex solution. ^{1}H NMR analysis indicated the product yield is 80% with a *trans:cis* ratio of 82:18.

Entry 4: With hexamethylbenzene as the internal standard. The general procedure was followed with Pd(0)/Senphos **3.105** complex solution. ^{1}H NMR analysis indicated the product yield is 71% with a *trans:cis* ratio of 82:18.

Entry 5: The general procedure was followed with Pd(0)/CC-Senphos **3.99** complex solution. ^{1}H NMR analysis indicated the product yield is 54% with a *trans:cis* ratio of 68:32.

3.5.3. X-ray crystallographic data

Crystal data and structure refinement for complex **3.76**.

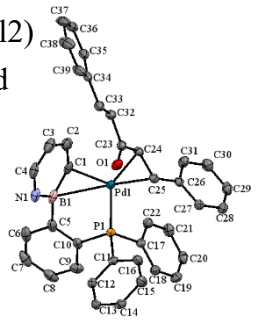

Identification code	C39H33BNOPPd(CH2Cl2)	
Empirical formula	C40 H35 B Cl2 N O P Pd	
Formula weight	764.77	
Temperature	100(2) K	
Wavelength	1.54178 Å	
Crystal system	Triclinic	
Space group	P-1	
Unit cell dimensions	a = 9.8969(3) Å	α = 115.5110(10)°.
	b = 14.1026(5) Å	β = 102.2530(10)°.
	c = 15.2451(5) Å	γ = 98.7000(10)°.
Volume	1804.16(10) Å^3	
Z	2	
Density (calculated)	1.408 Mg/m^3	
Absorption coefficient	6.174 mm^{-1}	
F(000)	780	
Crystal size	0.320 x 0.260 x 0.060 mm^3	
Theta range for data collection	3.380 to 66.810°.	
Index ranges	-11<=h<=11, -16<=k<=16, -18<=l<=18	
Reflections collected	21077	
Independent reflections	6335 [R(int) = 0.0313]	
Completeness to theta = 66.810°	99.0 %	
Absorption correction	Semi-empirical from equivalents	
Max. and min. transmission	0.7528 and 0.5905	
Refinement method	Full-matrix least-squares on F^2	
Data / restraints / parameters	6335 / 4 / 434	
Goodness-of-fit on F^2	1.035	
Final R indices [I>2sigma(I)]	R1 = 0.0431, wR2 = 0.1103	
R indices (all data)	R1 = 0.0444, wR2 = 0.1114	
Extinction coefficient	na	
Largest diff. peak and hole	2.060 and -1.558 e.Å^{-3}	

Crystal data and structure refinement for complex **3.77**.

Identification code	C22H19BCl2NPPd(CH2Cl2)
Empirical formula	C23 H21 B Cl4 N P Pd
Formula weight	601.39
Temperature	100(2) K
Wavelength	0.71073 Å
Crystal system	Monoclinic
Space group	$P2_1/c$
Unit cell dimensions	a = 10.889(2) Å α = 90°. b = 19.133(4) Å β = 100.678(3)°. c = 11.607(2) Å γ = 90°.
Volume	2376.2(8) $Å^3$
Z	4
Density (calculated)	1.681 Mg/m^3
Absorption coefficient	1.311 mm^{-1}
F(000)	1200
Crystal size	0.250 x 0.180 x 0.070 mm^3
Theta range for data collection	1.903 to 28.299°.
Index ranges	-14<=h<=14, -25<=k<=25, -15<=l<=15
Reflections collected	35058
Independent reflections	5897 [R(int) = 0.0385]
Completeness to theta = 25.242°	100.0 %
Absorption correction	Semi-empirical from equivalents
Max. and min. transmission	0.7457 and 0.6740
Refinement method	Full-matrix least-squares on F^2
Data / restraints / parameters	5897 / 0 / 283
Goodness-of-fit on F^2	1.038
Final R indices [I>2sigma(I)]	R1 = 0.0264, wR2 = 0.0581
R indices (all data)	R1 = 0.0365, wR2 = 0.0621
Extinction coefficient	n/a
Largest diff. peak and hole	0.821 and -0.507 $e.Å^{-3}$

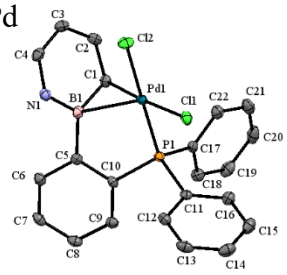

Crystal data and structure refinement for complex **3.78**.

Identification code	C40H35BNOPPd(C6H6)
Empirical formula	C46 H41 B N O P Pd
Formula weight	771.98
Temperature	100(2) K
Wavelength	1.54178 Å
Crystal system	Monoclinic
Space group	$P2_1/n$
Unit cell dimensions	a = 15.1440(5) Å α = 90°. b = 11.9285(4) Å β = 92.8867(10)°. c = 20.6366(7) Å γ = 90°.
Volume	3723.2(2) $Å^3$
Z	4
Density (calculated)	1.377 Mg/m^3
Absorption coefficient	4.701 mm^{-1}
F(000)	1592
Crystal size	0.320 x 0.200 x 0.160 mm^3
Theta range for data collection	3.536 to 66.630°.
Index ranges	-15<=h<=18, -14<=k<=14, -24<=l<=24
Reflections collected	33278
Independent reflections	6557 [R(int) = 0.0267]
Completeness to theta = 66.630°	99.8 %
Absorption correction	Semi-empirical from equivalents
Max. and min. transmission	0.7528 and 0.5980
Refinement method	Full-matrix least-squares on F^2
Data / restraints / parameters	6557 / 93 / 520
Goodness-of-fit on F^2	1.144
Final R indices [I>2sigma(I)]	R1 = 0.0266, wR2 = 0.0636
R indices (all data)	R1 = 0.0271, wR2 = 0.0639
Extinction coefficient	n/a
Largest diff. peak and hole	0.397 and -0.327 e.$Å^{-3}$

Crystal data and structure refinement for complex **3.79**.

Identification code	C23H21BBr2NPPd(CH2Cl2)
Empirical formula	C24 H23 B Br2 Cl2 N P Pd
Formula weight	704.33
Temperature	100(2) K
Wavelength	0.71073 Å
Crystal system	Triclinic
Space group	P-1
Unit cell dimensions	a = 9.0690(12) Å α = 88.992(3)°. b = 14.9993(18) Å β = 86.778(3)°. c = 19.563(3) Å γ = 75.831(4)°.
Volume	2576.1(6) Å^3
Z	4
Density (calculated)	1.816 Mg/m^3
Absorption coefficient	4.106 mm^{-1}
F(000)	1376
Crystal size	0.320 x 0.240 x 0.160 mm^3
Theta range for data collection	1.042 to 28.368°.
Index ranges	-12<=h<=12, -19<=k<=20, 0<=l<=26
Reflections collected	13641
Independent reflections	13641 [R(int) = ?]
Completeness to theta = 25.242°	97.5 %
Absorption correction	Semi-empirical from equivalents
Max. and min. transmission	0.4311 and 0.2567
Refinement method	Full-matrix least-squares on F^2
Data / restraints / parameters	13641 / 554 / 581
Goodness-of-fit on F^2	1.036
Final R indices [I>2sigma(I)]	R1 = 0.0516, wR2 = 0.1324
R indices (all data)	R1 = 0.0662, wR2 = 0.1432
Extinction coefficient	n/a
Largest diff. peak and hole	2.521 and -1.535 e.Å^{-3}

Crystal data and structure refinement for complex **3.80**.

Identification code	C42H39BNOPPd
Empirical formula	C42 H39 B N O P Pd
Formula weight	721.92
Temperature	100(2) K
Wavelength	1.54178 Å
Crystal system	Triclinic
Space group	P-1
Unit cell dimensions	a = 10.6537(7) Å α = 73.924(4)°. b = 17.4329(11) Å β = 76.945(3)°. c = 20.1210(15) Å γ = 88.247(3)°.
Volume	3496.0(4) Å^3
Z	4
Density (calculated)	1.372 Mg/m^3
Absorption coefficient	4.966 mm^{-1}
F(000)	1488
Crystal size	0.420 x 0.160 x 0.120 mm^3
Theta range for data collection	2.346 to 66.777°.
Index ranges	-12<=h<=12, -20<=k<=20, -23<=l<=19
Reflections collected	12309
Independent reflections	12309 [R(int) = 0.0742]
Completeness to theta = 66.777°	99.3 %
Absorption correction	Semi-empirical from equivalents
Max. and min. transmission	0.7528 and 0.4919
Refinement method	Full-matrix least-squares on F^2
Data / restraints / parameters	12309 / 0 / 853
Goodness-of-fit on F^2	1.045
Final R indices [I>2sigma(I)]	R1 = 0.0576, wR2 = 0.1690
R indices (all data)	R1 = 0.0668, wR2 = 0.1748
Extinction coefficient	n/a
Largest diff. peak and hole	1.233 and -0.714 e.Å^{-3}

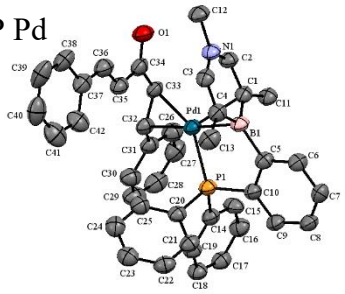

Crystal data and structure refinement for complex **3.81**.

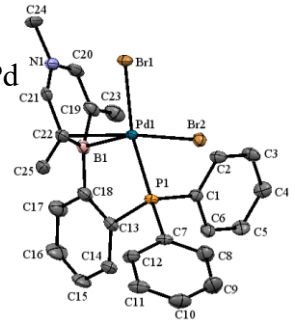

Identification code	C25H25BBr2NPPd
Empirical formula	C25 H25 B Br2 N P Pd
Formula weight	647.46
Temperature	100(2) K
Wavelength	1.54178 Å
Crystal system	Orthorhombic
Space group	Fdd2
Unit cell dimensions	a = 33.533(2) Å α = 90°. b = 35.484(2) Å β = 90°. c = 8.5203(5) Å γ = 90°.
Volume	10138.1(11) $Å^3$
Z	16
Density (calculated)	1.697 Mg/m^3
Absorption coefficient	10.283 mm^{-1}
F(000)	5088
Crystal size	0.480 x 0.220 x 0.130 mm^3
Theta range for data collection	3.627 to 66.914°.
Index ranges	-39<=h<=39, -34<=k<=42, -10<=l<=10
Reflections collected	29678
Independent reflections	4458 [R(int) = 0.0415]
Completeness to theta = 66.914°	99.5 %
Absorption correction	Semi-empirical from equivalents
Max. and min. transmission	0.7528 and 0.4050
Refinement method	Full-matrix least-squares on F^2
Data / restraints / parameters	4458 / 1 / 283
Goodness-of-fit on F^2	1.082
Final R indices [I>2sigma(I)]	R1 = 0.0204, wR2 = 0.0527
R indices (all data)	R1 = 0.0206, wR2 = 0.0527
Absolute structure parameter	0.012(3)
Extinction coefficient	n/a
Largest diff. peak and hole	0.999 and -0.397 $e.Å^{-3}$

3.5.4. NMR Spectra of New Compounds

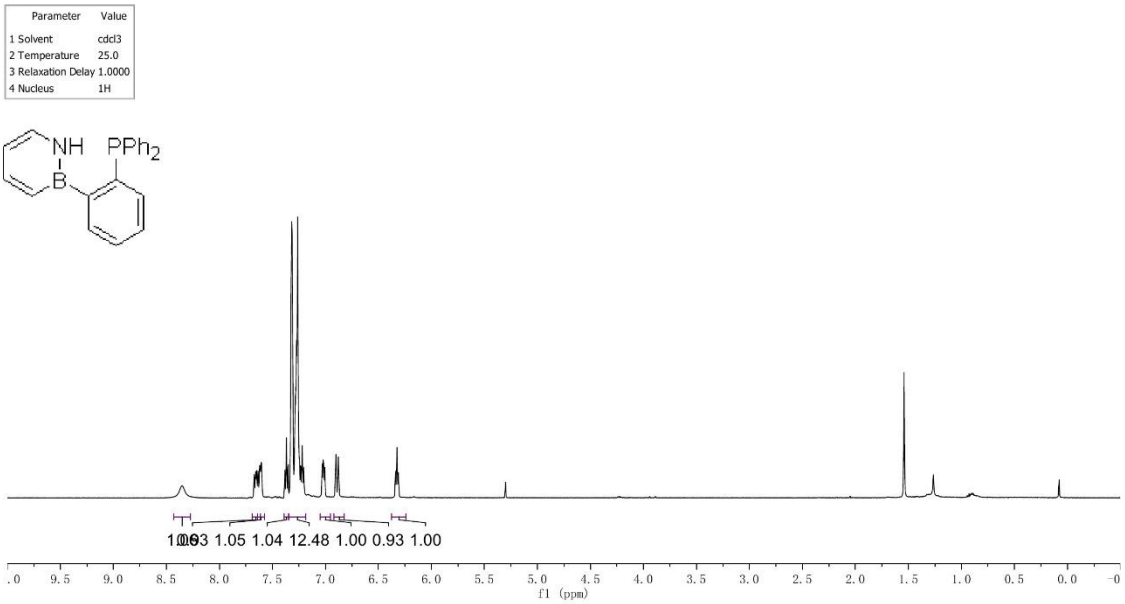

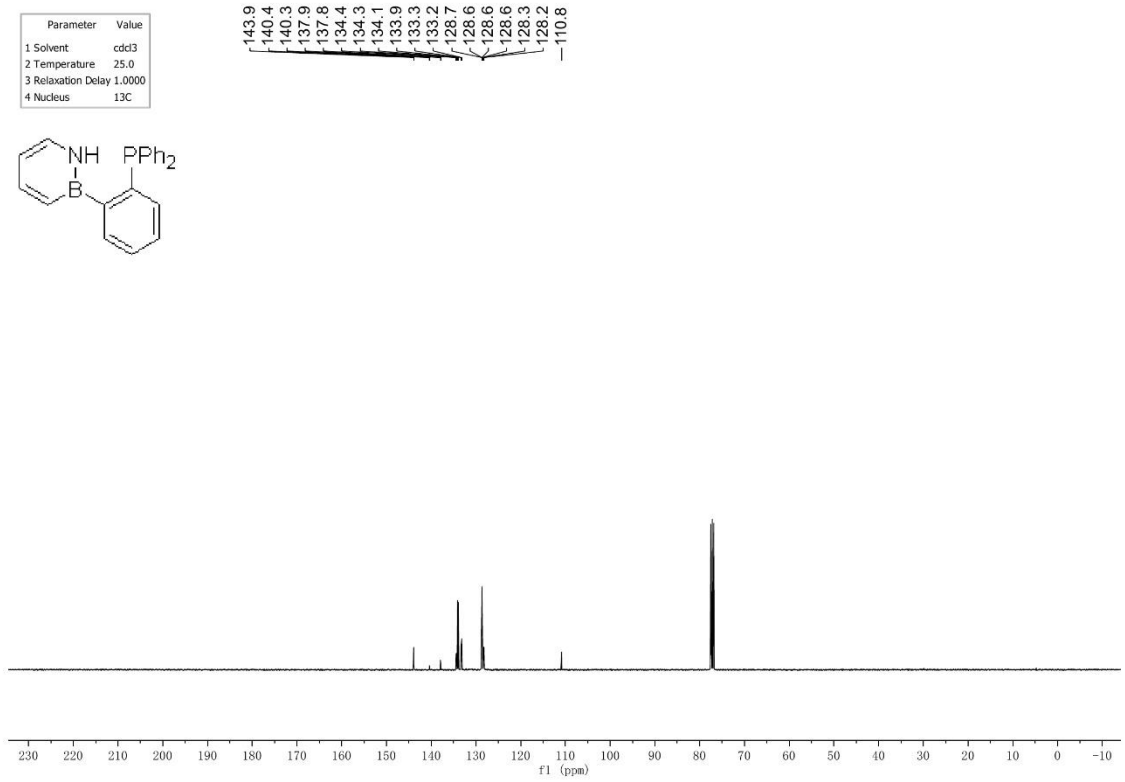

Parameter	Value
1 Solvent	cdcl3
2 Temperature	25.0
3 Relaxation Delay	0.0100
4 Nucleus	11B

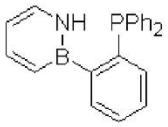

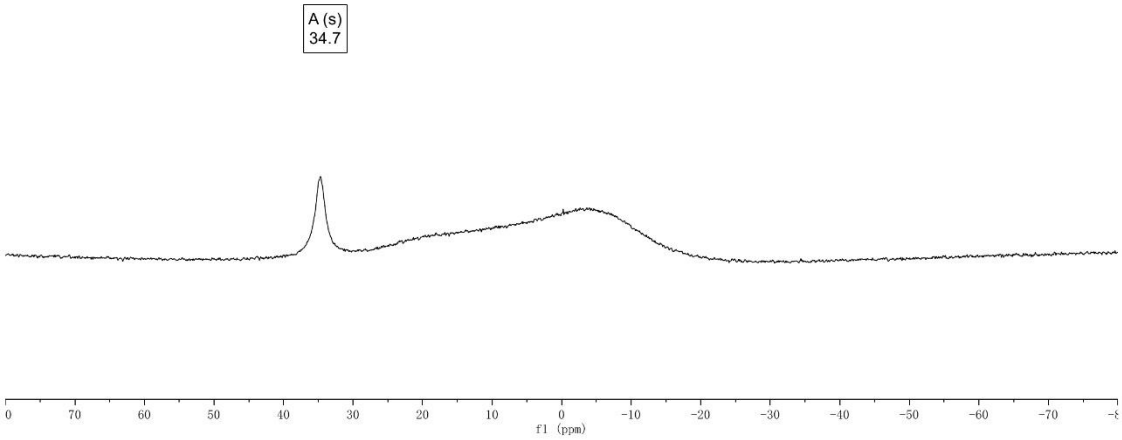

Parameter	Value
1 Solvent	cdcl3
2 Temperature	25.0
3 Relaxation Delay	1.0000
4 Nucleus	31P

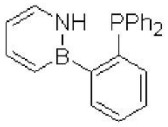

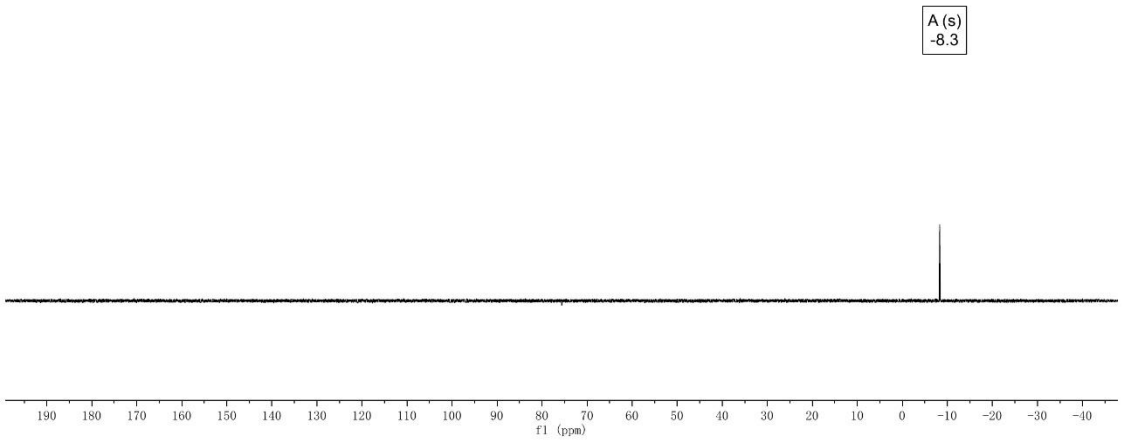

Parameter	Value
1 Solvent	cdcl3
2 Temperature	25.0
3 Relaxation Delay	10.0000
4 Nucleus	1H

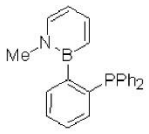

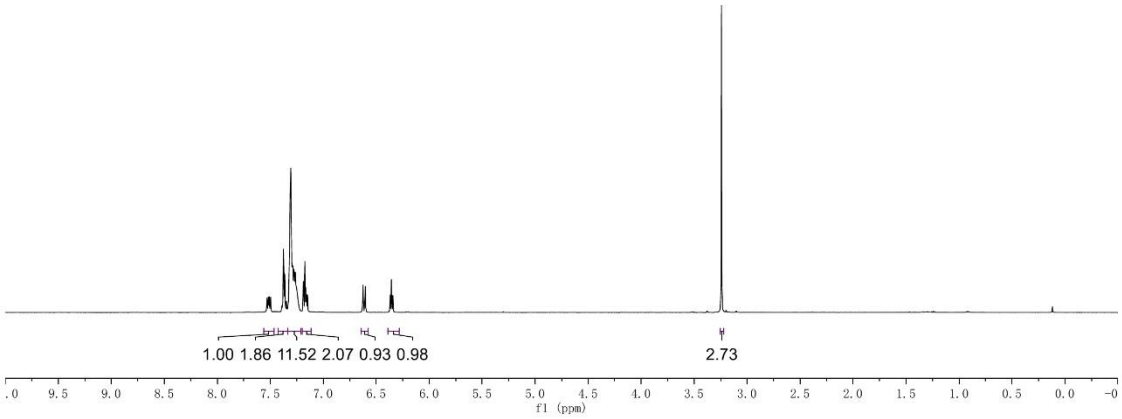

Parameter	Value
1 Solvent	cdcl3
2 Temperature	25.0
3 Relaxation Delay	1.0000
4 Nucleus	13C

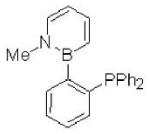

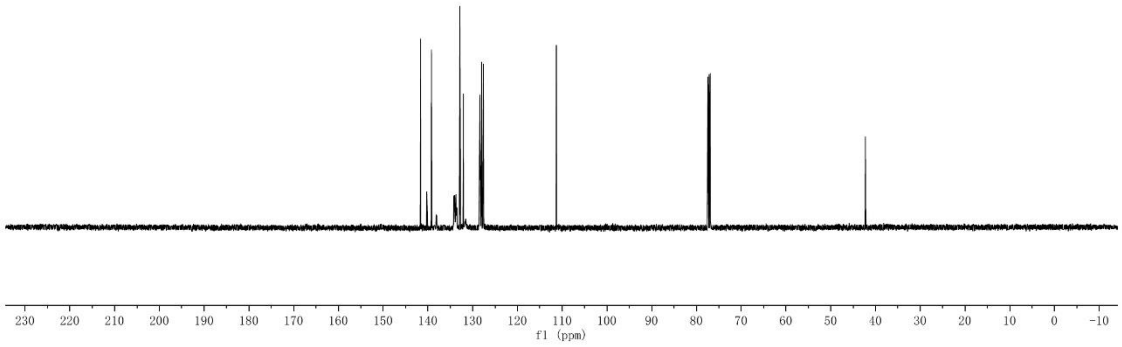

Parameter	Value
1 Solvent	cdcl3
2 Temperature	25.0
3 Relaxation Delay	0.0100
4 Nucleus	11B

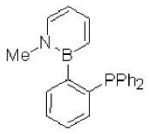

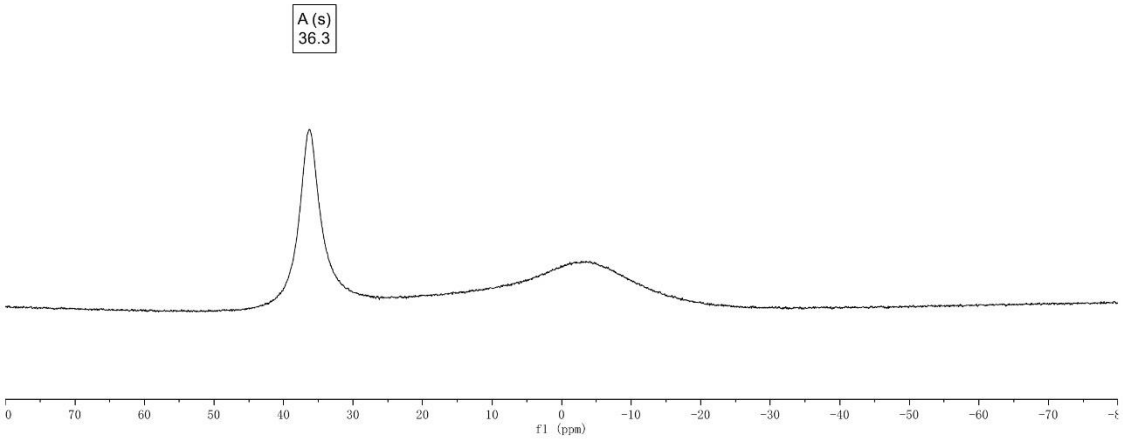

Parameter	Value
1 Solvent	cdcl3
2 Temperature	25.0
3 Relaxation Delay	1.0000
4 Nucleus	31P

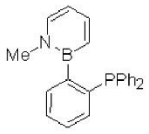

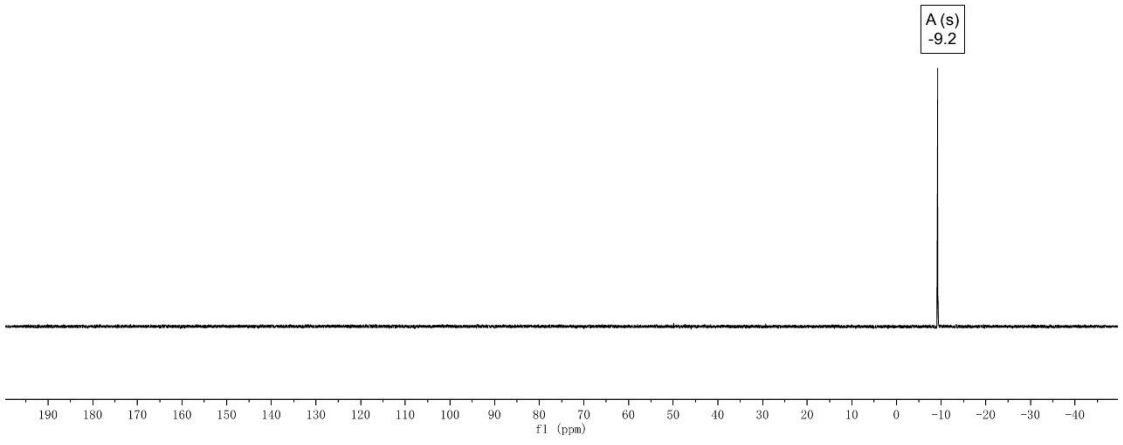

Parameter	Value
1 Solvent	cdcl3
2 Temperature	25.0
3 Relaxation Delay	10.0000
4 Nucleus	1H

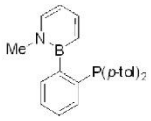

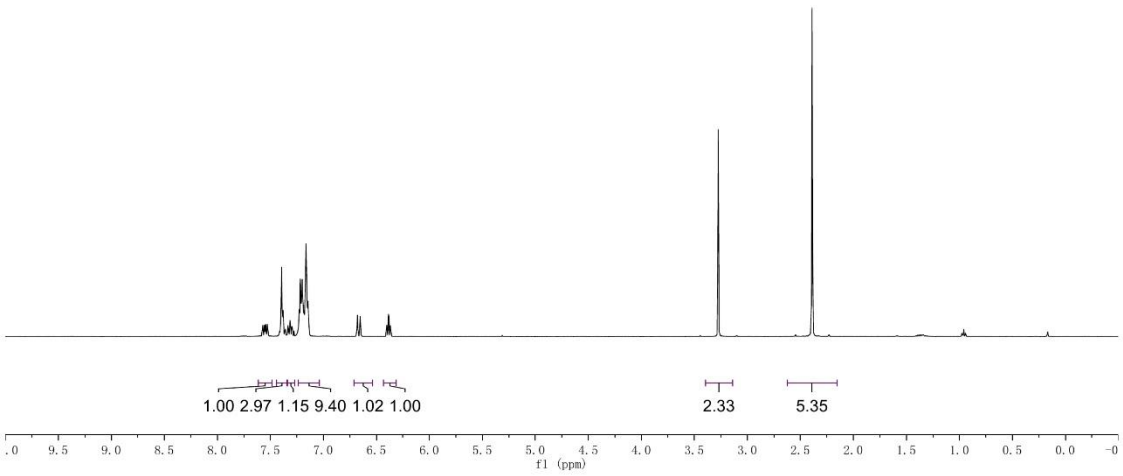

Parameter	Value
1 Solvent	cdcl3
2 Temperature	25.0
3 Relaxation Delay	1.0000
4 Nucleus	13C

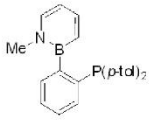

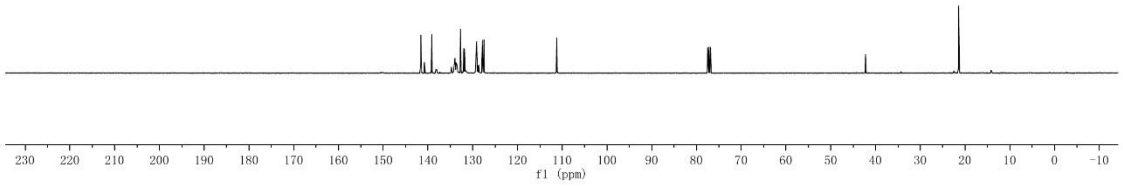

Parameter	Value
1 Solvent	cdcl3
2 Temperature	25.0
3 Relaxation Delay	0.0100
4 Nucleus	11B

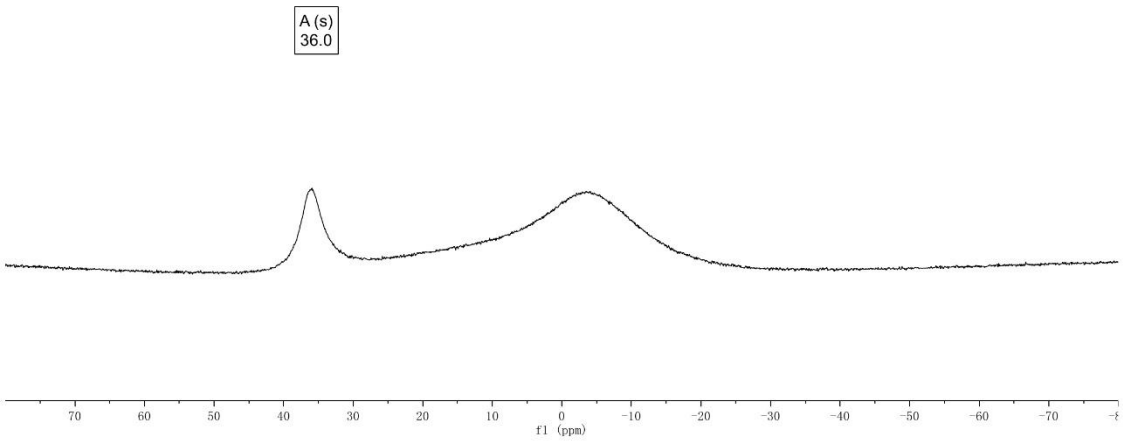

Parameter	Value
1 Solvent	cdcl3
2 Temperature	25.0
3 Relaxation Delay	1.0000
4 Nucleus	31P

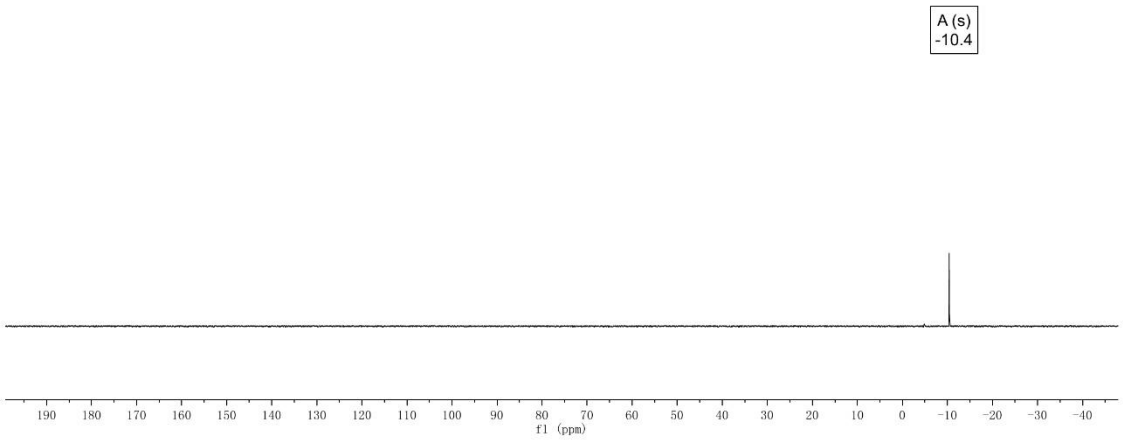

Parameter	Value
1 Solvent	cd2cl2
2 Temperature	25.0
3 Relaxation Delay	5.0000
4 Nucleus	1H

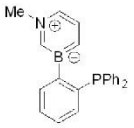

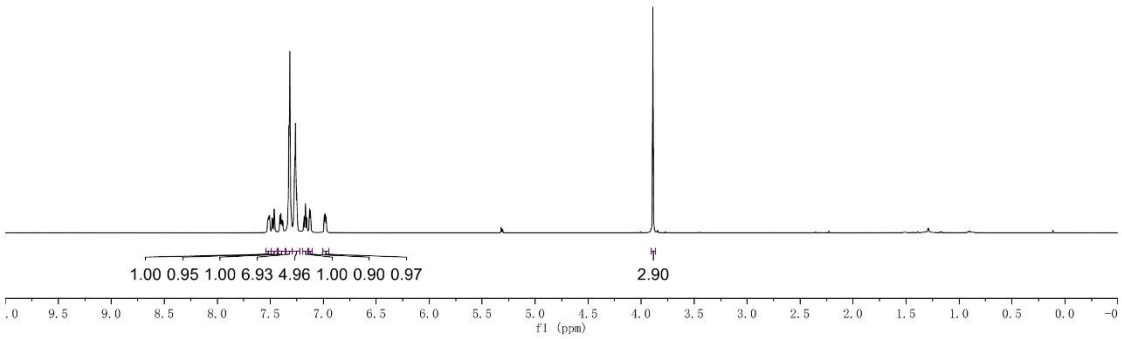

Parameter	Value
1 Solvent	cd2cl2
2 Temperature	25.0
3 Relaxation Delay	1.0000
4 Nucleus	13C

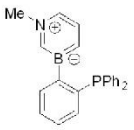

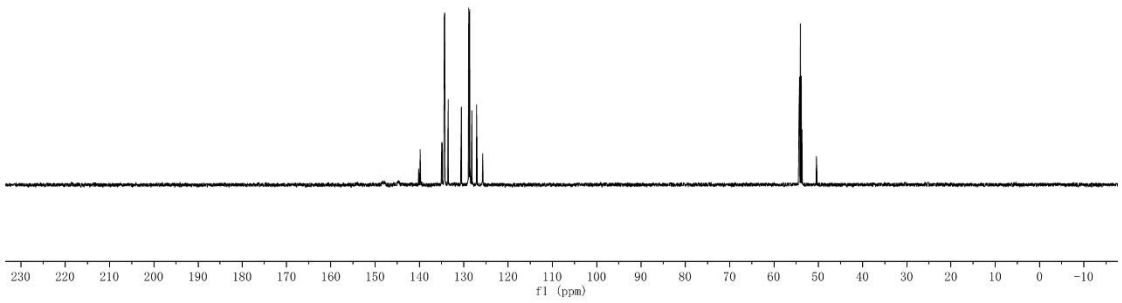

Parameter	Value
1 Solvent	cd2cl2
2 Temperature	25.0
3 Relaxation Delay	0.0100
4 Nucleus	11B

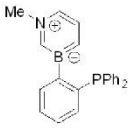

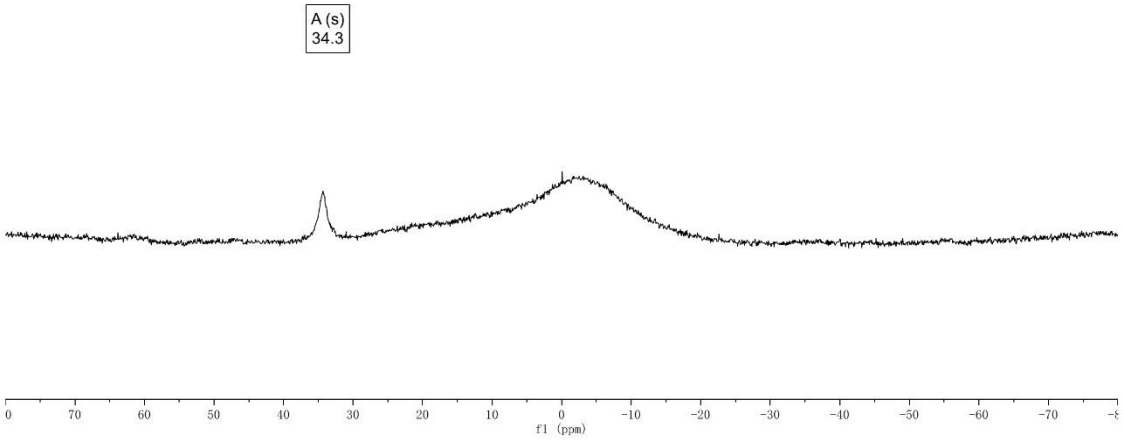

Parameter	Value
1 Solvent	cd2cl2
2 Temperature	25.0
3 Relaxation Delay	1.0000
4 Nucleus	31P

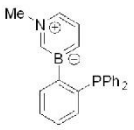

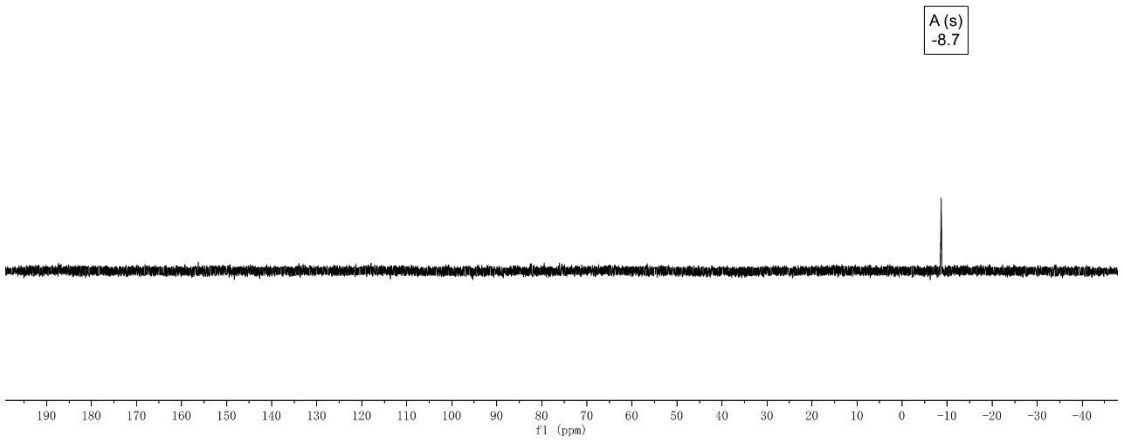

Parameter	Value
1 Solvent	cdcl3
2 Temperature	25.0
3 Relaxation Delay	10.0000
4 Nucleus	1H

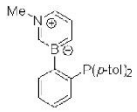

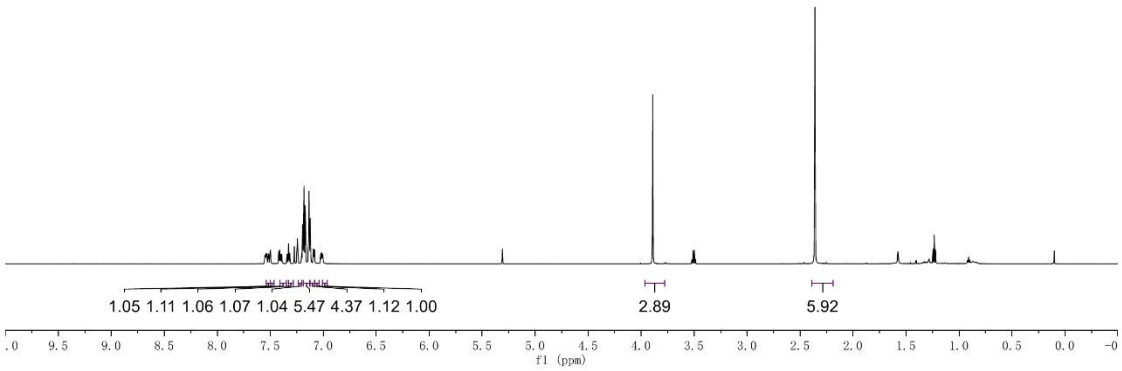

Parameter	Value
1 Solvent	cdcl3
2 Temperature	25.0
3 Relaxation Delay	1.0000
4 Nucleus	13C

153.1
147.6
144.6
140.2
140.1
137.9
136.0
135.9
134.4
134.4
134.1
134.0
133.0
130.4
129.2
127.5
126.7
125.1
49.9
21.4

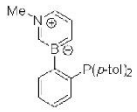

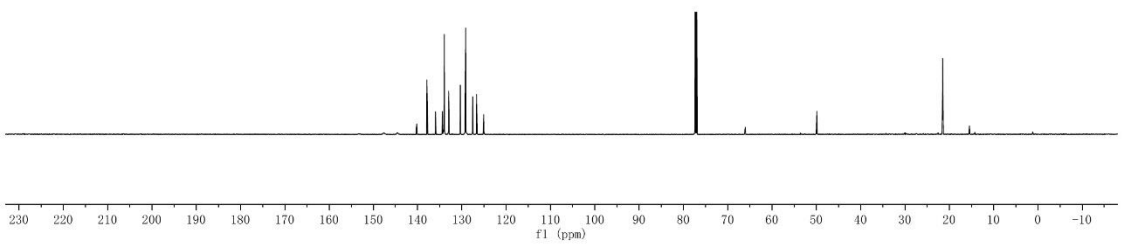

Parameter	Value
1 Solvent	cdcl3
2 Temperature	25.0
3 Relaxation Delay	0.0100
4 Nucleus	11B

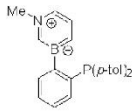

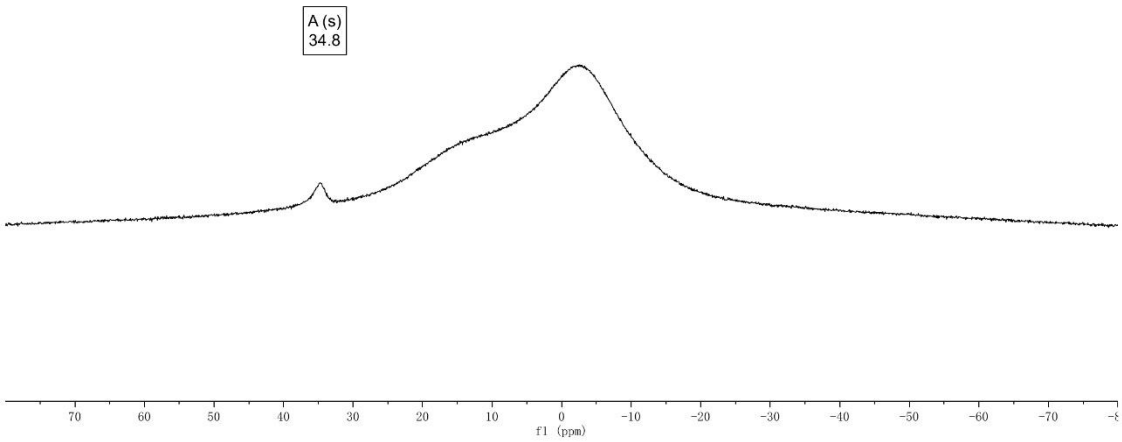

Parameter	Value
1 Solvent	cdcl3
2 Temperature	25.0
3 Relaxation Delay	1.0000
4 Nucleus	31P

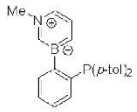

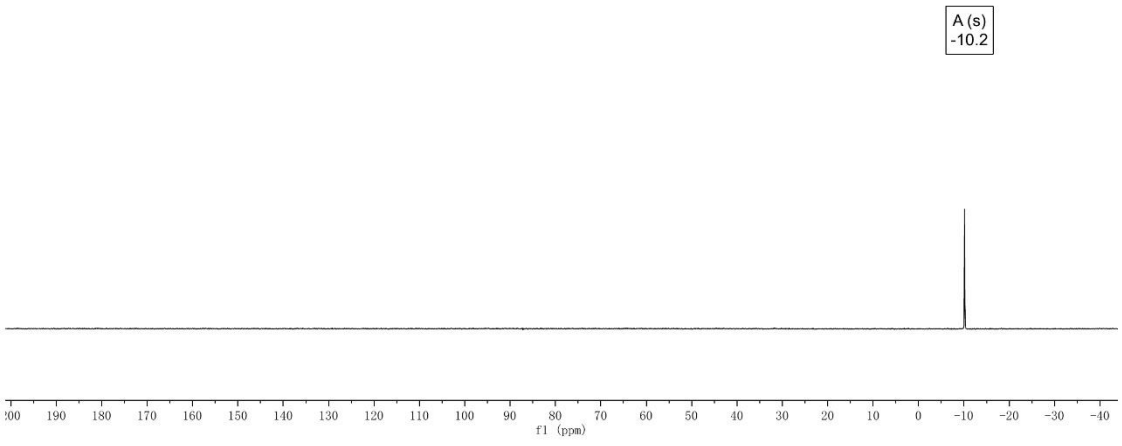

Parameter	Value
1 Solvent	cdcl3
2 Temperature	25.0
3 Relaxation Delay	10.0000
4 Nucleus	1H

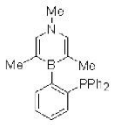

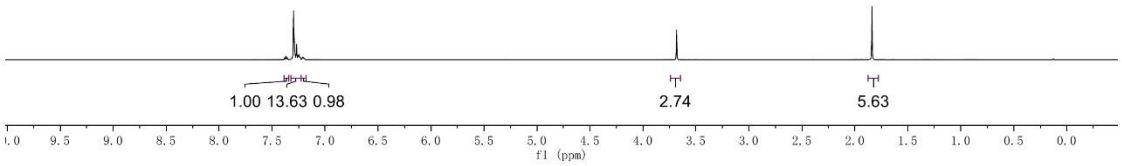

Parameter	Value
1 Solvent	cdcl3
2 Temperature	25.0
3 Relaxation Delay	1.0000
4 Nucleus	13C

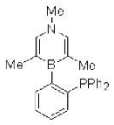

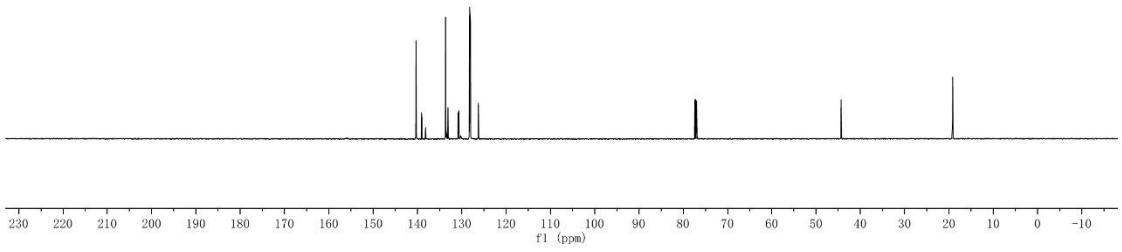

Parameter	Value
1 Solvent	cdcl3
2 Temperature	25.0
3 Relaxation Delay	0.0100
4 Nucleus	11B

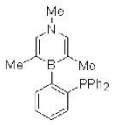

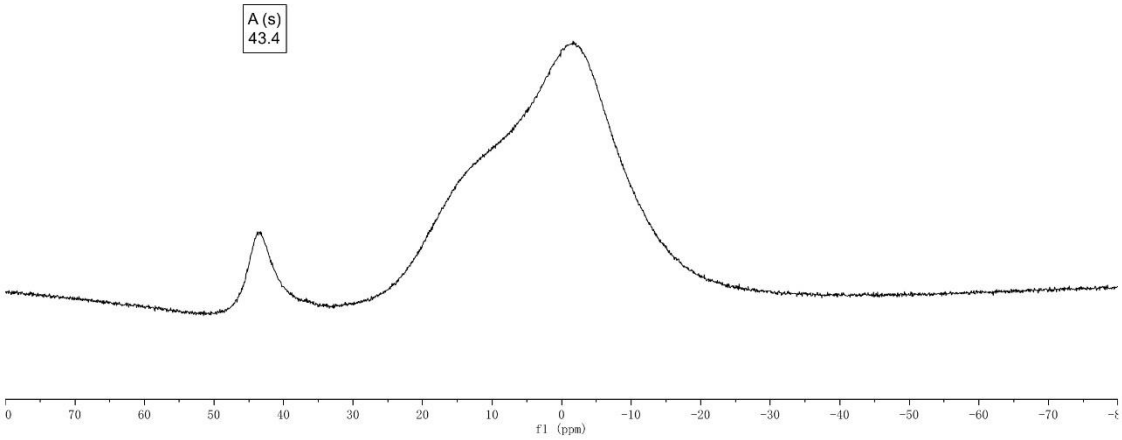

Parameter	Value
1 Solvent	cdcl3
2 Temperature	25.0
3 Relaxation Delay	1.0000
4 Nucleus	31P

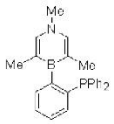

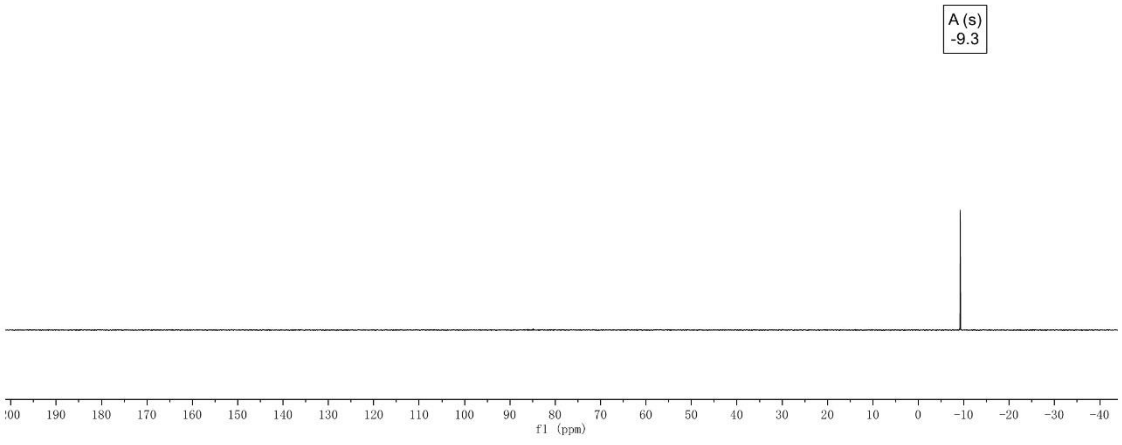

Parameter	Value
1 Solvent	cdcl3
2 Temperature	25.0
3 Relaxation Delay	10.0000
4 Nucleus	1H

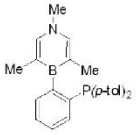

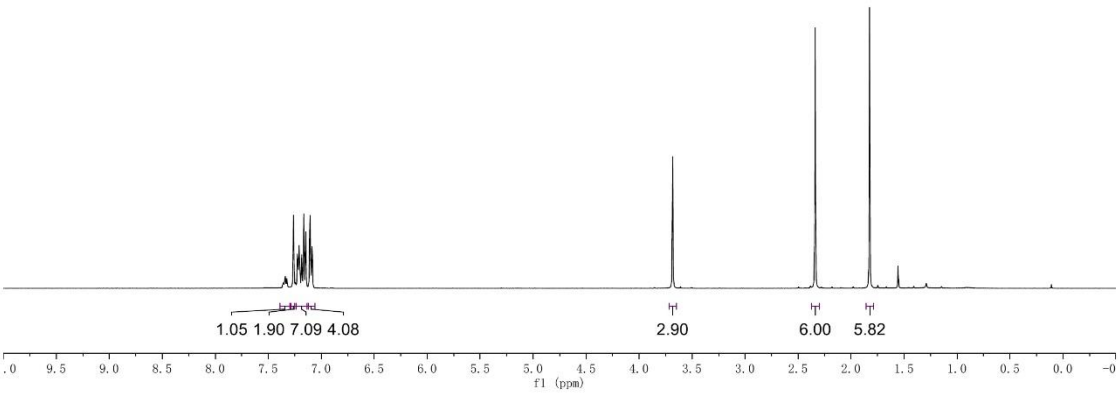

Parameter	Value
1 Solvent	cdcl3
2 Temperature	25.0
3 Relaxation Delay	1.0000
4 Nucleus	13C

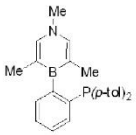

Parameter	Value
1 Solvent	cdcl3
2 Temperature	25.0
3 Relaxation Delay	0.0100
4 Nucleus	11B

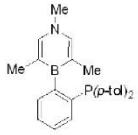

A (s)
43.3

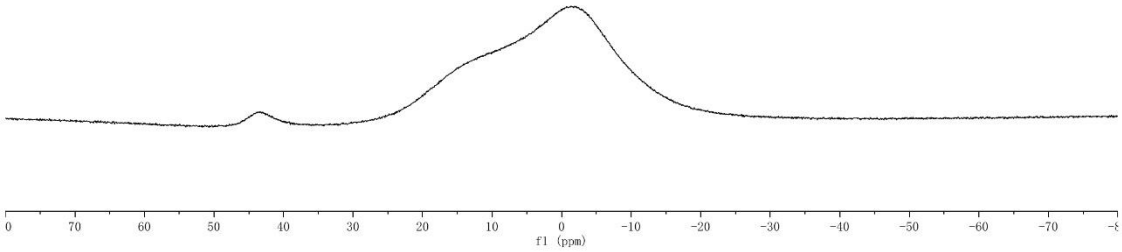

Parameter	Value
1 Solvent	cdcl3
2 Temperature	25.0
3 Relaxation Delay	1.0000
4 Nucleus	31P

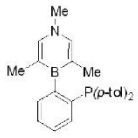

A (s)
-10.9

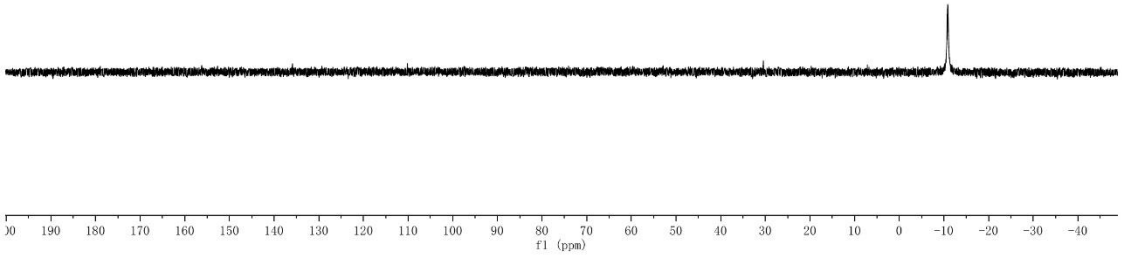

Parameter	Value
1 Solvent	cdcl3
2 Temperature	25.0
3 Relaxation Delay	10.0000
4 Nucleus	1H

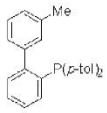

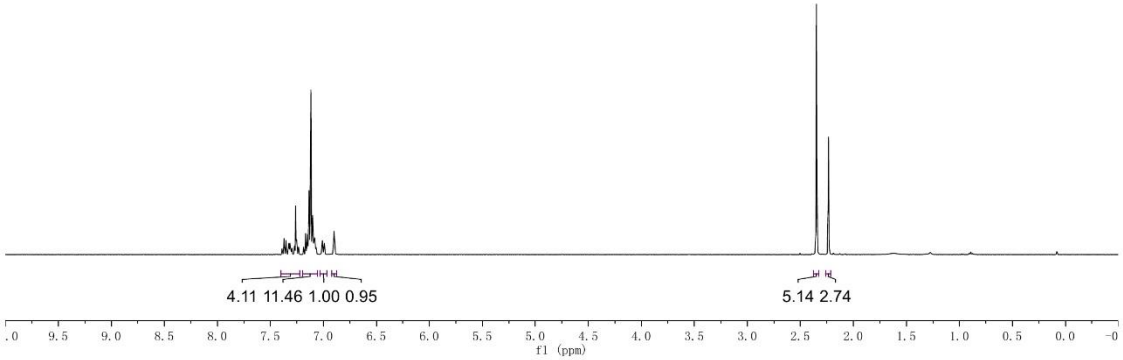

Parameter	Value
1 Solvent	cdcl3
2 Temperature	25.0
3 Relaxation Delay	1.0000
4 Nucleus	13C

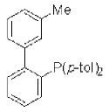

Parameter	Value
1 Solvent	cdcl3
2 Temperature	25.0
3 Relaxation Delay	1.0000
4 Nucleus	31P

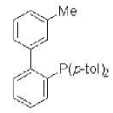

A (s)
-14.72

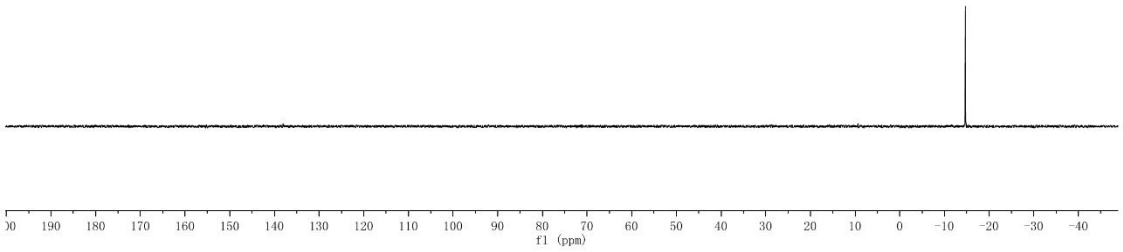

Parameter	Value
1 Solvent	cd2cl2
2 Temperature	25.0
3 Relaxation Delay	10.0000
4 Nucleus	1H

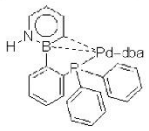

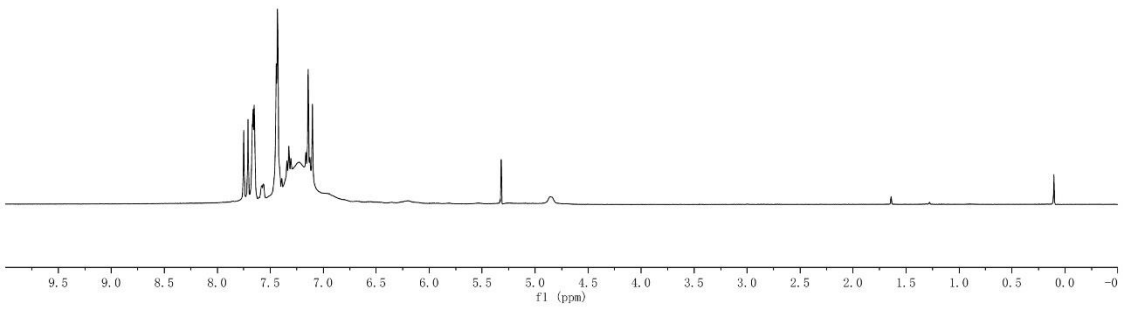

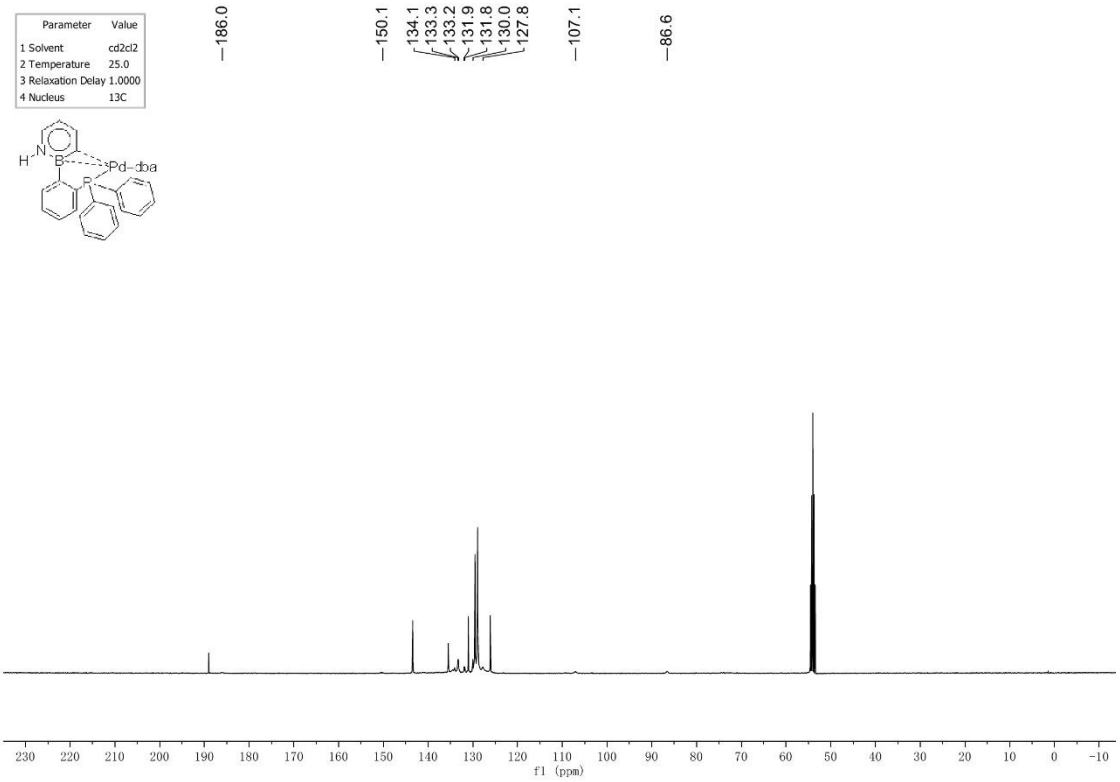
Parameter Value
1 Solvent cd2cl2
2 Temperature 25.0
3 Relaxation Delay 1.0000
4 Nucleus 13C
186.0
150.1
134.1
133.3
133.2
131.9
131.8
130.0
127.8
107.1
86.6
H
N
B
Pd-dba
P
230 220 210 200 190 180 170 160 150 140 130 120 110 100 90 80 70 60 50 40 30 20 10 0 -10
f1 (ppm)

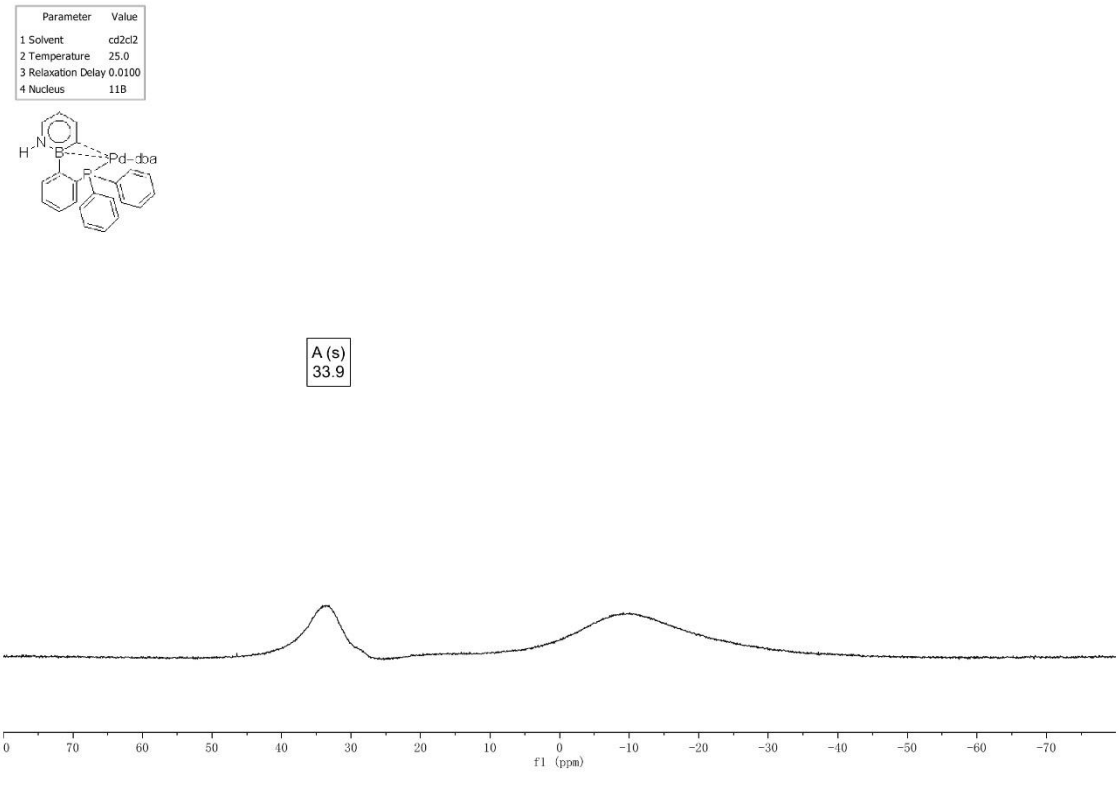
Parameter Value
1 Solvent cd2cl2
2 Temperature 25.0
3 Relaxation Delay 0.0100
4 Nucleus 11B
H
N
B
Pd-dba
P
A (s)
33.9
0 70 60 50 40 30 20 10 0 -10 -20 -30 -40 -50 -60 -70
f1 (ppm)

Parameter	Value
1 Solvent	cd2cl2
2 Temperature	25.0
3 Relaxation Delay	1.0000
4 Nucleus	31P

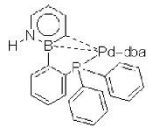

A (s)
24.3

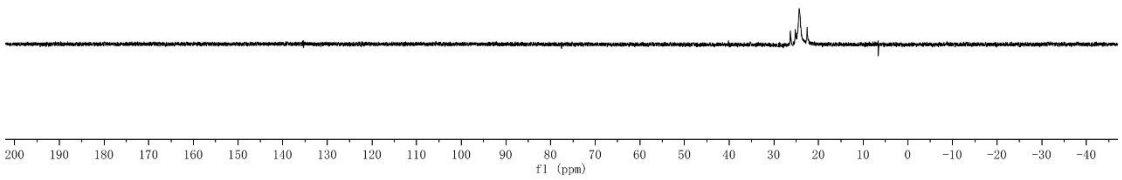

Parameter	Value
1 Solvent	cd3cn
2 Temperature	25.0
3 Relaxation Delay	10.0000
4 Nucleus	1H

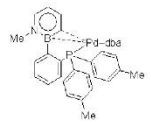

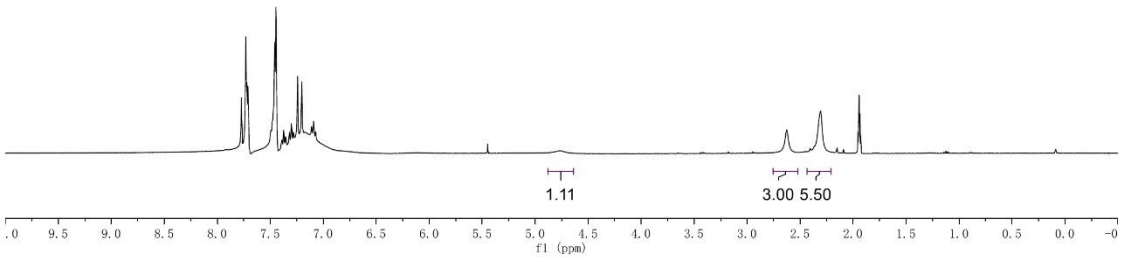

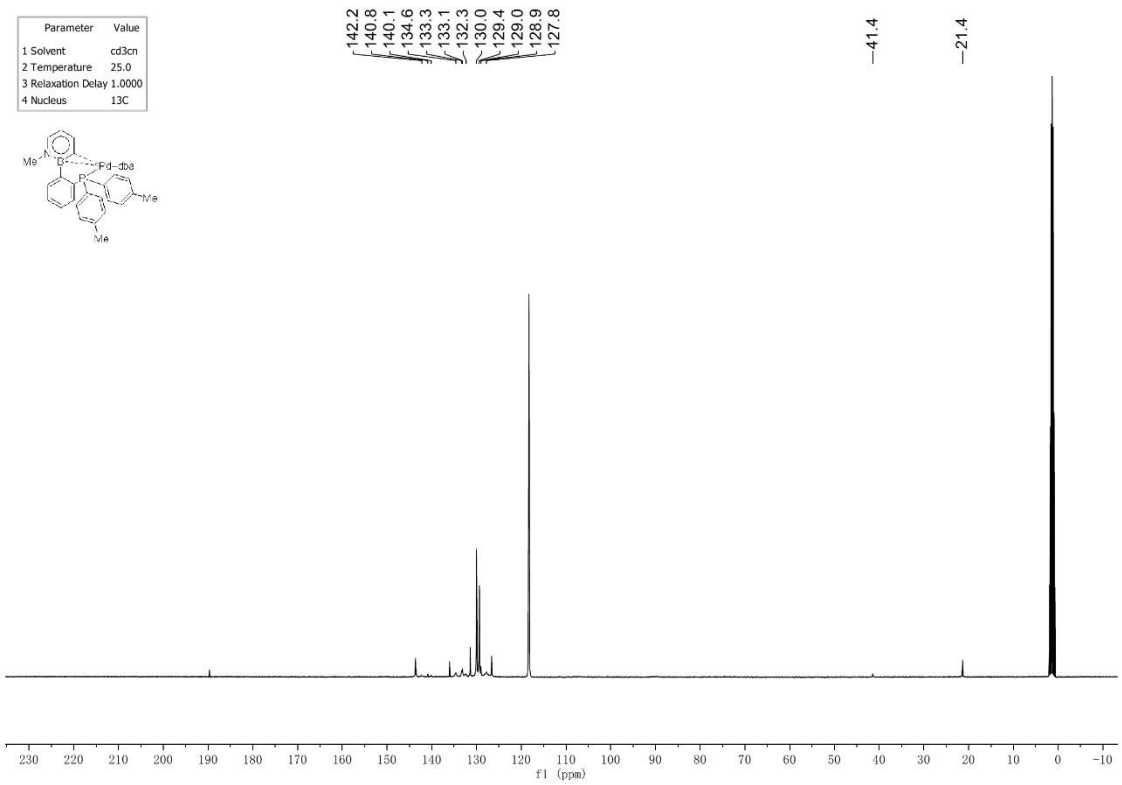
Parameter Value
1 Solvent cd3cn
2 Temperature 25.0
3 Relaxation Delay 1.0000
4 Nucleus 13C
142.2
140.8
140.1
134.6
133.3
133.1
132.3
130.0
129.4
129.0
128.9
127.8
41.4
21.4
Me
N
B
Pd-dba
P
Me
Me
f1 (ppm)

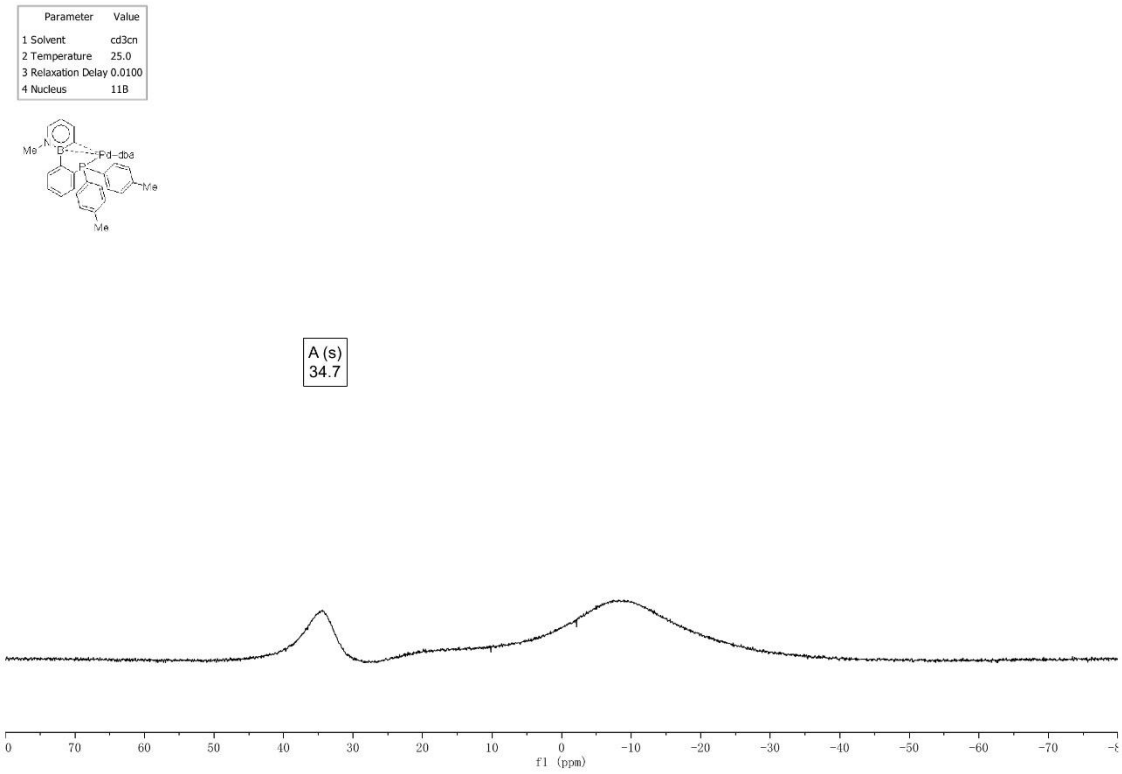
Parameter Value
1 Solvent cd3cn
2 Temperature 25.0
3 Relaxation Delay 0.0100
4 Nucleus 11B
A (s)
34.7
Me
N
B
Pd-dba
P
Me
Me
f1 (ppm)

Parameter	Value
1 Solvent	cd3cn
2 Temperature	25.0
3 Relaxation Delay	1.0000
4 Nucleus	31P

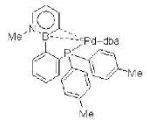

A (s)
26.0

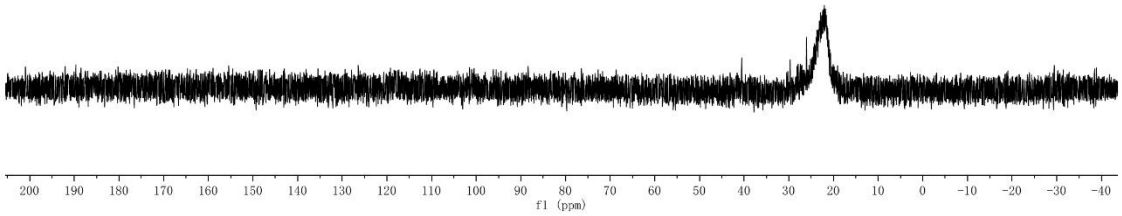

Parameter	Value
1 Solvent	cd3cn
2 Temperature	25.0
3 Relaxation Delay	10.0000
4 Nucleus	1H

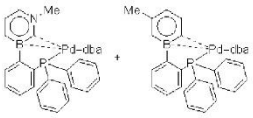

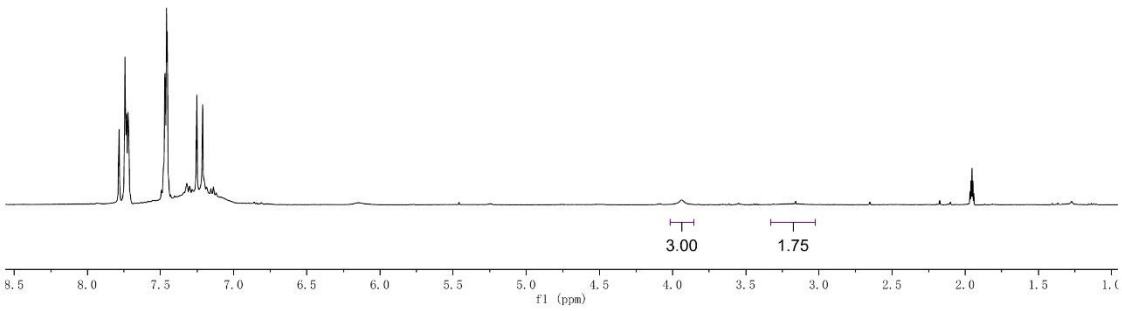

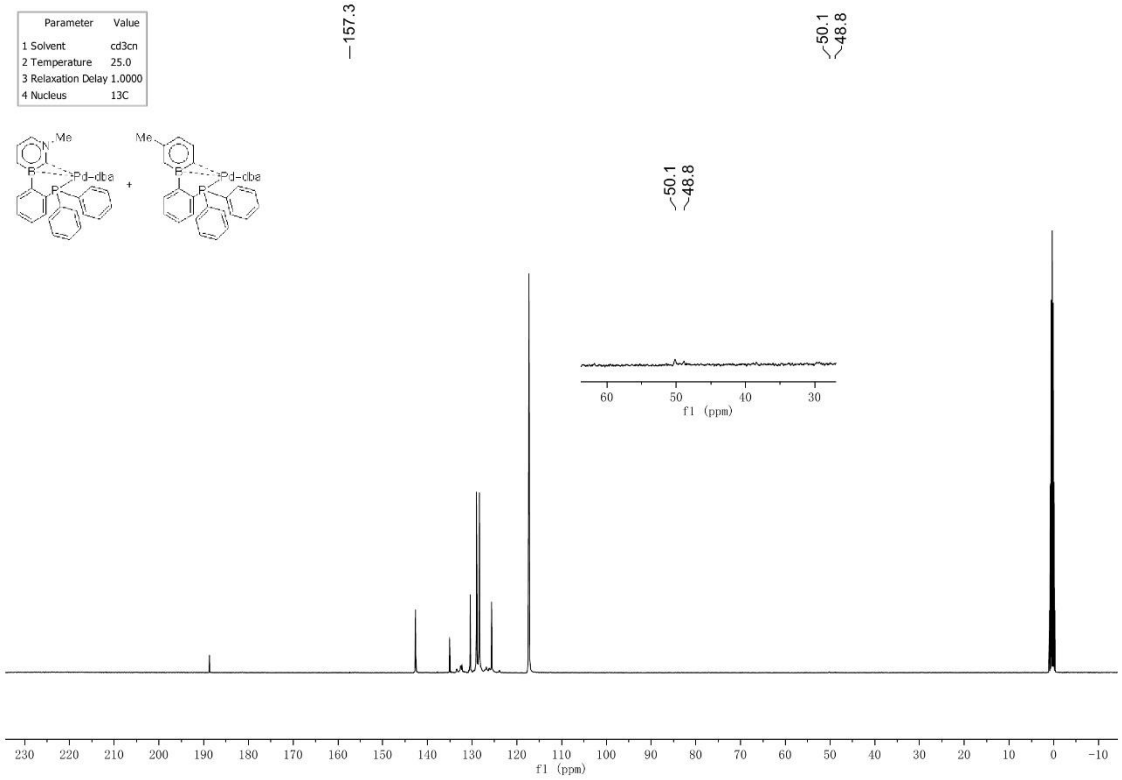
Parameter Value
1 Solvent cd3cn
2 Temperature 25.0
3 Relaxation Delay 1.0000
4 Nucleus 13C
Me
Pd-dba
Pd-dba
157.3
50.1
48.8
50.1
48.8
f1 (ppm)
f1 (ppm)

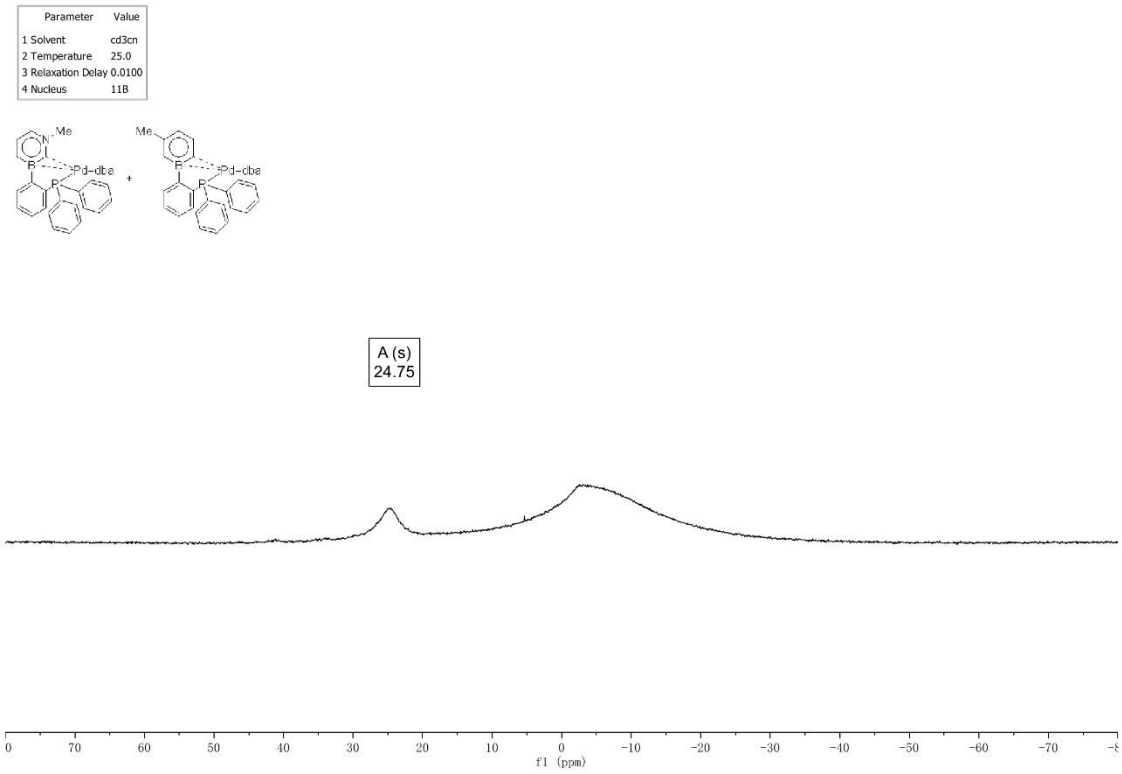
Parameter Value
1 Solvent cd3cn
2 Temperature 25.0
3 Relaxation Delay 0.0100
4 Nucleus 11B
Me
Pd-dba
Pd-dba
A (s)
24.75
f1 (ppm)

Parameter	Value
1 Solvent	cd3cn
2 Temperature	25.0
3 Relaxation Delay	1.0000
4 Nucleus	31P

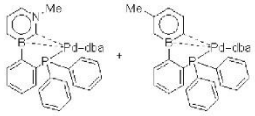

A (m)
29.3

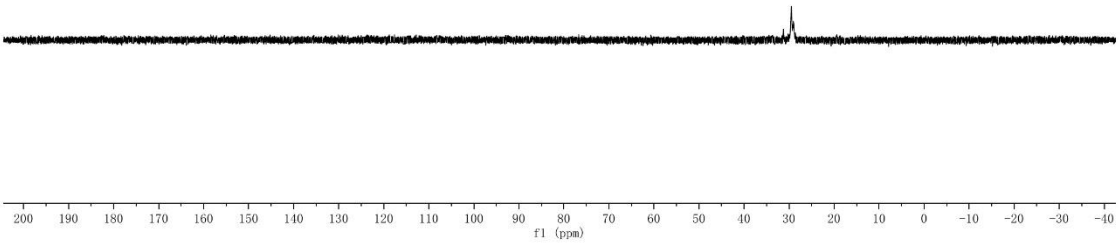

Parameter	Value
1 Solvent	cd3cn
2 Temperature	25.0
3 Relaxation Delay	10.0000
4 Nucleus	1H

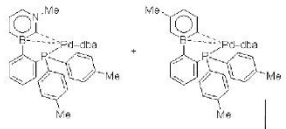

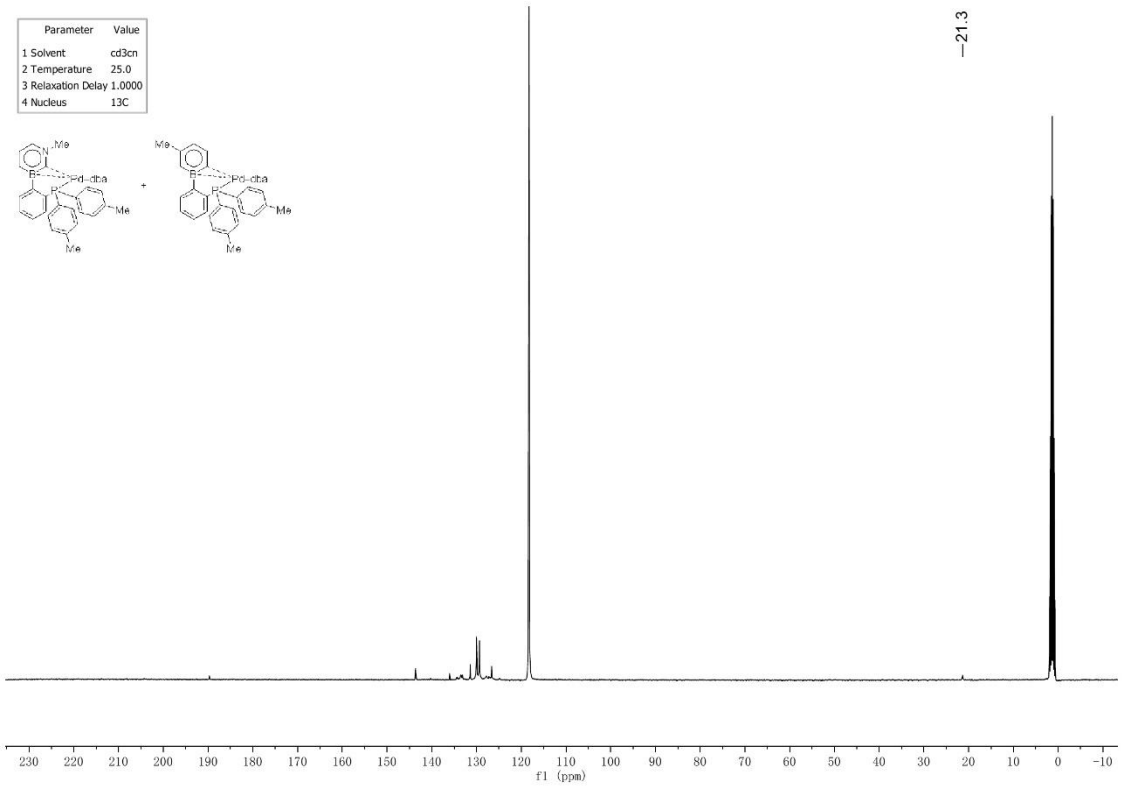
Parameter Value
1 Solvent cd3cn
2 Temperature 25.0
3 Relaxation Delay 1.0000
4 Nucleus 13C
21.3
f1 (ppm)

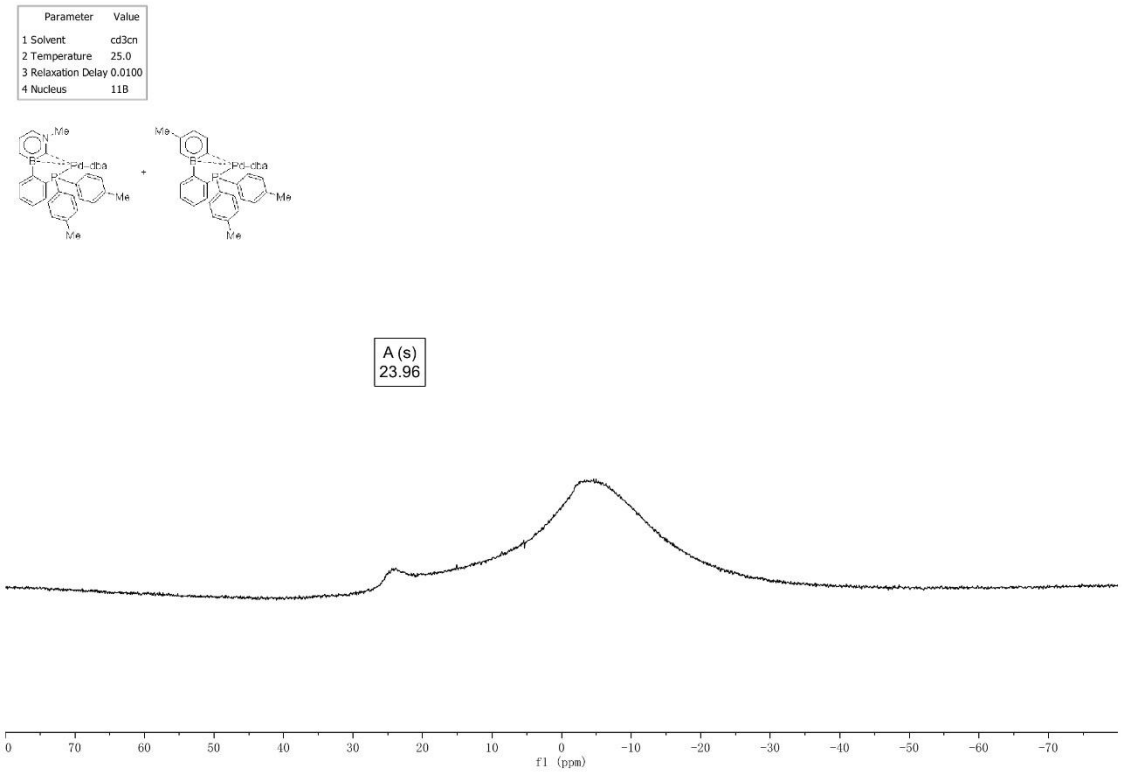
Parameter Value
1 Solvent cd3cn
2 Temperature 25.0
3 Relaxation Delay 0.0100
4 Nucleus 11B
A (s)
23.96
f1 (ppm)

Parameter	Value
1 Solvent	cd3cn
2 Temperature	25.0
3 Relaxation Delay	1.0000
4 Nucleus	31P

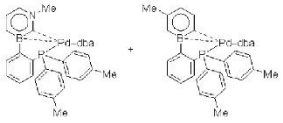

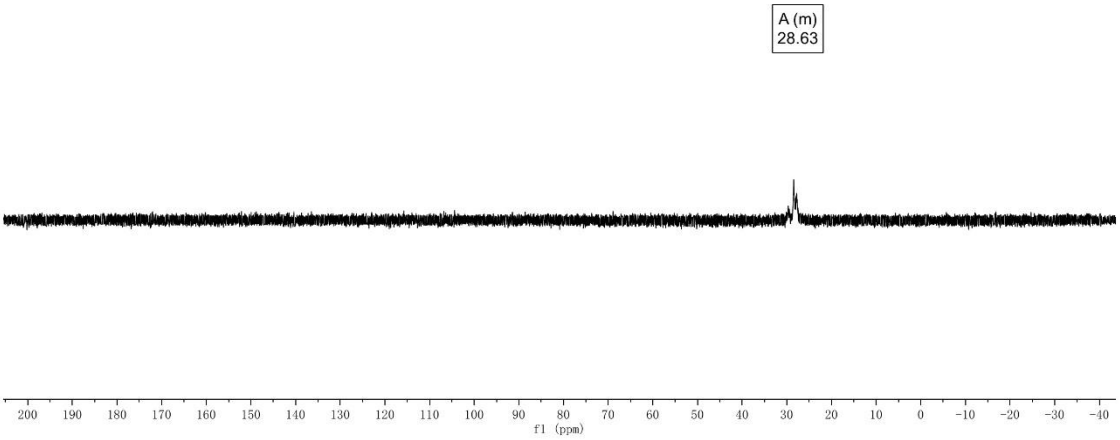

Parameter	Value
1 Solvent	cd3cn
2 Temperature	25.0
3 Relaxation Delay	10.0000
4 Nucleus	1H

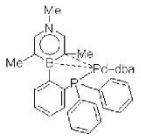

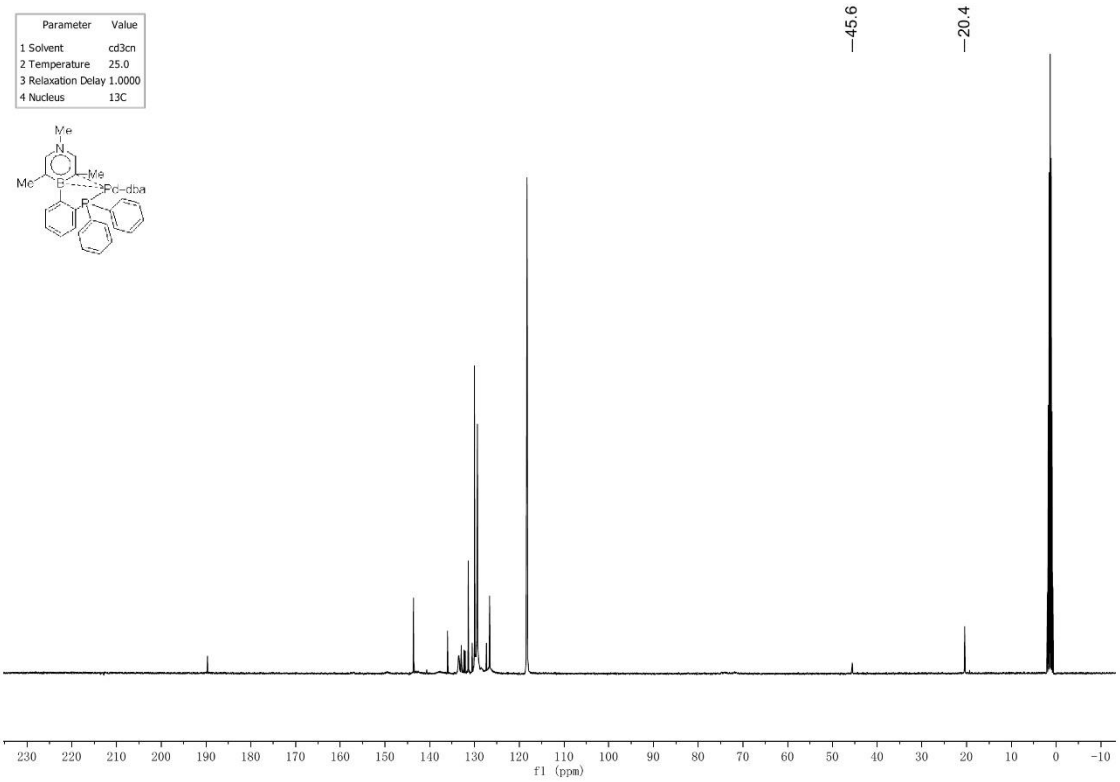
Parameter Value
1 Solvent cd3cn
2 Temperature 25.0
3 Relaxation Delay 1.0000
4 Nucleus 13C
Me
N
Me
Me
B
Pd-dba
P
45.6
20.4
230 220 210 200 190 180 170 160 150 140 130 120 110 100 90 80 70 60 50 40 30 20 10 0 -10
f1 (ppm)

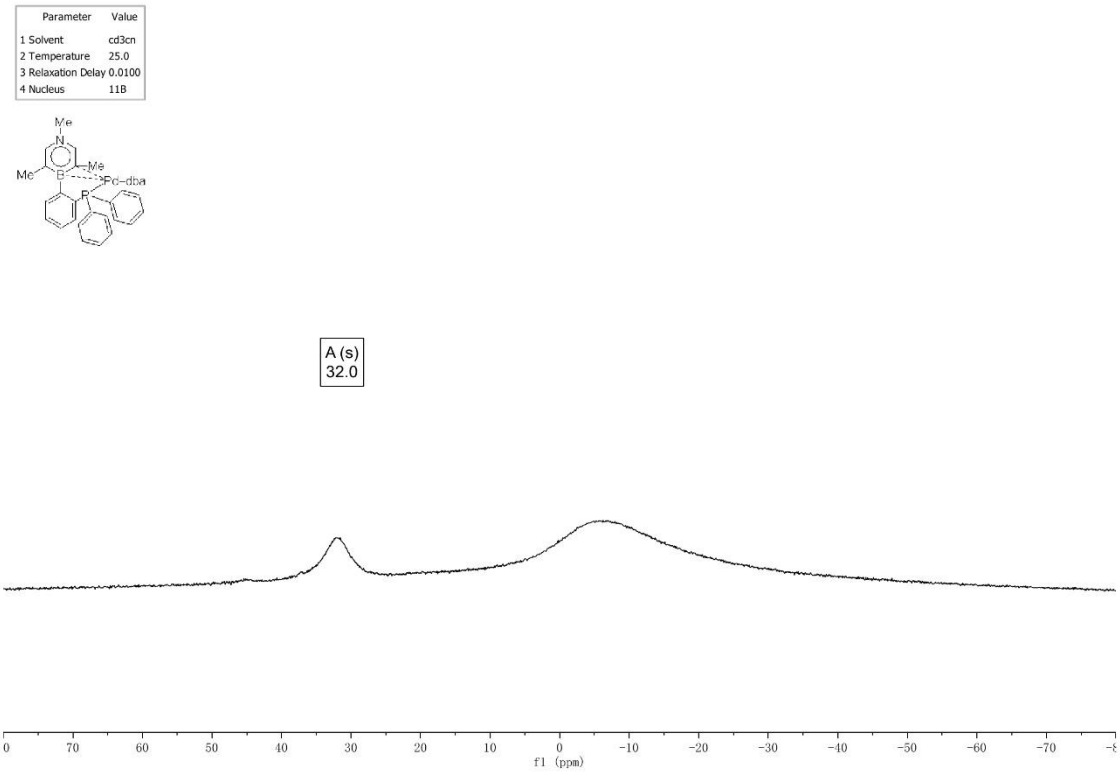
Parameter Value
1 Solvent cd3cn
2 Temperature 25.0
3 Relaxation Delay 0.0100
4 Nucleus 11B
Me
N
Me
Me
B
Pd-dba
P
A (s)
32.0
0 70 60 50 40 30 20 10 0 -10 -20 -30 -40 -50 -60 -70
f1 (ppm)

Parameter	Value
1 Solvent	cd3cn
2 Temperature	25.0
3 Relaxation Delay	1.0000
4 Nucleus	31P

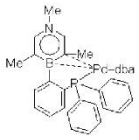

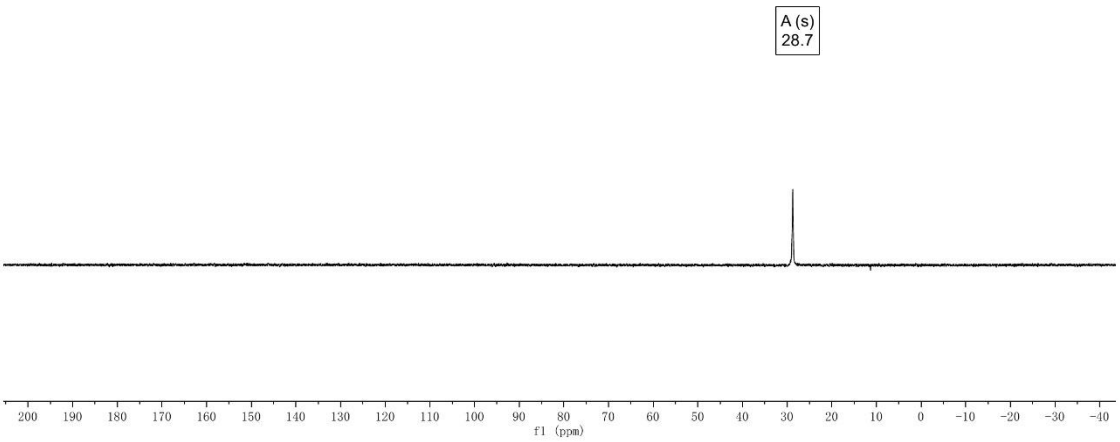

Parameter	Value
1 Solvent	cd3cn
2 Temperature	25.0
3 Receiver Gain	46
4 Relaxation Delay	10.0000
5 Nucleus	1H

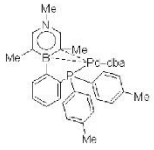

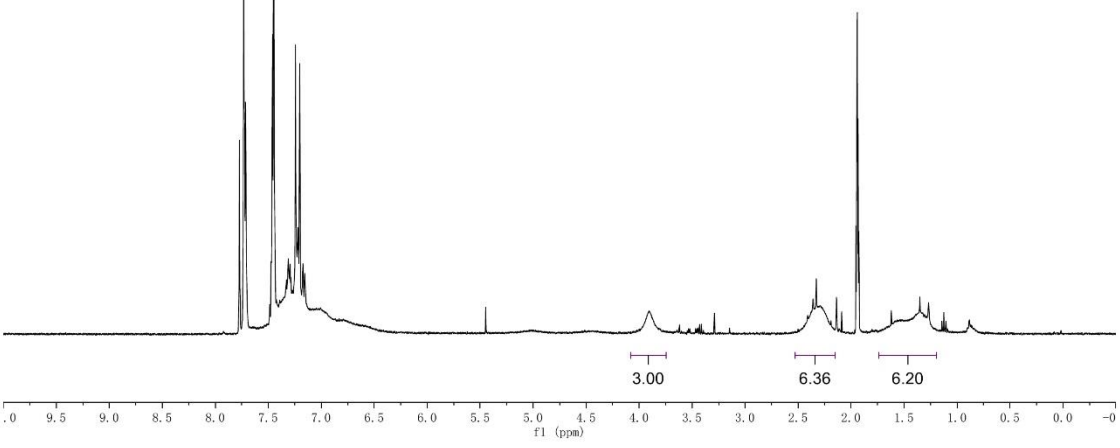

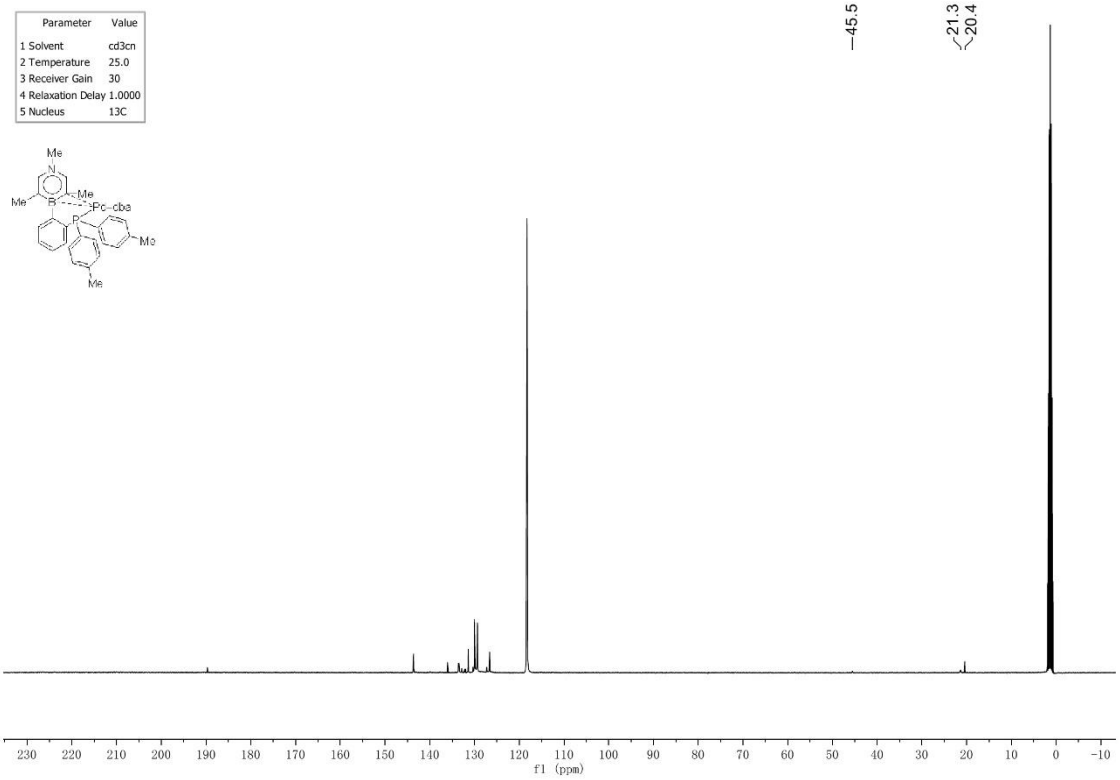
Parameter Value
1 Solvent cd3cn
2 Temperature 25.0
3 Receiver Gain 30
4 Relaxation Delay 1.0000
5 Nucleus 13C
45.5
21.3
20.4
f1 (ppm)

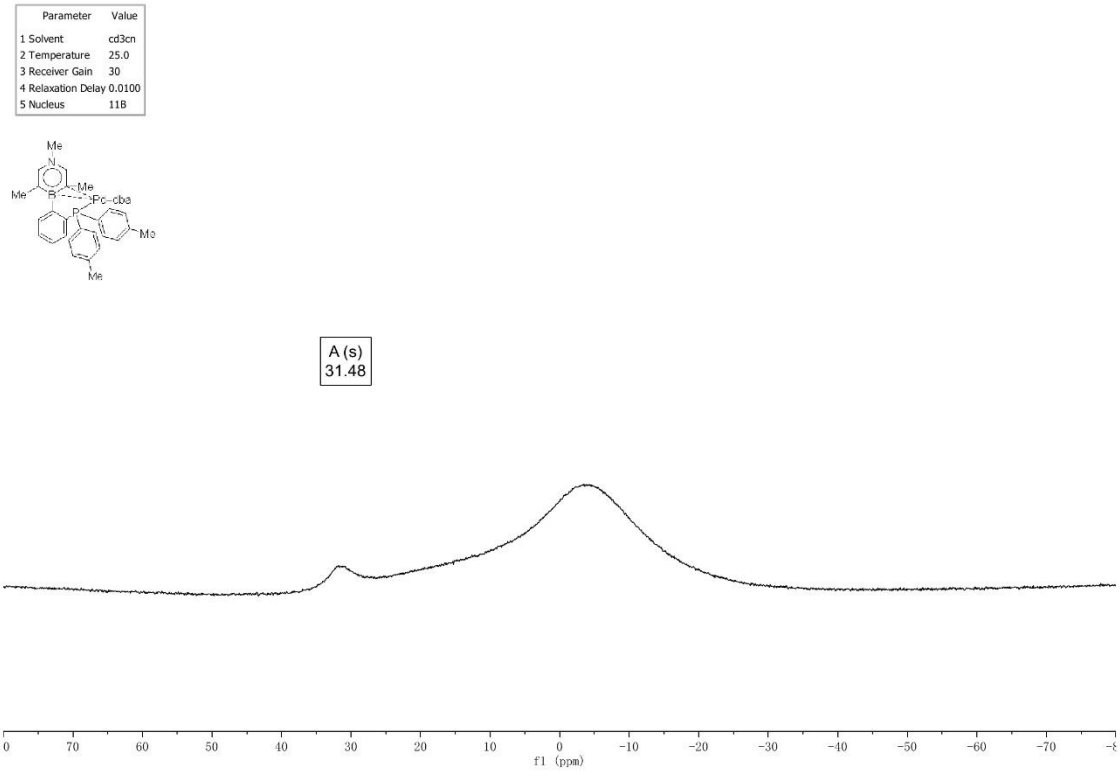
Parameter Value
1 Solvent cd3cn
2 Temperature 25.0
3 Receiver Gain 30
4 Relaxation Delay 0.0100
5 Nucleus 11B
A (s)
31.48
f1 (ppm)

Parameter	Value
1 Solvent	cd3cn
2 Temperature	25.0
3 Receiver Gain	50
4 Relaxation Delay	1.0000
5 Nucleus	31P

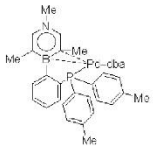

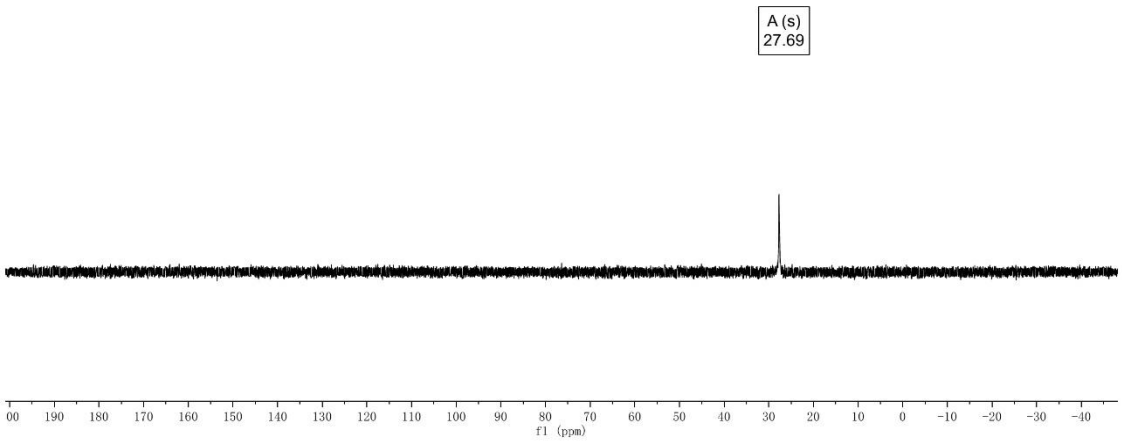

Parameter	Value
1 Solvent	cd3cn
2 Temperature	25.0
3 Relaxation Delay	1.0000
4 Nucleus	1H

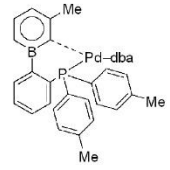

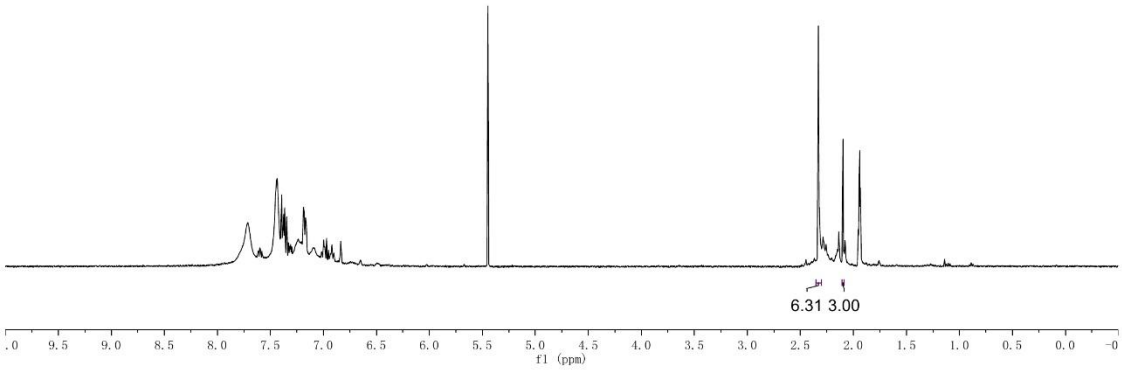

Parameter	Value
1 Solvent	cd3cn
2 Temperature	25.0
3 Relaxation Delay	1.0000
4 Nucleus	31P

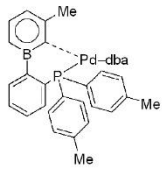

A (s)
27.9

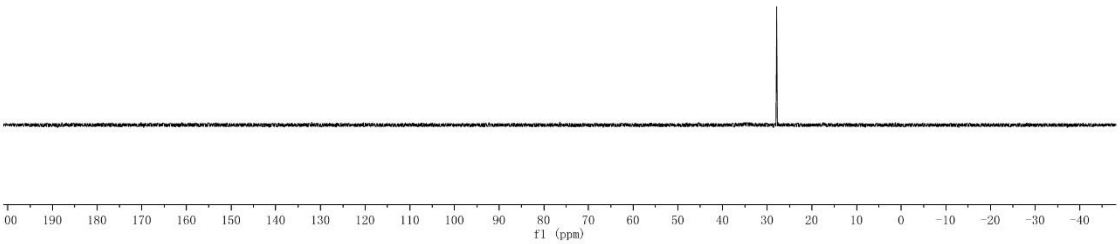

Parameter	Value
1 Solvent	cdcl3
2 Temperature	25.0
3 Relaxation Delay	1.0000
4 Nucleus	1H

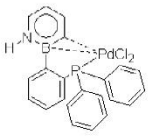

Parameter	Value
1 Solvent	cd2cl2
2 Temperature	25.0
3 Relaxation Delay	0.0100
4 Nucleus	11B

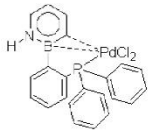

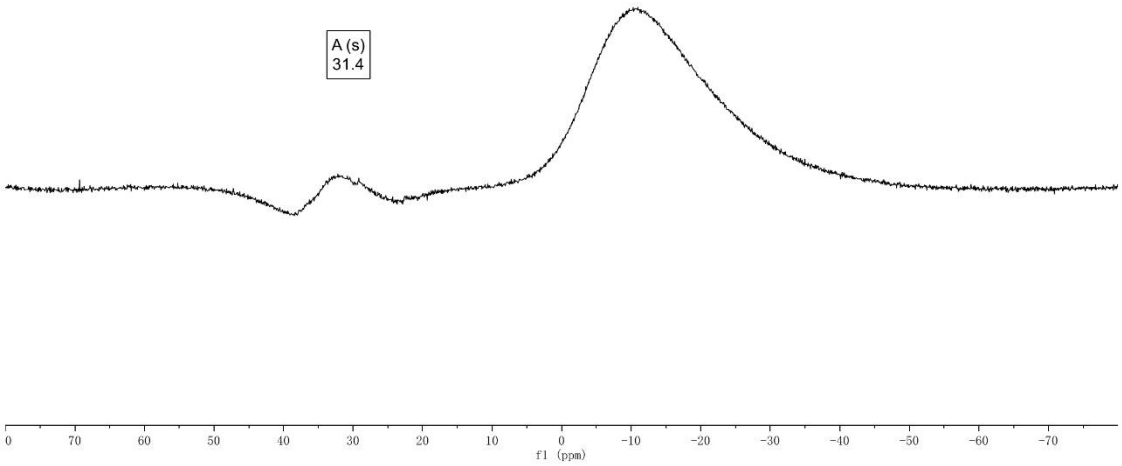

Parameter	Value
1 Solvent	cdcl3
2 Temperature	25.0
3 Relaxation Delay	1.0000
4 Nucleus	31P

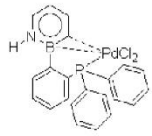

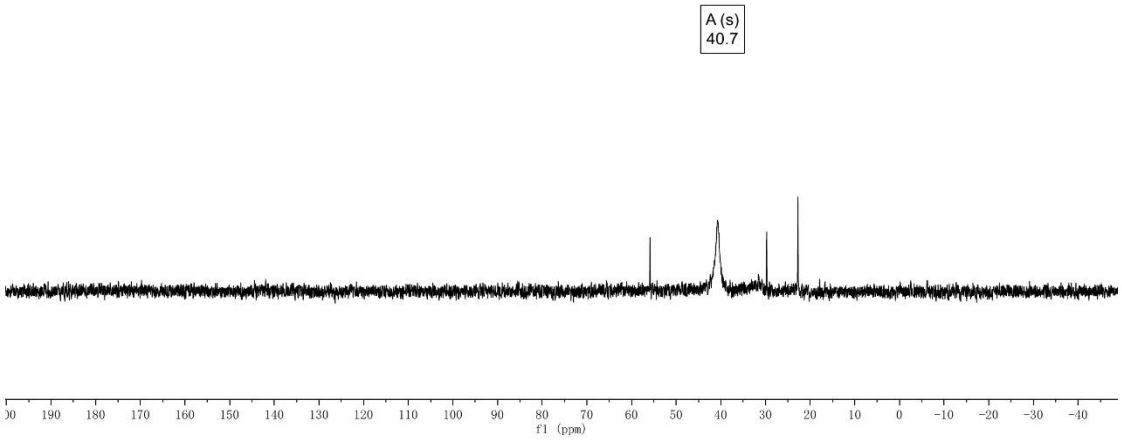

Parameter	Value
1 Solvent	cd3cn
2 Temperature	25.0
3 Relaxation Delay	10.0000
4 Nucleus	1H

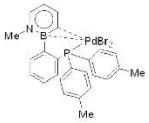

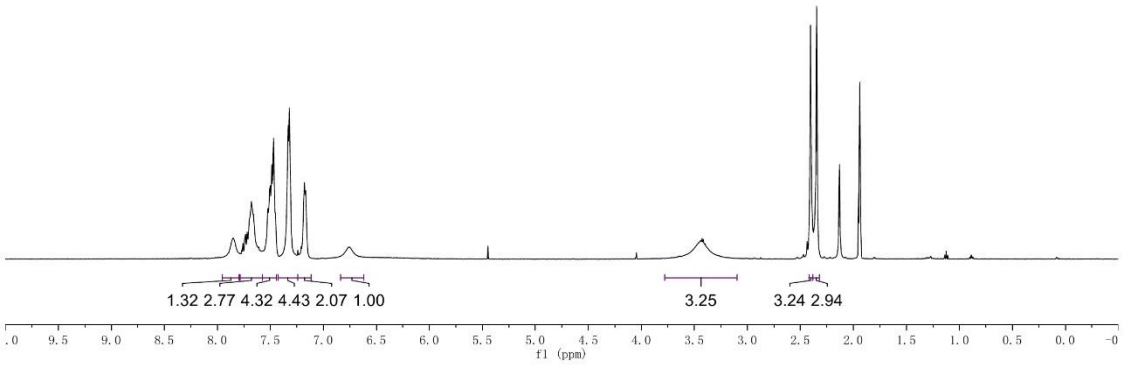

Parameter	Value
1 Solvent	cd3cn
2 Temperature	25.0
3 Relaxation Delay	1.0000
4 Nucleus	13C

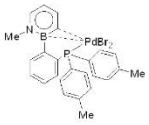

Parameter	Value
1 Solvent	cd3cn
2 Temperature	25.0
3 Relaxation Delay	0.0100
4 Nucleus	11B

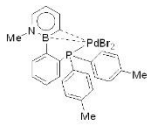

A (s)
34.3

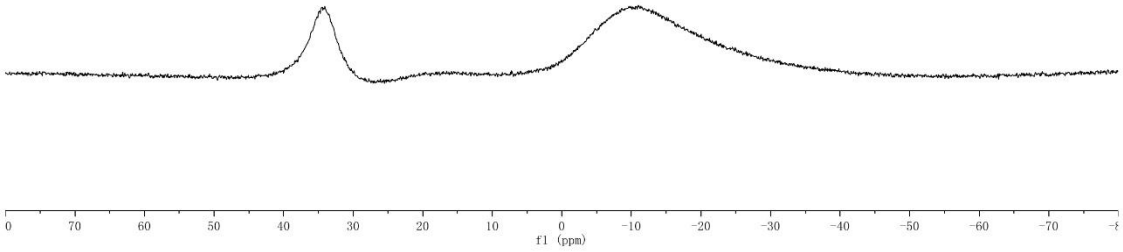

Parameter	Value
1 Solvent	cd3cn
2 Temperature	25.0
3 Relaxation Delay	1.0000
4 Nucleus	31P

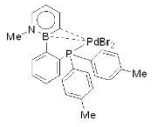

A (s)
33.9

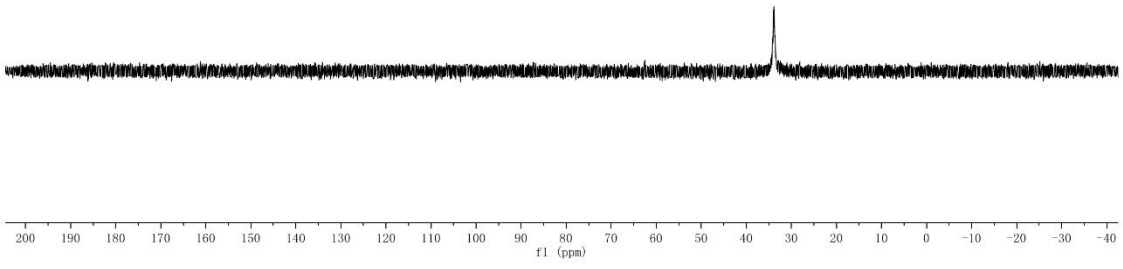

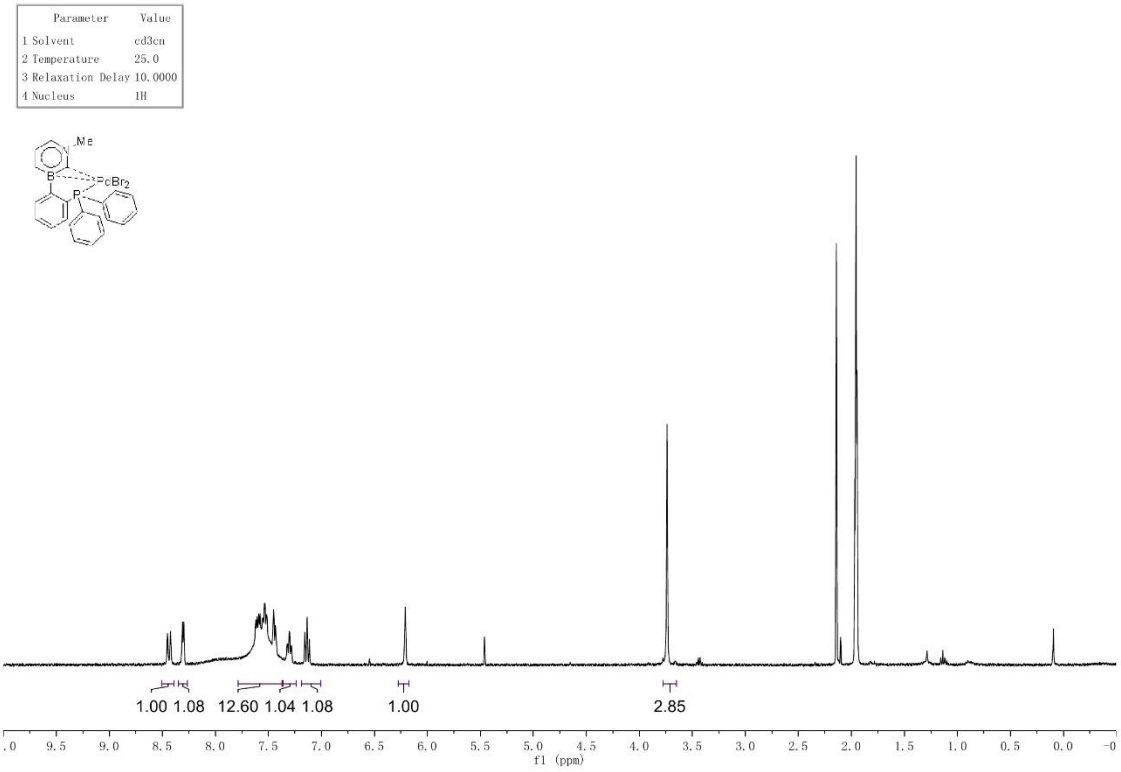
Parameter Value
1 Solvent cd3cn
2 Temperature 25.0
3 Relaxation Delay 10.0000
4 Nucleus 1H
Me
B
P
=cBr2
1.00 1.08 12.60 1.04 1.08 1.00 2.85
f1 (ppm)

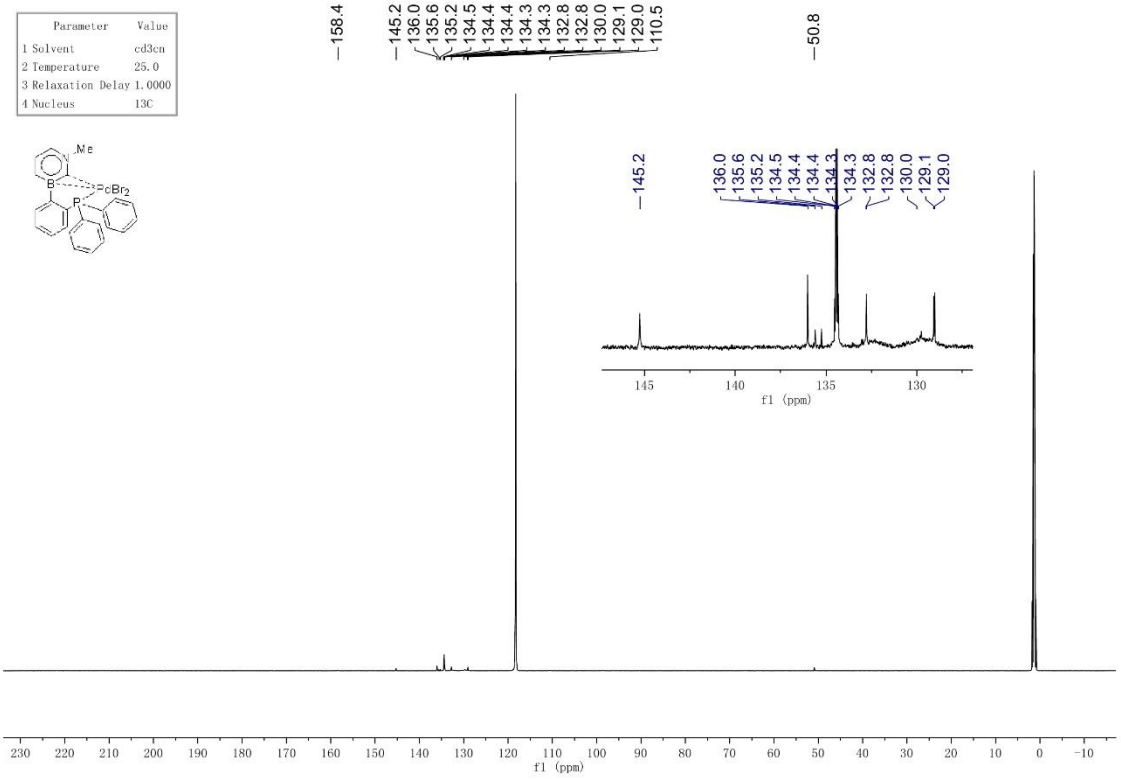
Parameter Value
1 Solvent cd3cn
2 Temperature 25.0
3 Relaxation Delay 1.0000
4 Nucleus 13C
Me
B
P
=cBr2
158.4
145.2
136.0
135.6
135.2
134.5
134.4
134.4
134.3
134.3
132.8
132.8
130.0
129.1
129.0
110.5
50.8
f1 (ppm)

Parameter	Value
1 Solvent	cd3cn
2 Temperature	25.0
3 Relaxation Delay	0.0100
4 Nucleus	11B

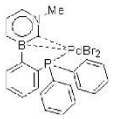

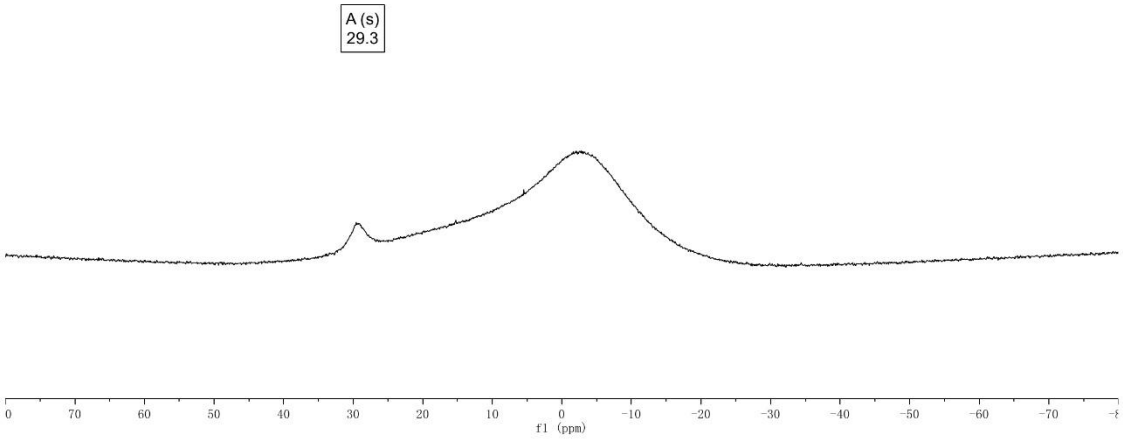

Parameter	Value
1 Solvent	cd3cn
2 Temperature	25.0
3 Relaxation Delay	1.0000
4 Nucleus	31P

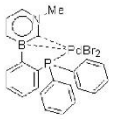

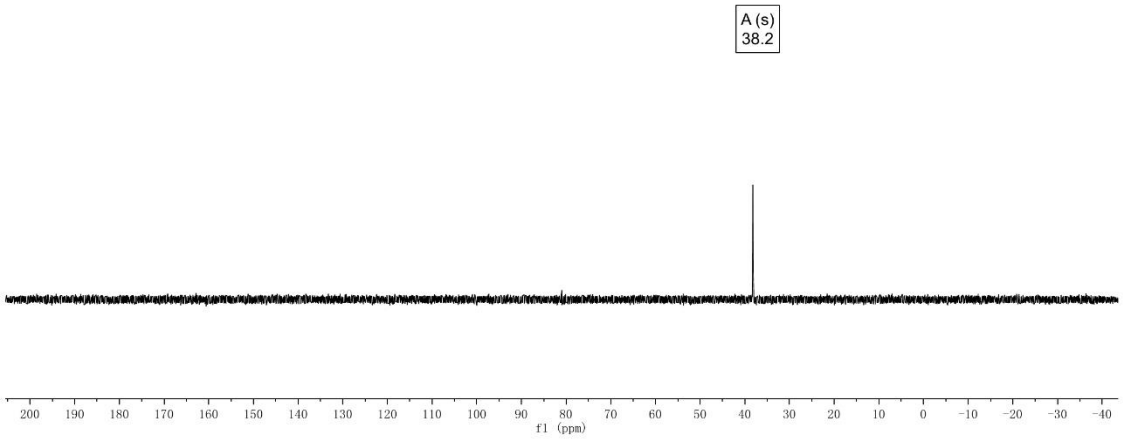

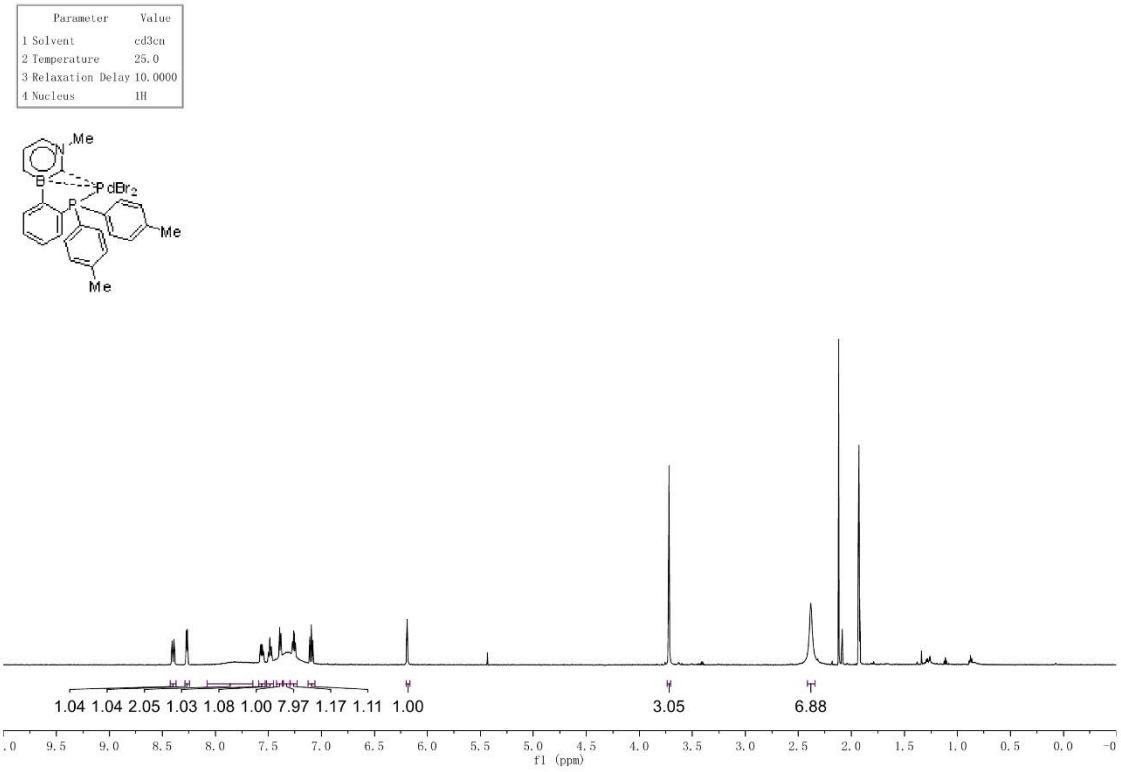
Parameter Value
1 Solvent cd3cn
2 Temperature 25.0
3 Relaxation Delay 10.0000
4 Nucleus 1H
Me
PdBr2
Me
Me
1.04 1.04 2.05 1.03 1.08 1.00 7.97 1.17 1.11 1.00
3.05
6.88
f1 (ppm)

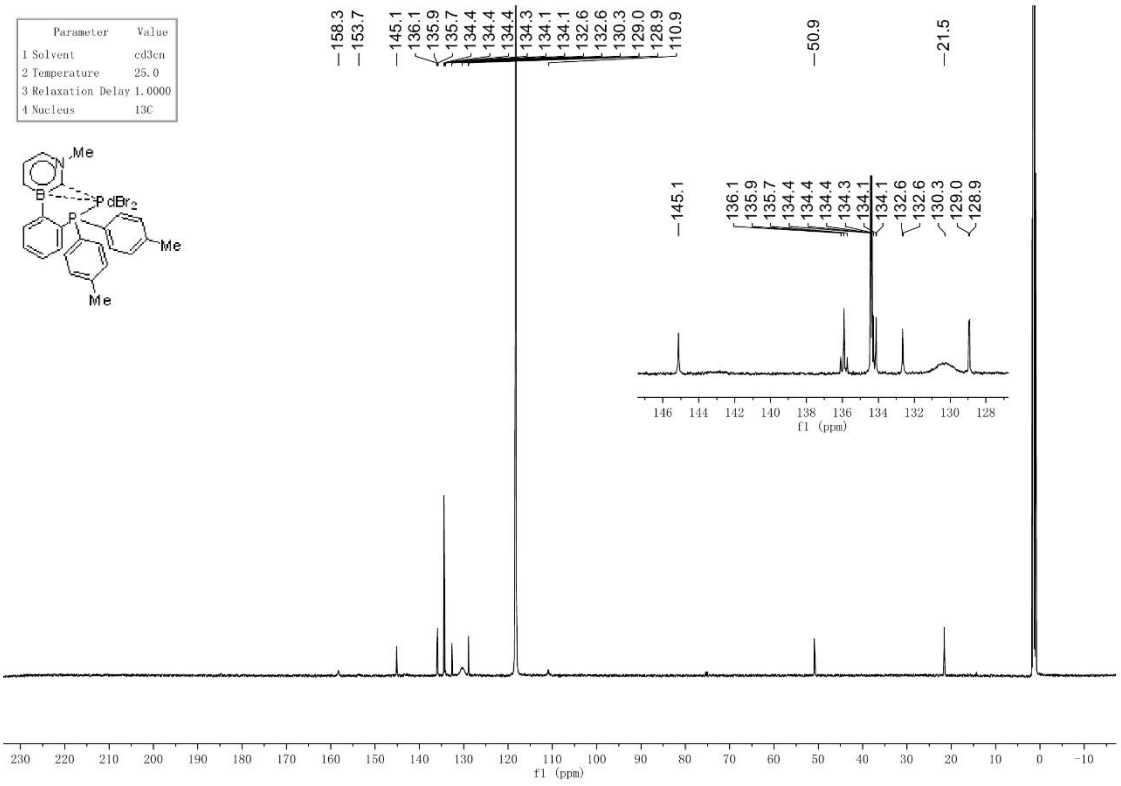
Parameter Value
1 Solvent cd3cn
2 Temperature 25.0
3 Relaxation Delay 1.0000
4 Nucleus 13C
Me
PdBr2
Me
Me
158.3
153.7
145.1
136.1
135.9
135.7
134.4
134.4
134.4
134.3
134.1
134.1
132.6
132.6
130.3
129.0
128.9
110.9
50.9
21.5
f1 (ppm)

Parameter	Value
1 Solvent	cd3cn
2 Temperature	25.0
3 Relaxation Delay	0.0100
4 Nucleus	11B

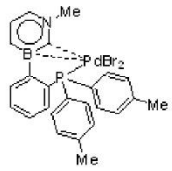

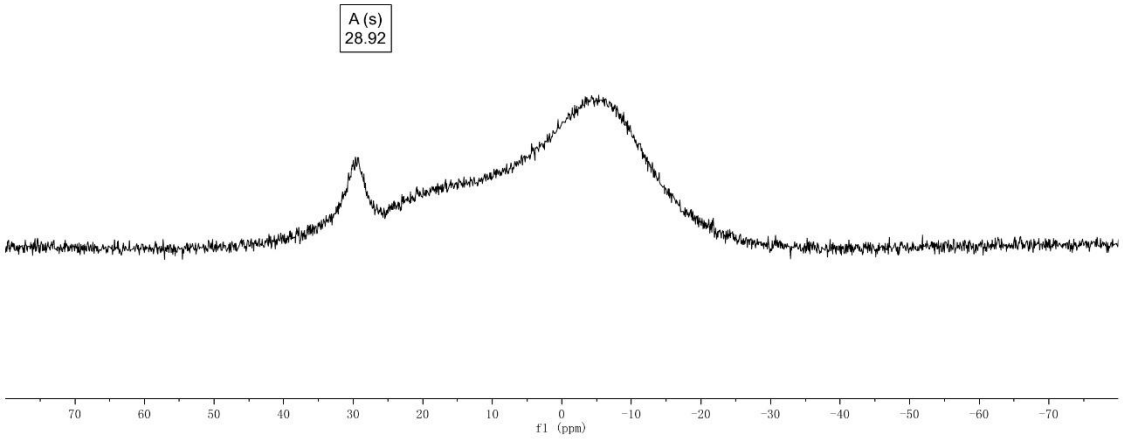

Parameter	Value
1 Solvent	cd3cn
2 Temperature	25.0
3 Relaxation Delay	1.0000
4 Nucleus	31P

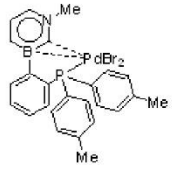

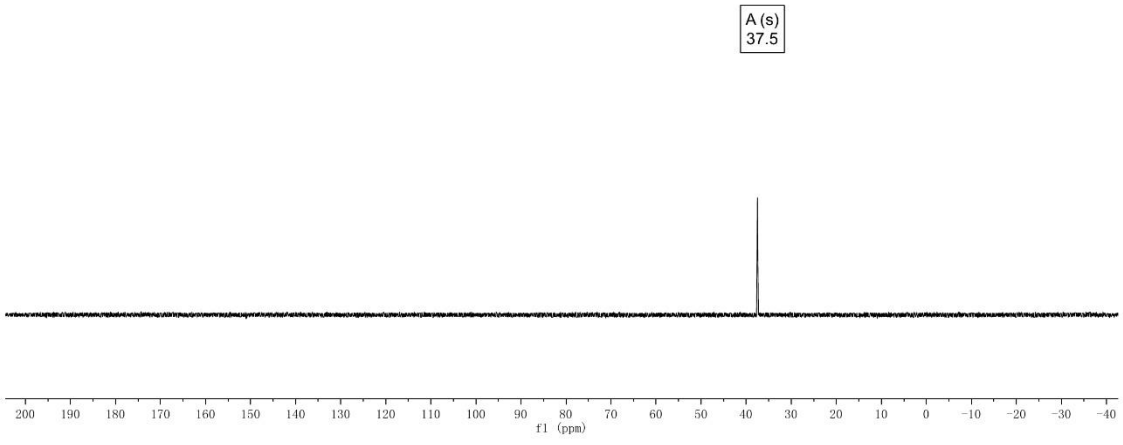

Parameter	Value
1 Solvent	cd3cn
2 Temperature	25.0
3 Relaxation Delay	10.0000
4 Nucleus	1H

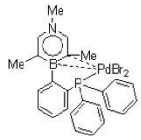

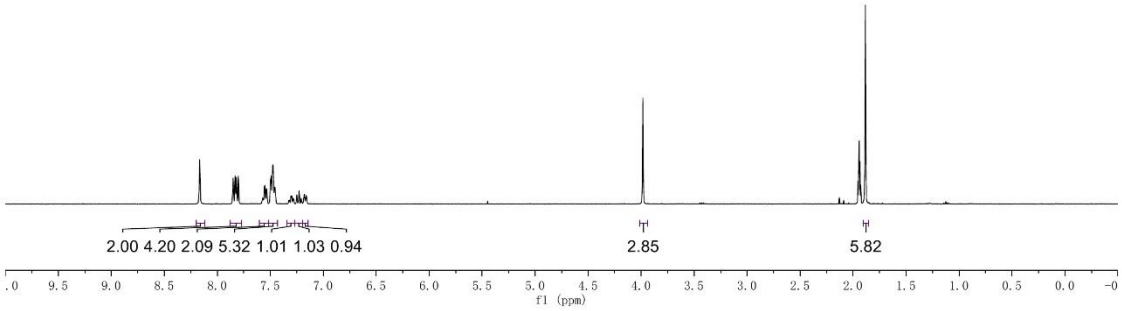

Parameter	Value
1 Solvent	cd3cn
2 Temperature	25.0
3 Relaxation Delay	1.0000
4 Nucleus	13C

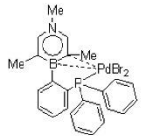

Parameter	Value
1 Solvent	cd3cn
2 Temperature	25.0
3 Relaxation Delay	0.0100
4 Nucleus	11B

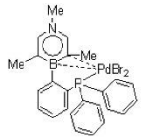

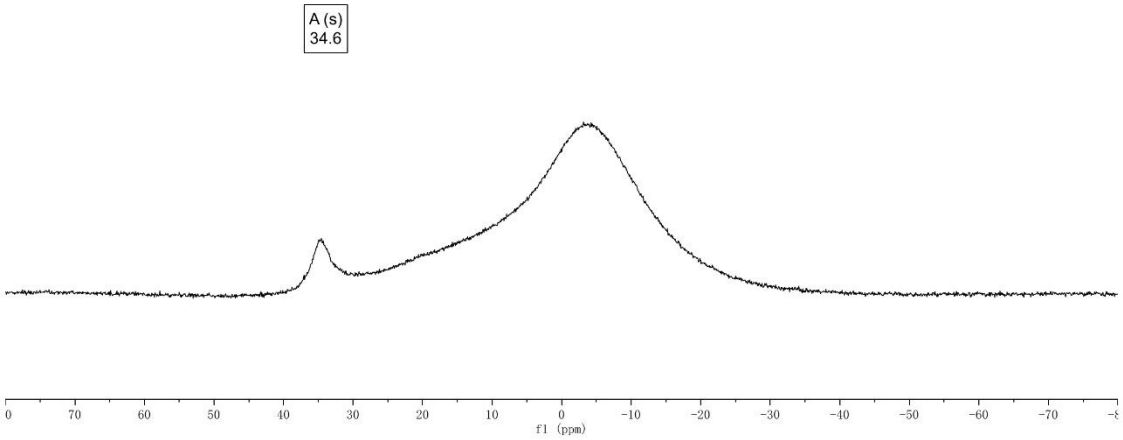

Parameter	Value
1 Solvent	cd3cn
2 Temperature	25.0
3 Relaxation Delay	1.0000
4 Nucleus	31P

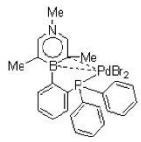

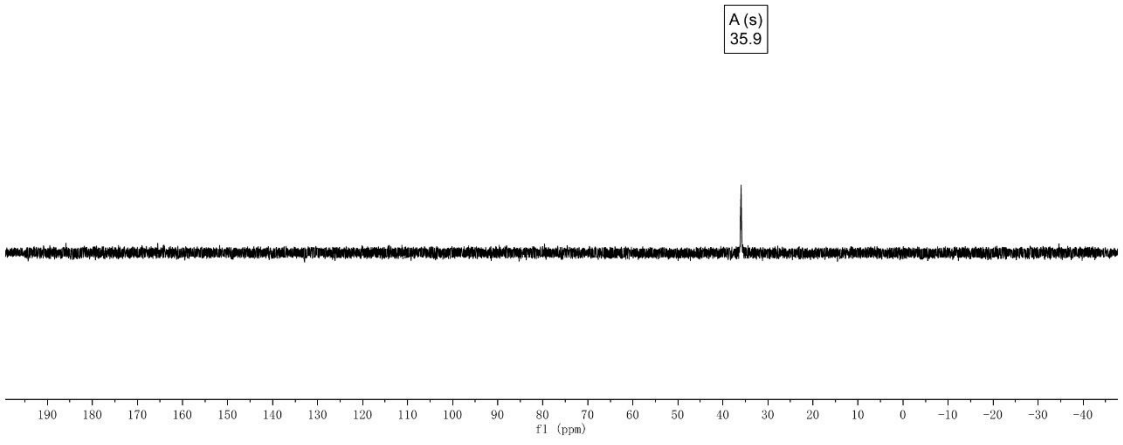

Parameter	Value
1 Solvent	cd3cn
2 Temperature	25.0
3 Relaxation Delay	10.0000
4 Nucleus	1H

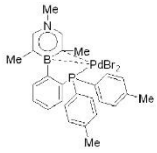

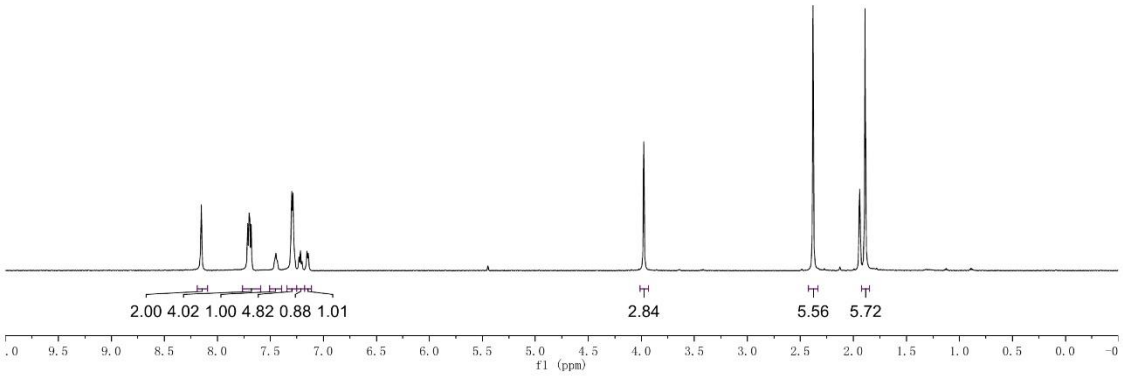

Parameter	Value
1 Solvent	cd3cn
2 Temperature	25.0
3 Relaxation Delay	1.0000
4 Nucleus	13C

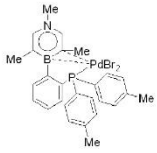

Parameter	Value
1 Solvent	cd3cn
2 Temperature	25.0
3 Relaxation Delay	0.0100
4 Nucleus	11B

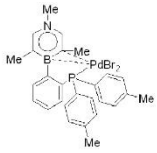

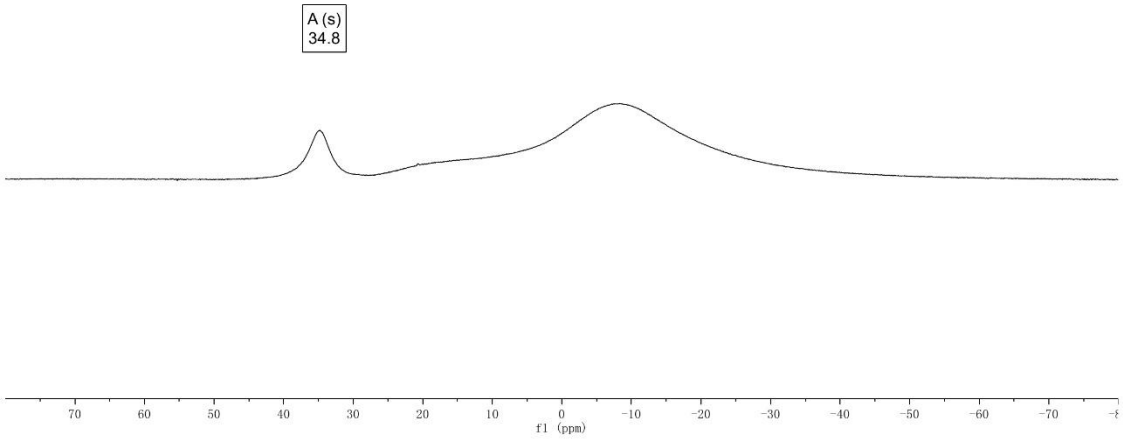

Parameter	Value
1 Solvent	cd3cn
2 Temperature	25.0
3 Relaxation Delay	1.0000
4 Nucleus	31P

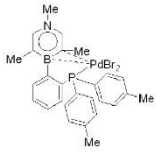

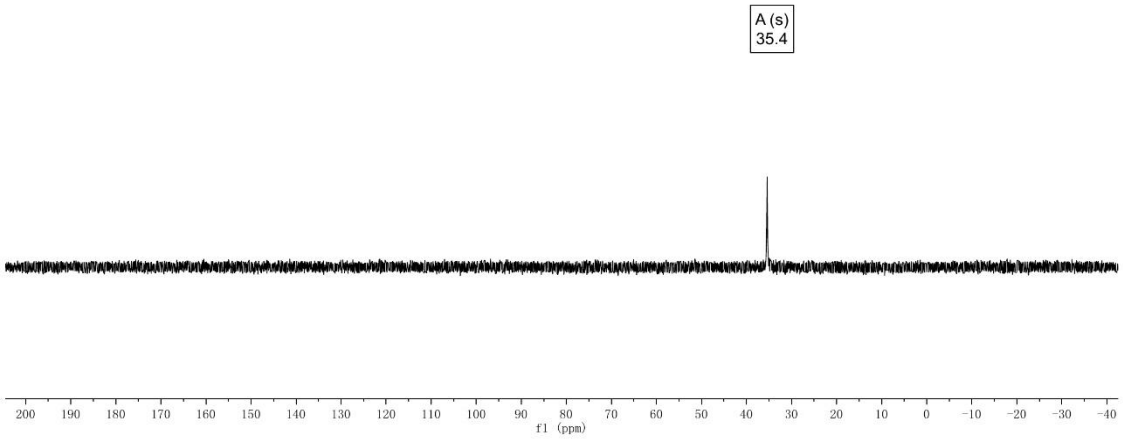

Parameter	Value
1 Solvent	cdcl3
2 Temperature	25.0
3 Relaxation Delay	10.0000
4 Nucleus	1H

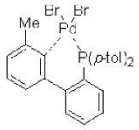

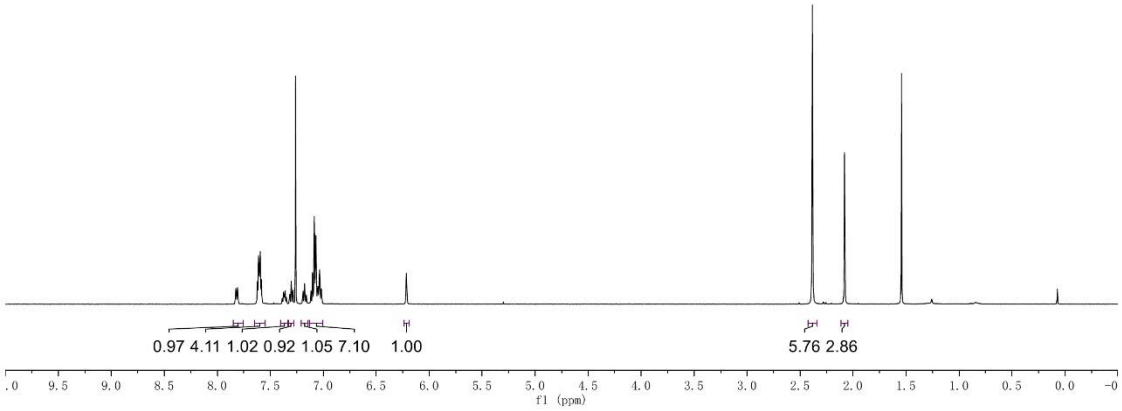

Parameter	Value
1 Solvent	cdcl3
2 Temperature	25.0
3 Relaxation Delay	1.0000
4 Nucleus	13C

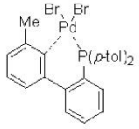

	Parameter	Value
1	Solvent	cdcl3
2	Temperature	25.0
3	Relaxation Delay	1.0000
4	Nucleus	31P